VIVEK SWARUP

Étude et caractérisation du rôle de protéines TDP-43 mutantes dans la pathogénèse de la sclérose latérale amyotrophique (SLA)

Study and characterization of the role of TDP-43 mutants in pathogenesis of amyotrophic lateral sclerosis (ALS)

Thèse présentée
à la Faculté des études supérieures et postdoctorales de l'Université Laval
dans le cadre du programme de doctorat en Physiologie-Endocrinologie
pour l'obtention du grade de Philosophiæ doctor (PhD)

FACULTÉ DE MEDECINE
UNIVERSITÉ LAVAL
QUÉBEC

2012

Résumé

La sclérose latérale amyotrophique (SLA) est une maladie mortelle caractérisée par une dégénérescence des neurones moteurs supérieurs et inférieurs. La présence d'inclusions ubiquitinylées de la protéine TDP-43 (Transactive response DNA-binding protein 43) est une caractéristique de la SLA. Afin de comprendre le mécanisme pathogène impliquant cette protéine, nous avons généré et étudié des souris transgéniques en utilisant des fragments génomiques codant pour la TDP-43 humain, de type sauvage ou mutant, associés aux cas familiaux de la SLA. Ces souris développent de nombreux changements liés au processus pathologique et biochimique de la SLA chez l'homme : présence d'inclusions de la protéine TDP-43 ubiquitinylées, anomalies au niveau des filaments intermédiaires, axonopathie et neuroinflammation. Pour mieux comprendre le rôle de la protéine TDP-43 dans la régénération des axones, nous avons utilisé des souris pré-symptomatiques et effectué une lésion du nerf sciatique sur celles-ci. Suite à cette intervention, les souris transgéniques ont eu une paralysie marquée du membre lésé, ont démontré une redistribution altéré de TDP-43 et une regénération plus lente des axones distaux par rapport aux souris non transgéniques. De plus, nous avons constaté que la protéine TDP-43 interagit et colocalise avec la sous-unité p65 du facteur nucléaire κB (NF-κB). Cette interaction se produit dans les cellules gliales et les neurones des souris transgéniques TDP-43 et aussi chez les patients atteints de la SLA. Nous avons démontré que les niveaux d'ARNm des protéines TDP-43 et NF-κB p65, sont plus élevés dans la moelle épinière des patients atteints de SLA que chez les individus sains et que la protéine TDP-43 agit comme un coactivateur de p65. Finalement, le traitement des souris transgéniques TDP-43 avec la Withaférine A, un inhibiteur de l'activité NF-κB, réduit le niveau de dénervation des jonctions neuromusculaires et des symptômes liés à la SLA. Nous suggérons donc que le dérèglement de la protéine TDP-43 contribue à la pathogenèse de la SLA en partie par l'augmentation de l'activation de NF-κB, et que NF-κB pourrait constituer une cible thérapeutique pour la maladie.

Abstract

Amyotrophic lateral sclerosis (ALS) is a lethal disease characterized by degeneration of lower and upper motor neurons. Transactive response DNA-binding protein 43 (TDP-43) ubiquitinated inclusions are a hallmark of ALS. In order to understand the pathogenic mechanism caused by TDP-43, we generated transgenic mice with genomic fragments encoding human TDP-43 wild-type or FALS-linked mutants TDP-43^{G348C} and TDP-43^{A315T}. These novel TDP-43 transgenic mice develop many age-related pathological and biochemical changes reminiscent of human ALS including ubiquitinated TDP-43 positive inclusions, intermediate filament abnormalities, axonopathy and neuroinflammation. In order to understand the role of TDP-43 in axon regeneration, we used pre-symptomatic 3-months old mice and performed sciatic nerve crush on them. After axonal crush, TDP-43 transgenic mice were noticeably paralyzed at the injured limb, have altered TDP-43 redistribution and the distal axons regenerated slowly as compared to non-transgenic mice. Moreover, we found that TDP-43 interacts with and colocalizes with p65, a NF-κB subunit, in glial and neuronal cells from TDP-43 transgenic mice and also from ALS patients. We report that TDP-43 and NF-κB p65 mRNA and protein expression is higher in spinal cords of ALS patients than healthy individuals. TDP-43 acted as a co-activator of p65, and glial cells expressing higher amounts of TDP-43 produced more proinflammatory cytokines and neurotoxic mediators after stimulation with lipopolysaccharide or reactive oxygen species. TDP-43 overexpression in neurons also increased their vulnerability to toxic mediators. Treatment of TDP-43 mice with Withaferin A, an inhibitor of NF-κB activity, reduced denervation in the neuromuscular junction and ALS disease symptoms. We propose that TDP-43 deregulation contributes to ALS pathogenesis in part by enhancing NF-κB activation, and that NF-κB may constitute a therapeutic target for the disease.

Foreword

A portion of introduction (Chapter 1), Chapter 2 and 4 are published manuscripts. Chapter 3 will be submitted to the Journal of Neuroscience

Introduction

Swarup V, Julien JP. ALS pathogenesis: recent insights from genetics and mouse models. Prog Neuropsychopharmacol Biol Psychiatry. 2011 Mar 30;35(2):363-9.

Both Vivek Swarup and JP Julien wrote the review. A portion of the review is included in the introduction section (chapter 1) of the thesis.

Chapter 2:

Swarup V, Phaneuf D, Bareil C, Robertson J, Rouleau GA, Kriz J, Julien JP (2011) Pathological hallmarks of amyotrophic lateral sclerosis/frontotemporal lobar degeneration in transgenic mice produced with TDP-43 genomic fragments. Brain. September,134(Pt 9):2610-26.

ln this paper, Vivek Swarup is responsible for the generation of all data, figures and writing of the manuscript. Daniel Phaneuf helped Vivek Swarup with cloning and generation of transgenic mice. Technical assistance was provided by Christine Bareil. Janice Robertson provided with peripherin 61 specific antibody. Jasna Kriz provided GFAP-luciferase mice and also provided access to live imaging system. Vivek Swarup and JP Julien wrote the paper.

Chapter 3:

Swarup V, Audet JN, Phaneuf D, Julien JP. Submitted to the Journal of Neuroscience.

Vivek Swarup is responsible for the generation of all data in figure 1. 2 and 3. Vivek Swarup analyzed all the figures and wrote the paper. Jean-Nicolas Audet is responsible for the generation of the data figure 4 as well as performed the axonal crush with Vivek

Swarup. Daniel Phaneuf helped Vivek Swarup with the generation of transgenic mice. Vivek Swarup and JP Julien wrote the paper.

Chapter 4

Swarup V, Phaneuf D, Dupré N, Petri S, Strong M, Kriz J, Julien JP Deregulation of TDP-43 in amyotrophic lateral sclerosis triggers nuclear factor κB-mediated pathogenic pathways. Journal of Experimental Medicine. 2011 Nov 21; 208(12):2429-47.

Vivek Swarup is responsible for the generation of all data (except qPCR- the Centre de Génomique de Québec, Mass Spectrometry – Proteomics Centre, CRCHUQ, Quebec), figures and the writing of the manuscript. Daniel Phaneuf helped Vivek Swarup with cloning and generation of transgenic mice. Nicolas Dupre, Susanne Petri and Michael Strong provided ALS and control spinal cord samples. Jasna Kriz provided GFAP-luciferase mice and also provided access to live imaging system. Vivek Swarup and JP Julien wrote the paper.

Acknowledgement

This thesis is the result of four years of work whereby I have been accompanied and supported by many people. It is a pleasant aspect that I now have the opportunity to express my gratitude for all of them.

First, I would like to express my deep sense of gratitude to my teacher and supervisor, Prof. Jean-Pierre Julien, Professor, Research Centre of CHUQ. The confidence and dynamism with which he guided the work requires no elaboration. His enthusiasm and passion for science on one hand and his integral but simplistic view on research has created a deep impression on me. I thank him whole-heartedly for his valuable guidance and his immense support all throughout my graduate studies. Besides, having him as my research guide, I would also cherish the personal relationship we share, throughout my life. I am really glad that I have come across Dr. Julien in my life.

I would also like to sincerely thank Dr. Jasna Kriz, Associate Professor, Research Centre of CHUQ for her constant support and words of encouragement during my research in Quebec.

It was also a great pleasure to work with my fellow lab mates. I specially thank Ms. Genevieve Soucy, Ms. Christine Bareil and Dr. Samer Abu Ezzi and Mr. Jean-Nicolas Audet for their immense patience in teaching me all the techniques related to my work. I shared great time working with Dr. Daniel Phaneuf as he taught me the nuances of molecular cloning. I will always be indebted to him for what he taught me. I would also like to thank, Ms Priyanka Patel, Mr. Pierre Cordeau Jr., Dr. Ana Sofia Correia and Ms. Renee Paridas for their constant help and valuable suggestions that helped me to trouble-shoot various scientific and technical problems. I thank all of them for patiently imparting me the skills; knowledge and the “art of doing laboratory science”, giving finer details on experimental procedure and analysis, motivating talk, sharing his expertise and experience and untiring support throughout the PhD.

I also would like to express my thanks to my friends Dr. Angana Mukherjee, Dr. Prasad Padmanabhan, Dr. Arpita Chakravarti, Mr. Debasis Mukhopadhay, Dr. Pallab Kumer

Sarker, Mrs. Dipa Dey for their unconditional help and support and for their unrelenting inspiration and understanding. I shared some happiest and joyous times of my PhD with my best friend Mr. Pravesh Mani Gungah. And my dear Arsh, what can I say. I am lucky to have you by my side. Dearest Uchasha, my heart fills with joy seeing you.

I would also like to thank all whose direct and indirect support helped me completing my thesis in time.

The chain of my gratitude would be definitely incomplete if I would forget to express my deepest regards and sincerest thanks to my parents who have been beside me through thick and thin and their invaluable support all throughout my life. A special word of thanks to my sister, Ms. Payel Chatterjee and my cousin Mr. Jit Chatterjee for the amazing times we shared together.

Omission(s) to thank a few helping hands, if any, is exclusively due to the forgetfulness of the foible neurons which may be absolved.

If you haven't found it yet, keep looking. Don't settle.

As with all matters of the heart, you'll know when you find it.

And, like any great relationship, it just gets better and better as the years roll on....

So keep looking until you find it. Don't settle...

Stay Hungry. Stay Foolish...

Steve Jobs, Stanford University, 14th June 2005

Table of Contents

List of Figures

List of Tables

List of Abbreviations

AD = Alzheimer's disease

ALS: Amyotrophic lateral sclerosis

AMPA: Alpha-amino-3-hydroxy-5-methyl-4-isoxazolepropionic acid receptor

ANG: Angiogenin

APC: Antigen presenting cell

APOE-4 : Apolipoprotein E

ATP: Adenosine triphosphate

ATXN2 : Ataxin-2 (gene)

BBB: Blood brain barrier

cDNA: Complementary DNA

CCS : Copper chaperone for SOD1

CHOP : C/EBP homologous protein

CHMP2B : Charged multivesicular protein 2B

CNS: Central nervous system

CNTF: Ciliary neurotrophic factor

CHGB : Chromogranin B (gene)

cRNA: Complementary RNA

CSF : Cerebrospinal fluid

Cu/Zn SOD: Cu/Zn superoxide dismutase

DAO : D-amino acid oxidase

DC: Dendritic cell

DCTN1: Dynactin 1

DNA: Desoxyribonucleic acid

DPP6: Dipeptidyl-peptidase 6

EAAT: Excitatory amino acid transporters

ELISA: Enzyme-linked immunosorbent assay

ESCRTIII : Endosomal secretory complex required for transport protein III

FALS: Familial amyotrophic lateral sclerosis

FTD= Frontotemporal lobar degeneration

FTLD-U : Frontotemporal lobar degeneration with ubiquitinated inclusions

FUS : Fused in sarcoma

GEF : Guanine nucleotide exchange factor

GLT: Glutamate transporter

GLUR: Glutamate receptor

GPCRs: G protein-coupled receptors

GTPase: Guanosine triphosphate hydrolase

GWAS : Genome-wide association studies

Hsp70: Heat shock protein 70

hnRNA : Heterogeneous nuclear RNA

hnRNP : Heterogeneous nuclear ribonucleoprotein

ICE: lnterleukin-1β-converting enzyme (caspase-1)

ICV: lntracerebroventricular

IF: Intermediate filament

IGF-l: Insulin-like growth factor 1

IL: lnterleukin

IFNγ: Interferon gamma

iNOS: Inducible NOS

IPC: Insoluble protein complexes

ITPR-2: lnositol1,4,5-triphosphate receptor, type 2

IκB: Inhibitor of nuclear factor kappa-light-chain-enhancer of activated B cells

IKK : inhibitor of nuclear factor kappa-B kinase subunit

Kb: Kilobase

kDa: KiloDalton

LPS: Lipopolysaccharide

MAPT : Microtubule-associated protein tau

MCP-1: Monocyte chemotactic protein-1

M-CSF: Macrophage colony stimulating factor

MHC: Major histocompatibility complex

MN : Motor neuron

MnSOD: Manganese superoxide dismutase

mRNA: Messenger ribonucleic acid

NADPH: Nicotinamide adenine dinucleotide phosphate

NEFH: Neurofilament heavy subunit (gene)

NEFL: Neurofilament light subunit (gene)

NEFM: Neurofilament medium subunit (gene)

NEMO : NF-kappa-B essential modulator

NF-H : Neurofilament heavy subunit (protein)

NF-M : Neurofilament medium subunit (protein)

NF-L: Neurofilament light subunit (protein)

NF-κB: Nuclear factor kappa-light-chain-enhancer of activated B cells

NMDA: N-methyi-D-aspartic acid

NMJ : Neuromuscular junction

Ntg : Non-transgenic

nNOS: Nitric oxide synthase

Nox-l: NADPH oxidase 1

Nrf2 : Nuclear erythroid-2-related factor 2

OPTN : Optineurin

PD : Parkinson disease

PDI : Protein disulphide isomerase

PNS: Peripheral nervous system

Prp : Prion promoter

Rac1: Ras-related C3 botulinum toxin substrate 1

RAG: Recombination activating genes

RANTES: Chemokine (C-C motif) ligand 5 (CCL-5)

RNA: Ribonucleic acid

RNP : Ribonucleoprotein

RRM : RNA recognition motif

RLD : Regulator of chromosome condensation 1 (RCC1)-like domain

RNS: Reactive nitrogen species

ROS: Reactive oxygen species

SALS: Sporadic amyotrophic lateral sclerosis

SCA2 : Spinocerebellar ataxia type 2

SETX: Senataxin

SPG11 : Spastic paraplegia 11

SLA: Sclerose laterale amyotrophique

SMA : Spinal muscular atrophy

SMN : Survival of motor neuron protein

SOD l:Cu/Zn superoxide dismutase

TAR : Transactive response element

TARDBP: Transactive response DNA-binding protein 43 (gene)

TCR: T-cell receptor

TDP-43: Transactive response DNA-binding protein 43 (protein)

TGF-β: Transforming growth factor beta

TLR: Toll-like receptor

TLS : Translocated in liposarcoma

TNFR: Tumor necrosis factor receptor

TNF-α: Tumor necrosis factor-alpha

UPS: Ubiquitin-proteasome system

μg: Microgram

μl: Microliter

μm: Micrometer

UBQLN2 : Ubiquilin 2

UPR : Unfolded protein response

VAPB: Vesicle-associated membrane protein (VAP)-associated protein B

VCP : Valosin containing protein

VEGF: Vascular endothelial growth factor

VPS9 : vacuolar protein sorting 9 domain

WT: Wild-type

Chapter 1: Introduction

1.1 Amyotrophic Lateral Sclerosis

Amyotrophic lateral sclerosis (ALS) is a neurodegenerative disorder of devastating impact that causes injury and cell death of lower motor neurons within the brainstem and spinal cord and upper motor neurons in the motor cortex, leading to progressive failure of the neuromuscular system usually resulting in death from respiratory failure. The world-wide incidence of about 2 per 100,000 is relatively uniform (Boillee et al., 2006a), except for a few high incidence foci, e.g. on the Kii peninsula and Guam (Steele and McGeer, 2008). The mean age of onset is 55 -60 years and the disease more commonly affects men compared to women. The average survival from symptom onset is approximately 3 years, though a proportion of patients have a slower disease course.

Although ALS has traditionally been considered a pure motor disorder, it is now regarded as a multi-system disorder in which the motor neurons (MNs) tend to be affected earliest and most severely (Andersen and Al-Chalabi, 2011). Involvement of sensory and spinocerebellar pathways and neuronal groups within the substantia nigra and the hippocampal dentate granule layer can be detected in a proportion of ALS patients. Gross pathological changes in ALS include atrophy of the precentral gyrus; shrinkage, sclerosis and pallor of the corticospinal tracts; thinning of the spinal ventral roots and hypoglossal nerves; and atrophy of the somatic and bulbar muscles (Ince et al., 1998a). At autopsy there is typically depletion of at least 50 percent of the spinal cord motor neurons accompanied by diffuse astrocytic gliosis in the spinal grey matter. Many of the surviving lower motor neurons show atrophic and basophilic changes (Ince et al., 1998a). A cardinal feature of the lower motor neuron pathology is the presence of ubiquitinated inclusion bodies, which may have the appearance of threads, skeins or compact bodies, within the soma, proximal dendrites and axons (Piao et al., 2003). TDP-43 protein is a major constituent of these ubiquitinated inclusions (Neumann et al., 2006). In the motor cortex, pathological changes are highly variable. Reduction in the population of giant pyramidal neurones (Betz cells) in the motor cortex and astroglyosis in the grey matter and underlying subcortical white matter may be observed. Evidence of microglial activation is detected in pathologically affected areas.

The primary pathogenetic processes underlying ALS are multifactorial and the precise mechanisms underlying motor neuron cell death are at present incompletely understood. Current understanding of the neurodegenerative process, derived predominantly from the subtype of disease cause by SOD1 mutations, highlights a complex interplay between multiple mechanisms including genetic factors, oxidative stress, excitotoxicity, protein aggregation as well as damage to critical cellular processes, including axonal transport and organelles such as mitochondria. There has been growing recent interest in the role played in motor neuron injury by neighboring glial cells (Ilieva et al., 2009); involvement of particular molecular signaling pathways in motor neuron survival and cell death (Kirby et al., 2005) and in the concept that the neuromuscular junction and distal axonal compartment is an early and important target of disease pathophysiology (Murray et al., 2010). New genetic discoveries have highlighted the likely importance of dysregulated RNA processing in motor neuron injury (Mackenzie et al., 2010). Evidence has also accumulated that the final process of motor neuron death is likely to occur via a caspase-dependent apoptotic cell death pathway (Sathasivam and Shaw, 2005).

1.1.1 Genetics of ALS

ALS is most commonly a sporadic disease (SALS), but 5-10% of cases are familial (FALS) and usually of autosomal dominant inheritance (**Table 1.1**). The identification of the genetic subtypes of ALS has established key pathogenic mechanisms which are applicable not only to the minority of cases which carry FALS mutations, but to sporadic ALS more broadly. All genes mutated in familial ALS have also been found mutated in patients diagnosed with sporadic ALS and, besides a lower mean age of onset, no clinical difference exists between the two groups.

1.1.1.1 Superoxide dismutase (SOD1)

Superoxide dismutase (*SOD1)* mutations were the first mutations associated with familial ALS in 1993 (Rosen et al., 1993). Since then more than 160 different mutations have been reported spanning the entire SOD1 protein and reviewed (Dion et al., 2009).

SOD1 is expressed in all cells mainly in the cytoplasm and the only known function of SOD1 is to convert superoxide, a toxic by-product of mitochondrial oxidative phosphorylation, to water or hydrogen peroxide (Danciger et al., 1986). *SOD1* gene has five exons which code for 153 evolutionarily conserved amino acids, which, together with a catalytic Cu^{2+} ion and a stabilizing Zn^{2+} ion, form a subunit. Through non-covalent binding, pairs of these subunits form SOD1 homodimers. All but one mutation (D90A mutation) are known to be inherited dominantly (Dion et al., 2009).

1.1.1.2 Alsin

Alsin is encoded by *ALS2* gene which is located in chromosome 2q33.1. Alsin has a molecular mass of 184 kDa, and has three putative guanine nucleotide exchange (GEF) domains: a regulator of chromosome condensation 1 (RCC1)-like domain (termed RLD), a diffuse B-cell lymphoma (Dbl) homology/pleckstrin homology (DH/PH) domain, and a vacuolar protein sorting 9 (VPS9) domain. Autosomal recessive mutations in the ALS2 gene have been linked to juvenile-onset amyotrophic lateral sclerosis (ALS2), primary lateral sclerosis and juvenile-onset ascending hereditary spastic paraplegia. Except for two identified missense mutations (Ben Hamida et al., 1990; Hadano et al., 2001a), all other mutations in the *ALS2* gene lead to a premature stop codon and likely abrogate all the potential functions of alsin, the protein encoded by the *ALS2* gene.

1.1.1.3 Senataxin

Mutations in the *SETX* gene, which codes for senataxin, at chromosome 9q34 are associated with both cerebellar and motor neuron degeneration. When inherited in an autosomal recessive pattern, a severe cerebellar ataxia syndrome with oculomotor apraxia ensues, while autosomal dominant inheritance gives rise to a slowly progressive motor neuronopathy with pyramidal signs but sparing of both bulbar and respiratory systems (Chen et al., 2004) and (Chen et al., 2006). A novel *SETX* mutation (Thr1118Ile) has been associated with a single SALS case, potentially expanding the phenotype of SETX mutations to include classical ALS (Zhao et al., 2009).

Table 1.1: Genetics of ALS categorized by pathophysiological mechanism

Gene Locus	Chromosomal Locus	Gene	Onset/ Inheritance	Reference
Oxidative Stress/Protein aggregation				
ALS1	21q22.1	Superoxide dismutase 1	Adult / AD	**Rosen et al, 1993**
Cell Signaling				
ALS2	2q33.2	Alsin (*ALS2*)	Juvenile/ AR	**Hentati et al, 1994**
ALS11	6q21	FIG4 phosphoinositide phosphatase	Adult / AD	**Chow et al, 2009**
RNA Processing				
ALS4	9q34	Senataxin (*SETX*)	Juvenile/ AD	**Chen et al, 2004**
ALS6	16p11.2	Fused in Sarcoma (*FUS*)	Adult / AD	**Kwiatkowski et al, 2009; Vance et al, 2009**
ALS9	14q11.2	Angiogenin (*ANG*)	Adult / AD	**Greenway et al, 2005**
ALS10	1p36.2	TAR DNA binding protein (*TARDBP*)	Adult / AD	**Sreedharan et al, 2008**
Endosomal Trafficking				

ALS8	20q13.3	VAMP associated protein type - B (*VAPB*)	Adult/ AD	**Nishimura et al, 2004**
Glutamate Excitotoxicity				
	12q24	D-amino acid oxidase (*DAO*)		**Mitchell et al, 2010**
Ubiquitin/protein degradation				
	9p13-p12	Valosin containing protein *VCP)*	Adult/ AD	**Johnson et al, 2010**
ALS-X	Xp11.23 to Xq13.1	Ubiquilin 2 (Ubqln2)	X-linked	**Deng et al.,2011**
Repeat Expansion				
ALS+FTD	9p21.3	C9orf72 (GGGGCC expansion)	Adult / AD	**Vance et al, 2006**
Cytoskeleton				
ALS+Dementia +PD	17q21	Microtubule associated protein tau *(MAPT)*	Adult / AD	**Hutton et al, 1998**
NF-κB Signaling				
ALS12	10p15-p14	Optineurin (*OPTN*)	Adult/ AD & AR	**Maruyama et al, 2010**
Others				
ALS5	15q21.1	Spastic paraplegia 11 (*SPG11*)	Juvenile/ AR	**Orlacchio et al, 2010**
ALS13	12q24	Ataxin-2 (*ATXN2*)	Adult/AD	**Elden et al, 2010**
ALS7	Not identified 20p13	Unknown	Adult /AD	**Sapp et al,2003**

Footnote: AD = Autosomal dominant, AR = Autosomal recessive, ALS= Amyotrophic lateral sclerosis, FTD= Frontotemporal lobar degeneration, PD= Parkinson disease.

1.1.1.4 TAR DNA Binding Protein (TARDBP)

Soon after the discovery that neuronal cytoplasmic inclusions in patients with ALS or FTLD-U contain TDP‑43, researchers around the world started analysis of TARDBP, the gene that encodes this protein, in FALS families. Mutation analysis of *TARDBP* has led to the discovery of missense mutations in sporadic and familial ALS (Kabashi et al., 2008; Kuhnlein et al., 2008; Rutherford et al., 2008; Sreedharan et al., 2008; Van Deerlin et al., 2008; Yokoseki et al., 2008; Corrado et al., 2009a; Del Bo et al., 2009; Lemmens et al., 2009; Tamaoka et al., 2010). Almost all of the mutations affect the C-terminus of TDP-43, and all but one are missense (Williams et al., 1988; Chio et al., 2011)the exception being Tyr374X (Daoud et al., 2009). These mutations are thought to result in redistribution of TDP-43 from the nucleus to the cytoplasm in neurons and glia in the spinal cord. Kabashi et al. (Kabashi et al., 2008) have shown that mutations increase the detergent insoluble fraction of TDP-43 and that some mutations are biochemically more toxic than others, suggesting various mutations may have differing roles. *TARDBP* mutations have been reported in 4–6% of FALS cases without *SOD1* mutations, and 0–2% cases of diagnosed SALS (Kabashi et al., 2008; Sreedharan et al., 2008). In all, *TARDBP* mutations account for about 2-3% of all ALS cases. Most cases have typical ALS, but ALS with cognitive impairment and FTD without ALS and ALS with extrapyramidal signs are also reported (Benajiba et al., 2009; Tsai et al., 2011).

1.1.1.5 Fused in Sarcoma (FUS)

TARDBP mutations prompted researchers around the globe to search for other RNA binding genes with similar structure to TDP-43 for mutations for a candidate in a known linkage region on 16q11.2, *FUS*. 2 reports in *Science* revealed FUS mutations (Kwiatkowski et al., 2009; Vance et al., 2009). With a secondary structure similar to TDP-43, FUS protein has been implicated in alternative splicing, genomic maintenance, and transcription factor regulation (Meissner et al., 2003; Wang et al., 2008b). Like *TARDBP* mutations, several missense mutations are predominantly in exons 14 and 15, which encode the C-terminus of FUS. Of the 42 known mutations in exons 3, 5, 6, 14 and 15 the

most common mutation is Arg521Cys (Kwiatkowski et al., 2009; Vance et al., 2009). The mutations are associated with typical ALS phenotype but some individuals also have cognitive impairment, or pure FTD without ALS (Ticozzi et al., 2009; Van Langenhove et al., 2010). *FUS* mutations have been reported in 4–6% of FALS cases without *SOD1* mutations, and 0.7–1.8% cases of diagnosed SALS (Yan et al., 2010; Tsai et al., 2011). In all, TARDBP mutations account for about 2-3% of all ALS cases, about the same as *TARDBP* mutations.

1.1.1.6 VAMP associated protein B (VAPB)

Mutations in vesicle-associated membrane protein-associated protein B (*VAPB*) was reported in 2004 by a Brazilian group (Nishimura et al., 2004b). The identified mutation is an autosomal-dominant mutation from a large Brazilian family (Nishimura et al., 2004b). Only one point mutation - Pro56Ser is known to cause autosomal-dominant ALS and adult-onset spinal muscular atrophy for a total of 200 patients who share a common ancient ancestor (Nishimura et al., 2004b). The VAP family proteins consisting of VAPA (synonym, VAP33), VAPB, and VAPC (a splicing variant of VAPB) in human were originally identified as homologues of vesicle-associated membrane protein (VAMP)-associated protein (VAP) that is involved in the release of neurotransmitters (Skehel et al., 1995). VAPB is a type II transmembrane protein localizing in the ER membrane and known to dimerize with VAPA, VAPB itself, VAMP1, and VAMP2 via the C-terminal transmembrane domain. VAPB is involved in intracellular membrane transportation and is primarily located in the endoplasmic reticulum. The Pro56Ser mutation in *VAPB* induces the formation of insoluble cytoplasmic aggregates containing the mutant protein. Pro56Ser mutation has been reported in ALS patients from Germany, Japan and the USA. Two other mutations of *VAPB* - Thr46Ile and Ser160del have been reported in ALS patients (Landers et al., 2008; Chen et al., 2010).

1.1.1.7 Angiogenin

Angiogenin (ANG) is a 14.1-kDa protein that belongs to the pancreatic ribonuclease superfamily. Lys17Ile mutation in *ANG* were originally identified in both familial and

sporadic ALS cases in the Irish and Scottish population because it shares a metabolic pathway with vascular endothelial growth factor (VEGF), which is implicated in ALS (Greenway et al., 2006b). Subsequently, more than 15 variants in the ANG gene have been reported (Conforti et al., 2008; Gellera et al., 2008; Fernandez-Santiago et al., 2009; van Es et al., 2009). ANG is a downstream effector of vascular endothelial growth factor (VEGF) in endothelial cells and is up-regulated in response to hypoxic/ ischemic events (Kishimoto et al., 2005). Angiogenin is widely expressed including vascular endothelial cells, fibroblasts, mast cells, and tumor cells (Moenner et al., 1994; Kulka et al., 2009). Angiogenin was also shown to be expressed by neurons in rat brain and motor neurons in humans (Huang et al., 2009). Endothelial cells are capable of endocytosing angiogenin which is then translocated to the nucleus and accumulates in the nucleolus (Moroianu and Riordan, 1994). Several lines of evidence demonstrate that the ANG protein promotes motor neuron survival. Knocking down angiogenin expression can cause excitotoxic motor neuron death, in contrast increased expression of angiogenin protects against stress-induced cell death (Kieran et al., 2008). In the $SOD1^{G93A}$ ALS mouse model, delivery of angiogenin increases lifespan and motor neuron survival, possibly through the Akt-1 signaling pathway (Kieran et al., 2008).

1.1.1.8 Optineurin

Japanese researchers have reported, using homozygosity mapping in consanguineous families, mutations in optineurin (*OPTN*), a gene already known to be mutated in primary open angle glaucoma and ataxia (POAG) (Maruyama et al., 2010). The mutations were found both in FALS and SALS cases. The researchers found three types of mutation of *OPTN*: a homozygous deletion of exon 5, a homozygous Q398X nonsense mutation and a heterozygous E478G missense mutation within its ubiquitin-binding domain. Of these mutations, the nonsense and missense mutations of *OPTN* abolished the inhibition of activation of nuclear factor kappa B (NF-κB), and the E478G mutation had a cytoplasmic distribution different from that of the wild type or a POAG mutation. A case with the E478G mutation showed OPTN-immunoreactive cytoplasmic inclusions. Recently, 10 novel heterozygous mutations in *OPTN* have been reported in a few SALS or FALS cases

of European descent (Belzil et al., 2011; Millecamps et al., 2011) and optineurin inclusions were reported in fairly large ALS cases.

1.1.1.9 Ataxin-2

Recent reports suggest intermediate-length polyQ expansion (27–33 repeats) on one allele in the ataxin-2 (*ATXN2*) as a significant genetic risk factor for ALS in four large populations of SALS and FALS cases (Elden et al., 2010). Normally *ATXN2* CAG-trinucleotide repeat expansion to 34 or more repeats is associated with spinocerebellar ataxia type 2 (SCA2). The findings raise the possibility that SCA2 and ALS represent opposite ends of a clinical spectrum, with intermediate-length repeat expansions presenting with more prominent motor neuron degeneration as in ALS and longer expansions resulting in cerebellar ataxia. This idea is further supported by the finding of ataxia in some patients with *SOD1* or *SETX* mutations (Yasser et al., 2010).

1.1.1.10 Ubiquilin 2

Mutations in the ubiquilin 2 (*UBQLN2*) gene, which encodes a ubiquitin-like protein, have been recently reported in a five-generation family showing X-linked dominant transmission of ALS (Deng et al., 2011). Interestingly, some affected individuals also had FTD. After careful analysis the group reported four other mutations in four unrelated families, all in a proline-repeat domain of ubiquilin 2. The age of ALS onset was significantly younger in males than females, presumably because the males are hemizygous and the females heterozygous for the mutation. Suggestive of a convergent pathway, ubiquilin 2 pathology was found in all the ALS cases examined, including SALS, FALS and ALS–FTD. Further research may reveal more mutations and associated mechanism, though the group reported that mutations in ubiquilin 2 render the ubiquitin-proteasome system ineffective (Deng et al., 2011).

1.1.1.11 Hexanucleotide expansion in C9orf72 gene

Linkage analysis in a large Swedish family and later in 13 similar pedigrees had pointed to a major locus on 9p21.2 for FALS, FALS–FTD and SALS cases (Dejesus-Hernandez et al., 2011; Murray et al., 2011; Renton et al., 2011). The causative gene defect has recently been reported as a massive hexanucleotide-repeat expansion, (GGGGCC)n, in the intron between noncoding exons 1a and 1b of the uncharacterized gene *C9orf72*. While normal individuals have, at most, 23 repeats, individuals with ALS /FTD-U can have up to 1,600 repeats. The expansion can account for a significant proportion of familial and apparently sporadic ALS and FTD cases. Speculatively, the dynamics of such a hexanucleotide-repeat expansion may explain the variability in phenotypes and disease penetrance previously reported in these families, and the association to the 9p21 locus of many cases with apparently sporadic disease (Dejesus-Hernandez et al., 2011; Murray et al., 2011; Renton et al., 2011). Only further research can tell whether all 9p21-linked families carry GGGGCC expansions in *C9ORF72*.

Several RNA processing genes have now been implicated in ALS, including TAR DNA binding protein (*TARDBP*) (Kabashi et al., 2008; Sreedharan et al., 2008) fused in sarcoma (*FUS*) (Vance et al., 2009), senataxin (*SETX*) (Chen et al., 2006) and angiogenin (*ANG*) (Conforti et al., 2008) highlighting the probability that disordered RNA processing contributes to motor neuron injury. Rare mutations in vesicle associated membrane protein (VAMP)-associated protein B (*VAPB*) (Nishimura et al., 2004a), optineurin (*OPTN*) (Maruyama et al., 2010) and the endosomal secretory complex required for transport (ESCRTIII) protein, charged multivesicular protein 2B (*CHMP2B) (Parkinson et al., 2006)*, implicate dysregulated endosomal trafficking as an important pathophysiological mechanism. Ironically, even though a large numbers of genes involved in ALS have been reported, the sheer volume of the genes pose challenges before researchers in finding pathogenic mechanisms associated with the disease. In any case, modern techniques like genome-wide association studies (GWAS), exome sequencing, next-gen deep sequencing have provided valuable genetics data for the scientific community.

1.1.2 Risk factors associated with ALS

Apart from genetic mutations contributing ALS pathogenesis, many other factors like environmental factors and Chromogranin polymorphism have been associated as risk factors for ALS. Though some of these factors are either semi-quantifiable or difficult to assess, reports have conclusively emphasized their role in the pathogenesis of the disease. These risk factors are summarized as:

1.1.2.1 Pesticides as risk factors. Systematic review of the literature reveals that exposure to pesticides is a potential environmental risk factor for ALS. Exposure to many industrial chemicals like benzene, styrene, herbicides (Welp et al., 1996; McGuire et al., 1997; Johnson and Atchison, 2009) and industrial metals like manganese, cadmium (McGuire et al., 1997) are significantly associated to ALS. Similarly, an increased ALS risk was reported for exposure to cleaning solvents or degreasers, alcohols or ketones, insecticides, fertilizers, selenium (McGuire et al., 1997), as well as for occupations potentially exposed to solvents (hairdressers and cosmetologists) or pesticides (farm-related occupations) (Park et al., 2005) .

1.1.2.2 Head injuries and APOE-4 carriers as risk factors. Studies have identified significant associations between ALS and a shorter interval between the last head injury indicating that head injuries experienced during childhood or young adulthood may not confer an increased ALS risk later in life, while head injuries experienced in later adulthood have a greater impact on risk (Scarmeas et al., 2002; Schmidt et al., 2010). These findings are consistent with evidences individuals with a lifetime history of vigorous physical activity like baseball players or boxers have a higher risk of developing ALS than those who aren't involved in such events. In addition to the observed main effect, results support the possibility of gene-environment interaction, since the association between ALS and head injuries was stronger in apolipoprotein E (APOE-4) carriers than non-carriers (Schmidt et al., 2010).

1.1.2.3 Chromogranin B (*CHGB*) variant as risk factor. Using DNA samples from ALS patients and matched controls from three different countries, researchers have identified that individuals who have P413L *CHGB* variant show a 2.2-fold greater risk of ALS than those who do not have this risk variant (Gros-Louis et al., 2009). Furthermore, the P413L *CHGB* variant is associated with an earlier age of onset by almost a decade in both sporadic ALS and familial ALS cases. Studies in human neuroblastoma cells have revealed that *CHGB* variants caused the abnormal sequestration of CHGB proteins within the ER-Golgi network. These results suggest that the P413L missense variation can impede the sorting and maturation of CHGB into secretory granules.

In general these risk factors along with the genetic factors discussed above contribute either individually or in a complex way interacting with gene-environment to play a critical role. Further studies are warranted in deciphering the role and contribution of these players in ALS pathogenesis.

1.1.3 Pathogenic mechanisms implicated in ALS

1.1.3.1 Excitotoxicity

Glutamate is the major excitatory neurotransmitter in the central nervous system (CNS) and exerts its effects through an array of ionotropic and metabotropic post-synaptic receptors. The excitatory signal is terminated by removal of glutamate from the synaptic cleft by glutamate re-uptake transporters, the most abundant of which is EAAT2/GLT1. Excitotoxicity, the neuronal injury resulting from excessive activation of calcium-permeable glutamate receptors, may be caused by increased synaptic levels of glutamate or by increased sensitivity of the post-synaptic neuron to normal glutamate levels resulting from alteration in neuronal energy homeostasis or glutamate receptor expression(Van Damme et al., 2005). Disruption of intracellular calcium homeostasis, with secondary activation of proteolytic and free radical generating enzyme systems, and perturbation of mitochondrial function and ATP production are key components of excitotoxicity (Bordet et al., 2007). AMPA receptors mediate much of the routine fast excitatory glutamatergic neurotransmission in the CNS and motor neuron (MN) are

especially vulnerable to AMPA-mediated excitotoxicity, including distal axonal injury(Carriedo et al., 1996; King et al., 2007). The calcium permeability of the AMPA receptor complex is largely determined by the GluR2 subunit, which is post-transcriptionally edited at the Q/R site 586 in the second transmembrane domain, to render the receptor complex calcium impermeable(Williams et al., 1997). Cell specific features of MN, including low expression of GluR283 and low expression of calcium buffering proteins (Ince et al., 1993), render these neurons vulnerable to AMPA-mediated toxicity (**Figure 1.1**). A body of evidence implicates excitotoxicity as a mechanism contributing to MN injury in ALS, though there is no clear evidence that it is a primary disease mechanism. Therapeutic intervention to ameliorate excitotoxicity is the only strategy that has so far had a positive effect on disease progression in ALS. Riluzole, which has several effects, including inhibition of pre- synaptic glutamate release(Cheah et al., 2010), causes a modest increase in survival (Lacomblez et al., 1996). However, other anti-glutamate agents including gabapentin, lamotrigine, topiramate and talampanel have not been effective in human trials. The evidence implicating excitotoxicity as a contributory factor in ALS includes: elevation of CSF glutamate in a subset of patients (Rothstein et al., 1990; Shaw et al., 1995b); reduced expression and function of the major astrocytic glutamate transporter EAAT2 in pathologically affected studies indicating hyperexcitability of the human motor system in the pre-symptomatic(Vucic et al., 2008) or early stages (Vucic and Kiernan, 2006) of ALS; calcium permeability of AMPA receptors in the spinal ventral horn may be dysregulated by failure of the normal editing of the GluR2 AMPA receptor subunit (Kwak et al., 2010). Experimental models have shown that mSOD1 causes: altered electrophysiological properties and increased sensitivity of MNs to excitotoxicity (Vucic and Kiernan, 2006); alteration in AMPA receptor subunit expression; reduced expression and function of the EAAT2/GLT1 glutamate transporter which may be mediated by oxidative damage and caspase 3 cleavage (Boston-Howes et al., 2006); increased glutamate efflux from spinal cord nerve terminals under basal and stimulated conditions(Milanese et al., 2011); reduction in the MN inhibitory/ excitatory synaptic ratio(Sunico et al., 2011); loss of regulation by astrocytes of the expression of GluR2 by neighboring MNs(Van Damme et al., 2007).

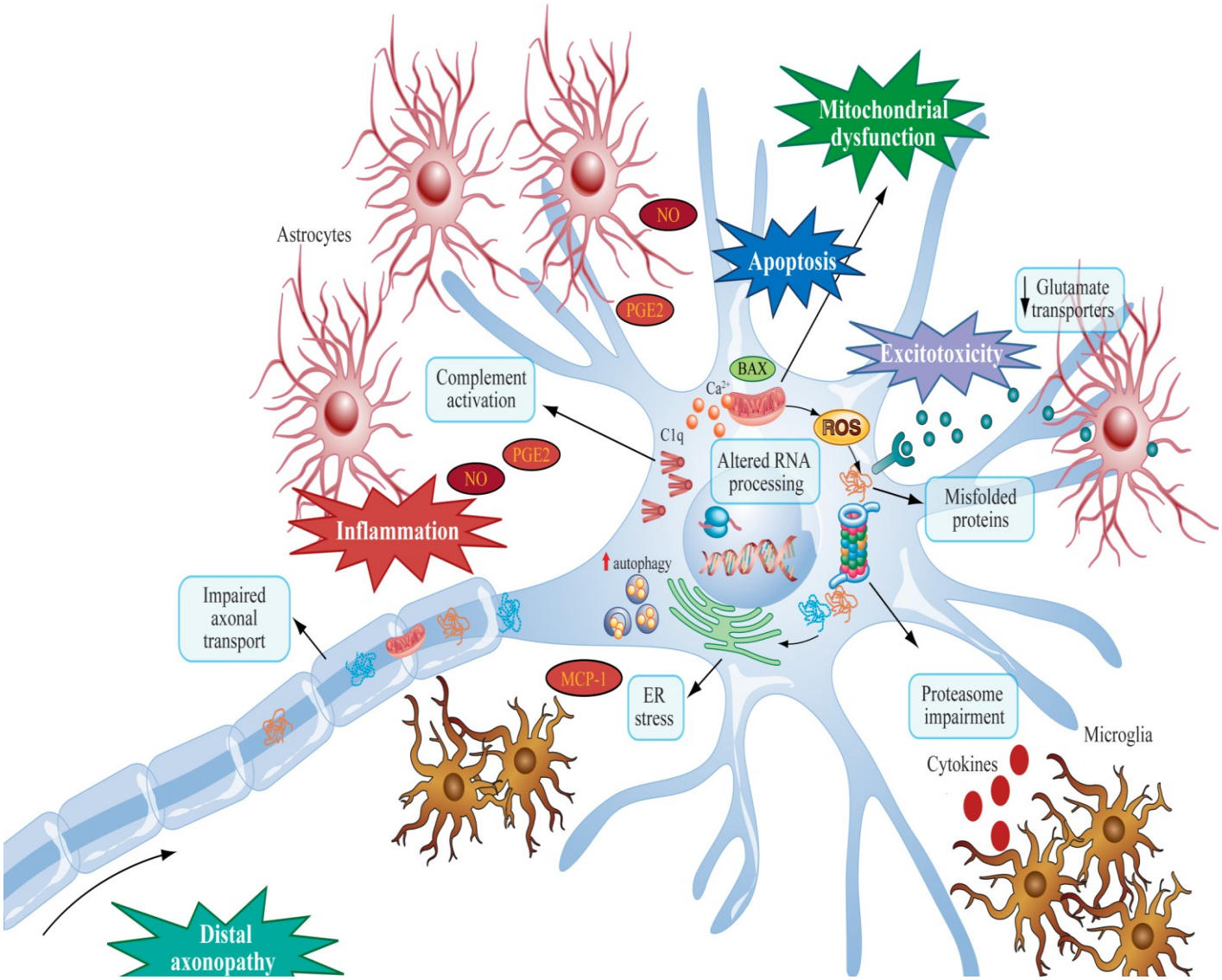

Figure 1.1 Summary of molecular mechanisms of motor neuron injury in ALS ALS is a complex disease involving the activation of several cellular pathways and entailing dysregulated interaction with neighboring glial cells. Microglia release MCP-1 and cytokines and astrocytes release nitric oxide (NO) and prostaglandin E2 (PGE2). There is evidence that MN undergo transcriptional dysregulation and abnormal RNA processing, which is, along with overproduction of reactive oxygen species (ROS), one of the causes of aberrant protein folding. Aberrant proteins can form aggregates and lead to proteasome impairment and endoplasmic reticulum (ER) stress, ultimately activating autophagy and apoptotic pathways. Mitochondrial impairment and dysregulation of calcium (Ca^{2+}) handling are two major components of MN injury which also ultimately lead to activation of the apoptotic cascade. Impaired axonal transport may contribute to a distal axonal energy deficit and the dying back axonopathy seen in ALS. Clq - complement protein

1.1.3.2 Oxidative stress

Oxidative stress arises from an alteration in the balance between the generation of reactive oxygen species (ROS) and their removal, together with the ability of the biological system to remove or repair ROS-induced damage. The accumulation of oxidative stress within non-replicating neurons with age, may be one important factor which tips the balance of homeostatic control mechanisms from an ability to cope with a toxic insult such as the presence of a disease causing mutation, into a vicious cycle of cellular injury culminating in neuronal death and an onset of neurodegeneration in middle or later life. Oxidative stress causes structural damage and also changes also in redox-sensitive signaling pathways. There has been particular interest in the role of oxidative stress in ALS, given that mutations in SOD1 which encodes a major anti-oxidant defense protein, accounts for 20% of cases of FALS.

Cellular ROS are generated as by-products of aerobic metabolism, predominantly due to leakage of electrons from the mitochondrial respiratory chain, but with contributions from other intracellular enzyme systems including xanthine oxidase and cytochrome P450. Initially formed ROS such as superoxide and hydrogen peroxide may undergo further reaction to produce more potent oxidant species including peroxynitrite and hydroxyl radicals. Biochemical indices of oxidative damage to proteins (Shaw et al., 1995a), lipids (Shibata et al., 2001) and DNA (Fitzmaurice et al., 1996), in excessive quantities compared to controls, can be found in post-mortem tissue from SALS and SOD1-related FALS cases. Oxidative damage to RNA species has also been documented (Chang et al., 2008), adding to the evidence that alteration in mRNA processing is an important pathophysiological mechanism in ALS. Indices of oxidative damage are also present in cellular and murine models of SOD1-related ALS (Barber and Shaw, 2010) and interestingly the SOD1 protein itself appears to be particularly susceptible to oxidative post-translational modification (Andrus et al., 1998). Other biosamples from ALS patients, including CSF, serum and urine also show elevation of markers of free radical damage (Smith et al., 1998; Simpson et al., 2004). It is clear that oxidative stress interacts with and potentially exacerbates other pathophysiological processes contributing to MN injury including exctitoxicity (Rao and

Weiss, 2004), mitochondrial impairment (Wood et al., 2003), protein aggregation (Kanekura et al., 2009), endoplasmic reticulum stress (Blackburn et al., 2009) and alterations in signaling from astrocytes and microglia (Blackburn et al., 2009).

Sources of oxidative stress in ALS have been investigated most thoroughly in mutant SOD1 models where several aberrant oxidative reactions have been proposed (Barber and Shaw, 2010). However, it is clear that enzymatically inactive SOD1, depleted of copper loading, is still capable of causing motor neuron degeneration (Subramaniam et al., 2002) and recent evidence suggests that mSOD1 may cause oxidative stress by mechanisms beyond its own catalytic activity. mSOD1 within microglia increases superoxide production by NADPH oxidase (Nox) enzymes. SOD1 stabilizes Rac1-GTP in the activated Nox2 complex and mutant SOD1 locks Rac1 into its active state, with resultant prolongation of ROS production (Harraz et al., 2008). Nox2 expression is increased in mSOD1 mice and human ALS, and survival of SOD1G93A mice is extended by knock-out of either Nox1 or Nox2 (Wu et al., 2006).

The transcription factor Nrf2 (nuclear erythroid-2-related factor2) is a master regulator of the anti-oxidant response and responds to oxidative stress by binding and upregulating anti-oxidant response element genes. Recent evidence has emerged that Nrf2-ARE signalling may be dysregulated in models of SOD1-related ALS8 and in the CNS of ALS patients (Sarlette et al., 2008).

1.1.3.3. Mitochondrial dysfunction

Mitochondria have major roles in intracellular energy production, calcium homeostasis and the control of apoptosis. In ALS there is a body of evidence implicating mitochondrial dysfunction as part of the disease process (**Figure 1.2**). Mutant SOD1 is located in the mitochondrial inter-membrane space, where vacuoles containing aggregates of mSOD1 are found (Wong et al., 1995). In mice, there is an age-dependent adherence of mSOD1 to the outer membrane of mitochondria, postulated to lead to organelle dysfunction by impeding protein import (Vande Velde et al., 2008). Defective respiratory chain function

associated with oxidative damage to mitochondrial proteins and lipids, has been described in tissue from ALS patients (Wiedemann et al., 2002), and experimental models of ALS expressing mSOD1 (Mattiazzi et al., 2002). Thus, dysregulated energy metabolism is likely to contribute to MN dysfunction in ALS. Mitochondrial calcium buffering is impaired in organelles purified from the CNS of mSOD1 mice (Damiano et al., 2006), which could increase MN susceptibility to excitotoxicity. Endoplasmic reticulum stress predicted to disrupt the ER/mitochondrial calcium cycle has been reported in models of ALS (Grosskreutz et al., 2010). Motor neuron cell death in ALS is considered to involve the activation of caspases and apoptosis, and damage to mitochondrial function could contribute to this process (Sathasivam et al., 2005). Altered mitochondrial morphology has been observed in skeletal muscle and in spinal MN from ALS patients (Sasaki and Iwata, 2007). Interestingly in some of the mSOD1 mouse models, mitochondrial vacuolation occurs during the pre-symptomatic disease stage, suggestive of an early event in the pathophysiological cascade of MN injury (Wong et al., 1995). Mitochondrial morphology is also altered in primary MNs and NSC34 cells expressing mutant but not wild type SOD1 (Menzies et al., 2002). Axonal transport of mitochondria is impaired in experimental models of ALS, and it is possible that damaged mitochondrial function combined with a reduction in the mitochondrial content of the distal axon leads to the dying back axonopathy seen in ALS (De Vos et al., 2007). Mitochondria represent an attractive target for ALS therapy development, and the novel mitochondrial-targeted neuroprotective compound olexisome (Bordet et al., 2007) is currently undergoing a Phase III clinical trial in ALS.

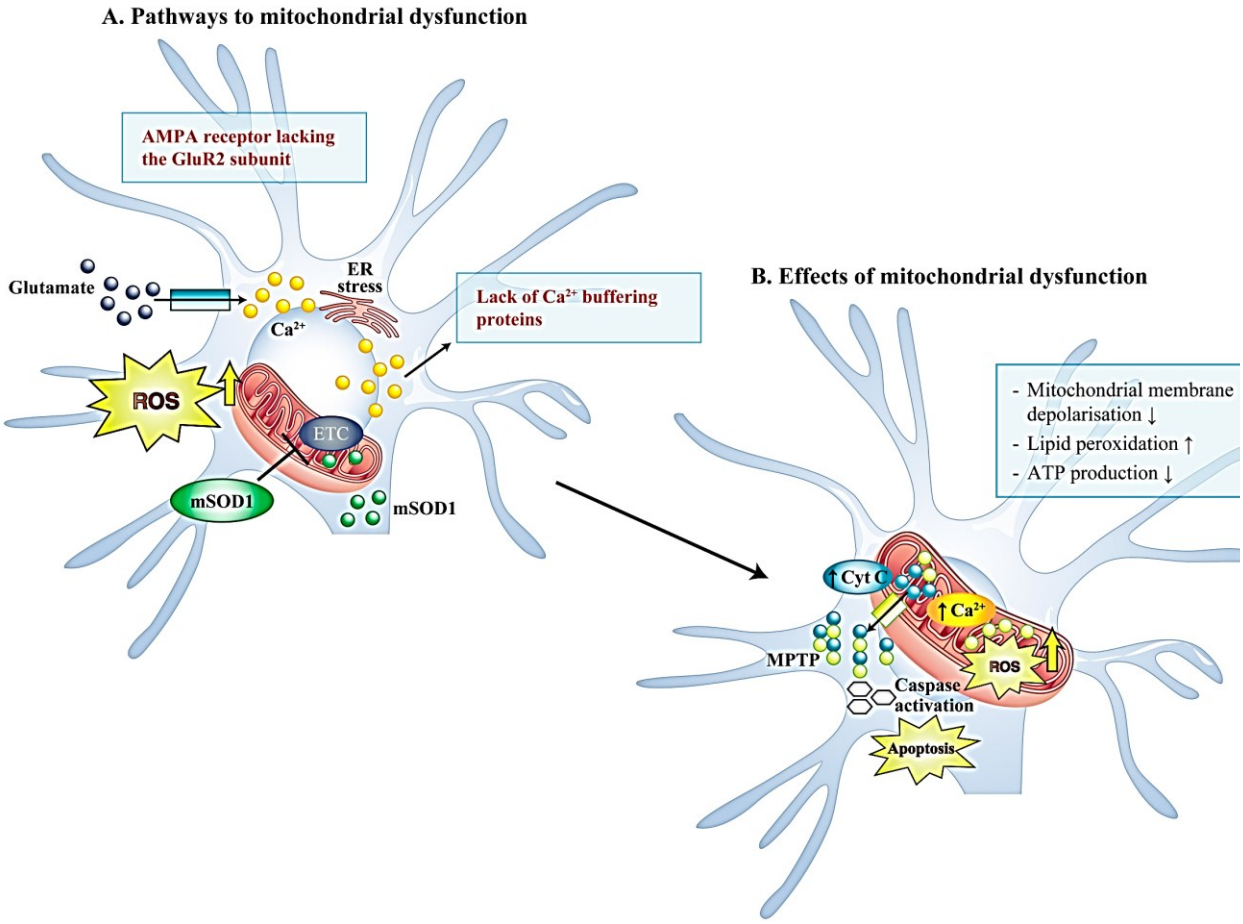

Figure 1.2 Mitochondrial dysfunction in ALS: mechanisms and downstream effects A. Post mortem tissue and animal models of ALS have indicated a decrease in the activity of the complexes forming the electron transport chain (ETC), which may be caused by oligomers of mSOD1 associated with mitochondria. These have been proposed to lead to alterations in mitochondrial redox state, damage to the mitochondrial protein import machinery, and sequestration of the anti-apoptotic factor Bcl-2. Loss of EAAT2, and an increase in expression of calcium permeable AMPA receptors lacking the edited form of the GluR2 subunit, leads to elevated intracellular calcium in motor neurons in ALS, which may result in a toxic shift of calcium from the ER to the mitochondria, leading to excitotoxicity. Defective ETC and calcium homeostasis are thought to underlie aberrant ROS generation. **B.** Together these pathways result in the depolarization of the mitochondrial membrane potential, reduced production of ATP, increased peroxidation of the mitochondrial membrane lipids, opening of the mitochondrial permeability transition pore, and the initiation of apoptosis.

1.1.3.4. Protein aggregation

Pathological protein aggregates, identified as compact or skein-like ubiquitinated inclusions, are a cardinal feature of ALS (Piao et al., 2003). The identification of TDP-43 as the major protein constituent of these inclusions initiated a major shift in our understanding of the pathobiology of ALS (Neumann et al., 2006). TDP-43 is normally predominantly localized within the nucleus, and loss of nuclear TDP-43 staining is seen in most cells containing TDP-43 positive cytoplasmic inclusions (Neumann et al., 2006). TDP-43 inclusions are not restricted to MNs, and it appears that cytoplasmic redistribution of TDP-43 is an early pathogenic event in ALS (Giordana et al., 2010). The discovery of TDP-43 mutations in several FALS pedigrees consolidated the evidence for TDP-43 dysfunction in ALS, and firmly established TDP-43 as a critical player in both sporadic and familial disease (Kabashi et al., 2008; Sreedharan et al., 2008). Neurofilament rich hyaline conglomerate inclusions are observed in the perikaryon or proximal dendrites of spinal cord motor neurons in some ALS cases, particularly those with SOD1 mutations (Ince et al., 1998b). Increased expression of phosphorylated neurofilament epitopes in the cell body of MN is also seen (Sobue et al., 1990). Small eosinophillic Bunina bodies containing cystatin C are seen within MN in up to 85% of cases (Okamoto et al., 1993). SOD1 inclusions are found in the spinal cord of FALS patients, as well as in mouse and cellular models expressing SOD1 mutations (Shibata et al., 1994). Monoclonal antibodies that are specific for epitopes present on misfolded SOD1 strongly label inclusions in SOD1 FALS patient samples (Rakhit et al., 2007), and appear to label similar structures in some SALS patients (Bosco et al., 2010). *FUS* mutations are reported in a subset of FALS pedigrees (Kwiatkowski et al., 2009; Vance et al., 2009; Hewitt et al., 2010), and where FUS immunohistochemistry has been performed, cytoplasmic inclusions containing FUS have been observed. However these have not been routinely observed in ALS cases without *FUS* mutations (Kwiatkowski et al., 2009; Vance et al., 2009; Hewitt et al., 2010). Proteins found in aggregates in ALS provide several important clues about the disease. Loss of nuclear TDP-43 or aggregation in cytoplasmic inclusions may be key pathogenic processes in both sporadic and familial ALS. The filamentous pathology observed suggests that neurofilament dysfunction is important in some forms of ALS (Hirano et al., 1984;

Sobue et al., 1990; Cote et al., 1993). The increase in phosphorylated neurofilament epitopes in MN perikarya may contribute to the observed slowing of axonal neurofilament transport (Blair et al., 2010).

1.1.3.5. Cytoskeletal dysfunction and disordered axonal transport

Axonal pathology is a key feature of ALS, which implicates damage to axons, or their constituent transport machinery, as critical to the pathophysiology of ALS. MNs are highly polarized cells with long axons, and axonal transport is required for delivery of essential components such as RNA, proteins and organelles to the axonal compartment including synaptic structures at the neuromuscular junction (NMJ). The principal machinery for axonal transport uses microtubule-dependent kinesin and cytoplasmic dynein molecular motors, which mediate transport towards the NMJ (anterograde) and towards the cell body (retrograde) respectively. Analysis of mSOD1 mice has demonstrated that defective axonal transport occurs early in the disease process (Zhang et al., 1997; Williamson and Cleveland, 1999; Kieran et al., 2005), supporting the hypothesis that dysregulation of axonal transport and the axonal compartment are mechanistic in ALS. Mutant SOD1 impairs both anterograde and retrograde transport of several cargoes, but the defects appear to be cargo-specific, since only anterograde transport of mitochondria is disrupted (Zhang et al., 1997; Williamson and Cleveland, 1999; Kieran et al., 2005). The mechanisms underlying defective axonal transport in mSOD1 models are unknown, but are likely to involve several different pathways. Impaired mitochondrial function leads to decreased axonal mitochondrial transport (Zhang et al., 1997), which could result in defective transport of other cargoes. The neuroinflammatory response in ALS and the demonstration that non-neuronal cells contribute to disease progression in ALS models, suggests that signals from non-neuronal cells might influence axonal transport *in vivo*. Tumor necrosis factor-alpha disrupts kinesin function via a mechanism involving p38 protein kinase (De Vos et al., 2000), activation of which has been demonstrated in models of ALS (Raoul et al., 2002; Ackerley et al., 2004). Excitotoxic damage by glutamate is thought to contribute to MN injury in ALS. In cultured neurons glutamate has been

shown to reduce axonal transport of neurofilaments, via activation of protein kinases that phosphorylate neurofilament proteins (Raoul et al., 2002). Lastly, damage to cargoes of axonal transport might lead to dysregulated binding to, or release from, molecular motors. For example, it has been demonstrated that neurofilament transport is negatively regulated by phosphorylation, and p38 and cdk5, two protein kinases that phosphorylate neurofilaments *in vivo*, are activated in ALS mouse models (Guidato et al., 1996). Evidence from both patients and disease models supports the concept that ALS is a dying back axonopathy (Pun et al., 2006). It is likely that axonal transport defects contribute to the dying back process, and in particular defects in anterograde axonal transport and mitochondrial dysfunction may combine to cause energy depletion specifically in the distal axon.

1.1.3.6. Neuroinflammation

Activated microglia and infiltrating lymphocytes indicate an inflammatory component in the CNS pathology of ALS (Henkel et al., 2004). Pro- inflammatory mediators including monocyte chemoattractive protein-1(MCP-1) and IL-8 (Kuhle et al., 2009) are detected in CSF, and biochemical indices of immune response activation are present in blood from ALS patients (Mantovani et al., 2009). Reduced blood CD4+ and CD25+ regulatory T (Treg) and monocytes (CD14+) counts are detected early in ALS, suggesting recruitment towards the CNS early in the neurodegenerative process. Treg cells interact with CNS microglia attenuating neuroinflammation by stimulating secretion of anti-inflammatory cytokines (Kipnis et al., 2004). Consistent with this, double transgenic mice carrying mSOD1, plus knock-out for CD4 (CD4-/-), develop a more aggressive phenotype, reversible by bone marrow transplantation (Kipnis et al., 2004). There is clearly a strong link between neuroinflammation and immune response activation. A recent study identified as a promising therapeutic target, CD40L, expressed by T cells which activates the immune response when bound by CD40 on antigen-presenting cells. Intraperitoneal injection of a monoclonal antibody to CD40L, MR1, in *SOD1*G93A mice delayed the complement system in both the mSOD1 mice (Ferraiuolo et al., 2007) and in human biosamples (Sta

et al., 2011) may trigger an adaptive immune response, involving antigen presenting cells, T-cells and B-cells, ultimately leading to inflammation. Astrocyte activation plays a central role in inflammation and mSOD1 astrocytes are reported to secrete inflammatory mediators including prostaglandin E2, leukotriene B4, iNOS, and NO under both basal and activated conditions (Hensley et al., 2006). Moreover co-cultures of human embryonic stem cell (ES)-derived MNs with either rodent or human astrocytes expressing mSOD1 showed MN toxicity which could be ameliorated by either inhibition of prostaglandin D2 receptors or NOX-2 (Di Giorgio et al., 2008; Marchetto et al., 2008). Taken together, these findings suggest that mSOD1 astrocytes are intrinsically more prone to enter an activated pro-inflammatory state, compared to their wild-type counterparts.

1.1.3.7. Non-cell autonomy

An important recent concept is that motor neuronal death in ALS is a non-cell-autonomous process, in which neighboring glial cells play a crucial role. Genetically engineered mouse models expressing mSOD1 in specific cell types have provided compelling evidence that alterations in the properties of glia conferred by mSOD1 contribute significantly to MN injury and that glial cells play an important role in disease progression. The use of chimeric mice showed that normal MN developed signs of ALS pathology when surrounded by mSOD1-expressing glia (Clement et al., 2003). The proportion of non-neuronal cells free of transgene correlated positively with the proportion of surviving mSOD1 expressing MN, and translated into a significant increase in the life span of the chimeric mice. To dissect the contribution of astrocytes and microglia to this finding, double transgenic mice were generated expressing the Cre/Lox recombinant system to exclude mutant SOD1 from MN or from the cells of myeloid lineage (Boillee et al., 2006b). Mice lacking mutant *G37R-SOD1* in MN showed delayed disease onset, but no alteration in the disease course once initiated. When mutant SOD1 was eliminated from microglia, disease onset was not altered, but disease progression was extended by nearly 50%. Thus, the onset of the disease and its subsequent progression/propagation are likely to represent two separate phases, highlighting distinct possibilities for therapeutic intervention. Although the targeted

expression of mSOD1 in astrocytes fails to produce an ALS phenotype (Gong et al., 2000), its selective silencing in astrocytes significantly slows disease progression in mSOD1 mice (Yamanaka et al., 2008b). Rodent primary astrocytes expressing mutant SOD1 have toxic effects on cultured primary MN and both embryonic mouse and human stem cell–derived MN (Nagai et al., 2007). This indicates that astrocytes expressing mSOD1 exert toxic effects or are unable to provide the required trophic support for motor neuron health. Conflicting results have been obtained when targeted expression of mSOD1 is limited to MN in murine models (Pramatarova et al., 2001a; Lino et al., 2002b; Jaarsma et al., 2008). The amount of SOD1 expressed seems to be crucial in triggering MN injury and disease onset. Mice lacking mutant *G37R-SOD1* in oligodendrocytes show a more aggressive disease course accompanied by reduced IGF-1 expression (Lobsiger et al., 2009). Expression of mutant *G93A-SOD1* exclusively in Schwann cells does not lead to MN pathology (Turner et al., 2010) and increasing mSOD1 expression in Schwann cells in does not exacerbate the phenotype (Turner et al., 2010). Thus, although mSOD1 expression in oligodendrocytes and Schwann cells alters the properties of these cells, it does not appear sufficient to cause MN degeneration. It is clear that glial cells play an important role in ALS, particularly influencing disease progression after onset. Understanding better the cross-talk between glial cells and motor neurons is likely to offer opportunities for therapeutic intervention to ameliorate the propagation of motor neuron injury in ALS.

1.1.3.8. Endoplasmic reticulum stress

Intracellular inclusions related to the accumulation of misfolded/unfolded proteins, are a pathological hallmark of ALS. Protein misfolding elicits the endoplasmic reticulum (ER) stress response pathway. The initial unfolded protein response (UPR) (Kaufman, 2002), involves the recognition of aberrant proteins by the ER through activation of ER-resident chaperones responsible for correct protein folding. Further steps to counteract the toxicity caused by accumulation of non-functional proteins are suppression of general translation and ER-associated protein degradation (Yamagishi et al., 2007). Although these

mechanisms are initially cytoprotective, prolongation of the UPR activates two ER-specific apoptotic signals, C/EBP homologous protein (CHOP) and caspase-4 (caspase-12 in rodents) (Hitomi et al., 2004).

There is therefore a body of evidence implicating ER stress as an early feature of MN injury in ALS. Protein disulphide isomerase (PDI), an ER-resident chaperone and a marker of the UPR, is activated in both transgenic mSOD1 mice, where it co-localizes with mSOD1 inclusions (Atkin et al., 2006), and in biosamples from sporadic ALS patients (Atkin et al., 2008). PDI and other UPR-induced proteins are upregulated prior to disease onset in mSOD1 rodents, suggesting that ER stress is involved in the early stages of MN injury (Atkin et al., 2008). Markers of ER-stress were also upregulated in the CSF and the spinal cord of sporadic ALS patients. Gene expression profiles of MN from mSOD1 mice either innervating fast fatigable fibers, vulnerable to disease, or fast fatigue-resistant and slow fibers, more resistant to the disease, indicated that vulnerable MN displayed differential upregulation of several UPR markers preceding muscle denervation (Saxena et al., 2009a). Similar changes eventually occurred in resistant MN, but with a delay of 25-30 days (Saxena et al., 2009a). Nerve crush experiments showed that vulnerable MNs are selectively more prone to UPR activation. Exposure of NSC34 cells and primary spinal MN to cerebrospinal fluid (CSF) from ALS patients leads to clear evidence of ER stress, including expression of UPR markers, ER fragmentation and caspase-12 activation (Vijayalakshmi et al., 2011). The CSF constituents responsible for these changes have not yet been identified. Although UPR activation is believed to be cytoprotective, at least in the initial phases of the disease (Hitomi et al., 2004), a surprising increase in survival was obtained in mSOD1 mice with knock-out of a key UPR transcription factor (X-box binding protein-1, XBP-1) (Matus et al., 2009) accompanied by greater activation of ER-associated protein degradation, with decreased mSOD1 aggregation and enhanced autophagy (Hetz et al., 2009). The protective role of autophagy in ALS is also supported by the evidence that *CHMP2B* mutations are found in some cases of ALS cases (Parkinson et al., 2006). Recent *in vitro* data showed that *CHMP2B* mutations disrupt autophagy, leading to formation of large cytoplasmic vacuoles and aberrant lysosomal localisation (Lee et al., 2009).

1.1.3.9. Dysregulation of transcription and RNA processing

Involvement of RNA processing in neurodegeneration was first implicated by the identification of mutations in survival motor neuron (*SMN1*) as a cause of spinal muscular atrophy (Lefebvre et al., 1995). Gene expression profiling demonstrated transcriptional repression in NSC34 cells stably expressing mSOD1^{G93A} and in isolated MN from SOD1^{G93A} mice at end stage disease (Ferraiuolo et al., 2007). Identification of TDP-43, a ubiquitously expressed RNA/DNA binding protein, as a major component of the ubiquitinated inclusions in ALS (Neumann et al., 2006), focused attention on altered RNA processing as a major potential pathophysiological mechanism in ALS.

TDP-43 (discussed in detail section 1.3) is a predominantly nuclear protein implicated in multiple aspects of RNA processing including splicing regulation (Buratti et al., 2001b), miRNA processing (Buratti and Baralle, 2008), mRNA stability (Strong et al., 2007), regulation of stress-granules (McDonald et al., 2011). TDP-43-positive cytoplasmic inclusions are present in both neuronal and glial cells of ALS cases, though not in mSOD1 related or FUS-related ALS (Mackenzie et al., 2010). This may signify an alternative neurodegenerative cascade in these genetic subtypes of ALS. TDP-43 expression is regulated by a negative feedback loop, with TDP-43 itself binding the 3'UTR of the mRNA, resulting in autoregulation (Polymenidou et al., 2011). At present it is unknown whether MN injury is caused by loss of normal nuclear functions of TDP-43 and FUS in RNA processing or whether other toxic gain(s) of function are responsible for the disease. TDP43 and FUS contain two RNA recognition domains, a structure that is common to many RNA interacting proteins, including proteins that are involved mRNA transport. TDP-43 and FUS may participate in such RNA transport complexes, and loss of axonal mRNA transport could thus contribute to MN injury (**Figure 1.3**). Alternatively, decreased nuclear expression and function of these proteins could disrupt pre mRNA splicing; nuclear mRNA export; sorting to distinct cytoplasmic compartments; or processing of noncoding RNAs. Thousands of RNA binding targets of TDP-43 have recently been identified and include RNAs from neurodegeneration- related genes FUS,

VCP and TARDBP, as well as being enriched for genes involved in RNA metabolism, synaptic function and CNS development (Polymenidou et al., 2011) and TDP-43 bound both exonic and intronic sequences. Further evidence of dysfunctional RNA metabolism is the presence of mutations in ALS of mutations in angiogenin (*ANG*) (Greenway et al., 2006a) and the DNA/RNA helicase senataxin (*SETX*). ANG, whose expression is increased during hypoxia to promote angiogenesis, also acts as a tRNA specific RNase and regulates ribosomal RNA transcription. Mutations in ANG are likely to act through a loss of function, as over-expression of ANG extends lifespan in mSOD1 mice (Kieran et al., 2008). *SETX* autosomal dominant mutations are associated with juvenile onset FALS (Chen et al., 2004). As a DNA/RNA helicase, the protein is predicted to be a component of large ribonucleoprotein complexes, with roles in maintaining genome integrity and RNA processing. The mechanism(s) by which mutant SETX causes ALS remain to be determined. Further evidence that dysregulated RNA processing may contribute to MN injury in ALS is highlighted by the finding that biomarkers of RNA oxidation are detectable in human ALS and as an early indicator of oxidative stress in mSOD1 mice.

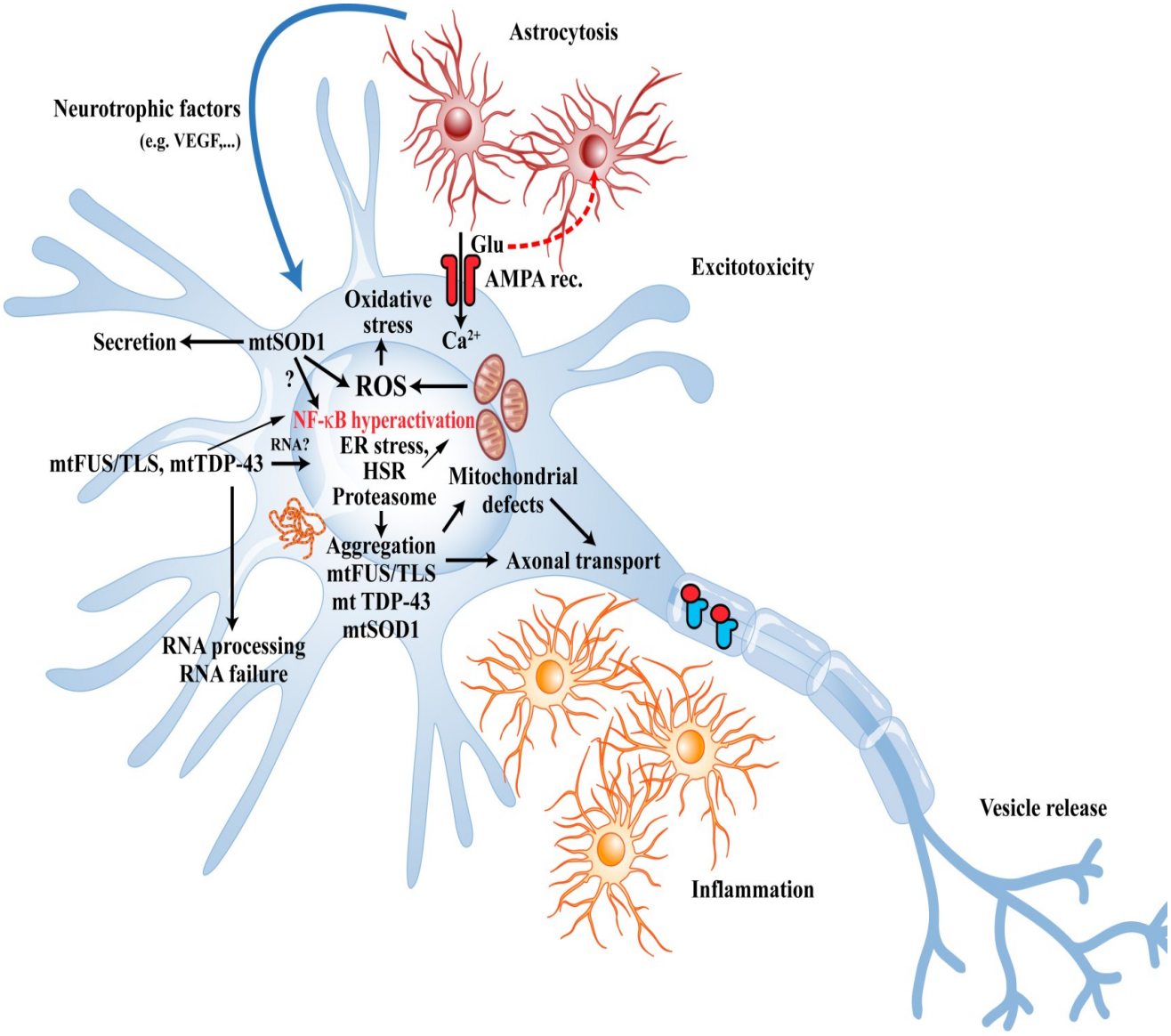

Figure 1.3. Major factors involved in ALS pathogenesis. A model showing interaction of major factors involved in ALS pathogenesis. RNA processing failure of FUS and TDP-43 as well as co-activation of NF-κB complex by TDP-43 may result in deregulation of a cascade of events resulting in astroglyosis, microgliosis, excitotoxicity, impairment of axonal transport, and oxidative stress. Factors like mitochondrial defects may contribute further to the pathogenesis of ALS.

1.1.3.10. Cell specific features of motor neurons that may underlie vulnerability to neurodegeneration

The selective vulnerability of particular neuronal groups to the neurodegenerative process is a key feature of ALS and other neurodegenerative disorders. The reason why MNs are particularly susceptible to injury in the presence of mutations affecting certain ubiquitously distributed proteins such as SOD1 and TDP-43 is not completely understood. The cell specific features of motor neurons which may predispose to age-related degeneration have are depicted in **Figure 1.4.** Important features are likely to include the large cell size, including long axons and large terminal arbors, which has implications for intracellular transport, energy metabolism and the requirement for mitochondrial and cytoskeletal support, as well as the spatial regulation of mRNA disposition for protein synthesis. The neurons vulnerable to injury in ALS have particular sensitivity to glutamatergic toxicity via AMPA receptor activation and differ from most other neuronal groups in their high expression levels of calcium-permeable AMPA receptors, lacking the GluR2 subunit (Williams et al., 1997) and their low expression of cytosolic calcium-buffering proteins (Ince et al., 1993). Vulnerable MNs also appear to have a high threshold for mounting a protective heat shock /chaperone protein response compared to other cell groups, increased sensitivity to ER stress (Saxena et al., 2009a) and mitochondrial features that predispose to oxidative damage and calcium overload (Sullivan et al., 2004). There is emerging evidence that MNs which are more resistant to the disease process such as fast-fatigue resistant and slow MNs within the spinal cord and those within the oculomotor nuclei of the brainstem and Onuf's nucleus in the sacral spinal cord, differ from the vulnerable spinal cord MNs in some of these key properties (Saxena et al., 2009a).

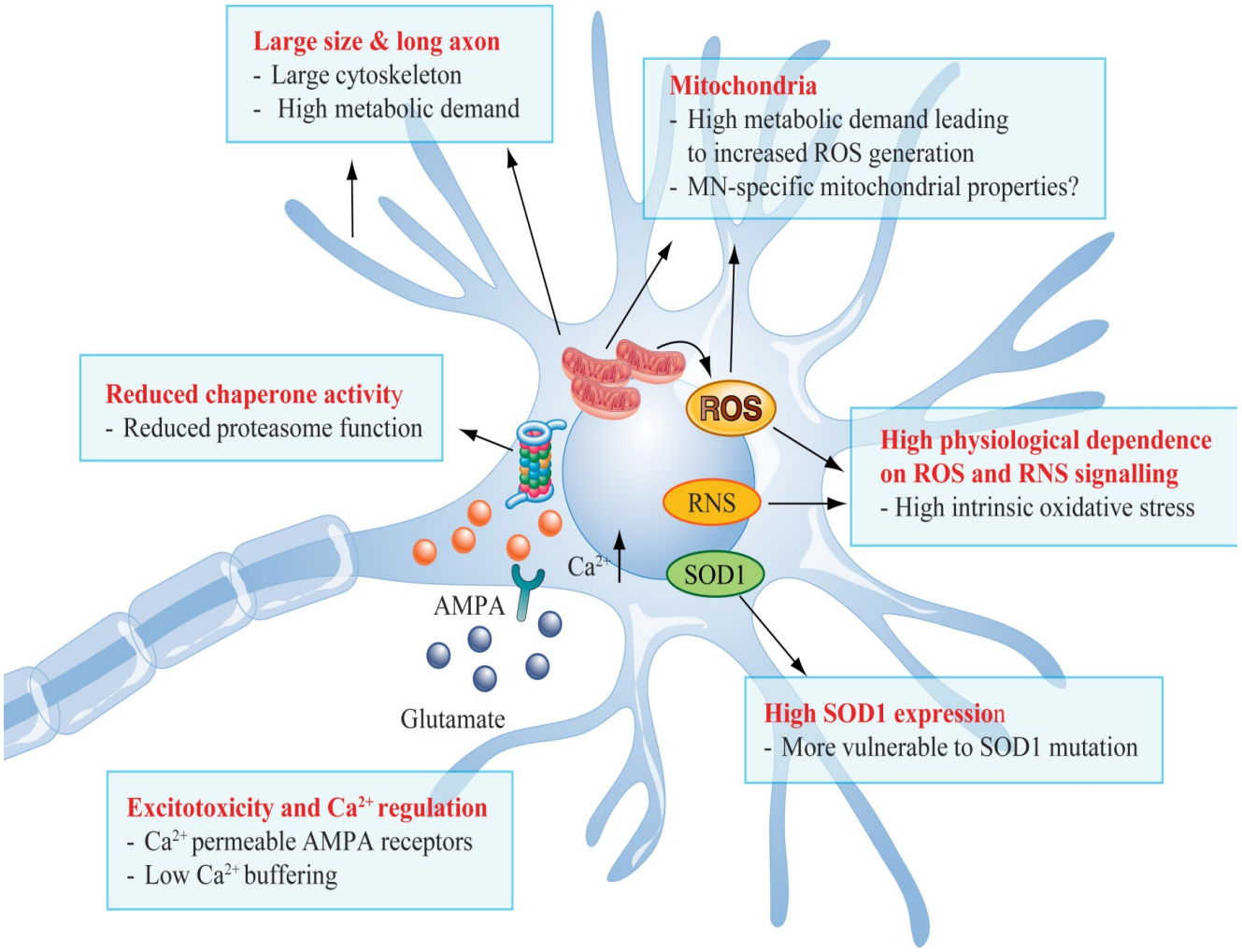

Figure 1.4 Cell specific features of motor neurons that may underlie vulnerability to neurodegeneration. The large size of the axons makes the neurons, especially motor neurons more vulnerable to toxic injury. An injury to large motor neuron may result in reduced proteasomal function combined with increased release of reactive oxygen species (ROS) and reactive nitrogen species (RNS). The neurons vulnerable to injury in ALS have particular sensitivity to glutamatergic toxicity via AMPA receptor activation and differ from most other neuronal groups in their high expression levels of calcium-permeable AMPA receptors, lacking the GluR2 subunit

1.2. Animal Models of ALS

1.2.1 Transgenic mice expressing ALS-linked SOD1 mutants

A breakthrough in the field of ALS came in 1993 with the discovery of missense mutations in the SOD1 gene of a subset of FALS cases (Rosen et al., 1993). SOD1 is a ubiquitously expressed cytosolic metalloenzyme of 153 amino acids encoded by 5 exons. To date, over 160 different mutations (mostly missense mutations) have been discovered in the SOD1 gene that account for 20% familial ALS cases (Andersen et al., 2003; Andersen, 2006). Most of our current knowledge of ALS pathogenic mechanisms came from the analysis of transgenic mice expressing mutant SOD1, especially from the widely used mouse strain SOD1G93A (B6SJL-TgN(SOD1-G93A)1Gur/J; 002726, Jackson Laboratory, Bar Harbor ME) originally generated by Gurney et al. (1994). Mouse studies led many unexpected findings described below.

1.2.1.1. A gain of toxicity due to misfolding and aggregation

Because of its normal function in catalyzing the conversion of superoxide anions to hydrogen peroxide, it was first thought that the toxicity of different SOD1 mutants could result from decreased free-radicals scavenging activity. However, SOD1 knockout mice did not develop motor neuron disease (Reaume et al., 1996) and mice expressing mutants $SOD1^{G93A}$ or $SOD1^{G37R}$ developed motor neuron disease despite elevation in SOD1 activity levels (Cleveland, 1999). These combined results suggested that the mutations in SOD1 provoke a gain of new toxic properties. Subsequently, two mouse studies further supported this view. The gene knockout for the copper chaperone for SOD1 (CCS) that delivers copper to SOD1 catalytic site had no effect on disease progression in mutant SOD1 mice (Subramanian et al. 2002). Second, transgenic mice overexpressing a mutant form of SOD1 lacking two of the four histidine residues coordinating the binding of the Cu at the catalytic site still developed motor neurodegeneration despite a marked reduction in SOD1 activity (Wang et al., 2002b).

To date, many transgenic mouse lines have been generated in which ALS-linked SOD1 mutants of different biochemical properties were expressed. High levels of mutant SOD1 mRNA are required for development of ALS-like phenotypes within the short life span of mice. Moreover, the life span of the ALS mice is inversely proportional to gene dosage. For example, in the $SOD1^{G127X}$, the survival time in hemizygous mice was twice as long as in mice homozygous for the transgene (Jonsson et al., 2006). The most widely used mouse strain $SOD1^{G93A}$ (B6SJL-TgN(SOD1-G93A)1Gur/J; 002726, Jackson Laboratory, Bar Harbor ME) with survival of approximately 130 days overexpress by 40 folds the normal mRNA levels of mouse SOD1 (Gurney et al., 1994; Jonsson et al., 2006). For many other transgenic strains (G85R, D90A, G93Adl and G127X) with later onset disease, the mRNA levels correspond to approximately 20 folds the level of endogenous SOD1 mRNA. It should be noted that the steady-state levels of mutant SOD1 proteins in the spinal cord can differ widely from one mouse strain to another. The level of human SOD1 protein in young mice of the G93A strain is of 17 fold higher than normal mouse SOD1 level whereas the G85R, G127X and L126Z mice exhibit at young age low levels of mutant SOD1 (**Table 1.2**). So, the different transgenic mouse strains express mutant SOD1 in a range of 0.5 to 20 folds the normal SOD1 levels. Such widely different steady state protein levels must reflect different stabilities and degradation of the various human SOD1 mutants. Surprisingly, despite low mutant SOD1 protein levels in the young G85R, G127X or L126Z mice, their life span remains similar to some G37R or G93A mice and they showed similar amounts of detergent-insoluble aggregates in the spinal cord at end-stage of disease (Bruijn et al., 1997; Wang et al., 2005a; Jonsson et al., 2006).

The combined studies suggest that the motor neuron disease may be caused by long-term exposure to noxious misfolded mutant SOD1 species with propensity to aggregate. However, the exact mechanism of toxicity of the misfolded SOD1 species remains unknown. Deleterious effects could result from overwhelming the capacity of the protein folding chaperones (Batulan et al., 2003)and/or of ubiquitin proteasome pathway to degrade important cellular regulatory factors (Urushitani et al., 2002). Somehow, the motor neuron death pathway is complex with multiple cascades of events including oxidative damage, excitotoxicity, alterations in calcium homeostasis, caspase activation,

mitochondrial defects (Liu et al., 2004; Pasinelli et al., 2004)and Fas transduction (Raoul et al., 2002). Moreover, the ER-Golgi pathway is a predominant site of uptake and age-dependent aggregation of misfolded mutant SOD1 linked to ALS (Urushitani et al., 2008), a phenomenon that could explain the endoplasmic reticulum (ER) stress responses detected in vulnerable motor neuron in G93A mice (Saxena et al., 2009b). Immuno-fluorescence staining with such antibodies revealed that the presence of misfolded SOD1 species was restricted to motor neurons at early pre-symptomatic stage in G93A-*SOD1* mice and intense punctate misfolded SOD1 aggregates localized in contiguous processes and in the neuropil were detected throughout the spinal cord in late disease stage (Gros-Louis et al., 2010). No immunostaining was detected in transgenic animals overexpressing wild-type human SOD1.

1.2.1.2. WT SOD1 can contribute to disease

In an initial study, the overexpression of human $SOD1^{WT}$ did not seem to affect the progression of motor neuron disease in transgenic mice expressing mutant $SOD1^{G85R}$ (Bruijn et al., 1998). However, more recent studies by other groups showed that overexpression of human $SOD1^{WT}$ caused dramatic exacerbation of disease in mice expressing different SOD1 mutants, including two SOD1 mutants ($SOD1^{G85R}$ and $SOD1^{L126Z}$) that express highly unstable and enzymatically inactive SOD1 (Deng et al., 2006; Deng et al., 2008; Jaarsma et al., 2008; Wang et al., 2009b). Remarkably, a $SOD1^{A4V}$ mouse line without phenotypes was converted to an ALS-like mouse model with death at 400 days through the generation of double-transgenic $SOD1^{A4V}$;wtSOD1. Evidence suggests that the $SOD1^{WT}$ may contribute to disease through interaction and perhaps stabilization of mutant SOD1. Interestingly, human $SOD1^{WT}$ overexpression did not affect the lifespan of mice overexpressing mouse $Sod1^{G86R}$ (Audet Jean-Nicolas, 2010). The analysis of spinal cord extracts revealed a lack of heterodimerization or aggregation between human $SOD1^{WT}$ and mouse $Sod1^{G86R}$ proteins. Thus, a direct interaction between wild type and mutant forms of SOD1 is required for exacerbation of ALS disease by $SOD1^{WT}$ protein.

Table 1.2: Different steady-state protein levels in mice expressing various mutant SOD1 transgenes

Mouse Strain	Human SOD1 mRNA levels relative to mouse SOD1	Spinal cord protein levels relative to mouse SOD1 in young mice	Life span	References
In vivo stable SOD-1 mutants				
G93A	40	17	124 days	(Jonsson et al., 2006)
G93Adl	20	8	253 days	(Jonsson et al., 2006)
D93A	20	20	407 days	(Jonsson et al., 2006)
G37R line 29	-	5	365 days	(Nguyen et al., 2001)
G37R line 42	-	12	154 days	(Nguyen et al., 2001)
In vivo unstable SOD-1 mutants				
G85R	17	0.9	345 days	(Jonsson et al., 2006)
G127x	25	0.45	250 days	(Jonsson et al., 2006)
L126Z	High	Low	210 days	(Wang et al., 2005a)

1.2.1.3. Involvement of non-neuronal cell types

A most significant contribution of transgenic mouse studies was the finding of a role for non-neuronal cells in motor neuron disease. For instance , the analyses of chimeric mice made of mixtures of normal and SOD1 mutant-expressing cells demonstrated that neurodegeneration is delayed or eliminated when motor neurons expressing mutant SOD1 are surrounded by healthy wild-type cells (Clement et al., 2003). To further clarify what cell types contribute to disease, very elegant studies were carried out with mice carrying $SOD1^{G37R}$ gene flanked by LoxP sequences, a system that allows excision by the Cre recombinase in specific cell types (Yamanaka et al., 2008a). These studies revealed that expression of mutant SOD1 within motor neurons is a modulator of onset of ALS disease whereas mutant SOD1 toxicity in glial cells can affect the progression of disease after onset (Figure 1.1). It should be noted that two studies, neuron-specific expression of SOD1 mutants with NF-L or Thy1 gene promoters did not induce motor neuron disease in mice (Pramatarova et al., 2001b; Lino et al., 2002a). However, subsequent studies reported motor neuron disease in mice overexpressing high levels of mutant SOD1 under the Prion gene or Thy1 gene promoters ((Wang et al., 2005b; Jaarsma et al., 2008). These apparent discrepancies can be explained by the degree of transgene overexpression in neurons.

1.2.1.4. Testing immunization approaches in mutant SOD1 mice

The existence of secretory pathways for SOD1 and for neurotoxicity of extracellular mutant SOD1 led us to test immunization protocols aiming to reduce the burden of extracellular SOD1 mutant in nervous tissue of mice models of ALS. A vaccination protocol, based on bacterially-purified recombinant SOD1 mutant protein as an immunogen, was tested on a $SOD1^{G37R}$ mouse strain exhibiting levels of mutant SOD1 protein at 5 folds the normal SOD1 levels. The vaccination was effective in delaying disease onset and extending life span of G37R *SOD1* mice by over 4 weeks and the analyses provided evidence of reduction of SOD1 species in the spinal cord of vaccinated G37R *SOD1* mice (Urushitani et al., 2007; Gros-Louis et al., 2010). Recently, passive immunization approach was tested based on intra-cerebroventricular infusion in G93A-*SOD1* mice of monoclonal antibodies specific to misfolded forms of SOD1. One antibody

succeeded in reducing the level of misfolded SOD1 by 23% in the spinal cord and in prolonging the lifespan of G93A-*SOD1* mice in proportion to the duration of treatment (Gros-Louis et al., 2010). These results suggest that passive immunization strategies should be considered as potential avenues for treatment of familial ALS caused by *SOD1* mutations.

1.2.2. Mice knockout for Als2

Deletion mutations were discovered in coding exons of a gene mapping to chromosome 2q33, *ALS2* coding for Alsin, from patients with an autosomal recessive form of juvenile ALS (JALS), primary lateral sclerosis and infantile-onset ascending hereditary spastic paralysis (IAHSP) (Hadano et al., 2001b; Yang et al., 2001; Eymard-Pierre et al., 2002; Gros-Louis et al., 2003). The ALS2 gene is ubiquitously expressed. It encodes a protein having guanine nucleotide exchange factor (GEF) homology domains which are known to activate small guanosine triphosphatase (GTPase) belonging to the Ras superfamily. Als2 knockout mice have been reported by three groups (Cai et al., 2005; Devon et al., 2006; Hadano et al., 2006). These studies demonstrate that absence of Als2 does not produce a severe phenotype in mice. However, the studies by Cai et al. (Cai et al., 2005) showed that the Als2 null mice develop age-dependent deficits in motor coordination and primary cultured motor neurons lacking Als2 were more susceptible to oxidative stress. Whereas Cai et al. detected no neuropathological changes in their Als2 null mice, Hadano et al. (Hadano et al., 2006) showed that Als2-null mice develop an age-dependent and slow progressive loss of cerebellar Purkinje Cells, a reduction in ventral motor axons during aging, astrogliosis and evidence of deficits in endosome trafficking. The Als2 knockout mouse exhibited degeneration of corticospinal axons and evidence of axonal transport defects (Gros-Louis et al., 2008).

1.2.3. Mice with disorganized Intermediate Filaments (IFs)

Neurofilament and peripherin proteins are two types of IFs detected in the majority of axonal inclusion bodies, called spheroids, in motor neurons of ALS patients (Hirano et al., 1984; Corbo and Hays, 1992). Multiple factors can potentially cause the accumulation of

IF proteins including deregulation of IF protein synthesis, proteolysis, defective axonal transport, abnormal phosphorylation, and other protein modifications. Even though genetic mutations in IF genes are not major causes of ALS, it is of potential relevance to ALS that transgenic mice with altered stoichiometry of neuronal IF develop pathological features of the disease (Cote et al., 1993; Beaulieu et al., 2000; Beaulieu and Julien, 2003; Millecamps et al., 2006). Of particular interest was the finding that sustained overexpression of wild-type peripherin in mice caused the selective loss of motor neurons during aging. This mouse model is characterized by the formation of perikaryal and axonal IF inclusions resembling spheroids in motor neurons of human ALS. The toxicity of peripherin overexpression in mice appears related in part to the axonal localization of IF aggregates, in line with the view that IF swellings might impair axonal transport (Beaulieu and Julien, 2003; Millecamps et al., 2006). Recently, a neurotoxic and assembly defective splicing variant of peripherin called Per28 was detected specifically in spinal cord samples from ALS cases (Xiao et al., 2008). In future, it would be of interest to test the in vivo toxicity of Per28 in motor neurons with the generation of transgenic mice.

1.2.4. Mice with microtubule-based transport defects

Axonal transport is essential to neurons because of the extreme polarity and size of these cells. In humans, spinal motor neurons may have axons of more than 1 meter in length. Most proteins must be synthesized in cell bodies and transported to nerve terminals through axonal transport. Various molecular motors, which are multi-subunit ATPases members of the kinesin family and dynein, move cargos along microtubules in the anterograde and retrograde directions, respectively. Impairment of axonal transport has recently emerged as a common factor in several neurodegenerative disorders. Mutations that disrupt either kinesin or the dynein complex cause impairment of axonal transport, blockade of membranous cargoes and axonal degeneration.

The creation of mice heterozygotes for disruption of the kinesin KIF1B gene provided the proof that defects in axonal transport can provoke neurodegeneration (Zhao et al., 2001). These mice showed defect in transporting synaptic vesicle precursors and they suffer from

progressive muscle weakness similar to human neuropathies. This discovery subsequently led to the identification of a loss-of-function mutation in the motor domain of the KIF1B gene in patients with Charcot–Marie–Tooth disease type 2A (Zhao et al., 2001). In addition, missense mutations in the conventional KIF5A are responsible for a hereditary form of spastic paraplegia (Reid et al., 2002) and disruption of KIF5A gene in mice was reported to cause neurofilament transport impairment (Xia et al., 2003).

Dynein is a molecular motor involved in retrograde axonal transport of organelles along microtubules. Dynein activity requires association with dynactin, a multiprotein complex that activates the motor function of dynein and participates in cargo attachment (Schroer, 2004). Transgenic mice overexpressing dynamitin developed a late-onset and progressive motor neuron disease resembling ALS with neurofilamentous swellings in motor axons (LaMonte et al., 2002; Hafezparast et al., 2003).

Few years ago, a family with a slowly progressive autosomal dominant lower motor neuron disease has been linked to a mutation in the $p150^{Glued}$ subunit (G59S) of the dynactin complex (Puls et al., 2003). Neuronal expression of mutant dynactin $p150^{Glued}$, but not wild type, caused motor neuron disease in transgenic mice (Laird et al., 2008). The disease was characterized by defects in vesicular transport in cell bodies of motor neurons, axonal swelling and axon terminal degeneration. Interestingly, evidence was provided that autophagic cell death was involved in the pathogenesis of mutant $p150^{Glued}$ transgenic mice. The mutant $p150^{Glued}$ mice share many pathological features of human sporadic ALS including ubiquitin positive inclusions, accumulations of neurofilaments and astrocytosis. None of these pathological changes occurred in mice expressing human wild-type $p150^{Glued}$.

1.2.5. Other Animal Models of ALS

Apart from transgenic mouse models of ALS, many other non-murine models of ALS have been reported in the past (**Table 1.3**). These non-murine models are particularly useful in their potential for large-scale chemical and genetic screening. Zebrafish (*Danio rerio*) has

been used as a model to study ALS. Overexpression of mutant human SOD1 in zebrafish embryos induced a motor axonopathy that was specific, dose-dependent and found for all mutations studied (Lemmens et al., 2007). Similarly, ALS-linked mutant SOD1 produced locomotor defects along with aggregation and synaptic dysfunction when expressed in neurons of *Caenorhabditis elegans* (Wang et al., 2009a). The fly model (*Drosophila melanogaster*) of ALS produced by overexpressing A4V and G85R mutants of SOD1 showed toxicity selectively in motor neurons and SOD1 protein aggregates (Watson et al., 2008). VAPB mutation model of ALS has also been reported in Drosophila (Ratnaparkhi et al., 2008). Apart from SOD1 and VAPB models, many non-murine models overexpressing TDP-43 and FUS have recently been reported. In the Drosophila model of FUS, ectopic expression of human ALS-causing FUS mutations caused an accumulation of ubiquitinated proteins, neurodegeneration, larval-crawling defect and early lethality. Mutant FUS localized to both the cytoplasm and nucleus, whereas wild-type FUS localized only to the nucleus, suggesting that the cytoplasmic localization of FUS is required for toxicity (Lanson et al., 2011). A brief description of murine and non-murine models of TDP-43 mutations is described in section 1.3.5.

Table 1.3 Animal models of motor neuron disease

Animal Models	Pathological Changes	References
ALS-linked SOD1 mutations Overexpressors of SOD1 mutants (G93A, G37R, G85R, G27X, L126Z) - Mouse models	Mitochondria swellings, vacuoles, SOD1 aggregates, neurofilament accumulations, motor neuron loss	(Bruijn et al., 1997; Durham et al., 1997; Bruijn et al., 1998; Johnston et al., 2000; Liu et al., 2004; Pasinelli et al., 2004; Wang et al., 2005b)
SOD1 – *C. elegans, D. melanogaster, D. rerio*	Locomotor defects along with aggregation and synaptic dysfunction	(Lemmens et al, 2007; Wang et al, 2009; Watson et al, 2008)
Intermediate filament disorganization		
hNF-H overexpressor	Perikaryal accumulations and axonal atrophy Altered conductivity but no neuronal loss	(Cote et al., 1993)
Mutant NF-L	Perikaryal and axonal NF accumulations No degeneration of sensory neurons but massive degeneration of spinal motor neurons	(Lee et al., 1994)
Peripherin overexpressor	Age-dependent IF aggregates in perikarya and axons 40% loss of spinal motor neurons	(Millecamps et al., 2006)
Defects in microtubule-based transport		
Dynamitin overexpressor	Abnormal gaits and decrease in strength	

	Axonal IF swellings 25% loss of motor axons at 16 months	(LaMonte et al., 2002)
KIF1B heterozygous Knockout	Staggering gait after 1-year of age Progressive muscle weakness	(Zhao et al., 2001)
Dynein mutations heterozygous	Progressive motor dysfunction Loss of 4–70% of motor neurons at 16 months	(LaMonte et al., 2002; Hafezparast et al., 2003)
pmn mouse	Axonal swellings and early onset motor neuron degeneration	(Bommel et al., 2002; Martin et al., 2002)
Defects in endosomal trafficking		
Als2 knockout and of corticospinal axons	Defects of endosome trafficking, late-onset degeneration of cerebellar Purkinje cells	(Yang et al., 2001; Eymard-Pierre et al., 2002; Gros-Louis et al., 2003; Hadano et al., 2006)
Trophic factor		
VEGF ΔHRE	Late-onset motor dysfunction Loss of 40% motor axons at 7 months	(Lambrechts et al., 2003; Moreau et al., 2006)

ALS Linked TDP-43		
Mice overexpressing A315T mutant of TDP-43	Gait abnormalities at 3 months of age and an average survival of 153 days.	(Wegorzewska et al., 2009)
Mice overexpressing wild-type TDP-43	Lack of Cytoplasmic TDP-43 aggregates Dose-dependent degeneration of cortical and spinal motor neurons and subsequent development of spastic quadriplegia	(Wils et al., 2010)
Mice overexpressing wild-type as well as A315T and M337V mutants of TDP-43	Develop Paralysis and death as early as 12 days	(Stallings et al., 2009) (Li et al., 2010)
Drosophila overexpressing wild-type TDP-43	Loss of ommatidia with signs of neurodegeneration	(Kabashi et al., 2010)
Zebrafish overexpressing wild-type as well as A315T, G348C and A382T mutants of TDP-43	Premature and excessive motor axonal branching.	
ALS linked FUS		
Drosophila overexpressing Wt or mutant FUS	Neurodegeneration, crawling defects, Early lethality. Mutant more toxic than wild-type	(Lanson et al., 2011)

1.3. Trans-activating response region (TAR) DNA Binding Protein- 43 (TDP-43)

1.3.1. TDP-43

TDP-43, a 414 amino acid 43 kDa protein, is encoded by the human *TARDBP* gene located on chromosome 1. Under normal physiological conditions, TDP-43 is predominantly nuclear (Wang et al., 2002a), although the protein is capable of shuttling between the nucleus and cytoplasm and is synthesized in the cytoplasmic compartment (Ayala et al., 2008; Winton et al., 2008). Though the physiological function of TDP-43 is still incompletely characterized; the available evidence suggests this protein has several roles like regulation of gene expression (Ou et al., 1995), splicing regulation (Buratti et al., 2001b), miRNA processing (Buratti and Baralle, 2008), mRNA stability (Strong et al., 2007), regulation of stress-granules (McDonald et al., 2011).

TDP-43 is ubiquitously expressed in all cell types including neurons, glia, and astrocytes, but the expression of TDP-43 differ among various cell types. The appearance of TDP-43 across neuronal and non-neuronal cell types differs markedly between healthy tissue and tissue affected by disease. Several studies have shown that TDP-43 is often hyperphosphorylated, cleaved into various fragments, poly-ubiquitinated, mislocalized in cytoplasm and detergent insoluble in tissues taken from cases of ALS/FTLD-U, but not in tissue taken from controls(Arai et al., 2006b; Neumann et al., 2006). These data raises the question of the functional consequences might ensue from the observed differences between normal and abnormal TDP-43. Hyperphosphorylation of TDP-43 at various amino acid residues, specifically at Serine residues S379, S403/404, S409 and S410, have been shown to clearly differentiate disease-associated TDP-43 from TDP-43 in normal brain tissue (Inukai et al., 2008; Neumann et al., 2009b). A study of the literature reveals that the biological activity of many proteins is regulated by their phosphorylation states and dysregulation of protein phosphorylation is an important feature of various neurodegenerative diseases. For example, researchers in Alzheimer's field have demonstrated that hyperphosphorylation of tau—a process implicated in the pathogenesis of FTLD-Tau and Alzheimer's Disease (AD)—leads to loss of the protein's normal ability to assemble and maintain microtubules, as well as a propensity for the molecule to

aggregate into paired helical filaments(Ballatore et al., 2007). These changes in tau, in turn, lead to neuronal dysfunction and degeneration. However the consequences of TDP-43 hyperphosphorylation or overexpression in ALS and FTLD-U remain unclear - loss-of function and/or gain-of-toxic-function or both mechanisms conferred by such post-translational modification might have a critical role in TDP-43-mediated neurodegeneration. TDP-43 extracted from disease-associated tissue is highly detergent insoluble than TDP-43 from normal tissue (Neumann et al., 2006). The functional consequence of this reduction in solubility is uncertain, although the propensity of insoluble TDP-43 to aggregate in the cytoplasm or in the nucleus may suggest a gain-of-toxic-function mechanism for TDP-43 in disease (Igaz et al., 2011). This gain-of-toxic property of TDP-43 might be linked to phosphorylation of the protein; small species of TDP-43 of ~25 kDa can be detected in pathological specimens from patients with ALS/FTLD-U, but not in normal brain tissue (Neumann et al., 2006). These species are believed to be carboxy-terminal (C-terminal) TDP-43 fragments generated through cleavage of the full-length protein (Hasegawa et al., 2008). Studies of the C-terminal fragments of TDP-43 are still in their early stages; however, work in yeast (Johnson et al., 2009) and in human cell lines (Nonaka et al., 2009) suggests that these fragments might cause inclusion formation and/or cellular toxicity.

1.3.2. TDP-43 Function

TDP-43 is a multifunctional protein involved in various steps of RNA processing including transcription, pre-mRNA splicing, mRNA transport and translation (**Figure 1.5**), although the exact cellular functions remain to be determined. TDP-43 acts as a transcription factor and has been shown to bind to TAR DNA of the human immunodeficiency virus type 1 (HIV-1) to repress its transcription (Ou et al., 1995). It has also been shown to bind to the promoter of the mouse SP-10 gene, which is required for spermatogenesis (Acharya et al., 2006)The C-terminal domain of TDP-43 is involved with exon skipping and splicing inhibitory activity through the interaction with other hnRNP family proteins. The pre-mRNA of cystic fibrosis transmembrane regulator (CFTR) contains an intronic UG tract that is recognized by TDP-43, thereby promoting skipping of exon 9 in CFTR mRNA

(**Figure 1.5**) (Buratti et al., 2001a). TDP-43 was also shown to affect the splicing of apolipoprotein A-II and survival motor neuron (SMN) transcripts (Mercado et al., 2005; Bose et al., 2008). The hnRNPs are RNA binding proteins that bind pre-mRNA in the nucleus and influence pre-mRNA splicing and other aspects of mRNA metabolism and transport. Some hnRNPs appear to shuttle between the nucleus and the cytoplasm, potentially transporting mRNAs. Pre-mRNAs may be alternatively spliced to generate multiple mRNA species for temporal and tissue-specific expression of a given gene (Dreyfuss et al., 2002). TDP-43 was reported to associate with a number of splicing regulator proteins, such as SC35 and hnRNP A2 (Wang et al., 2002a; D'Ambrogio et al., 2009). Other known RNA targets of TDP-43 include beta-actin and calcium/calmodulin kinase II alpha (Wang et al., 2008a). It is likely that other RNA targets are yet to be identified. Recently TDP-43 has been shown to bind to hundreds of intronic, pre-mRNA, NFL-mRNA, 3' and 5'UTRs of various RNAs (Polymenidou et al., 2011; Tollervey et al., 2011). Downregulation of TDP-43 using anti-sense RNA or gene knockout studies has shown that removing TDP-43 from the system alters splicing regulation and changes splicing pattern of various transcripts (Chiang et al., 2010; Polymenidou et al., 2011). TDP-43 also plays post-transcriptional roles other than splicing regulation (**Figure 1.6**). TDP-43 is recruited to stress granules (mRNA and RNP complexes where protein synthesis is temporarily arrested), indicating that TDP-43 may play a protective role against cellular insult (Colombrita et al., 2009; Liu-Yesucevitz et al., 2010; McDonald et al., 2011). TDP-43 also promotes the mRNA stability of human neurofilament light chain (hNFL) transcript (Strong et al., 2007). It can bind to UG repeats to repress expression of Cdk6, a gene that encodes the cell division protein kinase 6 (Ayala et al., 2008). TDP-43 may play a role in microRNA (miRNA; post-transcriptional regulators that bind to mRNA) biogenesis and processing as it has been found to associate with Drosha, the RNase III enzyme responsible for initiating the processing of miRNA. The C-terminal of TDP-43 is known to interact with proteins involved in miRNA processes, including argonaute 2 and DDX17 (Freibaum et al., 2010).

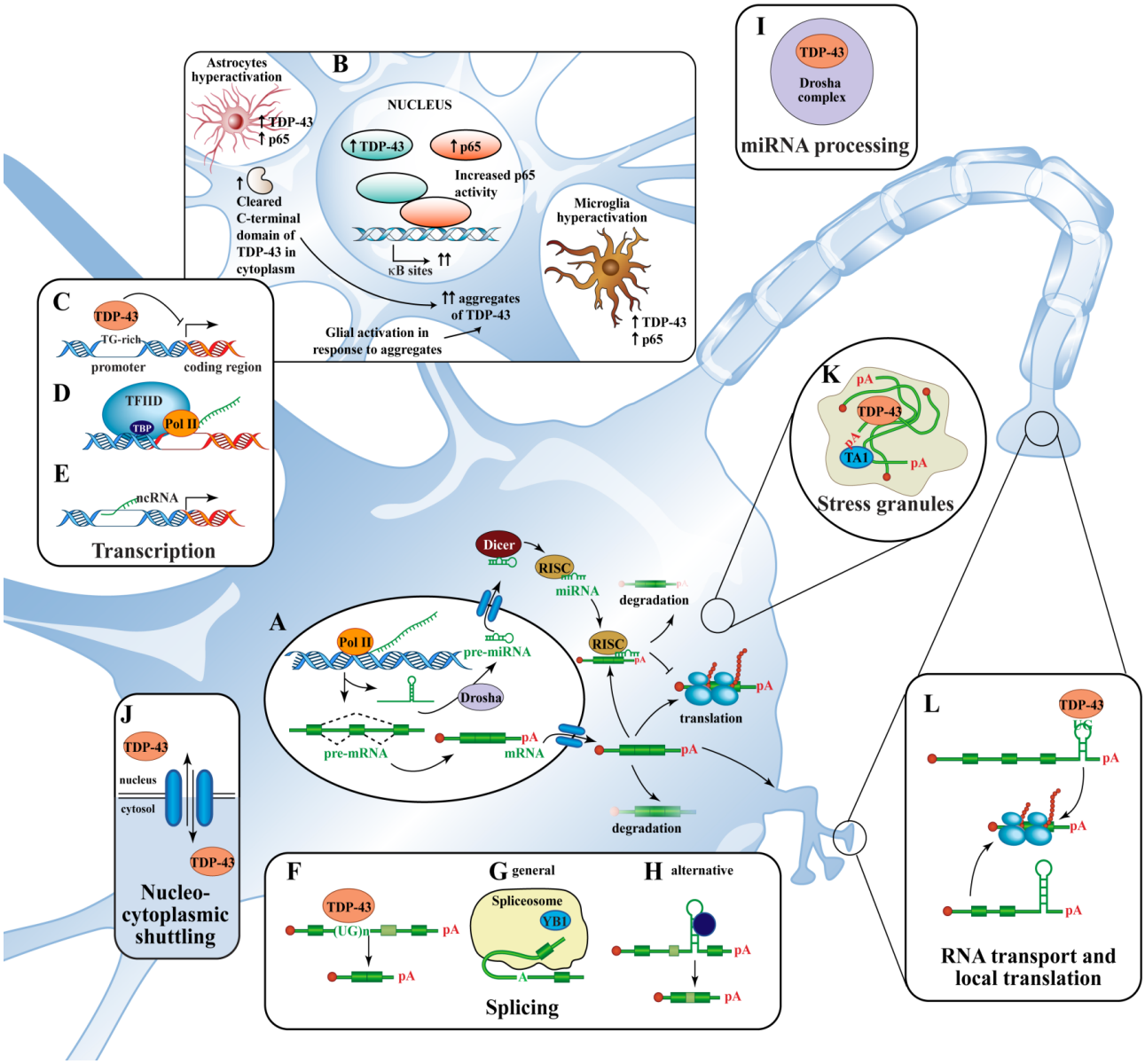

Figure 1.5 Multiple roles of TDP-43. Several different roles of TDP-43 have been proposed and reportedTDP-43 is involved in pre-mRNA processing (**A**), transcription inhibition (**C-E**), miRNA processing (**I**), as a component of stress granules (**K**), RNA transport and local translation (**L**), splicing regulator (**F-H**), nucleo-cytoplasmic shuttling (**J**), and as a co-activator of p65 NF-κB (**B**). Modified from Lagier-Tourenne et al, HMG, 2010.

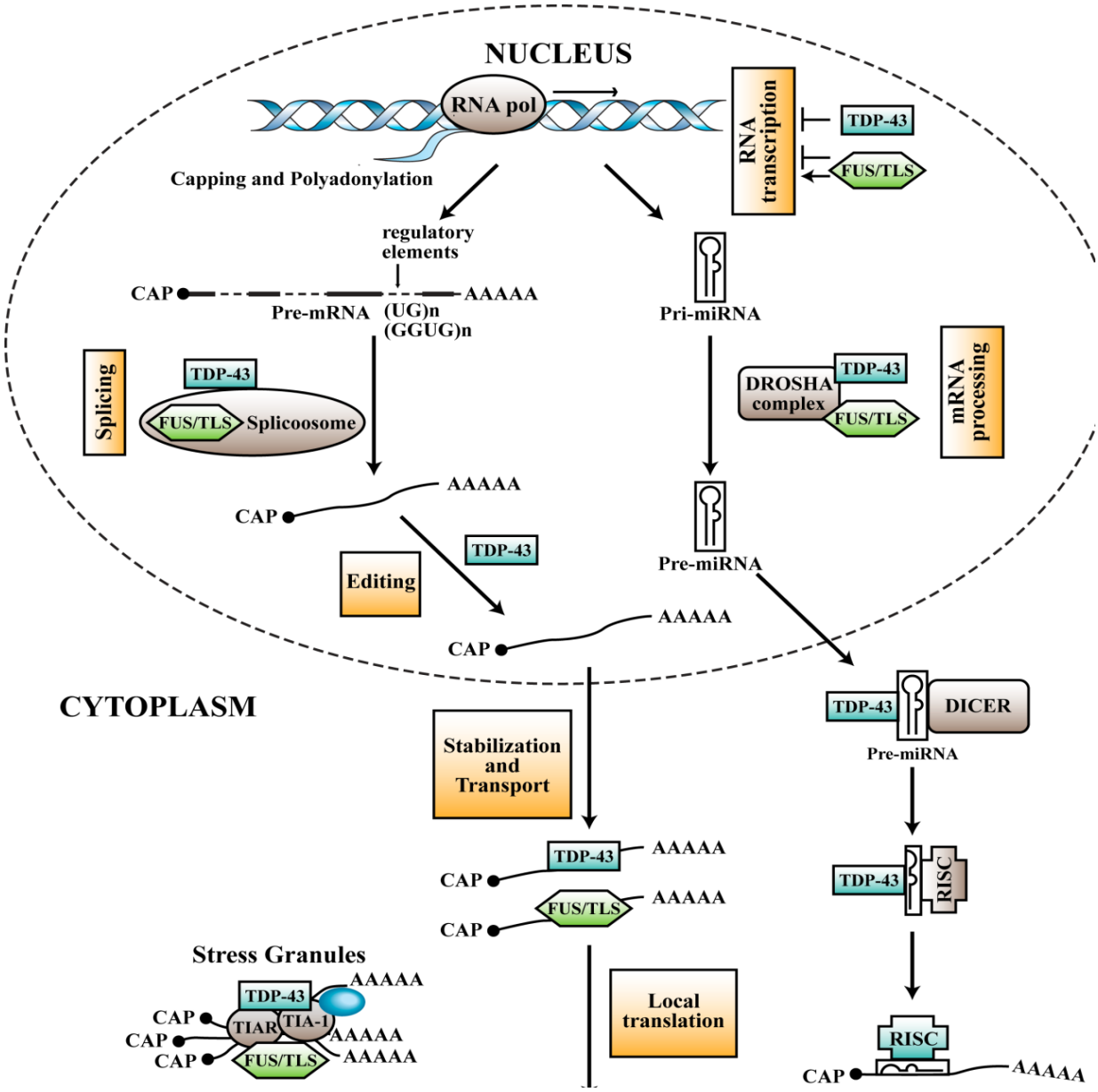

Figure 1.6 Role of TDP-43 and FUS in RNA processing and stress granule formation. TDP-43 and FUS are required for snRNA synthesis. TDP-43 interacts with SMN protein and forms complexes to regulate snRNA processing. In the cytoplasm, stress granules can be formed by injury to the axon. It is possible that prolonged stabilization of stress granules may result in formation of TDP-43 aggregates which are hyperphosphorylated. Modified from Colombrita et al, 20011.

1.3.3. TDP-43 in neurodegenerative diseases

TDP-43 pathology can be found in many neurodegenerative diseases – in some diseases TDP-43 is a major histopathological feature, while in other cases TDP-43 is a minor feature. In FTLD-U and ALS, TDP-43 pathology is the most prominent histopathological feature (Neumann et al., 2006; Ayala et al., 2008), while in Alzheimer's disease (AD), Parkinson disease (PD) and Huntington's disease (HD) (Dickson et al., 2007; Higashi et al., 2007; Nakashima-Yasuda et al., 2007; Schwab et al., 2008; Arai et al., 2009), TDP-43 pathology is an important but secondary histopathological feature of disease. In some patients, the topography of TDP-43 pathology accords with the primary clinical symptomology; for example, severe motor cortex pathology in ALS (Geser et al., 2008b; Geser et al., 2009a), but in other cases no such association exists like medial temporal lobe pathology in PD (Nakashima-Yasuda et al., 2007).

1.3.3.1. TDP-43 pathology in amyotrophic lateral sclerosis

Majority of ALS cases are sporadic, and about 90% of these cases have TDP-43 inclusions (Dickson et al., 2007; Geser et al., 2008a; McCluskey et al., 2009). TDP-43 inclusions (**Figure 1.7**) are found in familial ALS patients with the notable exception of cases associated with mutations in the superoxide dismutase gene (SOD1) (Mackenzie et al., 2007). Thus, SOD1- associated ALS might differ in terms of disease mechanism from the majority of sporadic and familial ALS cases with TDP-43 pathology. Histopathology of TDP-43 in ALS is characterized by skein-like cytoplasmic inclusions or a dense granular appearance and by nuclear clearance of TDP-43(Geser et al., 2008a). Some degree of TDP-43 pathology in ALS cases can be found throughout the brain; however, the most severely affected areas of the central nervous system are the motor cortex, the spinal cord, the basal ganglia, and the thalamus. This distribution of pathology in various regions of the CNS can explain as to why ALS with TDP-43 inclusions is considered to represent a distinct pathological subtype (Geser et al., 2008a). Many cases of FTLD-U or ALS can be readily categorized accordingly to the most prominent clinical features associated with each condition. However, a small yet substantial proportion of suspected ALS/FTLD-U cases

show features of both FTLD-U and MND (or ALS). Some of these patients first present with cognitive impairment (sometimes called FTLD–MND), while others initially present with motor impairment (sometimes called ALS+). TDP-43 pathology is the primary histopathological feature of such 'overlap' cases, and comprises TDP-43- positive inclusions or granular staining in the cytoplasm and an absence of nuclear TDP-43 immunoreactivity(Brandmeir et al., 2008). In these cases, the topographical distribution of TDP-43 lesions unsurprisingly lies somewhere between the distributions observed in FTLF-U and ALS (lesions mainly affecting upper and lower motor neurons) (Brandmeir et al., 2008; Geser et al., 2009b).

1.3.3.2. TDP-43 pathology in frontotemporal lobar degeneration

In FTLD-U, TDP-43 pathology is found throughout the central nervous system, although the occipital cortex and cerebellum remain relatively unaffected (Geser et al., 2009b). The TDP-43 histopathology in FTLD-U can be divided in 4 subtypes - **Type 1** the pathology is characterized by a relative abundance of cytoplasmic TDP-43 inclusions in long neuritic profiles in superficial cortical layers. **Type 2** the pathology is delineated by a predominance of cytoplasmic TDP-43 inclusions in both the superficial and deep cortical layers. **Type 3** the pathology is the abundance of cytoplasmic TDP-43 inclusions mainly in the superficial cortical layers, and in **Type 4** pathology, which is associated with VCP gene mutations, most TDP-43 inclusions are nuclear(Arai et al., 2006a; Sampathu et al., 2006; Brandmeir et al., 2008). Thus, ALS with TDP-43 inclusions is categorized as **Type 5** TDP-43 pathology (**Figure 1.7**) (Davidson et al., 2007). The importance of the various histopathological FTLD-U subtypes remains to be established. Curiously, all neuropathologically characterized cases of FTLD-U associated with *GRN* mutations have shown type 3-like TDP-43 pathology (Mackenzie et al., 2006; Josephs et al., 2007). These findings suggest mechanistic differences between subtypes of FTLD-U with varying TDP-43 pathology. A small proportion of FTLD-U cases (<10%) do not demonstrate TDP-43 pathology. many of these cases have been reported to have pathological inclusions containing the ALS-associated protein FUS mutations (Neumann et al., 2009a).

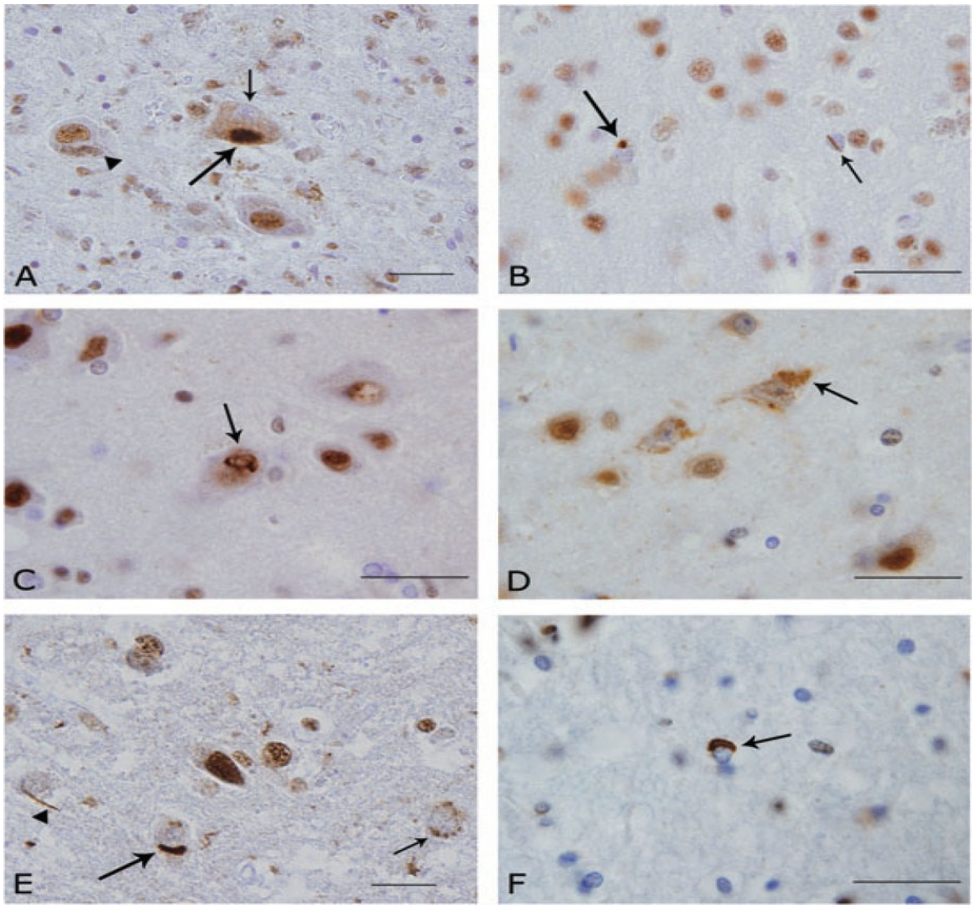

Figure 1.7 TDP-43 immunohistochemistry in ALS with dementia (A–D,F) and frontotemporal lobar degeneration (FTLD)-TDP (E) (bar = 20 μm). A. Lewy body-like inclusion (large arrow) in the substantia nigra; note the nucleus devoid of the endogenous TDP-43 staining ("cleared nucleus") (small arrow) that is present in the affected neuron, but not in an unaffected neuron (arrowhead). B. Neuronal cytoplasmic inclusions (large arrow) and neuronal intranuclear inclusion (short arrow) in the visual cortex. C. Fibrillar or skein-like curled inclusions in the sensory cortex (arrow). D. Cleared nuclei coupled with cytoplasmic, granular, or diffuse staining ("pre-inclusions") (large arrow) in Wernicke's area. E. Hypothalamus showing dense neuronal cytoplasmic inclusion (large arrow), smaller granular neuronal cytoplasmic TDP-43 immunoreactivity (small arrow), and dystrophic cellular processes (arrowhead). F. Oligodendrocyte with cytoplasmic inclusion in the white matter of cingulate gyrus. Published by (Geser et al., 2010) and reprinted with permission from John Wiley and sons publications vide license number # 2796650929569.

1.3.3.3. TDP-43 pathology in other neurodegenerative diseases

In addition to neurodegenerative diseases which have primary TDP-43 proteinopathies, TDP-43 inclusions have been detected in several disorders as secondary pathology or are referred to as secondary TDP-43 proteinopathies. TDP-43 inclusions have been also reported to be secondary pathological features of Alzheimer's disease (AD), Parkinson's disease (PD and related disorders), and Huntington disease (HD), as well as some rare diseases like Guam-ALS and Guam ALS–PD(Hasegawa et al., 2007; Geser et al., 2008b; Geser et al., 2009a). In Alzheimer's disease, TDP-43 pathology is found in over 50% of cases and is usually localized to the medial temporal lobe (Amador-Ortiz et al., 2007; Higashi et al., 2007; Hu et al., 2008). Recently in AD, detergent-insoluble TDP-43 was positively correlated with the accumulation of soluble Aβ42, amyloid plaques, and paired helical filament tau (Tremblay et al., 2011). The TDP-43 pathology observed in PD, PD with dementia, and dementia with Lewy bodies plus AD is also localized to this region of the brain, and affects up to 60% of cases(Higashi et al., 2007; Nakashima-Yasuda et al., 2007; Arai et al., 2009). Finally, a study has reported that in all cases of HD examined, pathological TDP-43 co-localized with mutant huntingtin in cytoplasmic inclusions (Schwab et al., 2008).

1.3.4. TARDBP mutations

Extensive mutation analysis of *TARDBP* has led to the discovery of missense mutations in sporadic and familial ALS (Kabashi et al., 2008; Kuhnlein et al., 2008; Rutherford et al., 2008; Sreedharan et al., 2008; Van Deerlin et al., 2008; Yokoseki et al., 2008; Corrado et al., 2009a; Del Bo et al., 2009; Lemmens et al., 2009; Tamaoka et al., 2010) as well as one frame-shift mutation that creates a premature stop codon (Y374X) leading to the expression of truncated TDP-43 (Daoud et al., 2009). All reported missense mutations cluster in exon 6 (**Figure 1.8**) of *TARDBP* except for one, D169G, which is localized in the RRM1 (Kabashi et al., 2008). TDP-43 mutations have been reported in only 2-3% of ALS cases; it is critical to understand how these mutations confer toxicity thereby providing insight on the role of TDP-43 in neurodegeneration. Mutations in C-terminal region of TDP-43 are

expected to influence protein–protein interactions and the exon skipping and splicing regulatory activity of TDP-43 as exon 6 encodes the highly conserved glycine-rich domain of TDP-43. Surprisingly mutations (Q331K, M337V and G348C) that occur in the C-terminal region required for hnRNP A2 interaction and splicing inhibition, fail to disrupt the binding of TDP-43 to hnRNP A2 and have no effect of TDP-43 CFTR exon 9 splicing inhibition (D'Ambrogio et al., 2009). Many mutations result in substitutions to threonine and serine residues (Kabashi et al., 2008; Sreedharan et al., 2008; Van Deerlin et al., 2008)and may thus increase TDP-43 phosphorylation, which could adversely impact various TDP-43 functions. Some mutations like - Q331K, M337V, Q343R, N345K, R361S and N390D accelerate the aggregation of TDP-43 *in vitro* and enhance aggregate formation and toxicity in yeast (Johnson et al., 2009). This suggests that pathogenic mutations, in combination with N-terminal truncation, promote abnormal TDP-43 accumulation in mammalian cells (Nonaka et al., 2009). Mutations in TDP-43 have been reported to have increased expression of toxic 25kDa fragment (Kabashi et al., 2008). Similarly, when lymphoblastoid cell lines derived from *TARDBP* mutation carriers are treated with the proteasome inhibitor, MG132, a marked increase in the accumulation of detergent insoluble TDP-43 fragments (approximately 25, 28 or 35 kDa), is observed that is not seen in lymphoblastoid cells from control individuals, suggesting that mutations increase TDP-43 truncation and its aggregation potential (Kabashi et al., 2008; Rutherford et al., 2008). Biochemical analysis of TDP-43 from spinal cord extracts of autopsied cases also reveal that a 25 kDa TDP-43 fragment, and a 45 kDa TDP-43 product, are increased in the 1% sarkosyl-soluble fraction from a patient with a Q343R mutation, compared with control and sporadic ALS patients (Yokoseki et al., 2008). Recently, however, the N267S mutation initially described in a sporadic ALS case (Corrado et al., 2009b) was identified in a patient with the behavioural variant of frontotemporal dementia without MND (Borroni et al., 2009). Additionally, an A90V mutation was identified in a FTLD-MND patient with a family history of dementia (Winton et al., 2008), a G295S mutation in exon 6 was identified in two unrelated patients with FTLD-MND (Benajiba et al., 2009), and a K263E *TARDBP* variant was identified in a subject who developed FTD but no signs of MND (Kovacs et al., 2009).

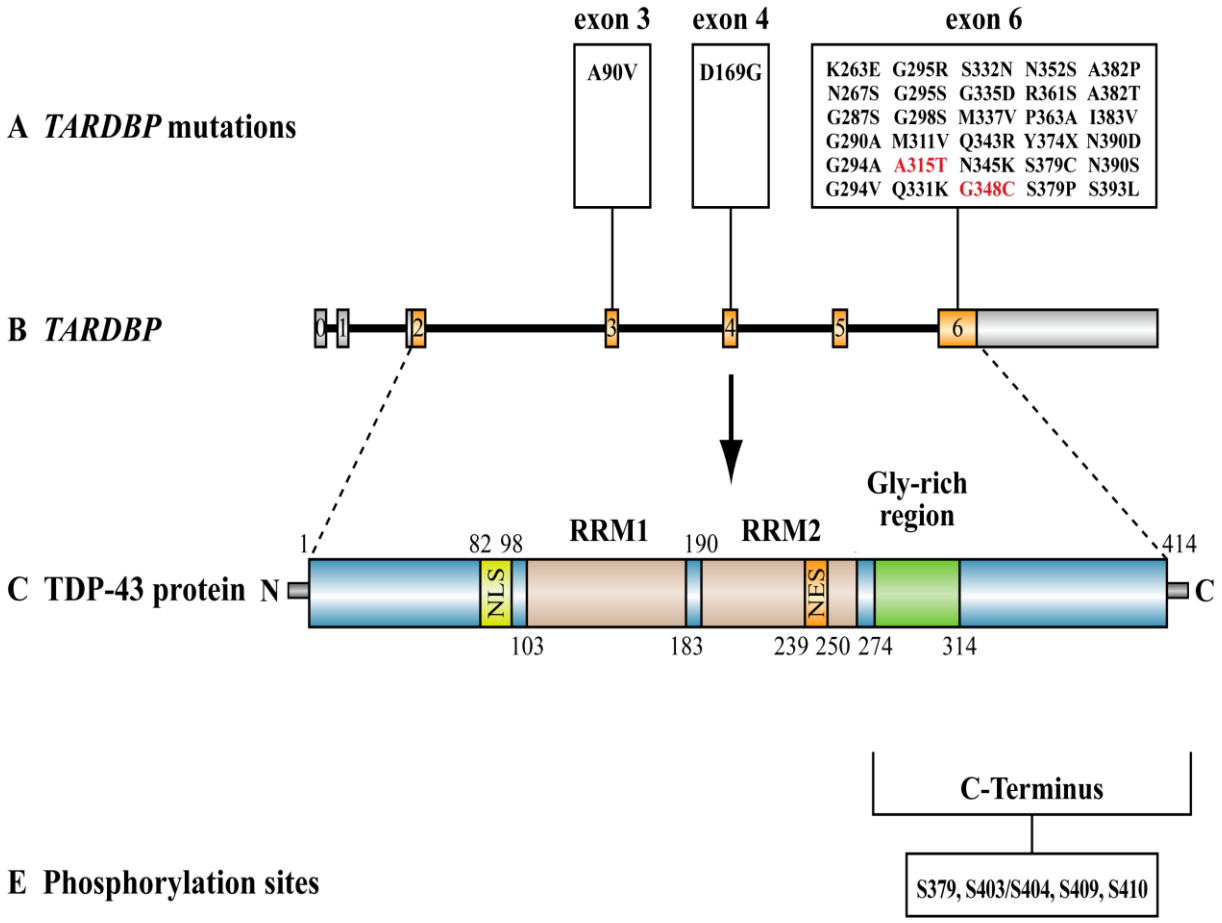

Figure 1.8 TARDBP mutations. Listed are several known TARDBP mutations in the exon 6 as well as one mutation each in exon 3and 4. Cartoons of TARDBP gene as well as TDP-43 primary protein structure along with known structural domains are shown. 2 mutations G348C and A315T are shown in red. Several groups have reported many phosphorylation sites of TDP-43 in its C-terminus. Modified from Gendron et al., 2010

1.3.5. Animal Models with TDP-43 abnormalities

The 43-kDa TAR DNA-binding protein (TDP-43), localized to the nucleus, was originally identified as a component of ubiquitinated inclusions in FTLD-U and ALS (Neumann et al., 2006; Cairns et al., 2007; Hasegawa et al., 2008). TDP-43 immunoreactive inclusions were observed in the cytoplasm and nucleus of both neurons and glial cells (Cairns et al., 2007; Mackenzie et al., 2007). The brains and spinal cords of patients with TDP-43 proteinopathy present a biochemical signature that is characterized by abnormal hyper-phosphorylation and ubiquitination of TDP-43 and the production of ~25 kDa C-terminal fragments that are missing their nuclear targeting domains (Neumann et al., 2006). TDP-43 is partly cleared from the nuclei of neurons containing cytoplasmic aggregates (Neumann et al., 2006; Van Deerlin et al., 2008) supporting the notion that pathogenesis of ALS in these cases may be driven, at least in part, by loss of normal TDP-43 function in the nucleus. Combined with a flurry of subsequent reports, TDP-43 inclusions are now recognized as a common characteristic of most ALS patients (Maekawa et al., 2009; Sumi et al., 2009).

The involvement of TDP-43 with ALS cases led to the discovery of TDP-43 mutations found in ALS patients. Dominant mutations in *TARDBP*, which codes for TDP-43, were reported by several groups as a primary cause of ALS (Gitcho et al., 2008; Kabashi et al., 2008; Sreedharan et al., 2008; Van Deerlin et al., 2008; Corrado et al., 2009b; Daoud et al., 2009). Mice homozygous knockout for TDP-43 are not viable. The TDP-43 deficient embryos die at 7.5 days of embryonic development thereby demonstrating the essential function of TDP-43 protein in development (Kraemer et al., 2010; Sephton et al., 2010; Wu et al., 2010). Mice heterozygous for TDP-43 disruption exhibit subtle muscle weakness with no evidence of motor neuron pathology. Since the discovery of TDP-43 mutations in ALS, there has been a flurry of reports of transgenic animal models of ALS (**Table 1.4**). Transgenic mice expressing a mutant form of human TDP-43 (A315T mutation) under the control of prion gene promoter develop a progressive and fatal neurodegenerative disease (Wegorzewska et al., 2009). These mice develop gait abnormalities at 3 months of age and an average survival of 153 days. Despite pan-neuronal transgene expression, pathologic

aggregates of ubiquitinated proteins accumulated only in specific neuronal populations, including layer 5 pyramidal neurons in frontal cortex, as well as spinal motor neurons. Surprisingly, these TDP-43^{A315T} mice did not exhibit cytoplasmic TDP-43 aggregates, a feature that led to the discovery of TDP-43 as a hallmark of ALS and FTLD-U. One possible reason for the lack of cytoplasmic ubiquitinated TDP-43 inclusions could be the premature cell death resulting from excessive and non-physiological expression levels of TDP-43 transgene under the strong prion gene promoter. The authors mentioned levels of TDP-43^{A315T} in excess of 3 to 5 folds the level of endogenous mouse TDP-43 in spinal cord extracts but these are likely underestimates of levels occurring within motor neurons because transgene expression was not ubiquitously expressed like the endogenous TDP-43 gene. Thus, it is unclear to what extent the disease in these mice is the result of excessive levels of TDP-43 species. Indeed, overexpression of wild-type human TDP-43 in mice caused a dose-dependent degeneration of cortical and spinal motor neurons with ensuing development of spastic quadriplegia (Wils et al., 2010). Neurons in the affected spinal cord and brain regions showed accumulation of TDP-43 nuclear and cytoplasmic aggregates that were both ubiquitinated and phosphorylated as observed in ALS/FTLD patients. However, the cytoplasmic accumulations did not contain TDP-43 like in human ALS situation. The characteristic ~25-kDa C-terminal fragments (CTFs) were recovered from nuclear fractions and correlated with disease development and progression in wild-type TDP-43 mice. Again, there is a concern with these mouse models about the excessive and neuronal-specific expression of human TDP-43 cDNA under the control of neuronal murine Thy-1 (mThy-1) promoter. Excessive levels of TDP-43 transgene expression may mask progressive and age-related pathways of higher relevance to ALS disease process. Moreover, this approach did not consider a possible role for TDP-43 in non-neuronal cell types and their contribution in disease pathology. Overexpression of mutant, but not normal, TDP-43 in a rat model caused widespread neurodegeneration that predominantly affected the motor system (Zhou et al., 2010). TDP-43 mutation (M337V) reproduced ALS phenotypes in transgenic rats, as seen by progressive degeneration of motor neurons and denervation atrophy of skeletal muscles. This rat model also recapitulated features of TDP-43 proteinopathies including the formation of TDP-43 inclusions, cytoplasmic localization

of phosphorylated TDP-43, and fragmentation of TDP-43 protein. Similar studies have been reported in many other transgenic models expressing high levels of mutant or wild-type TDP-43 (Xu et al., 2010; Igaz et al., 2011; Xu et al., 2011).

Non-rodent models have also been used to quickly and effectively model TDP-43 associated pathology. Transgenic *Drosophila* expressing human TDP-43 in various neuronal sub-populations have been used to investigate the role of wild-type TDP-43 in ALS pathogenesis (Li et al., 2010). Expression in the fly eyes of the full-length human TDP-43, but not a mutant lacking its amino-terminal domain, led to progressive loss of ommatidia with remarkable signs of neurodegeneration. Expressing TDP-43 in mushroom bodies resulted in dramatic axon losses and neuronal death. Furthermore, hTDP-43 expression in motor neurons led to axon swelling, reduction in axon branches and bouton numbers, and motor neuron loss together with functional deficits. Zebrafish (*Danio rerio*) has been used as another model to investigate the pathogenic nature of TDP-43 mutants (A315T, G348C and A382T) (Kabashi et al., 2010). Overexpression of mutant TDP-43 caused a motor phenotype in zebrafish embryos, consisting of shorter motor neuronal axons, premature and excessive branching as well as swimming deficits. Interestingly, knock-down of zebrafish TDP-43 led to a similar phenotype, which was rescued by co-expressing wild-type but not mutant human TDP-43. Together these approaches showed that TDP-43 mutations cause motor neuron defects and toxicity. Nonetheless, more animal studies are needed to provide further insights into mechanisms of disease caused by TDP-43 abnormalities. It is noteworthy that wobbler mice exhibit many of the features of TDP-43 proteinopathies including cytoplasmic localization and ubiquitinated TDP-43 positive inclusions (Dennis and Citron, 2009). Transgenic mice expressing a mutant *VAPB* gene ($VAPB^{P56S}$) linked to a subset of familial ALS developed cytoplasmic TDP-43 accumulations within spinal cord motor neurons at 18 months of age (Tudor et al., 2010). More recently, transgenic *Caenorhabditis elegans* with the neuronal expression of human TDP-43 exhibit an uncoordinated phenotype and have abnormal motor neuron synapses (Ash et al., 2010) and the toxicity is modulated by IGF-1 signaling (Zhang et al., 2011).

Table 1.4 Animal Models with TDP-43 abnormalities

Animal Models	Pathological Changes	References
Mice overexpressing A315T mutant of TDP-43	Gait abnormalities at 3 months of age and an average survival of 153 days.	(Wegorzewska et al., 2009)
Mice overexpressing wild-type TDP-43	Lack of Cytoplasmic TDP-43 aggregates Dose-dependent degeneration of cortical and spinal motor neurons and subsequent development of spastic quadriplegia	(Wils et al., 2010)
Mice overexpressing wild-type as well as A315T and M337V mutants of TDP-43	Develop Paralysis and death as early as 12 days	(Stallings et al., 2009)
Drosophila overexpressing wild-type TDP-43	Loss of ommatidia with signs of neurodegeneration	(Li et al., 2010)
Zebrafish overexpressing wild-type as well as A315T, G348C and A382T mutants of TDP-43	Premature and excessive motor axonal branching.	(Kabashi et al., 2010)
C. elegans overexpressing human TDP-43	Uncoordinated phenotype and have abnormal motor neuron synapses	(Ash et al., 2010)
Rat overexpressing TDP-43	Neurodegeneration, phosphorylated TDP-43 aggregates	(Zhou et al., 2010)

1.3.6. Prion-like properties of TDP-43: Interactions with other ALS associated genes

Prion diseases or transmissible spongiform encephalopathies are a class of neurodegenerative diseases that, as their name suggests, can be transmitted from individual to individual through ingestion or internalization of contaminated material on the native endogenous prion protein (Aguzzi, 2009). Prions replicate by recruiting PrP^{C} in the ordered PrP^{Sc}-containing aggregates and by inducing a pathological conformation. Although such modifications were thought to be unique for prion diseases, many proteins involved in neurodegenerative diseases have been reported to possess such "prion-like" properties. For example, Aβ aggregation propensity is increased by the presence of preformed Aβ aggregates or "seeds". Consistent with "prion-like" properties, intracerebral injection of brain extracts from autopsy material of human Alzheimer disease patients containing ordered aggregates of human Aβ into transgenic mice expressing human amyloid precursor protein (APP) accelerated the aggregation of human Aβ (Kane et al., 2000; Meyer-Luehmann et al., 2006). Similarly, tau, another protein involved in Alzheimer's disease, and α-synuclein, a protein involved in Parkinson's disease, have been reported to exhibit similar "prion-like" properties.

In ALS, mutant SOD1 is known to form toxic aggregates and has been recently reported to exhibit "prion-like" properties in cell-culture models (Grad et al., 2011). TDP-43 and FUS, RNA-binding proteins, are reported to aggregate in ALS/FTLD-U and mutations in the genes encoding these proteins are associated with both sporadic and familial ALS and rarely in FTLD-U (Borroni et al., 2010). In addition to sharing a role in ALS/FTLD-U, both TDP-43 and FUS proteins have similar secondary domains indicating possible convergent cellular functions[110]. Interestingly, using a bioinformatics approach, researchers have discovered a novel "prion-like" domain in TDP-43 and FUS (Fuentealba et al., 2010; Polymenidou and Cleveland, 2011; Udan and Baloh, 2011). This domain is enriched in uncharged polar amino acids (such as asparagine, glutamine and tyrosine) and glycine (Fuentealba et al., 2010). TDP-43 prion-like domain is at the C-terminal end (residues 277–414), whereas FUS prion-like domain is reported to be located in the N-terminal region of the protein - residues 1–239, with an additional region in the first RGG domain: residues

391–405 (Cushman et al., 2010). TDP-43 and TDP-43-derived peptides form aggregates in vitro (Johnson et al., 2008; Johnson et al., 2009; Cushman et al., 2010; Furukawa et al., 2011; Guo et al., 2011) and ALS-causing mutations enhance this behavior (Johnson et al., 2009; Guo et al., 2011). The C-terminal region of TDP-43 is apparently indispensable for aggregation (Johnson et al., 2008; Johnson et al., 2009; Furukawa et al., 2011), and truncation mutants consisting solely of TDP-43 C-terminal fragments show significantly increased aggregation propensities in vitro and in cells (Liu-Yesucevitz et al., 2010; Furukawa et al., 2011; Guo et al., 2011). Recent data confirm that aggregation of TDP-43 is driven by its prion-like C-terminal region and that ALS-linked mutations are likely to promote this process(Guo et al., 2011) . Compared to TDP-43 and SOD1, FUS demonstrates the highest aggregation propensity, but this property is not affected by ALS-causing mutations localized in its NLS (Dormann et al., 2010; Sun et al., 2011). Rather, these mutations clearly enhance the cytoplasmic accumulation/retention of FUS/TLS (Dormann et al., 2010; Ito et al., 2011). Even though SOD1, TDP-43, and FUS readily aggregate in vitro, the intracellular array of protein-folding chaperones must act to inhibit this. Thus, the unresolved questions in ALS are what factor(s) triggers the initiation of aggregation in disease and the selective vulnerability of the motor neurons? Only further research in this area can attempt to answer these questions.

Recently it has been reported that wild-type *FUS* could rescue the *TARDBP* knockdown phenotype, but not vice versa, suggesting that *TARDBP* is upstream of *FUS* in this pathway responsible for motor neuron disorder indicating that *TARDBP* acts upstream of *FUS* in a pathogenic pathway that is distinct from that of *SOD1* (Kabashi et al., 2011).

The discovery of TDP-43 in the ubiquitinated inclusions of FTLD-U and ALS, along with subsequent work characterizing both the normal functions of TDP-43 and the potential role of this protein in disease pathogenesis, has been an important chapter in a century-long effort to understand the etiologies of FTLD-U and MND. The identification of TDP-43 as a disease-associated protein now puts a ‘molecular face’ on the inclusions found in ALS, FTLD-U; overlap cases, and related disorders. Furthermore, the neuropathological and genetic findings for TDP-43 open up exciting new opportunities to improve the diagnosis

and treatment of these disorders. The intense interest in TDP-43 and reports of multiple animal models of TDP-43 proteinopathies provides optimism that proof of concept drug intervention studies in animal models could well be studied in a shorter time frame for TDP-43 proteinopathies as compared to taupathies.

1.4. NF-κB in neurodegeneration

Nuclear factor kappa B (NF-κB) family of transcription factors consisting of several proteins including p52, p50, RelB, c-Rel, RelA(p65) is responsible for the regulation of numerous genes involved in the inflammation, immune reactions, cell proliferation, apoptosis or central nervous system (CNS) functioning. NF-κB, thus, remains a central and crucial mediator of inducing various genes in response to varying stress stimuli. In most cells, homo and heterodimers are formed when the members of NF-κB family bind rendering them active resulting in their subsequent nuclear translocation. The hallmark feature of NF-κB family is a homology of N-terminal domain called Rel-homology domain (RHD) of approximately 300 amino acids which is identical in 35–61% in all family proteins (Baldwin, 1996; O'Neill and Kaltschmidt, 1997). The RHD is essential for DNA binding, dimerization and nuclear localization (Janssen-Heininger et al., 2000). Various dimeric complexes like p65-p50 are bound to inhibitor proteins IκB that keeps them in an inactive state in the cytoplasm (**Figure 1.9**). Phosphorylation of IκB results in its rapid proteasome-mediated degradation which in turn dissociates IκB from the dimer, making them active. Apart from inhibiting nuclear translocation of p65-p50 dimers, IκB also blocks NF-κB DNA-binding activity. Autoregulation is a very important aspect as transcription factors belonging to this family affect their own gene expression (Grilli and Memo, 1999). The inactive form of NF-κB is localized in the cytoplasm associated with the inhibitory subunit, IκB. IκB family consists of IκB-α IκB-β, Bcl3, IκB-R, p100 (IκB-δ), p105 (IκB-γ), and IκB-ε. Multiple copies of 30–33 amino acid sequences, called ankyrin repeats take part in the interaction of IκB with NF-κB complexes (Janssen-Heininger et al., 2000). The activation of NF-κB is preceded by the phosphorylation of IκB

by IκB kinase (IKK) complex which results in polyubiquitination and subsequent degradation of IκB with the involvement of the proteasome. IKK complex is composed of three proteins: two catalytic subunits IKK-α, IKK-β and the regulatory subunit IKK-γ. IKKs have a critical role in phosphorylation of two conserved serine residues in N-terminal domain of IκB proteins. The phosphorylated IκB is then ubiquitinated and finally degraded by the proteasome (Perkins, 2000). The released NF-κB in the form of an active heterodimer (p65-p50) is translocated to the nucleus, and in the presence of other transcription factors binds to the specific DNA fragments, called κB binding regions, and then activates the expression of the target genes. The ever growing list of factors activating NF-κB comprises neurotransmitters like glutamate, cytokines (e.g. tumor necrosis factor a (TNF-α), interleukin-1b (IL-1β), glycated tau, beta amyloid, phorbol esters, UV light, oxidized lipids, stress (e.g. oxidative, physiological, physical), growth factors, drugs and chemicals, viral and bacterial infections (Grilli and Memo, 1999; Pahl, 1999; Shi et al., 1999; Perkins, 2000).

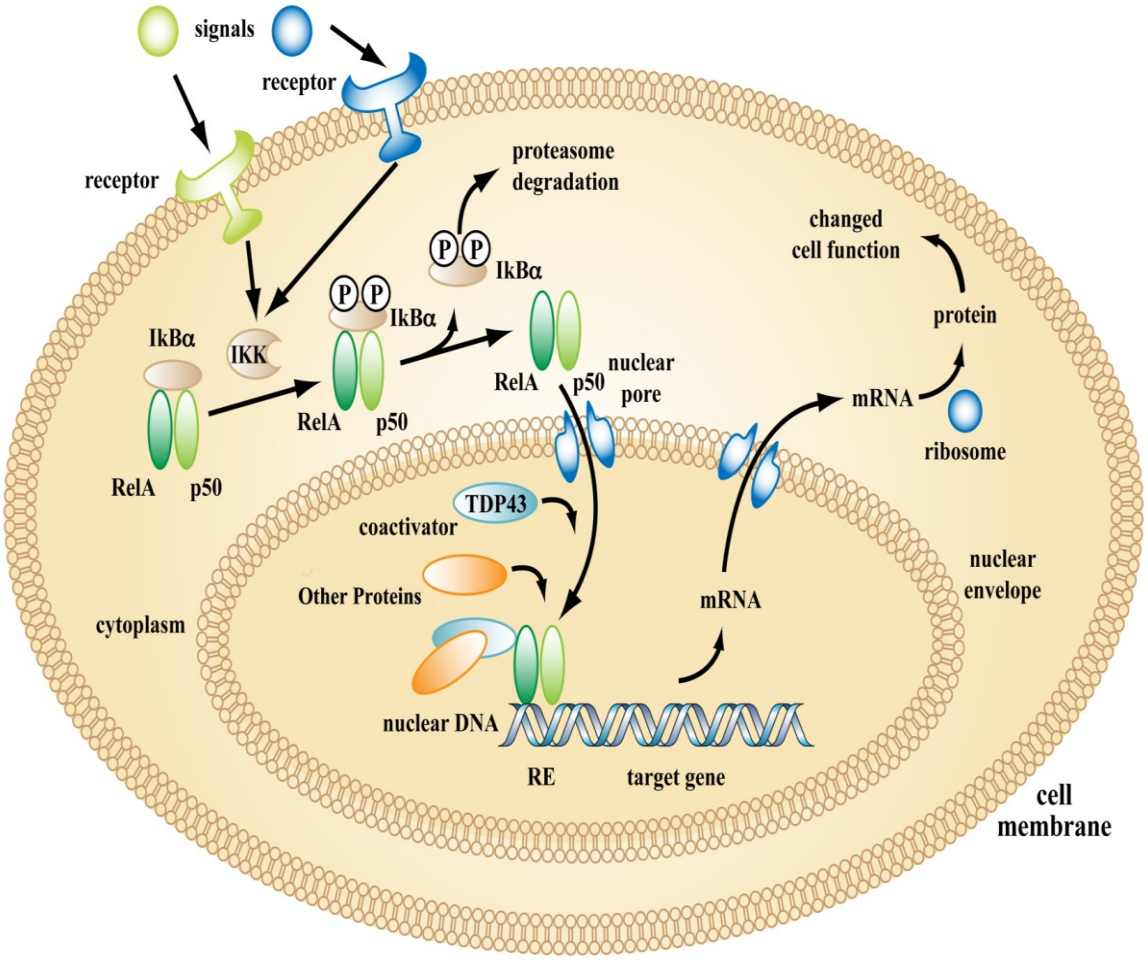

Figure 1.9 NF-κB signaling pathway. NF-κB family of transcription factors consist of two major factors – RelA (p65) and p50, which forms heterodimer. In the cytoplasm, NF-κB activity is inhibited by IκB which when phosphorylated by IKK (IκB kinase) degrades, thereby, releasing p65-p50 complex. Once activated and phosphorylayed p65-p50 complex is translocated into nucleus where it binds to κB binding sites and regulate transcription. NF-κB p65 requires co-activators like p300 and TDP-43 for its complete and proper activity. Modified from creative common license, Wikimedia.

1.4.1. The role of NF-κB in normal functioning of CNS

NF-κB signaling is important in embryogenesis and CNS development. There is a direct correlation between the activation of the CNS and NF-κB. Furthermore, NF-κB is known to protect hippocampal and cortical neurons from antioxidant stress (Grilli and Memo, 1999). Apart from the role of NF-κB activation in pathological conditions, non-pathological endogenous signals, such as neurotransmitters, can activate this factor in the CNS (Kaltschmidt et al., 1995). Non-toxic concentrations of glutamate can activate NF-κB in cerebellar granule neurons in vitro and this effect involved N-methyl-D-aspartate (NMDA) receptor activation (Guerrini et al., 1995; Kaltschmidt et al., 1995). NF-κB significantly participates in normal brain functioning (Kaltschmidt et al., 1994) including activation of glutamate transporter-1 in astrocytes (Ghosh et al., 2011). It has been speculated that changes during cerebellar development could be controlled by glutamate-induced gene expression involving NF-κB (Kaltschmidt et al., 1995). Glutamate induced NF-κB activation is also important during mouse cerebellum development but not in adult mice (Guerrini et al., 1997). As stimulation with glutamate, kainate, or potassium chloride resulted in a redistribution of NF-κB from neurites to the nucleus, NF-κB is likely to influence a great number of genes important for CNS action such as those encoding neuropeptides (dynorphin, proenkephalin), amyloid precursor protein (APP), p53, iNOS, MnSOD, COX-2, MHC class I, cytokines and chemokines (TNF-α, IL-6, IL-8, GM-CSF, CSF) (Grilli and Memo, 1999). NF-κB is regarded as signal transducer, which transmits transient glutamatergic signals from distant sites to the nucleus (Wellmann et al., 2001). Since NF-κB inducible activity is present not only in neuronal bodies but also in synapses and postsynaptic densities, it has been reported that NF-κB may be responsible for carrying synaptic information to the nucleus (Grilli and Memo, 1999). Depolarization, neurotransmitters (e.g. glutamate), opioid agonists, nerve growth factor (NGF), glycated tau, β-amyloid are all classified as factors triggering neuronal activation of NF-κB and translating it into CNS-specific signals.

1.4.2. Role of NF-κB in neurodegeneration

NF-κB takes part in initiation and acceleration of various neurodegenerative diseases such as Parkinson's disease (PD), Huntington's disease (HD) or Alzheimer's disease (AD). Many experimental as well as clinical studies have documented an increased activity of NF-κB in pathological conditions of the CNS. It is known that amyloid beta peptide (Aβ) neurotoxicity is linked with the pathogenesis of neurodegeneration in AD. Interestingly, NF-kB activation by low doses of Aβ and TNF-α leads to neuroprotection in primary neurons (Kaltschmidt et al., 1999). Furthermore, the overexpressing transdominant negative $I\kappa B^{SR}$ blocked NF-κB activation and potentiated Aβ-mediated neuronal apoptosis. Also activation of NF-κB by TNF-α has been reported to play a protective role on hippocampal neurons against Aβ toxicity. This effect was due to suppression of ROS and Ca^{2+} accumulation. In contrast, proinflammatory pathway in AD is connected with an induction of NF-κB dependent macrophage-colony stimulating factor (M-CSF) (Du Yan et al., 1997). In comparison with control postmortem cases, NF-κB immunoreactivity was upregulated in hippocampal and cerebral cortex areas in AD cases (Terai et al., 1996a). NF-κB is also activated in focal or global cerebral ischemia (Clemens, 2000); the activation is attributed to reactive oxygen species (ROS). As expected, acute inhibition of NF-κB activation using a recombinant adenovirus, expressing a dominant negative form of IκB, in the rat cortex reduced brain injury in a rat model of middle cerebral artery occlusion (MCAO) (Xu et al., 2002). Consequently, the infarct sizes as well as neurological deficits were reduced. In human postmortem brains, the NF-κB immunoreactivity was enhanced in glial cells of infarcted areas but not in those unaffected by infarction (Terai et al., 1996b). It has also been reported that delayed treatment (up to 6 hours after MCAO) with the IκB proteasomal inhibitor MLN519 was associated with the reduction of infarction and neurologic deficit caused by focal ischemic brain injury in rats and that this effect was due to the decreased activation of NF-κB, reduced blood proteasome level and neutrophil infiltration. Similarly, in a rat model of transient focal cerebral ischemia, another IκB proteasomal inhibitor, PS519, reduced infarction and improved neurological function and EEG activity (Phillips et al., 2000).

While these studies have emphasized the involvement of NF-κB deprivation in apoptosis, some studies have observed overexpression of NF-κB both in experimental model of epilepsy and in excitotoxicity (Lerner-Natoli et al., 2000). Also kainate-induced seizures resulted in a rapid NF-κB induction in adult rat limbic areas but not in juvenile rats (Rong and Baudry, 1996). These experimental data are consistent with the reports demonstrating significant and persistent overexpression of NF-κB in hippocampi surgically removed from patients with hippocampal sclerosis and medial temporal lobe epilepsy(Crespel et al., 2002). We still don't know, however, that this effect is due to deleterious or neuroprotective properties of NF-κB. In multiple sclerosis, (Gveric et al., 1998) NF-κB activation in macrophages may amplify the inflammatory reaction through upregulation of cytokines and adhesion molecules. In this regard kainate-induced neurotoxicity has been shown to upregulate NF-κB (Won et al., 1999) and that this effect was NMDA-dependent. In Parkinson's cases, NF -κB immunoreactivity was found to be 70-fold higher in the nuclei of dopaminergic neurons in the brains of PD patients than in control subjects. Similarly, in ataxia telangiectasia aberrant regulation of NF-κB has been reported to contribute to disease pathogenesis (Jung et al., 1995; Hadian and Krappmann, 2011). In an experimental model of HD, mice lacking the p50 subunit of NF-κB occurred to be more prone to damages to striatal neurons. The administration of mitochondrial toxin 3-nitropropionic acid resulted in intensified apoptosis indicated by DNA fragmentation and increased activation of caspases (Yu et al., 2000; Marcora and Kennedy, 2010). Finally, NF-κB has also been found to be upregulated in motor neurons and non-neuronal cells in amyotrophic lateral sclerosis patients (Jiang et al., 2005)

1.4.3. Therapeutic potential of NF-κB inhibitors

Many pathological conditions including inflammatory diseases, neurodegenerative diseases and cancers are associated with the aberrant NF-κB activity and inhibition of NF-κB signaling provides a great therapeutic strategy.

The molecular cascade of signaling events (**shown in Figure 1.9**) provides several steps for specific inhibition of NF-κB activity. Inhibition of NF-κB activation can occur by these mechanisms:

1.4.3.1. Blocking stimulatory signals which can activate NF-κB (e.g., binding of ligand to its receptor). One of the most common cytokine signaling pathways of NF-κB is the TNF-α pathway. Inhibiting the pathway by anti-TNF antibodies or agents that block the TNFR can be beneficial for diseases such as inflammatory bowel disease, arthritis and Crohn's disease (Song et al., 2002). Inhibiting kinases that can lead to activation of the IKK complex like NIK and MEKK1 are also effective therapeutic strategy. Eg. Geldanamycin (Chen et al., 2002), TNAP (Hu et al., 2004) and Rhein (Martin et al., 2003)

1.4.3.2. Inhibiting cytoplasmic signaling of NF-κB like inhibition of the IKK complex, or degradation of IκB. IKK has been a prime target for the development of NF-κB signaling inhibitors, in part due to its central role in transmitting upstream signals into the NF-κB activation pathways and in part due to other successes in developing kinase inhibitors for therapeutic applications. Compounds with allosteric effects on IKK structure like synthetic or natural ATP analogs as well as dominant-negative forms of IKK are capable of blocking activation of NF-κB (DiDonato et al., 1997; Mercurio et al., 1997; Regnier et al., 1997; Woronicz et al., 1997). Cell-permeable 10 amino-acid peptide corresponding to the NEMO-binding domain of IKKβ can block both the binding of NEMO to IKK and induction of NF-κB canonical pathway by TNF-α (May et al., 2000).This peptide has shown efficacy in mouse models of inflammation by both topical and systemic administration (May et al., 2000; di Meglio et al., 2005). Examples include Withaferin A (Grover et al., 2010), Rosmarinic acid (Moon et al., 2010), and Guggulsterone (Shishodia and Aggarwal, 2004)

1.4.3.3. Blockers of IκB ubiquitination. Inhibitors for ubiquitin ligase complex or the 26S proteasome are effective in inhibiting the ubiquitination of IκB, thereby targeting NF-κB signaling (Scheidereit, 2006). Among blockers of IκB ubiquitination are: Capsaicin

(8-methyl-N-vanillyl-6-nonenamide) (Mori et al., 2006), Glabridin (Park et al., 2010), and Tipifarnib (Lancet et al., 2011).

1.4.3.4. Blocking NF-κB nuclear signaling that is inhibiting its translocation to the nucleus, its binding to DNA, a nuclear modification of NF-κB that affects its activity or specificity. One approach has used cell-permeable peptides that contain the nuclear localizing sequence of p50. These peptides are thought to inhibit nuclear translocation of p50-containing dimers by saturating the nuclear import machinery responsible for the uptake of NF-κB dimers containing p50 (Lin et al., 1995; Torgerson et al., 1998; Letoha et al., 2005). Several sesquiterpene lactones (SLs) have anti-inflammatory activity and act as inhibitors of NF-κB DNA binding (Zhang et al., 2005). A molecular method to block specific NF-κB DNA binding is through the use of decoy oligonucleotides that have κB sites which competes out NF-κB dimer binding to specific genomic promoters (Morishita et al., 1997; Khaled et al., 1998; Karin et al., 2004). Eg. Dioxin (Singh et al., 2007), Leflunomide (Imose et al., 2004)

It has been shown (Bondeson et al., 1999) that using adenoviral technique IκB super repressor ($IκB^{SR}$) can be delivered and it reduces tissue destruction as well as the inflammatory mechanisms in rheumatoid arthritis. Use of a recombinant adenovirus, expressing a dominant negative form of IκB, protects the brain from ischemic injury (Xu et al., 2002). Switching the activity of NF-κB from anti-apoptotic to pro-apoptotic could be another potential strategy. Many currently used anti-inflammatory drugs like NSAIDs have a potential role in therapy of chronic inflammatory diseases like EAE (van Loo et al., 2010). Molecular studies revealed that acetylsalicylic acid and sodium salicylate (NSAIDs) have NF-κB -dependent neuroprotective abilities against glutamate-induced neurotoxicity in rat primary neuronal cultures and hippocampal slices (Grilli et al., 1996). Common NSAID ibuprofen was found to act not only as a cyclooxygenase (COX) inhibitor but also through the stabilization of IκB-α which resulted in the blockade of NF-κB translocation to the nucleus (Stuhlmeier et al., 1999).

Various natural compounds from plant extracts act as potent NF-κB inhibitor like Withaferin A, green tea extract and curcumin. Withaferin A, extract of *Withamnia somnifera*, is a potent NF-κB inhibitor which blocks the binding of NEMO/IKK complex (Grover et al., 2010). Traditionally, Withaferin A is used for the treatment of rheumatoid arthritis (RA). Green tea extracts (e.g. *Camellia sinensis*) was demonstrated to provide neuroprotection against 6-hydroxydopamine (6-OHDA)-induced neuronal damage (Guo et al., 2007). As 6-OHDA is known to induce NF-κB nuclear translocation green tea's polyphenols appear to inhibit NF-κB activity mainly due to potent antioxidant and iron chelating actions (Levites et al., 2002). Another NF-κB inhibitor, curcumin (main ingredient of *Curcuma longa*), blocked H_2O_2, TNF-α and phorbol ester-mediated activation of NF-κB (Singh and Aggarwal, 1995).

Under biological and pathological conditions, the promotion or inhibition of cell death pathway depends on the timing and location of NF-κB activation. As a central controlling gene responsible for cell survival or death in the nerve system, NF-κB is definitely a promising therapeutic target for nerve injury.

1.5 Objectives of the thesis

The work contained in this thesis has focused on determining the role of wild-type or mutant TDP-43 in the pathogenesis of ALS.

In chapter 2, we reported the generation and characterization of TDP-43 transgenic mice model. We generated transgenic mice using genomic fragments encoding full-length wild-type or FALS-linked mutants TDP-43^{G348C} and TDP-43^{A315T} human TDP-43. These transgenic mice recapitulate key features of ALS and FTLD-U.

In chapter 3, we used TDP-43 transgenic mice to determine genetic defects before onset of disease by using axonal crush model. Sciatic nerve crush in 3 months old mice revealed that TDP-43 transgenic mice were noticeably paralyzed at the injured limb, have altered TDP-43 redistribution and the distal axons regenerated slowly as compared to non-transgenic mice

In chapter 4, using lipopolysaccharide activated mouse microglial BV-2 cells, we discovered that TDP-43 acts as a co-activator of p65 subunit of NF-κB. We found that TDP-43 interacts with and colocalizes with p65 in glial and neuronal cells from TDP-43 transgenic mice and also from ALS patients. We report that TDP-43 and NF-κB p65 mRNA and protein expression is higher in spinal cords of ALS patients than healthy individuals. TDP-43 acted as a co-activator of p65, and glial cells expressing higher amounts of TDP-43 produced more proinflammatory cytokines and neurotoxic mediators after stimulation with lipopolysaccharide or reactive oxygen species. Treatment of TDP-43 mice with Withaferin A, an inhibitor of NF-κB activity, reduced denervation in the neuromuscular junction and ALS disease symptoms.

Chapter 2: Pathological hallmarks of ALS/FTLD in transgenic mice produced with genomic fragments encoding wild-type or mutant forms of human TDP-43

Article published in: Brain (2011) Sep; 134(9):2610-26

Vivek Swarup[1], Daniel Phaneuf[1], Christine Bareil[1], Janice Robertson[2], Jasna Kriz[1*] and Jean-Pierre Julien[1*]

[1]Centre de Recherche du Centre Hospitalier Universitaire de Québec, Department of Psychiatry and Neuroscience of Laval University, Québec, QC, Canada G1V 4G2

[2]Department of Laboratory Medicine and Pathobiology, Centre for Research in Neurodegenerative Diseases, University of Toronto, Tanz Neuroscience Building, Toronto, ON, Canada M5S 3H2.

2.1 Résumé

Les inclusions ubiquitinylées de la protéine TDP-43 (Transactive response DNA-binding protein 43) sont une caractéristique de la sclérose latérale amyotrophique (SLA) et de la dégénérescence lobaire fronto-temporale avec inclusions ubiquitine-positive (DLFT-U) . Nous pouvons aussi observer que des mutations dans le gène codant pour la protéine TDP-43 (TARDBP) sont associés seulement à 3% des cas de la SLA sporadique et familiale. Des études récentes sur des souris transgéniques, ont révélé un haut degré de toxicité de la protéine TDP-43 lorsqu'elle est surexprimée sous le contrôle de promoteurs de gènes neuronaux. Cette surexpression entraîne une paralysie précoce et la mort, et ce même sans la présence des inclusions positives ubiquitinylées présentes normalement dans la SLA. Pour avoir un modèle murin représentatif de la SLA chez l'humain, nous avons généré des souris transgéniques qui présentent une expression modérée et ubiquitaire de la protéine TDP-43 en utilisant des fragments génomiques codant pour la TDP-43 humain, de type sauvage ou mutant associé aux cas familiaux de SLA (FALS), soit les mutations TDP-43^{G348C} et TDP-43^{A315T} . Ces nouvelles souris transgéniques développent de nombreux changements liés au processus pathologique et biochimique de la SLA chez l'homme. Notamment, la présence d'inclusions de TDP-43 ubiquitinylées, des anomalies au niveau des filaments intermédiaires, une axonopathie et de la neuroinflammation. Les trois modèles de souris transgéniques (TDP-43^{WT}, TDP-43^{G348C} et TDP-43^{A315T}) que nous avons étudiées, présentaient des troubles d'apprentissage et de mémorisation au cours de leur vieillissement ainsi qu'un dysfonctionnement au niveau moteur. L'imagerie en temps réel de souris transgéniques TDP-43 biophotoniques, portant le gène rapporteur GFAP-Luc, a révélé que les déficits comportementaux ont été précédés par une astrogliose. Ces résultats concordent avec le fait que les astrocytes auraient un rôle dans la pathogenèse de la SLA. Ces nouvelles souris transgéniques exprimant la protéine TDP-43, reproduisent plusieurs caractéristiques de la SLA humaine et de la DLFT et ils devraient fournir de précieux modèles animaux pour tester des approches thérapeutiques.

2.2 Abstract

Transactive response DNA-binding protein 43 (TDP-43) ubiquitinated inclusions are a hallmark of amyotrophic lateral sclerosis (ALS) and of frontotemporal lobar degeneration with ubiquitin-positive inclusions (FTLD-U). Yet, mutations in *TARDBP*, the gene encoding TDP-43, are associated with only 3% of sporadic and familial ALS. Recent transgenic mouse studies revealed high degree of toxicity of TDP-43 proteins when overexpressed under the control of strong neuronal gene promoters resulting in early paralysis and death, but without the presence of ALS-like ubiquitinated TDP-43 positive inclusions. To better mimic the human ALS situation, we generated transgenic mice that exhibit moderate and ubiquitous expression of TDP-43 species using genomic fragments encoding human TDP-43 wild-type or FALS-linked mutants TDP-43^{G348C} and TDP-43^{A315T}. These novel TDP-43 transgenic mice develop many age-related pathological and biochemical changes reminiscent of human ALS including ubiquitinated TDP-43 positive inclusions, TDP-43 cleavage fragments, intermediate filament abnormalities, axonopathy and neuroinflammation. All three transgenic mouse models (TDP-43^{Wt}, TDP-43^{G348C} and TDP-43^{A315T} mice) exhibited during aging impaired learning and memory capabilities as well as motor dysfunction. Real-time imaging with the use of biophotonic TDP-43 transgenic mice carrying GFAP-luc reporter revealed that the behavioural defects were preceded by induction of astrogliosis, a finding consistent with a role for reactive astrocytes in ALS pathogenesis. These novel TDP-43 transgenic mice mimic several characteristics of human ALS/FTLD and they should provide valuable animal models for testing therapeutic approaches.

2.3 Introduction

Amyotrophic lateral sclerosis (ALS) is an adult-onset neurological disorder that is characterized by the selective loss of motor neurons leading to progressive weakness, muscle atrophy with eventual paralysis and death within 5 years of clinical onset. On the other hand frontotemporal lobar degeneration with ubiquitin inclusions (FTLD-U) is a relatively common cause of dementia among patients with onset before 65, typically manifesting with behavioural changes or language impairment due to degeneration of sub-populations of cortical neurons in the frontal, temporal and insular regions (Seeley, 2008). Interestingly, 50% of patients with ALS develop varying degrees of cognitive impairment (Lomen-Hoerth et al., 2003), and approximately 15% of FLTD-U patients also develop ALS (Hodges et al., 2004) and ALS and FTLD-U co-segregate in some families (Talbot and Ansorge, 2006). The discovery of TAR DNA-binding protein (TDP-43) being present in cytoplasmic aggregates in both ALS and FTLD-U provided the first conclusive molecular evidence that the two disorders share a common underlying mechanism (Neumann et al., 2006).

Identified first as a regulator of HIV gene expression (Ou et al., 1995), TDP-43 is a DNA/RNA-binding (Buratti et al., 2001) protein that contains a N-terminal domain, two RNA-recognition motifs and a glycine-rich C-terminal domain thought to be important for mediating protein–protein interactions (Forman et al., 2007; Lagier-Tourenne and Cleveland, 2009). Although TDP-43 has been implicated as a key factor regulating RNA splicing of human cystic fibrosis transmembrane conductance regulator (CFTR) (Buratti et al., 2001), Apolipoprotein A-II (Mercado et al., 2005), and Survival Motor Neuron (SMN) (Bose et al., 2008), the concept that TDP-43 can play a direct role in neurodegeneration was strengthened by recent reports that dominantly inherited missense mutations in TDP-43 are found in patients with familial ALS (Gitcho et al., 2008; Kabashi et al., 2008; Rutherford et al., 2008; Sreedharan et al., 2008; Van Deerlin et al., 2008; Yokoseki et al., 2008). Mutations in TDP-43 associated with ALS cluster in the C-terminal glycine-rich region, which is involved in protein-protein interactions between TDP-43 and other heterogeneous nuclear ribonuclear proteins (hnRNPs) (Lagier-Tourenne and Cleveland,

2009). The two TDP-43 mutations A315T and G348C used in this study were previously reported (Gitcho et al., 2008; Kabashi et al., 2008). In neurodegenerative diseases, TDP-43 can be found in cytoplasmic ubiquitinated inclusions, where the protein is poorly soluble, hyperphosphorylated and cleaved into small fragments, making TDP-43 aggregates a hallmark pathology of ALS and FTLD-U cases (Neumann et al., 2006). Many of transgenic mouse lines expressing TDP-43 WT or mutants reported to date exhibited early paralysis followed by death(Wegorzewska et al., 2009; Stallings et al., 2010; Wils et al., 2010). The available TDP-43 transgenic mouse models are based on high level neuronal expression of TDP-43 transgenes. Transgenic mice expressing either wild type or mutant TDP-43 (A315T and M337V) showed aggressive paralysis accompanied by increased ubiquitination (Stallings et al., 2009; Wegorzewska et al., 2009; Wils et al., 2010; Xu et al., 2010) but the lack of ubiquitinated TDP-43 inclusions raises concerns about their validity as models of human ALS disease (Wegorzewska et al., 2009). Another concern is the restricted expression of TDP-43 species with the use of Thy1.2 and Prion promoters.

To better mimic the ubiquitous and moderate levels of TDP-43 occurring in the human context, we describe here the generation of new transgenic mouse models of ALS/FTLD based on expression of genomicTDP-43 fragments resulting in moderate and ubiquitous expression of wild-type and mutant TDP-43 species (A315T and G348C).

2.4 Material and Methods

DNA Constructs and Generation of WT, A315T and G348C TDP-43 Transgenic Mice.

TARDBP (NM_007375) was amplified by PCR from a human BAC clone (clone RPCI-11, clone number: 829B14) along with the endogenous promoter (~4kb). A315T and G348C mutations in TDP-43 were inserted using site-directed mutagenesis (Supplemental Fig. 2.1). The full-length genomic *TARDBP* (TDP-43^{Wt,} TDP-43^{A315T}, and TDP-43^{G348C}) was linearized by Swa-1 restriction enzyme and an 18 kb DNA fragment microinjected in one-day mouse embryos (having a background of C3H X C57Bl/6). Founders were identified by southern blotting (Supplemental Fig. 2.1) and were bred with non-transgenic C57Bl/6 mice to establish stable transgenic lines. The transgenic mice were identified by PCR amplification of the human *TARDBP* gene using the following primer pairs as listed in Table 2.1. The mRNA was analysed in brain and spinal cord by real-time PCR and protein analyzed by by western blot using monoclonal human TDP-43 antibody (Clone E2-D3, Abnova, Walnut, CA, USA). To avoid the effects of genetic background, all experiments were performed on aged-matched littermates. The use and maintenance of the mice described in this article were performed in accordance to the Guide of Care and Use of Experimental Animals of the Canadian Council on Animal Care.

Co-immunoprecipitation and Western Blot Assays

Snap frozen spinal cords of mice were harvested with lysis buffer containing25 mM HEPES-NaOH (pH 7.9), 150 mM NaCl, 1.5 mM $MgCl_2$, 0.2 mM EDTA, 0.5% Triton-X-100, 1 mM dithiothreitol and protease inhibitor cocktail. Protein samples were estimated using Bradford method. The lysate was incubated with 50µl of Dynabeads (Protein-G beads, Invitrogen), anti-TDP-43 polyclonal (ProteinTech, Chicago, IL, USA) or anti-peripherin polyclonal antibody (AB1530, Chemicon, Billerica, MA, USA). After subsequent washing, the beads were incubated overnight at 4^{o}C with 400µg of tissue lysate. Antibody-bound complexes were eluted by boiling in Laemmli sample buffer. Supernatants were resolved by 10% SDS-PAGE and transferred on nitrocellulose membrane (Biorad, Hercules, CA, USA). The membrane was incubated with anti-ubiquitin antibody (1:1000,

Abcam, Cambridge, MA, USA). For other western blot assays, blots were incubated with primary antibodies against human monoclonal TARDBP antibody (1:1000, Abnova, clone E2-D3), peripherin polyclonal (1:1000, Chemcion - AB1530), peripherin monoclonal (1:500, Chemicon, AB1527), Clone NR4 for NF-L (1:1000, Sigma), Clone NN18 for NF-M (1:1000, Millipore) and Clone N52 for NF-H (1:1000, Millipore). Immunoreactive proteins were then visualized by chemiluminescence (Perkin and Elmer, Santa Clara, CA, USA) as described previously (Dequen et al., 2008). Actin (1:10000, Chemicon) is used as a loading control.

Immunohistochemistry/Immunofluorescence Microscopy

4% Paraformaldehyde (PFA) fixed spinal cord and brain sections of mice were sectioned and fixed on slides. For immunohistochemistry, tissues were treated with hydrogen-peroxide solution before permeabilisation. After blocking with 5% normal goat serum for 1hr at room temperature, primary antibody incubations were performed in 1% normal goat serum in PBST overnight, followed by an appropriate Alexa Fluor 488 or 594 secondary antibody (1:500, Invitrogen) for 1hr at room temperature. For immunohistochemistry, tissues were incubated in biotinylated secondary antibodies (1:500, Vector labs, Burlingame, CA, USA), incubated in avidin-biotin complex and developed using Dab Kit (Vector labs). Z-stacked sections were viewed using a 40X or 60 X oil immersion objectives on an Olympus Fluoview™ Confocal System (Olympus, Center Valley, PA, USA).

Neurofilament ELISA

Wells of microtiter plates were coated with 0.1% NaN3/TBS including the primary antibodies (NR4; 1:600, N52; 1:1000, NN18; 1:500). The coated wells were incubated with 10% normal goat serum/ 0.2% Tween 20/TBS for 30 min at 37 °C. After washing twice with TBS, an aliquot (100 μL) of the diluted samples was applied in each well, and incubated overnight at 4 °C. Further ELISA was performed using standard procedure as described elsewhere (Noto et al., 2010).

Quantitative Real-Time RT-PCR

Real-time RT-PCR was performed with a LightCycler 480 (Roche Diagnostics) sequence detection system using LightCycler SYBR Green I at the Quebec genomics Centre, Quebec. Total RNA was extracted from frozen spinal cord or brain tissues using Trizol reagent (Invitrogen). Total RNA was treated with DNase (Qiagen, Valencia, CA, USA) to get rid of genomic DNA contaminations. Total RNA was then quantified using Nanodrop and its purity verified by Bioanalyzer 2100 (Agilent Technologies, Santa Clara, CA, USA). Gene-specific primers were constructed using the GeneTools (Biotools Inc.) software v.3. Genes Atp5 and GAPDH were used as internal control genes. The primers used for the analysis of genes are given in Table 2.2. The presence of GFAP-luc transgene was assessed by PCR with HotStar Taq Master mix Kit (Quiagen, Mississauga, ON, Canada) in 15 mM $MgCl_2$ PCR buffer with the following primers: 5'GAAATGTCCGTTCGGTTGGCAGAAGC and 5'CCAAAACCGTGATGGAATGGAACAACA (Keller et al., 2009, 2010).

Table 2.1

Primers for genotyping transgenic mice

Gene Symbol	Forward Primer	Reverse Primer
TDP-43^{Wt}	CTCTTTGTGGAGAGGAC	CCCCAACTGCTCTGTAG
TDP-43^{A315T}	CTCTTTGTGGAGAGGAC	TTATTACCCGATGGGCA
TDP-43^{G348C}	CTCTTTGTGGAGAGGAC	GGATTAATGCTGAACGT
GFAP-luc	GAAATGTCCGTTCGGTTGGCAGAAGC	CCAAAACCGTGATGGAATGGAACAACA

Table 2.2 Primers for quantitative RT-PCR

Gene Symbol	Forward Primer Sequences	Reverse Primer Sequences
TNF-α	CCAGACCCTCACACTCAGATCATC	CCTTGAAGAGAACCTGGGAGTAGAC
IL-6	GTCCTTCCTACCCCAATTTCCAA	GAATGTCCACAAACTGATATGCTTAGG
IL-1β	GCCCATCCTCTGTGACTCAT	CGACAAAATACCTGTGGCCT
Nox2	TTGGAATTGCAGATGAGGAAGCGAG	CGATCCTGGGCATTGGTGAGT
IL-4	AGATCATCGGCATTTTGAACGAGG	CACTCTCTGTGGTGTTCTTCGTTG
IL-2	CAGCAGCAGCAGCAGCAGCAGC	CCTGGGGAGTTTCAGGTTCCTGTAAT
MCP-1	CCAGATGCAGTTAACGCCCCACTCACCT	TGCTGGTGATCCTCTTGTAGCTCTCCA
Per61	AGAGGAGTGGTATAAGTCGAAATATGC	CCCATCCACCTCGCACATCAG
Per58	TGGCCCTGGACATCGAGATAG	GCTCCATCTCAGGCACAGTCG
Per56	GGATCTCAGTGCCGGTTCATT	GGACTCTGTCACCACCTCCC
Human TDP-43	TTGACCCTTTTGAGATGGAACTTT	ATTTGACTTGAGACAACTTTTCAAATAAGT
Mouse TDP-43	ATTTGAGTCTCCAGGTGGGTGTGG	GTTTCACTATACCCAGCCCACTTTTCTTAGG
Atp5	GCTATGCAACCGCCCTGTACTCTG	ACGGTGCGCTTGATGTAGGGATTC
GAPDH	GGCTGCCCAGAACATCATCCCT	ATGCCTGCTTCACCACCTTCTTG

Barnes maze task.

For spatial learning test, the Barnes maze task was performed as described previously (Prut et al., 2007). The animals were subjected to four trials per session with an inter-trial interval (ITI) of 15 min. The probe trial takes 90 sec (half of the time used for the training trials) per mouse. Twelve days after the first probe trial mice are tested again in a second probe trial that takes 90 sec per mouse. Mice are not tested between the two probe trials. The time spent by the individual mice to reach the platform was recorded as the primary latency using video tracking software (ANY-maze, Wood Dale, IL, USA)

Step-Through Passive Avoidance Test

A two-compartment step-through passive avoidance apparatus (Ugo basile, Collegeville, PA, USA) was used. The apparatus is divided into bright and dark compartments by a wall with a guillotine door. The bright compartment was illuminated by a fluorescent light (8W). Mice at various ages were placed in the bright compartment and allowed to explore for 30 s, at which point the guillotine door was raised to allow the mice to enter the dark compartment. When the mice entered the dark compartment, the guillotine door was closed and an electrical foot shock (0.6 mA) was delivered for 4sec only on the 2^{nd} day. On the test day (3^{rd} day) mice were placed in the bright compartment, no shock was given, and their delay in latency to enter the dark compartment was recorded. The procedure was repeated every month to test the mice at different ages.

Neuromuscular junction staining and count

For monitoring the neuromuscular junctions, 25 mm thick muscle sections were incubated for 1 h in 0.1 M glycine in PBS for 2 h at RT and then stained with Alexa Fluor 594-conjugated α-bungarotoxin (1:2000, Molecular Probes/Invitrogen detection technologies, Carlsbad, CA, USA) diluted in 3% BSA in PBS for 3 h at RT. After washing in PBS, the muscle sections were blocked in 3% BSA, 10% goat serum and 0.5% Triton X-100 in PBS overnight at 48^0C. The next day, the sections were incubated with mouse antineurofilament antibody 160 K (1:2000, Temecula, CA, USA) and mouse anti-synaptophysin (Dako, Mississauga, ON, Canada) in the same blocking solution overnight at 48^0C. After washing

for 5 h, muscle sections were incubated with goat anti-mouse Alexa Fluor 488-conjugated secondary antibody (Probes/Invitrogen detection technologies, Carlsbad, CA, USA) diluted 1:500 in blocking buffer for 3 h at RT. Three hundred neuromuscular junctions were counted per animal sample, discriminating both innervated and denervated junctions as described above. Frequencies of innervation, partial denervation and denervation were then converted to percentages for statistical analyses (n =5, two-way ANOVA with Bonferroni post-test).

Accelerating rotarod.

Accelerating rotarod was performed on mice at 4rpm speed with 0.25rpm/sec acceleration as described elsewhere (Gros-Louis et al., 2008). Mice were subjected to three trials per session and every two weeks.

In vivo bioluminescence imaging

As previously described, (Keller et al., 2009, 2010) the images were gathered using IVIS® 200 Imaging System (CaliperLSXenogen, Alameda, CA, USA). Twenty-five minutes prior to imaging session, the mice received intraperitoneal (i.p.) injection of the luciferase substrate D-luciferine (150 mg/kg—for mice between 20 and 25 g, 150–187.5 ml of a solution of 20 mg/ml of D-luciferine dissolved in 0.9% saline was injected) (CaliperLS-Xenogen).

Statistical Analysis

For statistical analysis, the data obtained from independent experiments are presented as the mean ± SEM. A two-way analysis of variance (ANOVA) with repeated measures was used to study the effect of group (transgenic and non-transgenic mice) and time (in months or weeks) on latency to fall (accelerating rotarod test), latency to go to the dark chamber (passive avoidance test), primary errors and primary latency (Barnes maze test). Two-way ANOVA with repeated measures was also used for axonal calibre distribution and total flux of photons for *in vivo* imaging. The mixed procedure of the SAS software version 9.2 (SAS Institute Inc., Cary, NC, USA) was used with a repeated statement and covariance

structure that minimize the Akaike information criterion. The method of Kenward-Roger was used to calculate the degree of freedom. Pairwise comparisons were made using Bonferroni adjustment. One-way ANOVA was performed using GraphPad Prism Software version 5.0 (La Jolla, CA, USA) for real-time inflammation array, real-time RT-PCR and neurofilament ELISA analysis. Post-hoc comparisons were performed by Tukey's test, with the statistical significance set at $p<0.05$.

2.5 Results

2.5.1 Generation of transgenic mice carrying genomic TDP-43 fragments

We generated three transgenic mouse models using genomic DNA fragments coding for either TDP-43^{Wt}, TDP-43^{A315T} or TDP-43^{G348C} carrying mutations linked to human FALS (Kabashi et al., 2008). The transgenic mice (Wt, A315T and G348C) were generated by injection into one-cell embryos of DNA fragments, subcloned from *TARDBP* BAC using the endogenous ~4kB promoter. The A315T and G348C mutations were inserted using site directed mutagenesis (Fig. 2.1A). Founder TDP-43 transgenic mice were identified by the presence of the 1.8-kb EcoRV fragment on the Southern blot (Supplemental Fig 2.1A). RT-PCR analysis of the spinal cord lysates of TDP-43^{Wt}, TDP-43^{A315T} and TDP-43^{G348C} mice reveal bands corresponding to human TDP-43 (Supplemental Fig. 2.1B). As shown by immunoblot analysis the human TDP-43 transgenes (Wt and mutants) were expressed in all the tissues examined (Fig. 2.1B). Real-time RT-PCR showed that the mRNA expression of hTDP-43 in the spinal cord was elevated by ~3-fold in 3-months old TDP-43^{Wt}, TDP-43^{A315T} and TDP-43^{G348C} transgenic mice as compared to endogenous mouse TDP-43 (Fig. 2.1C). Whereas expression of human TDP-43 mRNA transcripts remained constant with age, the levels of endogenous mouse TDP-43 mRNA transcripts were decreased significantly in 10-months old transgenic mice (TDP-43^{Wt}, TDP-43^{A315T} and TDP-43^{G348C}) as compared to 3-months old mice (*$p<0.01$, Supplemental Fig. 2.1E). This is consistent with a TDP-43 autoregulation through TDP-43 binding and splicing-dependent RNA degradation as described as previously (Polymenidou et al., 2011). We next examined whether in our transgenic models we can detect pathological cytosolic TDP-43, characteristics of ALS. The immunohistochemical staining with anti-human TDP-43 antibodies of spinal cord sections from 10-months old transgenic mice revealed a cytoplasmic accumulation of TDP-43 in TDP-43^{G348C} mice and to a lower extent in TDP-43^{A315T} mice (Fig. 2.1D-G and Supplemental Fig. 2.3A-B). In contrast, the TDP-43 localization remained mostly nuclear in TDP-43^{Wt} and non-transgenic mice.

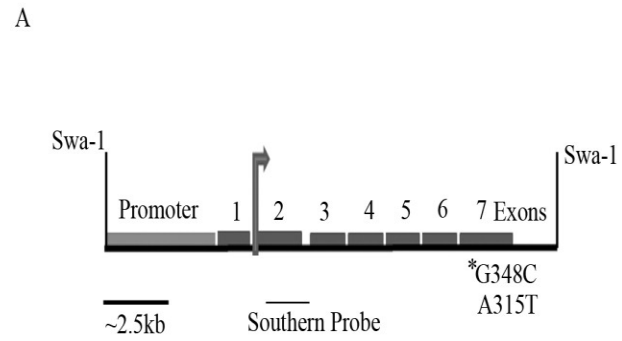
A
Swa-1
Swa-1
Promoter
1
2
3
4
5
6
7 Exons
*G348C
A315T
~2.5kb
Southern Probe

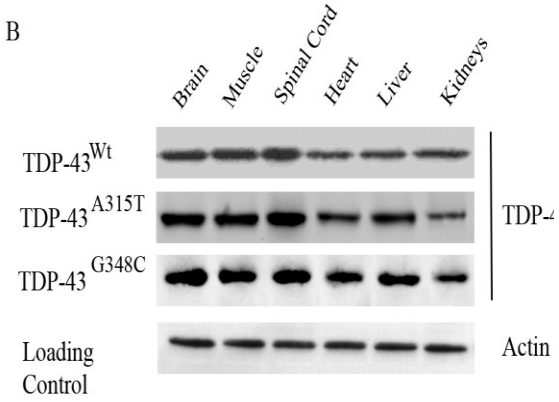
B
Brain
Muscle
Spinal Cord
Heart
Liver
Kidneys
TDP-43Wt
TDP-43A315T
TDP-43G348C
TDP-
Loading Control
Actin

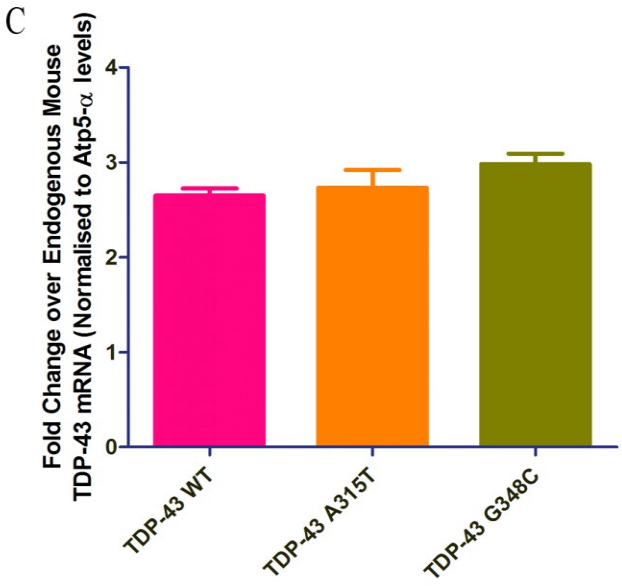
C
Fold Change over Endogenous Mouse TDP-43 mRNA (Normalised to Atp5-α levels)
4
3
2
1
0
TDP-43 WT
TDP-43 A315T
TDP-43 G348C

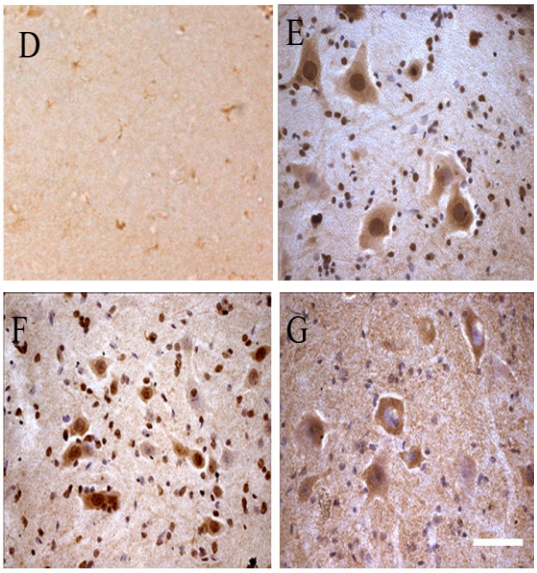
D
E
F
G

Figure 2.1. Generation and characterisation of TDP-43 transgenic mice. (**A)** Map of human TARDBP gene (Gene ID: 23435) showing upstream ~4kb promoter (un-characterized) and various exons (numbered 1-7) and introns. The orientation of transcription is shown by arrow. * showing position of 2 mutations – G348C (1176 G>T) and A315T (1077 G>A). The approximate locations of the Southern blotting probes are also indicated. (**B)** Western blots from lysates of various tissues from TDP-43^{Wt}, TDP-43^{A315T} and TDP-43^{G348C} transgenic mice at 2-months age using mouse monoclonal TDP-43 antibody that detect hTDP-43 only. Actin is shown as loading control. **(C)** Quantitative real-time PCR analysis of hTDP-43 mRNA expression in the spinal cord of TDP-43^{Wt}, TDP-43^{A315T} and TDP-43^{G348C} transgenic mice at 2-months age compared individually to their wild-type littermates and normalized to Atp-5α levels. Data shown are means ± SEM of 5 different mice from each group. **(D-G)** Immunohistochemistry shows hTDP-43 expression pattern in the spinal cord of ~8-months old TDP-43^{Wt}, TDP-43^{A315T} and TDP-43^{G348C} transgenic mice using TDP-43 monoclonal antibody. It is noteworthy that the expression of TDP-43 is mostly nuclear in TDP-43^{Wt} mice **(E)**, but TDP-43 is localized in the cytoplasm in TDP-43^{G348C} mice **(G)**, and to a lesser extent in TDP-43^{A315T} mice **(F)**.TDP-43 monoclonal antibody does not recognize endogenous mouse TDP-43 in non-transgenic control mice **(D)**. Scale bar = 20μm.

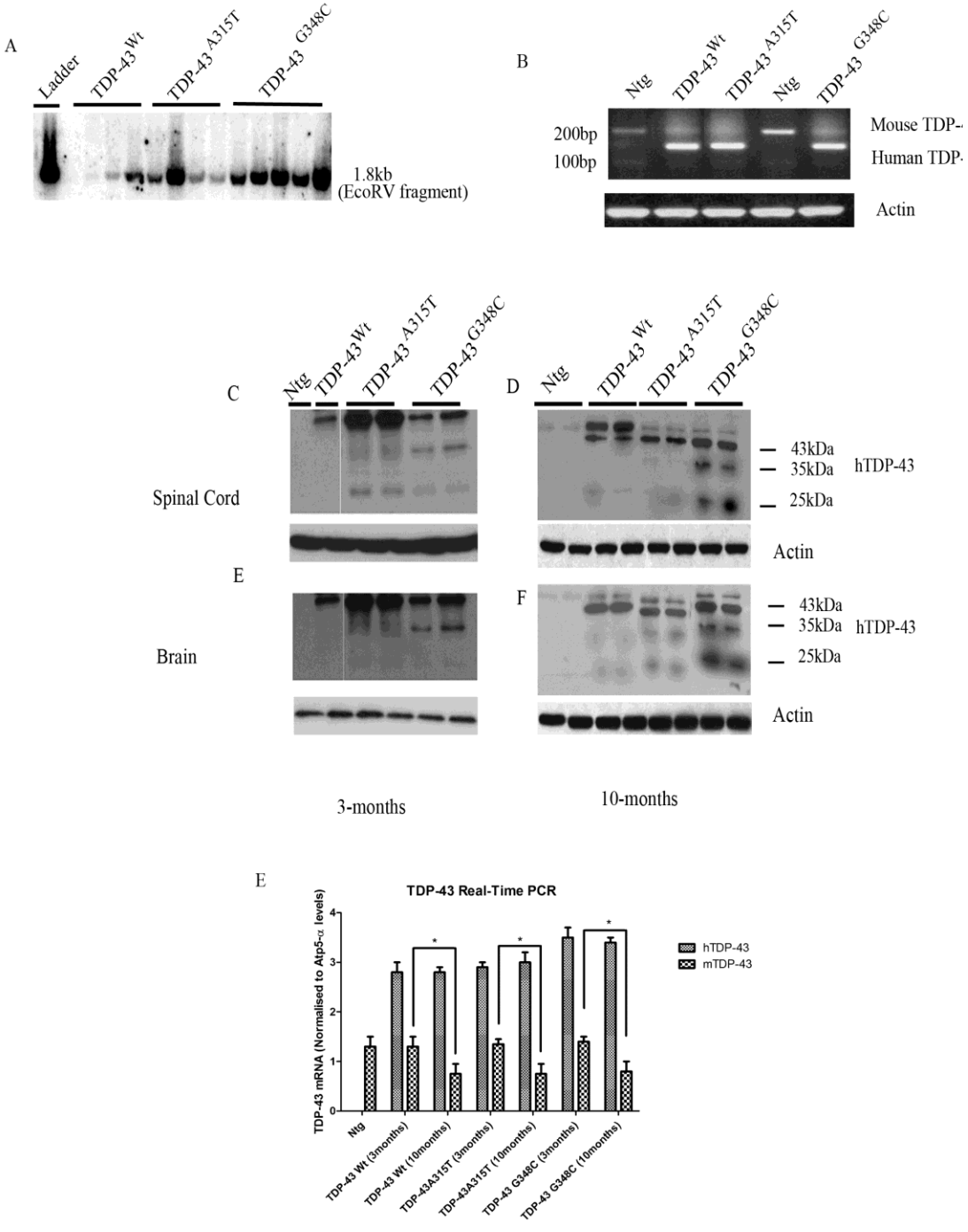
A
Ladder
TDP-43 Wt
TDP-43 A315T
TDP-43 G348C
1.8kb
(EcoRV fragment)
B
Ntg
TDP-43 Wt
TDP-43 A315T
Ntg
TDP-43 G348C
200bp
100bp
Mouse TDP-
Human TDP-
Actin
C
Ntg
TDP-43 Wt
TDP-43 A315T
TDP-43 G348C
Spinal Cord
D
Ntg
TDP-43 Wt
TDP-43 A315T
TDP-43 G348C
43kDa
35kDa
25kDa
hTDP-43
Actin
E
Brain
F
43kDa
35kDa
25kDa
hTDP-43
Actin
3-months
10-months

E
TDP-43 Real-Time PCR
TDP-43 mRNA (Normalised to Atp5-α levels)
hTDP-43
mTDP-43
Ntg
TDP-43 Wt (3months)
TDP-43 Wt (10months)
TDP-43A315T (3months)
TDP-43A315T (10months)
TDP-43 G348C (3months)
TDP-43 G348C (10months)

Supplemental Figure 2.1. Characterisation of TDP-43 transgenic mice. A. Founder TDP-43 transgenic mice were identified by the presence of the 1.8-kb EcoRV fragment on the Southern blot. Various lanes showing different transgenic lines. **B.** RT-PCR analysis of the spinal cord lysates of TDP-43^{Wt}, TDP-43^{A315T} and TDP-43^{G348C} mice reveal hTDP-43 (170bp). In some lanes, mouse TDP-43 is also visible (130bp). Actin is shown as internal control. **A-D.** Western blot analysis of spinal cord **(A-B)** and brain **(C-D)** lysates from 3-months and 10-months old mice were performed using TDP-43 human-specific monoclonal antibody. Blots reveal increased cytotoxic ~25-kDa TDP-43 fragment in the brain and spinal cord lysates of TDP-43^{G348C} and TDP-43^{A315T} mice at 10-months age as compared to 3-months old mice. TDP-43^{Wt} and Ntg (non-transgenic) mice had insignificant amounts of ~25-kDa fragments at both 3-months and 10-months age. Actin is shown as loading control. **(E)** Real-time PCR for human and mouse TDP-43 mRNA transcripts from non-transgenic (Ntg, 10-months old) and 3-months and 10-months old TDP-43Wt, TDP-43^{A315T} and TDP-43^{G348C} mice show reduced levels of endogenous mouse TDP-43 at 10-months in TDP-43 transgenic mice. Real-Time PCR were normalised against Atp-5α levels Two-way ANOVA was used with bonferroni adjustment for statistical analysis (n=5),*$p<0.01$.

2.5.2 Over-expression of WT and mutant TDP-43 is associated with the formation of cytosolic aggregates

Biochemically, ALS and FTLD-U cases are characterized by 25kDa C-terminal deposits which might contribute to pathogenesis (Cairns et al., 2007). Similar to ALS cases, TDP-43^{G348C} and TDP-43^{A315T} mice had ~25kDa fragments in the spinal cord (Fig. 2.2A-B). This ~25kDa fragment was more prominent at 10 months of age (Fig. 2.2B) than at 3 months of age (Fig. 2.2A). Blots probed with human TDP-43 specific monoclonal antibody reveal increased cytotoxic ~25-kDa TDP-43 fragment in the brain (Supplemental Fig. 2.1E-F) and spinal cord (Supplemental Fig. 2.1C-D) lysates of TDP-43^{G348C} and TDP-43^{A315T} mice at 10-months age as compared to 3-months old mice. Using immunofluorescence and monoclonal TDP-43 antibody, we detected the presence of cytoplasmic TDP-43 aggregates in TDP-43^{G348C} mice (Fig. 2.2H and Supplemental Fig. 2.2A-B) and TDP-43^{A315T} (Fig. 2.2G) mice at around 10-months of age, but not in TDP-43^{Wt} mice (Fig. 2.2F). Cytoplasmic localization as well as aggregates of TDP-43 were age dependent as they were absent in the spinal cord sections of 3-month old mice (Fig. 2.2C-E). In order to determine if the TDP-43 aggregates were ubiquitinated, we performed double immunofluorescence with TDP-43 and anti-ubiquitin antibodies. We found that ubiquitin specifically co-localized with cytoplasmic TDP-43 aggregates in the spinal cord (Fig. 2.2L-N), hippocampal (Fig. 2.2O-Q) and cortical sections (Fig. 2.2R-T) of 10-months old TDP-43^{G348C} mice, but not in the spinal cord sections of 3-months old (Fig. 2.2I-K) TDP-43^{G348C} mice. Ubiquitination of TDP-43 positive inclusions was further confirmed by the co-immunoprecipitation of ubiquitin (poly-ubiquitin) with hTDP-43. This immunoprecipitation experiment clearly demonstrates that proteins associated with TDP-43 inclusions especially in 10-months old TDP-43^{G348C} and TDP-43^{A315T} mice are massively ubiquitinated (Fig. 2.2U). However, probing the blot with anti-human TDP-43 monoclonal antibody (Fig. 2.2U) or with polyclonal antiTDP-43 (data not shown) did not reveal high molecular weight forms of TDP-43 suggesting that TDP-43 itself was not ubiquitinated. To further address this question, we have carried out immunoprecipitation of spinal cord extracts with anti-ubiquitin and probed the blot with anti-TDP-43 monoclonal antibody (Fig. 2.2U). As expected, TDP-43 was co-immunoprecipitated with anti-ubiquitin. However, only small

amount of high molecular weight forms of TDP-43 (i.e. poly-ubiquitinated) could be detected (Fig. 2.2V). This result is consistent with a report that TDP-43 is not in fact the major ubiquitinated target in ubiquitinated inclusions of ALS (Sanelli et al., 2007).

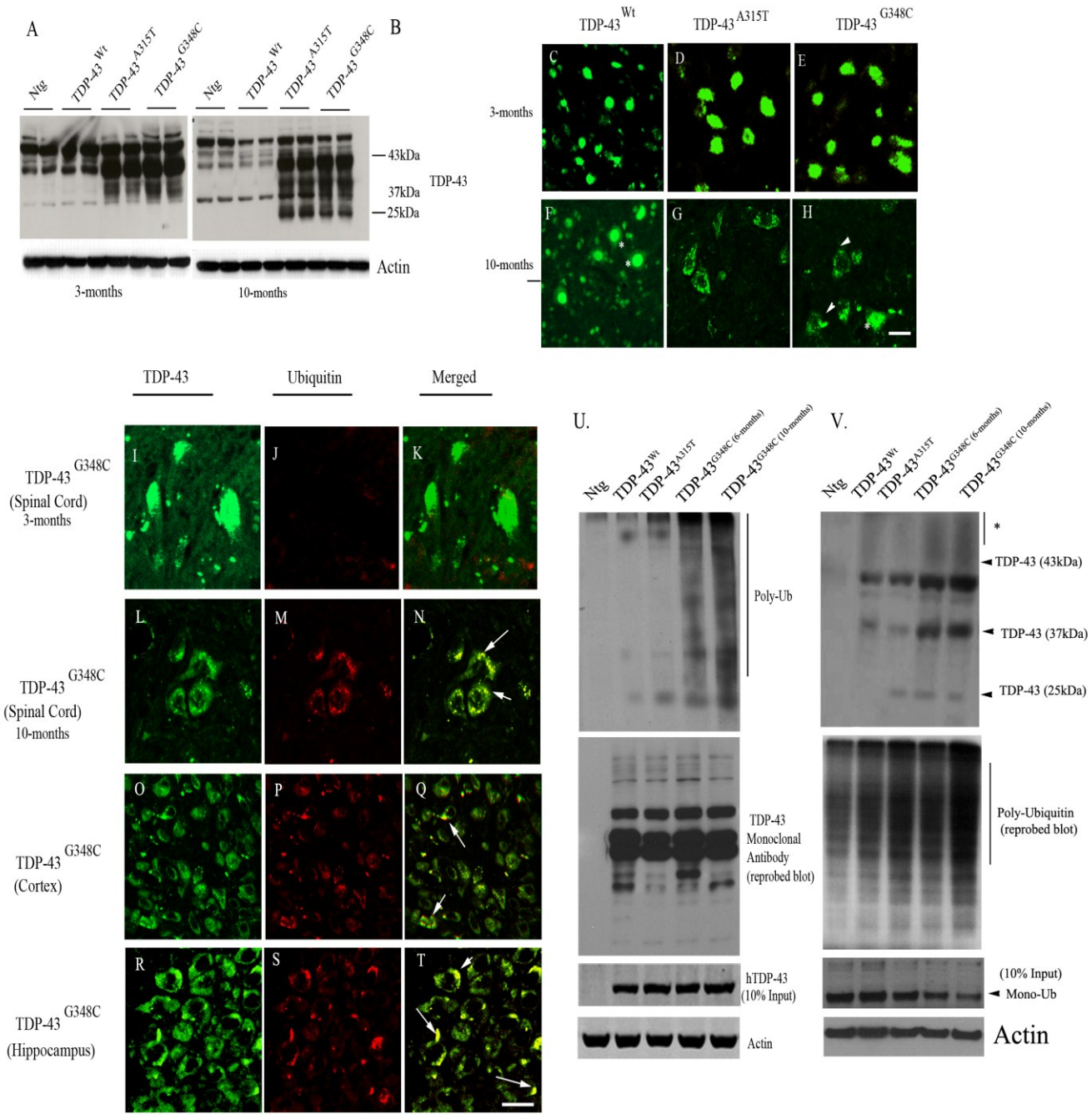
A
Ntg
TDP-43 Wt
TDP-43 A315T
TDP-43 G348C
B
43kDa
37kDa
25kDa
TDP-43
Actin
3-months
10-months
TDP-43 Wt
TDP-43 A315T
TDP-43 G348C
3-months
10-months
C
D
E
F
G
H
TDP-43
Ubiquitin
Merged
TDP-43 G348C (Spinal Cord) 3-months
TDP-43 G348C (Spinal Cord) 10-months
TDP-43 G348C (Cortex)
TDP-43 G348C (Hippocampus)
I
J
K
L
M
N
O
P
Q
R
S
T
U.
Ntg
TDP-43 Wt
TDP-43 A315T
TDP-43 G348C (6-months)
TDP-43 G348C (10-months)
Poly-Ub
TDP-43 Monoclonal Antibody (reprobed blot)
hTDP-43 (10% Input)
Actin
V.
Ntg
TDP-43 Wt
TDP-43 A315T
TDP-43 G348C (6-months)
TDP-43 G348C (10-months)
*
TDP-43 (43kDa)
TDP-43 (37kDa)
TDP-43 (25kDa)
Poly-Ubiquitin (reprobed blot)
(10% Input)
Mono-Ub
Actin

Figure 2.2. Biochemical and pathological features of ALS/FTLD in TDP-43 transgenic mice. (A-B) Western blot of spinal cord lysates from Ntg (non-transgenic), TDP-43^{Wt}, TDP-43^{A315T} and TDP-43^{G348C} mice using polyclonal TDP-43 antibody at 3 and 10-months show that TDP-43 (both G348C and A315T mutants) have ~35 and ~25kDa fragments which increase with age. Actin is shown as a loading control. (**C-H)** Immunofluorescence of the spinal cord of 10-month old TDP-43^{Wt} **(F)**, TDP-43^{A315T} **(G)** and TDP-43^{G348C} mice **(H)** using TDP-43 monoclonal antibody show cytoplasmic hTDP-43 aggregates (arrow-heads) especially in the spinal cord sections of TDP-43^{G348C} transgenic mice. Some of the TDP-43 is still in nucleus (asterisk). On the other hand, spinal cord sections of 3-month old transgenic mice show nuclear staining exclusively**(C-E)**. (**I-T)**. Double immunofluorescence of the brain and spinal cord sections of 10-months old TDP-43^{G348C} mice using monoclonal TDP-43 antibody and anti-ubiquitin antibody show ubiquitinated TDP-43 aggregates (arrows) in spinal cord **(L-N)**, cortex **(O-Q)** and hippocampal **(R-T)** regions. **(I-K)** Spinal cord sections of 3-months old TDP-43^{G348C} mice do not show intense ubiquitination. Background intensities were matched with 10-month old mice for consistency. **(U)** Co-immunoprecipitation of ubiquitin using mouse monoclonal TDP-43 from spinal cord lysates of transgenic mice show that proteins associated with hTDP-43 are poly-ubiquitinated (Poly-Ub), more in TDP-43^{G348C} mice. Note that the ubiquitination is more in 10-months old mice than in 6-months old TDP-43^{G348C} mice. Reprobed western blot is shown for TDP-43 using monoclonal antibody. Western blot of hTDP-43 using monoclonal antibody is shown as 10% input and actin as loading control. **(V)** Reverse co-immunoprecipitation with anti-ubiquitin antibody shows that TDP-43 was co-immunoprecipitated with anti-ubiquitin. However, only small amount of high molecular weight forms of TDP-43 (i.e. poly-ubiquitinated) could be detected. Western blot of ubiquitin using polyclonal antibody is shown as 10% input and actin as loading control. Scale bar: **C-H**, 50μm; **I-T**, 25μm.

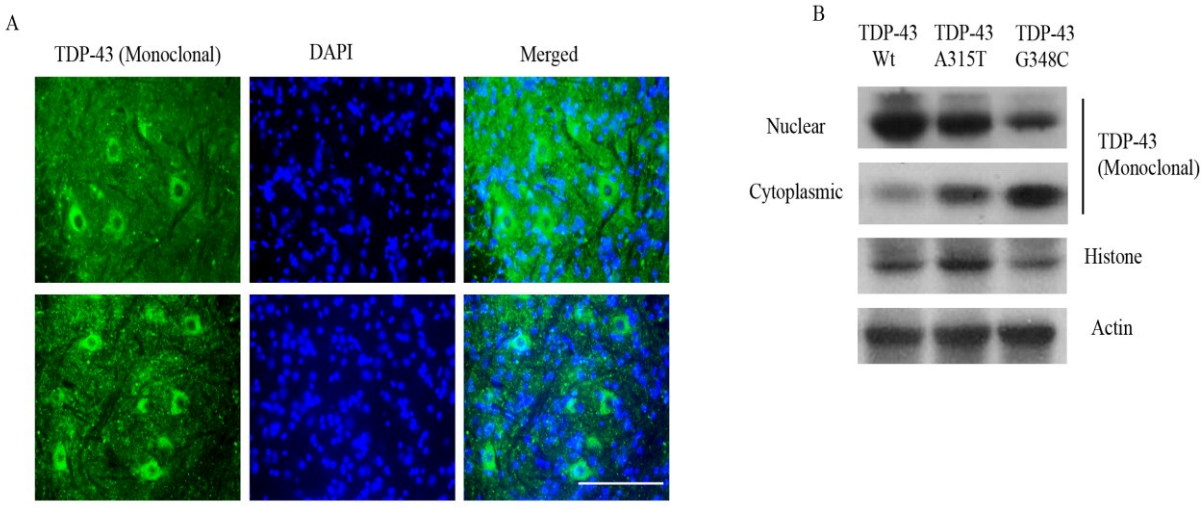

Supplemental Figure 2.2. Cytoplasmic Localization of TDP-43. (A) Immunofluorescence of spinal cord sections of TDP-43^{G348C} mice using human specific monoclonal TDP-43 reveals that human TDP-43 is cytoplasmic. 4',6-diamidino-2-phenylindole (DAPI) is used as nuclear marker. Scale bar: 50μm. **(B)** Nuclear and Cytoplasmic fractions were probed for human TDP-43 levels using monoclonal TDP-43 antibody. Cytoplasmic levels of TDP-43 were clearly increased in TDP-43^{G348C} mice as compared to TDP-43^{Wt} mice. Histone is used as a nuclear marker and actin as a cytoplasmic marker.

2.5.3 Peripherin overexpression and neurofilament disorganization in TDP-43 transgenic mice

A pathological hallmark of both sporadic and familial ALS is the presence of abnormal accumulations of neurofilament and peripherin proteins in motor neurons (Carpenter, 1968; Corbo and Hays, 1992; Migheli et al., 1993). Immunofluorescence analysis of the spinal cord sections by anti-peripherin polyclonal antibody, revealed presence of peripherin aggregates in large motor neurons of TDP- 43^{G348C}, TDP-43^{A315T} and to a lesser extent in TDP-43^{Wt} mice at 10-months of age as compared to 3-months old mice (Fig. 2.3A-E and Supplemental Fig 2.3A-D). Further analysis revealed that peripherin aggregates were also present in the brain. The aggregates in TDP-43^{G348C} and to a lesser extent in TDP-43^{A315T} and TDP-43^{Wt} mice were localized in the hippocampus (Fig. 2.3F-J) and in the cortex (Fig. 2.3K-O). Western blot analysis of the brain lysates of transgenic mice using polyclonal antibody against peripherin revealed abnormal splicing variants of peripherin in TDP-43^{G348C} and TDP-43^{A315T} transgenic mice, including a toxic Per61 fragment (Fig. 2.3P) along with other fragments like Per56 and the normal Per58. The use of anti-peripherin monoclonal antibody revealed overexpression of the peripherin ~58kDa fragment in TDP-43^{G348C}, TDP-43^{A315T} and to a lower extent in TDP-43^{Wt} mice compared to non-transgenic mice. Earlier reports have shown that Per61 is neurotoxic and is present in spinal cords of ALS patients (Robertson et al., 2003). We then determined the mRNA expression levels in the spinal cord extracts of various peripherin transcripts (Per61, Per58 and Per56) using real-time PCR. Though the levels of Per58 and Per56 are not significantly different between various transgenic mice, the levels of Per61 are significantly upregulated (~2.5 fold, $p<0.01$) in TDP-43^{G348C} mice compared to TDP-43^{Wt} mice (Fig. 2.3Q). Per61 was also upregulated in TDP-43^{A315T} mice (~1.5 fold) compared to TDP-43^{Wt} mice. Antibody specifically recognizing Per61 was used to detect Per61 in the spinal cord sections of TDP-43^{G348C} mice (Fig. 2.3S) and in TDP-43^{Wt} mice (Fig. 2.3R). As expected Per61 antibody stained Per61 aggregates in the axons and cell bodies in human ALS spinal cord sections (Fig. 2.3U) but not control spinal cord tissues (Fig. 2.3T).

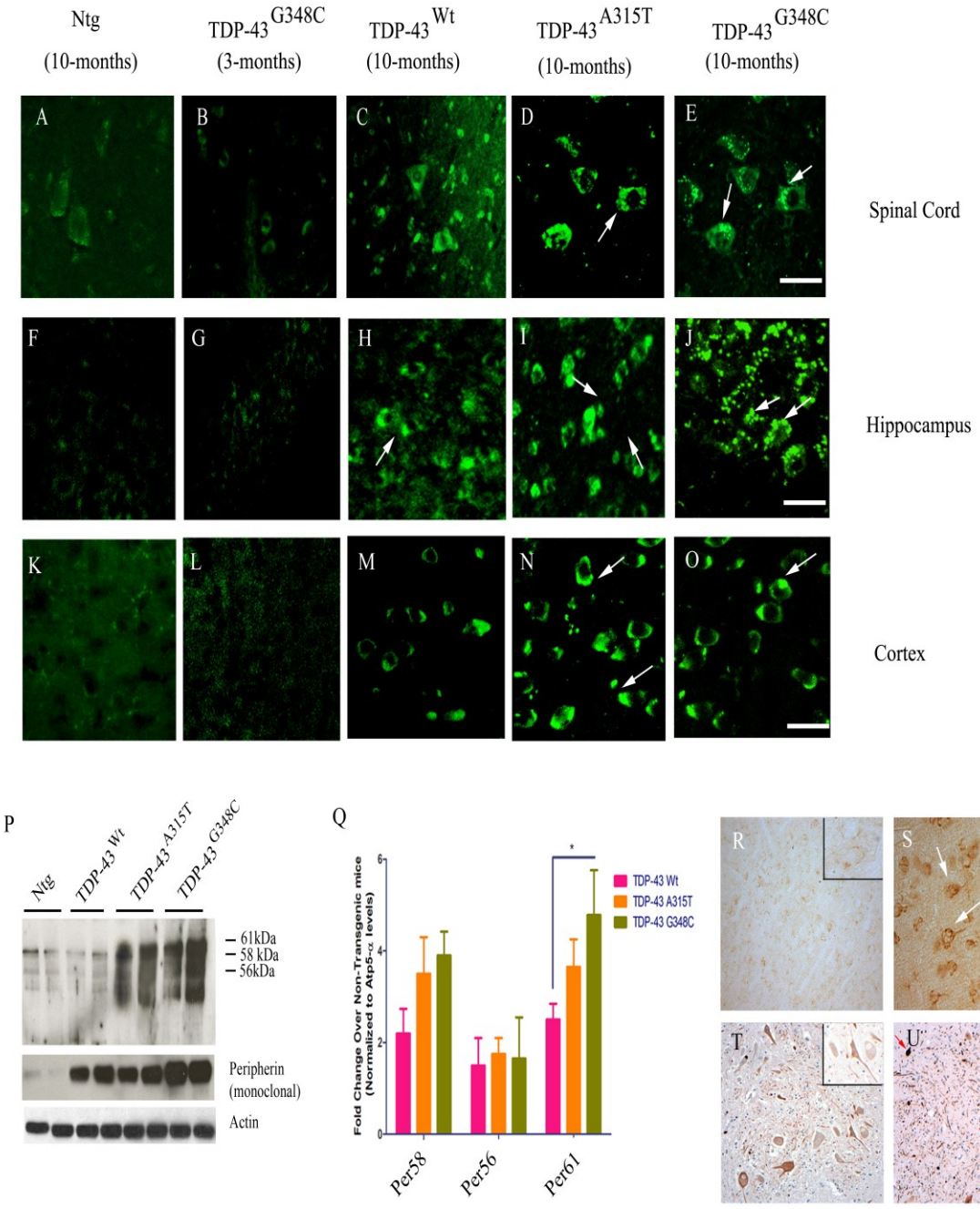
Ntg
(10-months)
TDP-43 G348C
(3-months)
TDP-43 Wt
(10-months)
TDP-43 A315T
(10-months)
TDP-43 G348C
(10-months)
A
B
C
D
E
Spinal Cord
F
G
H
I
J
Hippocampus
K
L
M
N
O
Cortex
P
Ntg
TDP-43 Wt
TDP-43 A315T
TDP-43 G348C
61kDa
58 kDa
56kDa
Peripherin
(monoclonal)
Actin
Q
Fold Change Over Non-Transgenic mice
(Normalized to Atp5-α levels)
TDP-43 Wt
TDP-43 A315T
TDP-43 G348C
Per58
Per56
Per61
R
S
T
U

Figure 2.3. Peripherin abnormalities in TDP-43 transgenic mice. A-O. Immunofluorescence of the brain **(F-O)** and spinal cord **(A-E)** sections of 10-months old Ntg (non-transgenic), TDP-43^{Wt}, TDP-43^{A315T} and TDP-43^{G348C} transgenic mice using polyclonal anti-peripherin antibody. Peripherin immunofluorescence of the spinal cord sections show peripherin aggregates more in TDP-43^{G348C} mice **(E)** (arrow), but also some in TDP-43^{A315T} mice **(C)** and very less in TDP-43^{Wt} mice **(C)** as compared to non-transgenic control **(A)**. Spinal cord sections of 3-months old TDP-43^{G348C} mice do not show peripherin overexpression or aggregates **(B). (F-J)** Hippocampal region of the brain of 10-month oldTDP-43^{G348C} mice show abundant peripherin aggregates **(J)**. Peripherin aggregates are also seen to a lesser extent in TDP-43^{A315T} mice **(I)** and very less in TDP-43^{Wt} mice **(H)** as compared to non-transgenic control **(F)** and 3-months old TDP-43G348C mice **(G)**. **(K-O)** Similarly, peripherin immunofluorescence in 10-months old TDP-43^{G348C} mice **(O)** in the cortical region of the brain show peripherin aggregates. These aggregates are also seen to a lesser extent in TDP-43^{A315T} mice **(N)** and very less in TDP-43^{Wt} mice **(M)** as compared to non-transgenic control **(K)** and 3-months old TDP-43G348C mice **(L)**. **(P)** Western blot analysis of the brain lysates of 10-months old Ntg, TDP-43^{Wt}, TDP-43^{A315T} and TDP-43^{G348C} transgenic mice using polyclonal peripherin antibody reveal various peripherin splice variants including the Per61, Per58 and Per56 fragments especially in TDP-43^{G348C} mice. Monoclonal peripherin antibody revealed overexpression of peripherin in TDP-43^{G348C}, TDP-43^{A315T} and to a lesser extent in TDP-43^{Wt} mice as compared to non-transgenic control. Actin is shown as loading control. **(Q)** Quantitative real-time PCR analysis of mRNA levels of peripherin splice variants – Per61, Per58 and Per56 in the spinal cord lysates show that TDP-43^{G348C} mice had ~2.5-fold higher Per61 transcript levels than in TDP-43^{Wt} spinal cord. Per58 levels are also higher in TDP-43^{G348C} mice compared to TDP-43^{Wt} mice, but no significant differences are observed in Per56 levels between different transgenic mice. Peripherin transcript levels are expressed as fold change over non-transgenic controls normalized to Atp-5α levels. One-way ANOVA was used with Tukey's post-hoc comparison for statistical analysis (n=3), *$p<0.01$ (**R-U**) Immuno-histochemistry on spinal cord tissues using Per61 specific antibody reveal Per61 specific aggregates in TDP-43^{G348C} mice **(S)** similar to sporadic ALS spinal cord tissues **(U)**. In contrast, Per61 antibody yielded weak staining of the spinal cord in human control **(T)** and in TDP-43^{Wt} transgenic mice **(R)**. Inset showing higher magnification images. Scale bars: **A-O** 25μm; **R-U** 50μm

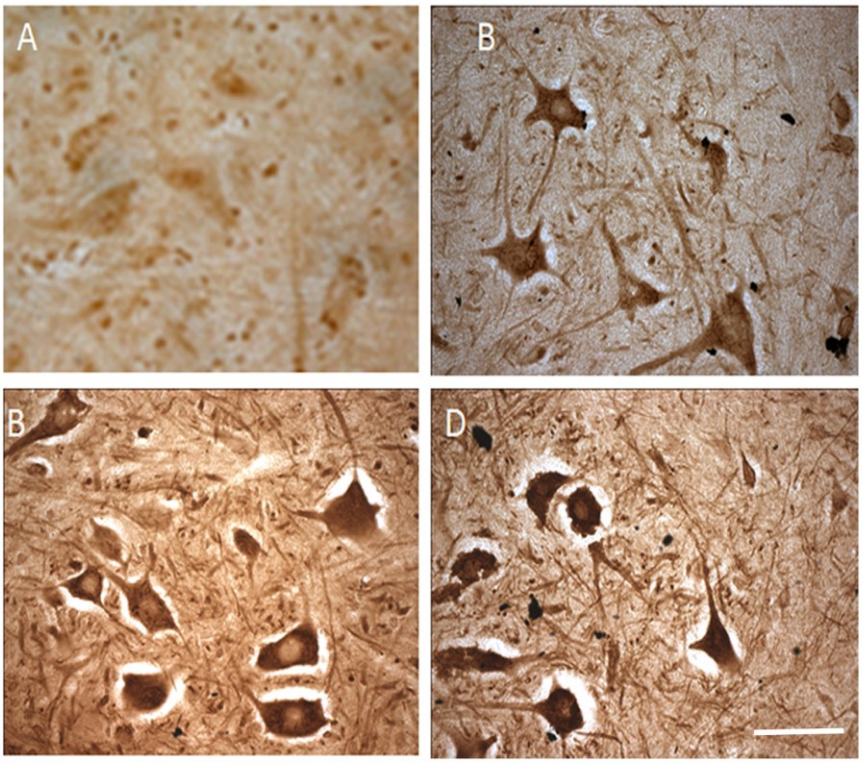

Supplemental Figure 2.3. Peripherin overexpression in spinal cord of TDP-43 transgenic mice. Immunohistochemistry of spinal cord sections of non-transgenic **(A)**, TDP-43^{Wt} **(B)**, TDP-43^{A315T} **(C)** and TDP-43^{G348C} **(D)** mice with polyclonal peripherin antibody show overexpression of peripherin the motor neurons, specifically in TDP-43^{G348C} mice. Scale bar: 25μm

The TDP-43 transgenic mice also exhibit altered levels of peripherin and neurofilament protein expression. As shown in Fig. 2.4A, western blotting revealed that NF-H is downregulated by about 1.5-fold and NF-L by about 2-fold in the spinal cord extracts of 10 months old TDP-43^{G348C} mice as compared to non-transgenic mice (Fig. 2.4A). The levels of NF-M on the other hand were not significantly altered in any of the transgenic mice. Since usual ELISA methods are not suitable for the quantitative measurement of neurofilament proteins because of their insolubility. However, neurofilament proteins are dissolved in urea at high concentration. Standard curves of NF-L, NF-M and NF-H dissolved in various concentrations of urea diluted with the dilution buffer were prepared as described elsewhere (Lu et al., 2011) (Supplemental Fig. 2.4A-C). A suitable concentration of urea for detection was estimated to be around 0.3 mol/L, because the sensitivity was higher in 0.3 mol/L urea than in the other concentrations examined. Analysis of ELISA revealed that NF-L levels are significantly reduced in 10-months old TDP-43G348C mice as compared to age-matched non-transgenic controls (**$p<0.001$, Supplemental Fig 2.4D). 10-months old spinal cord samples were fractionated in detergent soluble and insoluble fractions. Peripherin levels could be detected in both soluble and insoluble fractions (Supplemental Fig. 2.5A-B). We also determined the NF-H, NF-M and NF-L levels in the sciatic nerve of 3 and 10-months old transgenic mice. We observed a slight decrease in NF-L levels in 3-months old TDP-43^{G348C} mice as compared to age-matched TDP-43^{Wt} and TDP-43^{A315T} mice, which had levels similar to non-transgenic mice (Fig. 2.4B). At 10-months of age, TDP-43^{G348C} mice had about 50% reduction in NF-L levels in the sciatic nerve (Fig. 2.4B) as compared to TDP-43^{Wt} mice. We then used double immunofluorescence techniques to determine which neurofilament forms part of the aggregates with peripherin in TDP-43^{G348C} spinal cord sections. We found that NF-H clearly forms part of the aggregates (Fig. 2.4C-E), followed by NF-M to a lesser extent (Fig. 2.4F-H) and NF-L (Fig. 2.4I-K) does not form part of the aggregates. TDP-43 aggregates co-localize partially with NF-H and NF-M, but not with NF-L (Supplemental Fig. 2.6A-C).

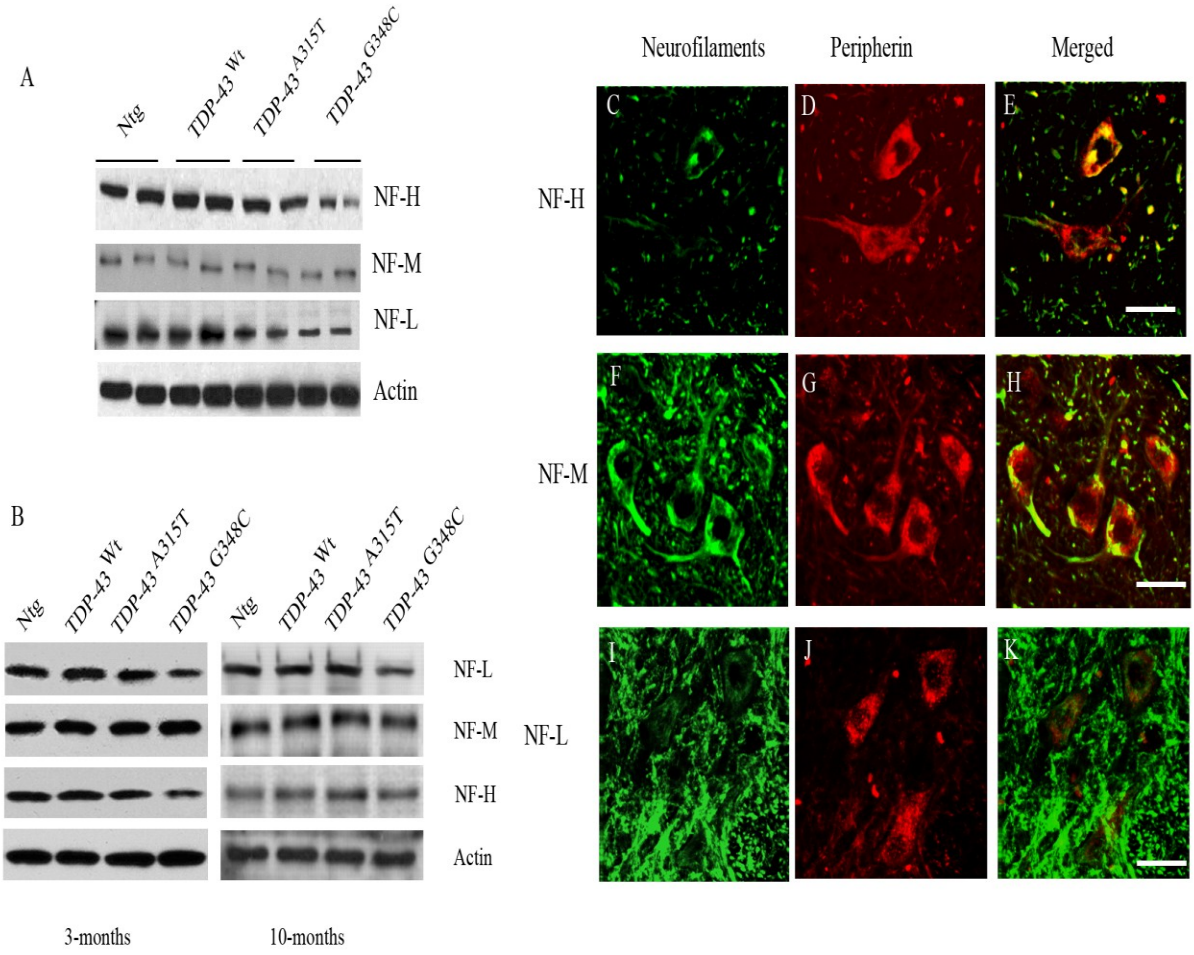

Figure 2.4. Neurofilament abnormalities in TDP-43 transgenic mice. (A) Western blots of various neurofilament proteins on the spinal cord lysates of 10-months old Ntg (non-transgenic), TDP-43^{Wt}, TDP-43^{A315T} and TDP-43^{G348C} transgenic mice using NF-H, NF-M and NF-L specific antibodies. Note the sharp reduction in the protein levels of NF-L and NF-H in TDP-43^{G348C} spinal cord lysates as compared to TDP-43^{Wt} lysates. Actin is shown as loading control. **(B)** Western blots of various neurofilament proteins on the spinal cord lysates of 3-months and 10-months old Ntg (non-transgenic), TDP-43^{Wt}, TDP-43^{A315T} and TDP-43^{G348C} transgenic mice using NF-H, NF-M and NF-L specific antibodies. Actin is shown as loading control. **C-K.** Double immuno-fluorescence of various neurofilaments (green) – NF-H **(C)**, NF-M **(F)** and NF-L **(I)** with polyclonal peripherin antibody (red) on the TDP-43^{G348C} spinal cord sections reveal that NF-H is recruited to peripherin aggregates (arrows, **E**), and to a lesser extent NF-H **(H)**, but not NF-L **(K)**. Scale bar: 25μm.

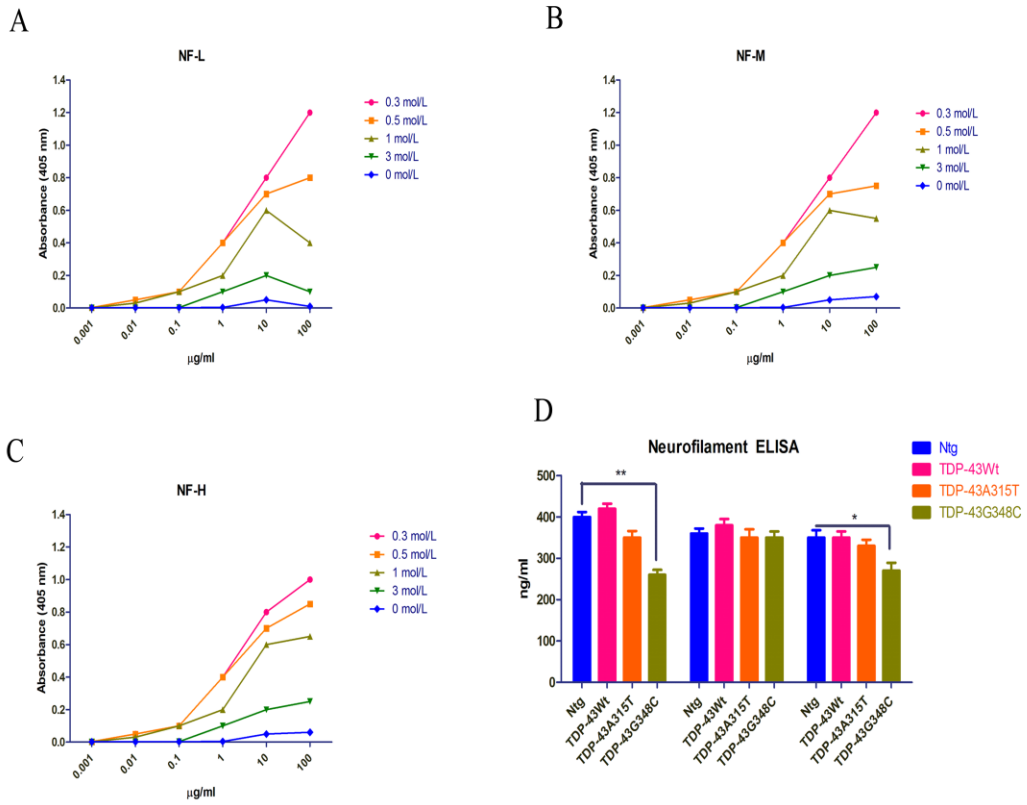

Supplemental Figure 2.4. Neurofilament ELISA. (A-C) Typical standard curves measuring neurofilament proteins in various concentrations of urea (0 mol/L, 0.3 mol/L, 0.5mol/L, 1 mol/L and 3 mol/L) - (A) NF-L (B) NF-M, (C) NF-H. Purified bovine NF-L, NF-M and NF-H were used as standard, respectively. The standard curve under 0 mol/L urea was obtained with the purified neurofilaments dialyzed against dilution buffer to remove urea. A suitable concentration of urea for ELISA detection was estimated to be around 0.3 mol/L, because the sensitivity was higher in 0.3 mol/L urea than in the other concentrations examined. **(D)** Measurement of total levels of neurofilaments by ELISA in spinal cord extracts of 10-months old non-transgenic (Ntg), TDP-43^{Wt}, TDP-43^{A315T} and TDP-43^{G348C} mice using phosphorylation independent N52 (NF-H), NN18 (NF-M), and NR4 (NF-L) antibodies reveal that NF-L and NF-H levels are reduced in TDP-43^{G348C} mice compared to non-transgenic control. One-way ANOVA was used with Tukey's post-hoc comparison for statistical analysis (n=3), *$p<0.01$, **$p<0.001$.

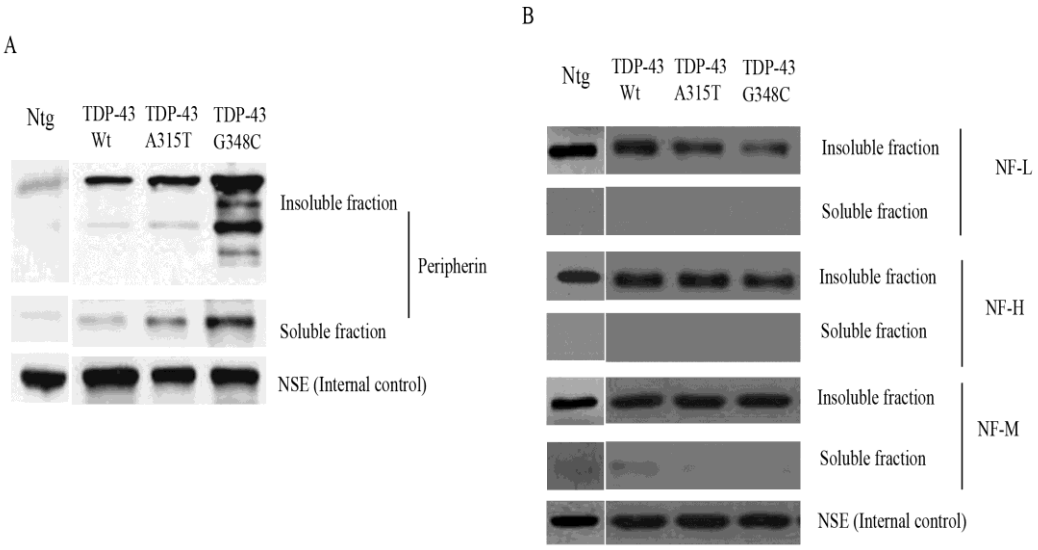

Supplemental Figure 2.5. Detergent soluble and insoluble fractionation of intermediate filaments. (A-B) For enrichment of neuronal intermediate filaments, spinal cords of non-transgenic (Ntg), TDP-43^{Wt}, TDP-43^{A315T} and TDP-43^{G348C} mice were homogenized at 4^{0}C in low salt extraction buffer [50 mM Tris (pH 7.5), 150 mM NaCl, 5 mM EDTA, and protease inhibitors]. The homogenates were then centrifuged at 16 000 g for 10 min at 4^{0}C. The pellet fractions were further homogenized in high salt Triton X-100 extraction buffer [20 mM Tris–HCl (pH 7.5), 750 mM NaCl, 1 mM EDTA, 1% (v/v) Triton X-100, and protease inhibitors] centrifuged at 16 000 g for 10 min at 4^{0}C. The resultant Triton-X 100 insoluble pellets were treated to a final homogenization in high salt buffer containing 1 M sucrose and re-centrifuged to remove contaminating lipids. The final pellet was solubilized in 2% (w/v) sodium dodecyl sulfate (SDS) in phosphate-buffered saline. Western blots of Triton X-100 soluble and insoluble fractions reveal that most of the neurofilaments (NF-L, NF-M and NF-H) were detergent insoluble, while peripherin bands were seen in both detergent soluble and insoluble fractions. NSE = Neuron specific enolase is used as an internal control.

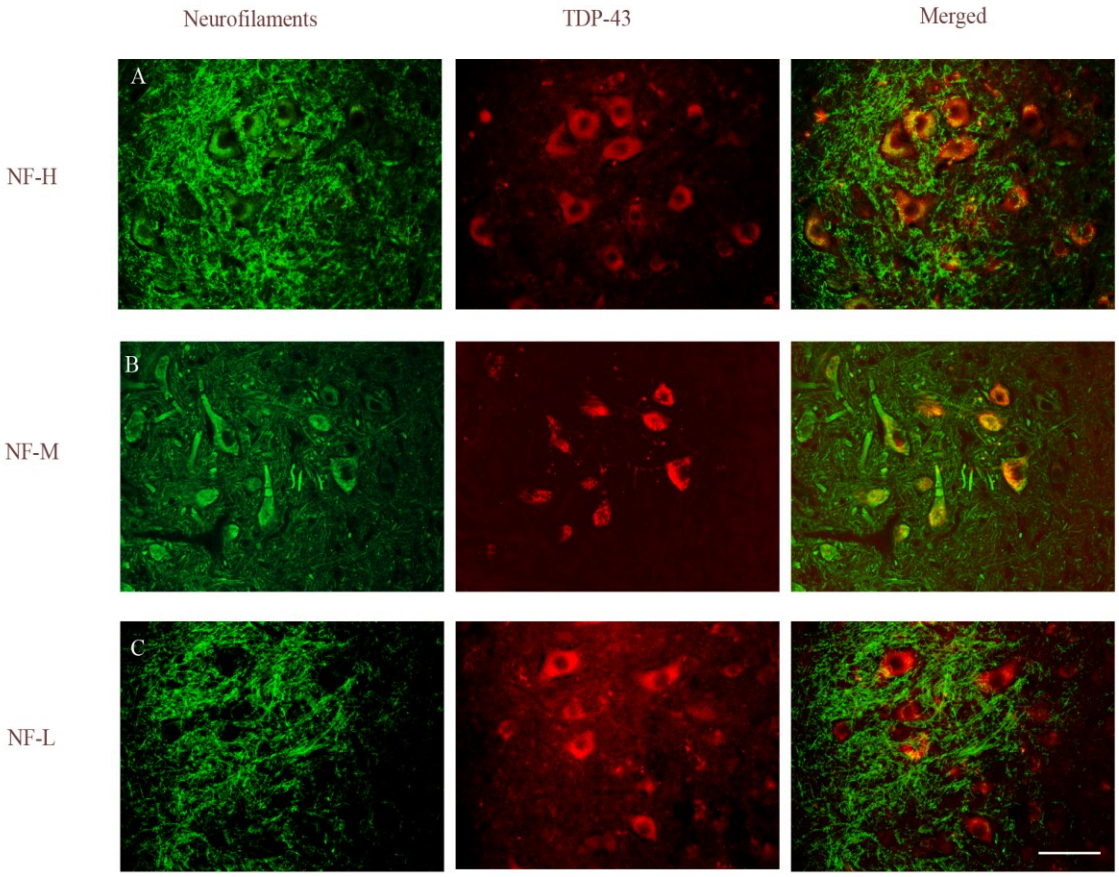

Supplemental Figure 2.6. Colocalization of cytoplasmic TDP-43 and neurofilaments. (A-C) Double immunofluorescence of spinal cord sections of 10-months old TDP-43^{G348C} mice was performed using human specific TDP-43 and NF-H (N52), NF-M (NN18) and NF-L (NR4) antibodies. Immunofluorescence studies reveal that TDP-43 co-localizes partially with NF-H and NF-M, but not with NF-L. Scale bar: 25μm

2.5.4 Smaller calibre of peripheral axons in TDP-43 transgenic mice

Our previous work has demonstrated that over-expression of the wild type peripherin, especially in context of NF-L loss, leads to a late onset motor neurons disease and axonal degeneration (Jacomy et al., 1999). We analysed at different time points the number of axons, the distribution of axonal calibre and their morphology. Axonal counts of the L5 ventral root from TDP-43 transgenic mice at 10-months age failed to reveal any significant differences in the number of motor axons (Fig. 2.5A-E). Normal mice exhibit a bimodal distribution of axonal calibre with peaks at ~2 μm and ~7 μm in diameter (Fig. 2.5F). In contrast, a skewed bimodal distribution is observed in TDP-43 transgenic mice. There was a 10% increase (an increase of 100 axons, $p<0.001$) in the number of motor axons with 1- to 3-μm calibre and a 12% decrease (a decrease of 120 axons) in the number of motor axons with 6- to 9-μm calibre in 10-months old TDP-43^{G348C} mice compared to non-transgenic mice. (Fig.5F). There was similar 7% increase (an increase of 70 axons, $p<0.01$) in the number of motor axons with 1- to 3-μm calibre and a 8% decrease (a decrease of 80 axons) in the number of motor axons with 6- to 9-μm calibre in 10-months old TDP-43^{A315T} mice as compared to non-transgenic mice. The increase in the number of motor axons with 1- to 3-μm calibre was less (about 5%) and a slight decrease of 6% in 10-month old TDP-43^{Wt} mice compared to non-transgenic mice (Fig. 2.5F). We have quantified the functional neuromuscular junctions (NMJs) through fluorescence. NMJ count revealed that 5 ± 4% of the analyzed NMJs were denervated in 10-month old TDP-43^{Wt} mice and 10 ± 5% were denervated in age-matched TDP-43^{G348C} mice as compared to non-transgenic controls (Supplemental Fig. 2.7D). Furthermore, over 20% of NMJs were partially denervated in both TDP-43^{Wt} mice and TDP-43^{G348C} mice. The severe alterations in motor axon morphology of TDP-43^{G348C} mice prompted us to examine whether this phenomenon was associated with caspase-3 activation, a sign of neuronal damage. Using double immunofluorescence and antibodies against cleaved caspase-3 and NeuN (a neuronal marker), we found many cleaved caspase-3 positive neurons in the spinal cord of TDP-43^{G348C} mice at 10-months age (Fig. 2.5J-L) compared to 3-months old TDP-43^{G348C} mice (Fig. 2.5G-I). Cleaved caspase-3 positive cells were also positive for cytoplasmic TDP-43

(Fig. 2.5M-O). However, no caspase-3 positive neurons were detected in TDP-43^{Wt} and TDP-43^{A315T} mice at 10 months of age (data not shown).

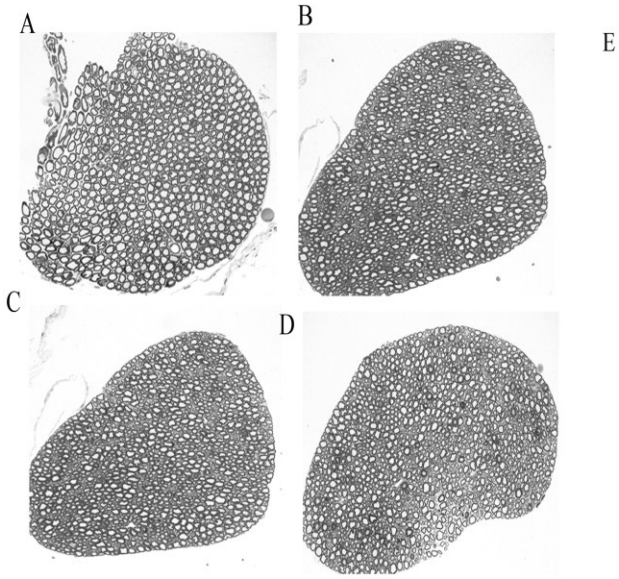
A
B
C
D

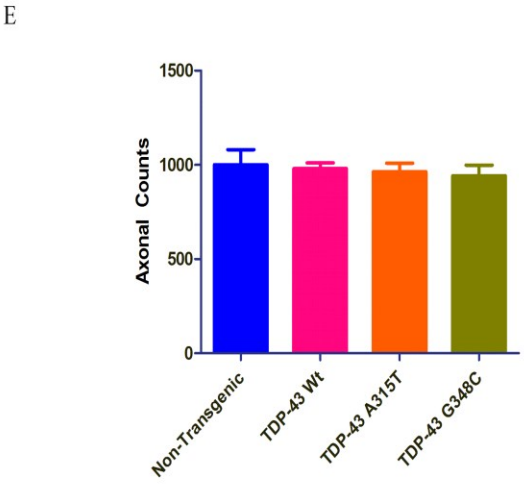
E
Axonal Counts
1500
1000
500
0
Non-Transgenic
TDP-43 Wt
TDP-43 A315T
TDP-43 G348C

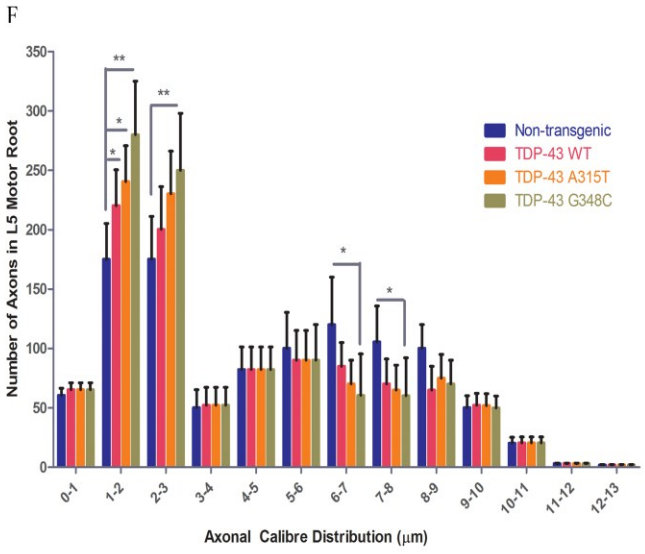
F
Number of Axons in L5 Motor Root
350
300
250
200
150
100
50
0
Non-transgenic
TDP-43 WT
TDP-43 A315T
TDP-43 G348C
0-1
1-2
2-3
3-4
4-5
5-6
6-7
7-8
8-9
9-10
10-11
11-12
12-13
Axonal Calibre Distribution (μm)

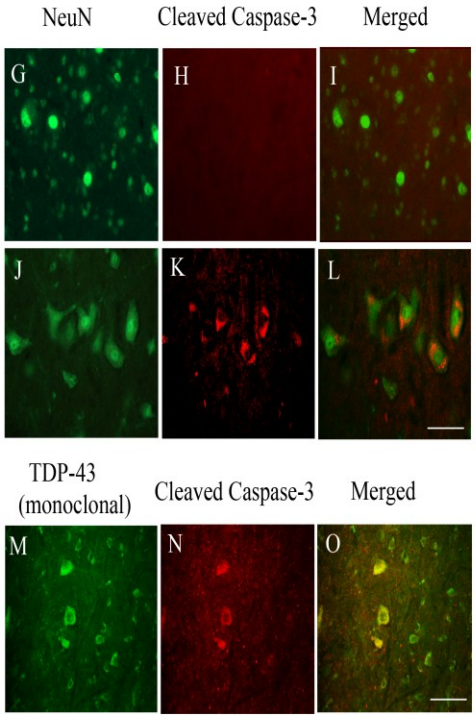
NeuN
Cleaved Caspase-3
Merged
G
H
I
TDP-43G348C
(3-months)
J
K
L
TDP-43G348C
(10-months)
TDP-43
(monoclonal)
Cleaved Caspase-3
Merged
M
N
O
TDP-43G348C
(10-months)

Figure 2.5. Reduced axonal calibre in ventral roots of TDP-43 transgenic mice. (A-D) Toluidine blue staining of thin sections of L5 ventral root axons from non-transgenic **(A)**, TDP-43^{Wt} **(B)**, TDP-43^{A315T} **(C)** and TDP-43^{G348C} **(D)** mice showing no significant differences in the motor neuron count. **(E)** Axonal counts of transgenic mouse at 10-months age failed to reveal any significant differences in the number of motor axons in the L5 ventral root. **(F)** Cumulative axon calibre distribution of axons at L5 ventral root of 10-months old non-transgenic and transgenic mice showing increased number of 1-to 3-μm axons and reduced number of 6-to 9-μm axons in TDP-43^{G348C} mice. A two-way ANOVA with repeated measures was used to study the effect of group (transgenic and non-transgenic mice) on axonal calibre distribution. Pairwise comparisons were made using Bonferroni adjustment *$p<0.01$ and **$p<0.001$. Data shown are means ± SEM of 5 different mice from each group. **(G-L)** Double immunofluorescence using NeuN (a neuronal marker) and cleaved caspase-3 show many cleaved caspase-3 positive neurons in the spinal cord of TDP-43^{G348C} mice at 10-months age (L) compared to 3-months old TDP-43^{G348C} mice **(I)**. **(M-O)** Double immunofluorescence using human specific TDP-43 and cleaved caspase-3 show many cleaved caspase-3 positive neurons in the spinal cord of TDP-43^{G348C} mice at 10-months age. Scale bar: 25μm

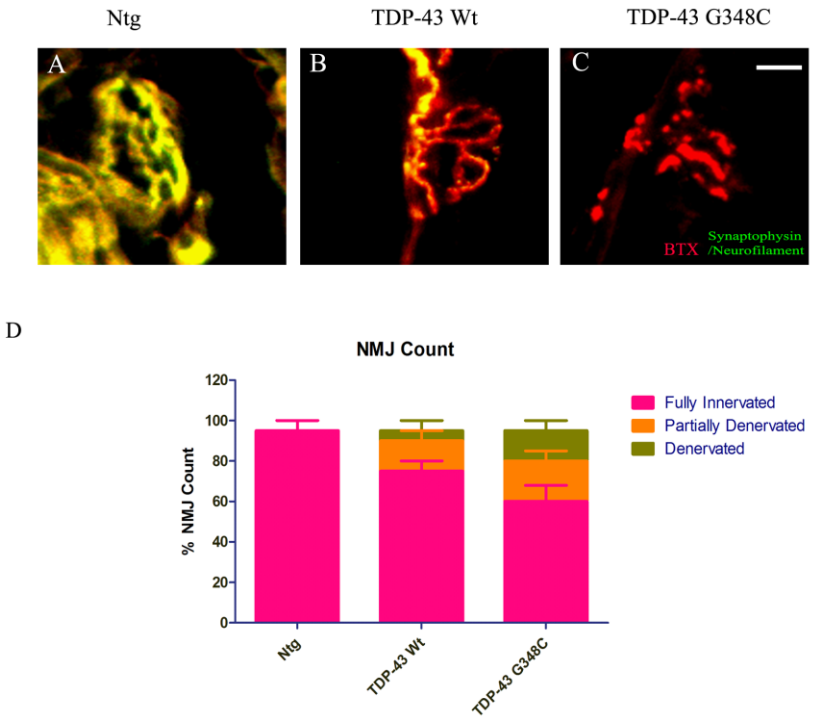

Supplemental Figure 2.7. Neuromuscular junction staining and count. (A-C) Neuromuscular junction (NMJ) staining was performed using anti-synaptophysin/neurofilament antibodies and α-bungarotoxin (BTX). Representative images showing fully innervated muscle in 10-months old non-transgenic mice **(A)**, partially denervated muscle in age-matched TDP-43^{Wt} mice **(B)** and fully denervated muscle in TDP-43^{G348C} mice **(C)**. (D) Three hundred neuromuscular junctions were counted per animal sample. Frequencies of innervation, partial denervation and denervation were then converted to percentages and plotted as graph. (n=5 per group)

2.5.5 TDP-43 transgenic mice develop motor dysfunction and cognitive deficits

Behavioural analysis of the TDP-43 transgenic mice revealed age-related cognitive defects, particularly learning and memory deficits. We used passive avoidance test to detect deficiencies in contextual memory. No defects were detected until 7 months of age. However, after 7 months TDP-43^{Wt}, TDP-43^{A315T} and TDP-43^{G348C} mice exhibited severe cognitive impairments, especially in the 11^{th} and 13^{th} months (Fig. 2.6A). The most robust memory deficit occurred in TDP-43^{G348C} mice. We then conducted Barnes maze test to specifically discern the spatial learning and memory deficits in these mice. The TDP-43^{G348C} and to a lesser extent TDP-43^{Wt} mice had significant learning impairment in the Barnes maze test at 10 months of age (Fig. 2.6B-C) as depicted by significant reduction in the time spent in the target quadrant and increased primary errors. In the probe trial (Day 5), TDP-43^{G348C} and TDP-43^{Wt} mice showed a significant reduction in the time spent in the target quadrant and increase in the total number of errors as compared to age-matched non-transgenic mice (Fig. 2.6B-C). Thus, 10-months old TDP-43^{G348C} mice had severe spatial learning and memory deficits. Transgenic mice overexpressing TDP-43^{G348C}, TDP-43^{A315T} or TDP-43^{Wt} exhibited also age-related motor deficits as depicted by significant reductions in latency in the accelerating rotarod tests starting at about 42-weeks of age (Fig. 2.6D).

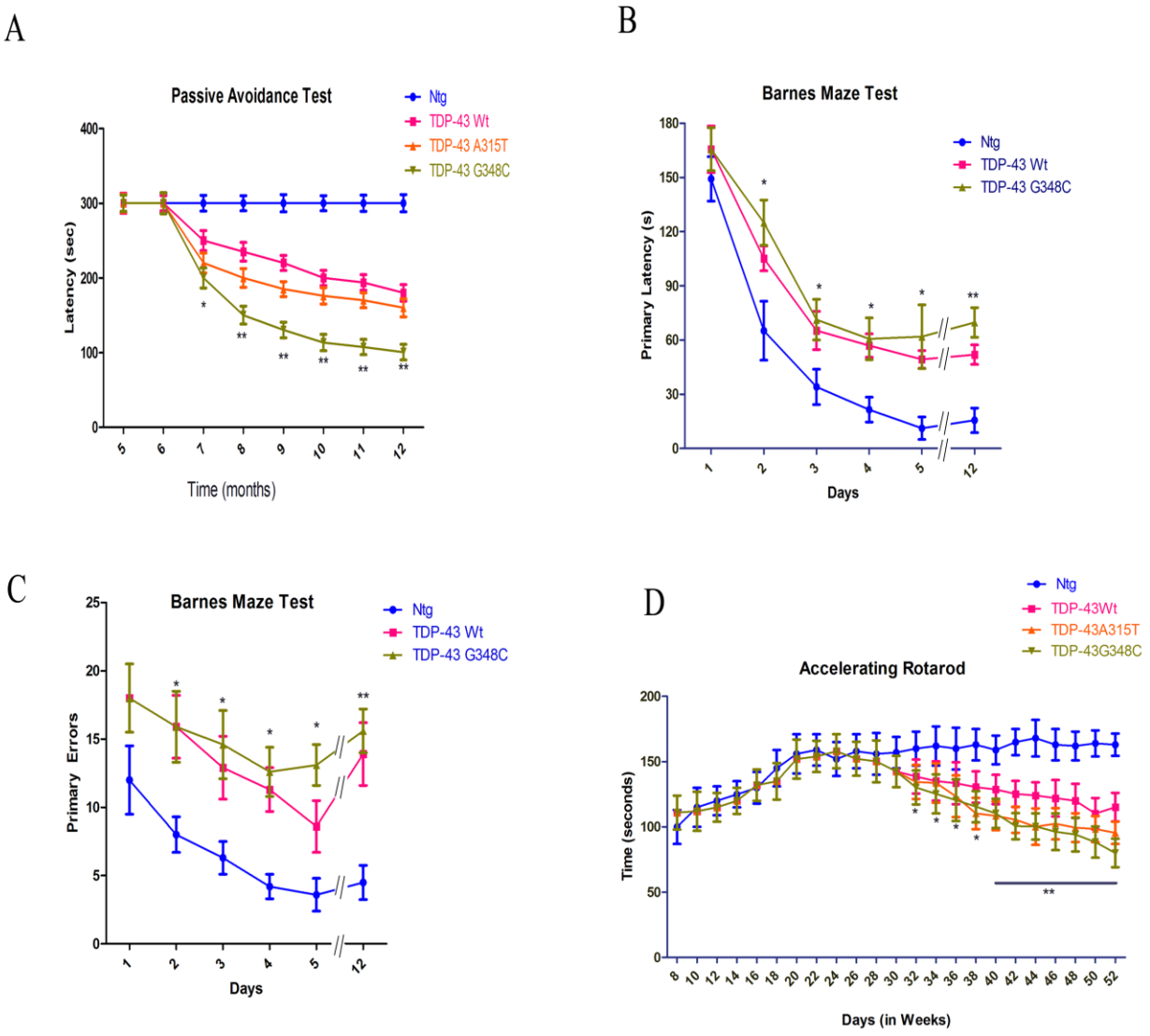

Figure 2.6. TDP-43 transgenic mice develop cognitive defects and motor dysfunction. A. Passive avoidance test of various transgenic mice was performed every month from 5 up to 12-months. Mice were placed in the light chamber, and mice entering in the dark chamber received a small shock. Each test set lasted for 2 days and on the 3rd day, contextual learning/memory of the mice was evaluated based on latency (in seconds) to enter the dark chamber. A two-way ANOVA with repeated measures was used to study the effect of group (transgenic and non-transgenic mice) and time (in months) on latency to go to the dark chamber. Pairwise comparisons were made using

Bonferroni adjustment. TDP-43^{G348C} mice showed significant deficits in contextual learning/memory at 7-months age (*p<0.01), while TDP-43^{A315T} and TDP-43^{Wt} mice showed significant deficiencies at 9-months age (**, p<0.001) as compared to non-transgenic control (Ntg). The cut-off time was 300sec; data shown are means ± SEM of 10 different mice from each group. **(B)** Barnes maze test was performed on 10-months old mice (TDP-43^{Wt}, TDP-43^{G348C} and Ntg). The spatial learning/memory capabilities are expressed as the primary latencies (latency to enter the target quadrant) exhibited in five consecutive sessions and one session at Day 12 of the test for long-term learning/memory analysis. A two-way ANOVA with repeated measures followed by bonferroni adjustment was used for statistical analysis. TDP-43^{G348C} and to a lesser extent TDP-43^{Wt} transgenic mice have severe spatial learning/memory deficits even at Day 2, which became increasingly prominent at Day 5. Long-term memory of TDP-43^{G348C} and TDP-43^{Wt} mice are also severely impaired as assessed at Day 12 (*p<0.01, **p<0.001). Results represent means ± SEM of three independent trials (n = 6 mice/group). **(C)** The spatial learning/memory capabilities are also expressed as the primary errors (number of errors before entering the target quadrant) exhibited in five consecutive sessions and one session at Day 12 of the test for long-term learning/memory analysis. TDP-43^{G348C} and to a lesser extent TDP-43^{Wt} transgenic mice have severe spatial learning/memory deficits even at Day 2, which became increasingly prominent at Day 5. Long-term memory of TDP-43^{G348C} and TDP-43^{Wt} mice are also severely impaired as assessed at Day 12 (*p<0.01, **p<0.001). Results represent means ± SEM of three independent trials (n = 6 mice/group). **(D)** Accelerating rotarod analysis of mice at various ages from 8-weeks to 52-weeks reveal that TDP-43^{G348C} mice had significant differences in rotarod latencies at 36-weeks of age, TDP-43^{A315T} at 38-weeks and TDP-43^{Wt} at 42-weeks of age as compared to non-transgenic control mice. A two-way ANOVA with repeated measures followed by bonferroni adjustment was used for statistical analysis, *p<0.01, **p<0.001. Data represent means ± SEM of three independent trials (n = 12 mice/group).

2.5.6 Age-related neuroinflammatory changes in TDP-43 mice precede behavioural defects

The microgliosis and astrogliosis were assessed in spinal cord and brains sections of different transgenic mice at presymptomatic stage (3 months) and after appearance of behavioural and sensorimotor deficits (10 months). Antibodies against Iba-1, a marker for microglial ion channel, revealed the existence of microgliosis in the brain and spinal cord sections of 10-months old TDP-43 transgenic mice (Fig. 2.7A-J). The microgliosis in the brain and spinal cord sections of 10-months old TDP-43^{Wt} and TDP-43^{A315T} mice was less pronounced than in 10-months TDP-43^{G348C} mice (Fig. E-H). Microgliosis was age-dependent as both spinal cord and brain sections of 3-months old TDP-43^{Wt}, TDP-43^{A315T} (Data not shown) and TDP-43^{G348C} mice (Fig. 2.7B&G) had far less microglial activation than 10-months old mice of same genotype. We also used antibodies against glial fibrillary acidic protein (GFAP) to detect astrogliosis in the brain (Fig. 2.7P-T) and spinal cord (Fig. 2.7K-O) sections of 10-months old TDP-43 transgenic mice. Again, astrogliosis in TDP-43^{Wt} and TDP-43^{A315T} mice was less severe than in TDP-43^{G348C} mice. Similar to microgliosis, astrogliosis was also age-dependent as both spinal cord and brain sections of 3-months old TDP-43^{Wt}, TDP-43^{A315T} (Data not shown) and TDP-43^{G348C} mice (Fig. 2.7L&Q) had far less astroglial activation than 10-months old mice of same genotype. We then quantified mRNA levels of various pro-inflammatory cytokines and chemokines in the spinal cord of 10-months old transgenic mice using quantitative real-time PCR. The mRNA levels of all studied cytokines and chemokines were upregulated in TDP-43^{Wt}, TDP-43^{A315T} and TDP-43^{G348C} mice when compared to their non-transgenic littermates. For instance, the levels of TNF-α (2.7-fold), IL-6 (2-fold), and MCP-1(2.5-fold) were all upregulated in TDP-43^{G348C} mice as compared to TDP-43^{Wt} mice (Fig. 2.7U).

We next asked the question whether neuroinflammatory signals can be detected in early, pre-onset staged of the disease. Previous results, using the sensitive live imaging approaches in SOD1 mutant models, revealed that one of the first signs of the disease is the transient induction of the GFAP signals (Keller et al., 2009). To investigate the temporal induction of gliosis and to relate it to sensorimotor and learning deficits, we generated by

breeding double transgenic mice carrying a TDP-43 transgene and a GFAP-luc transgene consisting of the reporter luciferase (luc) driven by the murine GFAP promoter.

To analyse the spatial and temporal dynamics of astrocytes activation/GFAP induction in TDP-43 mouse model, we performed series of live imaging experiments, starting at early 4–5 weeks of age until 52-weeks. Quantitative analysis of the imaging signals revealed an early (~20 weeks) and significant upregulation of GFAP promoter activity (Fig. 2.8A-H) in the brain of TDP-43^{G348C}/GFAP-luc mice. Starting at 20 weeks of age, the light signal intensity from the brain of TDP-43^{A315T}/GFAP-luc mice and TDP-43^{Wt}/GFAP-luc mice was also significantly elevated when compared to wild-type littermates, but the intensity was less than in GFAP-luc/TDP-43^{G348C} mice. The GFAP promoter activity in the brain progressively increased with age until it peaked at ~50 weeks for GFAP-luc/TDP-43^{G348C}, and at ~46 weeks for GFAP-luc/TDP-43^{A315T} (Supplemental Fig. 2.8) and GFAP-luc/TDP-43^{Wt} mice (Fig. 2.8Q). It is noteworthy that the induction of gliosis at 20 weeks in the brain of TDP-43 transgenic mice preceded the cognitive deficits first detected at ~28 weeks (Fig. 2.6). Likewise, in the spinal cord of all three TDP-43 mouse models, the induction of GFAP promoter activity signals at ~30 weeks of age (Fig. 2.8I-P & R and Supplemental Fig. 2.8) preceded the motor dysfunction first detected by the rotarod test at ~36 weeks of age. Hence, TDP-43 mediated pathogenesis is associated with an early induction of astrogliosis/GFAP signals and age dependent neuroinflammation.

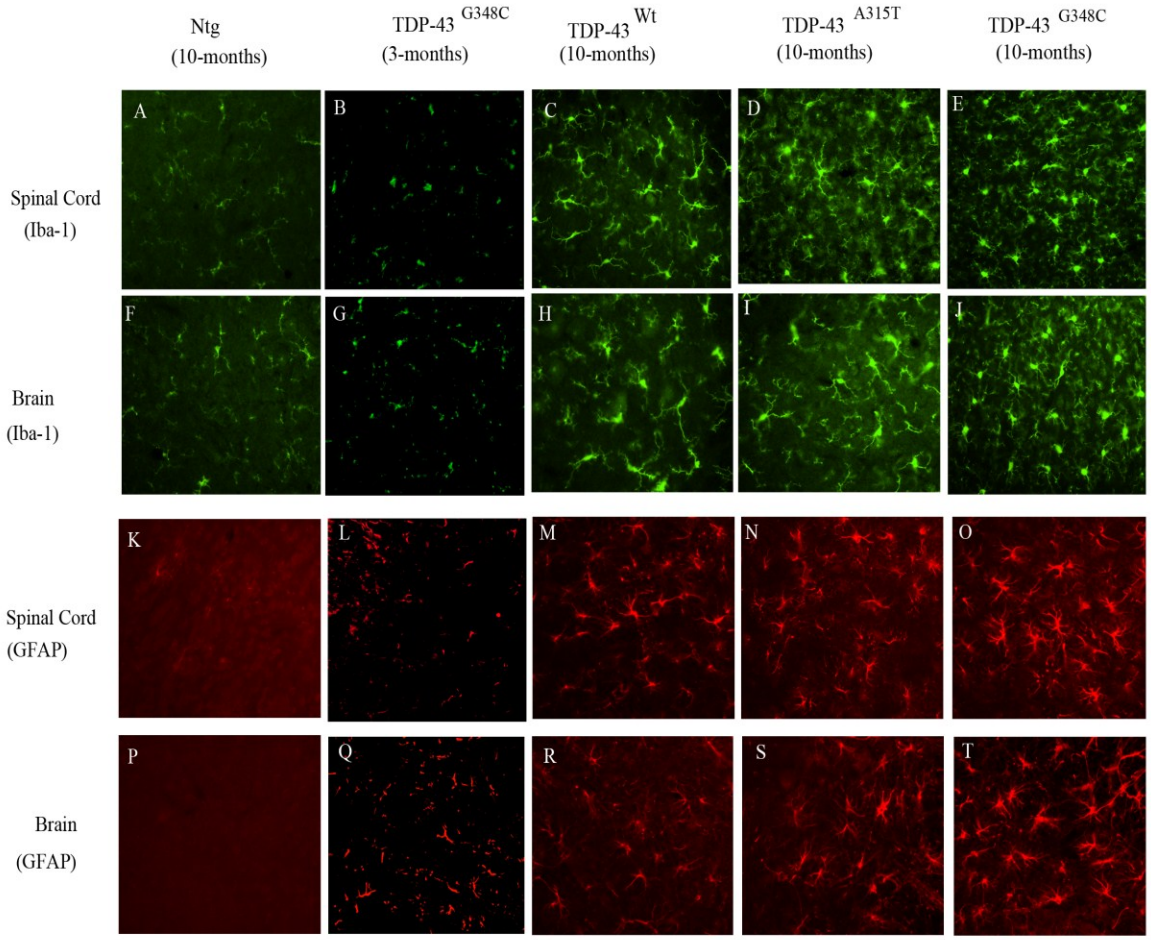
Ntg
(10-months)
TDP-43 G348C
(3-months)
TDP-43 Wt
(10-months)
TDP-43 A315T
(10-months)
TDP-43 G348C
(10-months)
Spinal Cord
(Iba-1)
Brain
(Iba-1)
Spinal Cord
(GFAP)
Brain
(GFAP)
A
B
C
D
E
F
G
H
I
J
K
L
M
N
O
P
Q
R
S
T

U

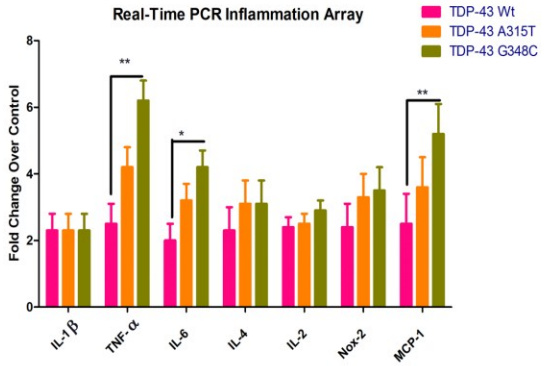
Real-Time PCR Inflammation Array
TDP-43 Wt
TDP-43 A315T
TDP-43 G348C
Fold Change Over Control
0
2
4
6
8
**
*
**
IL-1β
TNF-α
IL-6
IL-4
IL-2
Nox-2
MCP-1

Figure 2.7. Neuroinflammation in TDP-43 transgenic mice. A-H. Immunofluorescence of the spinal cord **(A-E)** and brain **(F-J)** sections of Ntg (non-transgenic), TDP-43^{Wt}, TDP-43^{A315T} and TDP-43^{G348C} mice was performed using anti-Iba-1 antibody. In the spinal cord microglial proliferation was abundant in 10-months old TDP-43^{G348C} mice **(E)**, followed by age-matched TDP-43^{A315T} **(D)** and TDP-43^{Wt} mice **(C)** as compared to non-transgenic control mice **(A)** and 3-months old TDP-43^{G348C} mice **(B)**. In brains sections also, microgliosis was intense in TDP-43^{G348C} mice **(J)** as well as in age-matched TDP-43^{A315T} **(I)** and TDP-43^{Wt} **(H)** as compared to non-transgenic control mice **(F)** and 3-months old TDP-43^{G348C} mice **(G)**. **K-T.** Immuno-fluorescence of the spinal cord **(K-O)** and brain **(P-T)** sections of Ntg, TDP-43^{Wt}, TDP-43^{A315T} and TDP-43^{G348C} mice was performed using anti-GFAP antibody. In the spinal cord astroglial proliferation was abundant in 10-months old TDP-43^{G348C} mice **(O)**, followed by age-matched TDP-43^{A315T} **(N)** and TDP-43^{Wt} **(M)** as compared to non-transgenic control mice **(K)** and 3-months old TDP-43^{G348C} mice **(L)**. In brains sections also, microgliosis was abundant in TDP-43^{G348C} mice **(T)** followed by age-matched TDP-43^{A315T} **(S)** and TDP-43^{Wt} **(R)** as compared to non-transgenic control mice **(P)** and 3-months old TDP-43^{G348C} mice **(Q)**. **(U).** Quantitative real-time PCR was performed on spinal cord tissue samples from 10-months old TDP-43^{Wt}, TDP-43^{A315T} and TDP-43^{G348C} transgenic mice and expressed as fold change over non-transgenic control littermates normalized to Atp-5α levels. One-way ANOVA was used with Tukey's post-hoc comparison for statistical analysis (n = 5 mice/group), *$p<0.01$, **$p<0.001$. The levels of TNF-α (2.7-fold, **$p<0.001$), IL-6 (2-fold, *$p<0.01$), and MCP-1(2.5-fold, **$p<0.001$) were upregulated in TDP-43^{G348C} mice as compared to TDP-43^{Wt} mice. Data represent means ± SEM of three independent experiments. Scale bars: **A-T** 50μm.

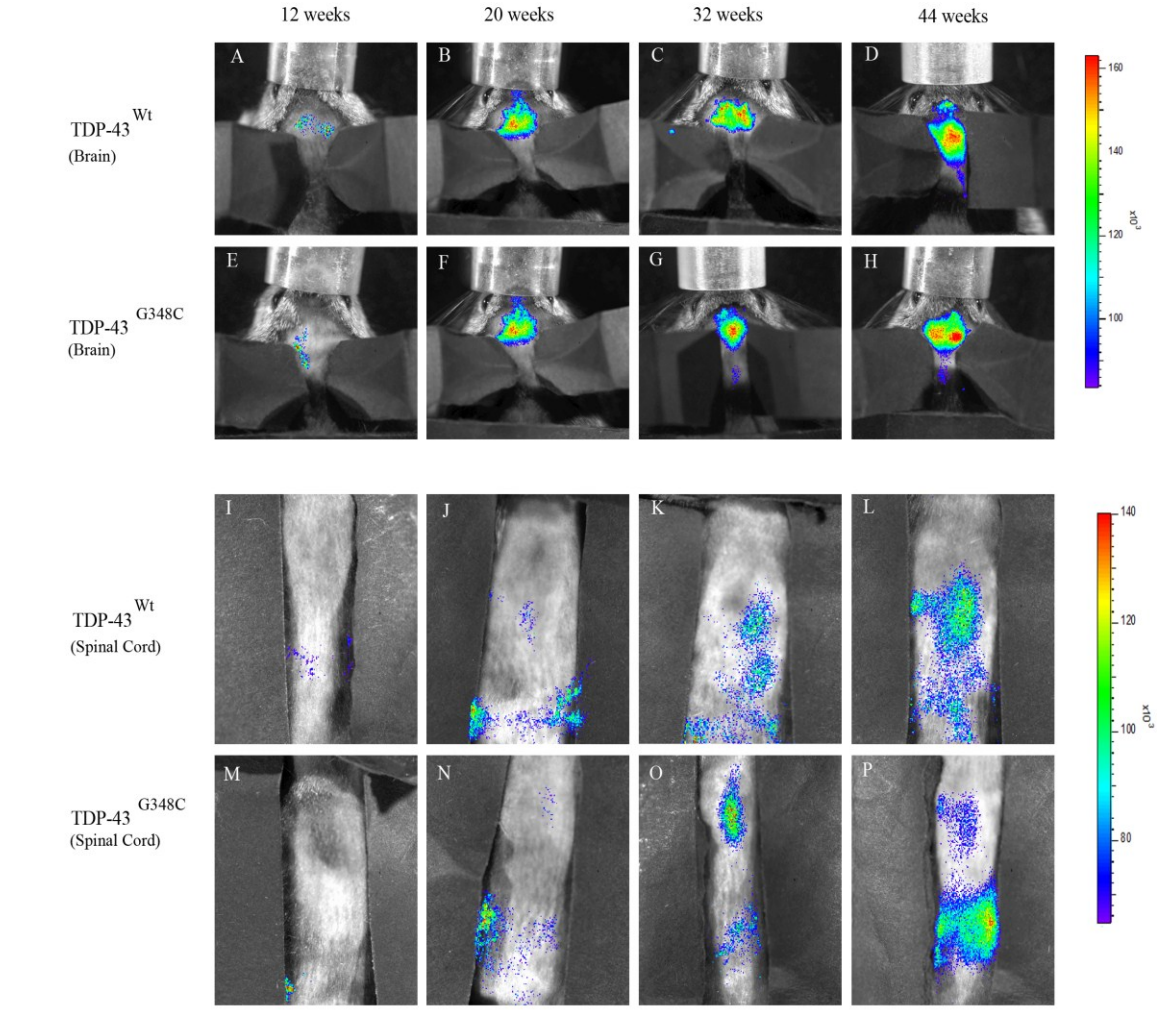
12 weeks
20 weeks
32 weeks
44 weeks
TDP-43 Wt (Brain)
TDP-43 G348C (Brain)
TDP-43 Wt (Spinal Cord)
TDP-43 G348C (Spinal Cord)
A
B
C
D
E
F
G
H
I
J
K
L
M
N
O
P
160
140
120
100
x10^3
140
120
100
80
x10^3

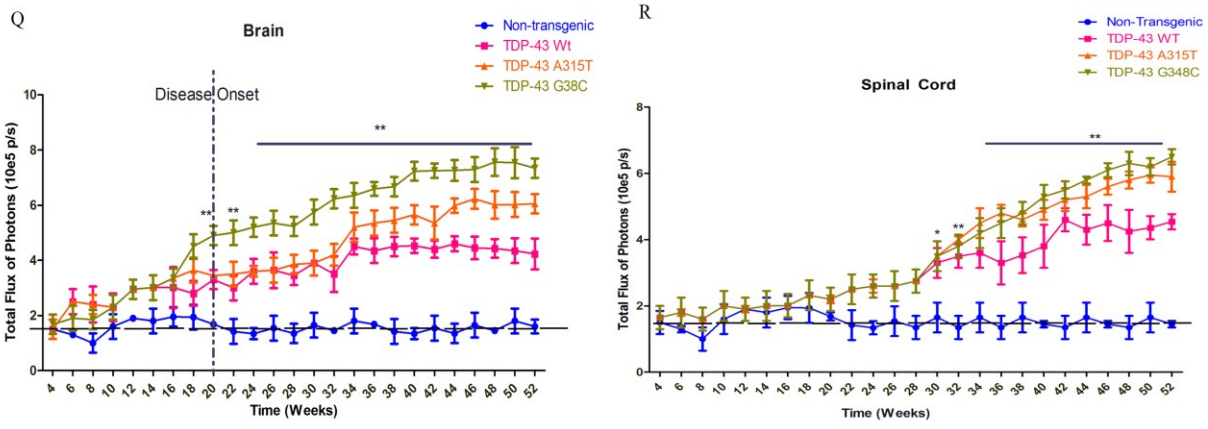
Q
Brain
Non-transgenic
TDP-43 Wt
TDP-43 A315T
TDP-43 G38C
Disease Onset
Total Flux of Photons (10e5 p/s)
Time (Weeks)
R
Spinal Cord
Non-Transgenic
TDP-43 WT
TDP-43 A315T
TDP-43 G348C
Total Flux of Photons (10e5 p/s)
Time (Weeks)

Figure 2.8. In vivo imaging revealed onset of astrocytosis before onset of behavioural impairments in doubly transgenic mice TDP-43/GFAP-luc. A-H. In vivo bioluminescence imaging of astrocytes activation was studied at various time points in the brain of GFAP-luc/TDP-43^{Wt} **(A-D)** and GFAP-luc/TDP-43^{G348C} **(E-H)** mice. Note that the GFAP-luc/TDP-43^{G348C} **(F)** mice had significant increase of GFAP promoter activity at 5-months (20-weeks) age compared to GFAP-luc/TDP-43^{Wt} **(B)** mice. **I-P.** Typical sequence of images of the spinal cord area obtained from of GFAP-luc/TDP-43^{Wt} **(I-L)** and GFAP-luc/TDP-43^{G348C} **(M-P)** mice at different time points by in vivo imaging. Significant GFAP promoter activity can be observed in GFAP-luc/TDP-43^{Wt} **(K)** and GFAP-luc/TDP-43^{G348C} **(O)** mice at 8-months (32-weeks) age. **Q-R:** Longitudinal quantitative analysis of the total photon GFAP-signal/ bioluminescence (total flux of photon/s) in GFAP-luc/TDP-$43^{Wt,}$ GFAP-luc/TDP-43^{A315T} and GFAP-luc/TDP-43^{G348C} mice in the brain **(Q)** and spinal cord **(R)**. A two-way ANOVA with repeated measures followed by bonferroni adjustment was used for statistical analysis, *$p<0.01$, **$p<0.001$.Data represent means ± SEM of three independent experiments (n = 12 mice/group).

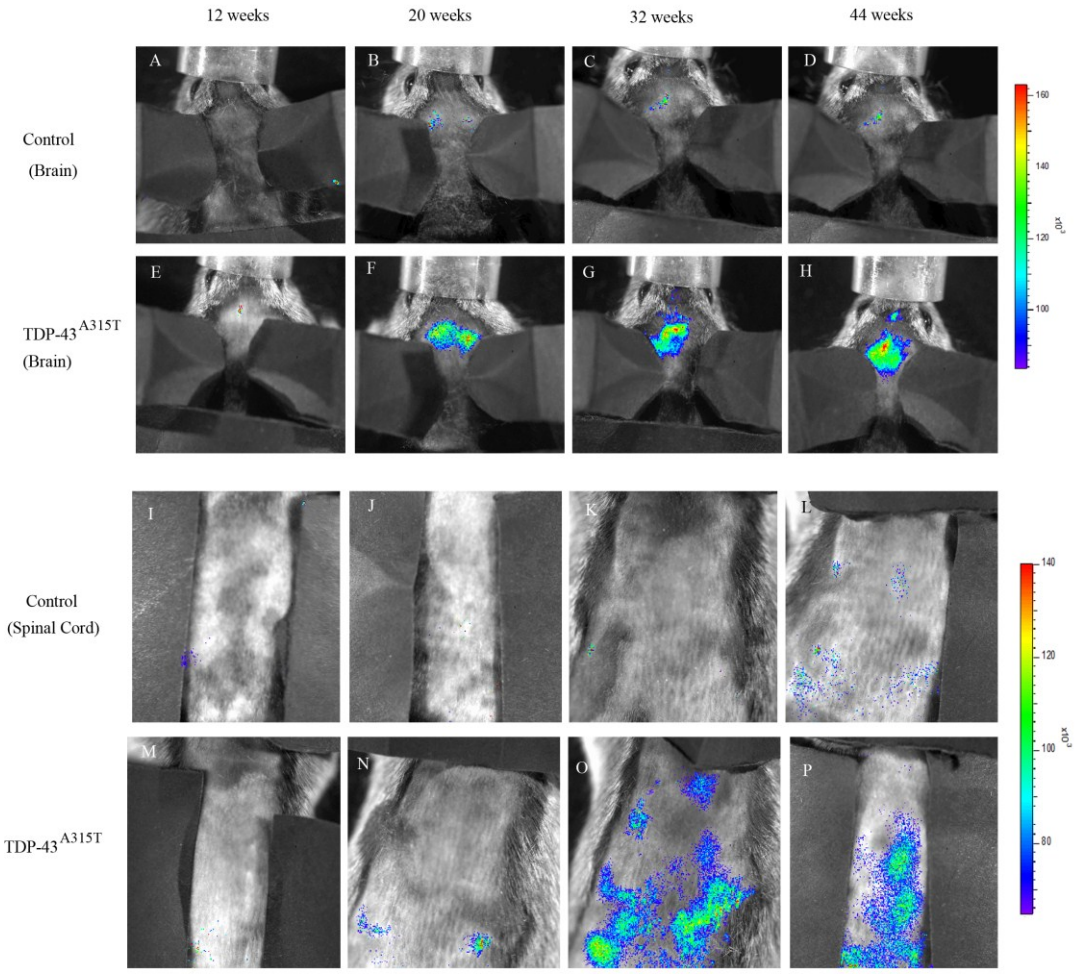

Supplemental Figure 2.8. GFAP induction in TDP-43^{A315T}/GFAP-luc transgenic mice

A-H. In vivo bioluminescence imaging of astrocytes activation was studied at various time points in the brain of GFAP-luc/control **(A-D)** and GFAP-luc/TDP-43^{A315T} **(E-H)** mice. Important to notice is that GFAP-luc/TDP-43^{A315T} **(F)** mice had significant GFAP promoter activity at 5-months (20-weeks) age compared to GFAP-luc/control **(B)** mice. **I-P.** Typical sequence of images of the spinal cord area obtained from of GFAP-luc/control **(I-L)** and GFAP-luc/TDP-43^{A315T} **(M-P)** mice at different time points by in vivo imaging. Significant GFAP promoter activity can be observed in GFAP-luc/control **(K)** and GFAP-luc/TDP-43^{A315T} **(O)** mice at 8-months (32-weeks) age.

2.6 Discussion

We report here the generation and characterization of novel transgenic mouse models of ALS-FTLD based on expression of genomic fragments encoding TDP-43 WT or mutants (A315T and G348C). The mouse models reported here carry TDP-43 transgenes under its own promoter resulting in ubiquitous and moderate expression (~3 fold) of hTDP-43 mRNA species. Most of the mouse models of TDP-43 reported previously have shown early paralysis followed by death. However, these mouse models are based on high expression levels of TDP-43 transgenes that can mask age-dependent pathogenic pathways. Mice expressing either wild-type or mutant TDP-43 (A315T and M337V) showed aggressive paralysis accompanied by increased ubiquitination (Wegorzewska et al., 2009; Stallings et al., 2010; Wils et al., 2010; Xu et al., 2010) but the lack of ubiquitinated TDP-43 positive inclusions raises concerns about their validity as models of human ALS disease. Another concern is the restricted expression of TDP-43 species with the use of Thy1.2 and Prion promoters. To better mimic the ubiquitous and moderate levels of TDP-43 occurring in the human context, it seems more appropriate to generate transgenic mice with genomic DNA fragments of TDP-43 gene including its own promoter. As in human neurodegenerative disease, our TDP-43 transgenic mice exhibited age-related phenotypic defects including impairment in contextual learning/memory and spatial learning/memory as determined by passive avoidance test and Barnes maze test. Long term memory of 10-months old TDP-43^{G348C} transgenic mice was severely impaired according to Barnes maze test. The TDP-43^{G348C}, TDP-43^{A315T} and to a lesser extent TDP-43^{Wt} mice exhibited also motor deficits as depicted by significant reductions in latency in the accelerating rotarod test.

Cognitive and motor deficits in TDP-43 transgenic mice prompted us to test the underlying pathological and biochemical changes in these mice. Western blot analysis of spinal cord lysates of transgenic mice revealed ~25-kDa and ~35-kDa TDP-43 cleavage fragments which increased in levels with age. Previous studies demonstrated cytotoxicity of the ~25-kDa fragment (Zhang et al., 2009). Immunofluorescence studies with human TDP-43 specific monoclonal antibodies revealed TDP-43 cytoplasmic aggregates in the spinal cord

of TDP-43^{G348C}, TDP-43^{A315T} and to lesser extent in TDP-43^{Wt} mice. The cytoplasmic TDP-43 positive inclusions were ubiquitinated. The TDP-43 positive ubiquitinated cytoplasmic inclusions along with ~25-kDa cytotoxic fragments are reminiscent of those described in studies on ALS and FTLD-U patients (Neumann et al., 2006). The co-immunoprecipitation of ubiquitin with anti-TDP-43 antibody and inversely of TDP-43 with anti-ubiquitin antibody (Fig. 2.2U&V) using spinal cord samples from TDP-43^{G348C} mice further confirmed the association of TDP-43 with ubiquitinated protein aggregates. However, TDP-43 itself was not extensively ubiquitinated. A thorough survey of articles on TDP-43 led us to the conclusion that there is no compelling biochemical evidence in literature supporting the general belief that TDP-43 is the major poly-ubiquitinated protein in the TDP-43 positive inclusions. We could find only one blot from one ALS case in one paper (Neumann et al., 2006) that revealed a very weak detection of high molecular weight smear with anti-TDP-43 after TDP-43 immunoprecipitation. A subsequent paper by (Sanelli et al., 2007) has concluded from 3D-deconvolution imaging that TDP-43 is not in fact the major ubiquitinated target in ubiquitinated inclusions of ALS.

The TDP-43 transgenic mice described here exhibit perikaryal and axonal aggregates of intermediate filaments, another hallmark of degenerating motor neurons in ALS (Carpenter, 1968; Corbo and Hays, 1992; Migheli et al., 1993). Before the onset of behavioural changes in these mice, there is formation of peripherin aggregates in the spinal cord and brain sections of TDP-43^{G348C} as well as in TDP-43^{A315T} transgenic mice. These peripherin inclusions were also seen in the hippocampal region of the brain of TDP-43^{G348C} mice. Normally peripherin is not expressed in brain. However, it is known that peripherin expression in the brain can be upregulated after injury or stroke (Beaulieu et al., 2002). The enhanced peripherin levels in these mice are probably due to an upregulation of IL-6, a cytokine that can trigger peripherin expression (Sterneck et al., 1996). Sustained peripherin overexpression by over 4 fold in transgenic mice was found previously to provoke progressive motor neuron degeneration during aging (Jacomy et al., 1999). In addition, we detected in TDP-43 transgenic mice the presence of abnormal splicing variants of peripherin, such as Per 61, that can contribute to formation of IF aggregates (Robertson et al., 2003). Using Per61 specific antibodies we detected peripherin inclusions in the spinal

cord sections of TDP-43^{G348C} mice, but not in TDP-43^{Wt} mice (Fig. 2.3). The occurrence of specific splicing peripherin variants has also been reported in human ALS cases (Xiao et al., 2008).

In addition we detected neurofilament protein anomalies in TDP-43^{G348C} mice. Double immunofluorescence revealed the detection of neurofilament NF-H and NF-M in inclusion bodies with peripherin in the spinal cord of TDP-43^{G348C} mice. Moreover, we found that neurofilament NF-L is downregulated in the spinal cord lysates of TDP-43^{G348C} mice, a phenomenon which has also been observed in motor neurons of ALS cases (Wong et al., 2000). A decrease in NF-L levels may explain in part the age-related axonal atrophy detected in TDP-43 mice. Previous studies with NF-L knockout mice demonstrated that such substantial shift in calibres of large myelinated axons provokes a reduction of axon conduction velocity by ~3 fold (Kriz et al., 2000). In large animals with long peripheral nerves this would cause neurological disease. A loss of neurofilaments due to a homozygous recessive mutation in the NEFL gene was found recently to cause a severe early-onset axonal neuropathy (Yum et al., 2009).

Age-related neuroinflammation constitutes another striking feature of the TDP-43 transgenic mice. In vivo imaging of biophotonic doubly transgenic mice bearing TDP-43 and GFAP-luc transgenes showed that astrocytes are activated as early as 20 weeks in the brain of GFAP-luc/TDP-43^{G348C} mice followed by activation in the spinal cord at ~30 weeks of age. The signal intensity for astrocytosis in GFAP-luc/TDP-43^{A315T} and GFAP-luc/TDP-43^{Wt} was less than in GFAP-luc/TDP-43^{G348C} mice. It is noteworthy that the induction of astrogliosis detected in the brain and spinal cord in all three TDP-43 mouse models preceded by 6 to 8 weeks the appearance of cognitive and motor defects. This finding is in line with the recent view of an involvement of reactive astrocytes in ALS pathogenesis (Barbeito et al., 2004; Di Giorgio et al., 2007; Julien, 2007; Nagai et al., 2007; Di Giorgio et al., 2008).

In conclusion, the TDP-43 transgenic mice described here mimic several aspects of the behavioural, pathological and biochemical features of human ALS/FTLD including age-related development of motor and cognitive dysfunction, cytoplasmic TDP-43 positive

ubiquitinated inclusions, intermediate filament abnormalities, axonopathy and neuroinflammation. Why there is no overt degeneration in our TDP-43 mouse models*?* Unlike previous TDP-43 transgenic mice, these transgenics were made with genomic fragment that contains 3' sequence autoregulating TDP-43 synthesis (Polymenidou *et al*., 2011). So, the TDP-43 levels remain moderate. The ubiquitous TDP-43 overexpression by about 3 folds in these mice mimics the ~2.5-fold increase of TDP-43 mRNA measured in the spinal cord of human sporadic ALS by quantitative real-time PCR (our unpublished result). We don't know why in human ALS cases carrying TDP-43 mutations, it takes many decades before ALS disease onset. This question remains unanswered but perhaps future studies with TDP-43 mouse models might provide some insights. In any case, our new TDP-43 mouse models should provide valuable tools for unravelling pathogenic pathways of ALS/FTLD and for preclinical drug testing.

2.7 Acknowledgement

We thank Genevieve Soucy for technical assistance. We are grateful to Jean-Nicolas Audet and the transgenic facility of Centre Hospitalier Universitaire de Québec (CHUQ) for generating and maintaining transgenic mice. This work was supported by the Canadian Institutes of Health Research (CIHR), the ALS Society of Canada, the Muscular Dystrophy of Canada and the Fondation André-Delambre. J.-P.J. holds a Canada Research Chair Tier 1 in mechanisms of neurodegeneration. J.K. holds a R&D/HRF/CIHR Career Award. V.S. is the recipient of the Merit Scholarship for Foreign Students (FQRNT, Quebec, Canada).

2.8 References

Barbeito LH, Pehar M, Cassina P, Vargas MR, Peluffo H, Viera L, Estevez AG, Beckman JS (2004) A role for astrocytes in motor neuron loss in amyotrophic lateral sclerosis. Brain Res Brain Res Rev 47:263-274.

Beaulieu JM, Kriz J, Julien JP (2002) Induction of peripherin expression in subsets of brain neurons after lesion injury or cerebral ischemia. Brain Res 946:153-161.

Bose JK, Wang IF, Hung L, Tarn WY, Shen CK (2008) TDP-43 overexpression enhances exon 7 inclusion during the survival of motor neuron pre-mRNA splicing. J Biol Chem 283:28852-28859.

Buratti E, Dork T, Zuccato E, Pagani F, Romano M, Baralle FE (2001) Nuclear factor TDP-43 and SR proteins promote in vitro and in vivo CFTR exon 9 skipping. EMBO J 20:1774-1784.

Cairns NJ et al. (2007) TDP-43 in familial and sporadic frontotemporal lobar degeneration with ubiquitin inclusions. Am J Pathol 171:227-240.

Carpenter S (1968) Proximal axonal enlargement in motor neuron disease. Neurology 18:841-851.

Corbo M, Hays AP (1992) Peripherin and neurofilament protein coexist in spinal spheroids of motor neuron disease. J Neuropathol Exp Neurol 51:531-537.

Dequen F, Bomont P, Gowing G, Cleveland DW, Julien JP (2008) Modest loss of peripheral axons, muscle atrophy and formation of brain inclusions in mice with targeted deletion of gigaxonin exon 1. J Neurochem 107:253-264.

Di Giorgio FP, Boulting GL, Bobrowicz S, Eggan KC (2008) Human embryonic stem cell-derived motor neurons are sensitive to the toxic effect of glial cells carrying an ALS-causing mutation. Cell Stem Cell 3:637-648.

Di Giorgio FP, Carrasco MA, Siao MC, Maniatis T, Eggan K (2007) Non-cell autonomous effect of glia on motor neurons in an embryonic stem cell-based ALS model. Nat Neurosci 10:608-614.

Forman MS, Trojanowski JQ, Lee VM (2007) TDP-43: a novel neurodegenerative proteinopathy. Curr Opin Neurobiol 17:548-555.

Gitcho MA, Baloh RH, Chakraverty S, Mayo K, Norton JB, Levitch D, Hatanpaa KJ, White CL, 3rd, Bigio EH, Caselli R, Baker M, Al-Lozi MT, Morris JC, Pestronk A, Rademakers R, Goate AM, Cairns NJ (2008) TDP-43 A315T mutation in familial motor neuron disease. Ann Neurol 63:535-538.

Gros-Louis F, Kriz J, Kabashi E, McDearmid J, Millecamps S, Urushitani M, Lin L, Dion P, Zhu Q, Drapeau P, Julien JP, Rouleau GA (2008) Als2 mRNA splicing variants detected in KO mice rescue severe motor dysfunction phenotype in Als2 knock-down zebrafish. Hum Mol Genet 17:2691-2702.

Hodges JR, Davies RR, Xuereb JH, Casey B, Broe M, Bak TH, Kril JJ, Halliday GM (2004) Clinicopathological correlates in frontotemporal dementia. Ann Neurol 56:399-406.

Jacomy H, Zhu Q, Couillard-Despres S, Beaulieu JM, Julien JP (1999) Disruption of type IV intermediate filament network in mice lacking the neurofilament medium and heavy subunits. J Neurochem 73:972-984.

Julien JP (2007) ALS: astrocytes move in as deadly neighbors. Nat Neurosci 10:535-537.

Kabashi E, Valdmanis PN, Dion P, Spiegelman D, McConkey BJ, Vande Velde C, Bouchard JP, Lacomblez L, Pochigaeva K, Salachas F, Pradat PF, Camu W, Meininger V, Dupre N, Rouleau GA (2008) TARDBP mutations in individuals with sporadic and familial amyotrophic lateral sclerosis. Nat Genet 40:572-574.

Keller AF, Gravel M, Kriz J (2009) Live imaging of amyotrophic lateral sclerosis pathogenesis: disease onset is characterized by marked induction of GFAP in Schwann cells. Glia 57:1130-1142.

Keller AF, Gravel M, Kriz J (2010) Treatment with minocycline after disease onset alters astrocyte reactivity and increases microgliosis in SOD1 mutant mice. Exp Neurol.

Kriz J, Meier J, Julien JP, Padjen AL (2000) Altered ionic conductances in axons of transgenic mouse expressing the human neurofilament heavy gene: A mouse model of amyotrophic lateral sclerosis. Exp Neurol 163:414-421.

Lagier-Tourenne C, Cleveland DW (2009) Rethinking ALS: the FUS about TDP-43. Cell 136:1001-1004.

Lomen-Hoerth C, Murphy J, Langmore S, Kramer JH, Olney RK, Miller B (2003) Are amyotrophic lateral sclerosis patients cognitively normal? Neurology 60:1094-1097.

Lu CH, Kalmar B, Malaspina A, Greensmith L, Petzold A (2011) A method to solubilise protein aggregates for immunoassay quantification which overcomes the neurofilament "hook" effect. J Neurosci Methods 195:143-150.

Mercado PA, Ayala YM, Romano M, Buratti E, Baralle FE (2005) Depletion of TDP 43 overrides the need for exonic and intronic splicing enhancers in the human apoA-II gene. Nucleic Acids Res 33:6000-6010.

Migheli A, Pezzulo T, Attanasio A, Schiffer D (1993) Peripherin immunoreactive structures in amyotrophic lateral sclerosis. Lab Invest 68:185-191.

Nagai M, Re DB, Nagata T, Chalazonitis A, Jessell TM, Wichterle H, Przedborski S (2007) Astrocytes expressing ALS-linked mutated SOD1 release factors selectively toxic to motor neurons. Nat Neurosci 10:615-622.

Neumann M, Sampathu DM, Kwong LK, Truax AC, Micsenyi MC, Chou TT, Bruce J, Schuck T, Grossman M, Clark CM, McCluskey LF, Miller BL, Masliah E, Mackenzie IR, Feldman H, Feiden W, Kretzschmar HA, Trojanowski JQ, Lee VM (2006) Ubiquitinated TDP-43 in frontotemporal lobar degeneration and amyotrophic lateral sclerosis. Science 314:130-133.

Noto YI, Shibuya K, Sato Y, Kanai K, Misawa S, Sawai S, Mori M, Uchiyama T, Isose S, Nasu S, Sekiguchi Y, Fujimaki Y, Kasai T, Tokuda T, Nakagawa M, Kuwabara S (2010) Elevated CSF TDP-43 levels in amyotrophic lateral sclerosis: Specificity, sensitivity, and a possible prognostic value. Amyotroph Lateral Scler.

Ou SH, Wu F, Harrich D, Garcia-Martinez LF, Gaynor RB (1995) Cloning and characterization of a novel cellular protein, TDP-43, that binds to human immunodeficiency virus type 1 TAR DNA sequence motifs. J Virol 69:3584-3596.

Polymenidou M, Lagier-Tourenne C, Hutt KR, Huelga SC, Moran J, Liang TY, Ling SC, Sun E, Wancewicz E, Mazur C, Kordasiewicz H, Sedaghat Y, Donohue JP, Shiue L, Bennett CF, Yeo GW, Cleveland DW (2011) Long pre-mRNA depletion and RNA missplicing contribute to neuronal vulnerability from loss of TDP-43. Nat Neurosci 14:459-468.

Prut L, Abramowski D, Krucker T, Levy CL, Roberts AJ, Staufenbiel M, Wiessner C (2007) Aged APP23 mice show a delay in switching to the use of a strategy in the Barnes maze. Behav Brain Res 179:107-110.

Robertson J, Doroudchi MM, Nguyen MD, Durham HD, Strong MJ, Shaw G, Julien JP, Mushynski WE (2003) A neurotoxic peripherin splice variant in a mouse model of ALS. J Cell Biol 160:939-949.

Rutherford NJ et al. (2008) Novel mutations in TARDBP (TDP-43) in patients with familial amyotrophic lateral sclerosis. PLoS Genet 4:e1000193.

Sanelli T, Xiao S, Horne P, Bilbao J, Zinman L, Robertson J (2007) Evidence that TDP-43 is not the major ubiquitinated target within the pathological inclusions of amyotrophic lateral sclerosis. Journal of neuropathology and experimental neurology 66:1147-1153.

Seeley WW (2008) Selective functional, regional, and neuronal vulnerability in frontotemporal dementia. Curr Opin Neurol 21:701-707.

Sreedharan J, Blair IP, Tripathi VB, Hu X, Vance C, Rogelj B, Ackerley S, Durnall JC, Williams KL, Buratti E, Baralle F, de Belleroche J, Mitchell JD, Leigh PN, Al-Chalabi A, Miller CC, Nicholson G, Shaw CE (2008) TDP-43 mutations in familial and sporadic amyotrophic lateral sclerosis. Science 319:1668-1672.

Stallings NR, Puttaparthi K, Luther CM, Elliott JL (2009) Generation and characterization of wild-type and mutant TDP-43 transgenic mice. Society For Neuroscience, Abstract Book 2009.

Stallings NR, Puttaparthi K, Luther CM, Burns DK, Elliott JL (2010) Progressive motor weakness in transgenic mice expressing human TDP-43. Neurobiol Dis 40:404-414.

Sterneck E, Kaplan DR, Johnson PF (1996) Interleukin-6 induces expression of peripherin and cooperates with Trk receptor signaling to promote neuronal differentiation in PC12 cells. J Neurochem 67:1365-1374.

Talbot K, Ansorge O (2006) Recent advances in the genetics of amyotrophic lateral sclerosis and frontotemporal dementia: common pathways in neurodegenerative disease. Hum Mol Genet 15 Spec No 2:R182-187.

Van Deerlin VM et al. (2008) TARDBP mutations in amyotrophic lateral sclerosis with TDP-43 neuropathology: a genetic and histopathological analysis. Lancet Neurol 7:409-416.

Wegorzewska I, Bell S, Cairns NJ, Miller TM, Baloh RH (2009) TDP-43 mutant transgenic mice develop features of ALS and frontotemporal lobar degeneration. Proc Natl Acad Sci U S A 106:18809-18814.

Wils H, Kleinberger G, Janssens J, Pereson S, Joris G, Cuijt I, Smits V, Ceuterick-de Groote C, Van Broeckhoven C, Kumar-Singh S (2010) TDP-43 transgenic mice develop spastic paralysis and neuronal inclusions characteristic of ALS and frontotemporal lobar degeneration. Proc Natl Acad Sci U S A 107:3858-3863.

Wong NK, He BP, Strong MJ (2000) Characterization of neuronal intermediate filament protein expression in cervical spinal motor neurons in sporadic amyotrophic lateral sclerosis (ALS). J Neuropathol Exp Neurol 59:972-982.

Xiao S, Tjostheim S, Sanelli T, McLean JR, Horne P, Fan Y, Ravits J, Strong MJ, Robertson J (2008) An aggregate-inducing peripherin isoform generated through

intron retention is upregulated in amyotrophic lateral sclerosis and associated with disease pathology. J Neurosci 28:1833-1840.

Xu YF, Gendron TF, Zhang YJ, Lin WL, D'Alton S, Sheng H, Casey MC, Tong J, Knight J, Yu X, Rademakers R, Boylan K, Hutton M, McGowan E, Dickson DW, Lewis J, Petrucelli L (2010) Wild-Type Human TDP-43 Expression Causes TDP-43 Phosphorylation, Mitochondrial Aggregation, Motor Deficits, and Early Mortality in Transgenic Mice. J Neurosci 30:10851-10859.

Yokoseki A, Shiga A, Tan CF, Tagawa A, Kaneko H, Koyama A, Eguchi H, Tsujino A, Ikeuchi T, Kakita A, Okamoto K, Nishizawa M, Takahashi H, Onodera O (2008) TDP-43 mutation in familial amyotrophic lateral sclerosis. Ann Neurol 63:538-542.

Yum SW, Zhang J, Mo K, Li J, Scherer SS (2009) A novel recessive Nefl mutation causes a severe, early-onset axonal neuropathy. Ann Neurol 66:759-770.

Zhang YJ, Xu YF, Cook C, Gendron TF, Roettges P, Link CD, Lin WL, Tong J, Castanedes-Casey M, Ash P, Gass J, Rangachari V, Buratti E, Baralle F, Golde TE, Dickson DW, Petrucelli L (2009) Aberrant cleavage of TDP-43 enhances aggregation and cellular toxicity. Proc Natl Acad Sci U S A 106:7607-7612.

Chapter 3 Impaired sciatic nerve regeneration following axotomy in transgenic mice overexpressing TDP-43 species.

Submitted to the Journal of Neuroscience

Vivek Swarup, Jean-Nicolas Audet, Daniel Phaneuf and Jean-Pierre Julien

Centre de Recherche du Centre Hospitalier Universitaire de Québec, Department of Psychiatry and Neuroscience of Laval University, Québec, QC, Canada G1V 4G2

3.1 Resume

Il a été démontré que dans la pathogenèse de la sclérose latérale amyotrophique (SLA) et de la démence lobaire fronto-temporale (DLFT-U), une mauvaise répartition de la protéine TDP-43 dans la cellule, est impliquée. Pour mieux comprendre les mécanismes pathogènes impliquant la protéine TDP-43, des lésions du nerf sciatique ont été effectuées chez des souris surexprimant la TDP-43 de type sauvage ou mutante (G348C). Suite à la lésion axonale, les souris non-transgéniques avaient retrouvé en grande partie leur mobilité habituelle, tandis que les souris transgéniques TDP-43, étaient encore nettement paralysées. Les analyses phénotypiques et histologiques ont été effectuées à différents moments jusqu'à 28 jours après la blessure et les niveaux d'expression de la TDP-43, de la périphérine et de l'ubiquitine, ont été analysés. Contrairement aux souris contrôles, la redistribution de TDP-43 du cytoplasme vers le noyau a été significativement retardée chez les souris transgéniques après lésion du nerf. Nous avons notées que les niveaux de périphérine et d'ubiquitine sont significativement plus élevés dans les souris transgéniques TDP-43 par rapport aux souris témoins. L'analyse du nerf sciatique 11 jours après la lésion, a montré que le nombre d'axones en régénération a été considérablement réduit dans la partie distale de la lésion chez les souris transgéniques. Par le fait même, l'analyse du calibre des ces mêmes axones, a également démontré que le calibre est légèrement inférieur par rapport aux souris normales. En outre, la microgliose et la production de cytokines ont été maintenues beaucoup plus longtemps dans les souris transgéniques surexprimant la TDP-43 de type sauvage ou mutant. Nos résultats suggèrent que l'expression de la protéine TDP-43, en particulier la forme mutante, est associée à un retard dans les processus de croissance et de récupération axonale suite à une lésion du nerf.

3.2 Abstract

Tar DNA Binding protein 43 (TDP-43) mislocalization and aggregation is a hallmark of in the pathogenesis of amyotrophic lateral sclerosis (ALS) and frontotemporal lobar dementia (FTLD-U). Here we have examined the effects of nerve injury in new transgenic mouse models overexpressing wild type (WT) or mutant (G348C) TDP-43. Four weeks after axonal crush of sciatic nerve, TDP-43 transgenic mice remained paralyzed at the injured limb unlike normal mice which had regained most of their normal mobility. Phenotypic and histological analyses were performed at different time points until 28 days after injury and TDP-43, peripherin and ubiquitin expression levels were analyzed. In contrast to control mice, redistribution of TDP-43 from cytoplasm to nucleus was significantly delayed in TDP-43 transgenic mice following nerve crush. Peripherin and ubiquitin levels were significantly elevated in TDP-43 transgenic mice compared to control mice. Analysis of the sciatic nerve 11 days after nerve crush showed that the number of regenerating axons in the distal portion of the lesion was considerably reduced in transgenic mice. Their caliber was also slightly lower compared to normal mice. In addition, microgliosis and increases cytokine profile were maintained much longer in transgenic mice overexpressing wild-type or mutant TDP-43. Our results suggest that TDP-43 expression, especially the mutant form, is associated with axonal growth impairment following injury.

3.3 Introduction

ALS is an adult-onset neurodegenerative disorder characterized by the progressive degeneration of motor neurons in the brain and spinal cord. TAR DNA binding protein 43 (TDP-43), a DNA/RNA-binding 43kDa protein, has been implicated in ALS (Arai et al., 2006; Neumann et al., 2006) and dominant mutations in *TARDBP*, which codes for TDP-43, were reported by several groups as a primary cause of ALS (Gitcho et al., 2008; Kabashi et al., 2008; Sreedharan et al., 2008; Van Deerlin et al., 2008) and may account for ~3% of familial ALS cases and ~1.5% of sporadic cases. TDP- 43, normally observed in the nucleus, is detected in pathological inclusions in the cytoplasm and nucleus of both neurons and glial cells of ALS and frontotemporal lobar degeneration with ubiquitin inclusions (FTLD-U) cases (Arai et al., 2006; Neumann et al., 2006).The inclusions consist prominently of TDP-43 C-terminal fragments (CTFs) of ~25kDa. The physiological role of TDP-43 and the pathogenic pathways of TDP-43 abnormalities are not well understood. TDP-43 is essential for embryogenesis (Sephton et al., 2010) and postnatal deletion of the TDP-43 gene in mice caused downregulation of *Tbc1d1*, a gene that alters body fat metabolism (Chiang et al., 2010). Neuronal overexpression at high levels of wild-type or mutant TDP-43 in transgenic mice caused a dose-dependent degeneration of cortical and spinal motor neurons but with no cytoplasmic TDP-43 aggregates (Wegorzewska et al., 2009; Stallings et al., 2010; Wils et al., 2010; Xu et al., 2010) raising up the possibility that an upregulation of TDP-43 in the nucleus rather than TDP-43 cytoplasmic aggregates may contribute to neurodegeneration. In fact TDP-43 has been reported to be upregulated in the cerebrospinal fluid of patients with ALS (Kasai et al., 2009) and in peripheral blood lymphocytes from ALS patients (Mougeot et al., 2011; Nardo et al., 2011). More recently work from our lab has shown that TDP-43 is upregulated in the spinal cord of sporadic ALS cases both at the mRNA and protein levels (Swarup et al., 2011a). Curiously, such upregulation of TDP-43 is also observed in the axotomized spinal motor neurons (Moisse et al., 2009b). The fact that TDP-43 is a NFL mRNA binding protein capable of stabilizing the mRNA transcript (Strong et al., 2007) suggests that TDP-43 has a critical role in mediating the response of the neuronal cytoskeleton to neuronal injury. In order to determine the effects of increased levels of TDP-43 on neuronal response to injury, we

used our transgenic mice bearing genomic fragments expressing ubiquitously moderate levels of human TDP-43 wild-type or mutant TDP-43^{G348C} (Swarup et al., 2011b). We determined the response to nerve crush injury prior to the development of clinical symptoms and pathological features

Overexpression of wild-type and mutant TDP-43 in transgenic mice resulted in altered cytoplasmic TDP-43 localization following axonal injury. Histochemical analyses of the spinal cord and sciatic nerve after crush provided evidence of persistent neuronal injury that was accompanied by sustained behavioral deficits. We observed altered levels of ubiquitin and peripherin after nerve-injury in transgenic mice. TDP-43^{Wt} and TDP-43^{G348C} mice exhibited exaggerated microglial response following nerve-injury as evidenced by increased Mac-2+ cell count and proinflammatory cytokine levels. Our data indicate that a deregulation of TDP-43 in ALS can contribute regeneration impairment after neuronal injury.

3.4 Materials and Methods:

Generation of TDP-43 transgenic mice

TARDBP (NM_007375) was amplified by PCR from a human BAC clone (clone RPCI-11, clone number: 829B14) along with the endogenous promoter (~4kB). A315T and G348C mutations in TDP-43 were inserted using site-directed mutagenesis. The full-length genomic *TARDBP* (TDP-43^{Wt} and TDP-43^{G348C}) was linearized by Swa-1 restriction enzyme and 18 kb DNA fragment microinjected in one-day mouse embryos (having a background of C3H X C57Bl/6). The embryos were implanted in pseudo-pregnant mothers (having ICR CD1 background). Founders were bred with non-transgenic C57Bl/6 mice to establish stable transgenic line (Swarup et al., 2011b). The use and maintenance of the mice described in this article were performed in accordance to the Guide of Care and Use of Experimental Animals of the Canadian Council on Animal Care.

Axonal crush studies

Non-transgenic, TDP-43^{Wt} and TDP-43^{G348C} mice of 3 to 4 months old have been used for these studies. The sciatic nerve was crushed at the level of obturator tendon three times for 20 s with No. 5 Dumont forceps either without (n= 6) or with (n=7) prechilling in liquid nitrogen. Spinal cord tissue from all strains was examined on post-injury days 1, 3, 7, 14, and 28. For neurobehavioral assessment scores, mice were also examined 42 days post-injury. At 11 days after crush injury, animals were sacrificed and sciatic nerves were dissected and processed for light microscopy as described (Zhu et al., 1997). The sections were stained with toluidine blue. At least six sections were examined for each experiment and the number of newly myelinated axons at 3 mm distal to the crush site was plotted. Statistics were carried out by the Student t test. Similarly, the number of myelinated axons

was counted at 3 mm proximal to the crush injury and at the corresponding level in the contralateral non-axotomixed sciatic nerve.

Immunohistochemistry/Immunofluorescence Microscopy

4% Paraformaldehyde (PFA) fixed spinal cord and brain sections of mice were sectioned and fixed on slides. For immunohistochemistry, tissues were treated with hydrogen-peroxide solution before permeabilisation. After blocking with 5% normal goat serum for 1hr at room temperature, primary antibody incubations were performed in 1% normal goat serum in PBST overnight, followed by an appropriate Alexa Fluor 488 or 594 secondary antibody (1:500, Invitrogen) for 1hr at room temperature. For immunohistochemistry, tissues were incubated in biotinylated secondary antibodies (1:500, Vector labs, Burlingame, CA, USA), incubated in avidin-biotin complex and developed using Dab Kit (Vector labs). Z-stacked sections were viewed using a 40X or 60 X oil immersion objectives on an Olympus Fluoview™ Confocal System (Olympus, Center Valley, PA, USA).

Evaluation of immunostaining

Immunoreactivity scores were assigned as described previously (Ravizza et al., 2006; Iyer et al., 2010) by a blinded investigator. Assigned scores represent averages for all cells in the sciatic motor neuron pool. This method was validated first by comparing scores assigned by a second blinded investigator and finding no significant difference, then by using Image J analysis system (National Institute of Mental Health, Bethesda, MD, USA) as described here (Carmona et al., 2007). The overall concordance was >90% and the overall κ value ranged from 0.86 to 0.95. In case of disagreement, independent re-evaluation was performed by both observers to define the final score. Briefly, day 28 post-axonal crush images containing TDP-43 immunostained cells were threshold weighted as described previously (Moisse et al., 2009). The percent immunostained area was measured

and the area occupied by Harris's Haematoxylin-counterstained nuclei was subtracted to give a quantitative cytosolic TDP-43 immunoreactivity value. A minimum of 4 mice per strain per time point were used for analysis (n=4– 6). Two spinal cord sections, >50 μm apart, were analyzed in 2 levels of lumbar cord between L3 and L5 (4 sections per mouse). For peripherin and ubiquitin staining, the percent immunostained area was measured as described previously using Image J imaging software (Carmona et al., 2007) .

Neurobehavioural assessment

Neurobehavioural symptoms of the axotomies were assessed on post-injury days 1, 3, 7, 14, and 28 using a rating scale published by (Marsala and Yaksh, 1994; Moisse et al., 2009a) consisting of two criteria: (A) walking with hind limbs: 0—normal; 1—toes flat under body when walking but ataxia is present; 2—knuckle walking; 3—movements in hind limbs but unable to walk; and 4—no hind limb movement/drags hind limbs; and (B) placing/stepping reflex: 0—normal; 1—weak; and 2—no stepping. The final score was obtained by adding the score from A with that from B for a total out of 6.

Mac-2 cell count

For Mac-2 cell count experiment, every sixth sample section of horizontal spinal cord sections were immunostained for Mac-2 for microglial cell counts or Nissl stained to identify motor neurons in the lumbar spinal cord as described in detail previously (Gowing et al., 2008). Briefly, the L3–L5 spinal cord sections were individually traced with a 4× objective and sampled using a 40× objective. Lumbar segments were identified during dissection and stereological analysis. An average distance for each segment was determined and was applied during stereological analyses. The density of labeled cells was estimated by the optical fractionator method using Stereo Investigator software (MBF Bioscience). For Mac-2-, positive cells to be counted, a distinct cell body had to be within the optical dissector height. The counting parameters were the distance between counting frames (600 μm), the counting frame size (150 × 150 μm), the dissector height (8 μm), and the guard zone thickness (1 μm).

ELISA

The levels of TNF-α, IL-1β, IL-6, MCP-1 and IFN-γ were assayed by multi-analyte ELISA and MIX-N-MATCH ELISAarray kits (mouse inflammatory cytokine array, SABiosciences, Frederick, MD, USA) and were carried out according to manufacturer's instructions.

Statistical Analysis

For statistical analysis, the data obtained from independent experiments are presented as the mean ± SEM. A two-way analysis of variance (ANOVA) with repeated measures was used for all IR score, Mac-2+ count and NBA data. Two-way ANOVA was used for axonal calibre distribution and ELISArray using GraphPad Software. Post-hoc comparisons were performed by Tukey's test, with the statistical significance set at $p<0.05$.

3.5 Results:

3.5.1 Sustained behavioral deficits in TDP-43 transgenic mice after nerve crush.

We used pre-symptomatic 3-months old mice in all these experiments. Clinical evaluation of the mice paralysis was performed by neurobehavioral assessment score (NBA). Mice undergoing nerve crush injury from all strains exhibited extreme left hindlimb paralysis immediately following crush such that they dragged the limb while walking and only extended toes slightly if at all when prompted to place the foot of the lesioned side on a bar and grasp. Although all the mice's scores were comparable one day after nerve crush, non-transgenic and TDP-43^{Wt} mice recovered significantly after 3 days as compared to TDP-43^{G348C} mice (Figure 3.1). NBA score of TDP43^{G348C} mice was significantly higher from three days after nerve crush and had a severely impaired mobility even at post-injury day 28 ($p < 0.001$, $n = 5$) as compared to non-transgenic mice. Behavioral scores for TDP-43^{G348C} mice improved at post-injury day 42, but still significantly different from non-transgenic mice ($p<0.05$). Similarly TDP-43^{Wt} mice recovered slowly than non-transgenic mice at post-injury days 14 and 28 ($p < 0.001$, $n = 5$) as compared to non-transgenic mice (Figure 3.1).

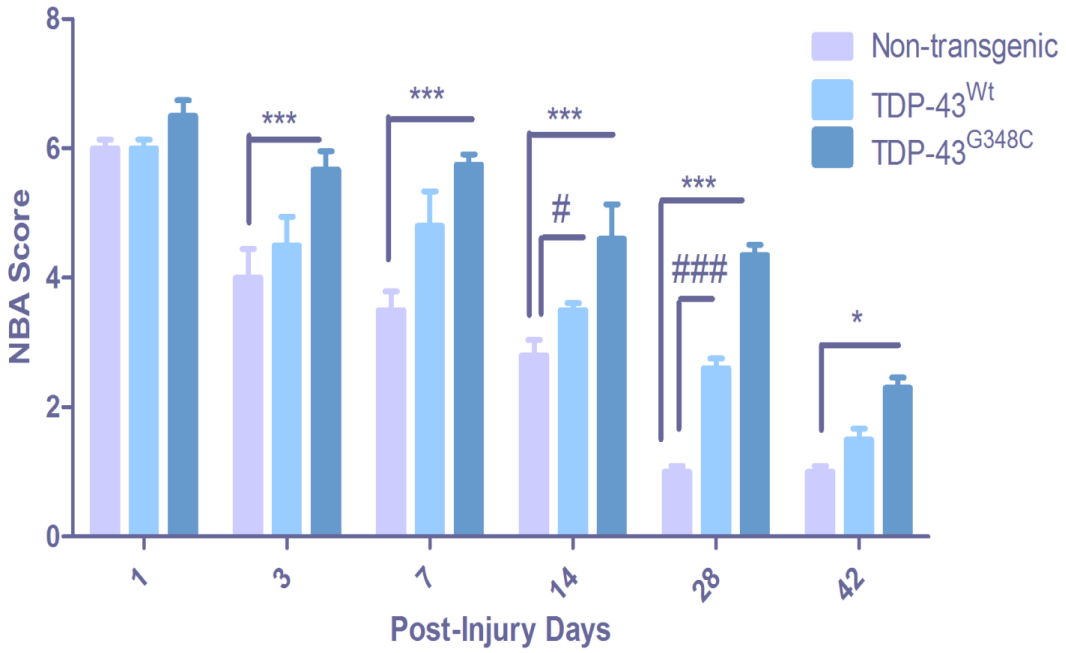

Figure 3.1.Clinical evaluation of the mice paralysis by neurobehavioral assessment score (NBA). Although all the mice's scores were comparable one day after nerve crush, TDP-43^{Wt} mice recovered slightly more slowly than non-transgenic mice and their NBA score was significantly higher 14 days (#, $p<0.05$) and 28 days after surgery (####, $p < 0.001$, $n = 5$, compared to non-transgenic mice). NBA score of TDP43^{G348C} mice was significantly higher from three days after nerve crush (*, $p<0.05$) and they still had a severely impaired mobility at 28 days (****, $p < 0.001$, $n = 5$, compared to non-transgenic mice) and 42 days (*$p<0.05$). Error bar represents mean ± SEM.

3.5.2 Sustained increases in cytoplasmic TDP-43 and peripherin immunoreactivity following axonal crush.

Cytoplasmic localization of TDP-43 following injury has been reported previously (Moisse et al., 2009a; Moisse et al., 2009b). We wanted to know if overexpression of wild-type or mutant TDP-43 in transgenic mice had any effect on the localization of TDP-43. We used TDP-43 polyclonal antibody which recognizes both endogenous mouse and human TDP-43. In non-transgenic control mice, TDP-43 was translocated in the cytoplasm ipsilateral to nerve-crush with peak immunoreactivity at 7 days after nerve crush, and sharply returned to the nucleus 14 and 28 days after the injury (Figure 3.2A-B). In the spinal cord sections, cytoplasmic TDP-43 was seen mostly in the neurons as determined by their shape and size in the staining. In TDP-43^{Wt} mice, the peak immunoreactivity in the cytoplasm was also seen at 7 days but it remained much higher than non-transgenic mice at 14 and 28 days post-injury (p<0.001). Moreover, in TDP-43^{G348C} mice cytosolic TDP-43 immunoreactivity was significantly higher 7 days after nerve crush and its mislocalization was substantially maintained at 28 days ($p < 0.001$) as compared to non-transgenic mice (Figure 3.2A-B). Nonetheless, in many neurons ipsilateral to the nerve-crush site, TDP-43 was found relocalized to the nucleus at 42 days after injury in both TDP-43^{Wt} and TDP-43^{G348C} mutant mice (Data not shown).

We then investigated the immunoreactivity and the distribution of peripherin, a type III neuronal intermediate filament (IF) protein, in axotomised TDP-43^{Wt} and TDP-43^{G348C} transgenic mice and compared them to non-transgenic mice. We chose to study peripherin immunoreactivity as peripherin inclusions are hallmark of ALS patients (Corbo and Hays, 1992; Migheli et al., 1993) and peripherin expression levels are increased by up to 300% in spinal motor neurons after injury of the sciatic nerve (Troy et al., 1990). In the spinal cord sections, peripherin immunoreactivity was highest in the cytoplasm 7 days post-injury in non-transgenic mice and gradually decreased in immunoreactivity at 14 and 28 days post-injury (Figure 3.2C-D). In both TDP-43^{Wt} and TDP-43^{G348C} transgenic mice, the peak

immunoreactivity of peripherin was at 7 days post-injury. However, TDP-43^{G348C} mice had significantly higher peripherin immunoreactivity at post-injury days 14 and 28 ($p<0.001$) and higher peripherin levels were also seen in TDP-43^{Wt} mice ($p<0.001$).

A

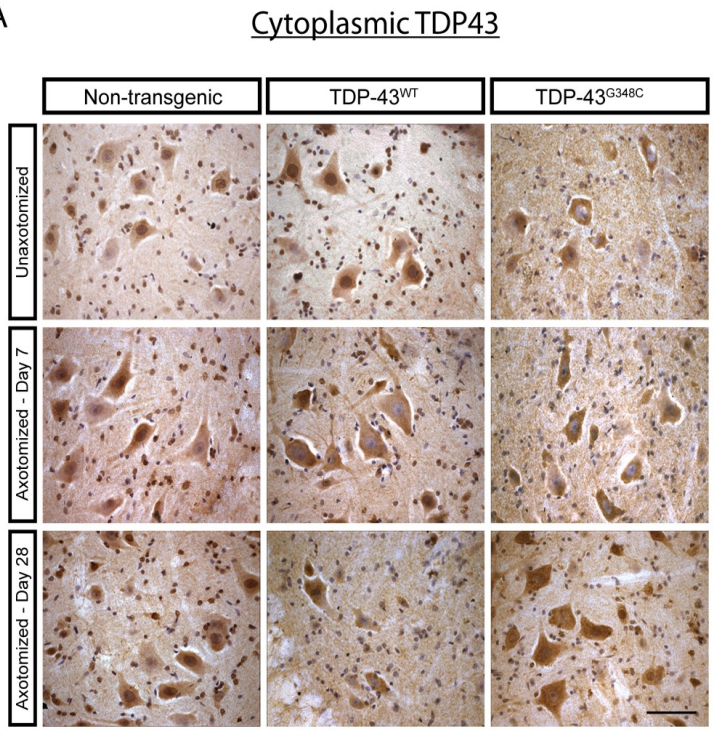
Cytoplasmic TDP43
Non-transgenic
TDP-43WT
TDP-43G348C
Unaxotomized
Axotomized - Day 7
Axotomized - Day 28

B

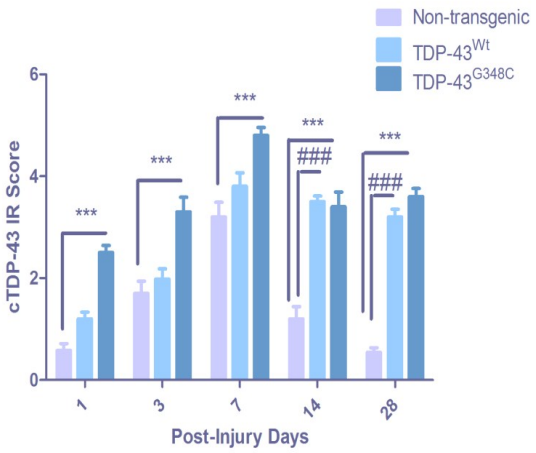
Non-transgenic
TDP-43Wt
TDP-43G348C
cTDP-43 IR Score
Post-Injury Days
***
###

C

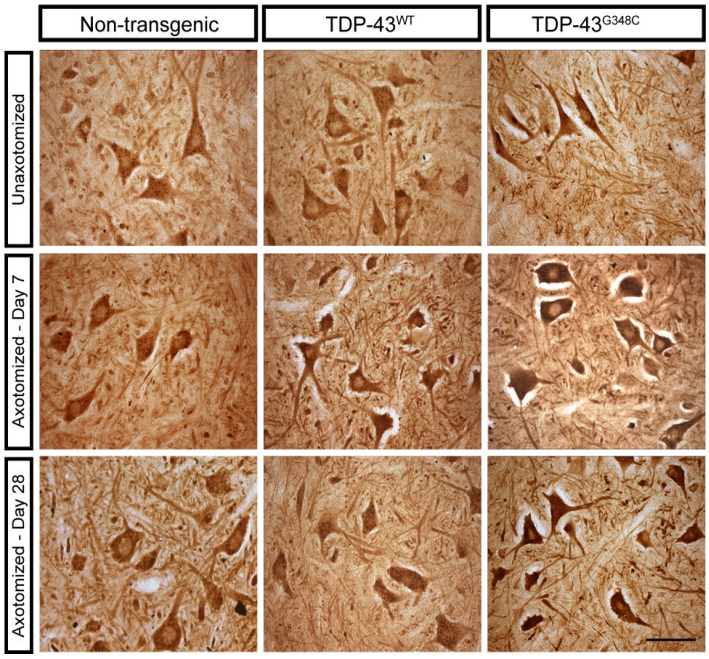
Peripherin
Non-transgenic
TDP-43WT
TDP-43G348C
Unaxotomized
Axotomized - Day 7
Axotomized - Day 28

D

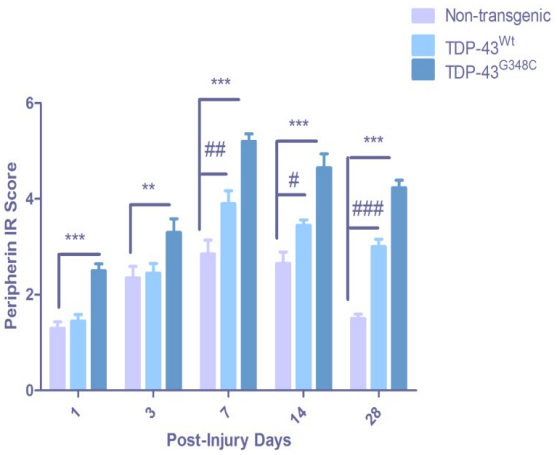
Non-transgenic
TDP-43Wt
TDP-43G348C
Peripherin IR Score
Post-Injury Days
***
**
##
#
###

Figure 3.2. Quantification of cytoplasmic TDP-43 and peripherin in spinal cord of mice following nerve crush by immunoreactivity (IR) score. (A-B) In non-transgenic mice, TDP-43 was translocated in the cytosol with a peak at 7 days after nerve crush, and mainly returned in the nucleus 28 days after injury. In TDP-43^{Wt} mice, the peak is also at 7 days but cytosolic TDP-43 was still much higher than non-transgenic mice at 14 and 28 days post-injury (###, $p < 0.001$, compared to non-transgenic mice). In TDP-43^{G348C} mice cytosolic TDP-43 was higher on all days after nerve crush and its mislocalization was substantially maintained at 28 days (***, $p < 0.001$, compared to non-transgenic mice) **(C-D)**. Peripherin was found to be unregulated 7 days after injury in non-transgenic mice and decreased rapidly on 14 and 28 days post-injury. In both TDP-43^{Wt} and TDP-43^{G348C} transgenic mice, the peak immunoreactivity was at 7 days but the peripherin levels were significantly upregulated 14 and 28 days post-injury (***, $p < 0.001$, ** $p < 0.01$, ###, $p < 0.001$, ## $p < 0.01$, #p<0.05 compared to non-transgenic mice). Scale bars: 50 μm, $n = 5$ for all quantifications. Error bar represents mean ± SEM.

3.5.3. Increased ubiquitin expression and microglial proliferation in TDP-43 transgenic mice following nerve crush

The role of increased ubiquitin expression in motor neurons have been reported before (Savedia and Kiernan, 1994). We thus analyzed immunoreactivity score for ubiquitin using commercially available polyclonal anti-ubiquitin antibody. In non-transgenic control mice ubiquitin immunoreactivity in the spinal cord showed peak levels at 7 days after injury and gradually decreased at 14 and 28 days post-injury (Figure 3.3A-B). Ubiquitin immunoreactivity also reached its peak at 7 days post-injury in TDP-43^{Wt} mice and TDP-43^{G348C} mice, but maintained significantly higher ubiquitin immunoreactivity at 14 and 28 days ($p < 0.001$) as compared to non-transgenic mice (Figure 3.3A-B).

We studied the inflammatory response to nerve crush in TDP-43 transgenic mice using Mac-2 positive microglial cell counts and mouse inflammatory multianalyte ELISArray (SABiosciences). Nerve crush provoked a progressive microgliosis in non-transgenic mice with highest Mac-2+ cells (15000 ± 750/mm^3) at 7 days post-injury and gradually declined at 14 and 28-days (2000 ± 200/mm^3) post-injury (Figure 3.3C). In TDP-43^{Wt} mice Mac-2+ cells were also highest at day 7, but their numbers were significantly higher (25000 ± 600/mm^3) than non-transgenic mice. At post-injury day 14 and 28, Mac-2+ counts were significantly higher in TDP-43^{Wt} mice as compared to non-transgenic mice. In contrast Mac-2+ cells counts were higher at 3, 7, 14 and 28 days in TDP-43^{G348C} mice compared to non-transgenic mice (Figure 3.3C).

To further evaluate the inflammatory response to nerve crush, we measured the protein levels of pro-inflammtory cytokines using mouse multianalyte ELISA system. We dissected ipsilateral and contralateral spinal cord and compared the ipsilateral side to nerve crush with the contralateral side for non-transgenic, TDP-43^{Wt} and TDP-43^{G348C} transgenic mice. The protein levels of all studied pro-inflammatory cytokines and chemokines were significantly upregulated in the ispsilateral side of TDP-43^{Wt} and TDP-43^{G348C} mice at 7 days post-injury when compared to their non-transgenic littermates. At 7 days post-injury, the levels of TNF-α (2.5-fold), IL-6 (2.5-fold), IL-1β (2-fold), IFNγ (1.5 fold) and MCP-1(2 -fold) were all upregulated in TDP-43^{Wt} mice compared to non-transgenic control and

the levels of TNF-α (2.8-fold), IL-6 (3.2 -fold), IL-1β (2.5-fold), IFNγ (2.5 fold) and MCP-1(3.2-fold) were all upregulated in TDP-43^{G348C} mice compared to non-transgenic control (Figure 3.3D). While most of the cytokine and chemokine levels had reduced 28-days after axonal crush in non-transgenic mice, the levels of TNF-α (1.5-fold in TDP-43^{Wt} and 2.0-fold in TDP-43^{G348C}), IL-6 (1.3-fold in TDP-43^{Wt} and 1.6-fold in TDP-43^{G348C}) and IL-1β (1.5-fold in TDP-43^{Wt} and 2.2-fold in TDP-43^{G348C}) were significantly upregulated as compared to non-transgenic control (Figure 3.3E).

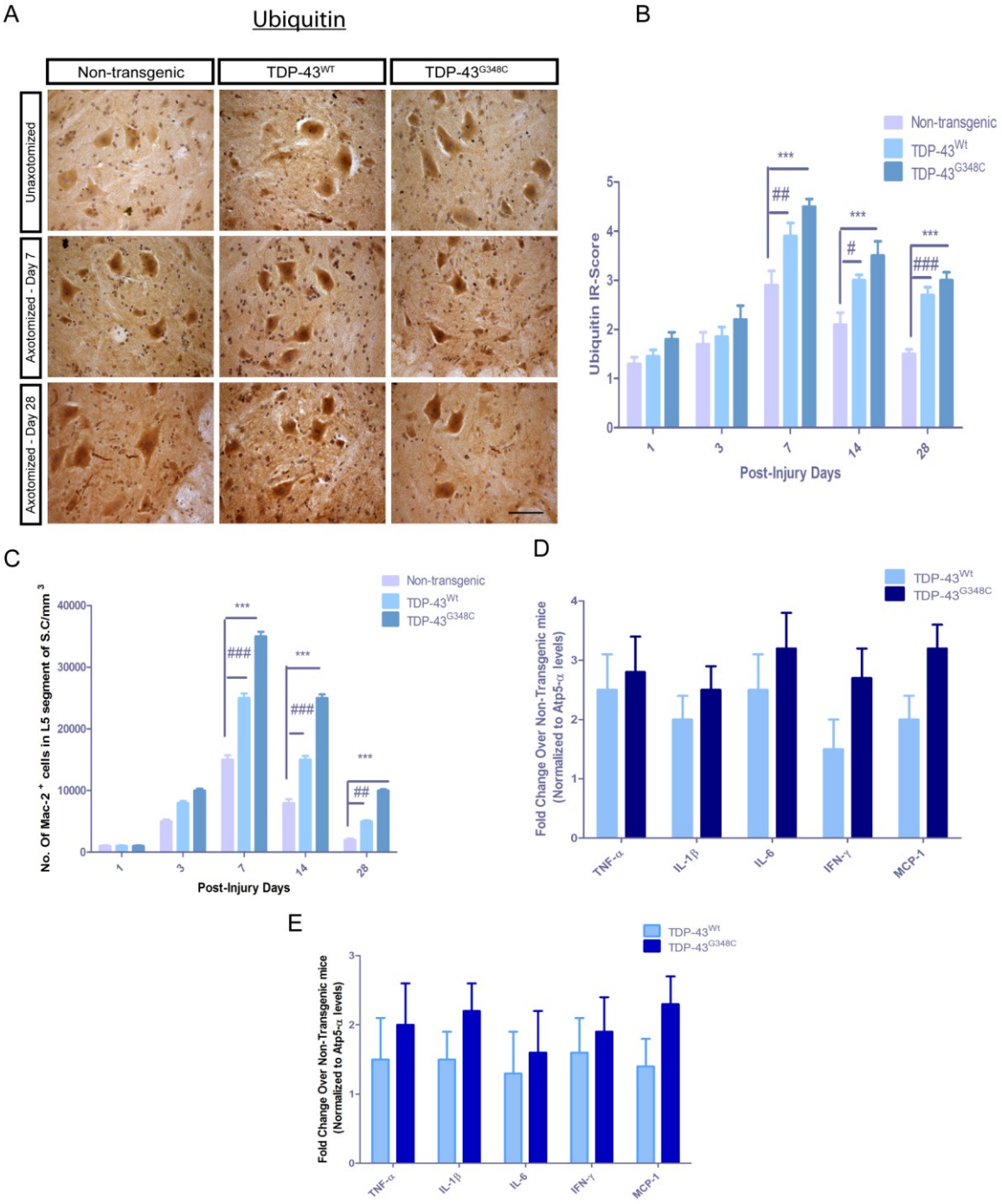
A
Ubiquitin
Non-transgenic
TDP-43Wt
TDP-43G348C
Unaxotomized
Axotomized - Day 7
Axotomized - Day 28
B
Non-transgenic
TDP-43Wt
TDP-43G348C
Ubiquitin IR-Score
Post-Injury Days
C
Non-transgenic
TDP-43Wt
TDP-43G348C
No. Of Mac-2+ cells in L5 segment of S.C/mm3
Post-Injury Days
D
TDP-43Wt
TDP-43G348C
Fold Change Over Non-Transgenic mice (Normalized to Atp5-α levels)
TNF-α
IL-1β
IL-6
IFN-γ
MCP-1
E
TDP-43Wt
TDP-43G348C
Fold Change Over Non-Transgenic mice (Normalized to Atp5-α levels)
TNF-α
IL-1β
IL-6
IFN-γ
MCP-1

Figure 3.3. Quantification of ubiquitin and microgliosis in spinal cord of mice following nerve crush by immunoreactivity (IR) score. (A-B) Nerve crush-induced upregulation of ubiquitin was at its highest level 7 days after injury in non-transgenic mice and in TDP-43^{Wt} mice. Nevertheless, TDP-43^{Wt} mice maintained more ubiquitin expression at 28 days (### $p < 0.001$, ##p<0.01, #p<0.05 compared to non-transgenic mice). The peak level of ubiquitin was also at 7 days in TDP-43^{G348C} mice and stayed higher at 14 and 28 days (***$p < 0.001$, compared to non-transgenic mice). **(C)** Nerve crush provoked a progressive microgliosis as seen by Mac-2+ cell count with a peak at 7 days in non-transgenic, TDP-43^{Wt} and TDP-43^{G348C} mice. In TDP-43^{Wt} mice Mac-2+ cell counts were significantly higher (25000 ± 600/mm^3) than non-transgenic mice (###p<0.001). At post-injury day 14 and 28, Mac-2+ counts were significantly higher in TDP-43^{Wt} mice as compared to non-transgenic mice (###p<0.001, ##p<0.01). Mac-2+ cells counts were higher at 3, 7, 14 and 28 days in TDP-43^{G348C} mice compared to non-transgenic mice TDP-43^{Wt} mice had its maximum number of Mac-2+ cells 7 days after injury and it was sustained until the end of the observations (***$p < 0.001$, compared to non-transgenic mice). **(D-E)** Mouse inflammatory multiplex ELISA was performed at 7 days (D) and 42 days (E). At 7 days post-injury, the levels of TNF-α (2.5-fold in TDP-43^{Wt} and 2.8-fold in TDP-43^{G348C}), IL-6 (2.5-fold in TDP-43^{Wt} and 3.2-fold in TDP-43^{G348C}), IL-1β (2-fold in TDP-43^{Wt} and 2.5-fold in TDP-43^{G348C}), IFNγ (1.5-fold in TDP-43^{Wt} and 2.5-fold in TDP-43^{G348C}) and MCP-1(2-fold in TDP-43^{Wt} and 3.2-fold in TDP-43^{G348C}) were all upregulated as compared to non-transgenic control. While most of the cytokine and chemokine levels had reduced 28-days after axonal crush in non-transgenic mice, the levels of TNF-α (1.5-fold in TDP-43^{Wt} and 2.0-fold in TDP-43^{G348C}), IL-6 (1.3-fold in TDP-43^{Wt} and 1.6-fold in TDP-43^{G348C}) and IL-1β (1.5-fold in TDP-43^{Wt} and 2.2-fold in TDP-43^{G348C}) were significantly upregulated as compared to non-transgenic control. Error bar represents mean ± SEM. Scale bars: 50 μm, $n = 5$ for all quantifications.

3.5.4. Delayed Regeneration of Myelinated Axons in TDP-43 transgenic mice following nerve crush

We wanted to examine how myelinated axons of peripheral nerves would regenerate in the presence of wild-type or mutant TDP-43 following axonal crush. We examined the sciatic nerve in the region proximal and distal to the initial crush 11 days after injury as illustrated in Figure 3.4A. Axonal responses in the dorsal root ganglia and in the distal sciatic nerve 11 days following nerve crush were evaluated. Electron microscopy of transversal sections of the distal nerve showed massive degeneration in ipsilateral sections to injury compared to contralateral control nerves (Figure 3.4B). No sign of degeneration of myelinated axons was evident in the nerve region 3 mm proximal to crush site (Data not shown). Quantifications of the total number of regenerating nerves (Figure 3.4C) surrounded by myelin (arrows in E.M.) reveals a significant difference between non-transgenic (mean = 571 ± 27) and TDP-43^{G348C} transgenic mice (mean = 335 ± 63). We conclude from these results that TDP-43^{G348C} mice had lower regeneration capacity of myelinated axons in the peripheral nerves as compared to non-transgenic controls. Similar to TDP-43^{G348C} mice, TDP-43^{Wt} mice also had lower regeneration capacity than non-transgenic mice but to a lesser extent than TDP-43^{G348C} mice.

We then investigated if nerve crush in TDP-43 transgenic mice change the number and distribution of axon caliber of the sciatic nerve. The axonal caliber was slightly lower in TDP-43^{G348C} and in TDP-43^{Wt} mice as compared to non-transgenic (Figure 3.4D-E). An analysis of the plotted distribution of axonal caliber confirms a significant shift of TDP-43^{G348C} axon caliber ($p = 0.0261$, $n = 3$, compared to non-transgenic mice) (Figure 3.4E). However, the numbers of axons in the ventral and dorsal root of the DRG are not significantly different (Figure 3.4F-G), neither between the contralateral and the ipsilateral sections nor between any of the transgenic or non-transgenic mice.

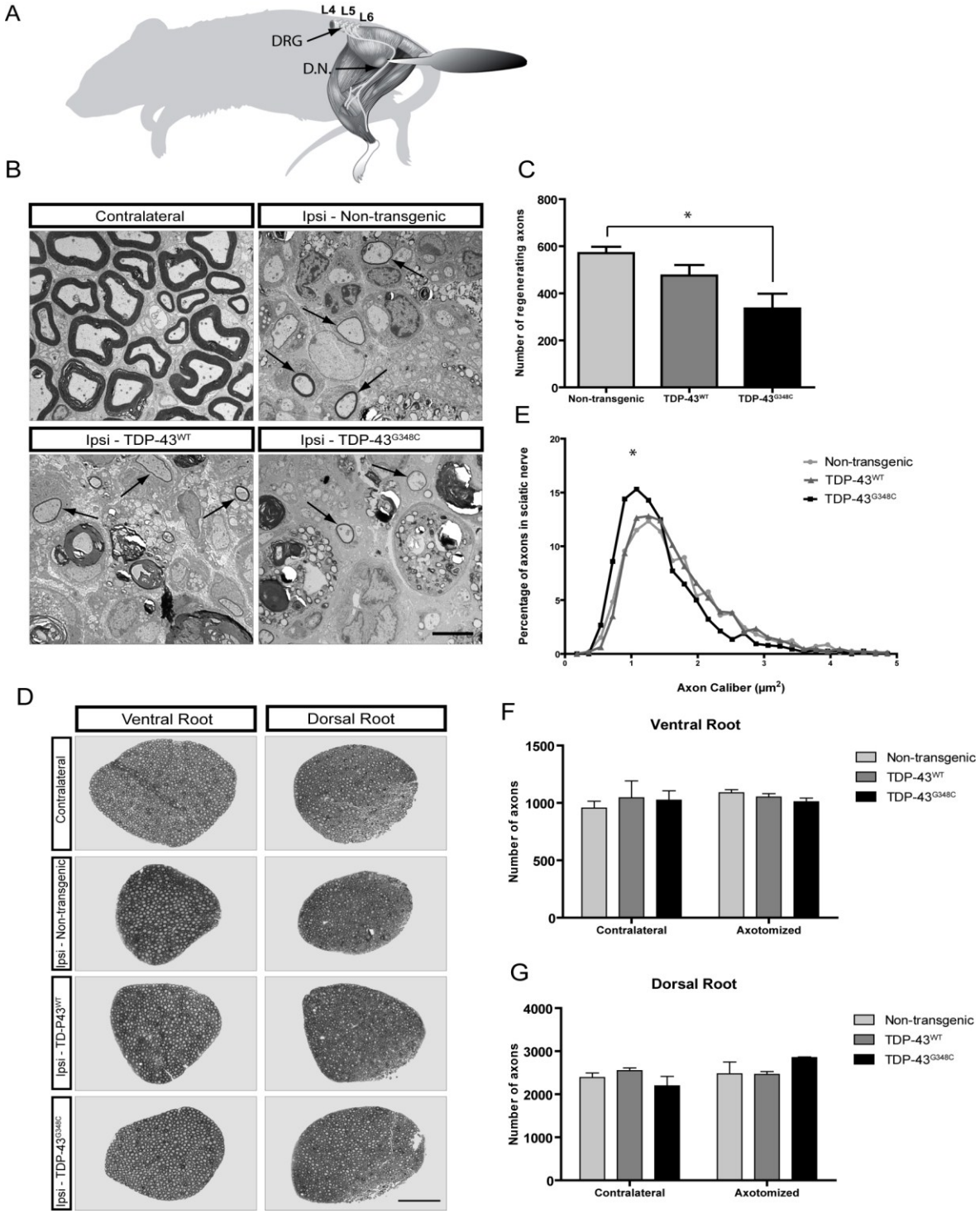
A
L4 L5 L6
DRG
D.N.
B
Contralateral
Ipsi - Non-transgenic
Ipsi - TDP-43WT
Ipsi - TDP-43G348C
C
Number of regenerating axons
800
600
400
200
0
*
Non-transgenic
TDP-43WT
TDP-43G348C
E
Percentage of axons in sciatic nerve
20
15
10
5
0
*
Non-transgenic
TDP-43WT
TDP-43G348C
0
1
2
3
4
5
Axon Caliber (μm2)
D
Ventral Root
Dorsal Root
Contralateral
Ipsi - Non-transgenic
Ipsi - TD-P43WT
Ipsi - TDP-43G348C
F
Ventral Root
Number of axons
1500
1000
500
0
Non-transgenic
TDP-43WT
TDP-43G348C
Contralateral
Axotomized
G
Dorsal Root
Number of axons
4000
3000
2000
1000
0
Non-transgenic
TDP-43WT
TDP-43G348C
Contralateral
Axotomized

Figure 3.4. Axonal responses in the dorsal root ganglia and in the distal sciatic nerve 11 days following nerve crush. (A) Schematic representation of the mice indicating the nerve crush site (forceps) and showing where the nerve analysis has been made (DRG: dorsal root ganglion sections; D.N.: distal nerve sections, 3 mm distal to the nerve crush site) **(B)**. Electron microscopy (E.M.) of transversal sections of the distal nerve shows massive degeneration in ipsilateral (axotomized) sections compared to contralateral (non-axotomized) control nerves (left panel in B). **(C)** Quantifications of the total number of regenerating nerves surrounded by myelin (arrows in E.M.) reveals a significant difference ($p = 0.0264$, $n = 3$) between non-transgenic (mean = 571 ± 27) and TDP-43^{G348C} transgenic mice (mean = 335 ± 63) (upper right panel in B). **(D)** Toluidine blue staining of thin sections of sciatic nerve from non-transgenic TDP-43^{Wt}, TDP-and TDP-43^{G348C} mice showing no significant differences in the axonal count.**(E)** The axonal caliber was measured 11 days post-injury in non-transgenic and transgenic mice and was slightly lower in TDP-43^{G348C} mice, mean = 74.31 compared to 91.48 in non-transgenic and 87.86 in TDP-43^{Wt} mice and an analysis of the plotted distribution confirms a significant shift the of TDP-43^{G348C} axon caliber ($p = 0.0261$, $n = 3$, compared to non-transgenic mice) **(F-G)** Axonal count was performed 11 days post-injury in the ventral (F) and dorsal root (G) of the DRG are not significantly different, neither between the contralateral and the ipsilateral sections nor between any of the axotomized sections groups. Error bar represents mean ± SEM. Scale bar: 5 μm (B) and 50 μm (D).

3.6 Discussion

The recent finding of cytosolic TDP-43 in ALS (Arai et al., 2006; Neumann et al., 2006) in particular its upregulation in spinal cord of sporadic ALS patients (Strong et al., 2007; Swarup et al., 2011a) prompted us to investigate whether overexpression of TDP-43 followed by nerve crush changes the biological response to neuronal injury. In sporadic ALS, TDP-43 expression is upregulated in both mRNA and protein levels with prominent cytosolic localization of TDP-43. We used our transgenic mice model overexpressing modest levels of TDP-43 encoded by genomic fragments to understand the effect of sciatic nerve crush on the overexpression of wild-type and mutant forms of TDP-43.

Neurobehavioral assessment score of TDP43^{G348C} mice was significantly higher from three days after nerve crush and had a severely impaired mobility even at post-injury day 28 and the behavioral score of TDP-43^{Wt} mice was significantly higher at 14 and 28 days post-injury as compared to non-transgenic mice. TDP-43^{G348C} mice did not recover from nerve crush after 28 days, in contrast to non-transgenic mice which recovered almost completely, and TDP-43^{Wt} recovered partially. NBA score of TDP-43^{Wt} and TDP-43^{G348C} mice after nerve injury suggests that these mice had slower recovery process compared to non-transgenic mice which can be attributed to inherent genetic defects of mice overexpressing wild-type or mutant TDP-43. TDP-43 has both nuclear export and import sequences (Strong et al., 2007; Winton et al., 2008) suggesting that TDP-43 may have a physiological role in the shuttling of mRNA from the nucleus to the cytosol. In response to axonal injury, TDP-43 relocalizes to the cytosol in a time-dependent manner (Moisse et al., 2009a). Immunohistochemical studies of the spinal cord sections indicate that sciatic nerve crush in TDP-43^{Wt} and TDP-43^{G348C} mice results in nuclear exclusion of TDP-43 followed by its cytoplasmic expression and the duration for cytoplasmic expression is significantly different from that in non-transgenic mice. Following nerve-crush injury, TDP-43 redistributes to the cytoplasm reaching peak cytoplasmic distribution 7 days post-injury in non-transgenic mice and expression patterns were restored 28 days post-injury. Interestingly the peak TDP-43 cytoplasmic distribution shifts to 14 days after nerve injury

in TDP-43^{Wt} and TDP-43^{G348C} mice and expression patterns were only restored 42 days post-injury.

Perikaryal and axonal aggregates of intermediate filaments is a hallmark of degenerating motor neurons in ALS (Carpenter, 1968; Corbo and Hays, 1992; Migheli et al., 1993). Peripherin is a type III intermediate filament whose expression is known to be upregulated in neuronal injury or stroke (Beaulieu et al., 2002). Using immunohisto-chemistry we found that peripherin was upregulated in a time-dependent manner reaching peak levels in cytoplasm 7 days post-injury in non-transgenic mice. Interestingly, peripherin levels in TDP-43^{G348C} mice were significantly higher at all days post-injury. Though peripherin levels returned back to normal levels 28 days post-injury in non-transgenic mice, peripherin was significantly upregulated at 28 days post-injury in TDP-43^{Wt} and TDP-43^{G348C} mice. Ubiquitin, another protein involved in injury (Yamauchi et al., 2008) was examined for its expression levels in our nerve-injury model. Ubiquitin levels were upregulated post-injury and were reversible events in that the baseline distribution and expression patterns were restored 28 days post-injury. It is important to note that ubiquitin expression levels were significantly upregulated 28 days post-injury in both TDP-43^{Wt} and TDP-43^{G348C} mice as compared to non-transgenic mice.

We then examined inflammatory response to sciatic nerve crush in transgenic mice and compared them to non-transgenic mice. Mac-2 positive microglial cell counts were highest at 7 days post-injury and gradually declined at 14 and 28-days post-injury in non-transgenic mice. In contrast Mac-2+ cells were significantly higher in both TDP-43^{Wt} and TDP-43^{G348C} mice. Higher number of Mac-2+ microglial cells prompted us to evaluate the cytokine and chemokine profile in the spinal cord tissue samples of 7 and 28 days post-injury mice. Consistent with Mac-2+ cell count, many inflammatory cytokines like TNF-α, IL-1β and chemokine like MCP-1 were upregulated 7 days post-injury in non-transgenic mice and gradually declined to normal levels 28 days post-injury. However, TDP-43^{Wt} and TDP-43^{G348C} mice had higher levels of cytokine levels at both 7 and 28 days post-injury compared to non-transgenic mice.

The slower recovery of TDP-43^{Wt} and TDP-43^{G348C} mice as assessed by NBA test compounded with increased cytoplasmic TDP-43 levels, peripherin and ubiquitin levels, and higher inflammatory repertoire in these mice prompted us to investigate if regeneration of myelinating axons is affected. We examined the sciatic nerve in the region proximal to the initial crush 11 days after injury (Fig 4A). Using electron microscopy in the transversal sections of the distal nerve massive degeneration in ipsilateral sections to injury can be seen as compared to contralateral control nerves. Quantifications of the total number of regenerating nerves surrounded by myelin reveals a significant decrease between non-transgenic and TDP-43^{Wt} or TDP-43^{G348C} transgenic mice. It can be concluded that TDP-43^{G348C} mice and to a lesser extent TDP-43^{Wt} mice had lower regeneration capacity of myelinated axons in the peripheral nerves as compared to non-transgenic controls.

The sciatic nerve crush model constitutes an acute injury model in which affected motor neurons recover following a series of highly regulated events involving the transport and stabilization of necessary mRNA species and their translation into protein at appropriate sites (Price and Porter, 1972; Zhu et al., 1997). Since TDP-43 is upregulated at protein and mRNA levels in sporadic ALS cases (Swarup et al., 2011a), we used transgenic TDP-43^{Wt} and TDP-43^{G348C} mice overexpressing modest levels of TDP-43 before the onset of disease (Swarup et al., 2011b) and performed sciatic nerve crush to understand their response to nerve injury. Our data suggest that TDP-43^{Wt} and TDP-43^{G348C} mice recover slowly following nerve crush. This fact is further substantiated by the observation that redistribution of cytoplasmic TDP-43 to the nucleus post injury is slower in TDP-43 transgenic mice, upregulated peripherin and ubiquitin levels return to normal more slowly in these mice and levels of pro-inflammatory cytokines are higher in these mice compared to control non-transgenic mice. As a result of these molecular changes, the regeneration of the myelinated axons is delayed in TDP-43^{Wt} and TDP-43^{G348C} mice. In all our data suggest that TDP-43^{Wt} and TDP-43^{G348C} mice have inherent genetic defects and provides new insights into the pathogenesis of ALS.

3.7. Acknowledgement

The authors acknowledge Ms. Christine Bareil and Genevieve Soucy for their excellent technical support. This work was supported by the Canadian Institutes of Health Research (CIHR), the ALS Society of Canada, the Muscular Dystrophy of Canada and the Fondation André-Delambre. J.-P.J. holds a Canada Research Chair Tier 1 in mechanisms of neurodegeneration. V.S. is the recipient of the Merit Scholarship for Foreign Students (FQRNT, Quebec, Canada).

3.8. References:

Arai T, Hasegawa M, Akiyama H, Ikeda K, Nonaka T, Mori H, Mann D, Tsuchiya K, Yoshida M, Hashizume Y, Oda T (2006) TDP-43 is a component of ubiquitin-positive tau-negative inclusions in frontotemporal lobar degeneration and amyotrophic lateral sclerosis. Biochemical and biophysical research communications 351:602-611.

Beaulieu JM, Kriz J, Julien JP (2002) Induction of peripherin expression in subsets of brain neurons after lesion injury or cerebral ischemia. Brain Res 946:153-161.

Carmona R, Macias D, Guadix JA, Portillo V, Perez-Pomares JM, Munoz-Chapuli R (2007) A simple technique of image analysis for specific nuclear immunolocalization of proteins. J Microsc 225:96-99.

Carpenter S (1968) Proximal axonal enlargement in motor neuron disease. Neurology 18:841-851.

Chiang PM, Ling J, Jeong YH, Price DL, Aja SM, Wong PC (2010) Deletion of TDP-43 down-regulates Tbc1d1, a gene linked to obesity, and alters body fat metabolism. Proceedings of the National Academy of Sciences of the United States of America 107:16320-16324.

Corbo M, Hays AP (1992) Peripherin and neurofilament protein coexist in spinal spheroids of motor neuron disease. J Neuropathol Exp Neurol 51:531-537.

Gitcho MA, Baloh RH, Chakraverty S, Mayo K, Norton JB, Levitch D, Hatanpaa KJ, White CL, 3rd, Bigio EH, Caselli R, Baker M, Al-Lozi MT, Morris JC, Pestronk A, Rademakers R, Goate AM, Cairns NJ (2008) TDP-43 A315T mutation in familial motor neuron disease. Ann Neurol 63:535-538.

Grover A, Shandilya A, Punetha A, Bisaria VS, Sundar D (2010) Inhibition of the NEMO/IKKbeta association complex formation, a novel mechanism associated with the NF-kappaB activation suppression by Withania somnifera's key metabolite withaferin A. BMC Genomics 11 Suppl 4:S25.

Gu Z, Cain L, Werrbach-Perez K, Perez-Polo JR (2000) Differential alterations of NF-kappaB to oxidative stress in primary basal forebrain cultures. Int J Dev Neurosci 18:185-192.

Guerreiro RJ, Schymick JC, Crews C, Singleton A, Hardy J, Traynor BJ (2008) TDP-43 is not a common cause of sporadic amyotrophic lateral sclerosis. PLoS One 3:e2450.

Guerrini L, Blasi F, Denis-Donini S (1995) Synaptic activation of NF-kappa B by glutamate in cerebellar granule neurons in vitro. Proceedings of the National Academy of Sciences of the United States of America 92:9077-9081.

Guerrini L, Molteni A, Wirth T, Kistler B, Blasi F (1997) Glutamate-dependent activation of NF-kappaB during mouse cerebellum development. The Journal of neuroscience : the official journal of the Society for Neuroscience 17:6057-6063.

Guidato S, Tsai LH, Woodgett J, Miller CC (1996) Differential cellular phosphorylation of neurofilament heavy side-arms by glycogen synthase kinase-3 and cyclin-dependent kinase-5. Journal of neurochemistry 66:1698-1706.

Gowing G, Philips T, Van Wijmeersch B, Audet JN, Dewil M, Van Den Bosch L, Billiau AD, Robberecht W, Julien JP (2008) Ablation of proliferating microglia does not affect motor neuron degeneration in amyotrophic lateral sclerosis caused by mutant superoxide dismutase. The Journal of neuroscience : the official journal of the Society for Neuroscience 28:10234-10244.

Iyer AM, Zurolo E, Boer K, Baayen JC, Giangaspero F, Arcella A, Di Gennaro GC, Esposito V, Spliet WG, van Rijen PC, Troost D, Gorter JA, Aronica E (2010) Tissue plasminogen activator and urokinase plasminogen activator in human epileptogenic pathologies. Neuroscience 167:929-945.

Jaarsma D, Teuling E, Haasdijk ED, De Zeeuw CI, Hoogenraad CC (2008) Neuron-specific expression of mutant superoxide dismutase is sufficient to induce amyotrophic lateral sclerosis in transgenic mice. J Neurosci 28:2075-2088.

Jacomy H, Zhu Q, Couillard-Despres S, Beaulieu JM, Julien JP (1999) Disruption of type IV intermediate filament network in mice lacking the neurofilament medium and heavy subunits. J Neurochem 73:972-984.

Janssen-Heininger YM, Poynter ME, Baeuerle PA (2000) Recent advances towards understanding redox mechanisms in the activation of nuclear factor kappaB. Free Radic Biol Med 28:1317-1327.

Jiang YM, Yamamoto M, Kobayashi Y, Yoshihara T, Liang Y, Terao S, Takeuchi H, Ishigaki S, Katsuno M, Adachi H, Niwa J, Tanaka F, Doyu M, Yoshida M, Hashizume Y, Sobue G (2005) Gene expression profile of spinal motor neurons in sporadic amyotrophic lateral sclerosis. Annals of neurology 57:236-251.

Johnson BS, McCaffery JM, Lindquist S, Gitler AD (2008) A yeast TDP-43 proteinopathy model: Exploring the molecular determinants of TDP-43 aggregation and cellular toxicity. Proc Natl Acad Sci U S A 105:6439-6444.

Johnson BS, Snead D, Lee JJ, McCaffery JM, Shorter J, Gitler AD (2009) TDP-43 is intrinsically aggregation-prone, and amyotrophic lateral sclerosis-linked mutations accelerate aggregation and increase toxicity. The Journal of biological chemistry 284:20329-20339.

Kabashi E, Valdmanis PN, Dion P, Spiegelman D, McConkey BJ, Vande Velde C, Bouchard JP, Lacomblez L, Pochigaeva K, Salachas F, Pradat PF, Camu W, Meininger V, Dupre N, Rouleau GA (2008) TARDBP mutations in individuals with sporadic and familial amyotrophic lateral sclerosis. Nat Genet 40:572-574.

Kasai T, Tokuda T, Ishigami N, Sasayama H, Foulds P, Mitchell DJ, Mann DM, Allsop D, Nakagawa M (2009) Increased TDP-43 protein in cerebrospinal fluid of patients with amyotrophic lateral sclerosis. Acta neuropathologica 117:55-62.

Marsala M, Yaksh TL (1994) Transient spinal ischemia in the rat: characterization of behavioral and histopathological consequences as a function of the duration of aortic occlusion. J Cereb Blood Flow Metab 14:526-535.

Migheli A, Pezzulo T, Attanasio A, Schiffer D (1993) Peripherin immunoreactive structures in amyotrophic lateral sclerosis. Lab Invest 68:185-191.

Moisse K, Mepham J, Volkening K, Welch I, Hill T, Strong MJ (2009a) Cytosolic TDP-43 expression following axotomy is associated with caspase 3 activation in NFL-/- mice: support for a role for TDP-43 in the physiological response to neuronal injury. Brain research 1296:176-186.

Moisse K, Volkening K, Leystra-Lantz C, Welch I, Hill T, Strong MJ (2009b) Divergent patterns of cytosolic TDP-43 and neuronal progranulin expression following axotomy: implications for TDP-43 in the physiological response to neuronal injury. Brain research 1249:202-211.

Mougeot JL, Li Z, Price AE, Wright FA, Brooks BR (2011) Microarray analysis of peripheral blood lymphocytes from ALS patients and the SAFE detection of the KEGG ALS pathway. BMC Med Genomics 4:74.

Nardo G, Pozzi S, Pignataro M, Lauranzano E, Spano G, Garbelli S, Mantovani S, Marinou K, Papetti L, Monteforte M, Torri V, Paris L, Bazzoni G, Lunetta C, Corbo M, Mora G, Bendotti C, Bonetto V (2011) Amyotrophic lateral sclerosis multiprotein biomarkers in peripheral blood mononuclear cells. PloS one 6:e25545.

Neumann M, Sampathu DM, Kwong LK, Truax AC, Micsenyi MC, Chou TT, Bruce J, Schuck T, Grossman M, Clark CM, McCluskey LF, Miller BL, Masliah E, Mackenzie IR, Feldman H, Feiden W, Kretzschmar HA, Trojanowski JQ, Lee VM (2006) Ubiquitinated TDP-43 in frontotemporal lobar degeneration and amyotrophic lateral sclerosis. Science 314:130-133.

Price DL, Porter KR (1972) The response of ventral horn neurons to axonal transection. The Journal of cell biology 53:24-37.

Ravizza T, Boer K, Redeker S, Spliet WG, van Rijen PC, Troost D, Vezzani A, Aronica E (2006) The IL-1beta system in epilepsy-associated malformations of cortical development. Neurobiology of disease 24:128-143.

Savedia S, Kiernan JA (1994) Increased production of ubiquitin mRNA in motor neurons after axotomy. Neuropathol Appl Neurobiol 20:577-586.

Sephton CF, Good SK, Atkin S, Dewey CM, Mayer P, 3rd, Herz J, Yu G (2010) TDP-43 is a developmentally regulated protein essential for early embryonic development. J Biol Chem 285:6826-6834.

Sreedharan J, Blair IP, Tripathi VB, Hu X, Vance C, Rogelj B, Ackerley S, Durnall JC, Williams KL, Buratti E, Baralle F, de Belleroche J, Mitchell JD, Leigh PN, Al-Chalabi A, Miller CC, Nicholson G, Shaw CE (2008) TDP-43 mutations in familial and sporadic amyotrophic lateral sclerosis. Science 319:1668-1672.

Stallings NR, Puttaparthi K, Luther CM, Burns DK, Elliott JL (2010) Progressive motor weakness in transgenic mice expressing human TDP-43. Neurobiol Dis 40:404-414.

Strong MJ, Volkening K, Hammond R, Yang W, Strong W, Leystra-Lantz C, Shoesmith C (2007) TDP43 is a human low molecular weight neurofilament (hNFL) mRNA-binding protein. Mol Cell Neurosci 35:320-327.

Swarup V, Phaneuf D, Dupre N, Petri S, Strong M, Kriz J, Julien JP (2011a) Deregulation of TDP-43 in amyotrophic lateral sclerosis triggers nuclear factor kappaB-mediated pathogenic pathways. J Exp Med 208:2429-2447.

Swarup V, Phaneuf D, Bareil C, Robertson J, Rouleau GA, Kriz J, Julien JP (2011b) Pathological hallmarks of amyotrophic lateral sclerosis/frontotemporal lobar degeneration in transgenic mice produced with TDP-43 genomic fragments. Brain : a journal of neurology 134:2610-2626.

Troy CM, Muma NA, Greene LA, Price DL, Shelanski ML (1990) Regulation of peripherin and neurofilament expression in regenerating rat motor neurons. Brain research 529:232-238.

Van Deerlin VM et al. (2008) TARDBP mutations in amyotrophic lateral sclerosis with TDP-43 neuropathology: a genetic and histopathological analysis. Lancet Neurol 7:409-416.

Wegorzewska I, Bell S, Cairns NJ, Miller TM, Baloh RH (2009) TDP-43 mutant transgenic mice develop features of ALS and frontotemporal lobar degeneration. Proc Natl Acad Sci U S A 106:18809-18814.

Wils H, Kleinberger G, Janssens J, Pereson S, Joris G, Cuijt I, Smits V, Ceuterick-de Groote C, Van Broeckhoven C, Kumar-Singh S (2010) TDP-43 transgenic mice develop spastic paralysis and neuronal inclusions characteristic of ALS and frontotemporal lobar degeneration. Proc Natl Acad Sci U S A 107:3858-3863.

Winton MJ, Igaz LM, Wong MM, Kwong LK, Trojanowski JQ, Lee VM (2008) Disturbance of nuclear and cytoplasmic TAR DNA-binding protein (TDP-43) induces disease-like redistribution, sequestration, and aggregate formation. J Biol Chem 283:13302-13309.

Xu YF, Gendron TF, Zhang YJ, Lin WL, D'Alton S, Sheng H, Casey MC, Tong J, Knight J, Yu X, Rademakers R, Boylan K, Hutton M, McGowan E, Dickson DW, Lewis J, Petrucelli L (2010) Wild-Type Human TDP-43 Expression Causes TDP-43 Phosphorylation, Mitochondrial Aggregation, Motor Deficits, and Early Mortality in Transgenic Mice. J Neurosci 30:10851-10859.

Yamauchi T, Sakurai M, Abe K, Matsumiya G, Sawa Y (2008) Ubiquitin-mediated stress response in the spinal cord after transient ischemia. Stroke 39:1883-1889.

Zhu Q, Couillard-Despres S, Julien JP (1997) Delayed maturation of regenerating myelinated axons in mice lacking neurofilaments. Exp Neurol 148:299-316.

Chapter 4 Deregulation of TDP-43 in ALS triggers nuclear factor-κB-mediated pathogenic pathways

Article published in : Journal of Experimental Medicine 2011 Nov 208 (12): 2429-2247

Vivek Swarup[1], Daniel Phaneuf[1], Nicolas Dupré[2], Susanne Petri[3], Michael Strong[4], Jasna Kriz[1] and Jean-Pierre Julien[1]*

[1]Centre de Recherche du Centre Hospitalier Universitaire de Québec, Department of Psychiatry and Neuroscience of Laval University, Quebec, QC, Canada

[2]Faculty of Medicine, Laval University, Department of Neurological Sciences, Enfant-Jesus Hospital, Quebec City, QC, Canada G1J 1Z4

[3]Hannover Medical School, Department of Neurology, Carl-Neuberg-Str. 1, 30625, Hannover, Germany

[4]Molecular Brain Research Group, Robarts Research Institute, London ON, Canada, N6A 5K8

4.1 Résumé

Les inclusions de la protéine TDP-43 sont une caractéristique de la sclérose latérale amyotrophique (SLA). Dans l'étude de nos modèles de souris transgéniques, nous démontrons que les niveaux d'expression d'ARNm des protéines TDP-43 et de la sous-unité p65 du NF-κB, sont plus élevées dans la moelle épinière des patients atteints de la SLA que chez les individus en bonne santé. La protéine TDP-43 interagit et colocalise avec la sous-unité p65 dans les cellules gliales et dans les neurones de patients atteints de la SLA, ainsi que chez les souris exprimant la TDP-43 de type sauvage et mutant. Par contre, cette interaction n'est pas présente dans les cellules de sujets sains ou chez des souris non transgéniques. TDP-43 agit donc comme un co-activateur de p65, et les cellules gliales exprimant des quantités plus importantes de la protéine TDP-43, produisent des cytokines pro-inflammatoires et des médiateurs plus neurotoxiques. Cette expression est causée par la stimulation des lipopolysaccharides ou des espèces oxygénées réactives. La surexpression de TDP-43 dans les neurones, concorde également avec une hausse de leur vulnérabilité aux médiateurs toxiques. Le traitement des souris transgéniques TDP-43 avec la Withaférine A, un inhibiteur de l'activité NF-κB, réduit le niveau de dénervation des jonctions neuromusculaires et des symptômes liés à la SLA. Nous suggérons donc que le dérèglement de la protéine TDP-43, contribue à la pathogenèse de la SLA en partie par l'augmentation de l'activation de NF-κB, et que NF-κB pourrait constituer une cible thérapeutique pour la maladie.

4.2 Abstract

TDP-43 inclusions are a hallmark of amyotrophic lateral sclerosis (ALS). Here, we report that TDP-43 and NF-κB p65 mRNA and protein expression is higher in spinal cords if ALS patients than healthy individuals. TDP-43 interacts with and colocalizes with p65 in glial and neuronal cells from ALS patients and mice expressing wild-type and mutant TDP-43 transgenes, but not in cells from healthy individuals or nontransgenic mice. TDP-43 acted as a co-activator of p65, and glial cells expressing higher amounts of TDP-43 produced more proinflammatory cytokines and neurotoxic mediators after stimulation with lipopolysaccharide or reactive oxygen species. TDP-43 overexpression in neurons also increased their vulnerability to toxic mediators. Treatment of TDP-43 mice with Withaferin A, an inhibitor of NF-κB activity, reduced denervation in the neuromuscular junction and ALS disease symptoms. We propose that TDP-43 deregulation contributes to ALS pathogenesis in part by enhancing NF-κB activation, and that NF-κB may constitute a therapeutic target for the disease.

4.3 Introduction

ALS is an adult-onset neurodegenerative disorder characterized by the progressive degeneration of motor neurons in the brain and spinal cord. Approximately 10% of ALS cases are familial and 90% are sporadic. Recently, TAR DNA binding protein 43 (TDP-43) has been implicated in ALS(Neumann et al., 2006). TDP-43 is a DNA/RNA-binding 43kDa protein that contains a N-terminal domain, two RNA recognition motifs (RRMs) and a glycine-rich C-terminal domain, characteristic of the heterogeneous nuclear ribonucleoprotein (hnRNP) class of proteins (Dreyfuss et al., 1993). TDP- 43, normally observed in the nucleus, is detected in pathological inclusions in the cytoplasm and nucleus of both neurons and glial cells of ALS and frontotemporal lobar degeneration with ubiquitin inclusions (FTLD-U) cases (Arai et al., 2006; Neumann et al., 2006). The inclusions consist prominently of TDP-43 C-terminal fragments (CTFs) of ~25kDa. The involvement of TDP-43 with ALS cases led to the discovery of TDP-43 mutations found in ALS patients. Dominant mutations in *TARDBP*, which codes for TDP-43, were reported by several groups as a primary cause of ALS(Corrado et al., 2009; Daoud et al., 2009; Gitcho et al., 2008; Kabashi et al., 2008; Sreedharan et al., 2008; Van Deerlin et al., 2008) and may account for ~3% of familial ALS cases and ~1.5% of sporadic cases.

Neuronal overexpression at high levels of wild-type or mutant TDP-43 in transgenic mice caused a dose-dependent degeneration of cortical and spinal motor neurons but with no cytoplasmic TDP-43 aggregates (Stallings et al., 2010; Wegorzewska et al., 2009; Wils et al., 2010; Xu et al., 2010), raising up the possibility that an upregulation of TDP-43 in the nucleus rather than TDP-43 cytoplasmic aggregates may contribute to neurodegeneration. The physiological role of TDP-43 and the pathogenic pathways of TDP-43 abnormalities are not well understood. TDP-43 is essential for embryogenesis(Sephton et al., 2010) and postnatal deletion of the TDP-43 gene in mice caused downregulation of Tbc1d1, a gene that alters body fat metabolism(Chiang et al., 2010). Proteins known to interact with TDP-43 have also been implicated in protein refolding or proteasomal degradation including ubiquitin, proteasome-beta subunits, SUMO-2/3 and Hsp70(Seyfried et al., 2010).

Because TDP-43 is ubiquitously expressed and several studies have supported the importance of glial cells in mediating motor neuron injury (Boillee et al., 2006a; Boillee et al., 2006b; Clement et al., 2003), we have searched for additional proteins which might interact with TDP-43 in LPS-stimulated microglial (BV-2) cells. Our rationale for choosing microglial BV-2 cells was that TDP-43 deregulation may occur not only in neurons but also in microglial cells. Moreover, there are recent reports of increased levels of LPS in the blood of ALS patients (Zhang et al., 2009a) and of an upregulation of LPS/TLR-4 signaling associated genes in peripheral blood monocytes from ALS patients (Zhang et al., 2011). Accordingly, we have biased our search for proteins interacting with TDP-43 when microglia are activated by LPS. Surprisingly, co-immunoprecipitation assays and mass spectrometry led to identify the p65 subunit of NF-κB as a binding partner of TDP-43. Furthermore, we discovered that TDP-43 mRNA was abnormally upregulated in the spinal cord of ALS subjects. These results reported here led us to further explore the physiological significance of the interaction between TDP-43 and p65 NF-κB.

4.4 Materials and Methods

Human subjects

The spinal cords of 16 subjects with sporadic ALS and 6 control cases were used in this study. The diagnosis of ALS was made on both clinical and pathological grounds. The ages at death ranged from 42 to 79 years, and the duration of illness ranged from 21 to 48 months (Table 4.1). TDP-43-positive inclusions were found in all ALS cases. We also used spinal cord samples from 6 neurologically normal individuals (normal controls), aged between 55 and 84 years. For routine histological examination, the spinal cord of each subject was fixed with 10% buffered formalin for 3 weeks and then embedded in paraffin; 4-µm-thick sections were cut and stained with hematoxylin. The use of the human tissue samples described in this article were performed in accordance to the committee on research ethics of Enfant-Jesus Hospital (comité d'éthique de la recherche de l'hôpital de l'Enfant-Jésus du CHA), Quebec.

Generation of TDP-43 transgenic mice

TARDBP (NM_007375) was amplified by PCR from a human BAC clone (clone RPCI-11, clone number: 829B14) along with the endogenous promoter (~4kB). A315T and G348C mutations in TDP-43 were inserted using site-directed mutagenesis. The full-length genomic *TARDBP* (TDP-43^{Wt} and TDP-43^{G348C}) was linearized by Swa-1 restriction enzyme and 18 kb DNA fragment microinjected in one-day mouse embryos (having a background of C3H X C57Bl/6). The embryos were implanted in pseudo-pregnant mothers (having ICR CD1 background). Founders were bred with non-transgenic C57Bl/6 mice to establish stable transgenic lines (Swarup et al., 2011a). Transgene expression was analyzed in brain and spinal cord by real-time PCR and in brain, spinal cord, muscle, liver by western blot using monoclonal human TDP-43 antibody (Clone E2-D3, Abnova). The use and maintenance of the mice described in this article were performed in accordance to the Guide of Care and Use of Experimental Animals of the Canadian Council on Animal Care.

Table 4.1 Details of Patients Examined During the Study

Patients	Sex	Age (yr)	Duration of Illness (yr)	Postmortem Delay (hr)	Diseases	Spinal Cord Neuropathology Motor neuron Loss/ Gliosis
ALS1	F	69	1.8	6	ALS(B,UL,LL)	Severe/severe
ALS2	F	72	1.9	5	ALS(LL,UL,B)	Severe/mild
ALS3	F	65	2.3	6	ALS(UL,LL,B)	Mild/moderate
ALS4	M	78	3.2	4	ALS(B,UL,LL)	Moderate/mild
ALS5	M	79	2.8	6	ALS(UL,LL)	Mild/mild
ALS6	F	65	2.6	5	ALS(UL,B)	Moderate/mild
ALS7	M	64	2.0	6	ALS(UL)	Mild/severe
ALS8	M	65	3.0	9	ALS(LL,B)	Moderate/severe
ALS9	M	53	3.5	5	ALS(UL,B)	Mild/mild
ALS10	M	59	2.2	10	ALS(LL,UL)	Mild/moderate
ALS11	F	42	2.5	7	ALS(B,UL,LL)	Moderate/mild
ALS12	M	69	1.9	9	ALS(UL,LL,B)	Severe/severe
ALS13	M	70	2.0	8	ALS(UL,LL,B)	Moderate/severe
ALS14	M	72	4.0	5	ALS(LL,B)	Mild/mild
ALS15	M	74	3.5	8	ALS(UL,B)	Mild/mild
ALS16	M	67	2.5	6	ALS(UL,LL,B)	Moderate/severe
Control1	M	57	-	7	Heart failure	No
Control2	F	55	-	10	Pneumonia	No
Control3	F	68	-	8	Heart Failure	No
Control4	M	72	-	8	Heart Failure	No

Control5	M	84	-	7	Pneumonia	No
Control6	M	74	-	5	Myocardial infarction	No

The age, duration of illness, and postmortem delay are indicated for the ALS and control cases. Predominant clinical features of ALS are shown: UL - upper limbs; LL - lower limbs; B - bulbar. Neuropathological involvement of spinal cords was graded as previously. All ALS and control samples were used for real-time RT-PCR and ELISA assays. Nine ALS (1–9) and all control samples were used for co-immunoprecipitation assays. Five ALS (1, 4, 8, 14, 15) and four control (1, 2, 4,6) samples were used for immunofluorescence. ALS -amyotrophic lateral sclerosis.

Withaferin A treatment

Withaferin A (Enzo life sciences, Plymouth meeting, PA, USA) were injected intra-peritoneally twice a week for 10-consecutive weeks at 3mg/kg body weight in 30-weeks old TDP-43^{Wt} mice (n=10). Age matched control non-transgenic animals (n=10) and in TDP-43^{Wt} (n=10) littermates were injected twice a week with 0.9% saline intra-peritoneally. All the behavioral and imaging experiments were conducted in a double blind manner as such the experimenter had no knowledge of the drug treatment or the genotype of animals.

Plasmids

Mammalian expression vector plasmids pCMV-p65, pCMV-p50, ICAM-luc (positions -340 to -25) and luciferase reporter plasmids 4κB^{Wt}-luc or 4κB^{mut}-luc, containing four tandem copies of the human immunodeficiency virus-κB sequence upstream of minimal SV40 promoter and mutant IκB-α (IκB^{SR}) containing Ser ^{32} and Ser ^{36}-to-alanine mutations were generous gifts from the lab of Dr. Michel J. Tremblay, CRCHUQ. To create a human pCMV-TDP43, the cDNA library from human myeloid cells was amplified by polymerase

chain reaction (PCR) using primers as described in Supplementary Table 1. These products were subcloned into TOPO-vector (Invitrogen, Carlsbad, CA, USA) and later digested with Kpn1-BamHI restriction enzymes and subcloned in frame into pcDNA3.0 vector to form pCMV-TDP43^{Wt}. The hemagglutinin (HA) tag was later added by PCR. HA tagged TDP-43$^{\Delta N}$, TDP-43$^{\Delta RRM-1}$, TDP-43$^{\Delta RRM-2}$ and TDP-43$^{\Delta C}$ deletion mutants were constructed by PCR amplification and cloned between Kpn1-BamHI sites using the primers described in Table 4.2. Point mutations (pCMV-TDP43^{A315T} and pCMV-TDP43^{G348C}) were inserted by PCR using site directed mutagenesis. Dual luciferase assay was used for ICAM-luc and kB-luc vectors (Clonetech).

Table 4.2

Primers for TDP-43 Cloning

Construct	Forward Primer	Reverse Primer
TDP-43^{Wt}	GCGGGAAAAGTAAAAGATGTC	ATTCCTGCAGCCCGGGGGATCC
TDP-43^{A315T}	GGGATGAACTTTGGTACGTTCAGCATTAATCC	GGATTAATGCTGAACGTACCAAAGTTCATCCC
TDP-43^{G348C}	CCAGCAGAACCAGTCATGCCCATCGGGTAA	GTTATTACCCGATGGGCATGACTGGTTCTGC
ΔN	CGGGAAAAGTAAAAGATGTTAATAGTGTT	ATTCCTGCAGCCCGGGGGATCC
ΔRRM-1	GCGGGAAAAGTAAAAGATGTC	AGAAAACATCCGATCTTCCTAATT

ΔRRM-2	GCGGGAAAAGTAAAAGATGTC	TTTGAGAAGCAAGCACAATAG
ΔC	GCGGGAAAAGTAAAAGATGTC	TTAGAAAGAAGTAGACAGTGGGG

Cell Culture and Transfection

Mouse microglial BV-2 and mouse neuroblastoma N2a cells were maintained in Dulbecco's modified Eagle's medium (Gibco, Carlsbad, CA, USA) with 10% fetal bovine serum and antibiotics. Cells were transfected using Lipofectamine 2000 transfection reagent (Invitrogen, Carlsbad, CA, USA) according to the manufacturer's instructions. At 48 h post-transfection, the cells were harvested, and the extracts were prepared for downstream assays.

Primary Cell Cultures

Primary microglial culture from brain tissues of neonatal (P0-P1) C57Bl/6 , TDP-43^{Wt}, TDP-43^{A315T} and TDP-43^{G348C} mice were prepared as described previously(Weydt et al., 2004). Briefly, the brain tissues were stripped of their meninges and minced with scissors under a dissecting microscope in DMEM. After trypsinization (0.5% trypsin, 10 min, 37°C/5% CO_2) the tissue was triturated. The cell suspension was washed in culture medium for glial cells [DMEM supplemented with 10% FBS (Gibco), L-glutamine (1 mM), sodium pyruvate (1 mM), penicillin (100 units/ml), and streptomycin (100 mg/ml)] and cultured at 37°C/5% CO_2 in 75-cm^2 Falcon tissue-culture flasks (BD, San Jose, CA, USA) coated with polyD-lysine (PDL) (10 mg/ml; Sigma-Aldrich) in borate buffer [2.37 g of borax and 1.55 g of boric acid dissolved in 500 ml of sterile water (pH 8.4)] for 1 h, then rinsed thoroughly with sterile, glass-distilled water. Half of the medium was changed after 6 h in culture and every second day thereafter, starting on day 2, for a total culture time of 10-14 days. Microglia were shaken off the primary mixed brain glial cell cultures (150 rpm, 37°C, 6 h) with maximum yields between days 12 and 16, seeded (10^5 cells per milliliter) onto PDL-pretreated 24-well plates (1 ml per well), and grown in culture medium for microglia [DMEM supplemented with 10% FBS, L-glutamine (1 mM), sodium pyruvate (1 mM), 2-

mercaptoethanol (50 mM), penicillin (100 units/ml), and streptomycin (100 mg/ml)]. The cells were allowed to adhere to the surface of a PDL-coated culture flask (30 min, 37°C/5% CO_2). After removal of primary microglial culture, the remaining cells were mainly astrocytes. Purity of the astrocytes was more than 90%. Astrocytes were maintained in a medium consisting of DMEM supplemented with 10% FBS, L-glutamine (1 mM), sodium pyruvate (1 mM), 2-mercaptoethanol (50 mM), penicillin (100 units/ml), and streptomycin (100 mg/ml). Primary cortical cultures from brain tissues of gestation day 16 (E16) C57Bl/6, TDP-43^{Wt}, TDP-43^{A315T} and TDP-43^{G348C} mice were prepared as described. Briefly, dissociated cortical cells (2.5–3.5 hemispheres) were plated onto PDL-coated 24-well , containing DMEM supplemented with 20 mM glucose, 2 mM glutamine, 5% fetal bovine serum, and 5% horse serum. Cytosine arabinoside was added 4–5 days after the plating to halt the groWth of non-neuronal cells. Cultures were maintained at 37°C in a humidified CO2 incubator and used for experiments between 14 and 21 days in vitro. Cells were treated with Withaferin A (Enzo life sciences, Plymouth meeting, PA, USA) at a final concentration of 1μM for 24 hrs. Bone-marrow derived macrophages (BMMs) were isolated and cultured using established protocols as described elsewhere(Davies and Gordon, 2005).

Co-immunoprecipitation and Western Blot Assays

After transfection of plasmids, BV-2 cells were cultured for 48 h and then harvested with lysis buffer (25 mM HEPES-NaOH (pH 7.9), 150 mM NaCl, 1.5 mM $MgCl_2$, 0.2 mM EDTA, 0.5% Triton-X-100, 1 mM dithiothreitol, protease inhibitor cocktail). Alternatively, spinal cords from TDP-43 transgenic mice or sporadic ALS subjects along with controls were lysed in the buffer. The lysate was incubated with 50μl of Dynabeads (Protein-G beads, Invitrogen), anti-TDP-43 polyclonal (ProteinTech, Chicago, IL, USA) and anti-HA antibody (clone 3F10, Roche, San Francisco, CA, USA). After subsequent washing, the beads were incubated overnight at 4^o with 400μg of cell lysate. Antibody-bound complexes were eluted by boiling in Laemmli sample buffer. Supernatants were resolved by 10% SDS-PAGE and transferred on nitrocellulose membrane (Biorad, Hercules, CA, USA). The membrane was incubated with anti-p65 antibody, and immunoreactive proteins were

visualized by chemiluminescence (Perkin and Elmer, Santa Clara, CA, USA) as described previously(Dequen et al., 2008). In some cases, phospho-p65^{Ser536} , (Cell Signaling, Boston, MA, USA) and phospho-p50^{337} (Santa Cruz) were used at a concentration of 1:1000.

Mass Spectrometer Analysis

BV-2 microglial cells were transiently transfected with plasmid vector pCMV-TDP43^{Wt} coding for TDP-43^{Wt} tagged with hemagglutinin (HA) and subsequently treated with LPS. 48 hrs after transfection, the LPS-challenged BV-2 cells were then harvested and cell extracts co-immunoprecipitated with anti-HA antibody. Proteins were resolved in 4-20% Tris-glycine gels (Precast gels, Biorad) and stained with Sypro-Ruby (Biorad). Protein bands from the gel were excised and subjected to mass spectrometer analysis at the Proteomics Platform, Quebec Genomics Centre, Quebec. The experiments were performed on a Thermo Surveyor MS pump connected to a LTQ linear ion trap mass spectrometer (Thermo Electron, San Jose, CA, USA) equipped with a nanoelectrospray ion source (Thermo Electron). Scaffold (version 1.7; Proteome Software Inc., Portland, OR, USA) was used to validate MS/MS-based peptide and protein identifications. Peptide identifications were accepted if they could be established at >90.0% probability as specified by the Peptide Prophet algorithm (Keller et al., 2002).

Immunofluorescence Microscopy

Cells were grown to 70% confluence on glass coverslips and fixed in 2% paraformaldehyde for 30 min. In some cases BV-2 cells were transiently transfected with the pCMV-TDP-43^{Wt} and pCMV-p65 vectors using the Lipofectamine2000 reagent. After fixation with 4% paraformaldehyde (PFA), cells were washed in phosphate-buffered saline (PBS), and permeabilized with 0.2% Triton X-100 in PBS for 15 min. After blocking coverslips with 5% normal goat serum for 1hr at room temperature, primary antibody incubations were performed in 1% normal goat serum in PBS overnight, followed by an appropriate Alexa Fluor 488 or 594 secondary antibody (Invitrogen) for 1hr at room temperature. Similar procedures were used for staining spinal cord sections from TDP-43

transgenic mice and sections of sporadic ALS cases. Cells were viewed using a 40X or 63 X oil immersion objectives on a Leica DM5000B microscope (Leica Microsystems, Bannockburn, IL, USA).

Quantitative Real-Time RT-PCR

Real-time RT-PCR was performed with a LightCycler 480 (Roche Diagnostics) sequence detection system using LightCycler SYBR Green I at the Quebec genomics Centre, Quebec. Total RNA was extracted from cell culture experiments using Trizol reagent (Invitrogen). Total RNA was treated with DNase (Qiagen, Valencia, CA, USA) to get rid of genomic DNA contaminations. Total RNA was the quantified using Nanodrop and its purity verified by Bioanalyzer 2100 (Agilent Technologies, Santa Clara, CA, USA). Gene-specific primers were constructed using the GeneTools (Biotools Inc.) software. 3 genes Atp5, Hprt1 and GAPDH were used as internal control genes. The primers used for the analysis of genes are given in Table 4.3.

Cytotoxicity Assay

N2a cells were transfected with pCMV-hTDP-43 (both wild type and mutants). 48 hrs after transfection, cells were treated with the conditioned media derived from BV-2 cells, some of which were treated with Lipopolysaccharide (0111:B4 serotype; Sigma). 24 hrs after challenging N2a cells, culture supernatants were assayed for CytoTox-ONE Homogeneous Membrane Integrity Assay (Promega, WI, USA), a fluorimetric assay which depends on the levels of lactate dehydrogenase (LDH) released due to cell death (Swarup et al., 2007a). The assay was performed according to the manufacturer's protocol. Fluorescence was measured using a SpectraMAX Gemini EM (Molecular Devices, Sunnyvale, CA, USA) fluorescence plate reader at an excitation wavelength of 560 nm and an emission wavelength of 590 nm. Similar techniques were used for primary cortical neurons derived from TDP-43 transgenic mice.

Table 4.3

Primers for quantitative RT-PCR

Gene Symbol	Forward Primer Sequences	Reverse Primer Sequences
TNF-α	CCAGACCCTCACACTCAGATCATC	CCTTGAAGAGAACCTGGGAGTAGAC
IL-6	GTCCTTCCTACCCCAATTTCCAA	GAATGTCCACAAACTGATATGCTTAGG
IL-1β	GCCCATCCTCTGTGACTCAT	CGACAAAATACCTGTGGCCT
Nox2	TTGGAATTGCAGATGAGGAAGCGAG	CGATCCTGGGCATTGGTGAGT
RelA (p65)	GAGCGACTGGGGTTGAGAAGC	CCCATAGGCACTGTCTTCTTTCACC
Tlr2	GCTCTTTGGCTCTTCTGGAT	AGGTTCTGATGTTGAAGTCC
MyD88	GGACTGCCAGAAATACTTAGGT	AGACTATCGGCTTAAGTTG
IL-12p40	TTAGCCAGTCCCGAAACCTGCTG	TGGAACTACACAAGAACGAGAGT
Cox-2	GCTGTACAAGCAGTGGCAAA	GCTCGGCTTCCAGTATTGAG
IP-10	AAGTGCTGCCGTCATTTTCT	CATTCTTTTTCATCGTGGCA
iNOS	AGTCCTTCATGAAGCACATGC	TTAGAGTCTTGGTGAAAGT
CXCL12	AGTAGTGGCTCCCCAGGTTT	GAGACAGTCTTGCGGACACA
CCL5	CCCTCACCATCATCCTCACT	CCTTCGAGTGACAAACACGA

CSF-1	GACCCTCGAGTCAACAGAGC	TGTCAGTCTCTGCCTGGATG
IL-1α	CCCGTCCTTAAAGCTGTCTG	AATTGGAATCCAGGGGAAAC
IL-18	ACGTGTTCCAGGACACAACA	ACAAACCCTCCCCACCTAAC
RANTES	CCCTCACCATCATCCTCACT	CTTCTTCTCTGGGTTGGCAC
Atp5α	GCTATGCAACCGCCCTGTACTCTG	ACGGTGCGCTTGATGTAGGGATTC
Hprt1	CAGGACTGAAAGACTTGCTCGAGAT	CAGCAGGTCAGCAAAGAACTTATAGC
GAPDH	GGCTGCCCAGAACATCATCCCT	ATGCCTGCTTCACCACCTTCTTG

ELISA

The levels of TNF-α, IL-1β, IL-6 and IFN-γ were assayed by multi-analyte ELISA and MIX-N-MATCH ELISAarray kits (mouse inflammatory cytokine array, SABiosciences, Frederick, MD, USA). Mouse p65 ELISA (Stressgen, Ann Arbor, MI, USA) and human p65 ELISA (SABiosciences) were carried out according to manufacturer's instructions. For TDP-43 ELISA, we used sandwich-ELISA protocol. Briefly ELISA plates were incubated in mouse monoclonal antibody against TDP-43 (Abnova, clone E2-D3) overnight and the total protein extracts (both soluble and insoluble fractions) were incubated in pre-coated plates. A second TDP-43 polyclonal antibody (ProteinTech) was further added and ELISA performed as described elsewhere(Kasai et al., 2009; Noto et al., 2010). The standard curve for the ELISA assay was carried out with triplicate measurements using 100 µl/well of recombinant TDP-43 protein (MW 54.3 kDa, AAH01487, recombinant protein with GST tag, Abnova Corporation, Walnut, USA) solution at different concentrations (0.24, 0.48, 0.97, 1.9, 3.9, 7.8, 15.6, 31.2, 62.5, 125, 250, 500, 1000 and 1250 ng/ml) of the protein in PBS. The relative concentration estimates of TDP-43 were calculated according to each standard curve.

Nitrite and Reactive Oxygen Species Assays

The cell culture supernatants from cortical neurons or N2a cells were assayed for nitrite concentration using Griess Reagent (Invitrogen) as described elsewhere (Swarup et al., 2007b). The supernatants were also assayed for reactive oxygen species (ROS) using H2DCFDA (Sigma, St. Louis, MO, USA).

Electrophoretic Mobility Shift Assay (EMSA)

48 hrs after transfection of CMV-p65 with pCMV-TDP43^{WT} or pCMV-TDP43^{G348C} and treatment with LPS, BV-2 cells were harvested and nuclear extracts prepared. Nuclear proteins were extracted using a protein extraction kit Panomics (Redwood City, CA, USA) as per the manufacturer's instructions. Concentrations of nuclear proteins were determined on diluted samples using a Bradford assay (Biorad). Interaction between p65 in the protein extract and DNA probe was investigated using EMSA kit from Panomics as per the manufacturer's instructions. These nuclear extracts were incubated with NF-κB binding site

specific oligonucleotides coated with streptavidin. Electrophoretic mobility shift assay (EMSA) was then performed using the NF-κB EMSA kit. For supershift assays, antibodies against p50, p65 or TDP-43 were added during the sample preparation step.

Reporter gene Assays

BV2 cells were harvested in 120 µl of cell lysis buffer (Promega, Madison, WI, USA), and an ensuing 1-min centrifugation step (20,000 ×*g*) yielded a luciferase-containing supernatant. In both cases aliquots of 20-µl supernatant were tested for luciferase activity (luciferase assay kit, Promega) and for β-galactosidase activity (β-galactosidase assay kit, Promega) to adjust for transfection efficiency.

RNA Intereference

To selectively prevent TDP-43 expression, we employed the RNA interference technology. A double-stranded RNA (siRNA) was employed to degrade TDP-43 mRNA and thus to limit the available protein. The siRNA experiments were designed and conducted as described earlier (Swarup et al., 2007a). The siRNAs directed against the murine TDP-43 mRNA (NM_145556.4) consisted of sequences with symmetrical 3'-UU overhangs using siRNA Target Finder (Ambion, TX, USA). The sequence of the most effective TDP-43 siRNAs represented is as follows: 5'- AGGAAUCAGCGUGCAUAUAUU-3', 5'-UAUAUGCACGCUGAUUCCUUU-3'. To account for the non-sequence-specific effects, scrambled siRNA was used. The sequence of scrambled siRNA is as follows: 5'-GUGCACAU GAGUGAGAUUU3' and 5'-CACGUGUACUCACUCUAAA-3'. TDP-43 siRNAs or the scrambled siRNAs were suspended in diethyl pyro-carbonate water to yield desired concentration. For *in vitro* transfection, cells were plated in 24-well plates and transfected with 0.6 µmol/L siRNAs with 2 µL Lipofectamine 2000 (Invitrogen). The cells were then kept for 72 h in OptiMEM medium (Gibco).

Accelerating rotarod.

Accelerating rotarod was performed on mice at 4rpm speed with 0.25rpm/sec acceleration as described elsewhere (Gros-Louis et al., 2008). Mice were subjected to three trials per session and every two weeks.

In vivo bioluminescence imaging

As previously described(Cordeau et al., 2008; Maysinger et al., 2007), the images were gathered using IVIS® 200 Imaging System (CaliperLSXenogen, Alameda, CA, USA). Twenty-five minutes prior to imaging session, the mice received intraperitoneal (i.p.) injection of the luciferase substrate D-luciferine (150 mg/kg—for mice between 20 and 25 g, 150–187.5 ml of a solution of 20 mg/ml of D-luciferine dissolved in 0.9% saline was injected) (CaliperLS-Xenogen).

Statistical Analysis

For statistical analysis, the data obtained from independent experiments are presented as the mean ± SEM; they were analyzed using a paired t-test with Mann-Whitney test, 1-way ANOVA with Kruskal-Wallis test or 2-way ANOVA with Bonferroni adjustment for multiple comparisons using the GraphPad Prism Software version 5.0 (La Jolla, CA, USA). For rotarod and GFAP imaging studies, repeated measures ANOVA was used. In some experiments, an unpaired t-test followed by a Welch's test was performed. Differences were considered significant at $p < 0.05$.

4.5 Results

4.5.1 TDP-43 interacts with p65 subunit of NF-κB

Mass spectrometry analysis and co-immunoprecipitation experiments were carried out to identify proteins which interact with TDP-43 in mouse microglia (BV-2) cells after LPS stimulation, as described in Materials and Methods. Many proteins were co-immunoprecitated with TDP-43, including proteins responsible for RNA granule transport (kinesin), molecular chaperones (Hsp70) and cytoskeletal proteins (*Data not shown*). In addition, our analysis revealed p65 (*REL-A*) as a novel protein interacting with TDP-43. An interaction between TDP-43 with p65 NF-κB was confirmed by a coimmunoprecipitation assay with a polyclonal antibody against TDP-43 using spinal cord extracts from transgenic mice overexpressing human TDP-43^{Wt} and TDP-43^{G348C} mutant (Swarup et al., 2011a) by 3-fold (Figure 4.1B). Additional coimmunoprecipitation experiments carried out using BV-2 cells which were transiently transfected with pCMV-TDP43^{Wt} and pCMV-p65 plasmids clearly show that TDP-43 interacts with p65.

To further determine the significance of TDP-43 interaction with p65 in context of human ALS, TDP-43 was pulled down with the polyclonal anti-TDP43 antibody using spinal cord extracts from 9 sporadic ALS cases and 6 control subjects (Figure 4.1A). In protein extracts from ALS cases, p65 NF-κB was co-immunoprecipitated with TDP-43. In contrast, no p65 was pulled down with TDP-43 using extracts of control spinal cords. To further validate, TDP-43:p65 interaction we performed reverse co-immunoprecipitation using p65 antibody to immunoprecipitate TDP-43 in human spinal cord tissues. Indeed p65 was able to co-immunoprecipitate TDP-43 in all 9 ALS cases, but not in 6 control cases (Supplemental Figure 4.1A). Along with p65, p50 was also co-immunoprecipitated with TDP-43 from the spinal cord samples of TDP-43^{Wt}, TDP-43^{G348C} mice and ALS samples, but not from non-transgenic or control spinal cord tissues, suggesting that TDP-43, p50 and p65 are a part of a complex (Figure 4.1B). To determine whether TDP-43 interacts directly with p65 or p50, we have carried out overexpression studies using pCMV-expression vectors transfected into mouse neuroblastoma Neuro2a cells (Figure 4.1C). Neuro2a cells were transfected with pCMV-p65 or pCMV-p50 expression vectors along with vectors encoding either HA-

tagged TDP-43^{Wt} or TDP-43$^{\Delta NR1-30}$, a deletion mutant lacking the region required for binding to p65 as described in section 4.5.3. It should be noted that the cells were not stimulated by LPS or any other means. After overexpression of p65 and TDP-43^{Wt} in the Neuro2a cells, p65 was co-immunoprecipitated with TDP-43^{Wt} but not with TDP-43$^{\Delta NR1-30}$ using anti-HA antibody. In contrast, p50 was not co-immunoprecipitated with TDP-43^{Wt} when overexpressed alone with TDP-43. These results suggest that TDP-43 interacts directly to p65, but not directly to p50 (Figure 4.1C and Supplemental Figure 4.2). Immunofluorescence microscopy corroborated these results. In the spinal cord of sporadic ALS subjects p65 was detected predominantly in the nucleus of cells in co-localization with TDP-43 (Figure 4.1M-O). On the contrary, in control spinal cord, there was absence of p65 in nucleus reflecting a lack of p65 activation (Figure 4.1J-L). It is remarkable that microscopy of the spinal cord from TDP-43^{Wt} transgenic mice revealed ALS-like immunofluorescence with active p65 that co-localized perfectly with TDP-43 in the nuclei of cells (Figure 4.1G-I). To elucidate which cell types in the spinal cord of ALS cases express TDP-43 and p65, we carried out three-color immunofluorescence with CD11b as microglial specific marker and GFAP as astroglial marker. We found that TDP-43 and p65 co-localize in many microglial and astroglial cells (Figure 4.2D-F; inset). We have quantified our data and found that 20±5% of microglia and 8±3% of astrocytes have TDP-43:p65 co-localization. We also found that many of the TDP-43 p65 co-localisation was in neurons, some also in motor neurons in many ALS cases (Figure 4.2A-C). In many ALS cases where TDP-43 forms aggregates in the cytoplasm, p65 is still in the nucleus (Figure 4.2A-C, arrow-heads). In non-transgenic C57Bl/6 mice, the lack of p65 activation resulted in partial co-localization of TDP-43 with p65 mainly in cytoplasm (Figure 4.1D-F). LPS-stimulated BV-2 cells transfected with pCMV-p65 and pCMV-TDP43^{Wt} had most p65 co-localized with nuclear TDP-43^{Wt} whereas in unstimulated cells p65 did not co-localize with nuclear TDP-43^{Wt}.While p65 was mainly cytoplasmic in 3-months old TDP-43^{Wt} spinal cord, there was gradual age dependent p65 activation in 6-months and 10-months old TDP-43^{Wt} spinal cord (Supplemental Figure 4.1D).

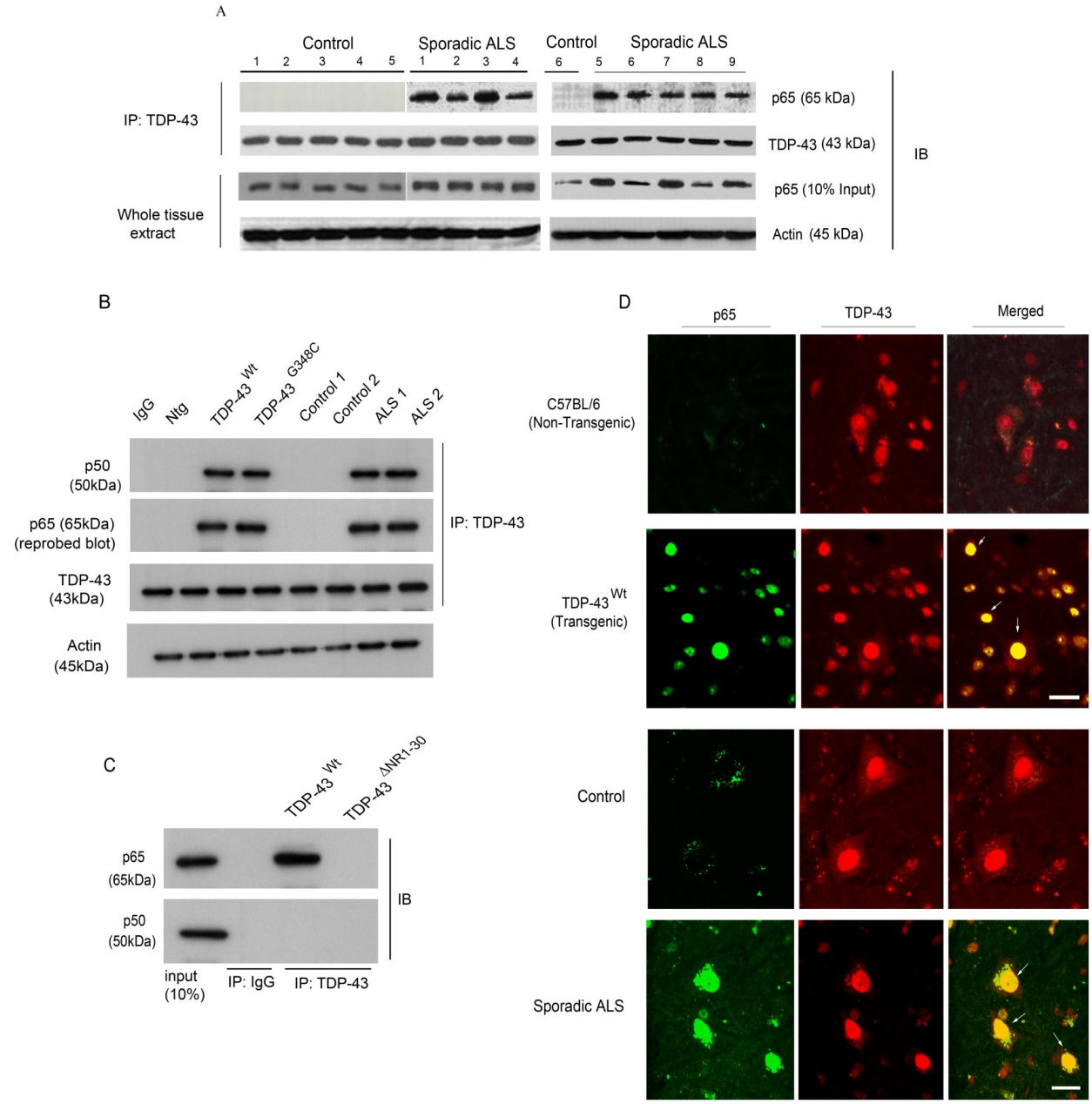
A
Control
Sporadic ALS
Control
Sporadic ALS
1 2 3 4 5 1 2 3 4 6 5 6 7 8 9
IP: TDP-43
p65 (65 kDa)
TDP-43 (43 kDa)
IB
Whole tissue extract
p65 (10% Input)
Actin (45 kDa)
B
IgG
Ntg
TDP-43 Wt
TDP-43 G348C
Control 1
Control 2
ALS 1
ALS 2
p50 (50kDa)
p65 (65kDa) (reprobed blot)
TDP-43 (43kDa)
Actin (45kDa)
IP: TDP-43
C
TDP-43 Wt
TDP-43 ΔNR1-30
p65 (65kDa)
p50 (50kDa)
IB
input (10%)
IP: IgG
IP: TDP-43
D
p65
TDP-43
Merged
C57BL/6 (Non-Transgenic)
TDP-43 Wt (Transgenic)
Control
Sporadic ALS

Figure 4.1. TDP-43 interacts with NF-κB p65. (A) Protein extracts from the spinal cords of nine sporadic ALS subjects (1-9) and six control individuals (1-6) were used for the immunoprecipitation (IP) with TDP-43 specific polyclonal antibody where indicated. Immunoprecipitates or whole cells extracts were subjected to immunoblot (IB) with indicated antibodies. Two experiments were performed (one with control 1-5 and ALS patients 1-4, and the other with control 6 and ALS patients 5-9). (B) Total protein extract from spinal cords of TDP-43^{Wt} and TDP-43^{G348C} transgenic mice, B6 nontransgenic mice (Ntg), 2 control individuals and 2 sporadic ALS patients were subjected to immunoprecipitation and immunoblot where indicated. Representative blot from two independent experiments is shown. (C) Neuro2a cells were transfected with pCMV-p65 and pCMV-p50 expression vectors along with TDP-43^{Wt} or TDP-$43^{\Delta NR1\text{-}30}$. Extracts were immunoprecipitated with anti-TDP-43 or control IgG where indicated, and immunoblotted with anti-p65 and anti-p50. Representative blot from two independent experiments is shown. (D) Spinal cords of B6 nontransgenic or TDP-43^{Wt} transgenic mice or control or ALS patients were stained with anti-p65 and anti-TDP-43 and analyzed by immunofluorescence. Brightness and contrast adjustments were made to the whole image to make background intensities equal in control and ALS cases. The images represent at least four sections from two experiments using ALS and control patient material. Scale bar = 20μm.

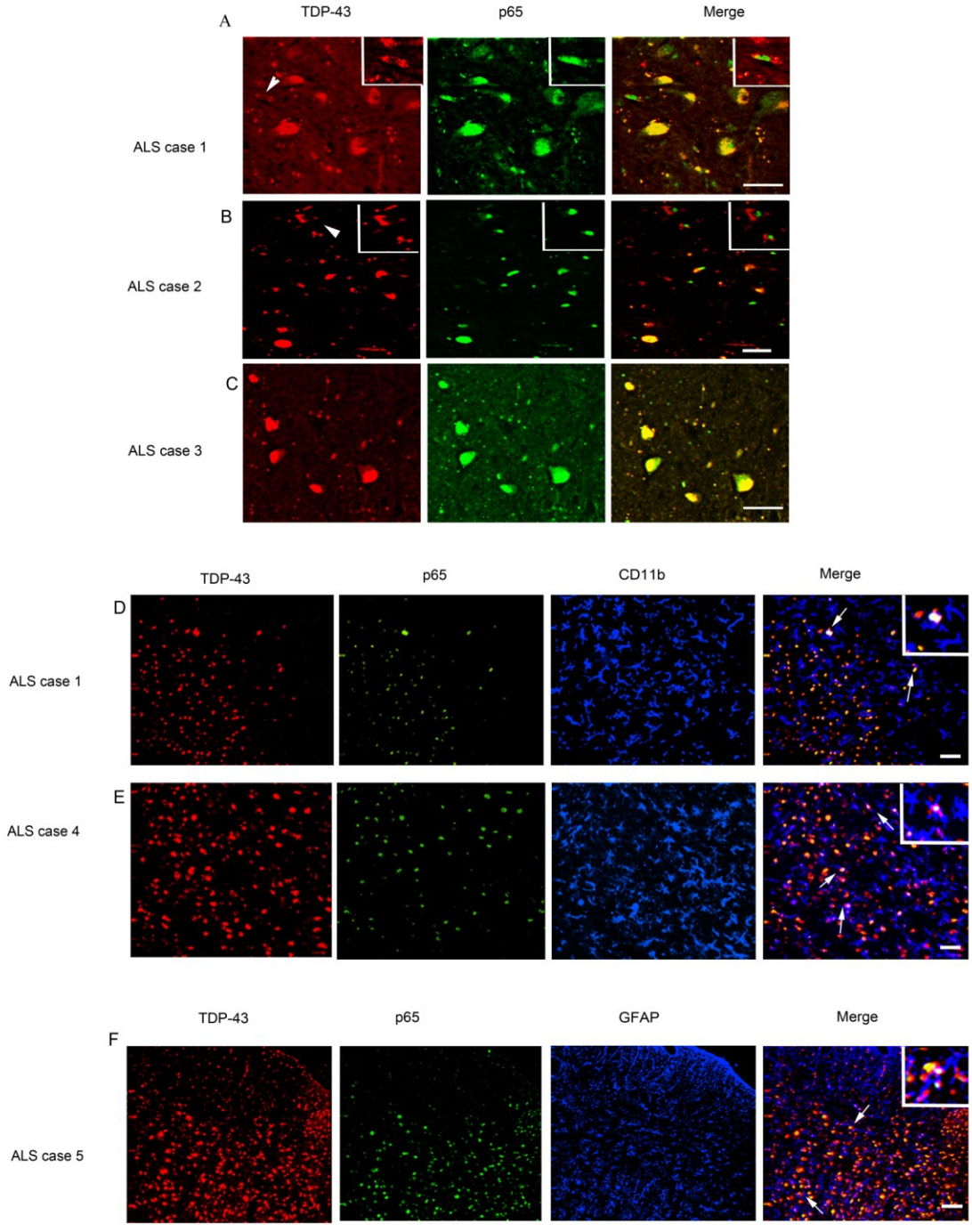
A
TDP-43
p65
Merge
ALS case 1
B
ALS case 2
C
ALS case 3
TDP-43
p65
CD11b
Merge
D
ALS case 1
E
ALS case 4
TDP-43
p65
GFAP
Merge
F
ALS case 5

Figure 4.2. TDP-43 co-localizes with p65 in neuronal and glial cells (A-C) TDP-43 and p65 double immunofluorescence was performed in different sporadic ALS cases as indicated. Double immunofluorescence pictures were taken at various magnifications. Arrowheads represent cytoplasmic localization of TDP-43 and nuclear p65 staining. The image shown is representative of at least four sections from two experiments from ALS patients. (D-E) A three-color immunofluorescence was performed using rabbit TDP-43, mouse p65 and rat CD11b (marker for microglia) as primary antibodies and Alexa Fluor 488 (Green), 594 (Red) and 633 (far-red, pseudo-color Blue) as secondary antibody. Inset of higher magnification, showing triple co-localization (white) of TDP-43, p65 and CD11b positive cells (arrows). The images shown are representative of at least four sections from two experiments from ALS patients. (F) A three-color immunofluorescence was performed using rabbit TDP-43, mouse p65 and rat GFAP (marker for astrocytes) as primary antibodies and Alexa Fluor 488 (Green), 594 (Red) and 633 (far-red, pseudo-color Blue) as secondary antibody. Inset of higher magnification, showing triple co-localization (white) of TDP-43, p65 and GFAP positive cells (arrows). The images shown are representative of at least four sections from two experiments from ALS patients. Scale bar = 20μm.

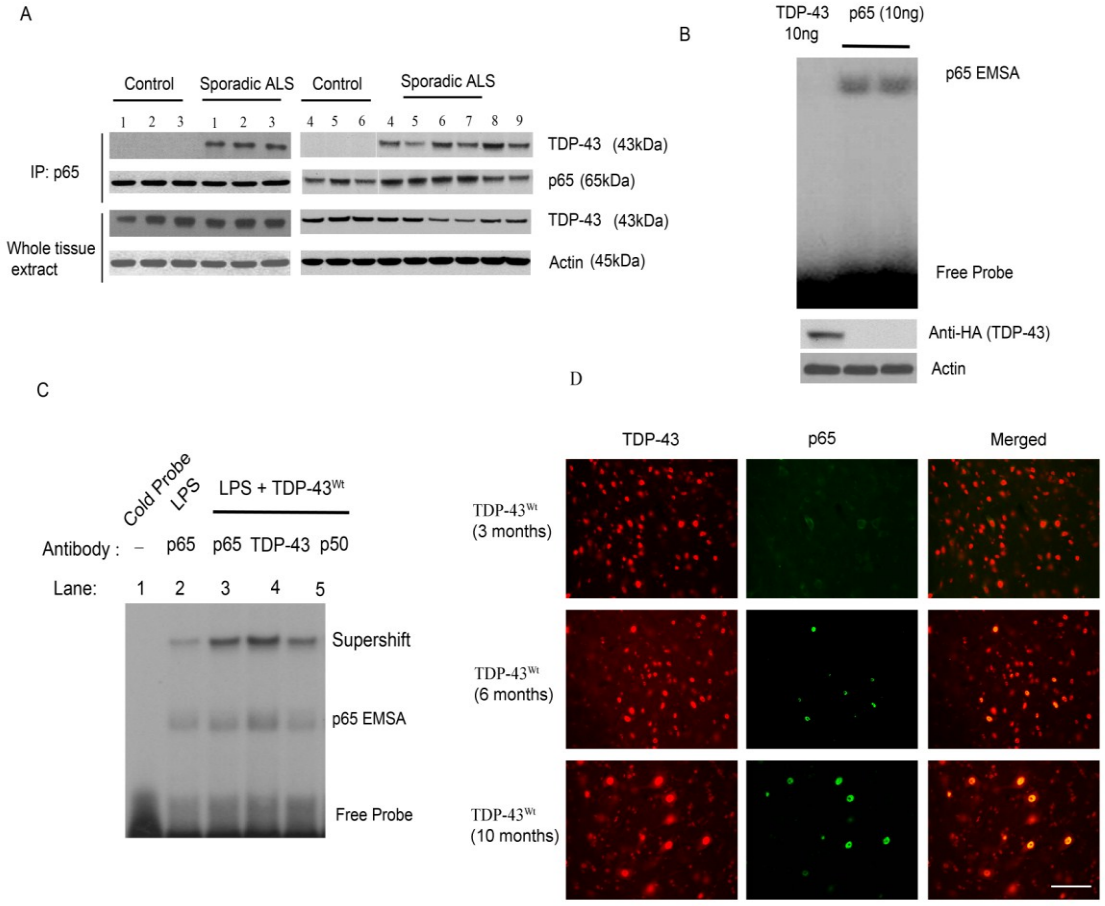

Supplemental Figure 4.1. TDP-43 co-immunoprecipitates with antibodies against p65 and age-dependent increase in p65 activation in TDP-43^{Wt} transgenic mice. (A) Protein extracts from the spinal cords of nine sporadic ALS subjects (1-9) and six control individuals (1-6) were used for the immunoprecipitation (IP) with p65 specific polyclonal antibody where indicated. Immunoprecipitates or whole cells extracts were subjected to immunoblot (IB) with indicated antibodies. (B) BV-2 cells were transfected with either 10ng TDP-43 or with 10ng p65. Nuclear extracts were subjected to p65 EMSA. Representative EMSA from two different experiments is shown. (C) Supershift p65 EMSA was performed with nuclear extracts from LPS stimulated BV-2 cells which were transfected with TDP-43^{Wt} (LPS+TDP-43^{Wt}) or empty vector (LPS only). Addition of p65, p50 or TDP-43 specific antibodies resulted in the supershift in the EMSA. Cold probe was added as a control. (D) Double immunofluorescence with TDP-43 (polyclonal) and p65 antibody in the spinal cord of TDP-43^{Wt} transgenic mice at various ages – 3 months, 6-months and 10-months as indicated. Scale bar = 20μm.

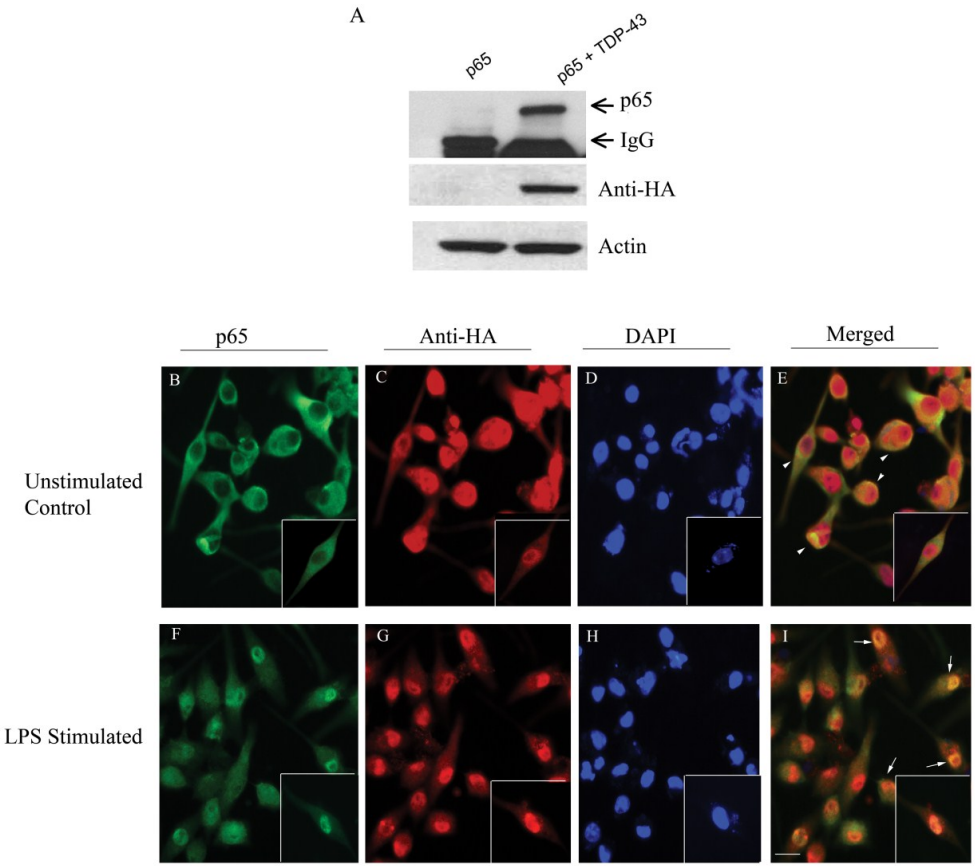

Supplemental Figure 4.2 TDP-43 co-immunoprecipitates with p65 in transfected BV-2 cells (A) pCMV-TDP43^{wt} (HA-tagged) and pCMV-p65 were co-transfected in BV-2 cells. 48 hrs after transfection, cells were harvested and total protein extracted. Cell extract was incubated with dynabeads magnetic beads coupled with anti-HA antibody. After incubation and further washing, the complexes were resolved by 10% SDS-PAGE and subjected to chemiluminescence detection. p65 was co-immunoprecipitated with anti-p65 mouse monoclonal antibody showing that TDP-43 interacts with p65 in vitro. The positions of TDP-43 and mouse IgG heavy chain are indicated. **(B-E)** A double immunofluorescence experiment was set up by transfecting BV-2 cells with pCMV-TDP43^{wt} and pCMV-p65. 24 hrs after transfection, cells were either LPS (100ng/ml) or mock-stimulated. 12 hrs after stimulation, cells were fixed in 4% PFA and stained with Anti-HA antibody (for TDP-43) and mouse monoclonal p65 antibody and counterstained with nuclear marker -DAPI. Mock stimulated TDP-43wt transfected cells show some co-localization (arrow heads) of p65 (mostly in cytoplasm) and TDP-43wt. **(F-I)** LPS stimulated TDP-43wt cells had significant co-localization (white arrow) of p65 and TDP-43^{wt}. Magnification 40X. Inset showing cells at a higher 63X magnification. Scale bar = 20μm.

4.5.2 TDP-43 acts as a co-activator of p65

A gene reporter assay was carried out to study the effect of TDP-43 on NF-κB-dependent gene expression. The effect of TDP-43 was studied on gene expression of the reporter plasmid $4\kappa B^{Wt}$-luc by transfecting pCMV-$TDP43^{Wt}$ in BV-2 cells with or without co-transfection of pCMV-p65 (Figure 4.3A). When expressed alone, TDP-43 had no detectable effect on the basal transcription level of plasmid $4\kappa B^{Wt}$-luc, suggesting that TDP-43 does not alter the basal transcription level of NF-κB. However, in co-expression with p65, TDP-43 augmented the gene expression of plasmid $4\kappa B^{Wt}$-luc in a dose-dependent manner. pCMV-p65 (20ng) alone activated gene expression of $4\kappa B^{Wt}$-luc by 10-fold (Figure 4.3A). However, upon co-transfection with pCMV-$TDP\text{-}43^{Wt}$ (20 ng), the extent of gene activation was elevated to 22-fold (2.2-fold augmentation by the effect of TDP-43). Further increase in NF-κB-dependent gene expression was recorded as the levels of $TDP\text{-}43^{Wt}$ were elevated to 50ng (2.8-fold activation) and 100ng (3.2- fold activation, $n=4$, $p<0.05$). The boosting effects of TDP-43 were not due to increased levels in p65 as shown by immunoblotting (Figure 4.3B). Similarly, pCMV-$TDP43^{A315T}$ and pCMV-$TDP43^{G348C}$ augmented p65-mediated gene expression from the reporter plasmid $4\kappa B^{Wt}$-luc (data not shown).

To further examine the effect of TDP-43 on the activation of p65, we performed p65 electrophoretic mobility shift assays (EMSA). Transfection in BV2 cells of pCMV-p65 with pCMV-$TDP43^{Wt}$ or pCMV-$TDP43^{G348C}$ and LPS treatment was followed by extraction of nuclear proteins. Subsequently the interaction between p65 in the protein extract and DNA probe was investigated using EMSA kit from Panomics (Redwood City, CA, USA) following the manufacturer's instructions.TDP-43 increased the binding of p65 to the NF-κB DNA probe in a dose-dependent manner. LPS alone induced the binding of p65 to the DNA probe by about 2-fold as compared to control (Figure 4.3C). The co-transfection of $TDP\text{-}43^{Wt}$ (50ng and 100ng) or of $TDP\text{-}43^{G348C}$ (100ng) resulted in a significant dose-dependent increase in the DNA binding of p65. The specificity of the gel shift assay was assessed by adding a cold probe. TDP-43 alone does not bind to p65 EMSA probes (Supplemental Figure 4.1B). Moreover, adding an anti-HA antibody which

recognizes the transfected TDP-43 or an anti-p65 antibody caused supershifts of bands in the p65 EMSA (Figure 4.3D). Along with p65 and TDP-43, p50 is also part of the activated complex as seen by supershifts of bands in p65 EMSA studies in BV-2 cells using antibodies specific to p65, TDP-43 and p50 (Supplemental Figure 4.1C).

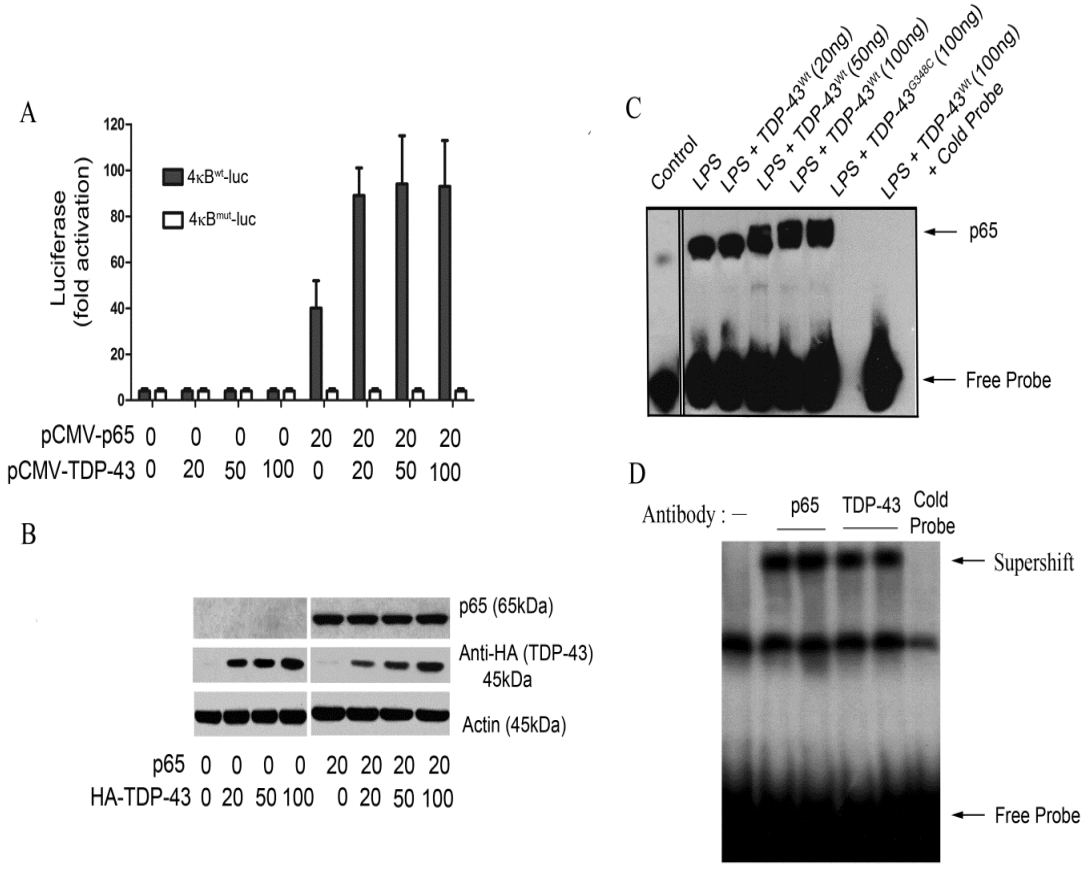

Figure 4.3. TDP-43 acts as a co-activator of NF-κB p65. (A) BV-2 cells were transfected with 20 ng of $4\kappa B^{Wt}$-luc (containing wild type NF-κB binding sites) or $4\kappa B^{mut}$-luc (containing mutated NF-κB binding sites) together with the indicated amounts of pCMV-$TDP43^{Wt}$ expression plasmid. Cells were harvested 48 h after transfection, and luciferase activity was measured. Values represent the luciferase activity mean ± SEM of three independent transfections and statistical analysis was done by two-way ANOVA with Bonferroni adjustment. (B) BV-2 cells were transfected with 20ng pCMV-p65 and various concentrations of pCMV-$TDP43^{Wt}$. TDP-43 levels are shown when blotted with Anti-HA antibody (Sigma), Actin is shown as a loading control. (C) 48 hrs after transfection, BV-2 cells were harvested and nuclear extracts were then incubated with NF-κB p65 binding site specific oligonucleotides coated with streptavidin. EMSA was then performed using the NF-κB EMSA kit. (D) Supershift assay was performed by adding anti-HA antibody, which specifically recognizes human TDP-43, during the EMSA assay.p65 antibody was also added in a separate lane as a positive control.

4.5.3 p65 interacts with the N-terminal and RRM-1 domains of TDP-43

To determine which domains of TDP-43 interacts with p65, we constructed a series of deletion mutants of various TDP-43 domains. Various pCMV-HA tagged deletion mutants like TDP-43$^{\Delta N}$ (1-105AAs), TDP-43$^{\Delta RRM-1}$ (106-176AAs), TDP-43$^{\Delta RRM-2}$ (191-262AAs) and TDP-43$^{\Delta C}$ (274-414AAs) were transfected in BV-2 cells with pCMV-p65 (Figure 4.4A). TDP-43$^{\Delta RRM-1}$ co-immunoprecipitated p65 partially whereas TDP-43$^{\Delta RRM-2}$ and TDP-43$^{\Delta C}$ interacted well with p65, suggesting that RRM-1 is important, but RRM-2 and C-terminal domains are dispensable for interaction with p65. Following transfection we found that TDP-43$^{\Delta N}$ had much reduced interaction with p65 (Figure 4.4B), thereby suggesting that N-terminal domain of TDP-43 is essential for the interaction of TDP-43 with p65. Since the nuclear localization signal (NLS) is in the N-terminal, the reduced interaction of TDP-43$^{\Delta N}$ to p65 could have been the result of a mislocalization of TDP-43$^{\Delta N}$. To address this issue and to further define the interacting domain, we constructed series of N-terminal and RRM-1 deletion mutants - TDP-43$^{\Delta NR1-81}$ (98-176AAs), TDP-43$^{\Delta NR1-50}$ (51-81 and 98-176 AAs) and TDP-43$^{\Delta NR1-30}$ (31-81 and 98-176 AAs) with the NLS signal attached so that the mutant proteins are able to be directed to the nucleus. Co-immunoprecipitation with these constructs suggested that even though TDP-43$^{\Delta NR1-30}$ is in the nucleus (Figure 4.4C), it cannot effectively interact with p65, TDP-43$^{\Delta NR1-81}$ and TDP-43$^{\Delta NR1-50}$ whereas can interact with p65 (Figure 4.4B). These results indicate that TDP-43 interacts with p65 through its N-terminal domain (31-81 and 98-106 AAs) and RRM-1 (107-176 AAs) domain.

To assess the effect of these deletion mutants on the activation of NF-κB gene, we used the gene reporter assay. Various deletion mutants of TDP-43 were co-transfected along with 4κB^{Wt}-luc or 4κB^{mut}-luc. When compared to full length TDP-43^{Wt}, TDP-43$^{\Delta N}$ had reduced effect (2-fold, n=3, $p<0.05$) on the gene activation. TDP-43$^{\Delta RRM-1}$ also exhibited attenuation of gene activation but to lesser extent than TDP-43$^{\Delta N}$ (Figure 4.4D). In contrast, TDP-43$^{\Delta RRM-2}$ and TDP-43$^{\Delta C}$ deletion mutants had effects similar to full length TDP-43^{Wt}. As expected, because TDP-43$^{\Delta NR1-30}$ does not effectively interact with p65, the level of NF-

κB activation detected by the 4κB^{Wt}-luc reporter assay was extremely low, 6-fold lower than full-length TDP-43^{Wt} (n=3, $p<0.001$) (Figure 4.4D). p65 and luciferase vectors were used as control for the experiment. Note that the amount of pCMV-p65 vector transfected in control was more than in other experiments to keep similar amounts of total transfected DNA. Transfection of a control luciferase reporter construct, 4κB^{mut}-luc, in which all four κB sites were mutated, had no effect on the basal-level activation of p65.To determine, if the interaction between TDP-43 and p65 is a protein-protein interaction, we performed immunoprecipitation experiments by adding either proteinase K, RNase A or DNase 1 (Figure 4.4E). Addition of proteinase K abolished TDP-43-p65 interaction, whereas RNase A or DNase 1 had no effect, suggesting that the interaction is not DNA/RNA dependent.

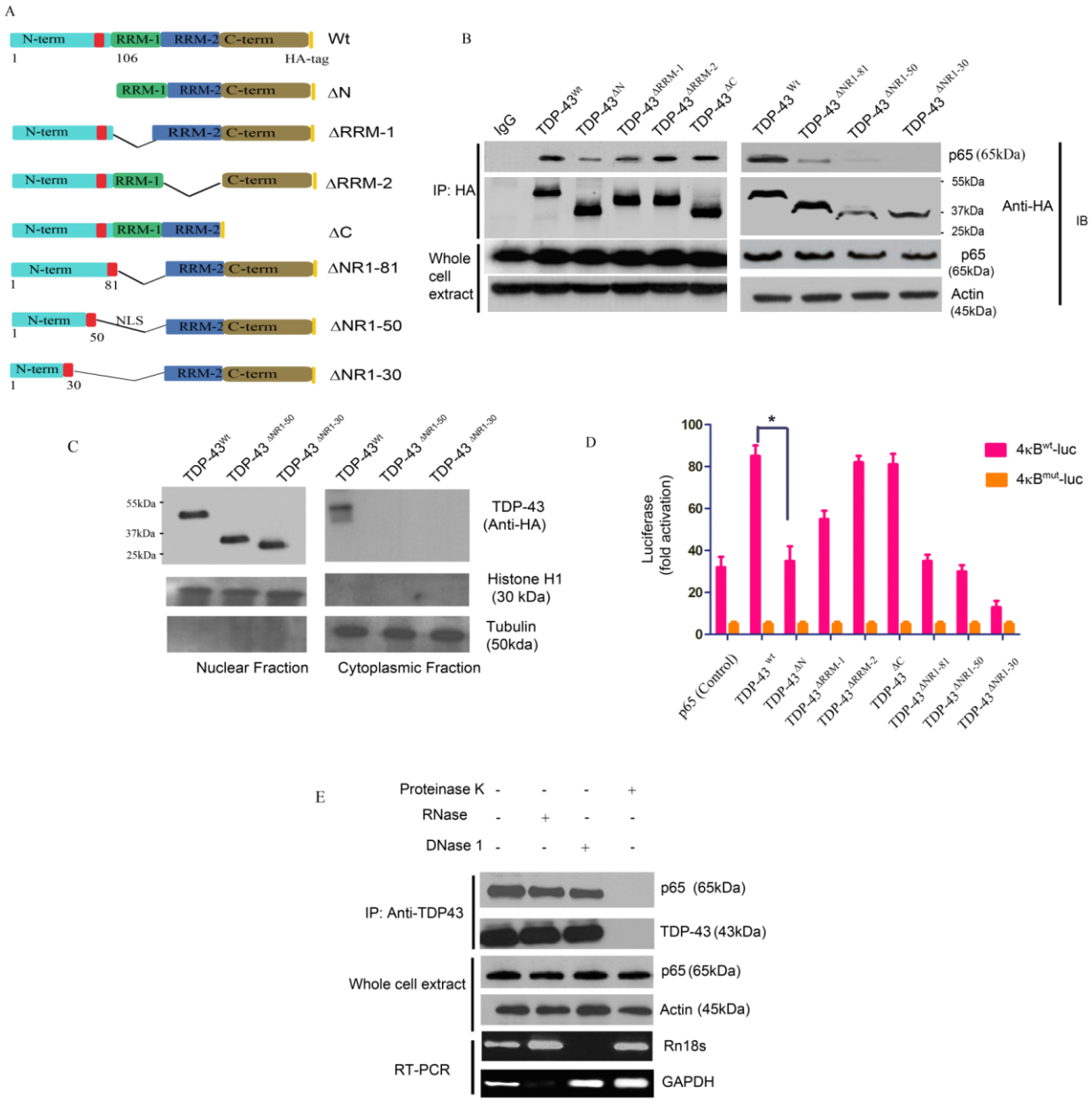
A
N-term
RRM-1
RRM-2
C-term
Wt
1
106
HA-tag
ΔN
ΔRRM-1
ΔRRM-2
ΔC
ΔNR1-81
81
ΔNR1-50
NLS
50
ΔNR1-30
30
B
IgG
TDP-43Wt
TDP-43ΔN
TDP-43ΔRRM-1
TDP-43ΔRRM-2
TDP-43ΔC
TDP-43 Wt
TDP-43 ΔNR1-81
TDP-43 ΔNR1-50
TDP-43 ΔNR1-30
IP: HA
Whole cell extract
p65 (65kDa)
55kDa
37kDa
25kDa
Anti-HA
p65 (65kDa)
Actin (45kDa)
IB
C
TDP-43Wt
TDP-43 ΔNR1-50
TDP-43 ΔNR1-30
55kDa
37kDa
25kDa
TDP-43 (Anti-HA)
Histone H1 (30 kDa)
Tubulin (50kda)
Nuclear Fraction
Cytoplasmic Fraction
D
Luciferase (fold activation)
100
80
60
40
20
0
*
4κBwt-luc
4κBmut-luc
p65 (Control)
TDP-43 wt
TDP-43ΔN
TDP-43ΔRRM-1
TDP-43ΔRRM-2
TDP-43 ΔC
TDP-43ΔNR1-81
TDP-43ΔNR1-50
TDP-43ΔNR1-30
E
Proteinase K - - - +
RNase - + - -
DNase 1 - - + -
IP: Anti-TDP43
p65 (65kDa)
TDP-43 (43kDa)
Whole cell extract
p65 (65kDa)
Actin (45kDa)
RT-PCR
Rn18s
GAPDH

Figure 4.4. The N-terminal and RRM-1 domains of TDP-43 are crucial for interaction with p65. (A) 2-dimensional cartoon of TDP-43 protein showing various deletion mutants used in this study. Deletion mutants TDP-43$^{\Delta N}$ (1-105AAs), TDP-43$^{\Delta RRM-1}$(106-176AAs), TDP-43$^{\Delta RRM-2}$ (191-262AAs) and TDP-43$^{\Delta C}$ (274-414AAs) and full-length TDP-43 (TDP-43^{Wt}) are shown. Serial N-terminal and RRM-1 domain deletion mutants are also shown. TDP-43$^{\Delta NR1-81}$ (98-176AAs), TDP-43$^{\Delta NR1-50}$ (51-81 and 98-176 AAs) and TDP-43$^{\Delta NR1-30}$ (31-81 and 98-176 AAs) were generated. (B) All constructs (Wt and deletion mutants) were cloned in pcDNA3.0 with HA tag at extreme C-terminal of the encoded protein. BV-2 cells were transfected with TDP-43^{Wt} or deletion constructs and pCMV-p65. 24 hrs after transfection, cells were harvested and immunoprecipitated (IP) with anti-HA antibody. Immunoprecipitates or whole cells extracts were subjected to immunoblot (IB) with indicated antibodies. A representative gel from three independent experiments is shown. (C) BV-2 cells transfected with TDP-43^{Wt}, TDP-43$^{\Delta NR1-50}$ or TDP-43$^{\Delta NR1-30}$ were fractionated into nuclear and cytoplasmic fractions using sucrose-density gradient centrifugation. These fractions were then probed with Anti-HA antibody for the expression of transfected TDP-43 species. Histone H1 is used as a nuclear and tubulin as a cytoplasmic marker. A representative gel from two independent experiments is shown. (D) Various deletion mutants of TDP-43 were co-transfected along with 4κB^{Wt}-luc (containing wild type NF-κB binding sites) or 4κB^{mut}-luc (containing mutated NF-κB binding sites). 48 h after transfection, luciferase activity was measured. Statistical analysis was done by two-way ANOVA with Bonferroni adjustment. Error bars represent mean ± SEM from three independent experiments. (E) TDP-43 antibody was added to BV-2 transfected cell lysates and proteins were immunoprecipitated (IP) with indicated antibody. After TDP-43 immunoprecipitation, samples were treated with either proteinase K (1μg/ml), RNase(1μg/ml) or DNase 1(1μg/ml). To monitor the effectiveness of RNase and DNase digestion, RNase or DNase were added to cell lysates before immunoprecipitation and subjected to PCR. GAPDH RT-PCR was used to monitor RNase digestion, while Rn18s gene (which codes for 18SrRNA) genomic PCR was used to monitor DNase digestion. Representative blots and gels from three different experiments are shown.

4.5.4. TDP-43 siRNA inhibits activation of NF-κB

If correct that TDP-43 acts as a co-activator of p65, then reducing the levels of TDP-43 should attenuate p65 activation. To reduce the expression levels of TDP-43, microglial BV-2 cells were transfected with either TDP-43 siRNA or scrambled siRNA together with $4\kappa B^{Wt}$-luc vectors. 72 hrs after transfection some of the cells were either stimulated with LPS (100ng/ml) or mock stimulated for 12 hrs. As shown in (Figure 4.5A), TDP-43 siRNA reduced the endogenous mouse TDP-43 levels significantly as compared to scrambled siRNA transfected cells in two different experiments. To examine the effect of reducing TDP-43 levels on NF-κB activation, BV-2 cells were transfected with pCMV-p65 and $4\kappa B^{Wt}$-luc vectors. TDP-43 siRNA decreased activation of NF-κB reporter gene in transfected cells. The decrease in NF-κB activation was about 3-fold for 5ng pCMV-p65 ($n=4$, $p<0.01$) and about 2.5-fold for 10 and 20ng pCMV-p65 ($n=4$, $p<0.05$) and 2-fold for 50ng pCMV-p65 ($n=4$, $p<0.05$) as compared to scrambled siRNA transfected cells (Figure 4.5B). To examine the physiological significance of TDP-43 inhibition by siRNA, we transfected BV-2 cells with ICAM1-luc vector together with TDP-43 siRNA or scrambled siRNA. 72 hrs after transfection, cells were stimulated with varying concentrations of TNF-α. When stimulated at 0.5ng/ml of TNF-α, TDP-43 siRNA transfected cells exhibited a 2-fold decrease in ICAM-1 luciferase activity ($n=4$, $p<0.05$) as compared to cells transfected with scrambled siRNA. Similarly, TDP-43 siRNA transfected BV-2 cells exhibited at 1.0ng/ml and 1.5ng/ml TNF-α concentrations decrease of 2.5-fold ($n=4$, $p<0.01$) and 2-fold ($n=4$, $p<0.05$) in ICAM-1 luciferase activity, respectively (Figure 4.5C). We also tested the effect of TDP-43 siRNA transfected in bone-marrow derived macrophages (BMMs) from normal mice. We compared the level of innate immunity activation when stimulated with LPS. BMMs transfected with TDP-43 siRNA had reduced levels of TLR2 mRNA (1.5-fold, $p<0.05$), p65 (3-fold, $p<0.01$), TNF-α (3-fold, $p<0.01$), IL-1β (2-fold, $p<0.05$), IP-10 (2-fold, $p<0.05$), IL-6 (2.5-fold, $p<0.01$) and Cox-2 (2-fold, $p<0.05$) as compared to scrambled siRNA transfected BMMs (Figure 4.5D).

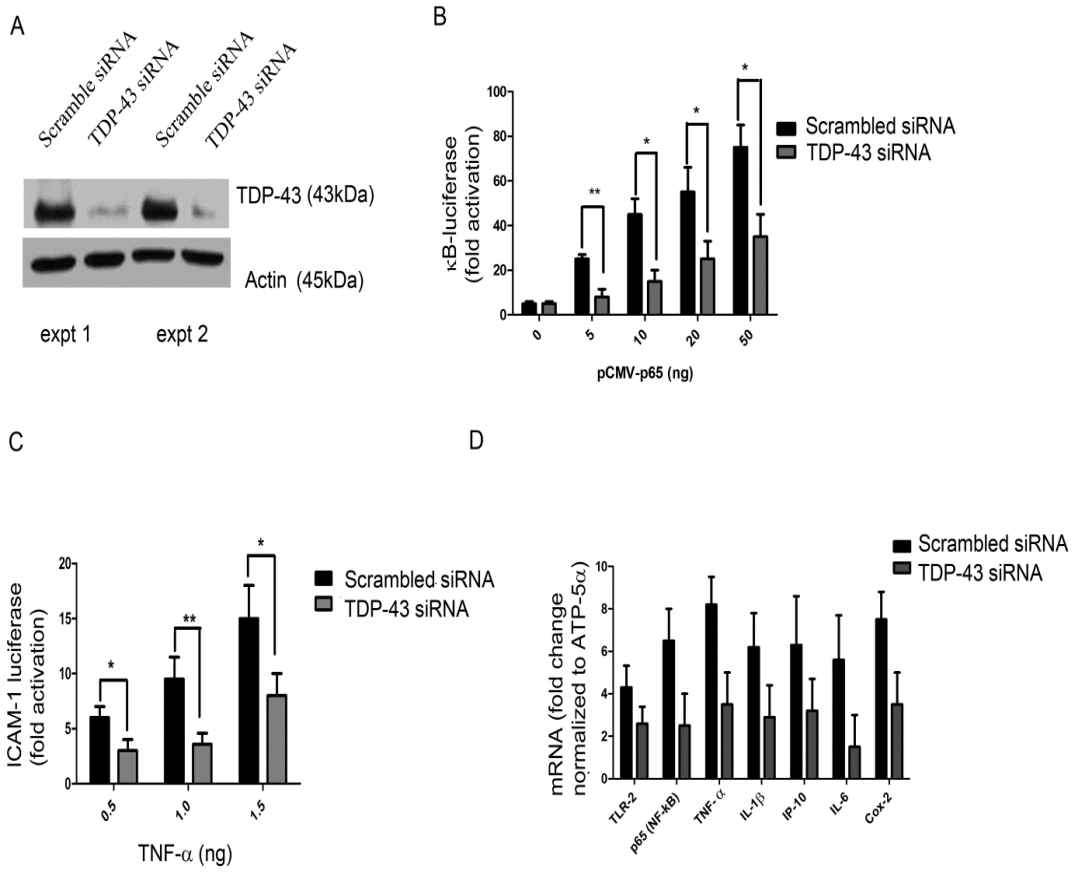

Figure 4.5. TDP-43 siRNA inhibits activation of NF-κB. BV-2 cells were transfected either with mouse TDP-43 siRNA or scrambled siRNA. 72 hrs after transfection some of the cells were either stimulated with LPS (100ng/ml) or mock stimulated for 12 hrs. (A) Protein extracted from siRNA experiment was subjected to western blot analysis. Mouse endogenous TDP-43 levels in TDP-43 siRNA or scrambled siRNA were compared in two different experiments (expt1 and expt2) as determined by rabbit polyclonal TDP-43 antibody. (B) Additionally BV-2 cells were transfected with pCMV-p65 (concentrations as indicated) and $4\kappa B^{Wt}$-luc vector and luciferase assay was performed. Statistical analysis was done by two-way ANOVA with Bonferroni adjustment. Error bars represent mean ± SEM from three independent experiments. (C) We transfected BV-2 cells with ICAM1-luc vector in addition to TDP-43 siRNA or scrambled siRNA in three different expeiments. 72 hrs after transfection, cells were stimulated with varying concentrations (as indicated) of TNF-α. Statistical analysis was done by two-way ANOVA with Bonferroni adjustment. (D) Real-time quantitative PCR levels of various mRNAs were compared with TDP-43 siRNA transfected (and LPS stimulated) bone-marrow derived macrophages (BMMs) and scrambled siRNA transfected (and LPS stimulated) BMMs. Statistical analysis was done by two-way ANOVA with Bonferroni adjustment. Error bars represent mean ± SEM from three different experiments.

4.5.5 TDP-43 and p65 mRNA levels are upregulated in the spinal cord of sporadic ALS patients

The findings that TDP-43 can interact with p65 and that TDP-43 overexpression in transgenic mice was sufficient to provoke abnormal nuclear co-localization of p65 as observed in sporadic ALS (Figure 4.1 M-O), prompted us to compare the levels of mRNA coding for TDP-43 and p65 NF-κB in spinal cord samples from sporadic ALS cases and control individuals. Real-time RT-PCR data revealed that the levels of TDP-43 mRNA in the spinal cord of sporadic ALS cases (n=16) were upregulated by about 2.5-fold ($p<0.01$) compared to controls (n=6) (Figure 4.6A). It is also noteworthy that the levels of p65 NF-κB mRNA were upregulated by about 4-fold ($p<0.001$) in ALS cases as compared to controls. Since TDP-43 forms many bands in western blot analysis, we quantified the total level of TDP-43 protein using sandwich ELISA as described in the materials and methods. The ELISA results suggest that TDP-43 protein levels are in fact upregulated in total spinal cord protein extracts of ALS cases (n=16) by 1.82-fold (241.2 ± 8.5 pg/μg of total protein) as compared to control cases (132.8 ± 5.6 pg/μg of total protein, n=6) (Figure 4.6B). For human p65 ELISA, we used an ELISA kit from SABioscience, Qiagen. The levels of p65 were also upregulated in total spinal cord extracts of ALS cases (n=16) by 3.5-fold (222.5 ± 11.5 pg/μg of total protein) as compared to control cases (62.83 ± 3.8 pg/μg of total protein, n=6) (Figure 4.6C).

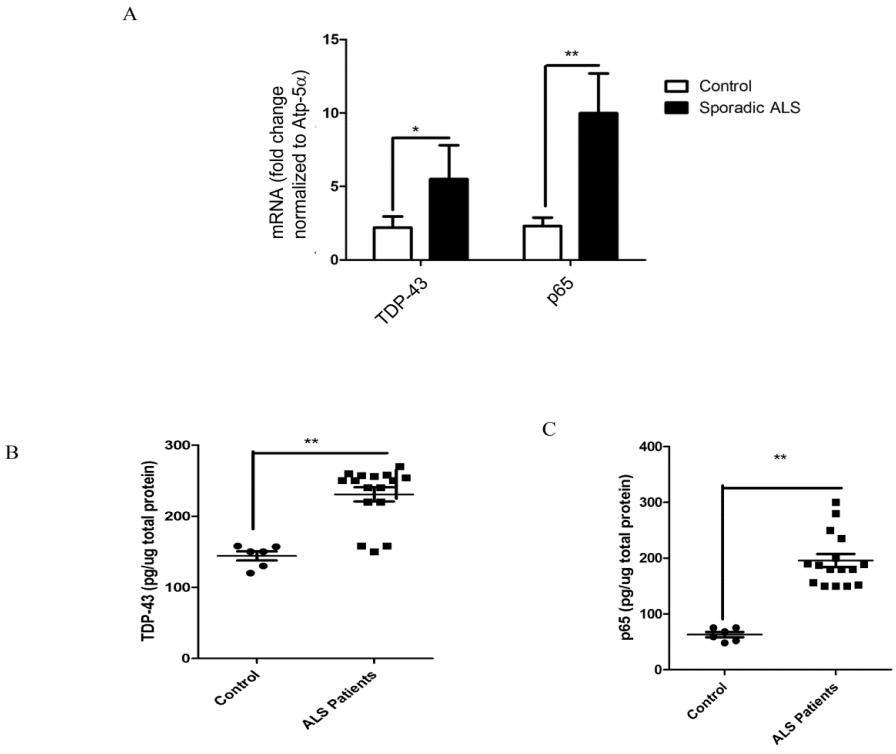

Figure 4.6. Analysis of TDP-43 and NF-κB p65 mRNA expression in sporadic ALS spinal cord. (A) Spinal cord tissue samples from 16 different sporadic ALS patients and 6 controls were subjected to real-time RT-PCR analysis using primers specific for TDP-43 (TARDBP) and p65 (RELA). Statistical analysis was done using unpaired student's t-test with Welch's correction. Error bars represent mean ± SEM from three different experiments. All real-time RT-PCR values are normalized to Atp-5α levels. (B) Sandwich ELISA was performed for TDP-43 using TDP-43 monoclonal and polyclonal antibodies. After coating the ELISA plates with TDP-43 monoclonal antibody, the plate were incubated with the protein lysates (containing both soluble and insoluble fragments in between) followed by TDP-43 polyclonal antibody and subsequent detection. Statistical analysis was done using unpaired student's t-test with Welch's correction. Error bars represent mean ± SEM from three different experiments. (C) For p65 ELISA, an ELISA kit from SABioscience, Qiagen was used. Statistical analysis was done using unpaired student's t-test with Welch's correction. Error bars represent mean ± SEM from three different experiments.

4.5.6 TDP-43 overexpression in glia or macrophages causes hyperactive inflammatory responses to LPS

Since NF-κB is involved in pro-inflammatory and innate immunity response, we tested the effects of increasing TDP-43 mRNA expression in BV-2 cells. Because LPS is a strong pro-inflammatory stimulator (Horvath et al., 2008), we used it to determine the differences in levels of pro-inflammatory cytokines produced by TDP-43-transfected or mock-transfected BV-2 cells. BV-2 cells were transiently transfected either with pCMV-TDP43^{Wt}, pCMV-TDP43^{A315T}, pCMV-TDP43^{G348C} or empty vector. 48 hrs after transfection and 12hrs after LPS challenge (100ng/ml), RNA extracted from various samples were subjected to real-time quantitative RT-PCR to determine the mRNA levels of various pro-inflammatory genes. As expected, there was a 4-fold increase in mRNA levels of TNF-α following LPS stimulation of BV-2 cells compared to controls (Figure 4.7A). However in LPS treated cells transfected with wild-type TDP-43, there was an additional 3-fold ($n=5$, $p<0.05$) increase in TNF-α levels. TDP-43 harboring the A315T and G348C mutations had similar effects on boosting the levels of TNF-α upon LPS stimulation. Similarly, in response to LPS, the extra levels of TDP-43 species in transfected microglial cells caused a significant 5-fold increase ($n=5$, $p<0.001$) in the mRNA levels of IL-1β (Figure 4.8A) and 9-fold increase in mRNA levels of IL-6 (Figure 4.7B, $n=5$, $p<0.001$) as compared to LPS-treated mock-transfected cells. The levels of NADPH oxidase 2 (Nox-2 gene) was increased by about 2.8-fold (Figure 4.8B, $n=5$, $p<0.05$) in LPS-challenged TDP-43 transfected cells as compared to LPS treated mock-transfected cells. Remarkably, overexpression of TDP-43 species resulted in 10-fold ($n=5$, $p<0.001$) increase in levels of p65 (RELA) mRNA in LPS-treated transfected cells as compared to LPS-treated mock-transfected cells (Figure 4.7C). Note that, in absence of LPS stimulation, microglial cells transfected with TDP-43 species (both wild-type and mutants) exhibited no significant differences in levels of TNF-α, IL-1β, Nox-2 and NF-κB when compared to mock-transfected controls.

To further evaluate the effect of LPS stimulation in TDP-43 overexpressing microglia, we prepared primary microglial cultures from C57Bl/6 mice and from transgenic mice

overexpressing by 3-fold TDP-43$^{Wt.}$ Primary microglial cells were challenged with LPS at a concentration of 100ng/ml of media. 12 hrs after LPS challenge, cells were harvested and total protein extracted and used for multi-analyte ELISA. LPS-treated TDP-43^{Wt} transgenic microglia had significantly higher levels of TNF-α (2.5-fold, $p<0.01$), IL-1β (2.3-fold, $p<0.01$), IL-6 (2-fold, $p<0.05$) and IFN-γ (2-fold, $p<0.05$) as compared to LPS-treated microglia from C57Bl/6 non-transgenic mice (Figure 4.7D). However, in absence of LPS stimulation, no significant differences in cytokines levels were detected between microglia from TDP-43^{Wt} transgenic mice and from non-transgenic mice (Data not shown). The p65 level was significantly higher (3-fold; $p<0.01$) in LPS-treated TDP-43^{Wt} microglia as compared to non-transgenic microglia (Figure 4.7D). We also treated primary microglial cultures with 1mM H_2O_2 for 1hr (and incubated in serum-free media for 12hrs) to study the effect of reactive-oxygen species (ROS) on primary microglial cultures. H_2O_2-treated TDP-43^{Wt} transgenic microglia had significantly higher levels of TNF-α (3-fold, $p<0.01$), IL-1β (2.5-fold, $p<0.01$), IL-6 (1.7-fold, $p<0.05$), IFN-γ (2-fold, $p<0.05$) and p65 (RELA) levels (2.2-fold, $p<0.05$) when compared to H_2O_2-treated microglia from C57Bl/6 non-transgenic mice (Figure 4.7E) as determined by multi-analyte ELISA.

LPS stimulation of primary microglial cells caused degradation of IkB-α as shown in Figure 4.7G. The decrease in IkB-α levels was more pronounced in microglia overexpressing TDP-43 species. After LPS treatment, the increases in levels of p65, phospho-p65$^{Ser\ 536}$, p50 and phospho-$^{p50Ser\ 337}$ were also more robust in transgenic microglia overexpressing TDP-43 species (Figure 4.7G). Similarly, H_2O_2-treatment led to reduction in IkB-α levels and increase in levels of p65 and phospho-p65^{Ser536} in TDP-43^{Wt} (Figure 4.8C). Again, the effects were more pronounced in transgenic microglia overexpressing TDP-43 species (Figure 4.8C). We then treated primary astrocytes with LPS and studied their response to LPS using real-time RT-PCR. LPS-treated TDP-43^{Wt} transgenic astrocytes had significantly higher levels of IL-α (1.75-fold, $p<0.05$), IL-1β (1.67-fold, $p<0.05$), IL-6 (2.8-fold, $p<0.01$), IL-18 (1.8-fold, $p<0.05$) and chemokines like colony stimulating factor (CSF) (1.6-fold, $p<0.05$), CCL5 (1.9-fold, $p<0.05$) and CXCL12 (2.67-

fold, $p<0.01$) as compared to LPS-treated microglia from C57Bl/6 non-transgenic mice (Figure 4.7F).

To further evaluate the innate immune response in TDP-43^{Wt} transgenic mice, we isolated bone-marrow derived macrophages (BMM) from TDP-43^{Wt} transgenic mice and from C57Bl/6 non-transgenic mice. In LPS-stimulated TDP-43^{Wt} macrophages there was an increase of 1.6-fold ($p<0.05$) in TLR2 mRNA levels, 1.8-fold ($p<0.05$) in MyD88 levels, 2.6-fold ($p<0.01$) in p65 (RELA, $p<0.01$) levels as compared to LPS stimulated control (non-transgenic) macrophages (Figure 4.7H). We also found in LPS-stimulated TDP-43^{Wt} macrophages that there was an increase of 3.2-fold ($p<0.01$) in TNF-α , 3.5-fold in IL-1β ($p<0.01$) and 2.6-fold in IL-12p40 levels, 2.5-fold ($p<0.01$) in IL-6 levels, 2-fold ($p<0.05$) in Cox-2 and iNOS levels, 3-fold in IP-10 levels ($p<0.01$) and 2.1-fold in RANTES ($p<0.05$) mRNA levels as compared to LPS stimulated control (non-transgenic) macrophages (Figure 4.7H).

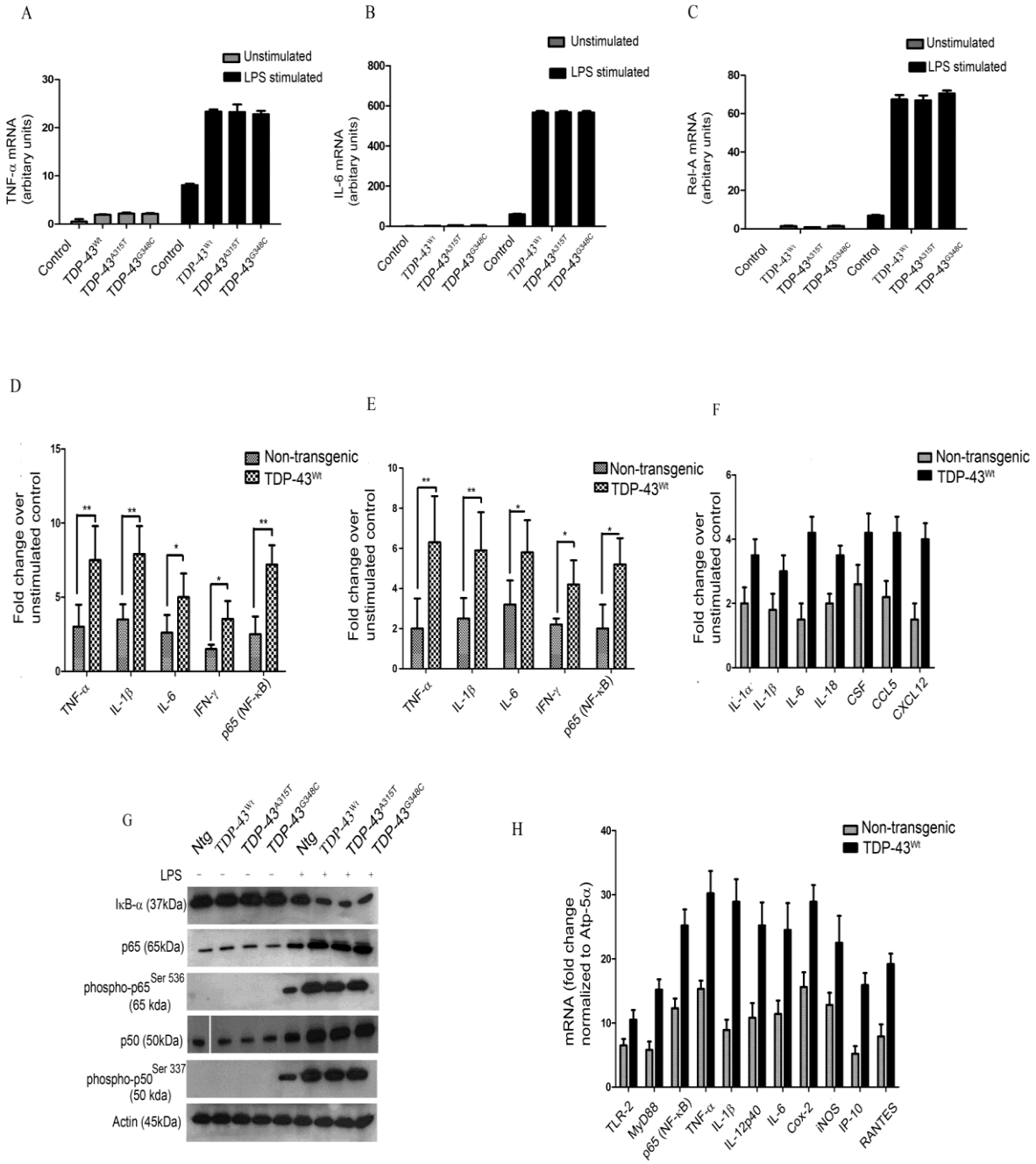
A
Unstimulated
LPS stimulated
TNF-α mRNA (arbitary units)
Control
TDP-43Wt
TDP-43A315T
TDP-43G348C
B
IL-6 mRNA (arbitary units)
C
Rel-A mRNA (arbitary units)
D
Non-transgenic
TDP-43Wt
Fold change over unstimulated control
TNF-α
IL-1β
IL-6
IFN-γ
p65 (NF-κB)
E
F
IL-1α
IL-18
CSF
CCL5
CXCL12
G
Ntg
LPS
IκB-α (37kDa)
p65 (65kDa)
phospho-p65 Ser 536 (65 kda)
p50 (50kDa)
phospho-p50 Ser 337 (50 kda)
Actin (45kDa)
H
mRNA (fold change normalized to Atp-5α)
TLR-2
MyD88
TNF-α
IL-1β
IL-12p40
IL-6
Cox-2
iNOS
IP-10
RANTES

Figure 4.7. Analysis of genes involved in inflammation of mouse microglial and macrophage cells overexpressing human TDP-43. Mouse microglial cells BV-2 were either transfected with pCMV-TDP43^{Wt}, pCMV-TDP43^{A315T}, and pCMV-TDP43^{G348C} or with empty vectors for 48 hrs. These cells were then either stimulated with LPS at a concentration of 100ng/ml or unstimulated (as indicated). 12hrs after stimulation, total RNA was extracted with Trizol. The total RNA samples were then subjected to real-time quantitative RT-PCR for TNF-α (A), IL-6 (B) and Rel-A (p65) (C). Error bars represent mean ± SEM from five different experiments. Statistical analysis was done by two-way ANOVA with Bonferroni adjustment. (D) Primary microglial cultures from TDP-43^{Wt} and B6 nontransgenic mice were stimulated with 100ng/ml of LPS. Proteins from LPS stimulated microglial cultures were subjected to multi-analyte ELISA for inflammatory cytokines and p65. Error bars represent mean ± SEM from four different experiments. Statistical analysis was done by two-way ANOVA with Bonferroni adjustment. (E) Primary microglial cultures from TDP-43^{Wt} and B6 nontransgenic mice were treated with 1mM H_2O_2 for 1hr and incubated in serum-free media for 12hrs to study the effect of reactive-oxygen species (ROS). Error bars represent mean ± SEM from three different experiments. Statistical analysis was done by two-way ANOVA with Bonferroni adjustment. (F) Pure (>90%) primary astrocytes from TDP-43^{Wt} and B6 nontransgenic mice were stimulated with LPS and their response studied using real-time PCR for various genes as indicated. Error bars represent mean ± SEM from three different experiments. Statistical analysis was done by two-way ANOVA with Bonferroni adjustment. (G) Primary microglial cells from TDP-43^{Wt}, TDP-43^{A315T}, TDP-43^{G348C} and B6 nontransgenic mice (Ntg) were stimulated or unstimulated with LPS. Immunoblots were run to determine the levels of various proteins using specific antibodies as indicated. Representative blot from two independent experiments is shown. (H) Bone marrow derived macrophages (BMMs) isolated from TDP-43^{Wt} and B6 nontransgenic mice were stimulated by 100ng/ml of LPS for 12 hrs. The total RNA samples were then subjected to real-time quantitative RT-PCR for various genes as indicated. Results are displayed as fold change over unstimulated control. All real-time RT-PCR values are normalized to Atp-5α levels. Error bars represent mean ± SEM from four different experiments. Statistical analysis was done by two-way ANOVA with Bonferroni adjustment.

4.5.7. TDP-43 upregulation increases microglia-mediated neurotoxicity

We then examined the effect of TDP-43 overexpression on toxicity of microglia towards neuronal cells. This was done with the use of primary microglia and of cortical neurons derived from transgenic mice overexpressing TDP-43 species (TDP-43^{Wt}, TDP-43^{A315T} or TDP-43^{G348C}) and C57Bl/6 non-transgenic mice. Primary cortical neurons were cultured for 12 hrs in conditioned media from LPS-stimulated microglial cells. All conditioned media from LPS-challenged microglia increased the death of cortical neurons in culture (Figure 4.8D). The media from LPS-stimulated non-transgenic microglial cells increased the neuronal death of non-transgenic mice by 3.5-fold ($p<0.01$). However, there were marked increases of neuronal death caused by conditioned media from LPS challenged microglia (of same genotype) overexpressing TDP-43 species: 5.5-fold ($p<0.001$) for TDP-43^{Wt}, 6.5-fold ($p<0.001$) for TDP-43^{A315T} and 7.5-fold ($p<0.001$) for TDP-43^{G348C}. The increased neurotoxicity of the conditioned media was associated with increased ROS and NO production. The ROS production, as determined by H2DCFDA fluorescence, was significantly higher in conditioned media challenged neurons from TDP-43^{Wt} (1.5-fold, $p<0.05$), TDP-43^{A315T} (1.8-fold, $p<0.05$) or TDP-43^{G348C} (2-fold, $p<0.05$) as compared individually to conditioned media challenged non-transgenic control neurons (Figure 4.8E). Similarly, the nitrite (NO) production was significantly higher in TDP-43^{Wt} (1.5-fold, $p<0.05$), TDP-43^{A315T} (2.3-fold, $p<0.05$) or TDP-43^{G348C} (3-fold, $p<0.01$) as compared individually to non-transgenic control (Figure 4.8F).

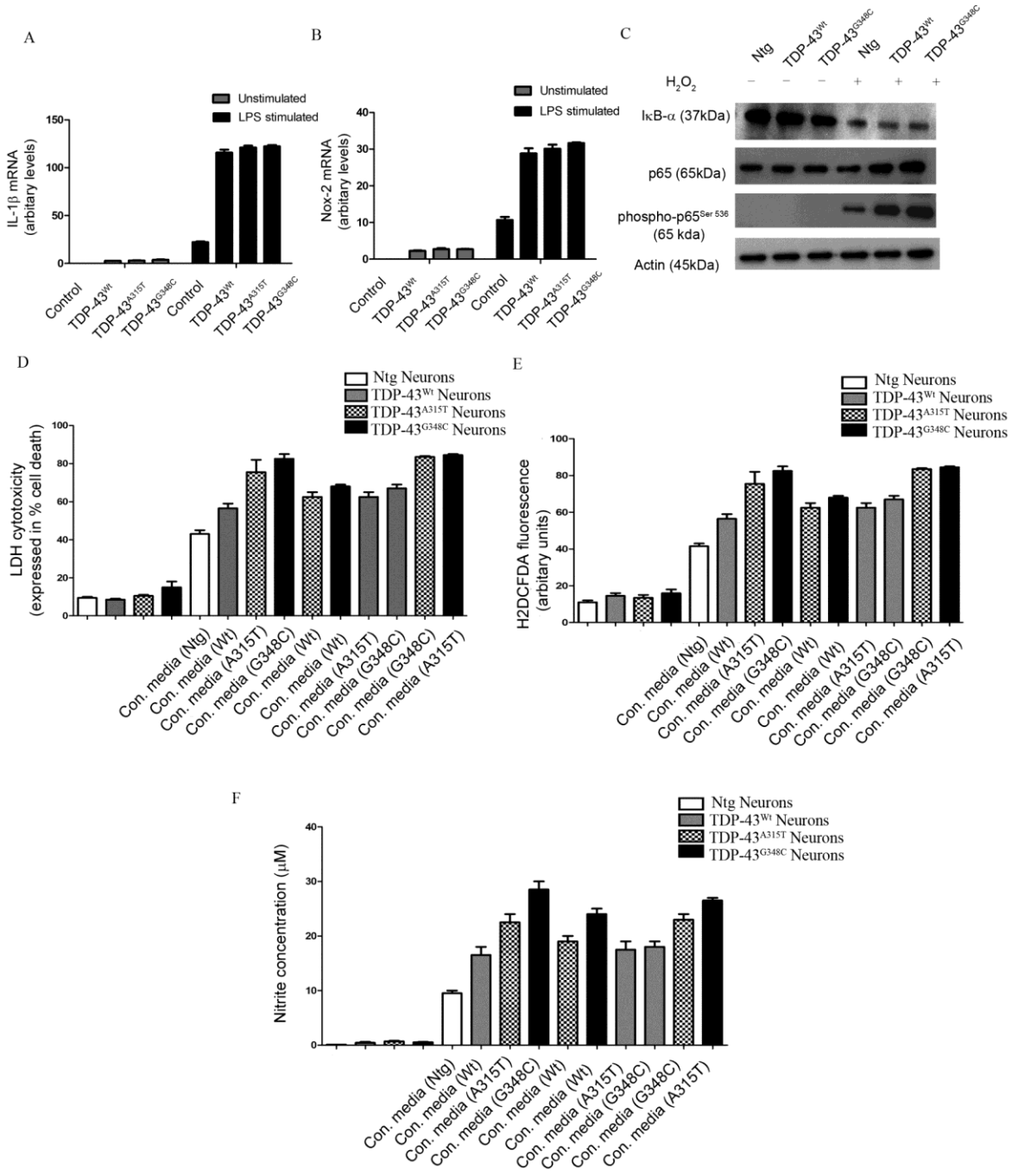
A
Unstimulated
LPS stimulated
IL-1β mRNA (arbitary levels)
Control
TDP-43Wt
TDP-43A315T
TDP-43G348C
B
Unstimulated
LPS stimulated
Nox-2 mRNA (arbitary levels)
C
Ntg
TDP-43Wt
TDP-43G348C
H2O2
IκB-α (37kDa)
p65 (65kDa)
phospho-p65Ser 536 (65 kda)
Actin (45kDa)
D
Ntg Neurons
TDP-43Wt Neurons
TDP-43A315T Neurons
TDP-43G348C Neurons
LDH cytotoxicity (expressed in % cell death)
Con. media (Ntg)
Con. media (Wt)
Con. media (A315T)
Con. media (G348C)
E
H2DCFDA fluorescence (arbitary units)
F
Nitrite concentration (μM)

Figure 4.8. TDP-43 upregulation enhances neuronal vulnerability to death by microglia-mediated cytotoxicity. (A-B) TDP-43 (Wt and mutants) transfected BV-2 cells were stimulated with LPS. 12hrs after stimulation, total RNA was extracted with Trizol. The total RNA samples were then subjected to real-time quantitative RT-PCR for IL1-β (A) and Nox-2 (B). Error bars represent mean ± SEM from five different experiments. Statistical analysis was done by two-way ANOVA with Bonferroni adjustment. (C) Primary microglial cells from TDP-43^{Wt}, TDP-43^{A315T}, TDP-43^{G348C} and B6 nontransgenic mice (Ntg) were stimulated or unstimulated with H_2O_2. Immunoblots were run to determine the levels of various proteins using specific antibodies as indicated. Representative blot from two independent experiments is shown. (D-F) Primary cortical neurons from TDP43^{Wt}, TDP43^{A315T}, TDP43^{G348C} and control B6 nontrangenic (Ntg) mice were incubated with the conditioned media (con. media) derived from primary microglial cells treated with 100ng/ml LPS. 12 hrs after challenging cortical cells, cell-culture supernatants were used for lactate dehydrogenase (LDH) assay (D). ROS production was determined by H2DCFDA fluorescence (E) and nitrite production was evaluated by griess reagent (F). Error bars represent mean ± SEM from four independent experiments.

4.5.8. Inhibition of NF-κB activation reduces vulnerability of TDP-43 overexpressing neurons to toxic injury

NF-κB is known to modulate p53-p38MAPK dependent apoptosis in neurons, when treated with DNA damage inducing chemicals like camptothecin (Aleyasin et al., 2004), glutamate excitotoxicity (Pizzi et al., 2005) or general bystander mediated killing of neurons by microglia (Sephton et al., 2010). To assess the potential contribution of NF-κB to the death of TDP-43 overexpressing neurons exposed to toxic injury, we prepared cultures of primary cortical neurons and microglia from transgenic mice overexpressing TDP-43^{Wt} or TDP-43 mutants. Cortical neurons were exposed to 10μM glutamate for 15 min, with or without 1μM withaferin A (WA), a known inhibitor of NF-κB (Oh et al., 2008). The LDH cytotoxicity was determined 24 hrs later (Figure 4.10A). We found that neurons overexpressing TDP-43 species were more vulnerable than non-transgenic neurons to glutamate cytotoxicity and that inhibition of NF-κB by WA resulted in marked decrease in cell death: TDP-43^{Wt} (2-fold, $p<0.01$), TDP-43^{A315T} (3-fold, $p<0.01$) and TDP-43^{G348C} (3-fold, $p<0.01$). The addition of WA inhibited NF-κB, as detected by reduced levels of phospho-$p65^{Ser536}$ (Figure 4.10B). We then incubated cortical neurons with the conditioned media from primary microglial culture, which were challenged with LPS at a concentration of 100ng/ml of media. Treatment of neuronal cultures with WA resulted in substantial decrease in microglia-mediated death of neurons overexpressing TDP-43^{Wt} (2-fold, $p<0.01$), TDP-43^{A315T} (3-fold, $p<0.01$) or TDP-43^{G348C} (3-fold, $p<0.01$). As WA might exert multiple pharmacological actions, we tested a more specific molecular approach for inhibiting NF-κB. We expressed a stable mutant super-repressive form of IκB-α (Ser 32/ Ser36-to-alanine mutant; $IκB^{SR}$) and evaluated its effects on neuronal death. $IκB^{SR}$ transfected cortical neurons from TDP-43 transgenic and non-transgenic mice were exposed to either 10μM glutamate for 30min or incubated in conditioned media from LPS-stimulated microglia of same genotype. Similar to WA treatment, we found that $IκB^{SR}$ inhibited NF-κB activation and it attenuated the glutamate-induced or microglia-mediated death of neurons overexpressing TDP-43^{Wt} (1.3-fold, $p<0.01$), TDP-43^{A315T} (1.5-fold, $p<0.01$) and TDP-43^{G348C} (2-fold, $p<0.01$) (Figure 4.9A and 4.9D).

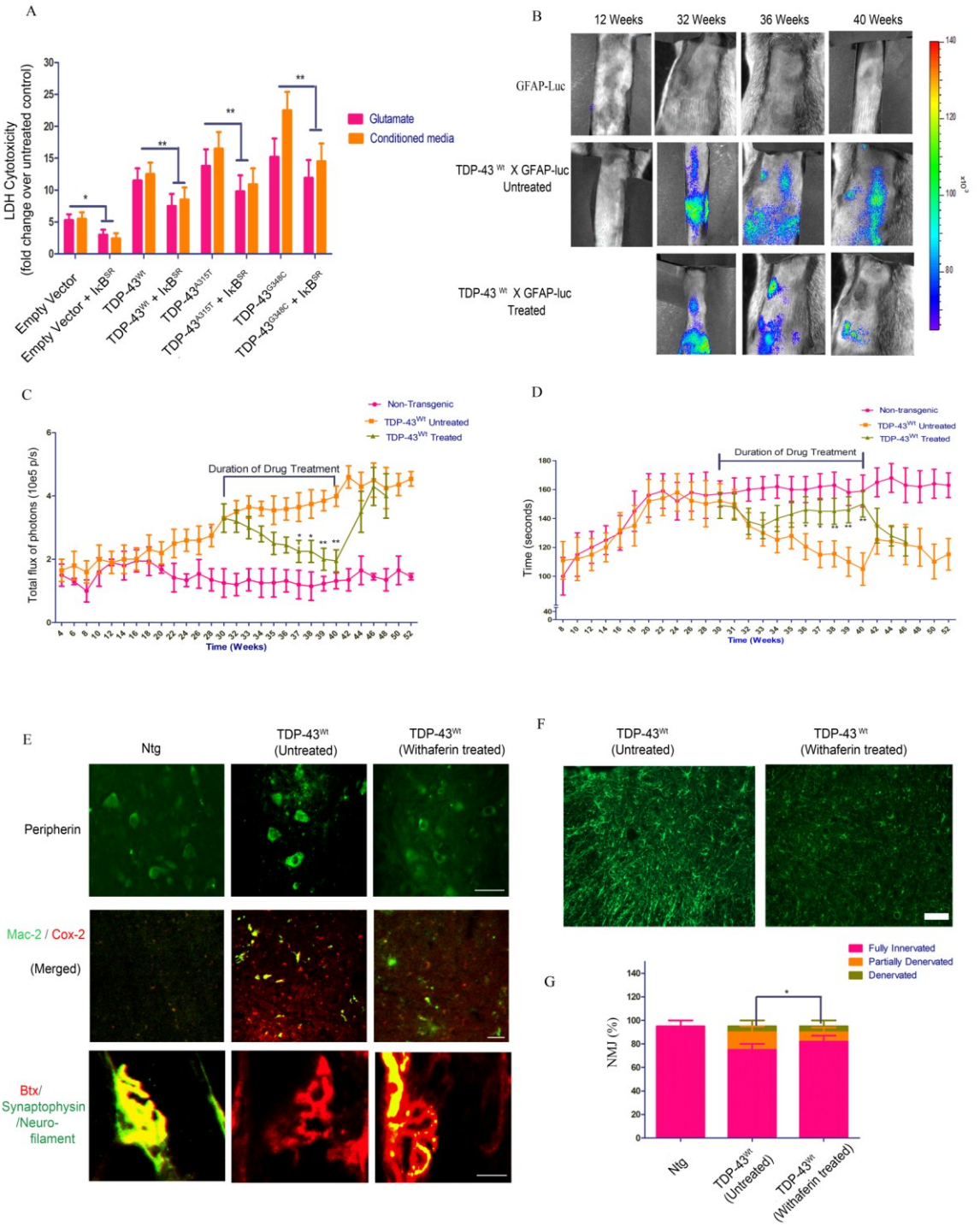
A
LDH Cytotoxicity
(fold change over untreated control)
Glutamate
Conditioned media
Empty Vector
Empty Vector + IκB^SR
TDP-43^Wt
TDP-43^Wt + IκB^SR
TDP-43^A315T
TDP-43^A315T + IκB^SR
TDP-43^G348C
TDP-43^G348C + IκB^SR
B
12 Weeks
32 Weeks
36 Weeks
40 Weeks
GFAP-Luc
TDP-43 Wt X GFAP-luc
Untreated
TDP-43 Wt X GFAP-luc
Treated
C
Non-Transgenic
TDP-43^Wt Untreated
TDP-43^Wt Treated
Duration of Drug Treatment
Total flux of photons (10e5 p/s)
Time (Weeks)
D
Non-transgenic
TDP-43^Wt Untreated
TDP-43^Wt Treated
Duration of Drug Treatment
Time (seconds)
Time (Weeks)
E
Ntg
TDP-43^Wt (Untreated)
TDP-43^Wt (Withaferin treated)
Peripherin
Mac-2 / Cox-2
(Merged)
Btx/
Synaptophysin
/Neuro-
filament
F
TDP-43^Wt (Untreated)
TDP-43 Wt (Withaferin treated)
G
Fully Innervated
Partially Denervated
Denervated
NMJ (%)
Ntg
TDP-43^Wt (Untreated)
TDP-43^Wt (Withaferin treated)

Figure 4.9. Withaferin A, an inhibitor of NF-κB, reduces neuronal vulnerability to toxic injury and ameliorates disease phenotypes in TDP-43 transgenic mice (A) A stable mutant super-repressive form of IκB-α ($IκB^{SR}$) was expressed and its effects on neuronal death were evaluated. The phosphorylation-defective IκBαS32A/S36A acts by sequestering the cytoplasmic NF-κB pool in a manner that is insensitive to extracellular stimuli. Cultured cortical neurons from TDP-43^{Wt}, TDP-43^{A315T}, TDP-43^{G348C} and B6 nontransgenic (Ntg) mice were transfected with a plasmid construct, expressing $IκB^{SR}$, and exposed to either 10μM glutamate for 30min or incubated in conditioned media from LPS-stimulated microglia of same genotype. Cytotoxicity to the cells was measured by lactate dehydrogenase (LDH) assay using a commercially available kit. Statistical analysis was done by two-way ANOVA with Bonferroni adjustment. Data represent mean ± SEM from three independent experiments. (B) In vivo bioluminescence imaging of astrocyte activation was analysed at various time points in the spinal cord of GFAP-luc/TDP-43^{Wt} mice. Typical sequence of images of the spinal cord area obtained from of GFAP-luc/TDP-43^{Wt} mice at different time points (12, 32, 36, and 40 weeks) by in vivo imaging (n=10, each group). Withaferin A was injected in GFAP-luc/TDP-43^{Wt} for 10 weeks starting at 30-weeks of age till 40-weeks. Representative images are shown. (C) Longitudinal quantitative analysis of the total photon GFAP-signal/ bioluminescence (total flux of photon/s) in withaferin A treated and untreated GFAP-luc/TDP-43^{Wt} mice and control GFAP-luc mice in the spinal cord are displayed. Duration of drug treatment is indicated. * represents a statistically significant difference between treated and untreated groups ($p<0.05$) and ** ($p<0.01$) using repeated-measures 2-way ANOVA (n=10, each group). (D) Accelerating rotarod analysis was performed in GFAP-luc/TDP-43^{Wt} mice at various ages from 8-weeks to 52-weeks and time taken by the mice to fall from the rotarod is used as rotarod performance. Withaferin A treatment period is marked as drug treatment period. * represents a statistically significant difference between treated and untreated groups ($p<0.05$) and ** ($p<0.01$) using repeated-measures 2-way ANOVA (n=10, each group). (E) Immunofluorescence of spinal cord sections of non-transgenic (control), TDP-43^{Wt} (untreated) and TDP-43^{Wt} (Withaferin treated) mice with polyclonal peripherin antibody is shown. Double immunofluorescence of spinal cord sections with activated microglial marker Mac-2 and cyclooxygenase -2 (Cox-2) is shown. Representative images from four different mice per genotype is shown. Neuromuscular junction (NMJ) staining was performed using anti-synaptophysin/neurofilament antibodies (green) and α-bungarotoxin (BTX - red). Representative images from four different mice per genotype showing fully innervated muscle in 10-months old non-transgenic mice, fully denervated muscle in TDP-43^{Wt} mice (untreated) and partially denervated muscle in age-matched withaferin treated TDP-43^{Wt} mice. Scale bar = 20μm. (F) Immunofluorescence using GFAP antibody was performed in the spinal cord sections of withaferin treated and untreated GFAP-luc/TDP-43^{Wt} mice Representative images from five different mice per genotype are shown. Scale bar = 20μm. (G) Three hundred neuromuscular junctions were counted per animal sample. Frequencies of innervation, partial denervation and denervation were then converted to percentages and plotted as graph. Statistical analysis was done by Student's t-test. * represents a statistically significant difference between treated and untreated groups ($p<0.01$) using repeated-measures 2-way ANOVA. Error bars represent mean ± SEM from three different experiments.

4.5.9. NF-κB inhibition by Withaferin A treatment reduces inflammation and ameliorates motor impairment of TDP-43 transgenic mice

To study the *in vivo* effect of NF-κB inhibition on disease progression, we injected TDP-43^{Wt};GFAP-luc double transgenic mice with 3mg/kg body weight of WA twice a week for 10-weeks starting at 30-weeks. The pharmacokinetic parameters of withaferin A has been published recently (Thaiparambil et al., 2011) and we have determined that this compound passes the blood-brain barrier (Supplemental Figure 4.3). We used TDP-43^{Wt};GFAP-luc double transgenic mice because the reporter luciferase (luc) allowed the longitudinal and non-invasive biophotonic imaging with CCD camera of the GFAP promoter activity which is a target of activated NF-κB**.** To analyse the spatial and temporal dynamics of astrocytes activation/GFAP induction in TDP-43 mouse model, we performed series of live imaging experiments. These live imaging experiments revealed that treatment of TDP-43^{Wt};GFAP-luc mice with WA caused progressive reduction in GFAP-luc expression in the spinal (Figure 4.9B,C) compared to untreated TDP-43^{Wt} mice which continued to exhibit high GFAP-luc expression. The downregulation of GFAP promoter activity was further confirmed in these mice using GFAP immunofluorescence of spinal cord sections of TDP-43^{Wt} mice (both drug-treated and untreated) (Figure 4.9F).This downregulation of GFAP in withaferin-treated mice was actually caused by reduced amount of active p65 in the nucleus of cells as indicated by p65 EMSA (Figure 4.10C). Analysis of motor behaviour using accelerating rotarod showed that withaferin-treated TDP-43^{Wt} mice had significantly better motor performance compared to untreated TDP-43^{Wt} mice as indicated by improved rotarod testing times (Figure 4.9D). We performed peripherin immunofluorescence and found reduction of peripherin aggregates in withaferin treated TDP-43Wt mice (Figure 4.9E). Peripherin levels were also reduced in withaferin treated TDP-43^{Wt} mice as seen by immunoblot (Figure 4.10E). Double immunofluorescence of activated microglial marker Mac-2 and cyclo-oxygenase-2 (Cox-2) shows a marked reduction in activated microglia in withaferin treated TDP-43^{Wt} mice (Figure 4.9E and Figure 4.10F). The withaferin-treated mice also had 40% reduction in the number of partially denervated neuromuscular junction (NMJ) (Figure 4.9E&G).

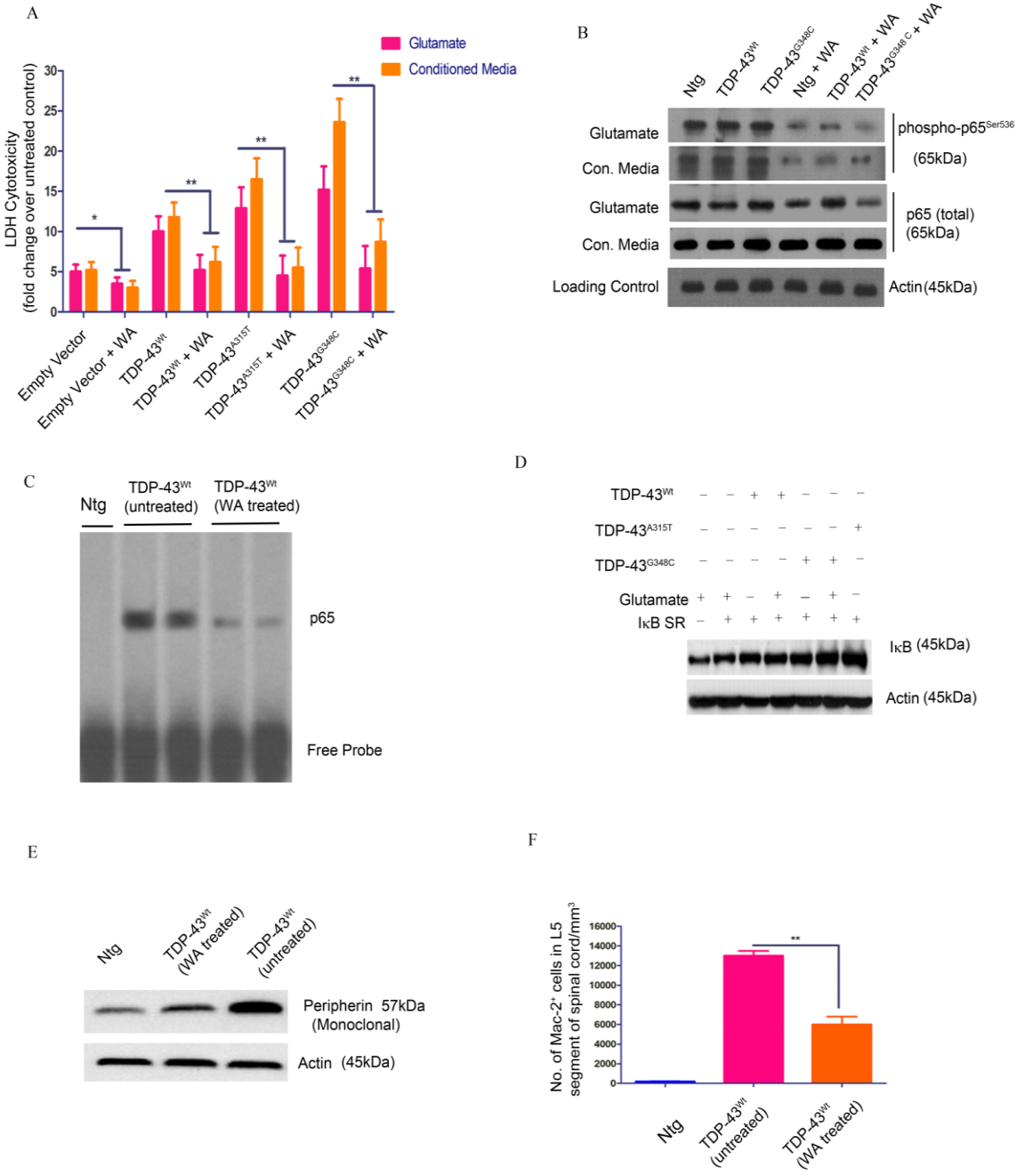
A
Glutamate
Conditioned Media
LDH Cytotoxicity
(fold change over untreated control)
Empty Vector
Empty Vector + WA
TDP-43Wt
TDP-43Wt + WA
TDP-43A315T
TDP-43A315T + WA
TDP-43G348C
TDP-43G348C + WA
B
Ntg
TDP-43Wt
TDP-43G348C
Ntg + WA
TDP-43Wt + WA
TDP-43G348C + WA
Glutamate
Con. Media
phospho-p65Ser536
(65kDa)
p65 (total)
(65kDa)
Loading Control
Actin(45kDa)
C
Ntg
TDP-43Wt
(untreated)
TDP-43Wt
(WA treated)
p65
Free Probe
D
TDP-43Wt
TDP-43A315T
TDP-43G348C
Glutamate
IκB SR
IκB (45kDa)
Actin (45kDa)
E
Ntg
TDP-43Wt
(WA treated)
TDP-43Wt
(untreated)
Peripherin 57kDa
(Monoclonal)
Actin (45kDa)
F
No. of Mac-2+ cells in L5
segment of spinal cord/mm3
Ntg
TDP-43Wt
(untreated)
TDP-43Wt
(WA treated)

Figure 4.10. Withaferin A ameliorates disease phenotypes in TDP-43 transgenic mice (A) Primary cortical neurons from TDP-43^{Wt}, TDP-43^{A315T}, TDP-43^{G348C} and B6 nontransgenic (Ntg) mice were exposed to 10μM glutamate for 15 min or incubated in conditioned media from LPS-stimulated microglia of same genotype with or without 1μM withaferin A (WA) and were evaluated for lactate dehydrogenase (LDH) cytotoxicity 24 hrs later. * represents a statistically significant difference between treated and untreated groups (*$p<0.05$) and ** ($p<0.01$) using repeated-measures 2-way ANOVA. Error bars represent mean ± SEM from three independent experiments. (B) Protein samples from cortical neurons (isolated from TDP-43^{Wt}, TDP-43^{A315T}, TDP-43^{G348C} and B6 nontransgenic (Ntg) mice) were subjected to immunoblot against various antibodies as indicated. (C) p65 EMSA was performed on the spinal cord tissue nuclear lysates from withaferin treated and untreated GFAP-luc/TDP-43^{Wt} mice. Representative EMSA of two independent experiments is shown. (D) IκB levels were measured by western blot analysis of the cell lysates from cortical neurons of various genotypes as indicated. Actin is shown as loading control. Various conditions are also shown. Representative blot from two different experiments is shown. (E) Western blot analysis of spinal cord sections of non-transgenic (control), TDP-43^{Wt} (untreated) and TDP-43^{Wt} (Withaferin treated) mice with monoclonal peripherin antibody. Representative blot from two different experiments is shown. (F**)** Quantification of microglial Mac-2 positive cells in the spinal cord sections of non-transgenic (control), TDP-43^{Wt} (untreated) and TDP-43^{Wt} (Withaferin treated) mice. Mac-2^{+} cells in TDP-43^{Wt} (untreated) L5 spinal cord 13000 ± 500/mm^3 and TDP-43^{Wt} (Withaferin treated) L5 spinal cord 6000 ± 300/mm^3 **$p<0.001$. Error bars represent mean ± SEM for four mice of each genotype.

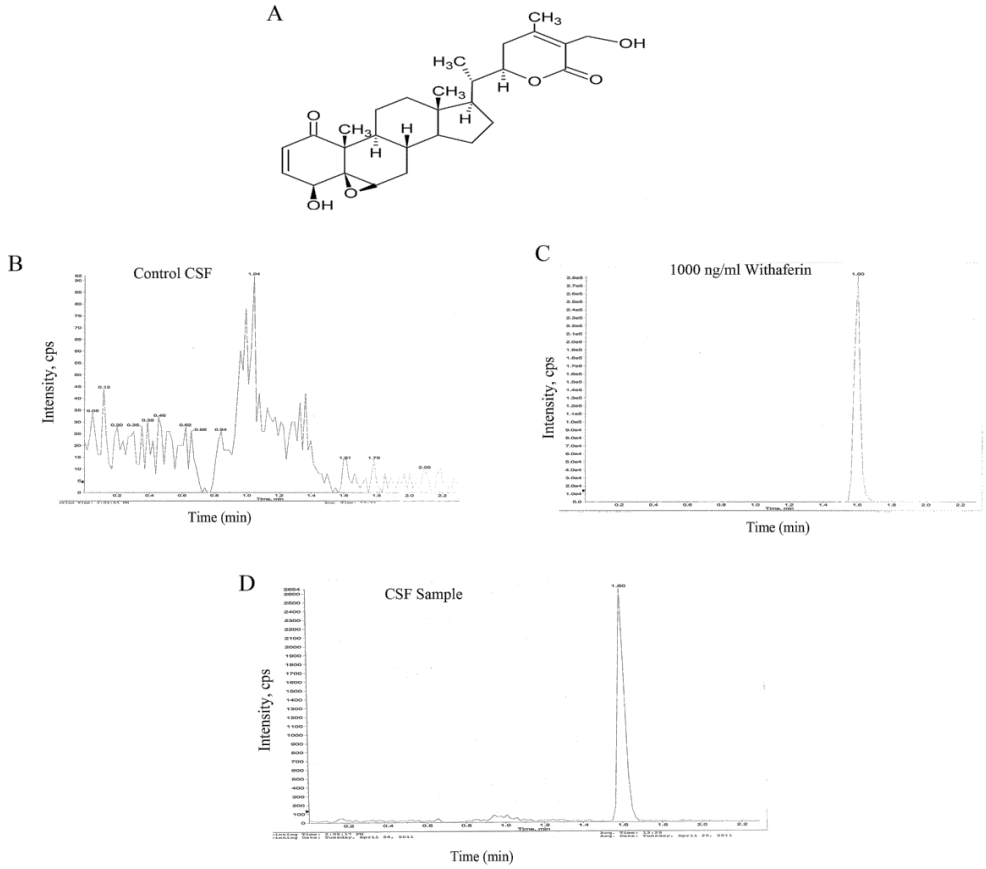

Supplemental Figure 4.3 Detection of Withaferin A in the CSF of mice using HPLC. (A) Chemical structure of withaferin A. **(B-D)** Withaferin A was injected (3mg/kg body weight) intra-peritoneally in 8-months old control non-transgenic and TDP-43^{Wt} mice. For blank samples (B), 0.9% saline was injected in non-transgenic mice. 1.5hrs after injection, CSF samples from the mice were obtained using stereotaxic injection into the cistern magna. 50µl of the sample was mixed with 60% ACN 0.1% formic acid, centrifuged and the supernatant was injected into HPLC. Blank CSF sample showing absence of Withaferin-A and drug injected CSF samples showing presence of Withaferin-A **(D)**. 1000ng/ml withaferin-a chemical served as a standard **(C)**. Withaferin retention time was 1.6mins. Data shown is a representative of three independent experiments.

4.6 Discussion

From the data presented here, we propose that a TDP-43 deregulation in ALS may contribute to pathogenic pathways through abnormal activation of p65 NF-κB. Several lines of evidence support this scheme: (i) proof of a direct interaction between TDP-43 and p65 NF-κB was provided by immunoprecipitation experiments using protein extracts from cultured cells, from TDP-43 transgenic mice and from human ALS spinal cord samples, (ii) reporter gene transcription assays and gel shift experiments demonstrated that TDP-43 was acting as co-activator of p65 NF-κB through binding of its N-terminal and RRM-1 domains to p65, (iii) the levels of mRNAs for both TDP-43 and p65 NF-κB were substantially elevated in the spinal cord of ALS subjects as compared to non-ALS subjects whereas immunofluorescence microscopy of ALS spinal cord samples revealed an abnormal nuclear localization p65 NF-κB, (iv) cell transfection studies demonstrated that an overexpression of TDP-43 can provoke hyperactive innate immune responses with ensuing enhanced toxicity on neuronal cells whereas in neurons TDP-43 overexpression increased their vulnerability to toxic environment, (v) in vivo treatment of TDP-43 transgenic mice with an inhibitor of NF-κB reduced inflammation and ameliorated motor deficits.

This is the first report of an upregulation of mRNAs encoding TDP-43 in post-mortem frozen spinal cords of sporadic ALS. A recent study has provided evidence of increased TDP-43 immuno-detection in the skin of ALS patients(Suzuki et al., 2010) but it failed to demonstrate whether this was due to upregulation in TDP-43 mRNA expression. The process that underlies a 2.5-fold increase in TDP-43 mRNA levels in ALS, whether it is transcriptional or mRNA stability remains to be investigated. It seems unlikely that copy number variants could explain an increase of TDP-43 gene transcription as variations in copy number of *TARDBP* have not been detected in cohorts of ALS (Baumer et al., 2009; Gitcho et al., 2009; Guerreiro et al., 2008). Actually, the pathogenic pathways of TDP-43 abnormalities in ALS are not well understood. To date, much attention has been focused of cytoplasmic C-terminal TDP-43 fragments that can elicit toxicity in cell culture systems (Dormann et al., 2009; Igaz et al., 2009; Johnson et al., 2008; Zhang et al., 2009b). However, it is noteworthy that neuronal overexpression at high levels of wild-type or

mutant TDP-43 in transgenic mice caused a dose-dependent degeneration of cortical and spinal motor neurons but without massive cytoplasmic TDP-43 aggregates (Wils et al., 2010). This suggests that an upregulation of TDP-43 in the nucleus rather than TDP-43 cytoplasmic aggregates may contribute to neurodegeneration in these mouse models. As shown here, an overexpression of TDP-43 can trigger pathogenic pathways via NF-κB activation.

The transcription factor NF-κB is a key regulator of hundreds of genes involved in innate immunity, cell survival and inflammation. Since the nuclear translocation and DNA binding of NF-κB are not sufficient for gene induction (Bergmann et al., 1998; Yoza et al., 1996), it has been suggested that interactions with other protein molecules through the transactivation domain (Gerritsen et al., 1997; Perkins et al., 1997; Schmitz et al., 1995b) as well as its modification by phosphorylation (Schmitz et al., 1995a) might play a critical role. It has been reported that transcriptional activation of NF-κB requires multiple co-activator proteins including CREB-binding protein (CBP)/p300 (Gerritsen et al., 1997; Perkins et al., 1997), CBP-associated factor, and steroid receptor coactivator 1(Sheppard et al., 1999). These coactivators have histone acetyltransferase activity to modify the chromatin structure and also provide molecular bridges to the basal transcriptional machinery. NF-κB p65 was also found to interact specifically with Fused in Sarcoma (FUS) protein, another DNA/RNA binding protein which is involved in ALS (Deng et al., 2010; Kwiatkowski et al., 2009; Vance et al., 2009).

Our results revealed robust effects of TDP-43 on the activation of NF-κB and innate immune responses. After transfection with TDP-43 species, microglial cells challenged with LPS exhibited much higher mRNA levels for pro-inflammatory cytokines, Nox-2 and NF-κB mRNA when compared to untransfected cells after LPS stimulation. TDP-43 overexpression makes microglia hyperactive to immune stimulation resulting in enhanced toxicity toward neighboring neuronal cells with involvement of reactive oxygen species (ROS) and increased nitrite levels (NO). Moreover, the adverse effects of TDP-43 upregulation are not limited to microglial cells. TDP-43 overexpression in transgenic astrocytes caused exaggerated responses to LPS (Figure 4.7F) whereas primary cortical

neurons overexpressing TDP-43 transgenes by ~3-fold exhibited increased susceptibility to the toxic effects of excess glutamate or LPS-activated microglia (Figure 4.9A and 8D).

The presence of ALS-linked mutations in TDP-43 (A315T or G348C) did not affect the binding and activation of p65 NF-κB. This is not surprising because our deletion mutant analysis revealed that a region spanning part of the N-terminal domain and RRM1 of TDP-43 is responsible for interaction with p65 whereas most TDP-43 mutations in ALS occur in the C-terminal domain, which is dispensable for p65 NF-κB activation (Figure 4.4). In fact, our cytotoxicity assays with primary cells from TDP-43 transgenic mice revealed that, at similar levels of mRNA expression, the adverse effects of mutant TDP-43 were more pronounced than TDP-43^{Wt}. These results could be explained by the observation that ALS-linked mutations in TDP-43 increase its protein stability (Ling et al., 2010). From the data presented here, we propose the involvement in ALS of a pathogenic pathway due to nuclear increase in TDP-43 levels (Figure 4.6). This scheme does not exclude adverse effects due to cytoplasmic TDP-43 aggregates that might occur concomitantly or later on during the disease process. Recent TDP-43 studies with Drosophila suggested that the TDP-43 toxicity may occur in absence of inclusions formation and that neurotoxicity requires TDP-43 RNA-binding domain (Voigt et al., 2010). These results are consistent with our model of TDP-43 toxicity and with data demonstrating interaction of TDP-43 with p65 via the RNA recognition motif RMM1.

Our finding that TDP-43 acts as co-activator of p65 suggests a key role for NF-κB signaling in ALS pathogenesis. This is corroborated by the abnormal 4-fold increase of p65 NF-κB mRNA in the spinal cord of human ALS (Figure 4.6) and by the nuclear localization of p65 (Figure 4.1M-O; Figure 4.2-inset). Remarkably, an overexpression of TDP-43 species by ~3-fold in transgenic mice (Swarup et al., 2011a), at levels similar to the human ALS situation (2.5-fold), was sufficient to cause during aging nuclear translocation of p65 NF-κB in the spinal cord (Figure 4.1G-I). It should be noted that TDP-43 itself does not cause NF-κB activation (Figure 4.7) and that it does not upregulate p65. It seems that a second hit is required. For example, LPS or other inducers such as pathogen-associated molecular patterns can trigger through TLR signaling p65 NF-κB

nuclear localization. Cytokines such as TNF-α and IL-1β can also trigger p65 activation. In ALS, the second hit(s) triggering innate immune responses remain to be identified. There is recent evidence for involvement of LPS in ALS (Zhang et al., 2011; Zhang et al., 2009a) and of endogenous retrovirus (HEVR-K) expression (Douville et al., 2011). Here we show that aging is associated with p65 nuclear translocation in the spinal cord of TDP-43 transgenic mice (Supplemental Figure 4.1D) but the exact factors underlying this phenomenon remain to be defined

There is a recent report of mutations in the gene coding for vasolin-containing protein (VCP) associated with 1-2% familial ALS cases (Johnson et al., 2010). It is well established that VCP is involved in the control of the NF-kB pathway through regulation of ubiquitin-dependent degradation of IκB-α. For instance, mutant VCP expression in mice resulted in increased TDP-43 levels and hyper-activation of NF-κB signalling (Badadani et al., 2010; Custer et al., 2010). Moreover, some ALS-linked mutations have been discovered in the gene coding for optineurin, a protein which activates the suppressor of NF-κB (Maruyama et al., 2010), further supporting a convergent NF-κB-pathogenic pathway. Thus, the data presented in our paper as well as ALS-linked mutations in the VCP and optineurin genes (Badadani et al., 2010; Johnson et al., 2010; Maruyama et al., 2010) are all supporting a convergent NF- κB pathogenic pathway in ALS. Recently the NF-κB signalling complex was identified as a major contributor of astrocyte mediated toxicity to motor neurons (Haidet-Phillips et al., 2011). Here, we show that inhibitors of NF-κB activation are able to attenuate the vulnerability of cultured neurons overexpressing TDP-43 species to glutamate-induced or microglia-mediated toxicity. Moreover, pharmacological inhibition of NF-κB by WA treatment attenuated disease phenotypes in TDP-43 transgenic mice. From these results, we propose that NF-κB signaling should be considered as potential therapeutic target in ALS treatment.

4.7 Acknowledgement

We thank Christine Bareil and Genevieve Soucy for technical assistance. We are grateful to the lab of Dr. Michel J. Tremblay of Research Center of Centre Hospitalier Universitaire de Québec (CHUQ) for p65, IκB^{SR} and luciferase plasmids. This work was supported by the Canadian Institutes of Health Research (CIHR), the Fondation André-Delambre and the Robert Packard Center for ALS Research at Johns Hopkins. J.-P.J. holds a Canada Research Chair Tier 1 in mechanisms of neurodegeneration. V.S. is the recipient of the Merit Scholarship for foreign students (FQRNT, Quebec, Canada). The authors have no conflicting financial interests.

4.8 References

Aleyasin, H., S.P. Cregan, G. Iyirhiaro, M.J. O'Hare, S.M. Callaghan, R.S. Slack, and D.S. Park. 2004. Nuclear factor-(kappa)B modulates the p53 response in neurons exposed to DNA damage. *J Neurosci*. 24:2963-2973.

Arai, T., M. Hasegawa, H. Akiyama, K. Ikeda, T. Nonaka, H. Mori, D. Mann, K. Tsuchiya, M. Yoshida, Y. Hashizume, and T. Oda. 2006. TDP-43 is a component of ubiquitin-positive tau-negative inclusions in frontotemporal lobar degeneration and amyotrophic lateral sclerosis. *Biochem Biophys Res Commun*. 351:602-611.

Badadani, M., A. Nalbandian, G.D. Watts, J. Vesa, M. Kitazawa, H. Su, J. Tanaja, E. Dec, D.C. Wallace, J. Mukherjee, V. Caiozzo, M. Warman, and V.E. Kimonis. 2010. VCP associated inclusion body myopathy and paget disease of bone knock-in mouse model exhibits tissue pathology typical of human disease. *PLoS One*. 5.

Baumer, D., N. Parkinson, and K. Talbot. 2009. TARDBP in amyotrophic lateral sclerosis: identification of a novel variant but absence of copy number variation. *J Neurol Neurosurg Psychiatry*. 80:1283-1285.

Bergmann, M., L. Hart, M. Lindsay, P.J. Barnes, and R. NeWton. 1998. IkappaBalpha degradation and nuclear factor-kappaB DNA binding are insufficient for interleukin-1beta and tumor necrosis factor-alpha-induced kappaB-dependent transcription. Requirement for an additional activation pathway. *J Biol Chem*. 273:6607-6610.

Boillee, S., C. Vande Velde, and D.W. Cleveland. 2006a. ALS: a disease of motor neurons and their nonneuronal neighbors. *Neuron*. 52:39-59.

Boillee, S., K. Yamanaka, C.S. Lobsiger, N.G. Copeland, N.A. Jenkins, G. Kassiotis, G. Kollias, and D.W. Cleveland. 2006b. Onset and progression in inherited ALS determined by motor neurons and microglia. *Science*. 312:1389-1392.

Chiang, P.M., J. Ling, Y.H. Jeong, D.L. Price, S.M. Aja, and P.C. Wong. 2010. Deletion of TDP-43 down-regulates Tbc1d1, a gene linked to obesity, and alters body fat metabolism. *Proc Natl Acad Sci U S A*.

Clement, A.M., M.D. Nguyen, E.A. Roberts, M.L. Garcia, S. Boillee, M. Rule, A.P. McMahon, W. Doucette, D. Siwek, R.J. Ferrante, R.H. Brown, Jr., J.P. Julien, L.S.

Goldstein, and D.W. Cleveland. 2003. Wild-type nonneuronal cells extend survival of SOD1 mutant motor neurons in ALS mice. *Science*. 302:113-117.

Cordeau, P., Jr., M. Lalancette-Hebert, Y.C. Weng, and J. Kriz. 2008. Live imaging of neuroinflammation reveals sex and estrogen effects on astrocyte response to ischemic injury. *Stroke*. 39:935-942.

Corrado, L., A. Ratti, C. Gellera, E. Buratti, B. Castellotti, Y. Carlomagno, N. Ticozzi, L. Mazzini, L. Testa, F. Taroni, F.E. Baralle, V. Silani, and S. D'Alfonso. 2009. High frequency of TARDBP gene mutations in Italian patients with amyotrophic lateral sclerosis. *Hum Mutat*. 30:688-694.

Custer, S.K., M. Neumann, H. Lu, A.C. Wright, and J.P. Taylor. 2010. Transgenic mice expressing mutant forms VCP/p97 recapitulate the full spectrum of IBMPFD including degeneration in muscle, brain and bone. *Hum Mol Genet*. 19:1741-1755.

Daoud, H., P.N. Valdmanis, E. Kabashi, P. Dion, N. Dupre, W. Camu, V. Meininger, and G.A. Rouleau. 2009. Contribution of TARDBP mutations to sporadic amyotrophic lateral sclerosis. *J Med Genet*. 46:112-114.

Davies, J.Q., and S. Gordon. 2005. Isolation and culture of murine macrophages. *Methods Mol Biol*. 290:91-103.

Deng, H.X., H. Zhai, E.H. Bigio, J. Yan, F. Fecto, K. Ajroud, M. Mishra, S. Ajroud-Driss, S. Heller, R. Sufit, N. Siddique, E. Mugnaini, and T. Siddique. 2010. FUS-immunoreactive inclusions are a common feature in sporadic and non-SOD1 familial amyotrophic lateral sclerosis. *Ann Neurol*. 67:739-748.

Dequen, F., P. Bomont, G. Gowing, D.W. Cleveland, and J.P. Julien. 2008. Modest loss of peripheral axons, muscle atrophy and formation of brain inclusions in mice with targeted deletion of gigaxonin exon 1. *J Neurochem*. 107:253-264.

Dormann, D., A. Capell, A.M. Carlson, S.S. Shankaran, R. Rodde, M. Neumann, E. Kremmer, T. Matsuwaki, K. Yamanouchi, M. Nishihara, and C. Haass. 2009. Proteolytic processing of TAR DNA binding protein-43 by caspases produces C-terminal fragments with disease defining properties independent of progranulin. *J Neurochem*. 110:1082-1094.

Douville, R., J. Liu, J. Rothstein, and A. Nath. 2011. Identification of active loci of a human endogenous retrovirus in neurons of patients with amyotrophic lateral sclerosis. *Ann Neurol*. 69:141-151.

Dreyfuss, G., M.J. Matunis, S. Pinol-Roma, and C.G. Burd. 1993. hnRNP proteins and the biogenesis of mRNA. *Annu Rev Biochem*. 62:289-321.

Gerritsen, M.E., A.J. Williams, A.S. Neish, S. Moore, Y. Shi, and T. Collins. 1997. CREB-binding protein/p300 are transcriptional coactivators of p65. *Proc Natl Acad Sci U S A*. 94:2927-2932.

Gitcho, M.A., R.H. Baloh, S. Chakraverty, K. Mayo, J.B. Norton, D. Levitch, K.J. Hatanpaa, C.L. White, 3rd, E.H. Bigio, R. Caselli, M. Baker, M.T. Al-Lozi, J.C. Morris, A. Pestronk, R. Rademakers, A.M. Goate, and N.J. Cairns. 2008. TDP-43 A315T mutation in familial motor neuron disease. *Ann Neurol*. 63:535-538.

Gitcho, M.A., E.H. Bigio, M. Mishra, N. Johnson, S. Weintraub, M. Mesulam, R. Rademakers, S. Chakraverty, C. Cruchaga, J.C. Morris, A.M. Goate, and N.J. Cairns. 2009. TARDBP 3'-UTR variant in autopsy-confirmed frontotemporal lobar degeneration with TDP-43 proteinopathy. *Acta Neuropathol*. 118:633-645.

Gros-Louis, F., J. Kriz, E. Kabashi, J. McDearmid, S. Millecamps, M. Urushitani, L. Lin, P. Dion, Q. Zhu, P. Drapeau, J.P. Julien, and G.A. Rouleau. 2008. Als2 mRNA splicing variants detected in KO mice rescue severe motor dysfunction phenotype in Als2 knock-down zebrafish. *Hum Mol Genet*. 17:2691-2702.

Guerreiro, R.J., J.C. Schymick, C. Crews, A. Singleton, J. Hardy, and B.J. Traynor. 2008. TDP-43 is not a common cause of sporadic amyotrophic lateral sclerosis. *PLoS One*. 3:e2450.

Haidet-Phillips, A.M., M.E. Hester, C.J. Miranda, K. Meyer, L. Braun, A. Frakes, S. Song, S. Likhite, M.J. Murtha, K.D. Foust, M. Rao, A. Eagle, A. Kammesheidt, A. Christensen, J.R. Mendell, A.H. Burghes, and B.K. Kaspar. 2011. Astrocytes from familial and sporadic ALS patients are toxic to motor neurons. *Nat Biotechnol*.

Horvath, R.J., N. Nutile-McMenemy, M.S. Alkaitis, and J.A. Deleo. 2008. Differential migration, LPS-induced cytokine, chemokine, and NO expression in immortalized

BV-2 and HAPI cell lines and primary microglial cultures. *J Neurochem*. 107:557-569.

Igaz, L.M., L.K. Kwong, A. Chen-Plotkin, M.J. Winton, T.L. Unger, Y. Xu, M. Neumann, J.Q. Trojanowski, and V.M. Lee. 2009. Expression of TDP-43 C-terminal Fragments in Vitro Recapitulates Pathological Features of TDP-43 Proteinopathies. *J Biol Chem*. 284:8516-8524.

Johnson, B.S., J.M. McCaffery, S. Lindquist, and A.D. Gitler. 2008. A yeast TDP-43 proteinopathy model: Exploring the molecular determinants of TDP-43 aggregation and cellular toxicity. *Proc Natl Acad Sci U S A*. 105:6439-6444.

Johnson, J.O., J. Mandrioli, M. Benatar, Y. Abramzon, V.M. Van Deerlin, J.Q. Trojanowski, J.R. Gibbs, M. Brunetti, S. Gronka, J. Wuu, J. Ding, L. McCluskey, M. Martinez-Lage, D. Falcone, D.G. Hernandez, S. Arepalli, S. Chong, J.C. Schymick, J. Rothstein, F. Landi, Y.D. Wang, A. Calvo, G. Mora, M. Sabatelli, M.R. Monsurro, S. Battistini, F. Salvi, R. Spataro, P. Sola, G. Borghero, G. Galassi, S.W. Scholz, J.P. Taylor, G. Restagno, A. Chio, and B.J. Traynor. 2010. Exome sequencing reveals VCP mutations as a cause of familial ALS. *Neuron*. 68:857-864.

Kabashi, E., P.N. Valdmanis, P. Dion, D. Spiegelman, B.J. McConkey, C. Vande Velde, J.P. Bouchard, L. Lacomblez, K. Pochigaeva, F. Salachas, P.F. Pradat, W. Camu, V. Meininger, N. Dupre, and G.A. Rouleau. 2008. TARDBP mutations in individuals with sporadic and familial amyotrophic lateral sclerosis. *Nat Genet*. 40:572-574.

Kasai, T., T. Tokuda, N. Ishigami, H. Sasayama, P. Foulds, D.J. Mitchell, D.M. Mann, D. Allsop, and M. Nakagawa. 2009. Increased TDP-43 protein in cerebrospinal fluid of patients with amyotrophic lateral sclerosis. *Acta Neuropathol*. 117:55-62.

Keller, A., A.I. Nesvizhskii, E. Kolker, and R. Aebersold. 2002. Empirical statistical model to estimate the accuracy of peptide identifications made by MS/MS and database search. *Anal Chem*. 74:5383-5392.

Kwiatkowski, T.J., Jr., D.A. Bosco, A.L. Leclerc, E. Tamrazian, C.R. Vanderburg, C. Russ, A. Davis, J. Gilchrist, E.J. Kasarskis, T. Munsat, P. Valdmanis, G.A. Rouleau, B.A. Hosler, P. Cortelli, P.J. de Jong, Y. Yoshinaga, J.L. Haines, M.A. Pericak-Vance, J.

Yan, N. Ticozzi, T. Siddique, D. McKenna-Yasek, P.C. Sapp, H.R. Horvitz, J.E. Landers, and R.H. Brown, Jr. 2009. Mutations in the FUS/TLS gene on chromosome 16 cause familial amyotrophic lateral sclerosis. *Science*. 323:1205-1208.

Ling, S.C., C.P. Albuquerque, J.S. Han, C. Lagier-Tourenne, S. Tokunaga, H. Zhou, and D.W. Cleveland. 2010. ALS-associated mutations in TDP-43 increase its stability and promote TDP-43 complexes with FUS/TLS. *Proc Natl Acad Sci U S A*. 107:13318-13323.

Maruyama, H., H. Morino, H. Ito, Y. Izumi, H. Kato, Y. Watanabe, Y. Kinoshita, M. Kamada, H. Nodera, H. Suzuki, O. Komure, S. Matsuura, K. Kobatake, N. Morimoto, K. Abe, N. Suzuki, M. Aoki, A. Kawata, T. Hirai, T. Kato, K. Ogasawara, A. Hirano, T. Takumi, H. Kusaka, K. Hagiwara, R. Kaji, and H. Kawakami. 2010. Mutations of optineurin in amyotrophic lateral sclerosis. *Nature*. 465:223-226.

Maysinger, D., M. Behrendt, M. Lalancette-Hebert, and J. Kriz. 2007. Real-time imaging of astrocyte response to quantum dots: in vivo screening model system for biocompatibility of nanoparticles. *Nano Lett*. 7:2513-2520.

Neumann, M., D.M. Sampathu, L.K. Kwong, A.C. Truax, M.C. Micsenyi, T.T. Chou, J. Bruce, T. Schuck, M. Grossman, C.M. Clark, L.F. McCluskey, B.L. Miller, E. Masliah, I.R. Mackenzie, H. Feldman, W. Feiden, H.A. Kretzschmar, J.Q. Trojanowski, and V.M. Lee. 2006. Ubiquitinated TDP-43 in frontotemporal lobar degeneration and amyotrophic lateral sclerosis. *Science*. 314:130-133.

Noto, Y.I., K. Shibuya, Y. Sato, K. Kanai, S. Misawa, S. Sawai, M. Mori, T. Uchiyama, S. Isose, S. Nasu, Y. Sekiguchi, Y. Fujimaki, T. Kasai, T. Tokuda, M. Nakagawa, and S. Kuwabara. 2010. Elevated CSF TDP-43 levels in amyotrophic lateral sclerosis: Specificity, sensitivity, and a possible prognostic value. *Amyotroph Lateral Scler*.

Oh, J.H., T.J. Lee, J.W. Park, and T.K. Kwon. 2008. Withaferin A inhibits iNOS expression and nitric oxide production by Akt inactivation and down-regulating LPS-induced activity of NF-kappaB in RAW 264.7 cells. *Eur J Pharmacol*. 599:11-17.

Perkins, N.D., L.K. Felzien, J.C. Betts, K. Leung, D.H. Beach, and G.J. Nabel. 1997. Regulation of NF-kappaB by cyclin-dependent kinases associated with the p300 coactivator. *Science*. 275:523-527.

Pizzi, M., I. Sarnico, F. Boroni, A. Benetti, M. Benarese, and P.F. Spano. 2005. Inhibition of IkappaBalpha phosphorylation prevents glutamate-induced NF-kappaB activation and neuronal cell death. *Acta Neurochir Suppl*. 93:59-63.

Schmitz, M.L., M.A. dos Santos Silva, and P.A. Baeuerle. 1995a. Transactivation domain 2 (TA2) of p65 NF-kappa B. Similarity to TA1 and phorbol ester-stimulated activity and phosphorylation in intact cells. *J Biol Chem*. 270:15576-15584.

Schmitz, M.L., G. Stelzer, H. Altmann, M. Meisterernst, and P.A. Baeuerle. 1995b. Interaction of the COOH-terminal transactivation domain of p65 NF-kappa B with TATA-binding protein, transcription factor IIB, and coactivators. *J Biol Chem*. 270:7219-7226.

Sephton, C.F., S.K. Good, S. Atkin, C.M. Dewey, P. Mayer, 3rd, J. Herz, and G. Yu. 2010. TDP-43 is a developmentally regulated protein essential for early embryonic development. *J Biol Chem*. 285:6826-6834.

Seyfried, N.T., Y.M. Gozal, E.B. Dammer, Q. Xia, D.M. Duong, D. Cheng, J.J. Lah, A.I. Levey, and J. Peng. 2010. Multiplex SILAC analysis of a cellular TDP-43 proteinopathy model reveals protein inclusions associated with SUMOylation and diverse polyubiquitin chains. *Mol Cell Proteomics*. 9:705-718.

Sheppard, K.A., D.W. Rose, Z.K. Haque, R. Kurokawa, E. McInerney, S. Westin, D. Thanos, M.G. Rosenfeld, C.K. Glass, and T. Collins. 1999. Transcriptional activation by NF-kappaB requires multiple coactivators. *Mol Cell Biol*. 19:6367-6378.

Sreedharan, J., I.P. Blair, V.B. Tripathi, X. Hu, C. Vance, B. Rogelj, S. Ackerley, J.C. Durnall, K.L. Williams, E. Buratti, F. Baralle, J. de Belleroche, J.D. Mitchell, P.N. Leigh, A. Al-Chalabi, C.C. Miller, G. Nicholson, and C.E. Shaw. 2008. TDP-43 mutations in familial and sporadic amyotrophic lateral sclerosis. *Science*. 319:1668-1672.

Stallings, N.R., K. Puttaparthi, C.M. Luther, D.K. Burns, and J.L. Elliott. 2010. Progressive motor weakness in transgenic mice expressing human TDP-43. *Neurobiol Dis*.

Suzuki, M., H. Mikami, T. Watanabe, T. Yamano, T. Yamazaki, M. Nomura, K. Yasui, H. Ishikawa, and S. Ono. 2010. Increased expression of TDP-43 in the skin of amyotrophic lateral sclerosis. *Acta Neurol Scand*.

Swarup, V., S. Das, S. Ghosh, and A. Basu. 2007a. Tumor necrosis factor receptor-1-induced neuronal death by TRADD contributes to the pathogenesis of Japanese encephalitis. *J Neurochem*. 103:771-783.

Swarup, V., J. Ghosh, R. Duseja, S. Ghosh, and A. Basu. 2007b. Japanese encephalitis virus infection decrease endogenous IL-10 production: correlation with microglial activation and neuronal death. *Neurosci Lett*. 420:144-149.

Swarup, V., D. Phaneuf, C. Bareil, J. Robertson, G.A. Rouleau, J. Kriz, and J.P. Julien. 2011a. Pathological hallmarks of amyotrophic lateral sclerosis/frontotemporal lobar degeneration in transgenic mice produced with TDP-43 genomic fragments. *Brain* 134:2610-2626.

Thaiparambil, J.T., L. Bender, T. Ganesh, E. Kline, P. Patel, Y. Liu, M. Tighiouart, P.M. Vertino, R.D. Harvey, A. Garcia, and A.I. Marcus. 2011. Withaferin A inhibits breast cancer invasion and metastasis at sub-cytotoxic doses by inducing vimentin disassembly and serine 56 phosphorylation. *Int J Cancer*.

Van Deerlin, V.M., J.B. Leverenz, L.M. Bekris, T.D. Bird, W. Yuan, L.B. Elman, D. Clay, E.M. Wood, A.S. Chen-Plotkin, M. Martinez-Lage, E. Steinbart, L. McCluskey, M. Grossman, M. Neumann, I.L. Wu, W.S. Yang, R. Kalb, D.R. Galasko, T.J. Montine, J.Q. Trojanowski, V.M. Lee, G.D. Schellenberg, and C.E. Yu. 2008. TARDBP mutations in amyotrophic lateral sclerosis with TDP-43 neuropathology: a genetic and histopathological analysis. *Lancet Neurol*. 7:409-416.

Vance, C., B. Rogelj, T. Hortobagyi, K.J. De Vos, A.L. Nishimura, J. Sreedharan, X. Hu, B. Smith, D. Ruddy, P. Wright, J. Ganesalingam, K.L. Williams, V. Tripathi, S. Al-Saraj, A. Al-Chalabi, P.N. Leigh, I.P. Blair, G. Nicholson, J. de Belleroche, J.M. Gallo, C.C. Miller, and C.E. Shaw. 2009. Mutations in FUS, an RNA processing

protein, cause familial amyotrophic lateral sclerosis type 6. *Science*. 323:1208-1211.

Voigt, A., D. Herholz, F.C. Fiesel, K. Kaur, D. Muller, P. Karsten, S.S. Weber, P.J. Kahle, T. Marquardt, and J.B. Schulz. 2010. TDP-43-mediated neuron loss in vivo requires RNA-binding activity. *PLoS One*. 5:e12247.

Wegorzewska, I., S. Bell, N.J. Cairns, T.M. Miller, and R.H. Baloh. 2009. TDP-43 mutant transgenic mice develop features of ALS and frontotemporal lobar degeneration. *Proc Natl Acad Sci U S A*. 106:18809-18814.

Weydt, P., E.C. Yuen, B.R. Ransom, and T. Moller. 2004. Increased cytotoxic potential of microglia from ALS-transgenic mice. *Glia*. 48:179-182.

Wils, H., G. Kleinberger, J. Janssens, S. Pereson, G. Joris, I. Cuijt, V. Smits, C. Ceuterick-de Groote, C. Van Broeckhoven, and S. Kumar-Singh. 2010. TDP-43 transgenic mice develop spastic paralysis and neuronal inclusions characteristic of ALS and frontotemporal lobar degeneration. *Proc Natl Acad Sci U S A*. 107:3858-3863.

Xu, Y.F., T.F. Gendron, Y.J. Zhang, W.L. Lin, S. D'Alton, H. Sheng, M.C. Casey, J. Tong, J. Knight, X. Yu, R. Rademakers, K. Boylan, M. Hutton, E. McGowan, D.W. Dickson, J. Lewis, and L. Petrucelli. 2010. Wild-Type Human TDP-43 Expression Causes TDP-43 Phosphorylation, Mitochondrial Aggregation, Motor Deficits, and Early Mortality in Transgenic Mice. *J Neurosci*. 30:10851-10859.

Yoza, B.K., J.Y. Hu, and C.E. McCall. 1996. Protein-tyrosine kinase activation is required for lipopolysaccharide induction of interleukin 1beta and NFkappaB activation, but not NFkappaB nuclear translocation. *J Biol Chem*. 271:18306-18309.

Zhang, R., K.G. Hadlock, H. Do, S. Yu, R. Honrada, S. Champion, D. Forshew, C. Madison, J. Katz, R.G. Miller, and M.S. McGrath. 2011. Gene expression profiling in peripheral blood mononuclear cells from patients with sporadic amyotrophic lateral sclerosis (sALS). *J Neuroimmunol*. 230:114-123.

Zhang, R., R.G. Miller, R. Gascon, S. Champion, J. Katz, M. Lancero, A. Narvaez, R. Honrada, D. Ruvalcaba, and M.S. McGrath. 2009a. Circulating endotoxin and systemic immune activation in sporadic amyotrophic lateral sclerosis (sALS). *J Neuroimmunol*. 206:121-124.

Zhang, Y.J., Y.F. Xu, C. Cook, T.F. Gendron, P. Roettges, C.D. Link, W.L. Lin, J. Tong, M. Castanedes-Casey, P. Ash, J. Gass, V. Rangachari, E. Buratti, F. Baralle, T.E. Golde, D.W. Dickson, and L. Petrucelli. 2009b. Aberrant cleavage of TDP-43 enhances aggregation and cellular toxicity. *Proc Natl Acad Sci U S A*. 106:7607-7612.

Chapter 5. General Discussion and Conclusion

5.1 Lessons learned from TDP-43 transgenic models

With the implication of TDP-43 in ALS and FTLD-U (Arai et al., 2006; Neumann et al., 2006), there has been a boom in the reports of animal models of TDP-43. Most of the mouse models of TDP-43 reported show early paralysis followed by death. However, these mouse models are based on high expression levels of TDP-43 transgenes that can mask age-dependent pathogenic pathways (Swarup and Julien, 2010). Mice expressing either wild type or mutant TDP-43 (A315T and M337V) showed aggressive paralysis accompanied by increased ubiquitination (Wegorzewska et al., 2009; Stallings et al., 2010; Wils et al., 2010; Zhou et al., 2010; Igaz et al., 2011; Xu et al., 2011) but the lack of ubiquitinated TDP-43 inclusions raises concerns about their validity as models of human ALS disease (Wegorzewska et al., 2009). Another concern is restricted expression of TDP-43 species with the use of Thy1.2 and Prion promoters. Are these models based on TDP-43 transgene overexpression mimicking the human ALS disease? To better mimic the ubiquitous and moderate levels of TDP-43 occurring in the human context, it seems more appropriate to generate transgenic mice with genomic DNA fragments of TDP-43 gene including its own promoter. While different approaches are needed to reveal the mechanism of pathogenicity of TDP-43, it would be essential to critically evaluate each one of them to judge their usefulness in modeling the human disease.

Our new TDP-43 transgenic mouse model (Swarup et al., 2011a) as well as other models (summarized in chapter 1.2) recapitulate key features of ALS and FTLD (Figure 5.1). What insight do they provide into the pathogenic mechanism of TDP-43- associated neurodegeneration as witnessed in ALS/FTLD-U and possibly other disorders where abnormal TDP-43 pathology like cytoplasmic inclusions, nuclear clearing, etc. is present? Based on observations from human pathological samples and studies in cultured cells, (Chen-Plotkin et al., 2010; Lagier-Tourenne et al., 2010). These can be broadly divided into 2 phenomenon nuclear toxicity and cytoplasmic toxicity -

1. The nuclear toxicity hypothesis postulates that either gain or loss of TDP-43 nuclear function like transcription, splicing, miRNA processing, altered protein-protein interaction etc. leads to toxicity.

2. The cytoplasmic toxicity theory states that TDP-43 is mislocalized to the cytoplasm (either soluble or insoluble, full length or cleaved into C-terminal fragments) which triggers chain of events leading to protein aggregation and neurotoxicity. This cytoplasmic toxicity may occur either by sequestering and inactivating endogenous nuclear TDP-43 or through some other unrelated toxic gain of function like promotion of stress granule formation, etc.

In the following sections insights into these proposed mechanisms will be discussed that have come to light from existing rodent models. It is important to note that one cannot exclude mechanism(s) where both of the above hypotheses or some part of them causes the toxicity. Let's examine what lessons have we actually learned from the various animal models of TDP-43 so far.

Figure 5.1 Key features of transgenic mice encoding genomic fragments of TDP-43 The diagram highlights the key pathological and behavioral changes seen in transgenic mice expressing human wild-type or mutant TDP-43 (G348C and A315T) encoded by genomic fragments. Many key features of ALS and FTLD-U are recapitulated in this mouse model described in Chapter 2 and published Swarup et al., 2011a Brain; Sep;134(9):2610-26. IF = intermediate filaments

5.1.1 TDP-43 autoregulation – a reason for toxicity?

It has been recently reported that TDP-43 can bind to its own 3'-untranslated region (3'UTR) and regulate its expression, a phenomenon called autoregulation and common in hnRNP class of proteins, of which TDP-43 is a member (Buratti and Baralle, 2008; Polymenidou et al., 2011). Reports from our transgenic mouse models as well from others (Swarup et al., 2011a; Xu et al., 2011) suggest that overexpression of full-length human TDP-43 actually downregulates mouse endogenous TDP-43 levels. So how does this autoregulatory process influence ALS pathogenesis?

It is probable to assume that the export of TDP-43 from the nucleus to the cytoplasm for various reasons like injury as seen in our axotomy results (Chapter 3) and its sequestration in insoluble aggregates can stimulate the autoregulatory system. This autoregulatory stimulation will cause a major increase in the rate of TDP-43 production that would be needed to overcome any 'loss-of-function' effects in the nucleus. Ironically, such an 'auto-protective' process even when successful may have potential drawbacks. Increased overall production of TDP-43 may also lead to an increase in aggregate formation or aberrant cleavage/phosphorylation within the cytoplasm, and thus to an increase in any eventual 'gain-of-toxic-function' (in the cytoplasm) effects that might occur as a consequence. With regard to this issue it is important to note that our studies have observed increased TDP-43 mRNA and protein levels in the spinal cord of sporadic ALS patients (Swarup et al., 2011b) and other studies have also revealed upregulation of TDP-43 mRNA in the brains of patients affected by frontotemporal lobar degeneration (Mishra et al., 2007; Chen-Plotkin et al., 2008). Moreover, overexpression of TDP-43 in several animal models has consistently been demonstrated to be pathogenic in a dose-dependent manner (Wegorzewska et al., 2009; Stallings et al., 2010). In addition to the full-length protein, numerous reports have also demonstrated that overexpressing different portions of TDP-43 C-terminal region, including the 25- and 35-kDa, can induce aggregation, and this process may also recruit the full-length TDP-43 into these aggregates (Arai et al., 2010; Chen et al., 2010; Brady et al., 2011). A potential mechanism explaining how TDP-43 C-terminal fragments may trigger aggregation has been recently proposed in a "two-hit" model which

suggests that C-terminal fragments can efficiently enhance this phenomenon only if coupled with loss of their association with RNA (either direct or indirect) or RNP transport (Pesiridis et al., 2011). Additionally, many disease-associated mutations that fall in the C-terminal region of TDP-43 (Barmada and Finkbeiner, 2010; Barmada et al., 2010; Lagier-Tourenne et al., 2010) have been suggested to enhance the aggregation properties of TDP-43 in cell culture (Johnson et al., 2009; Nonaka et al., 2009). Recently, prion like Q/N domain have been reported in the C-terminus of TDP-43 (Udan and Baloh, 2011); wild-type protein is prone to aggregates and mutation associated with ALS in this protein increase the aggregation propensity (Guo et al., 2011). At the moment, the role of aggregation in causing neurodegeneration is still controversial, especially based on recent results obtained in rodent models where the evident neurodegeneration does not always correlate with the observation of insoluble TDP-43 inclusions (Wegorzewska et al., 2009; Stallings et al., 2010; Wils et al., 2010; Xu et al., 2010; Zhou et al., 2010; Igaz et al., 2011; Xu et al., 2011). However, it is conceivable to think that uncontrolled TDP-43 expression levels, due to a loss in the autoregulation mechanism, could generate TDP-43 aggregate formation through an increased production of this mRNA in the nucleus and hence of protein in the cytoplasm. As supported by a previous observation from other aggregation proteins (Furukawa et al., 2009)and TDP-43 itself (Furukawa et al., 2011), these aggregates would then serve as a seed by recruiting more overexpressed TDP-43, causing inclusion body formations, mislocalization of TDP-43, and both gain- and loss-of-functions. Taken together, all these evidences suggest that overproduction of TDP-43 caused by misregulation of its autoregulatory mechanism is an important mechanism and may therefore enhance both its intrinsic aggregation potential and the production of potentially toxic, aggregation prone, CTF fragments. Increased sequestration of TDP-43 in the cytoplasm by the aggregates would then lead to a major increase of its production in an attempt to overcome eventual loss-of-function effects in the nucleus, setting up a vicious circle that in the long run could prove to be very harmful for the cell. With regard to the overproduction issue, it is important to note that two studies have observed increased TDP-43 mRNA levels in the brains of patients affected by various forms of FTLD (Mishra et al., 2007; Chen-Plotkin et al., 2008)in the presence of a nucleotide substitution in the 3′UTR

region of TDP-43 (Gitcho et al., 2009) and in several other types of pathological samples (Weihl et al., 2008; Swarup et al., 2011b).

5.1.2. Cytoplasmic TDP-43 inclusions causing toxicity

Cytoplasmic TDP-43 inclusions are present in more than 90% cases of ALS and FTLD-U (Arai et al., 2006; Neumann et al., 2006). Abnormal protein inclusions are a hallmark finding in many other neurodegenerative diseases including AD, PD and HD and research continues in each of these diseases as to whether inclusions are toxic to neurons, are neuroprotective, or are simply a by-product of another toxic process involving the protein in question. Cytoplasmic inclusions of TDP-43 form the basis of the cytoplasmic toxicity theory which states that inclusions of TDP-43 themselves mediate neurodegeneration. While our mouse models have cytoplasmic TDP-43 aggregates that are ubiquitin positive as seen by double immunofluorescence and co-immunoprecipitation with ubiquitin and TDP-43 antibodies (Swarup et al., 2011a), most of the reported rodent models have ubiquitinated inclusions that are common in vulnerable neurons prior to degeneration and these inclusions either rarely (Stallings et al., 2010; Wils et al., 2010; Xu et al., 2011) or never (Wegorzewska et al., 2009; Shan et al., 2010) stain for TDP-43 itself. Antibodies staining phosphorylated TDP-43 appear to be more sensitive at detecting these rare TDP-43 positive inclusions (Stallings et al., 2010; Xu et al., 2010). Thus, the fact remains that the majority of ubiquitinated inclusions in the reported TDP-43 transgenic rodent models do not stain for TDP-43 or phospho-TDP-43, except that in our model (Swarup et al., 2011a). If not TDP-43, what do the frequent ubiquitinated inclusions in TDP-43- based transgenic models (other than our model) contain? Two reports used electron microscopy and immunostaining to show that spinal motor neurons of TDP-43 transgenic animals contained large perinuclear accumulations of mitochondria (Shan et al., 2010; Xu et al., 2010). These mitochondrial accumulations were observed whether wild-type TDP-43 was driven with Thy-1.2 or mPrp, indicating this is not specific to a particular promoter or expression of wild-type versus ALS disease mutant constructs. The only common underlying factor among these studies is the fact that these studies focus on high expression levels of TDP-43 in restricted cell lineage, resulting in misregulation of TDP-43 function

and causing disease distinct from classical ALS. Clearly, the fact that TDP-43 inclusions are rare in these rodent models (Wegorzewska et al., 2009; Shan et al., 2010; Wils et al., 2010; Xu et al., 2010) despite widespread neurodegeneration is in contrary to the hypothesis that cytoplasmic inclusions of TDP-43 are a necessary step for TDP-43-related neurodegeneration. TDP-43 is an inherently aggregation-prone protein (Johnson et al., 2009) as has been recently reported that the C-terminal region of TDP-43 contains a Q/N rich prion-related domain (Fuentealba et al., 2010).Thus our mouse model which show age-dependent increase in C-terminal fragments and ubiquitinated TDP-43 will provide an invaluable tool in determining the role of cytoplasmic TDP-43 associated toxicity.

5.1.3. Gain of nuclear function of TDP-43 as a mechanism of neurodegeneration

While loss of nuclear TDP-43 function is frequently discussed (see section 5.1.4) as a potential basis of TDP-43-related neurodegeneration, our recent data suggest that it is more probable that ALS-associated TDP-43 mutations or increased levels of wild-type TDP-43 may alter protein binding partners or DNA/RNA targets thus leading to toxicity, either through changes in alternative splicing, transcriptional regulation, or other nuclear TDP-43 functions (Swarup et al., 2011b). In this respect, our finding suggests that increased protein and mRNA levels of TDP-43, which acts as a co-activator of p65 NF-κB, can result in altered innate immune response and increased neurotoxicity (Swarup et al., 2011b). Interestingly, it has also been reported that overexpression of wild-type TDP-43 in mice led to an increased number of Gemini bodies in the nucleus (Shan et al., 2010). Gemini bodies are rich in SMN (survival motor neuron) protein, and are required for assembling snRNPs, critical components of the pre-mRNA splicing apparatus. Overexpression of TDP-43 especially the mutations associated with ALS is known to be aggregate prone and toxic to cultured mouse primary neurons (Johnson et al., 2009; Barmada et al., 2010). The reports of TDP-43 binding to literally hundreds of RNA species in human and murine samples further raises the possibility that overexpression of TDP-43 can misregulate RNA metabolism (Polymenidou et al., 2011; Tollervey et al., 2011).

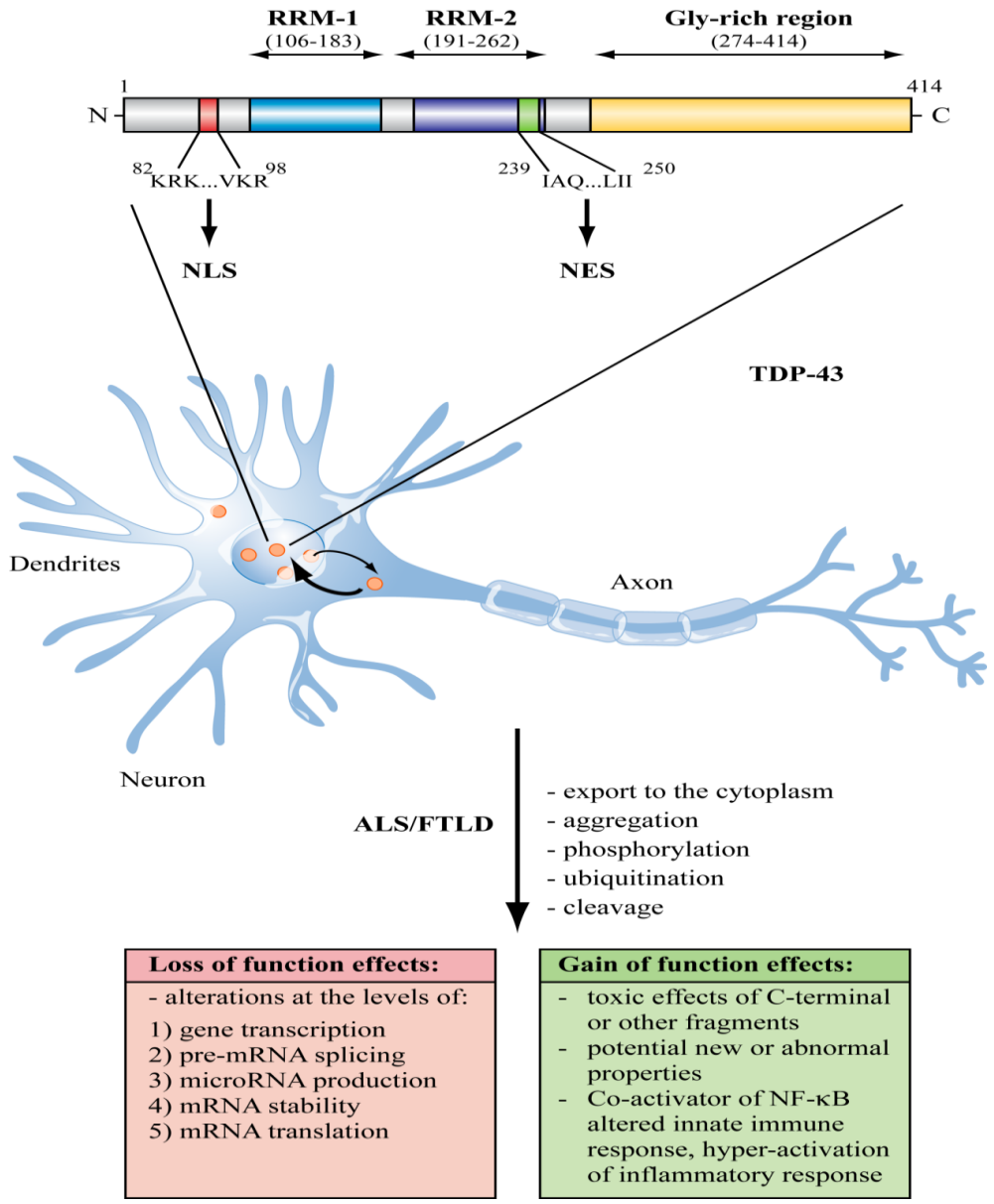

Figure 5.2 Possible pathogenic mechanisms involving TDP-43. Cytoplsmic exclusion of TDP-43, a toxic gain of function in cytoplasm, or a potential loss- of function in the cytoplasm or a combination of all of these may contribute to the pathogenesis of TDP-43. Modified from Buratti et al., 2010

5.1.4. Loss of nuclear function of TDP-43 as a mechanism of neurodegeneration

In striking contrast to gain of TDP-43 functions, loss of nuclear TDP-43 staining is commonly observed in affected neurons in ALS and FTLD [9] leading to the suggestion that a secondary loss of TDP-43 function may be involved in neurodegeneration [13] .While at first it seemed obvious that redistribution of TDP-43 from the nucleus to cytoplasm is a potential loss-of function in the nucleus, recent reports have suggested just the opposite. Contrary to the popular belief TDP-43 is actually upregulated in the spinal cord (Swarup et al., 2011b) and in PBMCs of ALS patients (Nardo et al., 2011). To understand the effects of loss of TDP-43, several groups have generated TDP-43 knockout in mice (Kraemer et al., 2010; Sephton et al., 2010; Wu et al., 2010) . In all cases, homozygous null mice showed early embryonic lethality due to defective outgrowth of the inner cell mass. The importance of this finding supporting loss-of-function theory is weak as this toxicity can also be attributed to the fact that TDP-43 acts as a co-activator of NF-κB, and absence of TDP-43 (siRNA or knockout in mice) fails to activate NF-κB properly which is essential in embryogenesis (Swarup et al., 2011b). Heterozygous mutant mice were normal and did not display pathologic changes in the brain or spinal cord, though a group reported subtle behavioral abnormalities in aged mice (Kraemer et al., 2010) . These studies indicate that TDP-43 is essential for embryonic development, and are consistent with a role for TDP-43 in fundamental aspects of RNA metabolism. Furthermore it is consistent with the observation that loss of TDP-43 is toxic even in cultured cells (Ayala et al., 2008), and may relate to why TDP-43 shows such marked toxicity when overexpressed during development. Whether loss of TDP-43 in mature neurons causes neurodegeneration in ALS or FTLD may never be answered, as a recent report showed that removal of TDP-43 globally from adult mice using a floxed *Tardbp* allele crossed to *Rosa26-ErCre* mice, treated as adults with tamoxifen led to rapid demise within 9 days (Chiang et al., 2010) resulting to study TDP-43 downregulation in adult mice difficult. These mice had selective loss of body fat due to increased fatty acid oxidation, possibly from to misregulation of the putative TDP-43 target gene Tbc1d1, though the relevance of this finding to neurodegeneration in ALS and FTLD remains unclear. Similar to observations in human ALS and FTLD brains and spinal cords, several of the transgenic rodent models showed

loss of nuclear TDP-43 staining in selectively vulnerable neurons prior to overt degeneration (Wegorzewska et al., 2009; Wils et al., 2010). One consideration is that translocation of TDP-43 from the nucleus to the cytosol has also been observed in motor neurons after axotomy (Moisse et al., 2009) and our unpublished data, and therefore further studies are needed to determine if this change in the subcellular distribution of TDP-43 is pathogenic and contributing to the disease or is simply a response to injury.

Thus the evidences till date heavy point that TDP-43 and associated mutations in ALS are responsible for toxic gain-of-function. This is especially looking convincing as more researchers are reporting that TDP-43 is actually upregulated in ALS/FTLD-U and that overexpression of TDP-43 (wild-type or mutations) are neurotoxic.

5.2 TDP-43 as a novel co-activator of NF-κB

The transcription factor NF-κB is a key regulator of hundreds of genes involved in innate immunity, cell survival and inflammation. Since the nuclear translocation and DNA binding of NF-κB are not sufficient for gene induction (Yoza et al., 1996; Bergmann et al., 1998), it has been suggested that interactions with other protein molecules through the transactivation domain (Schmitz et al., 1995b; Gerritsen et al., 1997; Perkins et al., 1997) as well as its modification by phosphorylation (Schmitz et al., 1995a) might play a critical role. It has been reported that transcriptional activation of NF-κB requires multiple co-activator proteins including CREB-binding protein (CBP)/p300 (Gerritsen et al., 1997; Perkins et al., 1997), CBP-associated factor, and steroid receptor coactivator 1(Sheppard et al., 1999). These coactivators have histone acetyltransferase (HAT) activity to modify the chromatin structure and also provide molecular bridges to the basal transcriptional machinery. NF-κB p65 was also found to interact specifically with Fused in Sarcoma (FUS) protein (Uranishi et al., 2001), another DNA/RNA binding protein which is involved in ALS (Kwiatkowski et al., 2009; Vance et al., 2009; Deng et al., 2010).

A study of literature reveals that several approaches have been made to demonstrate that multiple co-activators are required for NF-κB dependent gene expression. Notably, steroid receptor-coactivator-1(SRC-1) or nuclear receptor coactivator-1 (NCoA-1) interacts with p65 and potentiates NF-κB-mediated transactivation (Sheppard et al., 1998). Similarly in vivo approaches were used to establish that both CBP and p/CAF are essential coactivators (Zhong et al., 1998). Multiple interactions are involved in the assembly of the NF-κB transcription complex. Transcriptional activation by p65 requires CBP, or its homolog p300, which also exerts an essential co-activator role for many other classes of regulated transcription factors (Shiama, 1997). Our work suggests that TDP-43 acts as a co-activator of NF-κB. We provide many pathbreaking discoveries listed as below:

1. We have provided proof of a direct interaction between TDP-43 and p65 NF-κB by co-immunoprecipitation experiments using protein extracts from cultured cells, from TDP-43 transgenic mice and from human ALS spinal cord samples. This interaction of TDP-43 with p65 is not affected by mutations in the C-terminal domain of TDP-43.
2. Reporter gene transcription assays and gel shift experiments demonstrated that TDP-43 acts as co-activator of p65 NF-κB through binding of its N-terminal domain to p65. Using deletion mutants of TDP-43, we mapped the region where TDP-43 binds to p65. Our results indicate that p65 interacts with the N-terminal and RRM-1 domains of TDP-43. In particular, TDP-43 interacts with p65 through its N-terminal domain (31-81 and 98-106 AAs) and RRM-1 (107-176 AAs) domain.
3. The presence of ALS-linked mutations in TDP-43 (A315T or G348C) did not affect the binding and activation of p65 NF-κB. This is not surprising because our deletion mutant analysis revealed that a region spanning part of the N-terminal domain and RRM1 of TDP-43 is responsible for interaction with p65 whereas most TDP-43 mutations in ALS occur in the C-terminal domain, which is dispensable for p65 NF-κB activation.
4. The levels of mRNAs for both TDP-43 and p65 NF-κB were substantially elevated in the spinal cord of ALS subjects as compared to non-ALS subjects whereas

immunofluorescence microscopy of ALS spinal cord samples revealed an abnormal nuclear localization p65 NF-κB.

5. In vitro studies have demonstrated that reducing the levels of TDP-43 by siRNA in a cell-culture model led to attenuation of p65 activation. TDP-43 siRNA transfected mouse microglial BV-2 cells exhibited at varying TNF-α concentrations decrease of 2 to 2.5-fold in ICAM-1 luciferase activity.
6. Cell transfection studies have demonstrated that an overexpression of TDP-43 can provoke hyperactive innate immune responses with ensuing enhanced toxicity on neuronal cells whereas in neurons TDP-43 overexpression increased their vulnerability to toxic environment.
7. Using primary cortical neuronal and microglial culture from TDP-43 transgenic mice, we showed that media from LPS-stimulated transgenic microglial cells were more neurotoxic than that from non-transgenic microglia.
8. In vivo treatment of TDP-43 transgenic mice with an inhibitor of NF-κB, Withaferin A, reduced inflammation, ameliorated motor deficits, restored NMJ innervation and reduced peripherin pathology.

This is the first report of an upregulation of mRNAs encoding TDP-43 in post-mortem frozen spinal cords of sporadic ALS. A recent study has provided evidence of increased TDP-43 immunodetection in the skin of ALS patients(Suzuki et al., 2010) but it failed to demonstrate whether this was due to upregulation in TDP-43 mRNA expression. The process that underlies a 2.5-fold increase in TDP-43 mRNA levels in ALS, whether it is transcriptional or mRNA stability remains to be investigated. It seems unlikely that copy number variants could explain an increase of TDP-43 gene transcription as variations in copy number of *TARDBP* have not been detected in cohorts of ALS (Guerreiro et al., 2008; Baumer et al., 2009; Gitcho et al., 2009). Actually, the pathogenic pathways of TDP-43 abnormalities in ALS are not well understood. To date, much attention has been focused of cytoplasmic C-terminal TDP-43 fragments that can elicit toxicity in cell culture systems (Johnson et al., 2008; Dormann et al., 2009; Igaz et al., 2009; Zhang et al., 2009). However, it is noteworthy that neuronal overexpression at high levels of wild-type or mutant TDP-43 in transgenic mice caused a dose-dependent degeneration of cortical and

spinal motor neurons but without massive cytoplasmic TDP-43 aggregates (Wils et al., 2010). This suggests that an upregulation of TDP-43 in the nucleus rather than TDP-43 cytoplasmic aggregates may contribute to neurodegeneration in these mouse models. As shown here, an overexpression of TDP-43 can trigger pathogenic pathways via NF-κB activation.

In fact, our cytotoxicity assays with primary cells from TDP-43 transgenic mice revealed that, at similar levels of mRNA expression, the adverse effects of mutant TDP-43 were more pronounced than TDP-43^{wt}. These results could be explained by the observation that ALS-linked mutations in TDP-43 increase its protein stability(Ling et al., 2010). From the data presented here, we propose the involvement in ALS of a pathogenic pathway due to nuclear increase in TDP-43 levels. Even in cells that exhibit cytoplasmic TDP-43 accumulations in ALS, as commonly detected with antibodies against the C-terminal region, evidence is presented here that TDP-43 N-terminal cleavage fragments could remain in the nuclear compartment as detected with antibody against N-terminal sequences. Accordingly, hyperactivation of p65 by nuclear accumulation of N-terminal TDP-43 fragments may occur concomitantly with cytoplasmic accumulations of TDP-43 C-terminal species.

Our results revealed robust effects of TDP-43 on the activation of NF-κB and innate immune responses. After transfection with TDP-43 species, microglial cells challenged with LPS exhibited much higher mRNA levels for pro-inflammatory cytokines, Nox-2 and NF-κB mRNA when compared to untransfected cells after LPS stimulation. TDP-43 overexpression makes microglia hyperactive to immune stimulation resulting in enhanced toxicity toward neighboring neuronal cells with involvement of reactive oxygen species (ROS) and increased nitrite levels (NO). Moreover, the adverse effects of TDP-43 upregulation are not limited to microglial cells. Primary cortical neurons overexpressing TDP-43 transgenes by ~3-folds exhibited increased susceptibility to the toxic effects of excess glutamate or LPS-activated microglia.

Our finding that TDP-43 acts as co-activator of p65 suggests a key role for NF-κB signaling in ALS pathogenesis. This is corroborated by the abnormal 4-folds increase of p65 NF-κB mRNA in the spinal cord of human ALS and by the nuclear localization of p65. Remarkably, an overexpression of TDP-43 species by ~3-folds in transgenic mice, at levels similar to the human ALS situation (2.5-folds), was sufficient to cause nuclear translocation of p65 NF-κB in the spinal cord. Recently, some ALS-linked mutations have been discovered in the gene coding for optineurin, a protein which activates the suppressor of NF-κB (Maruyama et al., 2010), further supporting a convergent NF-κB-pathogenic pathway. Here, we show that inhibitors of NF-κB activation are able to attenuate the vulnerability of cultured neurons overexpressing TDP-43 species to glutamate-induced or microglia-mediated toxicity. Moreover, pharmacological inhibition of NF-κB by WA treatment attenuated disease phenotypes in TDP-43 transgenic mice. From these results, we propose that NF-κB signaling should be considered as potential therapeutic target in ALS treatment.

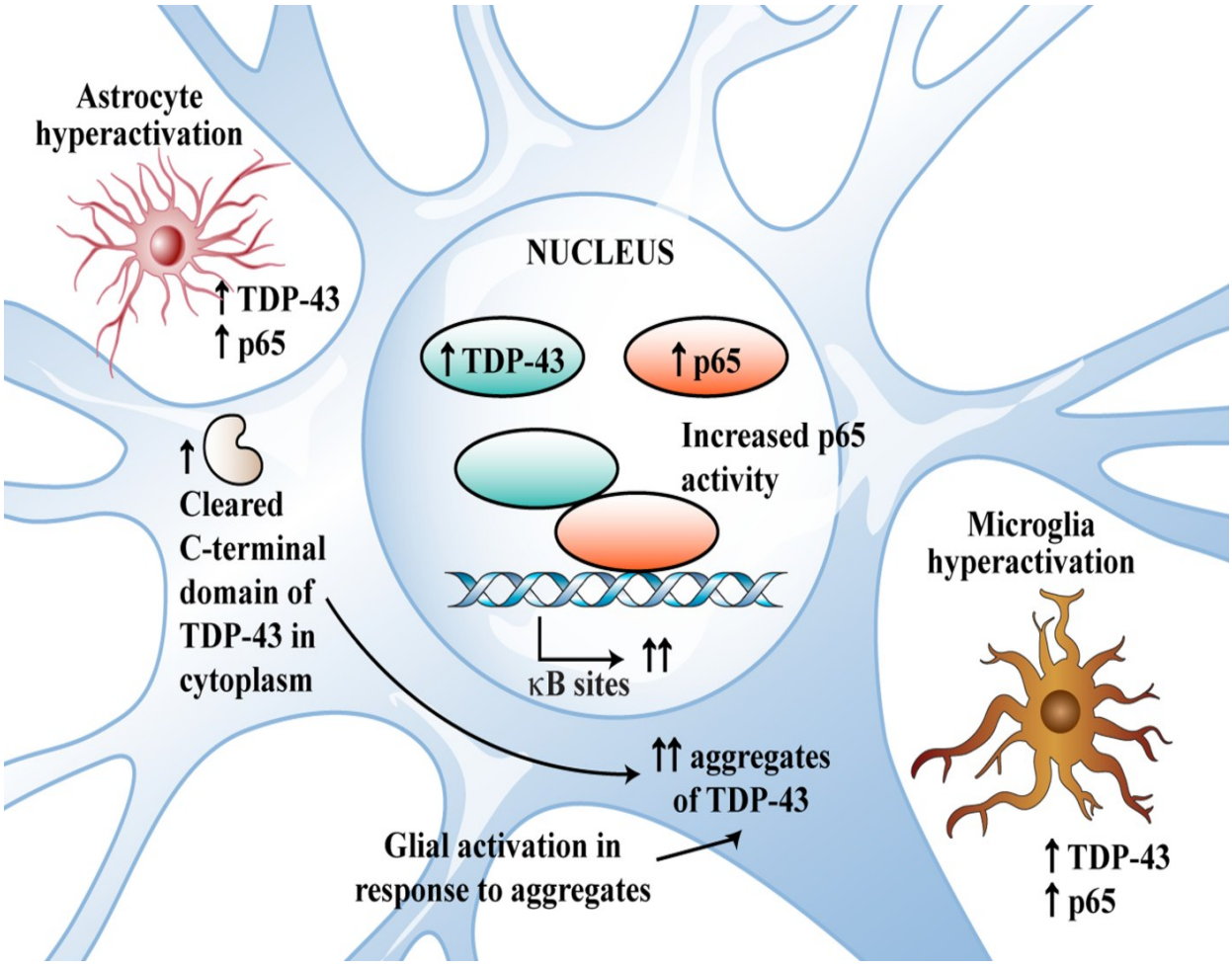

Figure 5.3 Model of TDP-43 acting as a co-activator of NF-κB p65. A model explains how TDP-43 can act as a co-activator of p65 subunit of NF-κB. In different cell-types, TDP-43 can acts in different ways modulating numerous pathogenic pathways involved in ALS. The role of C-terminal fragments of TDP-43 causing TDP-43 aggregates and acting as a substrate for microglial activation remains to be investigated. The model is based on the work presented in chapter 4 and published Swarup et al, 2011b; Journal of Experimental Medicine 2011 Nov 208 (12): 2429-2247

5.3 TDP-43 as a potential biomarker in ALS

There is increasing evidence that a number of potentially informative ALS biomarkers can improve the accuracy of diagnosing ALS, especially when they are used as a panel of diagnostic assays and interpreted in the context of neuroimaging and clinical data. However, further studies are needed that use fully bioanalytically validated immunoassays and other test formats which can cover the heterogeneity of the disease, but studies are also needed that follow patients longitudinally to autopsy in order to correlate biomarker findings with definitive neuropathological diagnoses. Of these TDP-43 can be used an important biomarker of ALS/FTLD-U for the following reasons:

1. TDP-43 inclusions are wide-spread and account to over 90% of all ALS cases (Arai et al., 2006; Neumann et al., 2006). As such TDP-43 can cut across the disease heterogeneity and can be used as a biomarker for ALS.
2. Increased TDP-43 levels have been reported in peripheral blood mononuclear cells (PBMCs) and in cerebrospinal fluid by 2 independent groups (Kasai et al., 2009; Nardo et al., 2011).
3. Increased TDP-43 levels are reported by our group in the spinal cord sections of post-mortem ALS cases both at the mRNA and protein levels (Swarup et al., 2011b).
4. Increased TDP-43 levels have also been reported and being actively considered as a biomarker of FTLD-U cases (Geser et al., 2011).

Although hypothesis-driven candidate biomarkers should continue to be the focus of ALS biomarker research, it is timely to pursue the identification of biomarkers using unbiased strategies based on proteomics, metabolomics or related technologies. TDP-43 has several advantages as an ALS biomarker and further studies should be done to better understand the metabolism and turnover of TDP-43. the importance of the public health benefits that will come from validating informative biomarkers to translate laboratory advances in understanding mechanisms of ALS into better diagnostic strategies and accelerate the pace of developing more meaningful disease-modifying therapies for ALS and related neurodegenerative disorders.

5.4 Conclusion

In accordance with the evidence shown in the thesis, accumulating evidence show that overexpressing moderate levels of TDP-43 (wild-type or mutants) encoded by genomic fragments in a mouse model recapitulate key features of ALS and FTLD-U. Additionally, the mouse model show age-dependent progressive cytoplasmic TDP-43 aggregates, inflammation, intermediate filament pathology and axon caliber changes. The thesis also shows how increased levels of TDP-43 in ALS cases and TDP-43 acting as a co-activator of p65 NF-κB contribute to the pathogenesis of ALS.

References

Acharya KK, Govind CK, Shore AN, Stoler MH, Reddi PP (2006) cis-requirement for the maintenance of round spermatid-specific transcription. Dev Biol 295:781-790.

Ackerley S, Grierson AJ, Banner S, Perkinton MS, Brownlees J, Byers HL, Ward M, Thornhill P, Hussain K, Waby JS, Anderton BH, Cooper JD, Dingwall C, Leigh PN, Shaw CE, Miller CC (2004) p38alpha stress-activated protein kinase phosphorylates neurofilaments and is associated with neurofilament pathology in amyotrophic lateral sclerosis. Molecular and cellular neurosciences 26:354-364.

Aguzzi A (2009) Cell biology: Beyond the prion principle. Nature 459:924-925.

Ahn HJ, Hernandez CM, Levenson JM, Lubin FD, Liou HC, Sweatt JD (2008) c-Rel, an NF-kappaB family transcription factor, is required for hippocampal long-term synaptic plasticity and memory formation. Learn Mem 15:539-549.

Aleyasin H, Cregan SP, Iyirhiaro G, O'Hare MJ, Callaghan SM, Slack RS, Park DS (2004) Nuclear factor-(kappa)B modulates the p53 response in neurons exposed to DNA damage. J Neurosci 24:2963-2973.

Amador-Ortiz C, Lin WL, Ahmed Z, Personett D, Davies P, Duara R, Graff-Radford NR, Hutton ML, Dickson DW (2007) TDP-43 immunoreactivity in hippocampal sclerosis and Alzheimer's disease. Annals of neurology 61:435-445.

Andersen PM (2006) Amyotrophic lateral sclerosis associated with mutations in the CuZn superoxide dismutase gene. Curr Neurol Neurosci Rep 6:37-46.

Andersen PM, Al-Chalabi A (2011) Clinical genetics of amyotrophic lateral sclerosis: what do we really know? Nat Rev Neurol 7:603-615.

Andersen PM, Sims KB, Xin WW, Kiely R, O'Neill G, Ravits J, Pioro E, Harati Y, Brower RD, Levine JS, Heinicke HU, Seltzer W, Boss M, Brown RH, Jr. (2003) Sixteen novel mutations in the Cu/Zn superoxide dismutase gene in amyotrophic lateral sclerosis: a decade of discoveries, defects and disputes. Amyotroph Lateral Scler Other Motor Neuron Disord 4:62-73.

Andrus PK, Fleck TJ, Gurney ME, Hall ED (1998) Protein oxidative damage in a transgenic mouse model of familial amyotrophic lateral sclerosis. Journal of neurochemistry 71:2041-2048.

Arai T, Mackenzie IR, Hasegawa M, Nonoka T, Niizato K, Tsuchiya K, Iritani S, Onaya M, Akiyama H (2009) Phosphorylated TDP-43 in Alzheimer's disease and dementia with Lewy bodies. Acta neuropathologica 117:125-136.

Arai T, Hasegawa M, Akiyama H, Ikeda K, Nonaka T, Mori H, Mann D, Tsuchiya K, Yoshida M, Hashizume Y, Oda T (2006) TDP-43 is a component of ubiquitin-positive tau-negative inclusions in frontotemporal lobar degeneration and amyotrophic lateral sclerosis. Biochemical and biophysical research communications 351:602-611.

Arai T, Hasegawa M, Nonoka T, Kametani F, Yamashita M, Hosokawa M, Niizato K, Tsuchiya K, Kobayashi Z, Ikeda K, Yoshida M, Onaya M, Fujishiro H, Akiyama H (2010) Phosphorylated and cleaved TDP-43 in ALS, FTLD and other neurodegenerative disorders and in cellular models of TDP-43 proteinopathy. Neuropathology : official journal of the Japanese Society of Neuropathology 30:170-181.

Ash PE, Zhang YJ, Roberts CM, Saldi T, Hutter H, Buratti E, Petrucelli L, Link CD (2010) Neurotoxic effects of TDP-43 overexpression in C. elegans. Human molecular genetics 19:3206-3218.

Atkin JD, Farg MA, Walker AK, McLean C, Tomas D, Horne MK (2008) Endoplasmic reticulum stress and induction of the unfolded protein response in human sporadic amyotrophic lateral sclerosis. Neurobiology of disease 30:400-407.

Atkin JD, Farg MA, Turner BJ, Tomas D, Lysaght JA, Nunan J, Rembach A, Nagley P, Beart PM, Cheema SS, Horne MK (2006) Induction of the unfolded protein response in familial amyotrophic lateral sclerosis and association of protein-disulfide isomerase with superoxide dismutase 1. The Journal of biological chemistry 281:30152-30165.

Audet Jean-Nicolas GGaJJ-P (2010) Wild-type human SOD1 overexpression does not accelerate motor neuron disease in mice expressing murine Sod1 G86R. Neurobiology of Disease doi:10.1016/j.nbd.2010.05.031.

Ayala YM, Zago P, D'Ambrogio A, Xu YF, Petrucelli L, Buratti E, Baralle FE (2008) Structural determinants of the cellular localization and shuttling of TDP-43. J Cell Sci 121:3778-3785.

Ayala YM, Pantano S, D'Ambrogio A, Buratti E, Brindisi A, Marchetti C, Romano M, Baralle FE (2005) Human, Drosophila, and C.elegans TDP43: nucleic acid binding properties and splicing regulatory function. J Mol Biol 348:575-588.

Badadani M, Nalbandian A, Watts GD, Vesa J, Kitazawa M, Su H, Tanaja J, Dec E, Wallace DC, Mukherjee J, Caiozzo V, Warman M, Kimonis VE (2010) VCP associated inclusion body myopathy and paget disease of bone knock-in mouse model exhibits tissue pathology typical of human disease. PLoS One 5.

Baeuerle PA, Baichwal VR (1997) NF-kappa B as a frequent target for immunosuppressive and anti-inflammatory molecules. Adv Immunol 65:111-137.

Bakalkin G, Yakovleva T, Terenius L (1993) NF-kappa B-like factors in the murine brain. Developmentally-regulated and tissue-specific expression. Brain Res Mol Brain Res 20:137-146.

Baldwin AS, Jr. (1996) The NF-kappa B and I kappa B proteins: new discoveries and insights. Annu Rev Immunol 14:649-683.

Ballatore C, Lee VM, Trojanowski JQ (2007) Tau-mediated neurodegeneration in Alzheimer's disease and related disorders. Nat Rev Neurosci 8:663-672.

Banerjee R, Mosley RL, Reynolds AD, Dhar A, Jackson-Lewis V, Gordon PH, Przedborski S, Gendelman HE (2008) Adaptive immune neuroprotection in G93A-SOD1 amyotrophic lateral sclerosis mice. PLoS One 3:e2740.

Barbeito LH, Pehar M, Cassina P, Vargas MR, Peluffo H, Viera L, Estevez AG, Beckman JS (2004) A role for astrocytes in motor neuron loss in amyotrophic lateral sclerosis. Brain Res Brain Res Rev 47:263-274.

Barber SC, Shaw PJ (2010) Oxidative stress in ALS: key role in motor neuron injury and therapeutic target. Free Radic Biol Med 48:629-641.

Barmada SJ, Finkbeiner S (2010) Pathogenic TARDBP mutations in amyotrophic lateral sclerosis and frontotemporal dementia: disease-associated pathways. Rev Neurosci 21:251-272.

Barmada SJ, Skibinski G, Korb E, Rao EJ, Wu JY, Finkbeiner S (2010) Cytoplasmic mislocalization of TDP-43 is toxic to neurons and enhanced by a mutation associated with familial amyotrophic lateral sclerosis. J Neurosci 30:639-649.

Batulan Z, Shinder GA, Minotti S, He BP, Doroudchi MM, Nalbantoglu J, Strong MJ, Durham HD (2003) High threshold for induction of the stress response in motor neurons is associated with failure to activate HSF1. J Neurosci 23:5789-5798.

Baumer D, Parkinson N, Talbot K (2009) TARDBP in amyotrophic lateral sclerosis: identification of a novel variant but absence of copy number variation. J Neurol Neurosurg Psychiatry 80:1283-1285.

Beaulieu JM, Julien JP (2003) Peripherin-mediated death of motor neurons rescued by overexpression of neurofilament NF-H proteins. J Neurochem 85:248-256.

Beaulieu JM, Nguyen MD, Julien JP (1999) Late onset of motor neurons in mice overexpressing wild-type peripherin. J Cell Biol 147:531-544.

Beaulieu JM, Jacomy H, Julien JP (2000) Formation of intermediate filament protein aggregates with disparate effects in two transgenic mouse models lacking the neurofilament light subunit. J Neurosci 20:5321-5328.

Beaulieu JM, Kriz J, Julien JP (2002) Induction of peripherin expression in subsets of brain neurons after lesion injury or cerebral ischemia. Brain Res 946:153-161.

Beckman JS, Carson M, Smith CD, Koppenol WH (1993) ALS, SOD and peroxynitrite. Nature 364:584.

Belzil VV, Daoud H, Desjarlais A, Bouchard JP, Dupre N, Camu W, Dion PA, Rouleau GA (2011) Analysis of OPTN as a causative gene for amyotrophic lateral sclerosis. Neurobiol Aging 32:555 e513-554.

Ben Hamida M, Hentati F, Ben Hamida C (1990) Hereditary motor system diseases (chronic juvenile amyotrophic lateral sclerosis). Conditions combining a bilateral pyramidal syndrome with limb and bulbar amyotrophy. Brain : a journal of neurology 113 (Pt 2):347-363.

Benajiba L, Le Ber I, Camuzat A, Lacoste M, Thomas-Anterion C, Couratier P, Legallic S, Salachas F, Hannequin D, Decousus M, Lacomblez L, Guedj E, Golfier V, Camu W, Dubois B, Campion D, Meininger V, Brice A (2009) TARDBP mutations in motoneuron disease with frontotemporal lobar degeneration. Annals of neurology 65:470-473.

Bergmann M, Hart L, Lindsay M, Barnes PJ, Newton R (1998) IkappaBalpha degradation and nuclear factor-kappaB DNA binding are insufficient for interleukin-1beta and tumor necrosis factor-alpha-induced kappaB-dependent transcription. Requirement for an additional activation pathway. J Biol Chem 273:6607-6610.

Bhakar AL, Tannis LL, Zeindler C, Russo MP, Jobin C, Park DS, MacPherson S, Barker PA (2002) Constitutive nuclear factor-kappa B activity is required for central neuron survival. J Neurosci 22:8466-8475.

Blackburn D, Sargsyan S, Monk PN, Shaw PJ (2009) Astrocyte function and role in motor neuron disease: a future therapeutic target? Glia 57:1251-1264.

Blair IP, Williams KL, Warraich ST, Durnall JC, Thoeng AD, Manavis J, Blumbergs PC, Vucic S, Kiernan MC, Nicholson GA (2010) FUS mutations in amyotrophic lateral sclerosis: clinical, pathological, neurophysiological and genetic analysis. Journal of neurology, neurosurgery, and psychiatry 81:639-645.

Blair WS, Bogerd HP, Madore SJ, Cullen BR (1994) Mutational analysis of the transcription activation domain of RelA: identification of a highly synergistic minimal acidic activation module. Mol Cell Biol 14:7226-7234.

Boillee S, Vande Velde C, Cleveland DW (2006a) ALS: a disease of motor neurons and their nonneuronal neighbors. Neuron 52:39-59.

Boillee S, Yamanaka K, Lobsiger CS, Copeland NG, Jenkins NA, Kassiotis G, Kollias G, Cleveland DW (2006b) Onset and progression in inherited ALS determined by motor neurons and microglia. Science 312:1389-1392.

Bommel H, Xie G, Rossoll W, Wiese S, Jablonka S, Boehm T, Sendtner M (2002) Missense mutation in the tubulin-specific chaperone E (Tbce) gene in the mouse mutant progressive motor neuronopathy, a model of human motoneuron disease. J Cell Biol 159:563-569.

Bondeson J, Foxwell B, Brennan F, Feldmann M (1999) Defining therapeutic targets by using adenovirus: blocking NF-kappaB inhibits both inflammatory and destructive mechanisms in rheumatoid synovium but spares anti-inflammatory mediators. Proceedings of the National Academy of Sciences of the United States of America 96:5668-5673.

Bordet T, Buisson B, Michaud M, Drouot C, Galea P, Delaage P, Akentieva NP, Evers AS, Covey DF, Ostuni MA, Lacapere JJ, Massaad C, Schumacher M, Steidl EM, Maux D, Delaage M, Henderson CE, Pruss RM (2007) Identification and characterization of cholest-4-en-3-one, oxime (TRO19622), a novel drug candidate for amyotrophic lateral sclerosis. J Pharmacol Exp Ther 322:709-720.

Borroni B, Bonvicini C, Alberici A, Buratti E, Agosti C, Archetti S, Papetti A, Stuani C, Di Luca M, Gennarelli M, Padovani A (2009) Mutation within TARDBP leads to frontotemporal dementia without motor neuron disease. Human mutation 30:E974-983.

Borroni B, Archetti S, Del Bo R, Papetti A, Buratti E, Bonvicini C, Agosti C, Cosseddu M, Turla M, Di Lorenzo D, Pietro Comi G, Gennarelli M, Padovani A (2010) TARDBP mutations in frontotemporal lobar degeneration: frequency, clinical features, and disease course. Rejuvenation Res 13:509-517.

Bosco DA, Morfini G, Karabacak NM, Song Y, Gros-Louis F, Pasinelli P, Goolsby H, Fontaine BA, Lemay N, McKenna-Yasek D, Frosch MP, Agar JN, Julien JP, Brady ST, Brown RH, Jr. (2010) Wild-type and mutant SOD1 share an aberrant conformation and a common pathogenic pathway in ALS. Nature neuroscience 13:1396-1403.

Bose JK, Wang IF, Hung L, Tarn WY, Shen CK (2008) TDP-43 overexpression enhances exon 7 inclusion during the survival of motor neuron pre-mRNA splicing. J Biol Chem 283:28852-28859.

Boston-Howes W, Gibb SL, Williams EO, Pasinelli P, Brown RH, Jr., Trotti D (2006) Caspase-3 cleaves and inactivates the glutamate transporter EAAT2. The Journal of biological chemistry 281:14076-14084.

Brady OA, Meng P, Zheng Y, Mao Y, Hu F (2011) Regulation of TDP-43 aggregation by phosphorylation and p62/SQSTM1. Journal of neurochemistry 116:248-259.

Brandmeir NJ, Geser F, Kwong LK, Zimmerman E, Qian J, Lee VM, Trojanowski JQ (2008) Severe subcortical TDP-43 pathology in sporadic frontotemporal lobar degeneration with motor neuron disease. Acta neuropathologica 115:123-131.

Bruening W, Roy J, Giasson B, Figlewicz DA, Mushynski WE, Durham HD (1999) Up-regulation of protein chaperones preserves viability of cells expressing toxic Cu/Zn-superoxide dismutase mutants associated with amyotrophic lateral sclerosis. J Neurochem 72:693-699.

Bruijn LI, Houseweart MK, Kato S, Anderson KL, Anderson SD, Ohama E, Reaume AG, Scott RW, Cleveland DW (1998) Aggregation and motor neuron toxicity of an ALS-linked SOD1 mutant independent from wild-type SOD1. Science 281:1851-1854.

Bruijn LI, Becher MW, Lee MK, Anderson KL, Jenkins NA, Copeland NG, Sisodia SS, Rothstein JD, Borchelt DR, Price DL, Cleveland DW (1997) ALS-linked SOD1 mutant G85R mediates damage to astrocytes and promotes rapidly progressive disease with SOD1-containing inclusions. Neuron 18:327-338.

Buratti E, Baralle FE (2008) Multiple roles of TDP-43 in gene expression, splicing regulation, and human disease. Front Biosci 13:867-878.

Buratti E, Dork T, Zuccato E, Pagani F, Romano M, Baralle FE (2001) Nuclear factor TDP-43 and SR proteins promote in vitro and in vivo CFTR exon 9 skipping. EMBO J 20:1774-1784.

Buratti E, Brindisi A, Giombi M, Tisminetzky S, Ayala YM, Baralle FE (2005) TDP-43 binds heterogeneous nuclear ribonucleoprotein A/B through its C-terminal tail: an important region for the inhibition of cystic fibrosis transmembrane conductance regulator exon 9 splicing. J Biol Chem 280:37572-37584.

Cai H, Lin X, Xie C, Laird FM, Lai C, Wen H, Chiang HC, Shim H, Farah MH, Hoke A, Price DL, Wong PC (2005) Loss of ALS2 function is insufficient to trigger motor neuron degeneration in knock-out mice but predisposes neurons to oxidative stress. J Neurosci 25:7567-7574.

Cairns NJ et al. (2007) TDP-43 in familial and sporadic frontotemporal lobar degeneration with ubiquitin inclusions. Am J Pathol 171:227-240.

Carmona R, Macias D, Guadix JA, Portillo V, Perez-Pomares JM, Munoz-Chapuli R (2007) A simple technique of image analysis for specific nuclear immunolocalization of proteins. J Microsc 225:96-99.

Carpenter S (1968) Proximal axonal enlargement in motor neuron disease. Neurology 18:841-851.

Carriedo SG, Yin HZ, Weiss JH (1996) Motor neurons are selectively vulnerable to AMPA/kainate receptor-mediated injury in vitro. The Journal of neuroscience : the official journal of the Society for Neuroscience 16:4069-4079.

Casafont I, Bengoechea R, Tapia O, Berciano MT, Lafarga M (2009) TDP-43 localizes in mRNA transcription and processing sites in mammalian neurons. J Struct Biol 167:235-241.

Chang Y, Kong Q, Shan X, Tian G, Ilieva H, Cleveland DW, Rothstein JD, Borchelt DR, Wong PC, Lin CL (2008) Messenger RNA oxidation occurs early in disease pathogenesis and promotes motor neuron degeneration in ALS. PloS one 3:e2849.

Chau CH, Clavijo CA, Deng HT, Zhang Q, Kim KJ, Qiu Y, Le AD, Ann DK (2005) Etk/Bmx mediates expression of stress-induced adaptive genes VEGF, PAI-1, and iNOS via multiple signaling cascades in different cell systems. Am J Physiol Cell Physiol 289:C444-454.

Cheah BC, Vucic S, Krishnan AV, Kiernan MC (2010) Riluzole, neuroprotection and amyotrophic lateral sclerosis. Curr Med Chem 17:1942-1199.

Chen-Plotkin AS, Lee VM, Trojanowski JQ (2010) TAR DNA-binding protein 43 in neurodegenerative disease. Nat Rev Neurol 6:211-220.

Chen-Plotkin AS, Geser F, Plotkin JB, Clark CM, Kwong LK, Yuan W, Grossman M, Van Deerlin VM, Trojanowski JQ, Lee VM (2008) Variations in the progranulin gene affect global gene expression in frontotemporal lobar degeneration. Human molecular genetics 17:1349-1362.

Chen AK, Lin RY, Hsieh EZ, Tu PH, Chen RP, Liao TY, Chen W, Wang CH, Huang JJ (2010a) Induction of amyloid fibrils by the C-terminal fragments of TDP-43 in amyotrophic lateral sclerosis. J Am Chem Soc 132:1186-1187.

Chen G, Cao P, Goeddel DV (2002) TNF-induced recruitment and activation of the IKK complex require Cdc37 and Hsp90. Mol Cell 9:401-410.

Chen HJ, Anagnostou G, Chai A, Withers J, Morris A, Adhikaree J, Pennetta G, de Belleroche JS (2010b) Characterization of the properties of a novel mutation in VAPB in familial amyotrophic lateral sclerosis. The Journal of biological chemistry 285:40266-40281.

Chen YZ, Hashemi SH, Anderson SK, Huang Y, Moreira MC, Lynch DR, Glass IA, Chance PF, Bennett CL (2006) Senataxin, the yeast Sen1p orthologue: characterization of a unique protein in which recessive mutations cause ataxia and dominant mutations cause motor neuron disease. Neurobiology of disease 23:97-108.

Chen YZ, Bennett CL, Huynh HM, Blair IP, Puls I, Irobi J, Dierick I, Abel A, Kennerson ML, Rabin BA, Nicholson GA, Auer-Grumbach M, Wagner K, De Jonghe P, Griffin JW, Fischbeck KH, Timmerman V, Cornblath DR, Chance PF (2004) DNA/RNA helicase gene mutations in a form of juvenile amyotrophic lateral sclerosis (ALS4). American journal of human genetics 74:1128-1135.

Chiang PM, Ling J, Jeong YH, Price DL, Aja SM, Wong PC (2010) Deletion of TDP-43 down-regulates Tbc1d1, a gene linked to obesity, and alters body fat metabolism. Proceedings of the National Academy of Sciences of the United States of America 107:16320-16324.

Chio A et al. (2011) Large proportion of amyotrophic lateral sclerosis cases in Sardinia due to a single founder mutation of the TARDBP gene. Arch Neurol 68:594-598.

Chiu IM, Phatnani H, Kuligowski M, Tapia JC, Carrasco MA, Zhang M, Maniatis T, Carroll MC (2009) Activation of innate and humoral immunity in the peripheral nervous system of ALS transgenic mice. Proc Natl Acad Sci U S A 106:20960-20965.

Clemens JA (2000) Cerebral ischemia: gene activation, neuronal injury, and the protective role of antioxidants. Free Radic Biol Med 28:1526-1531.

Clement AM, Nguyen MD, Roberts EA, Garcia ML, Boillee S, Rule M, McMahon AP, Doucette W, Siwek D, Ferrante RJ, Brown RH, Jr., Julien JP, Goldstein LS, Cleveland DW (2003) Wild-type nonneuronal cells extend survival of SOD1 mutant motor neurons in ALS mice. Science 302:113-117.

Cleveland DW (1999) From Charcot to SOD1: mechanisms of selective motor neuron death in ALS. Neuron 24:515-520.

Colombrita C, Zennaro E, Fallini C, Weber M, Sommacal A, Buratti E, Silani V, Ratti A (2009) TDP-43 is recruited to stress granules in conditions of oxidative insult. Journal of neurochemistry 111:1051-1061.

Conforti FL, Sprovieri T, Mazzei R, Ungaro C, La Bella V, Tessitore A, Patitucci A, Magariello A, Gabriele AL, Tedeschi G, Simone IL, Majorana G, Valentino P, Condino F, Bono F, Monsurro MR, Muglia M, Quattrone A (2008) A novel Angiogenin gene mutation in a sporadic patient with amyotrophic lateral sclerosis from southern Italy. Neuromuscul Disord 18:68-70.

Corbo M, Hays AP (1992) Peripherin and neurofilament protein coexist in spinal spheroids of motor neuron disease. J Neuropathol Exp Neurol 51:531-537.

Cordeau P, Jr., Lalancette-Hebert M, Weng YC, Kriz J (2008) Live imaging of neuroinflammation reveals sex and estrogen effects on astrocyte response to ischemic injury. Stroke 39:935-942.

Corrado L, Ratti A, Gellera C, Buratti E, Castellotti B, Carlomagno Y, Ticozzi N, Mazzini L, Testa L, Taroni F, Baralle FE, Silani V, D'Alfonso S (2009) High frequency of TARDBP gene mutations in Italian patients with amyotrophic lateral sclerosis. Hum Mutat 30:688-694.

Cote F, Collard JF, Julien JP (1993) Progressive neuronopathy in transgenic mice expressing the human neurofilament heavy gene: a mouse model of amyotrophic lateral sclerosis. Cell 73:35-46.

Crespel A, Coubes P, Rousset MC, Brana C, Rougier A, Rondouin G, Bockaert J, Baldy-Moulinier M, Lerner-Natoli M (2002) Inflammatory reactions in human medial temporal lobe epilepsy with hippocampal sclerosis. Brain research 952:159-169.

Cushman M, Johnson BS, King OD, Gitler AD, Shorter J (2010) Prion-like disorders: blurring the divide between transmissibility and infectivity. J Cell Sci 123:1191-1201.

Custer SK, Neumann M, Lu H, Wright AC, Taylor JP (2010) Transgenic mice expressing mutant forms VCP/p97 recapitulate the full spectrum of IBMPFD including degeneration in muscle, brain and bone. Hum Mol Genet 19:1741-1755.

D'Ambrogio A, Buratti E, Stuani C, Guarnaccia C, Romano M, Ayala YM, Baralle FE (2009) Functional mapping of the interaction between TDP-43 and hnRNP A2 in vivo. Nucleic acids research 37:4116-4126.

Daily D, Vlamis-Gardikas A, Offen D, Mittelman L, Melamed E, Holmgren A, Barzilai A (2001) Glutaredoxin protects cerebellar granule neurons from dopamine-induced apoptosis by activating NF-kappa B via Ref-1. J Biol Chem 276:1335-1344.

Damiano M, Starkov AA, Petri S, Kipiani K, Kiaei M, Mattiazzi M, Flint Beal M, Manfredi G (2006) Neural mitochondrial Ca2+ capacity impairment precedes the onset of motor symptoms in G93A Cu/Zn-superoxide dismutase mutant mice. Journal of neurochemistry 96:1349-1361.

Danciger E, Dafni N, Bernstein Y, Laver-Rudich Z, Neer A, Groner Y (1986) Human Cu/Zn superoxide dismutase gene family: molecular structure and characterization of four Cu/Zn superoxide dismutase-related pseudogenes. Proceedings of the National Academy of Sciences of the United States of America 83:3619-3623.

Daoud H, Valdmanis PN, Kabashi E, Dion P, Dupre N, Camu W, Meininger V, Rouleau GA (2009) Contribution of TARDBP mutations to sporadic amyotrophic lateral sclerosis. J Med Genet 46:112-114.

Davidson Y, Kelley T, Mackenzie IR, Pickering-Brown S, Du Plessis D, Neary D, Snowden JS, Mann DM (2007) Ubiquitinated pathological lesions in frontotemporal lobar degeneration contain the TAR DNA-binding protein, TDP-43. Acta neuropathologica 113:521-533.

Davies JQ, Gordon S (2005) Isolation and culture of murine macrophages. Methods Mol Biol 290:91-103.

De Jonghe P, Mersivanova I, Nelis E, Del Favero J, Martin JJ, Van Broeckhoven C, Evgrafov O, Timmerman V (2001) Further evidence that neurofilament light chain gene mutations can cause Charcot-Marie-Tooth disease type 2E. Ann Neurol 49:245-249.

De Vos K, Severin F, Van Herreweghe F, Vancompernolle K, Goossens V, Hyman A, Grooten J (2000) Tumor necrosis factor induces hyperphosphorylation of kinesin light chain and inhibits kinesin-mediated transport of mitochondria. The Journal of cell biology 149:1207-1214.

De Vos KJ, Chapman AL, Tennant ME, Manser C, Tudor EL, Lau KF, Brownlees J, Ackerley S, Shaw PJ, McLoughlin DM, Shaw CE, Leigh PN, Miller CC, Grierson AJ (2007) Familial amyotrophic lateral sclerosis-linked SOD1 mutants perturb fast axonal transport to reduce axonal mitochondria content. Human molecular genetics 16:2720-2728.

Dejesus-Hernandez M et al. (2011) Expanded GGGGCC Hexanucleotide Repeat in Noncoding Region of C9ORF72 Causes Chromosome 9p-Linked FTD and ALS. Neuron 72:245-256.

Del Bo R, Ghezzi S, Corti S, Pandolfo M, Ranieri M, Santoro D, Ghione I, Prelle A, Orsetti V, Mancuso M, Soraru G, Briani C, Angelini C, Siciliano G, Bresolin N, Comi GP (2009) TARDBP (TDP-43) sequence analysis in patients with familial and sporadic ALS: identification of two novel mutations. Eur J Neurol 16:727-732.

Deng HX, Jiang H, Fu R, Zhai H, Shi Y, Liu E, Hirano M, Dal Canto MC, Siddique T (2008) Molecular dissection of ALS-associated toxicity of SOD1 in transgenic mice using an exon-fusion approach. Hum Mol Genet 17:2310-2319.

Deng HX, Zhai H, Bigio EH, Yan J, Fecto F, Ajroud K, Mishra M, Ajroud-Driss S, Heller S, Sufit R, Siddique N, Mugnaini E, Siddique T (2010) FUS-immunoreactive inclusions are a common feature in sporadic and non-SOD1 familial amyotrophic lateral sclerosis. Ann Neurol 67:739-748.

Deng HX, Shi Y, Furukawa Y, Zhai H, Fu R, Liu E, Gorrie GH, Khan MS, Hung WY, Bigio EH, Lukas T, Dal Canto MC, O'Halloran TV, Siddique T (2006) Conversion to the amyotrophic lateral sclerosis phenotype is associated with intermolecular linked insoluble aggregates of SOD1 in mitochondria. Proc Natl Acad Sci U S A 103:7142-7147.

Deng HX et al. (2011) Mutations in UBQLN2 cause dominant X-linked juvenile and adult-onset ALS and ALS/dementia. Nature 477:211-215.

Dennis JS, Citron BA (2009) Wobbler mice modeling motor neuron disease display elevated transactive response DNA binding protein. Neuroscience 158:745-750.

Dequen F, Bomont P, Gowing G, Cleveland DW, Julien JP (2008) Modest loss of peripheral axons, muscle atrophy and formation of brain inclusions in mice with targeted deletion of gigaxonin exon 1. J Neurochem 107:253-264.

Devon RS, Orban PC, Gerrow K, Barbieri MA, Schwab C, Cao LP, Helm JR, Bissada N, Cruz-Aguado R, Davidson TL, Witmer J, Metzler M, Lam CK, Tetzlaff W, Simpson EM, McCaffery JM, El-Husseini AE, Leavitt BR, Hayden MR (2006) Als2-deficient mice exhibit disturbances in endosome trafficking associated with motor behavioral abnormalities. Proc Natl Acad Sci U S A 103:9595-9600.

Di Giorgio FP, Boulting GL, Bobrowicz S, Eggan KC (2008) Human embryonic stem cell-derived motor neurons are sensitive to the toxic effect of glial cells carrying an ALS-causing mutation. Cell stem cell 3:637-648.

Di Giorgio FP, Carrasco MA, Siao MC, Maniatis T, Eggan K (2007) Non-cell autonomous effect of glia on motor neurons in an embryonic stem cell-based ALS model. Nat Neurosci 10:608-614.

di Meglio P, Ianaro A, Ghosh S (2005) Amelioration of acute inflammation by systemic administration of a cell-permeable peptide inhibitor of NF-kappaB activation. Arthritis Rheum 52:951-958.

Dickson DW, Josephs KA, Amador-Ortiz C (2007) TDP-43 in differential diagnosis of motor neuron disorders. Acta neuropathologica 114:71-79.

DiDonato JA, Hayakawa M, Rothwarf DM, Zandi E, Karin M (1997) A cytokine-responsive IkappaB kinase that activates the transcription factor NF-kappaB. Nature 388:548-554.

Dion PA, Daoud H, Rouleau GA (2009) Genetics of motor neuron disorders: new insights into pathogenic mechanisms. Nat Rev Genet 10:769-782.

Dormann D, Capell A, Carlson AM, Shankaran SS, Rodde R, Neumann M, Kremmer E, Matsuwaki T, Yamanouchi K, Nishihara M, Haass C (2009) Proteolytic processing of TAR

DNA binding protein-43 by caspases produces C-terminal fragments with disease defining properties independent of progranulin. J Neurochem 110:1082-1094.

Dormann D, Rodde R, Edbauer D, Bentmann E, Fischer I, Hruscha A, Than ME, Mackenzie IR, Capell A, Schmid B, Neumann M, Haass C (2010) ALS-associated fused in sarcoma (FUS) mutations disrupt Transportin-mediated nuclear import. The EMBO journal 29:2841-2857.

Douville R, Liu J, Rothstein J, Nath A (2011) Identification of active loci of a human endogenous retrovirus in neurons of patients with amyotrophic lateral sclerosis. Annals of neurology 69:141-151.

Dreyfuss G, Kim VN, Kataoka N (2002) Messenger-RNA-binding proteins and the messages they carry. Nat Rev Mol Cell Biol 3:195-205.

Dreyfuss G, Matunis MJ, Pinol-Roma S, Burd CG (1993) hnRNP proteins and the biogenesis of mRNA. Annu Rev Biochem 62:289-321.

Du Yan S, Zhu H, Fu J, Yan SF, Roher A, Tourtellotte WW, Rajavashisth T, Chen X, Godman GC, Stern D, Schmidt AM (1997) Amyloid-beta peptide-receptor for advanced glycation endproduct interaction elicits neuronal expression of macrophage-colony stimulating factor: a proinflammatory pathway in Alzheimer disease. Proceedings of the National Academy of Sciences of the United States of America 94:5296-5301.

Duan W, Li X, Shi J, Guo Y, Li Z, Li C (2010) Mutant TAR DNA-binding protein-43 induces oxidative injury in motor neuron-like cell. Neuroscience 169:1621-1629.

Dubois M, Lalonde R, Julien JP, Strazielle C (2005) Mice with the deleted neurofilament of low-molecular-weight (Nefl) gene: 1. Effects on regional brain metabolism. J Neurosci Res 80:741-750.

Duffy LM, Chapman AL, Shaw PJ, Grierson AJ (2011) Review: The role of mitochondria in the pathogenesis of amyotrophic lateral sclerosis. Neuropathol Appl Neurobiol 37:336-352.

Durham HD, Roy J, Dong L, Figlewicz DA (1997) Aggregation of mutant Cu/Zn superoxide dismutase proteins in a culture model of ALS. J Neuropathol Exp Neurol 56:523-530.

Elden AC et al. (2010) Ataxin-2 intermediate-length polyglutamine expansions are associated with increased risk for ALS. Nature 466:1069-1075.

Elder GA, Friedrich VL, Jr., Margita A, Lazzarini RA (1999) Age-related atrophy of motor axons in mice deficient in the mid-sized neurofilament subunit. J Cell Biol 146:181-192.

Elder GA, Friedrich VL, Jr., Kang C, Bosco P, Gourov A, Tu PH, Zhang B, Lee VM, Lazzarini RA (1998) Requirement of heavy neurofilament subunit in the development of axons with large calibers. J Cell Biol 143:195-205.

Eymard-Pierre E, Lesca G, Dollet S, Santorelli FM, di Capua M, Bertini E, Boespflug-Tanguy O (2002) Infantile-onset ascending hereditary spastic paralysis is associated with mutations in the alsin gene. Am J Hum Genet 71:518-527.

Fernandez-Santiago R, Hoenig S, Lichtner P, Sperfeld AD, Sharma M, Berg D, Weichenrieder O, Illig T, Eger K, Meyer T, Anneser J, Munch C, Zierz S, Gasser T, Ludolph A (2009) Identification of novel Angiogenin (ANG) gene missense variants in German patients with amyotrophic lateral sclerosis. Journal of neurology 256:1337-1342.

Ferraiuolo L, Heath PR, Holden H, Kasher P, Kirby J, Shaw PJ (2007) Microarray analysis of the cellular pathways involved in the adaptation to and progression of motor neuron injury in the SOD1 G93A mouse model of familial ALS. The Journal of neuroscience : the official journal of the Society for Neuroscience 27:9201-9219.

Fisher AL, Caudy M (1998) Groucho proteins: transcriptional corepressors for specific subsets of DNA-binding transcription factors in vertebrates and invertebrates. Genes Dev 12:1931-1940.

Fitzmaurice PS, Shaw IC, Kleiner HE, Miller RT, Monks TJ, Lau SS, Mitchell JD, Lynch PG (1996) Evidence for DNA damage in amyotrophic lateral sclerosis. Muscle Nerve 19:797-798.

Forman MS, Trojanowski JQ, Lee VM (2007) TDP-43: a novel neurodegenerative proteinopathy. Curr Opin Neurobiol 17:548-555.

Freibaum BD, Chitta RK, High AA, Taylor JP (2010) Global analysis of TDP-43 interacting proteins reveals strong association with RNA splicing and translation machinery. J Proteome Res 9:1104-1120.

Fuentealba RA, Udan M, Bell S, Wegorzewska I, Shao J, Diamond MI, Weihl CC, Baloh RH (2010) Interaction with polyglutamine aggregates reveals a Q/N-rich domain in TDP-43. The Journal of biological chemistry 285:26304-26314.

Furukawa Y, Kaneko K, Matsumoto G, Kurosawa M, Nukina N (2009) Cross-seeding fibrillation of Q/N-rich proteins offers new pathomechanism of polyglutamine diseases. The Journal of neuroscience : the official journal of the Society for Neuroscience 29:5153-5162.

Furukawa Y, Kaneko K, Watanabe S, Yamanaka K, Nukina N (2011) A seeding reaction recapitulates intracellular formation of Sarkosyl-insoluble transactivation response element (TAR) DNA-binding protein-43 inclusions. The Journal of biological chemistry 286:18664-18672.

Gellera C, Colombrita C, Ticozzi N, Castellotti B, Bragato C, Ratti A, Taroni F, Silani V (2008) Identification of new ANG gene mutations in a large cohort of Italian patients with amyotrophic lateral sclerosis. Neurogenetics 9:33-40.

Gerritsen ME, Williams AJ, Neish AS, Moore S, Shi Y, Collins T (1997) CREB-binding protein/p300 are transcriptional coactivators of p65. Proc Natl Acad Sci U S A 94:2927-2932.

Geser F, Lee VM, Trojanowski JQ (2010) Amyotrophic lateral sclerosis and frontotemporal lobar degeneration: a spectrum of TDP-43 proteinopathies. Neuropathology : official journal of the Japanese Society of Neuropathology 30:103-112.

Geser F, Martinez-Lage M, Kwong LK, Lee VM, Trojanowski JQ (2009a) Amyotrophic lateral sclerosis, frontotemporal dementia and beyond: the TDP-43 diseases. Journal of neurology 256:1205-1214.

Geser F, Prvulovic D, O'Dwyer L, Hardiman O, Bede P, Bokde AL, Trojanowski JQ, Hampel HJ (2011) On the development of markers for pathological TDP-43 in amyotrophic lateral sclerosis with and without dementia. Prog Neurobiol.Sept 3, Epub Ahead of Print.

Geser F, Brandmeir NJ, Kwong LK, Martinez-Lage M, Elman L, McCluskey L, Xie SX, Lee VM, Trojanowski JQ (2008a) Evidence of multisystem disorder in whole-brain map of pathological TDP-43 in amyotrophic lateral sclerosis. Arch Neurol 65:636-641.

Geser F, Winton MJ, Kwong LK, Xu Y, Xie SX, Igaz LM, Garruto RM, Perl DP, Galasko D, Lee VM, Trojanowski JQ (2008b) Pathological TDP-43 in parkinsonism-dementia complex and amyotrophic lateral sclerosis of Guam. Acta neuropathologica 115:133-145.

Geser F, Martinez-Lage M, Robinson J, Uryu K, Neumann M, Brandmeir NJ, Xie SX, Kwong LK, Elman L, McCluskey L, Clark CM, Malunda J, Miller BL, Zimmerman EA, Qian J, Van Deerlin V, Grossman M, Lee VM, Trojanowski JQ (2009b) Clinical and pathological continuum of multisystem TDP-43 proteinopathies. Arch Neurol 66:180-189.

Ghosh M, Yang Y, Rothstein JD, Robinson MB (2011) Nuclear factor-kappaB contributes to neuron-dependent induction of glutamate transporter-1 expression in astrocytes. The Journal of neuroscience : the official journal of the Society for Neuroscience 31:9159-9169.

Ghosh S, May MJ, Kopp EB (1998) NF-kappa B and Rel proteins: evolutionarily conserved mediators of immune responses. Annu Rev Immunol 16:225-260.

Giordana MT, Piccinini M, Grifoni S, De Marco G, Vercellino M, Magistrello M, Pellerino A, Buccinna B, Lupino E, Rinaudo MT (2010) TDP-43 redistribution is an early event in sporadic amyotrophic lateral sclerosis. Brain Pathol 20:351-360.

Gitcho MA, Bigio EH, Mishra M, Johnson N, Weintraub S, Mesulam M, Rademakers R, Chakraverty S, Cruchaga C, Morris JC, Goate AM, Cairns NJ (2009) TARDBP 3'-UTR variant in autopsy-confirmed frontotemporal lobar degeneration with TDP-43 proteinopathy. Acta Neuropathol 118:633-645.

Gitcho MA, Baloh RH, Chakraverty S, Mayo K, Norton JB, Levitch D, Hatanpaa KJ, White CL, 3rd, Bigio EH, Caselli R, Baker M, Al-Lozi MT, Morris JC, Pestronk A, Rademakers R, Goate AM, Cairns NJ (2008) TDP-43 A315T mutation in familial motor neuron disease. Ann Neurol 63:535-538.

Gong YH, Parsadanian AS, Andreeva A, Snider WD, Elliott JL (2000) Restricted expression of G86R Cu/Zn superoxide dismutase in astrocytes results in astrocytosis but does not cause motoneuron degeneration. The Journal of neuroscience : the official journal of the Society for Neuroscience 20:660-665.

Gowing G, Philips T, Van Wijmeersch B, Audet JN, Dewil M, Van Den Bosch L, Billiau AD, Robberecht W, Julien JP (2008) Ablation of proliferating microglia does not affect motor neuron degeneration in amyotrophic lateral sclerosis caused by mutant superoxide dismutase. The Journal of neuroscience : the official journal of the Society for Neuroscience 28:10234-10244.

Grad LI, Guest WC, Yanai A, Pokrishevsky E, O'Neill MA, Gibbs E, Semenchenko V, Yousefi M, Wishart DS, Plotkin SS, Cashman NR (2011) Intermolecular transmission of superoxide dismutase 1 misfolding in living cells. Proceedings of the National Academy of Sciences of the United States of America 108:16398-16403.

Greenway MJ, Andersen PM, Russ C, Ennis S, Cashman S, Donaghy C, Patterson V, Swingler R, Kieran D, Prehn J, Morrison KE, Green A, Acharya KR, Brown RH, Jr., Hardiman O (2006) ANG mutations segregate with familial and 'sporadic' amyotrophic lateral sclerosis. Nature genetics 38:411-413.

Grilli M, Memo M (1999) Nuclear factor-kappaB/Rel proteins: a point of convergence of signalling pathways relevant in neuronal function and dysfunction. Biochem Pharmacol 57:1-7.

Grilli M, Pizzi M, Memo M, Spano P (1996) Neuroprotection by aspirin and sodium salicylate through blockade of NF-kappaB activation. Science 274:1383-1385.

Gros-Louis F, Soucy G, Lariviere R, Julien JP (2010) Intracerebroventricular infusion of monoclonal antibody or its derived Fab fragment against misfolded forms of SOD1 mutant delays mortality in a mouse model of ALS. J Neurochem. 113(5):1188-99

Gros-Louis F, Lariviere R, Gowing G, Laurent S, Camu W, Bouchard JP, Meininger V, Rouleau GA, Julien JP (2004) A frameshift deletion in peripherin gene associated with amyotrophic lateral sclerosis. J Biol Chem 279:45951-45956.

Gros-Louis F, Meijer IA, Hand CK, Dube MP, MacGregor DL, Seni MH, Devon RS, Hayden MR, Andermann F, Andermann E, Rouleau GA (2003) An ALS2 gene mutation causes hereditary spastic paraplegia in a Pakistani kindred. Ann Neurol 53:144-145.

Gros-Louis F, Kriz J, Kabashi E, McDearmid J, Millecamps S, Urushitani M, Lin L, Dion P, Zhu Q, Drapeau P, Julien JP, Rouleau GA (2008) Als2 mRNA splicing variants detected in KO mice rescue severe motor dysfunction phenotype in Als2 knock-down zebrafish. Hum Mol Genet 17:2691-2702.

Gros-Louis F, Andersen PM, Dupre N, Urushitani M, Dion P, Souchon F, D'Amour M, Camu W, Meininger V, Bouchard JP, Rouleau GA, Julien JP (2009) Chromogranin B P413L variant as risk factor and modifier of disease onset for amyotrophic lateral sclerosis. Proceedings of the National Academy of Sciences of the United States of America 106:21777-21782.

Grosskreutz J, Van Den Bosch L, Keller BU (2010) Calcium dysregulation in amyotrophic lateral sclerosis. Cell Calcium 47:165-174.

Grover A, Shandilya A, Punetha A, Bisaria VS, Sundar D (2010) Inhibition of the NEMO/IKKbeta association complex formation, a novel mechanism associated with the NF-kappaB activation suppression by Withania somnifera's key metabolite withaferin A. BMC Genomics 11 Suppl 4:S25.

Gu Z, Cain L, Werrbach-Perez K, Perez-Polo JR (2000) Differential alterations of NF-kappaB to oxidative stress in primary basal forebrain cultures. Int J Dev Neurosci 18:185-192.

Guerreiro RJ, Schymick JC, Crews C, Singleton A, Hardy J, Traynor BJ (2008) TDP-43 is not a common cause of sporadic amyotrophic lateral sclerosis. PLoS One 3:e2450.

Guerrini L, Blasi F, Denis-Donini S (1995) Synaptic activation of NF-kappa B by glutamate in cerebellar granule neurons in vitro. Proceedings of the National Academy of Sciences of the United States of America 92:9077-9081.

Guerrini L, Molteni A, Wirth T, Kistler B, Blasi F (1997) Glutamate-dependent activation of NF-kappaB during mouse cerebellum development. The Journal of neuroscience : the official journal of the Society for Neuroscience 17:6057-6063.

Guidato S, Tsai LH, Woodgett J, Miller CC (1996) Differential cellular phosphorylation of neurofilament heavy side-arms by glycogen synthase kinase-3 and cyclin-dependent kinase-5. Journal of neurochemistry 66:1698-1706.

Guo S, Yan J, Yang T, Yang X, Bezard E, Zhao B (2007) Protective effects of green tea polyphenols in the 6-OHDA rat model of Parkinson's disease through inhibition of ROS-NO pathway. Biol Psychiatry 62:1353-1362.

Guo W et al. (2011) An ALS-associated mutation affecting TDP-43 enhances protein aggregation, fibril formation and neurotoxicity. Nat Struct Mol Biol 18:822-830.

Gurney ME, Pu H, Chiu AY, Dal Canto MC, Polchow CY, Alexander DD, Caliendo J, Hentati A, Kwon YW, Deng HX, et al. (1994) Motor neuron degeneration in mice that express a human Cu,Zn superoxide dismutase mutation. Science 264:1772-1775.

Gveric D, Kaltschmidt C, Cuzner ML, Newcombe J (1998) Transcription factor NF-kappaB and inhibitor I kappaBalpha are localized in macrophages in active multiple sclerosis lesions. Journal of neuropathology and experimental neurology 57:168-178.

Hadano S, Benn SC, Kakuta S, Otomo A, Sudo K, Kunita R, Suzuki-Utsunomiya K, Mizumura H, Shefner JM, Cox GA, Iwakura Y, Brown RH, Jr., Ikeda JE (2006) Mice deficient in the Rab5 guanine nucleotide exchange factor ALS2/alsin exhibit age-dependent neurological deficits and altered endosome trafficking. Hum Mol Genet 15:233-250.

Hadano S et al. (2001) A gene encoding a putative GTPase regulator is mutated in familial amyotrophic lateral sclerosis 2. Nature genetics 29:166-173.

Hadian K, Krappmann D (2011) Signals from the nucleus: activation of NF-kappaB by cytosolic ATM in the DNA damage response. Sci Signal 4:pe2.

Hafezparast M et al. (2003) Mutations in dynein link motor neuron degeneration to defects in retrograde transport. Science 300:808-812.

Haidet-Phillips AM, Hester ME, Miranda CJ, Meyer K, Braun L, Frakes A, Song S, Likhite S, Murtha MJ, Foust KD, Rao M, Eagle A, Kammesheidt A, Christensen A, Mendell JR, Burghes AH, Kaspar BK (2011) Astrocytes from familial and sporadic ALS patients are toxic to motor neurons. Nat Biotechnol. 29:824-828

Harraz MM, Marden JJ, Zhou W, Zhang Y, Williams A, Sharov VS, Nelson K, Luo M, Paulson H, Schoneich C, Engelhardt JF (2008) SOD1 mutations disrupt redox-sensitive Rac regulation of NADPH oxidase in a familial ALS model. J Clin Invest 118:659-670.

Hasegawa M, Arai T, Akiyama H, Nonaka T, Mori H, Hashimoto T, Yamazaki M, Oyanagi K (2007) TDP-43 is deposited in the Guam parkinsonism-dementia complex brains. Brain : a journal of neurology 130:1386-1394.

Hasegawa M, Arai T, Nonaka T, Kametani F, Yoshida M, Hashizume Y, Beach TG, Buratti E, Baralle F, Morita M, Nakano I, Oda T, Tsuchiya K, Akiyama H (2008) Phosphorylated

TDP-43 in frontotemporal lobar degeneration and amyotrophic lateral sclerosis. Ann Neurol 64:60-70.

Hay DC, Kemp GD, Dargemont C, Hay RT (2001) Interaction between hnRNPA1 and IkappaBalpha is required for maximal activation of NF-kappaB-dependent transcription. Mol Cell Biol 21:3482-3490.

Henkel JS, Engelhardt JI, Siklos L, Simpson EP, Kim SH, Pan T, Goodman JC, Siddique T, Beers DR, Appel SH (2004) Presence of dendritic cells, MCP-1, and activated microglia/macrophages in amyotrophic lateral sclerosis spinal cord tissue. Annals of neurology 55:221-235.

Hensley K, Abdel-Moaty H, Hunter J, Mhatre M, Mou S, Nguyen K, Potapova T, Pye QN, Qi M, Rice H, Stewart C, Stroukoff K, West M (2006) Primary glia expressing the G93A-SOD1 mutation present a neuroinflammatory phenotype and provide a cellular system for studies of glial inflammation. J Neuroinflammation 3:2.

Hetz C, Thielen P, Matus S, Nassif M, Court F, Kiffin R, Martinez G, Cuervo AM, Brown RH, Glimcher LH (2009) XBP-1 deficiency in the nervous system protects against amyotrophic lateral sclerosis by increasing autophagy. Genes & development 23:2294-2306.

Hewitt C, Kirby J, Highley JR, Hartley JA, Hibberd R, Hollinger HC, Williams TL, Ince PG, McDermott CJ, Shaw PJ (2010) Novel FUS/TLS mutations and pathology in familial and sporadic amyotrophic lateral sclerosis. Arch Neurol 67:455-461.

Higashi S, Iseki E, Yamamoto R, Minegishi M, Hino H, Fujisawa K, Togo T, Katsuse O, Uchikado H, Furukawa Y, Kosaka K, Arai H (2007) Concurrence of TDP-43, tau and alpha-synuclein pathology in brains of Alzheimer's disease and dementia with Lewy bodies. Brain research 1184:284-294.

Hirano A, Nakano I, Kurland LT, Mulder DW, Holley PW, Saccomanno G (1984) Fine structural study of neurofibrillary changes in a family with amyotrophic lateral sclerosis. J Neuropathol Exp Neurol 43:471-480.

Hitomi J, Katayama T, Eguchi Y, Kudo T, Taniguchi M, Koyama Y, Manabe T, Yamagishi S, Bando Y, Imaizumi K, Tsujimoto Y, Tohyama M (2004) Involvement of caspase-4 in endoplasmic reticulum stress-induced apoptosis and Abeta-induced cell death. The Journal of cell biology 165:347-356.

Hodges JR, Davies RR, Xuereb JH, Casey B, Broe M, Bak TH, Kril JJ, Halliday GM (2004) Clinicopathological correlates in frontotemporal dementia. Ann Neurol 56:399-406.

Hortobagyi T, Troakes C, Nishimura AL, Vance C, van Swieten JC, Seelaar H, King A, Al-Sarraj S, Rogelj B, Shaw CE (2011) Optineurin inclusions occur in a minority of TDP-43 positive ALS and FTLD-TDP cases and are rarely observed in other neurodegenerative disorders. Acta neuropathologica 121:519-527.

Horvath RJ, Nutile-McMenemy N, Alkaitis MS, Deleo JA (2008) Differential migration, LPS-induced cytokine, chemokine, and NO expression in immortalized BV-2 and HAPI cell lines and primary microglial cultures. J Neurochem 107:557-569.

Houseweart MK, Cleveland DW (1999) Bcl-2 overexpression does not protect neurons from mutant neurofilament-mediated motor neuron degeneration. J Neurosci 19:6446-6456.

Hu JH, Zhang H, Wagey R, Krieger C, Pelech SL (2003) Protein kinase and protein phosphatase expression in amyotrophic lateral sclerosis spinal cord. J Neurochem 85:432-442.

Hu WH, Mo XM, Walters WM, Brambilla R, Bethea JR (2004) TNAP, a novel repressor of NF-kappaB-inducing kinase, suppresses NF-kappaB activation. The Journal of biological chemistry 279:35975-35983.

Hu WT, Josephs KA, Knopman DS, Boeve BF, Dickson DW, Petersen RC, Parisi JE (2008) Temporal lobar predominance of TDP-43 neuronal cytoplasmic inclusions in Alzheimer disease. Acta neuropathologica 116:215-220.

Huang L, Huang Y, Guo H (2009) Dominant expression of angiogenin in NeuN positive cells in the focal ischemic rat brain. J Neurol Sci 285:220-223.

Igaz LM, Kwong LK, Chen-Plotkin A, Winton MJ, Unger TL, Xu Y, Neumann M, Trojanowski JQ, Lee VM (2009) Expression of TDP-43 C-terminal Fragments in Vitro Recapitulates Pathological Features of TDP-43 Proteinopathies. J Biol Chem 284:8516-8524.

Igaz LM, Kwong LK, Lee EB, Chen-Plotkin A, Swanson E, Unger T, Malunda J, Xu Y, Winton MJ, Trojanowski JQ, Lee VM (2011) Dysregulation of the ALS-associated gene TDP-43 leads to neuronal death and degeneration in mice. J Clin Invest 121:726-738.

Ilieva H, Polymenidou M, Cleveland DW (2009) Non-cell autonomous toxicity in neurodegenerative disorders: ALS and beyond. The Journal of cell biology 187:761-772.

Imose M, Nagaki M, Kimura K, Takai S, Imao M, Naiki T, Osawa Y, Asano T, Hayashi H, Moriwaki H (2004) Leflunomide protects from T-cell-mediated liver injury in mice through inhibition of nuclear factor kappaB. Hepatology 40:1160-1169.

Ince P, Stout N, Shaw P, Slade J, Hunziker W, Heizmann CW, Baimbridge KG (1993) Parvalbumin and calbindin D-28k in the human motor system and in motor neuron disease. Neuropathol Appl Neurobiol 19:291-299.

Ince PG, Lowe J, Shaw PJ (1998a) Amyotrophic lateral sclerosis: current issues in classification, pathogenesis and molecular pathology. Neuropathol Appl Neurobiol 24:104-117.

Ince PG, Tomkins J, Slade JY, Thatcher NM, Shaw PJ (1998b) Amyotrophic lateral sclerosis associated with genetic abnormalities in the gene encoding Cu/Zn superoxide dismutase: molecular pathology of five new cases, and comparison with previous reports and 73 sporadic cases of ALS. Journal of neuropathology and experimental neurology 57:895-904.

Inukai Y, Nonaka T, Arai T, Yoshida M, Hashizume Y, Beach TG, Buratti E, Baralle FE, Akiyama H, Hisanaga S, Hasegawa M (2008) Abnormal phosphorylation of Ser409/410 of TDP-43 in FTLD-U and ALS. FEBS Lett 582:2899-2904.

Ito D, Seki M, Tsunoda Y, Uchiyama H, Suzuki N (2011) Nuclear transport impairment of amyotrophic lateral sclerosis-linked mutations in FUS/TLS. Annals of neurology 69:152-162.

Iyer AM, Zurolo E, Boer K, Baayen JC, Giangaspero F, Arcella A, Di Gennaro GC, Esposito V, Spliet WG, van Rijen PC, Troost D, Gorter JA, Aronica E (2010) Tissue plasminogen activator and urokinase plasminogen activator in human epileptogenic pathologies. Neuroscience 167:929-945.

Jaarsma D, Teuling E, Haasdijk ED, De Zeeuw CI, Hoogenraad CC (2008) Neuron-specific expression of mutant superoxide dismutase is sufficient to induce amyotrophic lateral sclerosis in transgenic mice. J Neurosci 28:2075-2088.

Jacomy H, Zhu Q, Couillard-Despres S, Beaulieu JM, Julien JP (1999) Disruption of type IV intermediate filament network in mice lacking the neurofilament medium and heavy subunits. J Neurochem 73:972-984.

Janssen-Heininger YM, Poynter ME, Baeuerle PA (2000) Recent advances towards understanding redox mechanisms in the activation of nuclear factor kappaB. Free Radic Biol Med 28:1317-1327.

Jiang YM, Yamamoto M, Kobayashi Y, Yoshihara T, Liang Y, Terao S, Takeuchi H, Ishigaki S, Katsuno M, Adachi H, Niwa J, Tanaka F, Doyu M, Yoshida M, Hashizume Y, Sobue G (2005) Gene expression profile of spinal motor neurons in sporadic amyotrophic lateral sclerosis. Annals of neurology 57:236-251.

Johnson BS, McCaffery JM, Lindquist S, Gitler AD (2008) A yeast TDP-43 proteinopathy model: Exploring the molecular determinants of TDP-43 aggregation and cellular toxicity. Proc Natl Acad Sci U S A 105:6439-6444.

Johnson BS, Snead D, Lee JJ, McCaffery JM, Shorter J, Gitler AD (2009) TDP-43 is intrinsically aggregation-prone, and amyotrophic lateral sclerosis-linked mutations accelerate aggregation and increase toxicity. The Journal of biological chemistry 284:20329-20339.

Johnson FO, Atchison WD (2009) The role of environmental mercury, lead and pesticide exposure in development of amyotrophic lateral sclerosis. Neurotoxicology 30:761-765.

Johnson JO et al. (2010) Exome sequencing reveals VCP mutations as a cause of familial ALS. Neuron 68:857-864.

Johnston JA, Dalton MJ, Gurney ME, Kopito RR (2000) Formation of high molecular weight complexes of mutant Cu, Zn-superoxide dismutase in a mouse model for familial amyotrophic lateral sclerosis. Proc Natl Acad Sci U S A 97:12571-12576.

Jonsson PA, Graffmo KS, Andersen PM, Brannstrom T, Lindberg M, Oliveberg M, Marklund SL (2006) Disulphide-reduced superoxide dismutase-1 in CNS of transgenic amyotrophic lateral sclerosis models. Brain 129:451-464.

Josephs KA, Ahmed Z, Katsuse O, Parisi JF, Boeve BF, Knopman DS, Petersen RC, Davies P, Duara R, Graff-Radford NR, Uitti RJ, Rademakers R, Adamson J, Baker M, Hutton ML, Dickson DW (2007) Neuropathologic features of frontotemporal lobar degeneration with ubiquitin-positive inclusions with progranulin gene (PGRN) mutations. Journal of neuropathology and experimental neurology 66:142-151.

Julien JP (2001) Amyotrophic lateral sclerosis. unfolding the toxicity of the misfolded. Cell 104:581-591.

Julien JP (2007) ALS: astrocytes move in as deadly neighbors. Nat Neurosci 10:535-537.

Jung M, Zhang Y, Lee S, Dritschilo A (1995) Correction of radiation sensitivity in ataxia telangiectasia cells by a truncated I kappa B-alpha. Science 268:1619-1621.

Kabashi E, Bercier V, Lissouba A, Liao M, Brustein E, Rouleau GA, Drapeau P (2011) FUS and TARDBP but not SOD1 interact in genetic models of amyotrophic lateral sclerosis. PLoS genetics 7:e1002214.

Kabashi E, Lin L, Tradewell ML, Dion PA, Bercier V, Bourgouin P, Rochefort D, Bel Hadj S, Durham HD, Vande Velde C, Rouleau GA, Drapeau P (2010) Gain and loss of function of ALS-related mutations of TARDBP (TDP-43) cause motor deficits in vivo. Hum Mol Genet 19:671-683.

Kabashi E, Valdmanis PN, Dion P, Spiegelman D, McConkey BJ, Vande Velde C, Bouchard JP, Lacomblez L, Pochigaeva K, Salachas F, Pradat PF, Camu W, Meininger V, Dupre N,

Rouleau GA (2008) TARDBP mutations in individuals with sporadic and familial amyotrophic lateral sclerosis. Nat Genet 40:572-574.

Kajino S, Suganuma M, Teranishi F, Takahashi N, Tetsuka T, Ohara H, Itoh M, Okamoto T (2000) Evidence that de novo protein synthesis is dispensable for anti-apoptotic effects of NF-kappaB. Oncogene 19:2233-2239.

Kaltschmidt B, Baeuerle PA, Kaltschmidt C (1993) Potential involvement of the transcription factor NF-kappa B in neurological disorders. Mol Aspects Med 14:171-190.

Kaltschmidt B, Sparna T, Kaltschmidt C (1999a) Activation of NF-kappa B by reactive oxygen intermediates in the nervous system. Antioxid Redox Signal 1:129-144.

Kaltschmidt B, Uherek M, Volk B, Baeuerle PA, Kaltschmidt C (1997) Transcription factor NF-kappaB is activated in primary neurons by amyloid beta peptides and in neurons surrounding early plaques from patients with Alzheimer disease. Proc Natl Acad Sci U S A 94:2642-2647.

Kaltschmidt B, Uherek M, Wellmann H, Volk B, Kaltschmidt C (1999b) Inhibition of NF-kappaB potentiates amyloid beta-mediated neuronal apoptosis. Proceedings of the National Academy of Sciences of the United States of America 96:9409-9414.

Kaltschmidt C, Kaltschmidt B, Baeuerle PA (1995) Stimulation of ionotropic glutamate receptors activates transcription factor NF-kappa B in primary neurons. Proceedings of the National Academy of Sciences of the United States of America 92:9618-9622.

Kaltschmidt C, Kaltschmidt B, Neumann H, Wekerle H, Baeuerle PA (1994) Constitutive NF-kappa B activity in neurons. Molecular and cellular biology 14:3981-3992.

Kane MD, Lipinski WJ, Callahan MJ, Bian F, Durham RA, Schwarz RD, Roher AE, Walker LC (2000) Evidence for seeding of beta -amyloid by intracerebral infusion of Alzheimer brain extracts in beta -amyloid precursor protein-transgenic mice. The Journal of neuroscience : the official journal of the Society for Neuroscience 20:3606-3611.

Kanekura K, Suzuki H, Aiso S, Matsuoka M (2009) ER stress and unfolded protein response in amyotrophic lateral sclerosis. Mol Neurobiol 39:81-89.

Karin M, Yamamoto Y, Wang QM (2004) The IKK NF-kappa B system: a treasure trove for drug development. Nat Rev Drug Discov 3:17-26.

Kasai T, Tokuda T, Ishigami N, Sasayama H, Foulds P, Mitchell DJ, Mann DM, Allsop D, Nakagawa M (2009) Increased TDP-43 protein in cerebrospinal fluid of patients with amyotrophic lateral sclerosis. Acta neuropathologica 117:55-62.

Kaufman RJ (2002) Orchestrating the unfolded protein response in health and disease. J Clin Invest 110:1389-1398.

Keller A, Nesvizhskii AI, Kolker E, Aebersold R (2002) Empirical statistical model to estimate the accuracy of peptide identifications made by MS/MS and database search. Anal Chem 74:5383-5392.

Keller AF, Gravel M, Kriz J (2009) Live imaging of amyotrophic lateral sclerosis pathogenesis: disease onset is characterized by marked induction of GFAP in Schwann cells. Glia 57:1130-1142.

Keller AF, Gravel M, Kriz J (2010) Treatment with minocycline after disease onset alters astrocyte reactivity and increases microgliosis in SOD1 mutant mice. Exp Neurol. 228(1):69-79

Kerr LD, Ransone LJ, Wamsley P, Schmitt MJ, Boyer TG, Zhou Q, Berk AJ, Verma IM (1993) Association between proto-oncoprotein Rel and TATA-binding protein mediates transcriptional activation by NF-kappa B. Nature 365:412-419.

Khaled AR, Butfiloski EJ, Sobel ES, Schiffenbauer J (1998) Use of phosphorothioate-modified oligodeoxynucleotides to inhibit NF-kappaB expression and lymphocyte function. Clin Immunol Immunopathol 86:170-179.

Kieran D, Hafezparast M, Bohnert S, Dick JR, Martin J, Schiavo G, Fisher EM, Greensmith L (2005) A mutation in dynein rescues axonal transport defects and extends the life span of ALS mice. The Journal of cell biology 169:561-567.

Kieran D, Sebastia J, Greenway MJ, King MA, Connaughton D, Concannon CG, Fenner B, Hardiman O, Prehn JH (2008) Control of motoneuron survival by angiogenin. The Journal of neuroscience : the official journal of the Society for Neuroscience 28:14056-14061.

King AE, Dickson TC, Blizzard CA, Foster SS, Chung RS, West AK, Chuah MI, Vickers JC (2007) Excitotoxicity mediated by non-NMDA receptors causes distal axonopathy in long-term cultured spinal motor neurons. Eur J Neurosci 26:2151-2159.

Kipnis J, Avidan H, Caspi RR, Schwartz M (2004) Dual effect of CD4+CD25+ regulatory T cells in neurodegeneration: a dialogue with microglia. Proceedings of the National Academy of Sciences of the United States of America 101 Suppl 2:14663-14669.

Kirby J, Halligan E, Baptista MJ, Allen S, Heath PR, Holden H, Barber SC, Loynes CA, Wood-Allum CA, Lunec J, Shaw PJ (2005) Mutant SOD1 alters the motor neuronal transcriptome: implications for familial ALS. Brain : a journal of neurology 128:1686-1706.

Kishimoto K, Liu S, Tsuji T, Olson KA, Hu GF (2005) Endogenous angiogenin in endothelial cells is a general requirement for cell proliferation and angiogenesis. Oncogene 24:445-456.

Kovacs GG, Murrell JR, Horvath S, Haraszti L, Majtenyi K, Molnar MJ, Budka H, Ghetti B, Spina S (2009) TARDBP variation associated with frontotemporal dementia, supranuclear gaze palsy, and chorea. Mov Disord 24:1843-1847.

Kraemer BC, Schuck T, Wheeler JM, Robinson LC, Trojanowski JQ, Lee VM, Schellenberg GD (2010) Loss of murine TDP-43 disrupts motor function and plays an essential role in embryogenesis. Acta Neuropathol. 119(4):409-19

Krecic AM, Swanson MS (1999) hnRNP complexes: composition, structure, and function. Curr Opin Cell Biol 11:363-371.

Kriz J, Zhu Q, Julien JP, Padjen AL (2000a) Electrophysiological properties of axons in mice lacking neurofilament subunit genes: disparity between conduction velocity and axon diameter in absence of NF-H. Brain Res 885:32-44.

Kriz J, Meier J, Julien JP, Padjen AL (2000b) Altered ionic conductances in axons of transgenic mouse expressing the human neurofilament heavy gene: A mouse model of amyotrophic lateral sclerosis. Exp Neurol 163:414-421.

Kuhle J, Lindberg RL, Regeniter A, Mehling M, Steck AJ, Kappos L, Czaplinski A (2009) Increased levels of inflammatory chemokines in amyotrophic lateral sclerosis. Eur J Neurol 16:771-774.

Kuhnlein P, Sperfeld AD, Vanmassenhove B, Van Deerlin V, Lee VM, Trojanowski JQ, Kretzschmar HA, Ludolph AC, Neumann M (2008) Two German kindreds with familial amyotrophic lateral sclerosis due to TARDBP mutations. Arch Neurol 65:1185-1189.

Kulka M, Fukuishi N, Metcalfe DD (2009) Human mast cells synthesize and release angiogenin, a member of the ribonuclease A (RNase A) superfamily. J Leukoc Biol 86:1217-1226.

Kwak S, Hideyama T, Yamashita T, Aizawa H (2010) AMPA receptor-mediated neuronal death in sporadic ALS. Neuropathology : official journal of the Japanese Society of Neuropathology 30:182-188.

Kwiatkowski TJ, Jr. et al. (2009) Mutations in the FUS/TLS gene on chromosome 16 cause familial amyotrophic lateral sclerosis. Science 323:1205-1208.

Lacomblez L, Bensimon G, Leigh PN, Guillet P, Meininger V (1996) Dose-ranging study of riluzole in amyotrophic lateral sclerosis. Amyotrophic Lateral Sclerosis/Riluzole Study Group II. Lancet 347:1425-1431.

Lagier-Tourenne C, Cleveland DW (2009) Rethinking ALS: the FUS about TDP-43. Cell 136:1001-1004.

Lagier-Tourenne C, Polymenidou M, Cleveland DW (2010) TDP-43 and FUS/TLS: emerging roles in RNA processing and neurodegeneration. Human molecular genetics 19:R46-64.

Laird FM, Farah MH, Ackerley S, Hoke A, Maragakis N, Rothstein JD, Griffin J, Price DL, Martin LJ, Wong PC (2008) Motor neuron disease occurring in a mutant dynactin mouse model is characterized by defects in vesicular trafficking. J Neurosci 28:1997-2005.

Lambrechts D et al. (2003) VEGF is a modifier of amyotrophic lateral sclerosis in mice and humans and protects motoneurons against ischemic death. Nat Genet 34:383-394.

LaMonte BH, Wallace KE, Holloway BA, Shelly SS, Ascano J, Tokito M, Van Winkle T, Howland DS, Holzbaur EL (2002) Disruption of dynein/dynactin inhibits axonal transport in motor neurons causing late-onset progressive degeneration. Neuron 34:715-727.

Lancet JE, Duong VH, Winton EF, Stuart RK, Burton M, Zhang S, Cubitt C, Blaskovich MA, Wright JJ, Sebti S, Sullivan DM (2011) A phase I clinical-pharmacodynamic study of the farnesyltransferase inhibitor tipifarnib in combination with the proteasome inhibitor bortezomib in advanced acute leukemias. Clin Cancer Res 17:1140-1146.

Landers JE, Leclerc AL, Shi L, Virkud A, Cho T, Maxwell MM, Henry AF, Polak M, Glass JD, Kwiatkowski TJ, Al-Chalabi A, Shaw CE, Leigh PN, Rodriguez-Leyza I, McKenna-Yasek D, Sapp PC, Brown RH, Jr. (2008) New VAPB deletion variant and exclusion of VAPB mutations in familial ALS. Neurology 70:1179-1185.

Lanson NA, Jr., Maltare A, King H, Smith R, Kim JH, Taylor JP, Lloyd TE, Pandey UB (2011) A Drosophila model of FUS-related neurodegeneration reveals genetic interaction between FUS and TDP-43. Human molecular genetics 20:2510-2523.

Lariviere RC, Julien JP (2004) Functions of intermediate filaments in neuronal development and disease. J Neurobiol 58:131-148.

Lariviere RC, Nguyen MD, Ribeiro-da-Silva A, Julien JP (2002) Reduced number of unmyelinated sensory axons in peripherin null mice. J Neurochem 81:525-532.

Lee JA, Liu L, Gao FB (2009) Autophagy defects contribute to neurodegeneration induced by dysfunctional ESCRT-III. Autophagy 5:1070-1072.

Lee MK, Marszalek JR, Cleveland DW (1994) A mutant neurofilament subunit causes massive, selective motor neuron death: implications for the pathogenesis of human motor neuron disease. Neuron 13:975-988.

Lefebvre S, Burglen L, Reboullet S, Clermont O, Burlet P, Viollet L, Benichou B, Cruaud C, Millasseau P, Zeviani M, et al. (1995) Identification and characterization of a spinal muscular atrophy-determining gene. Cell 80:155-165.

Lemmens R, Van Hoecke A, Hersmus N, Geelen V, D'Hollander I, Thijs V, Van Den Bosch L, Carmeliet P, Robberecht W (2007) Overexpression of mutant superoxide dismutase 1 causes a motor axonopathy in the zebrafish. Human molecular genetics 16:2359-2365.

Lemmens R, Race V, Hersmus N, Matthijs G, Van Den Bosch L, Van Damme P, Dubois B, Boonen S, Goris A, Robberecht W (2009) TDP-43 M311V mutation in familial amyotrophic lateral sclerosis. Journal of neurology, neurosurgery, and psychiatry 80:354-355.

Lerner-Natoli M, Montpied P, Rousset MC, Bockaert J, Rondouin G (2000) Sequential expression of surface antigens and transcription factor NFkappaB by hippocampal cells in excitotoxicity and experimental epilepsy. Epilepsy Res 41:141-154.

Letoha T, Somlai C, Takacs T, Szabolcs A, Jarmay K, Rakonczay Z, Jr., Hegyi P, Varga I, Kaszaki J, Krizbai I, Boros I, Duda E, Kusz E, Penke B (2005) A nuclear import inhibitory peptide ameliorates the severity of cholecystokinin-induced acute pancreatitis. World J Gastroenterol 11:990-999.

Levavasseur F, Zhu Q, Julien JP (1999) No requirement of alpha-internexin for nervous system development and for radial growth of axons. Brain Res Mol Brain Res 69:104-112.

Levites Y, Youdim MB, Maor G, Mandel S (2002) Attenuation of 6-hydroxydopamine (6-OHDA)-induced nuclear factor-kappaB (NF-kappaB) activation and cell death by tea extracts in neuronal cultures. Biochem Pharmacol 63:21-29.

Li Y, Ray P, Rao EJ, Shi C, Guo W, Chen X, Woodruff EA, 3rd, Fushimi K, Wu JY (2010) A Drosophila model for TDP-43 proteinopathy. Proc Natl Acad Sci U S A 107:3169-3174.

Lin YZ, Yao SY, Veach RA, Torgerson TR, Hawiger J (1995) Inhibition of nuclear translocation of transcription factor NF-kappa B by a synthetic peptide containing a cell membrane-permeable motif and nuclear localization sequence. The Journal of biological chemistry 270:14255-14258.

Ling SC, Albuquerque CP, Han JS, Lagier-Tourenne C, Tokunaga S, Zhou H, Cleveland DW (2010) ALS-associated mutations in TDP-43 increase its stability and promote TDP-43 complexes with FUS/TLS. Proc Natl Acad Sci U S A 107:13318-13323.

Lino MM, Schneider C, Caroni P (2002) Accumulation of SOD1 mutants in postnatal motoneurons does not cause motoneuron pathology or motoneuron disease. The Journal of neuroscience : the official journal of the Society for Neuroscience 22:4825-4832.

Liu-Yesucevitz L, Bilgutay A, Zhang YJ, Vanderweyde T, Citro A, Mehta T, Zaarur N, McKee A, Bowser R, Sherman M, Petrucelli L, Wolozin B (2010) Tar DNA binding protein-43 (TDP-43) associates with stress granules: analysis of cultured cells and pathological brain tissue. PloS one 5:e13250.

Liu J, Lillo C, Jonsson PA, Vande Velde C, Ward CM, Miller TM, Subramaniam JR, Rothstein JD, Marklund S, Andersen PM, Brannstrom T, Gredal O, Wong PC, Williams DS, Cleveland DW (2004) Toxicity of familial ALS-linked SOD1 mutants from selective recruitment to spinal mitochondria. Neuron 43:5-17.

Lobsiger CS, Boillee S, McAlonis-Downes M, Khan AM, Feltri ML, Yamanaka K, Cleveland DW (2009) Schwann cells expressing dismutase active mutant SOD1 unexpectedly slow disease progression in ALS mice. Proceedings of the National Academy of Sciences of the United States of America 106:4465-4470.

Lomen-Hoerth C, Murphy J, Langmore S, Kramer JH, Olney RK, Miller B (2003) Are amyotrophic lateral sclerosis patients cognitively normal? Neurology 60:1094-1097.

Lu CH, Kalmar B, Malaspina A, Greensmith L, Petzold A (2011) A method to solubilise protein aggregates for immunoassay quantification which overcomes the neurofilament "hook" effect. J Neurosci Methods 195:143-150.

Lubin FD, Ren Y, Xu X, Anderson AE (2007) Nuclear factor-kappa B regulates seizure threshold and gene transcription following convulsant stimulation. J Neurochem 103:1381-1395.

Mackenzie IR, Rademakers R, Neumann M (2010) TDP-43 and FUS in amyotrophic lateral sclerosis and frontotemporal dementia. Lancet neurology 9:995-1007.

Mackenzie IR, Baker M, Pickering-Brown S, Hsiung GY, Lindholm C, Dwosh E, Gass J, Cannon A, Rademakers R, Hutton M, Feldman HH (2006) The neuropathology of frontotemporal lobar degeneration caused by mutations in the progranulin gene. Brain : a journal of neurology 129:3081-3090.

Mackenzie IR, Bigio EH, Ince PG, Geser F, Neumann M, Cairns NJ, Kwong LK, Forman MS, Ravits J, Stewart H, Eisen A, McClusky L, Kretzschmar HA, Monoranu CM, Highley JR, Kirby J, Siddique T, Shaw PJ, Lee VM, Trojanowski JQ (2007) Pathological TDP-43 distinguishes sporadic amyotrophic lateral sclerosis from amyotrophic lateral sclerosis with SOD1 mutations. Ann Neurol 61:427-434.

Maekawa S, Leigh PN, King A, Jones E, Steele JC, Bodi I, Shaw CE, Hortobagyi T, Al-Sarraj S (2009) TDP-43 is consistently co-localized with ubiquitinated inclusions in sporadic and Guam amyotrophic lateral sclerosis but not in familial amyotrophic lateral sclerosis with and without SOD1 mutations. Neuropathology.

Mantovani S, Garbelli S, Pasini A, Alimonti D, Perotti C, Melazzini M, Bendotti C, Mora G (2009) Immune system alterations in sporadic amyotrophic lateral sclerosis patients suggest an ongoing neuroinflammatory process. J Neuroimmunol 210:73-79.

Marchetto MC, Muotri AR, Mu Y, Smith AM, Cezar GG, Gage FH (2008) Non-cell-autonomous effect of human SOD1 G37R astrocytes on motor neurons derived from human embryonic stem cells. Cell stem cell 3:649-657.

Marcora E, Kennedy MB (2010) The Huntington's disease mutation impairs Huntingtin's role in the transport of NF-kappaB from the synapse to the nucleus. Human molecular genetics 19:4373-4384.

Marsala M, Yaksh TL (1994) Transient spinal ischemia in the rat: characterization of behavioral and histopathological consequences as a function of the duration of aortic occlusion. J Cereb Blood Flow Metab 14:526-535.

Martin G, Bogdanowicz P, Domagala F, Ficheux H, Pujol JP (2003) Rhein inhibits interleukin-1 beta-induced activation of MEK/ERK pathway and DNA binding of NF-kappa B and AP-1 in chondrocytes cultured in hypoxia: a potential mechanism for its disease-modifying effect in osteoarthritis. Inflammation 27:233-246.

Martin N, Jaubert J, Gounon P, Salido E, Haase G, Szatanik M, Guenet JL (2002) A missense mutation in Tbce causes progressive motor neuronopathy in mice. Nat Genet 32:443-447.

Maruyama H et al. (2010) Mutations of optineurin in amyotrophic lateral sclerosis. Nature 465:223-226.

Mattiazzi M, D'Aurelio M, Gajewski CD, Martushova K, Kiaei M, Beal MF, Manfredi G (2002) Mutated human SOD1 causes dysfunction of oxidative phosphorylation in mitochondria of transgenic mice. The Journal of biological chemistry 277:29626-29633.

Matus S, Nassif M, Glimcher LH, Hetz C (2009) XBP-1 deficiency in the nervous system reveals a homeostatic switch to activate autophagy. Autophagy 5:1226-1228.

May MJ, D'Acquisto F, Madge LA, Glockner J, Pober JS, Ghosh S (2000) Selective inhibition of NF-kappaB activation by a peptide that blocks the interaction of NEMO with the IkappaB kinase complex. Science 289:1550-1554.

Maysinger D, Behrendt M, Lalancette-Hebert M, Kriz J (2007) Real-time imaging of astrocyte response to quantum dots: in vivo screening model system for biocompatibility of nanoparticles. Nano Lett 7:2513-2520.

McCluskey LF, Elman LB, Martinez-Lage M, Van Deerlin V, Yuan W, Clay D, Siderowf A, Trojanowski JQ (2009) Amyotrophic lateral sclerosis-plus syndrome with TAR DNA-binding protein-43 pathology. Arch Neurol 66:121-124.

McDonald KK, Aulas A, Destroismaisons L, Pickles S, Beleac E, Camu W, Rouleau GA, Vande Velde C (2011) TAR DNA-binding protein 43 (TDP-43) regulates stress granule dynamics via differential regulation of G3BP and TIA-1. Human molecular genetics 20:1400-1410.

McGuire V, Longstreth WT, Jr., Nelson LM, Koepsell TD, Checkoway H, Morgan MS, van Belle G (1997) Occupational exposures and amyotrophic lateral sclerosis. A population-based case-control study. Am J Epidemiol 145:1076-1088.

Meffert MK, Baltimore D (2005) Physiological functions for brain NF-kappaB. Trends Neurosci 28:37-43.

Meffert MK, Chang JM, Wiltgen BJ, Fanselow MS, Baltimore D (2003) NF-kappa B functions in synaptic signaling and behavior. Nat Neurosci 6:1072-1078.

Meier J, Couillard-Despres S, Jacomy H, Gravel C, Julien JP (1999) Extra neurofilament NF-L subunits rescue motor neuron disease caused by overexpression of the human NF-H gene in mice. J Neuropathol Exp Neurol 58:1099-1110.

Meissner M, Lopato S, Gotzmann J, Sauermann G, Barta A (2003) Proto-oncoprotein TLS/FUS is associated to the nuclear matrix and complexed with splicing factors PTB, SRm160, and SR proteins. Exp Cell Res 283:184-195.

Menzies FM, Cookson MR, Taylor RW, Turnbull DM, Chrzanowska-Lightowlers ZM, Dong L, Figlewicz DA, Shaw PJ (2002) Mitochondrial dysfunction in a cell culture model of familial amyotrophic lateral sclerosis. Brain : a journal of neurology 125:1522-1533.

Mercado PA, Ayala YM, Romano M, Buratti E, Baralle FE (2005) Depletion of TDP 43 overrides the need for exonic and intronic splicing enhancers in the human apoA-II gene. Nucleic Acids Res 33:6000-6010.

Mercurio F, Manning AM (1999) Multiple signals converging on NF-kappaB. Curr Opin Cell Biol 11:226-232.

Mercurio F, Zhu H, Murray BW, Shevchenko A, Bennett BL, Li J, Young DB, Barbosa M, Mann M, Manning A, Rao A (1997) IKK-1 and IKK-2: cytokine-activated IkappaB kinases essential for NF-kappaB activation. Science 278:860-866.

Mersiyanova IV, Perepelov AV, Polyakov AV, Sitnikov VF, Dadali EL, Oparin RB, Petrin AN, Evgrafov OV (2000) A new variant of Charcot-Marie-Tooth disease type 2 is probably the result of a mutation in the neurofilament-light gene. Am J Hum Genet 67:37-46.

Meyer-Luehmann M, Coomaraswamy J, Bolmont T, Kaeser S, Schaefer C, Kilger E, Neuenschwander A, Abramowski D, Frey P, Jaton AL, Vigouret JM, Paganetti P, Walsh DM, Mathews PM, Ghiso J, Staufenbiel M, Walker LC, Jucker M (2006) Exogenous induction of cerebral beta-amyloidogenesis is governed by agent and host. Science 313:1781-1784.

Migheli A, Pezzulo T, Attanasio A, Schiffer D (1993) Peripherin immunoreactive structures in amyotrophic lateral sclerosis. Lab Invest 68:185-191.

Migheli A, Piva R, Atzori C, Troost D, Schiffer D (1997) c-Jun, JNK/SAPK kinases and transcription factor NF-kappa B are selectively activated in astrocytes, but not motor neurons, in amyotrophic lateral sclerosis. J Neuropathol Exp Neurol 56:1314-1322.

Milanese M, Zappettini S, Onofri F, Musazzi L, Tardito D, Bonifacino T, Messa M, Racagni G, Usai C, Benfenati F, Popoli M, Bonanno G (2011) Abnormal exocytotic release of glutamate in a mouse model of amyotrophic lateral sclerosis. Journal of neurochemistry 116:1028-1042.

Millecamps S, Robertson J, Lariviere R, Mallet J, Julien JP (2006) Defective axonal transport of neurofilament proteins in neurons overexpressing peripherin. J Neurochem 98:926-938.

Millecamps S, Boillee S, Chabrol E, Camu W, Cazeneuve C, Salachas F, Pradat PF, Danel-Brunaud V, Vandenberghe N, Corcia P, Le Forestier N, Lacomblez L, Bruneteau G, Seilhean D, Brice A, Feingold J, Meininger V, LeGuern E (2011) Screening of OPTN in French familial amyotrophic lateral sclerosis. Neurobiol Aging 32:557 e511-553.

Mishra M, Paunesku T, Woloschak GE, Siddique T, Zhu LJ, Lin S, Greco K, Bigio EH (2007) Gene expression analysis of frontotemporal lobar degeneration of the motor neuron disease type with ubiquitinated inclusions. Acta neuropathologica 114:81-94.

Moenner M, Gusse M, Hatzi E, Badet J (1994) The widespread expression of angiogenin in different human cells suggests a biological function not only related to angiogenesis. Eur J Biochem 226:483-490.

Moisse K, Strong MJ (2006) Innate immunity in amyotrophic lateral sclerosis. Biochim Biophys Acta 1762:1083-1093.

Moisse K, Mepham J, Volkening K, Welch I, Hill T, Strong MJ (2009a) Cytosolic TDP-43 expression following axotomy is associated with caspase 3 activation in NFL-/- mice:

support for a role for TDP-43 in the physiological response to neuronal injury. Brain research 1296:176-186.

Moisse K, Volkening K, Leystra-Lantz C, Welch I, Hill T, Strong MJ (2009b) Divergent patterns of cytosolic TDP-43 and neuronal progranulin expression following axotomy: implications for TDP-43 in the physiological response to neuronal injury. Brain research 1249:202-211.

Moon DO, Kim MO, Lee JD, Choi YH, Kim GY (2010) Rosmarinic acid sensitizes cell death through suppression of TNF-alpha-induced NF-kappaB activation and ROS generation in human leukemia U937 cells. Cancer Lett 288:183-191.

Moore PA, Ruben SM, Rosen CA (1993) Conservation of transcriptional activation functions of the NF-kappa B p50 and p65 subunits in mammalian cells and Saccharomyces cerevisiae. Mol Cell Biol 13:1666-1674.

Moreau C, Devos D, Brunaud-Danel V, Defebvre L, Perez T, Destee A, Tonnel AB, Lassalle P, Just N (2006) Paradoxical response of VEGF expression to hypoxia in CSF of patients with ALS. J Neurol Neurosurg Psychiatry 77:255-257.

Mori A, Lehmann S, O'Kelly J, Kumagai T, Desmond JC, Pervan M, McBride WH, Kizaki M, Koeffler HP (2006) Capsaicin, a component of red peppers, inhibits the growth of androgen-independent, p53 mutant prostate cancer cells. Cancer Res 66:3222-3229.

Morishita R, Sugimoto T, Aoki M, Kida I, Tomita N, Moriguchi A, Maeda K, Sawa Y, Kaneda Y, Higaki J, Ogihara T (1997) In vivo transfection of cis element "decoy" against nuclear factor-kappaB binding site prevents myocardial infarction. Nat Med 3:894-899.

Moroianu J, Riordan JF (1994) Nuclear translocation of angiogenin in proliferating endothelial cells is essential to its angiogenic activity. Proceedings of the National Academy of Sciences of the United States of America 91:1677-1681.

Mougeot JL, Li Z, Price AE, Wright FA, Brooks BR (2011) Microarray analysis of peripheral blood lymphocytes from ALS patients and the SAFE detection of the KEGG ALS pathway. BMC Med Genomics 4:74.

Murray LM, Talbot K, Gillingwater TH (2010) Review: neuromuscular synaptic vulnerability in motor neurone disease: amyotrophic lateral sclerosis and spinal muscular atrophy. Neuropathol Appl Neurobiol 36:133-156.

Murray ME, Dejesus-Hernandez M, Rutherford NJ, Baker M, Duara R, Graff-Radford NR, Wszolek ZK, Ferman TJ, Josephs KA, Boylan KB, Rademakers R, Dickson DW (2011) Clinical and neuropathologic heterogeneity of c9FTD/ALS associated with hexanucleotide repeat expansion in C9ORF72. Acta neuropathologica. 122(6):673-90.

Naar AM, Beaurang PA, Zhou S, Abraham S, Solomon W, Tjian R (1999) Composite co-activator ARC mediates chromatin-directed transcriptional activation. Nature 398:828-832.

Nagai M, Re DB, Nagata T, Chalazonitis A, Jessell TM, Wichterle H, Przedborski S (2007) Astrocytes expressing ALS-linked mutated SOD1 release factors selectively toxic to motor neurons. Nat Neurosci 10:615-622.

Nakashima-Yasuda H et al. (2007) Co-morbidity of TDP-43 proteinopathy in Lewy body related diseases. Acta neuropathologica 114:221-229.

Naor S, Keren Z, Bronshtein T, Goren E, Machluf M, Melamed D (2009) Development of ALS-like disease in SOD-1 mice deficient of B lymphocytes. J Neurol 256:1228-1235.

Nardo G, Pozzi S, Pignataro M, Lauranzano E, Spano G, Garbelli S, Mantovani S, Marinou K, Papetti L, Monteforte M, Torri V, Paris L, Bazzoni G, Lunetta C, Corbo M, Mora G, Bendotti C, Bonetto V (2011) Amyotrophic lateral sclerosis multiprotein biomarkers in peripheral blood mononuclear cells. PloS one 6:e25545.

Neumann M, Rademakers R, Roeber S, Baker M, Kretzschmar HA, Mackenzie IR (2009a) A new subtype of frontotemporal lobar degeneration with FUS pathology. Brain : a journal of neurology 132:2922-2931.

Neumann M, Kwong LK, Lee EB, Kremmer E, Flatley A, Xu Y, Forman MS, Troost D, Kretzschmar HA, Trojanowski JQ, Lee VM (2009b) Phosphorylation of S409/410 of TDP-43 is a consistent feature in all sporadic and familial forms of TDP-43 proteinopathies. Acta neuropathologica 117:137-149.

Neumann M, Sampathu DM, Kwong LK, Truax AC, Micsenyi MC, Chou TT, Bruce J, Schuck T, Grossman M, Clark CM, McCluskey LF, Miller BL, Masliah E, Mackenzie IR, Feldman H, Feiden W, Kretzschmar HA, Trojanowski JQ, Lee VM (2006) Ubiquitinated TDP-43 in frontotemporal lobar degeneration and amyotrophic lateral sclerosis. Science 314:130-133.

Nguyen MD, Lariviere RC, Julien JP (2001) Deregulation of Cdk5 in a mouse model of ALS: toxicity alleviated by perikaryal neurofilament inclusions. Neuron 30:135-147.

Nishimura AL, Mitne-Neto M, Silva HC, Richieri-Costa A, Middleton S, Cascio D, Kok F, Oliveira JR, Gillingwater T, Webb J, Skehel P, Zatz M (2004) A mutation in the vesicle-trafficking protein VAPB causes late-onset spinal muscular atrophy and amyotrophic lateral sclerosis. American journal of human genetics 75:822-831.

Nonaka T, Kametani F, Arai T, Akiyama H, Hasegawa M (2009) Truncation and pathogenic mutations facilitate the formation of intracellular aggregates of TDP-43. Human molecular genetics 18:3353-3364.

Noto YI, Shibuya K, Sato Y, Kanai K, Misawa S, Sawai S, Mori M, Uchiyama T, Isose S, Nasu S, Sekiguchi Y, Fujimaki Y, Kasai T, Tokuda T, Nakagawa M, Kuwabara S (2010) Elevated CSF TDP-43 levels in amyotrophic lateral sclerosis: Specificity, sensitivity, and a possible prognostic value. Amyotroph Lateral Scler. 12(2):140-3

O'Neill LA, Kaltschmidt C (1997) NF-kappa B: a crucial transcription factor for glial and neuronal cell function. Trends Neurosci 20:252-258.

Oh JH, Lee TJ, Park JW, Kwon TK (2008) Withaferin A inhibits iNOS expression and nitric oxide production by Akt inactivation and down-regulating LPS-induced activity of NF-kappaB in RAW 264.7 cells. Eur J Pharmacol 599:11-17.

Okamoto K, Hirai S, Amari M, Watanabe M, Sakurai A (1993) Bunina bodies in amyotrophic lateral sclerosis immunostained with rabbit anti-cystatin C serum. Neuroscience letters 162:125-128.

Okamoto T, Sakurada S, Yang JP, Merin JP (1997) Regulation of NF-kappa B and disease control: identification of a novel serine kinase and thioredoxin as effectors for signal transduction pathway for NF-kappa B activation. Curr Top Cell Regul 35:149-161.

Oosthuyse B et al. (2001) Deletion of the hypoxia-response element in the vascular endothelial growth factor promoter causes motor neuron degeneration. Nat Genet 28:131-138.

Ou SH, Wu F, Harrich D, Garcia-Martinez LF, Gaynor RB (1995) Cloning and characterization of a novel cellular protein, TDP-43, that binds to human immunodeficiency virus type 1 TAR DNA sequence motifs. J Virol 69:3584-3596.

Pahl HL (1999) Activators and target genes of Rel/NF-kappaB transcription factors. Oncogene 18:6853-6866.

Park RM, Schulte PA, Bowman JD, Walker JT, Bondy SC, Yost MG, Touchstone JA, Dosemeci M (2005) Potential occupational risks for neurodegenerative diseases. Am J Ind Med 48:63-77.

Park SH, Kang JS, Yoon YD, Lee K, Kim KJ, Lee KH, Lee CW, Moon EY, Han SB, Kim BH, Kim HM, Park SK (2010) Glabridin inhibits lipopolysaccharide-induced activation of a microglial cell line, BV-2, by blocking NF-kappaB and AP-1. Phytother Res 24 Suppl 1:S29-34.

Parkhurst SM (1998) Groucho: making its Marx as a transcriptional co-repressor. Trends Genet 14:130-132.

Parkinson N, Ince PG, Smith MO, Highley R, Skibinski G, Andersen PM, Morrison KE, Pall HS, Hardiman O, Collinge J, Shaw PJ, Fisher EM (2006) ALS phenotypes with mutations in CHMP2B (charged multivesicular body protein 2B). Neurology 67:1074-1077.

Pasinelli P, Belford ME, Lennon N, Bacskai BJ, Hyman BT, Trotti D, Brown RH, Jr. (2004) Amyotrophic lateral sclerosis-associated SOD1 mutant proteins bind and aggregate with Bcl-2 in spinal cord mitochondria. Neuron 43:19-30.

Perkins ND (2000) The Rel/NF-kappa B family: friend and foe. Trends Biochem Sci 25:434-440.

Perkins ND, Felzien LK, Betts JC, Leung K, Beach DH, Nabel GJ (1997) Regulation of NF-kappaB by cyclin-dependent kinases associated with the p300 coactivator. Science 275:523-527.

Pesiridis GS, Tripathy K, Tanik S, Trojanowski JQ, Lee VM (2011) A "two-hit" hypothesis for inclusion formation by carboxyl-terminal fragments of TDP-43 protein linked to RNA depletion and impaired microtubule-dependent transport. The Journal of biological chemistry 286:18845-18855.

Phillips JB, Williams AJ, Adams J, Elliott PJ, Tortella FC (2000) Proteasome inhibitor PS519 reduces infarction and attenuates leukocyte infiltration in a rat model of focal cerebral ischemia. Stroke 31:1686-1693.

Piao YS, Wakabayashi K, Kakita A, Yamada M, Hayashi S, Morita T, Ikuta F, Oyanagi K, Takahashi H (2003) Neuropathology with clinical correlations of sporadic amyotrophic lateral sclerosis: 102 autopsy cases examined between 1962 and 2000. Brain Pathol 13:10-22.

Pizzi M, Sarnico I, Boroni F, Benetti A, Benarese M, Spano PF (2005) Inhibition of IkappaBalpha phosphorylation prevents glutamate-induced NF-kappaB activation and neuronal cell death. Acta Neurochir Suppl 93:59-63.

Polymenidou M, Cleveland DW (2011) The Seeds of Neurodegeneration: Prion-like Spreading in ALS. Cell 147:498-508.

Polymenidou M, Lagier-Tourenne C, Hutt KR, Huelga SC, Moran J, Liang TY, Ling SC, Sun E, Wancewicz E, Mazur C, Kordasiewicz H, Sedaghat Y, Donohue JP, Shiue L, Bennett CF, Yeo GW, Cleveland DW (2011) Long pre-mRNA depletion and RNA missplicing contribute to neuronal vulnerability from loss of TDP-43. Nat Neurosci 14:459-468.

Pramatarova A, Laganiere J, Roussel J, Brisebois K, Rouleau GA (2001) Neuron-specific expression of mutant superoxide dismutase 1 in transgenic mice does not lead to motor

impairment. The Journal of neuroscience : the official journal of the Society for Neuroscience 21:3369-3374.

Price DL, Porter KR (1972) The response of ventral horn neurons to axonal transection. The Journal of cell biology 53:24-37.

Prut L, Abramowski D, Krucker T, Levy CL, Roberts AJ, Staufenbiel M, Wiessner C (2007) Aged APP23 mice show a delay in switching to the use of a strategy in the Barnes maze. Behav Brain Res 179:107-110.

Puls I, Jonnakuty C, LaMonte BH, Holzbaur EL, Tokito M, Mann E, Floeter MK, Bidus K, Drayna D, Oh SJ, Brown RH, Jr., Ludlow CL, Fischbeck KH (2003) Mutant dynactin in motor neuron disease. Nat Genet 33:455-456.

Pun S, Santos AF, Saxena S, Xu L, Caroni P (2006) Selective vulnerability and pruning of phasic motoneuron axons in motoneuron disease alleviated by CNTF. Nature neuroscience 9:408-419.

Rakhit R, Robertson J, Vande Velde C, Horne P, Ruth DM, Griffin J, Cleveland DW, Cashman NR, Chakrabartty A (2007) An immunological epitope selective for pathological monomer-misfolded SOD1 in ALS. Nat Med 13:754-759.

Rao MV, Houseweart MK, Williamson TL, Crawford TO, Folmer J, Cleveland DW (1998) Neurofilament-dependent radial growth of motor axons and axonal organization of neurofilaments does not require the neurofilament heavy subunit (NF-H) or its phosphorylation. J Cell Biol 143:171-181.

Rao SD, Weiss JH (2004) Excitotoxic and oxidative cross-talk between motor neurons and glia in ALS pathogenesis. Trends in neurosciences 27:17-23.

Raoul C, Estevez AG, Nishimune H, Cleveland DW, deLapeyriere O, Henderson CE, Haase G, Pettmann B (2002) Motoneuron death triggered by a specific pathway downstream of Fas. potentiation by ALS-linked SOD1 mutations. Neuron 35:1067-1083.

Ratnaparkhi A, Lawless GM, Schweizer FE, Golshani P, Jackson GR (2008) A Drosophila model of ALS: human ALS-associated mutation in VAP33A suggests a dominant negative mechanism. PloS one 3:e2334.

Ravati A, Ahlemeyer B, Becker A, Klumpp S, Krieglstein J (2001) Preconditioning-induced neuroprotection is mediated by reactive oxygen species and activation of the transcription factor nuclear factor-kappaB. J Neurochem 78:909-919.

Ravizza T, Boer K, Redeker S, Spliet WG, van Rijen PC, Troost D, Vezzani A, Aronica E (2006) The IL-1beta system in epilepsy-associated malformations of cortical development. Neurobiology of disease 24:128-143.

Reaume AG, Elliott JL, Hoffman EK, Kowall NW, Ferrante RJ, Siwek DF, Wilcox HM, Flood DG, Beal MF, Brown RH, Jr., Scott RW, Snider WD (1996) Motor neurons in Cu/Zn superoxide dismutase-deficient mice develop normally but exhibit enhanced cell death after axonal injury. Nat Genet 13:43-47.

Regnier CH, Song HY, Gao X, Goeddel DV, Cao Z, Rothe M (1997) Identification and characterization of an IkappaB kinase. Cell 90:373-383.

Reid E, Kloos M, Ashley-Koch A, Hughes L, Bevan S, Svenson IK, Graham FL, Gaskell PC, Dearlove A, Pericak-Vance MA, Rubinsztein DC, Marchuk DA (2002) A kinesin heavy chain (KIF5A) mutation in hereditary spastic paraplegia (SPG10). Am J Hum Genet 71:1189-1194.

Renton AE et al. (2011) A Hexanucleotide Repeat Expansion in C9ORF72 Is the Cause of Chromosome 9p21-Linked ALS-FTD. Neuron 72:257-268.

Robertson J, Beaulieu JM, Doroudchi MM, Durham HD, Julien JP, Mushynski WE (2001) Apoptotic death of neurons exhibiting peripherin aggregates is mediated by the proinflammatory cytokine tumor necrosis factor-alpha. J Cell Biol 155:217-226.

Robertson J, Doroudchi MM, Nguyen MD, Durham HD, Strong MJ, Shaw G, Julien JP, Mushynski WE (2003) A neurotoxic peripherin splice variant in a mouse model of ALS. J Cell Biol 160:939-949.

Rohn TT (2008) Caspase-cleaved TAR DNA-binding protein-43 is a major pathological finding in Alzheimer's disease. Brain Res 1228:189-198.

Rollinson S, Snowden JS, Neary D, Morrison KE, Mann DM, Pickering-Brown SM (2007) TDP-43 gene analysis in frontotemporal lobar degeneration. Neuroscience letters 419:1-4.

Rong Y, Baudry M (1996) Seizure activity results in a rapid induction of nuclear factor-kappa B in adult but not juvenile rat limbic structures. Journal of neurochemistry 67:662-668.

Rosen DR, Siddique T, Patterson D, Figlewicz DA, Sapp P, Hentati A, Donaldson D, Goto J, O'Regan JP, Deng HX, et al. (1993) Mutations in Cu/Zn superoxide dismutase gene are associated with familial amyotrophic lateral sclerosis. Nature 362:59-62.

Rothstein JD, Tsai G, Kuncl RW, Clawson L, Cornblath DR, Drachman DB, Pestronk A, Stauch BL, Coyle JT (1990) Abnormal excitatory amino acid metabolism in amyotrophic lateral sclerosis. Annals of neurology 28:18-25.

Rutherford NJ et al. (2008) Novel mutations in TARDBP (TDP-43) in patients with familial amyotrophic lateral sclerosis. PLoS Genet 4:e1000193.

Sampathu DM, Neumann M, Kwong LK, Chou TT, Micsenyi M, Truax A, Bruce J, Grossman M, Trojanowski JQ, Lee VM (2006) Pathological heterogeneity of frontotemporal lobar degeneration with ubiquitin-positive inclusions delineated by ubiquitin immunohistochemistry and novel monoclonal antibodies. The American journal of pathology 169:1343-1352.

Sanelli T, Xiao S, Horne P, Bilbao J, Zinman L, Robertson J (2007) Evidence that TDP-43 is not the major ubiquitinated target within the pathological inclusions of amyotrophic lateral sclerosis. Journal of neuropathology and experimental neurology 66:1147-1153.

Sarlette A, Krampfl K, Grothe C, Neuhoff N, Dengler R, Petri S (2008) Nuclear erythroid 2-related factor 2-antioxidative response element signaling pathway in motor cortex and spinal cord in amyotrophic lateral sclerosis. Journal of neuropathology and experimental neurology 67:1055-1062.

Sarnico I, Lanzillotta A, Boroni F, Benarese M, Alghisi M, Schwaninger M, Inta I, Battistin L, Spano P, Pizzi M (2009) NF-kappaB p50/RelA and c-Rel-containing dimers: opposite regulators of neuron vulnerability to ischaemia. J Neurochem 108:475-485.

Sasaki S, Iwata M (2007) Mitochondrial alterations in the spinal cord of patients with sporadic amyotrophic lateral sclerosis. Journal of neuropathology and experimental neurology 66:10-16.

Sathasivam S, Shaw PJ (2005) Apoptosis in amyotrophic lateral sclerosis--what is the evidence? Lancet neurology 4:500-509.

Sathasivam S, Grierson AJ, Shaw PJ (2005) Characterization of the caspase cascade in a cell culture model of SOD1-related familial amyotrophic lateral sclerosis: expression, activation and therapeutic effects of inhibition. Neuropathol Appl Neurobiol 31:467-485.

Savedia S, Kiernan JA (1994) Increased production of ubiquitin mRNA in motor neurons after axotomy. Neuropathol Appl Neurobiol 20:577-586.

Saxena S, Cabuy E, Caroni P (2009) A role for motoneuron subtype-selective ER stress in disease manifestations of FALS mice. Nature neuroscience 12:627-636.

Scarmeas N, Shih T, Stern Y, Ottman R, Rowland LP (2002) Premorbid weight, body mass, and varsity athletics in ALS. Neurology 59:773-775.

Scheidereit C (2006) IkappaB kinase complexes: gateways to NF-kappaB activation and transcription. Oncogene 25:6685-6705.

Schmidt S, Kwee LC, Allen KD, Oddone EZ (2010) Association of ALS with head injury, cigarette smoking and APOE genotypes. J Neurol Sci 291:22-29.

Schmitz ML, Baeuerle PA (1991) The p65 subunit is responsible for the strong transcription activating potential of NF-kappa B. EMBO J 10:3805-3817.

Schmitz ML, dos Santos Silva MA, Baeuerle PA (1995a) Transactivation domain 2 (TA2) of p65 NF-kappa B. Similarity to TA1 and phorbol ester-stimulated activity and phosphorylation in intact cells. J Biol Chem 270:15576-15584.

Schmitz ML, Stelzer G, Altmann H, Meisterernst M, Baeuerle PA (1995b) Interaction of the COOH-terminal transactivation domain of p65 NF-kappa B with TATA-binding protein, transcription factor IIB, and coactivators. J Biol Chem 270:7219-7226.

Schroer TA (2004) Dynactin. Annu Rev Cell Dev Biol 20:759-779.

Schwab C, Arai T, Hasegawa M, Yu S, McGeer PL (2008) Colocalization of transactivation-responsive DNA-binding protein 43 and huntingtin in inclusions of Huntington disease. Journal of neuropathology and experimental neurology 67:1159-1165.

Seeley WW (2008) Selective functional, regional, and neuronal vulnerability in frontotemporal dementia. Curr Opin Neurol 21:701-707.

Sephton CF, Good SK, Atkin S, Dewey CM, Mayer P, 3rd, Herz J, Yu G (2010) TDP-43 is a developmentally regulated protein essential for early embryonic development. J Biol Chem 285:6826-6834.

Sephton CF, Cenik C, Kucukural A, Dammer EB, Cenik B, Han Y, Dewey CM, Roth FP, Herz J, Peng J, Moore MJ, Yu G (2011) Identification of neuronal RNA targets of TDP-43-containing ribonucleoprotein complexes. The Journal of biological chemistry 286:1204-1215.

Seyfried NT, Gozal YM, Dammer EB, Xia Q, Duong DM, Cheng D, Lah JJ, Levey AI, Peng J (2010) Multiplex SILAC analysis of a cellular TDP-43 proteinopathy model reveals protein inclusions associated with SUMOylation and diverse polyubiquitin chains. Mol Cell Proteomics 9:705-718.

Shan X, Chiang PM, Price DL, Wong PC (2010) Altered distributions of Gemini of coiled bodies and mitochondria in motor neurons of TDP-43 transgenic mice. Proceedings of the National Academy of Sciences of the United States of America 107:16325-16330.

Shaw PJ, Eggett CJ (2000) Molecular factors underlying selective vulnerability of motor neurons to neurodegeneration in amyotrophic lateral sclerosis. Journal of neurology 247 Suppl 1:I17-27.

Shaw PJ, Ince PG, Falkous G, Mantle D (1995a) Oxidative damage to protein in sporadic motor neuron disease spinal cord. Annals of neurology 38:691-695.

Shaw PJ, Forrest V, Ince PG, Richardson JP, Wastell HJ (1995b) CSF and plasma amino acid levels in motor neuron disease: elevation of CSF glutamate in a subset of patients. Neurodegeneration 4:209-216.

Sheppard KA, Phelps KM, Williams AJ, Thanos D, Glass CK, Rosenfeld MG, Gerritsen ME, Collins T (1998) Nuclear integration of glucocorticoid receptor and nuclear factor-kappaB signaling by CREB-binding protein and steroid receptor coactivator-1. The Journal of biological chemistry 273:29291-29294.

Shi X, Dong Z, Huang C, Ma W, Liu K, Ye J, Chen F, Leonard SS, Ding M, Castranova V, Vallyathan V (1999) The role of hydroxyl radical as a messenger in the activation of nuclear transcription factor NF-kappaB. Mol Cell Biochem 194:63-70.

Shiama N (1997) The p300/CBP family: integrating signals with transcription factors and chromatin. Trends Cell Biol 7:230-236.

Shibata N, Nagai R, Uchida K, Horiuchi S, Yamada S, Hirano A, Kawaguchi M, Yamamoto T, Sasaki S, Kobayashi M (2001) Morphological evidence for lipid peroxidation and protein glycoxidation in spinal cords from sporadic amyotrophic lateral sclerosis patients. Brain research 917:97-104.

Shibata N, Hirano A, Kobayashi M, Sasaki S, Kato T, Matsumoto S, Shiozawa Z, Komori T, Ikemoto A, Umahara T, et al. (1994) Cu/Zn superoxide dismutase-like immunoreactivity in Lewy body-like inclusions of sporadic amyotrophic lateral sclerosis. Neuroscience letters 179:149-152.

Shishodia S, Aggarwal BB (2004) Guggulsterone inhibits NF-kappaB and IkappaBalpha kinase activation, suppresses expression of anti-apoptotic gene products, and enhances apoptosis. The Journal of biological chemistry 279:47148-47158.

Simpson EP, Henry YK, Henkel JS, Smith RG, Appel SH (2004) Increased lipid peroxidation in sera of ALS patients: a potential biomarker of disease burden. Neurology 62:1758-1765.

Singh NP, Nagarkatti M, Nagarkatti PS (2007) Role of dioxin response element and nuclear factor-kappaB motifs in 2,3,7,8-tetrachlorodibenzo-p-dioxin-mediated regulation of Fas and Fas ligand expression. Mol Pharmacol 71:145-157.

Singh S, Aggarwal BB (1995) Activation of transcription factor NF-kappa B is suppressed by curcumin (diferuloylmethane) [corrected]. The Journal of biological chemistry 270:24995-25000.

Skehel PA, Martin KC, Kandel ER, Bartsch D (1995) A VAMP-binding protein from Aplysia required for neurotransmitter release. Science 269:1580-1583.

Smith RG, Henry YK, Mattson MP, Appel SH (1998) Presence of 4-hydroxynonenal in cerebrospinal fluid of patients with sporadic amyotrophic lateral sclerosis. Annals of neurology 44:696-699.

Sobue G, Hashizume Y, Yasuda T, Mukai E, Kumagai T, Mitsuma T, Trojanowski JQ (1990) Phosphorylated high molecular weight neurofilament protein in lower motor neurons in amyotrophic lateral sclerosis and other neurodegenerative diseases involving ventral horn cells. Acta neuropathologica 79:402-408.

Song XY, Torphy TJ, Griswold DE, Shealy D (2002) Coming of age: anti-cytokine therapies. Mol Interv 2:36-46.

Sreedharan J, Blair IP, Tripathi VB, Hu X, Vance C, Rogelj B, Ackerley S, Durnall JC, Williams KL, Buratti E, Baralle F, de Belleroche J, Mitchell JD, Leigh PN, Al-Chalabi A, Miller CC, Nicholson G, Shaw CE (2008) TDP-43 mutations in familial and sporadic amyotrophic lateral sclerosis. Science 319:1668-1672.

Sta M, Sylva-Steenland RM, Casula M, de Jong JM, Troost D, Aronica E, Baas F (2011) Innate and adaptive immunity in amyotrophic lateral sclerosis: evidence of complement activation. Neurobiology of disease 42:211-220.

Stallings NR, Puttaparthi K, Luther CM, Burns DK, Elliott JL (2010) Progressive motor weakness in transgenic mice expressing human TDP-43. Neurobiol Dis 40:404-414.

Steele JC, McGeer PL (2008) The ALS/PDC syndrome of Guam and the cycad hypothesis. Neurology 70:1984-1990.

Sterneck E, Kaplan DR, Johnson PF (1996) Interleukin-6 induces expression of peripherin and cooperates with Trk receptor signaling to promote neuronal differentiation in PC12 cells. J Neurochem 67:1365-1374.

Straube-West K, Loomis PA, Opal P, Goldman RD (1996) Alterations in neural intermediate filament organization: functional implications and the induction of pathological changes related to motor neuron disease. J Cell Sci 109 (Pt 9):2319-2329.

Strong MJ, Volkening K, Hammond R, Yang W, Strong W, Leystra-Lantz C, Shoesmith C (2007) TDP43 is a human low molecular weight neurofilament (hNFL) mRNA-binding protein. Mol Cell Neurosci 35:320-327.

Stuhlmeier KM, Li H, Kao JJ (1999) Ibuprofen: new explanation for an old phenomenon. Biochem Pharmacol 57:313-320.

Subramaniam JR, Lyons WE, Liu J, Bartnikas TB, Rothstein J, Price DL, Cleveland DW, Gitlin JD, Wong PC (2002) Mutant SOD1 causes motor neuron disease independent of copper chaperone-mediated copper loading. Nat Neurosci 5:301-307.

Sullivan PG, Rabchevsky AG, Keller JN, Lovell M, Sodhi A, Hart RP, Scheff SW (2004) Intrinsic differences in brain and spinal cord mitochondria: Implication for therapeutic interventions. J Comp Neurol 474:524-534.

Sumi H, Kato S, Mochimaru Y, Fujimura H, Etoh M, Sakoda S (2009) Nuclear TAR DNA binding protein 43 expression in spinal cord neurons correlates with the clinical course in amyotrophic lateral sclerosis. J Neuropathol Exp Neurol 68:37-47.

Sun SC, Ganchi PA, Beraud C, Ballard DW, Greene WC (1994) Autoregulation of the NF-kappa B transactivator RelA (p65) by multiple cytoplasmic inhibitors containing ankyrin motifs. Proc Natl Acad Sci U S A 91:1346-1350.

Sun Z, Diaz Z, Fang X, Hart MP, Chesi A, Shorter J, Gitler AD (2011) Molecular determinants and genetic modifiers of aggregation and toxicity for the ALS disease protein FUS/TLS. PLoS Biol 9:e1000614.

Sunesson L, Hellman U, Larsson C (2008) Protein kinase Cepsilon binds peripherin and induces its aggregation, which is accompanied by apoptosis of neuroblastoma cells. J Biol Chem 283:16653-16664.

Sunico CR, Dominguez G, Garcia-Verdugo JM, Osta R, Montero F, Moreno-Lopez B (2011) Reduction in the motoneuron inhibitory/excitatory synaptic ratio in an early-symptomatic mouse model of amyotrophic lateral sclerosis. Brain Pathol 21:1-15.

Suzuki M, Mikami H, Watanabe T, Yamano T, Yamazaki T, Nomura M, Yasui K, Ishikawa H, Ono S (2010) Increased expression of TDP-43 in the skin of amyotrophic lateral sclerosis. Acta Neurol Scand. 122(5):367-72

Swarup V, Julien JP (2011) ALS pathogenesis: recent insights from genetics and mouse models. Progress in neuro-psychopharmacology & biological psychiatry 35:363-369.

Swarup V, Das S, Ghosh S, Basu A (2007a) Tumor necrosis factor receptor-1-induced neuronal death by TRADD contributes to the pathogenesis of Japanese encephalitis. J Neurochem 103:771-783.

Swarup V, Ghosh J, Duseja R, Ghosh S, Basu A (2007b) Japanese encephalitis virus infection decrease endogenous IL-10 production: correlation with microglial activation and neuronal death. Neurosci Lett 420:144-149.

Swarup V, Phaneuf D, Bareil C, Robertson J, Rouleau GA, Kriz J, Julien JP (2011a) Pathological hallmarks of amyotrophic lateral sclerosis/frontotemporal lobar degeneration in transgenic mice produced with TDP-43 genomic fragments. Brain : a journal of neurology 134:2610-2626

Swarup V, Phaneuf D, Dupre N, Petri S, Strong M, Kriz J, Julien JP (2011a) Deregulation of TDP-43 in amyotrophic lateral sclerosis triggers nuclear factor kappaB-mediated pathogenic pathways. J Exp Med 208:2429-2447

Talbot K, Ansorge O (2006) Recent advances in the genetics of amyotrophic lateral sclerosis and frontotemporal dementia: common pathways in neurodegenerative disease. Hum Mol Genet 15 Spec No 2:R182-187.

Tamaoka A, Arai M, Itokawa M, Arai T, Hasegawa M, Tsuchiya K, Takuma H, Tsuji H, Ishii A, Watanabe M, Takahashi Y, Goto J, Tsuji S, Akiyama H (2010) TDP-43 M337V mutation in familial amyotrophic lateral sclerosis in Japan. Intern Med 49:331-334.

Terai K, Matsuo A, McGeer EG, McGeer PL (1996) Enhancement of immunoreactivity for NF-kappa B in human cerebral infarctions. Brain research 739:343-349.

Terry PD, Kamel F, Umbach DM, Lehman TA, Hu H, Sandler DP, Taylor JA (2004) VEGF promoter haplotype and amyotrophic lateral sclerosis (ALS). J Neurogenet 18:429-434.

Tetsuka T, Uranishi H, Imai H, Ono T, Sonta S, Takahashi N, Asamitsu K, Okamoto T (2000) Inhibition of nuclear factor-kappaB-mediated transcription by association with the amino-terminal enhancer of split, a Groucho-related protein lacking WD40 repeats. J Biol Chem 275:4383-4390.

Thaiparambil JT, Bender L, Ganesh T, Kline E, Patel P, Liu Y, Tighiouart M, Vertino PM, Harvey RD, Garcia A, Marcus AI (2011) Withaferin A inhibits breast cancer invasion and metastasis at sub-cytotoxic doses by inducing vimentin disassembly and serine 56 phosphorylation. Int J Cancer. 129:2744-2755

Ticozzi N, Silani V, LeClerc AL, Keagle P, Gellera C, Ratti A, Taroni F, Kwiatkowski TJ, Jr., McKenna-Yasek DM, Sapp PC, Brown RH, Jr., Landers JE (2009) Analysis of FUS gene mutation in familial amyotrophic lateral sclerosis within an Italian cohort. Neurology 73:1180-1185.

Toder V, Fein A, Carp H, Torchinsky A (2003) TNF-alpha in pregnancy loss and embryo maldevelopment: a mediator of detrimental stimuli or a protector of the fetoplacental unit? J Assist Reprod Genet 20:73-81.

Tollervey JR, Curk T, Rogelj B, Briese M, Cereda M, Kayikci M, Konig J, Hortobagyi T, Nishimura AL, Zupunski V, Patani R, Chandran S, Rot G, Zupan B, Shaw CE, Ule J (2011) Characterizing the RNA targets and position-dependent splicing regulation by TDP-43. Nature neuroscience 14:452-458.

Torgerson TR, Colosia AD, Donahue JP, Lin YZ, Hawiger J (1998) Regulation of NF-kappa B, AP-1, NFAT, and STAT1 nuclear import in T lymphocytes by noninvasive delivery of peptide carrying the nuclear localization sequence of NF-kappa B p50. J Immunol 161:6084-6092.

Toth ZE, Mezey E (2007) Simultaneous visualization of multiple antigens with tyramide signal amplification using antibodies from the same species. J Histochem Cytochem 55:545-554.

Tremblay C, St-Amour I, Schneider J, Bennett DA, Calon F (2011) Accumulation of transactive response DNA binding protein 43 in mild cognitive impairment and Alzheimer disease. Journal of neuropathology and experimental neurology 70:788-798.

Troy CM, Muma NA, Greene LA, Price DL, Shelanski ML (1990) Regulation of peripherin and neurofilament expression in regenerating rat motor neurons. Brain research 529:232-238.

Tsai CP, Soong BW, Lin KP, Tu PH, Lin JL, Lee YC (2011) FUS, TARDBP, and SOD1 mutations in a Taiwanese cohort with familial ALS. Neurobiol Aging 32:553 e513-521.

Tudor EL, Galtrey CM, Perkinton MS, Lau KF, De Vos KJ, Mitchell JC, Ackerley S, Hortobagyi T, Vamos E, Leigh PN, Klasen C, McLoughlin DM, Shaw CE, Miller CC (2010) Amyotrophic lateral sclerosis mutant vesicle-associated membrane protein-associated protein-B transgenic mice develop TAR-DNA-binding protein-43 pathology. Neuroscience 167:774-785.

Turner BJ, Ackerley S, Davies KE, Talbot K (2010) Dismutase-competent SOD1 mutant accumulation in myelinating Schwann cells is not detrimental to normal or transgenic ALS model mice. Human molecular genetics 19:815-824.

Udan M, Baloh RH (2011) Implications of the prion-related Q/N domains in TDP-43 and FUS. Prion 5:1-5.

Uranishi H, Tetsuka T, Yamashita M, Asamitsu K, Shimizu M, Itoh M, Okamoto T (2001) Involvement of the pro-oncoprotein TLS (translocated in liposarcoma) in nuclear factor-kappa B p65-mediated transcription as a coactivator. J Biol Chem 276:13395-13401.

Urushitani M, Ezzi SA, Julien JP (2007) Therapeutic effects of immunization with mutant superoxide dismutase in mice models of amyotrophic lateral sclerosis. Proc Natl Acad Sci U S A 104:2495-2500.

Urushitani M, Kurisu J, Tsukita K, Takahashi R (2002) Proteasomal inhibition by misfolded mutant superoxide dismutase 1 induces selective motor neuron death in familial amyotrophic lateral sclerosis. J Neurochem 83:1030-1042.

Van Damme P, Dewil M, Robberecht W, Van Den Bosch L (2005) Excitotoxicity and amyotrophic lateral sclerosis. Neurodegener Dis 2:147-159.

Van Damme P, Bogaert E, Dewil M, Hersmus N, Kiraly D, Scheveneels W, Bockx I, Braeken D, Verpoorten N, Verhoeven K, Timmerman V, Herijgers P, Callewaert G, Carmeliet P, Van Den Bosch L, Robberecht W (2007) Astrocytes regulate GluR2 expression in motor neurons and their vulnerability to excitotoxicity. Proceedings of the National Academy of Sciences of the United States of America 104:14825-14830.

Van Deerlin VM et al. (2008) TARDBP mutations in amyotrophic lateral sclerosis with TDP-43 neuropathology: a genetic and histopathological analysis. Lancet Neurol 7:409-416.

van Es MA, Diekstra FP, Veldink JH, Baas F, Bourque PR, Schelhaas HJ, Strengman E, Hennekam EA, Lindhout D, Ophoff RA, van den Berg LH (2009) A case of ALS-FTD in a large FALS pedigree with a K17I ANG mutation. Neurology 72:287-288.

Van Langenhove T, van der Zee J, Sleegers K, Engelborghs S, Vandenberghe R, Gijselinck I, Van den Broeck M, Mattheijssens M, Peeters K, De Deyn PP, Cruts M, Van Broeckhoven C (2010) Genetic contribution of FUS to frontotemporal lobar degeneration. Neurology 74:366-371.

van Loo G, Sze M, Bougarne N, Praet J, Mc Guire C, Ullrich A, Haegeman G, Prinz M, Beyaert R, De Bosscher K (2010) Antiinflammatory properties of a plant-derived nonsteroidal, dissociated glucocorticoid receptor modulator in experimental autoimmune encephalomyelitis. Mol Endocrinol 24:310-322.

Van Vught PW, Sutedja NA, Veldink JH, Koeleman BP, Groeneveld GJ, Wijmenga C, Uitdehaag BM, de Jong JM, Baas F, Wokke JH, Van den Berg LH (2005) Lack of association between VEGF polymorphisms and ALS in a Dutch population. Neurology 65:1643-1645.

Vance C et al. (2009) Mutations in FUS, an RNA processing protein, cause familial amyotrophic lateral sclerosis type 6. Science 323:1208-1211.

Vande Velde C, Miller TM, Cashman NR, Cleveland DW (2008) Selective association of misfolded ALS-linked mutant SOD1 with the cytoplasmic face of mitochondria. Proceedings of the National Academy of Sciences of the United States of America 105:4022-4027.

Vijayalakshmi K, Alladi PA, Ghosh S, Prasanna VK, Sagar BC, Nalini A, Sathyaprabha TN, Raju TR (2011) Evidence of endoplasmic reticular stress in the spinal motor neurons exposed to CSF from sporadic amyotrophic lateral sclerosis patients. Neurobiology of disease 41:695-705.

Voigt A, Herholz D, Fiesel FC, Kaur K, Muller D, Karsten P, Weber SS, Kahle PJ, Marquardt T, Schulz JB (2010) TDP-43-mediated neuron loss in vivo requires RNA-binding activity. PLoS One 5:e12247.

Volkening K, Leystra-Lantz C, Yang W, Jaffee H, Strong MJ (2009) Tar DNA binding protein of 43 kDa (TDP-43), 14-3-3 proteins and copper/zinc superoxide dismutase (SOD1) interact to modulate NFL mRNA stability. Implications for altered RNA processing in amyotrophic lateral sclerosis (ALS). Brain Res 1305:168-182.

Vucic S, Kiernan MC (2006) Novel threshold tracking techniques suggest that cortical hyperexcitability is an early feature of motor neuron disease. Brain : a journal of neurology 129:2436-2446.

Vucic S, Nicholson GA, Kiernan MC (2008) Cortical hyperexcitability may precede the onset of familial amyotrophic lateral sclerosis. Brain : a journal of neurology 131:1540-1550.

Wang HY, Wang IF, Bose J, Shen CK (2004) Structural diversity and functional implications of the eukaryotic TDP gene family. Genomics 83:130-139.

Wang IF, Reddy NM, Shen CK (2002a) Higher order arrangement of the eukaryotic nuclear bodies. Proceedings of the National Academy of Sciences of the United States of America 99:13583-13588.

Wang IF, Wu LS, Shen CK (2008a) TDP-43: an emerging new player in neurodegenerative diseases. Trends Mol Med 14:479-485.

Wang J, Farr GW, Hall DH, Li F, Furtak K, Dreier L, Horwich AL (2009a) An ALS-linked mutant SOD1 produces a locomotor defect associated with aggregation and synaptic dysfunction when expressed in neurons of Caenorhabditis elegans. PLoS genetics 5:e1000350.

Wang J, Xu G, Gonzales V, Coonfield M, Fromholt D, Copeland NG, Jenkins NA, Borchelt DR (2002b) Fibrillar inclusions and motor neuron degeneration in transgenic mice expressing superoxide dismutase 1 with a disrupted copper-binding site. Neurobiol Dis 10:128-138.

Wang J, Xu G, Li H, Gonzales V, Fromholt D, Karch C, Copeland NG, Jenkins NA, Borchelt DR (2005a) Somatodendritic accumulation of misfolded SOD1-L126Z in motor neurons mediates degeneration: alphaB-crystallin modulates aggregation. Hum Mol Genet 14:2335-2347.

Wang J, Xu G, Slunt HH, Gonzales V, Coonfield M, Fromholt D, Copeland NG, Jenkins NA, Borchelt DR (2005b) Coincident thresholds of mutant protein for paralytic disease and protein aggregation caused by restrictively expressed superoxide dismutase cDNA. Neurobiol Dis 20:943-952.

Wang J, Farr GW, Zeiss CJ, Rodriguez-Gil DJ, Wilson JH, Furtak K, Rutkowski DT, Kaufman RJ, Ruse CI, Yates JR, 3rd, Perrin S, Feany MB, Horwich AL (2009b) Progressive aggregation despite chaperone associations of a mutant SOD1-YFP in transgenic mice that develop ALS. Proc Natl Acad Sci U S A 106:1392-1397.

Wang X, Arai S, Song X, Reichart D, Du K, Pascual G, Tempst P, Rosenfeld MG, Glass CK, Kurokawa R (2008b) Induced ncRNAs allosterically modify RNA-binding proteins in cis to inhibit transcription. Nature 454:126-130.

Watson MR, Lagow RD, Xu K, Zhang B, Bonini NM (2008) A drosophila model for amyotrophic lateral sclerosis reveals motor neuron damage by human SOD1. The Journal of biological chemistry 283:24972-24981.

Wegorzewska I, Bell S, Cairns NJ, Miller TM, Baloh RH (2009) TDP-43 mutant transgenic mice develop features of ALS and frontotemporal lobar degeneration. Proc Natl Acad Sci U S A 106:18809-18814.

Weihl CC, Temiz P, Miller SE, Watts G, Smith C, Forman M, Hanson PI, Kimonis V, Pestronk A (2008) TDP-43 accumulation in inclusion body myopathy muscle suggests a common pathogenic mechanism with frontotemporal dementia. Journal of neurology, neurosurgery, and psychiatry 79:1186-1189.

Wellmann H, Kaltschmidt B, Kaltschmidt C (2001) Retrograde transport of transcription factor NF-kappa B in living neurons. The Journal of biological chemistry 276:11821-11829.

Welp E, Kogevinas M, Andersen A, Bellander T, Biocca M, Coggon D, Esteve J, Gennaro V, Kolstad H, Lundberg I, Lynge E, Partanen T, Spence A, Boffetta P, Ferro G, Saracci R (1996) Exposure to styrene and mortality from nervous system diseases and mental disorders. Am J Epidemiol 144:623-633.

Weydt P, Yuen EC, Ransom BR, Moller T (2004) Increased cytotoxic potential of microglia from ALS-transgenic mice. Glia 48:179-182.

Wiedau-Pazos M, Goto JJ, Rabizadeh S, Gralla EB, Roe JA, Lee MK, Valentine JS, Bredesen DE (1996) Altered reactivity of superoxide dismutase in familial amyotrophic lateral sclerosis. Science 271:515-518.

Wiedemann FR, Manfredi G, Mawrin C, Beal MF, Schon EA (2002) Mitochondrial DNA and respiratory chain function in spinal cords of ALS patients. Journal of neurochemistry 80:616-625.

Williams DB, Floate DA, Leicester J (1988) Familial motor neuron disease: differing penetrance in large pedigrees. J Neurol Sci 86:215-230.

Williams TL, Day NC, Ince PG, Kamboj RK, Shaw PJ (1997) Calcium-permeable alpha-amino-3-hydroxy-5-methyl-4-isoxazole propionic acid receptors: a molecular determinant of selective vulnerability in amyotrophic lateral sclerosis. Annals of neurology 42:200-207.

Williamson TL, Cleveland DW (1999) Slowing of axonal transport is a very early event in the toxicity of ALS-linked SOD1 mutants to motor neurons. Nature neuroscience 2:50-56.

Williamson TL, Bruijn LI, Zhu Q, Anderson KL, Anderson SD, Julien JP, Cleveland DW (1998) Absence of neurofilaments reduces the selective vulnerability of motor neurons and slows disease caused by a familial amyotrophic lateral sclerosis-linked superoxide dismutase 1 mutant. Proc Natl Acad Sci U S A 95:9631-9636.

Wils H, Kleinberger G, Janssens J, Pereson S, Joris G, Cuijt I, Smits V, Ceuterick-de Groote C, Van Broeckhoven C, Kumar-Singh S (2010) TDP-43 transgenic mice develop spastic paralysis and neuronal inclusions characteristic of ALS and frontotemporal lobar degeneration. Proc Natl Acad Sci U S A 107:3858-3863.

Won SJ, Ko HW, Kim EY, Park EC, Huh K, Jung NP, Choi I, Oh YK, Shin HC, Gwag BJ (1999) Nuclear factor kappa B-mediated kainate neurotoxicity in the rat and hamster hippocampus. Neuroscience 94:83-91.

Wong NK, He BP, Strong MJ (2000) Characterization of neuronal intermediate filament protein expression in cervical spinal motor neurons in sporadic amyotrophic lateral sclerosis (ALS). J Neuropathol Exp Neurol 59:972-982.

Wong PC, Pardo CA, Borchelt DR, Lee MK, Copeland NG, Jenkins NA, Sisodia SS, Cleveland DW, Price DL (1995) An adverse property of a familial ALS-linked SOD1 mutation causes motor neuron disease characterized by vacuolar degeneration of mitochondria. Neuron 14:1105-1116.

Wood JD, Beaujeux TP, Shaw PJ (2003) Protein aggregation in motor neurone disorders. Neuropathol Appl Neurobiol 29:529-545.

Woronicz JD, Gao X, Cao Z, Rothe M, Goeddel DV (1997) IkappaB kinase-beta: NF-kappaB activation and complex formation with IkappaB kinase-alpha and NIK. Science 278:866-869.

Wu DC, Re DB, Nagai M, Ischiropoulos H, Przedborski S (2006) The inflammatory NADPH oxidase enzyme modulates motor neuron degeneration in amyotrophic lateral sclerosis mice. Proceedings of the National Academy of Sciences of the United States of America 103:12132-12137.

Wu LS, Cheng WC, Hou SC, Yan YT, Jiang ST, Shen CK (2010) TDP-43, a neuro-pathosignature factor, is essential for early mouse embryogenesis. Genesis 48:56-62.

Xia CH, Roberts EA, Her LS, Liu X, Williams DS, Cleveland DW, Goldstein LS (2003) Abnormal neurofilament transport caused by targeted disruption of neuronal kinesin heavy chain KIF5A. J Cell Biol 161:55-66.

Xiao S, Tjostheim S, Sanelli T, McLean JR, Horne P, Fan Y, Ravits J, Strong MJ, Robertson J (2008) An aggregate-inducing peripherin isoform generated through intron retention is upregulated in amyotrophic lateral sclerosis and associated with disease pathology. J Neurosci 28:1833-1840.

Xu L, Zhan Y, Wang Y, Feuerstein GZ, Wang X (2002) Recombinant adenoviral expression of dominant negative IkappaBalpha protects brain from cerebral ischemic injury. Biochemical and biophysical research communications 299:14-17.

Xu X, Prorock C, Ishikawa H, Maldonado E, Ito Y, Gelinas C (1993a) Functional interaction of the v-Rel and c-Rel oncoproteins with the TATA-binding protein and association with transcription factor IIB. Mol Cell Biol 13:6733-6741.

Xu YF, Zhang YJ, Lin WL, Cao X, Stetler C, Dickson DW, Lewis J, Petrucelli L (2011) Expression of mutant TDP-43 induces neuronal dysfunction in transgenic mice. Mol Neurodegener 6:73.

Xu YF, Gendron TF, Zhang YJ, Lin WL, D'Alton S, Sheng H, Casey MC, Tong J, Knight J, Yu X, Rademakers R, Boylan K, Hutton M, McGowan E, Dickson DW, Lewis J, Petrucelli L (2010) Wild-Type Human TDP-43 Expression Causes TDP-43 Phosphorylation, Mitochondrial Aggregation, Motor Deficits, and Early Mortality in Transgenic Mice. J Neurosci 30:10851-10859.

Xu Z, Cork LC, Griffin JW, Cleveland DW (1993b) Increased expression of neurofilament subunit NF-L produces morphological alterations that resemble the pathology of human motor neuron disease. Cell 73:23-33.

Xu Z, Chen S, Li X, Luo G, Li L, Le W (2006) Neuroprotective effects of (-)-epigallocatechin-3-gallate in a transgenic mouse model of amyotrophic lateral sclerosis. Neurochem Res 31:1263-1269.

Yamagishi S, Koyama Y, Katayama T, Taniguchi M, Hitomi J, Kato M, Aoki M, Itoyama Y, Kato S, Tohyama M (2007) An in vitro model for Lewy body-like hyaline inclusion/astrocytic hyaline inclusion: induction by ER stress with an ALS-linked SOD1 mutation. PloS one 2:e1030.

Yamanaka K, Boillee S, Roberts EA, Garcia ML, McAlonis-Downes M, Mikse OR, Cleveland DW, Goldstein LS (2008a) Mutant SOD1 in cell types other than motor neurons and oligodendrocytes accelerates onset of disease in ALS mice. Proc Natl Acad Sci U S A 105:7594-7599.

Yamanaka K, Chun SJ, Boillee S, Fujimori-Tonou N, Yamashita H, Gutmann DH, Takahashi R, Misawa H, Cleveland DW (2008b) Astrocytes as determinants of disease progression in inherited amyotrophic lateral sclerosis. Nature neuroscience 11:251-253.

Yamauchi T, Sakurai M, Abe K, Matsumiya G, Sawa Y (2008) Ubiquitin-mediated stress response in the spinal cord after transient ischemia. Stroke 39:1883-1889.

Yamit-Hezi A, Dikstein R (1998) TAFII105 mediates activation of anti-apoptotic genes by NF-kappaB. EMBO J 17:5161-5169.

Yamit-Hezi A, Nir S, Wolstein O, Dikstein R (2000) Interaction of TAFII105 with selected p65/RelA dimers is associated with activation of subset of NF-kappa B genes. J Biol Chem 275:18180-18187.

Yan J, Deng HX, Siddique N, Fecto F, Chen W, Yang Y, Liu E, Donkervoort S, Zheng JG, Shi Y, Ahmeti KB, Brooks B, Engel WK, Siddique T (2010) Frameshift and novel mutations in FUS in familial amyotrophic lateral sclerosis and ALS/dementia. Neurology 75:807-814.

Yang JP, Hori M, Sanda T, Okamoto T (1999) Identification of a novel inhibitor of nuclear factor-kappaB, RelA-associated inhibitor. J Biol Chem 274:15662-15670.

Yang Y, Hentati A, Deng HX, Dabbagh O, Sasaki T, Hirano M, Hung WY, Ouahchi K, Yan J, Azim AC, Cole N, Gascon G, Yagmour A, Ben-Hamida M, Pericak-Vance M, Hentati F, Siddique T (2001) The gene encoding alsin, a protein with three guanine-nucleotide exchange factor domains, is mutated in a form of recessive amyotrophic lateral sclerosis. Nat Genet 29:160-165.

Yasser S, Fecto F, Siddique T, Sheikh KA, Athar P (2010) An unusual case of familial ALS and cerebellar ataxia. Amyotrophic lateral sclerosis : official publication of the World Federation of Neurology Research Group on Motor Neuron Diseases 11:568-570.

Yokoseki A, Shiga A, Tan CF, Tagawa A, Kaneko H, Koyama A, Eguchi H, Tsujino A, Ikeuchi T, Kakita A, Okamoto K, Nishizawa M, Takahashi H, Onodera O (2008) TDP-43 mutation in familial amyotrophic lateral sclerosis. Annals of neurology 63:538-542.

Yoza BK, Hu JY, McCall CE (1996) Protein-tyrosine kinase activation is required for lipopolysaccharide induction of interleukin 1beta and NFkappaB activation, but not NFkappaB nuclear translocation. The Journal of biological chemistry 271:18306-18309.

Yu Z, Zhou D, Cheng G, Mattson MP (2000) Neuroprotective role for the p50 subunit of NF-kappaB in an experimental model of Huntington's disease. J Mol Neurosci 15:31-44.

Yum SW, Zhang J, Mo K, Li J, Scherer SS (2009) A novel recessive Nefl mutation causes a severe, early-onset axonal neuropathy. Ann Neurol 66:759-770.

Zandi E, Karin M (1999) Bridging the gap: composition, regulation, and physiological function of the IkappaB kinase complex. Mol Cell Biol 19:4547-4551.

Zhang B, Tu P, Abtahian F, Trojanowski JQ, Lee VM (1997) Neurofilaments and orthograde transport are reduced in ventral root axons of transgenic mice that express human SOD1 with a G93A mutation. The Journal of cell biology 139:1307-1315.

Zhang R, Miller RG, Gascon R, Champion S, Katz J, Lancero M, Narvaez A, Honrada R, Ruvalcaba D, McGrath MS (2009a) Circulating endotoxin and systemic immune activation in sporadic amyotrophic lateral sclerosis (sALS). J Neuroimmunol 206:121-124.

Zhang R, Hadlock KG, Do H, Yu S, Honrada R, Champion S, Forshew D, Madison C, Katz J, Miller RG, McGrath MS (2011a) Gene expression profiling in peripheral blood mononuclear cells from patients with sporadic amyotrophic lateral sclerosis (sALS). J Neuroimmunol 230:114-123.

Zhang S, Won YK, Ong CN, Shen HM (2005) Anti-cancer potential of sesquiterpene lactones: bioactivity and molecular mechanisms. Curr Med Chem Anticancer Agents 5:239-249.

Zhang T, Mullane PC, Periz G, Wang J (2011b) TDP-43 neurotoxicity and protein aggregation modulated by heat shock factor and insulin/IGF-1 signaling. Human molecular genetics 20:1952-1965.

Annex I: Published paper in PDF format

ALS pathogenesis: Recent insights from genetics and mouse models

Progress in Neuro-Psychopharmacology & Biological Psychiatry 35 (2011) 363–369

Contents lists available at ScienceDirect

Progress in Neuro-Psychopharmacology & Biological Psychiatry

journal homepage: www.elsevier.com/locate/pnp

ALS pathogenesis: Recent insights from genetics and mouse models

Vivek Swarup, Jean-Pierre Julien *

Centre de Recherche du Centre Hospitalier Universitaire de Québec, Department of Psychiatry and Neuroscience of Laval University, Quebec, QC, Canada

ARTICLE INFO

Article history:
Received 9 June 2010
Received in revised form 15 July 2010
Accepted 11 August 2010
Available online 20 August 2010

Keywords:
Amyotrophic lateral sclerosis
Animal models
Dynactin
SOD1
TDP-43
VAPB

ABSTRACT

For the vast majority of cases of amyotrophic lateral sclerosis (ALS) the etiology remains unknown. After the discovery of missense mutations in the gene coding for the Cu/Zn superoxide dismutase 1 (SOD1) in subsets of familial ALS, several transgenic mouse lines have been generated with various forms of SOD1 mutants overexpressed at different levels. Studies with these mice yielded complex results with multiple targets of damage in disease including mitochondria, proteasomes, and secretory pathways. Many unexpected discoveries were made. For instance, the toxicity of mutant SOD1 seems unrelated to copper-mediated catalysis but rather to formation of misfolded SOD1 species and aggregates. Transgenic studies revealed a potential role of wtSOD1 in exacerbating mutant SOD1-mediated disease. Another key finding came from chimeric mouse studies and from Cre-lox mediated gene deletion experiments which have highlighted the importance of non-neuronal cells in the disease progression. Involvement of cytoskeletal components in ALS pathogenesis is supported by several mouse models of motor neuron disease with neurofilament abnormalities and with genetic defects in microtubule-based transport. Recently, the generation of new animal models of ALS has been made possible with the discovery of ALS-linked mutations in other genes encoding for alsin, dynactin, senataxin, VAPB, TDP-43 and FUS. Following the discovery of mutations in the *TARDBP* gene linked to ALS, there have been some reports of transgenic mice with high level overexpression of WT or mutant forms of TDP-43 under strong gene promoters. However, these TDP-43 transgenic mice do not exhibit all pathological features the human ALS disease. Here, we will describe these new TDP-43 transgenic mice and discuss their validity as animal models of human ALS.

1. Introduction

Amyotrophic lateral sclerosis (ALS) is an adult-onset neurological disorder that is characterized by the selective loss of motor neurons leading to progressive weakness, muscle atrophy with eventual paralysis and death within 5 years of clinical onset. Approximately 10% of ALS cases are familial; the remainder ALS cases being diagnosed as sporadic (90%). The discovery 17 years ago of missense mutations in the gene coding for the Cu/Zn superoxide dismutase 1 (SOD1) in subsets of familial cases directed most ALS research to elucidating the mechanism of SOD1-mediated disease. Subsequently, rare mutations associated with motor neuron disease were also discovered in other genes including ALSIN (Eymard-Pierre et al., 2002; Hadano et al., 2001; Yang et al., 2001), VAPB (Nishimura et al., 2004), SETX (Chen et al., 2004), ANG (Greenway et al., 2006) and DCTN1 (Puls et al., 2003). Recently, much attention has been devoted to two genes coding for DNA/RNA binding proteins which have been implicated in the pathogenesis of ALS. Dominant mutations in the *TARDBP* gene, which codes for TDP-43, were reported by several groups as a primary cause of ALS for ~3% familial cases and ~1.5% sporadic cases (Corrado et al., 2009; Daoud et al., 2009; Gitcho et al., 2008; Kabashi et al., 2008; Sreedharan et al., 2008; Van Deerlin et al., 2008). Mutations in the FUS/TLS gene were also detected in ~4% of familial ALS cases (Kwiatkowski et al., 2009; Vance et al., 2009). A list of genes involved in ALS is provided in Table 1. The discovery of gene mutations linked to human ALS has provided opportunities to develop model systems for investigating mechanisms of disease. Here we will review various transgenic mouse models that have been used to study the toxicity of ALS-linked gene mutations and also to investigate pathological hallmarks of the disease.

2. Transgenic mice expressing ALS-linked SOD1 mutants

A breakthrough in the field of ALS came in 1993 with the discovery of missense mutations in the SOD1 gene of a subset of FALS cases (Rosen et al., 1993). SOD1 is a ubiquitously expressed cytosolic metalloenzyme of 153 amino acids encoded by 5 exons. To date, over 150 different mutations (mostly missense mutations) have been discovered in the SOD1 gene that account for 20% familial ALS cases

Abbreviations: ALS, amyotrophic lateral sclerosis; ER, endoplasmic reticulum; FTLD-U, frontotemporal lobar dementia with ubiquitinated inclusions; FUS, fused in sarcoma; GEF, guanine nucleotide exchange factor; IAHSP, infantile ascending hereditary spastic paralysis; IF, intermediate filament; NF-L, neurofilament-light chain; SOD1, superoxide dismutase-1; TDP-43, TAR DNA binding protein-43; TLS, translocated in liposarcoma; VAPB, vesicle-associated membrane protein-associated protein-B.

* Corresponding author. Pavillon CHUL, 2705 Boulevard Laurier, Quebec, QC, Canada G1V 4G2. Fax: +1 418 654 2761.
E-mail address: jean-pierre.julien@crchul.ulaval.ca (J.-P. Julien).

0278-5846/$ – see front matter © 2010 Elsevier Inc. All rights reserved.
doi:10.1016/j.pnpbp.2010.08.006

Table 1
Familial ALS (fALS) gene mutations.

FALS type	Locus	Gene	Inheritence	Clinical Pattern	Mutations	Causes SALS
ALS1	21q	SOD1	AD	Classical	>120	Yes
ALS2	2q33	ALSIN	AR	Young Onset, UMN	10	No
ALS3	18q21	?	AD	Classical	?	?
ALS4	9q34	SETX	AD	Young Onset, Slow	3	?
ALS5	15q15	?	AR	Young Onset	?	?
ALS6	16q21	FUS-TLS	AD	Classical	14	?
ALS7	20ptel-p13	?	AD	Classical	?	?
ALS8	20q13.3	VAPB	AD	Varied	1	No
ALS-FTD	9q21-q22	?	AD	With FTD	?	?
ALS-FTD	9q21.3	?	AD	With FTD	?	?
ALS	14q11.2	Angiogenin	AD	Classical	6	Yes
FTD (FTD3)	3	CHMP2B	AD	FTD (ALS)	2	?
ALS	1	TDP-43	AD	ALS	30	Yes
LMND	2p13	DCTN1	AD	LMND	1(+4 in ALS?)	?

Genes involved in RNA metabolism.
Genes involved in trafficking and transport.
Most ALS cases are sporadic (SALS) and about 10% of cases are familial (FALS). 20% of FALS have a mutation in the SOD1 gene and about 2–5% has mutations of the TARDBP (TDP-43) gene. 2% of SALS patients have SOD1 mutations. TARDBP mutations also occur in sporadic cases.

(Andersen, 2006; Andersen et al., 2003). Most of our current knowledge of ALS pathogenic mechanisms came from the analysis of transgenic mice expressing mutant SOD1, especially from the widely used mouse strain SOD1G93A (B6SJL-TgN(SOD1-G93A)1Gur/J; 002726, Jackson Laboratory, Bar Harbor ME) originally generated by Gurney et al. (1994). Mouse studies led many unexpected findings described below.

2.1. A gain of toxicity due to misfolding and aggregation

Because of its normal function in catalyzing the conversion of superoxide anions to hydrogen peroxide, it was first thought that the toxicity of different SOD1 mutants could result from decreased free-radicals scavenging activity. However, SOD1 knockout mice did not develop motor neuron disease (Reaume et al., 1996) and mice expressing mutants $SOD1^{G93A}$ or $SOD1^{G37R}$ developed motor neuron disease despite elevation in the SOD1 activity levels (Cleveland, 1999). These combined results suggested that the mutations in SOD1 provoke a gain of new toxic properties. Subsequently, two mouse studies further supported this view. The gene knockout for the copper chaperone for SOD1 (CCS) that delivers copper to SOD1 catalytic site had no effect on disease progression in mutant SOD1 mice (Subramaniam et al. 2002). Second, transgenic mice overexpressing a mutant form of SOD1 lacking two of the four histidine residues coordinating the binding of the Cu at the catalytic site still developed motor neurodegeneration despite a marked reduction in SOD1 activity (Wang et al., 2002).

To date, many transgenic mouse lines have been generated in which ALS-linked SOD1 mutants of different biochemical properties were expressed. High levels of mutant SOD1 mRNA are required for development of ALS-like phenotypes within the short life span of mice. Moreover, the life span of the ALS mice is inversely proportional to gene dosage. For example, in the $SOD1^{G127X}$, the survival time in hemizygous mice was twice as long as in mice homozygous for the transgene (Jonsson et al., 2006). The most widely used mouse strain $SOD1^{G93A}$ (B6SJL-TgN(SOD1-G93A)1Gur/J; 002726, Jackson Laboratory, Bar Harbor ME) with survival of approximately 130 days overexpress by 40 folds the normal mRNA levels of mouse SOD1 (Gurney et al., 1994; Jonsson et al., 2006). For many other transgenic strains (G85R, D90A, G93Adl and G127X) with later onset disease, the mRNA levels correspond to approximately 20 folds the level of endogenous SOD1 mRNA. It should be noted that the steady state levels of mutant SOD1 proteins in the spinal cord can differ widely from one mouse strain to another. The level of human SOD1 protein in young mice of the G93A strain is of 17 fold higher than normal mouse SOD1 level whereas the G85R, G127X and L126Z mice exhibit at young age low levels of mutant SOD1. So, the different transgenic mouse strains express mutant SOD1 in a range of 0.5 to 20 folds the normal SOD1 levels. Such widely different steady state protein levels must reflect different stabilities and degradation of the various human SOD1 mutants. Surprisingly, despite low mutant SOD1 protein levels in the young G85R, G127X or L126Z mice, their life span remains similar to some G37R or G93A mice and they showed similar amounts of detergent-insoluble aggregates in the spinal cord at end-stage of disease (Bruijn et al., 1997; Jonsson et al., 2006; Wang et al., 2005a).

The combined studies suggest that the motor neuron disease may be caused by long-term exposure to noxious misfolded mutant SOD1 species with propensity to aggregate. However, the exact mechanism of toxicity of the misfolded SOD1 species remains unknown. Deleterious effects could result from overwhelming the capacity of the protein folding chaperones (Batulan et al., 2003) and/or of ubiquitin proteasome pathway to degrade important cellular regulatory factors (Urushitani et al., 2002). Somehow, the motor neuron death pathway is complex with multiple cascades of events including oxidative damage, excitotoxicity, alterations in calcium homeostasis, caspase activation, mitochondrial defects (Liu et al., 2004; Pasinelli et al., 2004) and Fas transduction (Raoul et al., 2002). Moreover, the ER–Golgi pathway is a predominant site of uptake and age-dependent aggregation of misfolded mutant SOD1 linked to ALS (Urushitani et al., 2008), a phenomenon that could explain the endoplasmic reticulum (ER) stress responses detected in vulnerable motor neuron in G93A mice (Saxena et al., 2009). Recently, our group generated a collection of monoclonal antibodies that recognize specifically misfolded forms from mutant SOD1 but not the intact wild-type (WT) SOD1. Immunofluorescence staining with such antibodies revealed that the presence of misfolded SOD1 species was restricted to motor neurons at early pre-symptomatic stage in G93A-*SOD1* mice and intense punctate misfolded SOD1 aggregates localized in contiguous processes and in the neuropil were detected throughout the spinal cord in late disease stage (Gros-Louis et al., 2010). No immunostaining was detected in transgenic animals overexpressing wild-type human SOD1.

2.2. WT SOD1 can contribute to disease

In an initial study, the overexpression of human $SOD1^{WT}$ did not seem to affect the progression of motor neuron disease in transgenic mice expressing mutant $SOD1^{G85R}$ (Bruijn et al., 1998). However, more recent studies by other groups showed that overexpression of human

$SOD1^{WT}$ caused dramatic exacerbation of disease in mice expressing different SOD1 mutants, including two SOD1 mutants ($SOD1^{G85R}$ and $SOD1^{L126Z}$) that express highly unstable and enzymatically inactive SOD1 (Deng et al., 2006, 2008; Jaarsma et al., 2008; Wang et al., 2009). Remarkably, a $SOD1^{A4V}$ mouse line without phenotypes was converted to an ALS-like mouse model with death at 400 days through the generation of double-transgenic $SOD1^{A4V}$;wtSOD1. Evidence suggests that the $SOD1^{WT}$ may contribute to disease through interaction and perhaps stabilization of mutant SOD1. Interestingly, human $SOD1^{WT}$ overexpression did not affect the lifespan of mice overexpressing mouse $Sod1^{G86R}$ (Audet et al., 2010). The analysis of spinal cord extracts revealed a lack of heterodimerization or aggregation between human $SOD1^{WT}$ and mouse $Sod1^{G86R}$ proteins. Thus, a direct interaction between wild-type and mutant forms of SOD1 is required for exacerbation of ALS disease by $SOD1^{WT}$ protein.

2.3. Involvement of non-neuronal cell types

A most significant contribution of transgenic mouse studies was the finding of a role for non-neuronal cells in motor neuron disease. For instance, the analyses of chimeric mice made of mixtures of normal and SOD1 mutant-expressing cells demonstrated that neurodegeneration is delayed or eliminated when motor neurons expressing mutant SOD1 are surrounded by healthy wild-type cells (Clement et al., 2003). To further clarify what cell types contribute to disease, very elegant studies were carried out with mice carrying $SOD1^{G37R}$ gene flanked by LoxP sequences, a system that allows excision by the Cre recombinase in specific cell types (Yamanaka et al., 2008). These studies revealed that expression of mutant SOD1 within motor neurons is a modulator of onset of ALS disease whereas mutant SOD1 toxicity in glial cells can affect the progression of disease after onset (Fig. 1). It should be noted that two studies, neuron-specific expression of SOD1 mutants with NF-L or Thy1 gene promoters did not induce motor neuron disease in mice (Lino et al., 2002; Pramatarova et al., 2001). However, subsequent studies reported motor neuron disease in mice overexpressing high levels of mutant SOD1 under the Prion gene or Thy1 gene promoters (Jaarsma et al., 2008; Wang et al., 2005b). These apparent discrepancies can be explained by the degree of transgene overexpression in neurons.

2.4. Testing immunization approaches in mutant SOD1 mice

The existence of secretory pathways for SOD1 and for neurotoxicity of extracellular mutant SOD1 led us to test immunization protocols aiming to reduce the burden of extracellular SOD1 mutant in nervous tissue of mice models of ALS. A vaccination protocol, based on bacterially-purified recombinant SOD1 mutant protein as an immunogen, was tested on a $SOD1^{G37R}$ mouse strain exhibiting levels of mutant SOD1 protein at 5 folds the normal SOD1 levels. The vaccination was effective in delaying disease onset and extending life span of G37R *SOD1* mice by over 4 weeks and our analyses provided evidence of reduction of SOD1 species in the spinal cord of vaccinated G37R *SOD1* mice (Gros-Louis et al., 2010; Urushitani et al., 2007). Recently, we tested a passive immunization approach based on intracerebroventricular infusion in G93A-*SOD1* mice of monoclonal antibodies specific to misfolded forms of SOD1. One antibody succeeded in reducing the level of misfolded SOD1 by 23% in the spinal cord and in prolonging the lifespan of G93A-*SOD1* mice in proportion to the duration of treatment (Gros-Louis et al., 2010). These results suggest that passive immunization strategies should be considered as potential avenues for treatment of familial ALS caused by *SOD1* mutations.

3. Mice knockout for Als2

Deletion mutations were discovered in coding exons of a gene mapping to chromosome 2q33, *ALS2* coding for Alsin, from patients with an autosomal recessive form of juvenile ALS (JALS), primary lateral

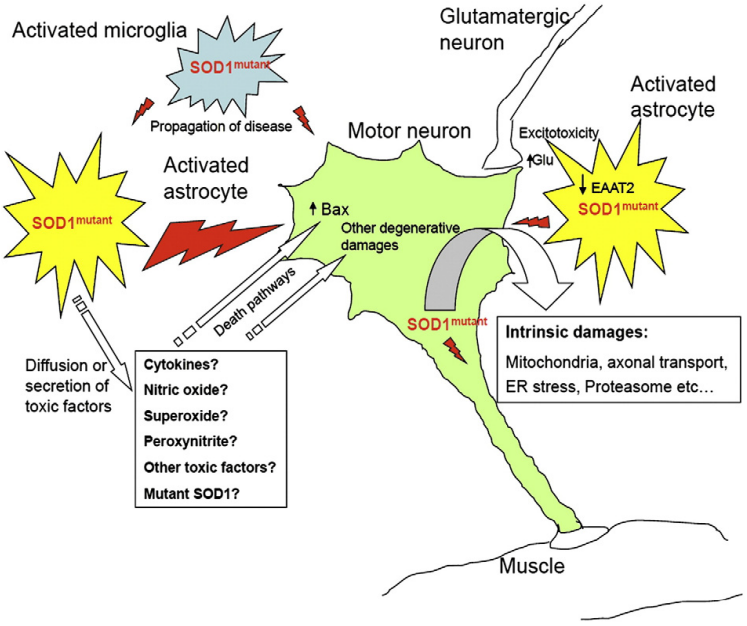

Fig. 1.

sclerosis and infantile-onset ascending hereditary spastic paralysis (IAHSP) (Eymard-Pierre et al., 2002; Gros-Louis et al., 2003; Hadano et al., 2001; Yang et al., 2001). The ALS2 gene is ubiquitously expressed. It encodes a protein having guanine nucleotide exchange factor (GEF) homology domains which are known to activate small guanosine triphosphatase (GTPase) belonging to the Ras superfamily. Als2 knockout mice have been reported by four groups (Cai et al., 2005; Devon et al., 2006; Hadano et al., 2006; Gros-Louis et al., 2008). These studies demonstrate that absence of Als2 does not produce a severe phenotype in mice. However, the studies by Cai et al. (2005) showed that the Als2 null mice develop age-dependent deficits in motor coordination and primary motor cultured motor neurons lacking Als2 were more susceptible to oxidative stress. Whereas Cai et al. detected no neuropathological changes in their Als2 null mice, Hadano et al. (2006) showed that Als2-null mice develop an age-dependent and slow progressive loss of cerebellar Purkinje Cells, a reduction in ventral motor axons during aging, astrogliosis and evidence of deficits in endosome trafficking. The Als2 knockout mouse generated by our group exhibited degeneration of corticospinal axons and evidence of axonal transport defects (Gros-Louis et al., 2008).

4. Mice with disorganized Intermediate Filaments (IFs)

Neurofilament and peripherin proteins are two types of IFs detected in the majority of axonal inclusion bodies, called spheroids, in motor neurons of ALS patients (Corbo and Hays, 1992; Hirano et al., 1984). Multiple factors can potentially cause the accumulation of IF proteins including deregulation of IF protein synthesis, proteolysis, defective axonal transport, abnormal phosphorylation, and other protein modifications. Even though genetic mutations in IF genes are not major causes of ALS, it is of potential relevance to ALS that transgenic mice with altered stoichiometry of neuronal IF develop pathological features of the disease (Beaulieu et al., 2000; Beaulieu and Julien, 2003; Cote et al., 1993; Millecamps et al., 2006) (Table 2). Of particular interest was the finding that sustained overexpression of wild-type peripherin in mice caused the selective loss of motor neurons during aging. This mouse model is characterized by the formation of perikaryal and axonal IF inclusions resembling spheroids in motor neurons of human ALS. The toxicity of peripherin overexpression in mice appears related in part to the axonal localization of IF aggregates, in line with the view that IF swellings might impair axonal (Beaulieu and Julien, 2003; Millecamps et al., 2006). Recently, a neurotoxic and assembly defective splicing variant of peripherin called Per28 was detected specifically in spinal cord samples from ALS cases (Xiao et al., 2008). In the future, it would be of interest to test the in vivo toxicity of Per28 in motor neurons with the generation of transgenic mice.

5. Mice with microtubule-based transport defects

Axonal transport is essential to neurons because of the extreme polarity and size of these cells. In humans, spinal motor neurons may have axons of more than 1 m in length. Most proteins must be synthesized in cell bodies and transported to nerve terminals through axonal transport. Various molecular motors, which are multi-subunit ATPases members of the kinesin family and dynein, move cargos along microtubules in the anterograde and retrograde directions, respectively. Impairment of axonal transport has recently emerged as a common factor in several neurodegenerative disorders. Mutations that disrupt either kinesin or the dynein complex cause impairment of axonal transport, blockade of membranous cargoes and axonal degeneration.

The creation of mice heterozygotes for disruption of the kinesin KIF1B gene provided the proof that defects in axonal transport can provoke neurodegeneration (Zhao et al., 2001). These mice showed defect in transporting synaptic vesicle precursors and they suffer from progressive muscle weakness similar to human neuropathies. This discovery subsequently led to the identification of a loss-of-function mutation in the motor domain of the KIF1B gene in patients with Charcot-Marie-Tooth disease type 2A (Zhao et al., 2001). In addition, missense mutations in the conventional KIF5A are responsible for a hereditary form of spastic paraplegia (Reid et al., 2002) and disruption of KIF5A gene in mice was reported to cause neurofilament transport impairment (Xia et al., 2003).

Dynein is a molecular motor involved in retrograde axonal transport of organelles along microtubules. Dynein activity requires association with dynactin, a multiprotein complex that activates the motor function of dynein and participates in cargo attachment (Schroer, 2004). Transgenic mice overexpressing dynamitin developed a late-onset and progressive motor neuron disease resembling ALS with neurofilamentous swellings in motor axons (Hafezparast et al., 2003; LaMonte et al., 2002).

Few years ago, a family with a slowly progressive autosomal dominant lower motor neuron disease has been linked to a mutation in the $p150^{Glued}$ subunit (G59S) of the dynactin complex (Puls et al., 2003). Neuronal expression of mutant dynactin $p150^{Glued}$, but not wild-type, caused motor neuron disease in transgenic mice (Laird et al., 2008). The disease was characterized by defects in vesicular transport in cell bodies of motor neurons, axonal swelling and axon terminal degeneration. Interestingly, evidence was provided that autophagic cell death was involved in the pathogenesis of mutant $p150^{Glued}$ transgenic mice. The mutant $p150^{Glued}$ mice share many pathological features of human sporadic ALS including ubiquitin positive inclusions, accumulations of neurofilaments and astrocytic gliosis. None of these pathological changes occurred in mice expressing human wild-type $p150^{Glued}$.

6. Animal models with TDP-43 abnormalities

The 43-kDa TAR DNA binding protein (TDP-43), localized to the nucleus, was originally identified as a component of ubiquitinated inclusions in FTLD-U and ALS (Cairns et al., 2007; Hasegawa et al., 2008; Neumann et al., 2006). TDP-43 immunoreactive inclusions were observed in the cytoplasm and nucleus of both neurons and glial cells (Cairns et al., 2007; Mackenzie et al., 2007). The brains and spinal cords of patients with TDP-43 proteinopathy present a biochemical signature that is characterized by abnormal hyper-phosphorylation and ubiquitination of TDP-43 and the production of ~25 kDa C-terminal fragments that are missing their nuclear targeting domains (Neumann et al., 2006). TDP-43 is partly cleared from the nuclei of neurons containing cytoplasmic aggregates (Neumann et al., 2006; Van Deerlin et al., 2008) supporting the notion that pathogenesis of ALS in these cases may be driven, at least in part, by loss of normal TDP-43 function in the nucleus. TDP-43 inclusions are now recognized as a common characteristic of most ALS patients (Maekawa et al., 2009; Sumi et al., 2009).

The involvement of TDP-43 with ALS cases led to the discovery of TDP-43 mutations found in ALS patients. Dominant mutations in *TARDBP*, which codes for TDP-43, were reported by several groups as a primary cause of ALS (Corrado et al., 2009; Daoud et al., 2009; Gitcho et al., 2008; Kabashi et al., 2008; Sreedharan et al., 2008; Van Deerlin et al., 2008). These studies collectively provided persuasive evidence that the aberrant form of TDP-43 can directly trigger neurodegeneration. A total of 30 different mutations is now known in 22 unrelated families (~3% of familial ALS cases) and in 29 sporadic cases of ALS (~1.5% of sporadic cases).

Mice homozygous knockout for TDP-43 are not viable. The TDP-43 deficient embryos die at 7.5 days of embryonic development thereby demonstrating the essential function of TDP-43 protein in development (Kraemer et al., 2010; Sephton et al., 2010; Wu et al., 2010). Mice heterozygous for TDP-43 disruption exhibit subtle muscle weakness with no evidence of motor neuron pathology. There is a recent report that transgenic mice expressing a mutant form of human TDP-43 (A315T mutation) under the control of prion gene

Table 2
Animal models of motor neuron disease.

Animal models	Pathological changes	References
ALS-linked SOD1 mutations		
Overexpressors of SOD1 mutants (G93A, G37R, G85R, G27X, L126Z)	Mitochondria swellings, vacuoles, SOD1 aggregates, neurofilament accumulations, motor neuron loss	(Bruijn et al., 1997, 1998; Durham et al., 1997; Johnston et al., 2000; Liu et al., 2004; Pasinelli et al., 2004; Wang et al., 2005b)
Intermediate filament disorganization		
hNF-H overexpressor	Perikaryal accumulations and axonal atrophy Altered conductivity but no neuronal loss	(Cote et al., 1993)
Mutant NF-L	Perikaryal and axonal NF accumulations No degeneration of sensory neurons but massive degeneration of spinal motor neurons	(Lee et al., 1994)
Peripherin overexpressor	Age-dependent IF aggregates in perikarya and axons 40% loss of spinal motor neurons	(Millecamps et al., 2006)
Defects in microtubule-based transport		
Dynamitin overexpressor	Abnormal gaits and decrease in strength Axonal IF swellings 25% loss of motor axons at 16 months	(LaMonte et al., 2002)
KIF1B heterozygous	Staggering gait after 1-year of age	(Zhao et al., 2001)
Knockout	Progressive muscle weakness	(Hafezparast et al., 2003; LaMonte et al., 2002)
Dynein mutations heterozygous	Progressive motor dysfunction Loss of 4–70% of motor neurons at 16 months	(Bommel et al., 2002; Martin et al., 2002)
pmn mouse	Axonal swellings and early onset motor neuron degeneration	(Laird et al., 2008)
Dynactin mouse	Defects in vesicular transport in cell bodies of motor neurons, axonal swelling and axo-terminal degeneration	
Defects in endosomal trafficking		
ALS2 knockout and of corticospinal axons	Defects of endosome trafficking, late-onset degeneration of cerebellar Purkinje cells	(Eymard-Pierre et al., 2002; Gros-Louis et al., 2003; Hadano et al., 2006; Yang et al., 2001)
ALS linked TDP-43		
Mice overexpressing A315T mutant of TDP-43	Gait abnormalities at 3 months of age and an average survival of 153 days.	(Wegorzewska et al., 2009)
Mice overexpressing wild-type TDP-43	Lack of cytoplasmic TDP-43 aggregates Dose-dependent degeneration of cortical and spinal motor neurons and subsequent development of spastic quadriplegia	(Wils et al., 2010)
Mice overexpressing wild-type as well as A315T and M337V mutants of TDP-43	Develop paralysis and death as early as 12 days	(Stallings et al., 2009)
Drosophila overexpressing wild-type TDP-43	Loss of ommatidia with signs of neurodegeneration	(Li et al., 2010)
Zebrafish overexpressing wild-type as well as A315T, G348C and A382T mutants of TDP-43	Premature and excessive motor axonal branching	(Kabashi et al., 2010)

promoter develop a progressive and fatal neurodegenerative disease (Wegorzewska et al., 2009). These mice develop gait abnormalities at 3 months of age and an average survival of 153 days (Table 2). Despite pan-neuronal transgene expression, pathologic aggregates of ubiquitinated proteins accumulated only in specific neuronal populations, including layer 5 pyramidal neurons in frontal cortex, as well as spinal motor neurons. Surprisingly, these TDP-43^{A315T} mice did not exhibit cytoplasmic TDP-43 aggregates, a feature that led to the discovery of TDP-43 as a hallmark of ALS and FTLD-U. One possible reason for the lack of cytoplasmic ubiquitinated TDP-43 inclusions could be the premature cell death resulting from excessive and non-physiological expression levels of TDP-43 transgene under the strong prion gene promoter. The authors mentioned levels of TDP-43^{A315T} in excess of 3 to 5 folds the level of endogenous mouse TDP-43 in spinal cord extracts but these are likely underestimates of levels occurring within motor neurons because transgene expression was not ubiquitously expressed like the endogenous TDP-43 gene. Thus, it is unclear to what extent the disease in these mice is the result of excessive levels of TDP-43 species. Indeed, there is a recent report that overexpression of wild-type human TDP-43 in mice caused a dose-dependent degeneration of cortical and spinal motor neurons with ensuing development of spastic quadriplegia (Wils et al., 2010). Neurons in the affected spinal cord and brain regions showed accumulation of TDP-43 nuclear and cytoplasmic aggregates that were both ubiquitinated and phosphorylated as observed in ALS/FTLD patients. However, the cytoplasmic accumulations did not contain TDP-43 like in human ALS situation. The characteristic ~25-kDa C-terminal fragments (CTFs) were recovered from nuclear fractions and correlated with disease development and progression in wild-type TDP-43 mice. Again, there is a concern with these mouse models about the excessive and neuronal-specific expression of human TDP-43 cDNA under the control of neuronal murine Thy-1 (mThy-1) promoter. Excessive levels of TDP-43 transgene expression may mask progressive and age-related pathways of higher relevance to ALS disease process. Moreover, this approach did not consider a possible role for TDP-43 in non-neuronal cell types and their contribution in disease pathology. Recently, overexpression of mutant, but not normal, TDP-43 in a rat model caused widespread neurodegeneration that predominantly affected the motor system (Zhou et al., 2010). TDP-43 mutation (M337V) reproduced ALS phenotypes in transgenic rats, as seen by progressive degeneration of motor neurons and denervation atrophy of skeletal muscles. This rat model also recapitulated features of TDP-43 proteinopathies including the formation of TDP-43 inclusions, cytoplasmic localization of phosphorylated TDP-43, and fragmentation of TDP-43 protein.

Non-rodent models have also been used to quickly and effectively model TDP-43 associated pathology. Transgenic *Drosophila* expressing human TDP-43 in various neuronal sub-populations has been used to investigate the role of wild-type TDP-43 in ALS pathogenesis (Li et al., 2010). Expression in the fly eyes of the full-length human TDP-43, but not a mutant lacking its amino-terminal domain, led to progressive loss of ommatidia with remarkable signs of neurodegeneration. Expressing TDP-43 in mushroom bodies resulted in dramatic axon losses and neuronal death. Furthermore, hTDP-43 expression in motor neurons led to axon swelling, reduction in axon branches and bouton numbers, and motor neuron loss together with functional deficits.

Zebrafish (*Danio rerio*) has been used as another model to investigate the pathogenic nature of TDP-43 mutants (A315T, G348C and A382T) (Kabashi et al., 2010). Overexpression of mutant TDP-43 species, but less so of wild-type human TDP-43 caused a motor phenotype in zebrafish embryos, consisting of shorter motor neuronal axons, premature and excessive branching as well as swimming deficits. Interestingly, knock-down of zebrafish TDP-43 led to a similar phenotype, which was rescued by co-expressing wild-type but not mutant human TDP-43. Together these approaches showed that TDP-43 mutations cause motor neuron defects and toxicity, suggesting that both a toxic gain of function as well as a novel loss of function may be involved in the molecular mechanism by which mutant TDP-43 contributes to disease pathogenesis. Nonetheless, more animal studies are needed to provide further insights into mechanisms of disease caused by TDP-43 abnormalities. It is noteworthy that wobbler mice exhibit many of the features of TDP-43 proteinopathy including cytoplasmic localization and ubiquitinated TDP-43 positive inclusions (Dennis and Citron, 2009). Moreover, there seems to be a link between TDP-43 mislocalization and abnormalities in vesicle-associated membrane protein-associated protein-B (VAPB). Transgenic mice expressing a mutant VAPB gene ($VAPB^{P56S}$) linked to a subset of familial ALS developed cytoplasmic TDP-43 accumulations within spinal cord motor neurons at 18 months of age (Tudor et al., 2010).

7. Conclusion

Despite important effort devoted in the past decade toward elucidating the mechanism of disease caused by SOD1 mutations, the neurodegeneration mechanism is still not fully understood. The SOD1 mutants cause disease through acquisition of toxicity. Yet, it is not resolved how SOD1 mutants can trigger through protein misfolding some death pathways selectivity in neuronal subsets. With the recent implication of TDP-43 in ALS and FTLD-U, there has been a boom in the reports of animal models of TDP-43. Most of the mouse models of TDP-43 reported shown early paralysis followed by death. However, these mouse models are based on high levels expression of TDP-43 transgenes that can mask age-dependent pathogenic pathways. Mice expressing either wild-type or mutant TDP-43 (A315T and M337V) showed aggressive paralysis accompanied by increased ubiquitination (Stallings et al., 2009; Wegorzewska et al., 2009; Wils et al., 2010) but the lack of ubiquitinated TDP-43 inclusions raises concerns about their validity as models of human ALS disease (Wegorzewska et al., 2009). Another concern is the restricted expression of TDP-43 species with the use of Thy1.2 and Prion promoters. Are these models based on TDP-43 transgene overexpression mimicking the human ALS disease? To better mimic the ubiquitous and moderate levels of TDP-43 occurring in the human context, it seems more appropriate to generate transgenic mice with genomic DNA fragments of TDP-43 gene including its own promoter. While different approaches are needed to reveal the mechanism of pathogenecity of TDP-43, it would be essential to critically evaluate each one of them to judge their usefulness in modeling the human disease. In any case, the transgenic studies to date are suggesting that excess TDP-43 can be neurotoxic. Thus, it would be of interest in the future to determine whether there is an upregulation of TDP-43 mRNA in motor neurons of sporadic ALS cases.

Acknowledgements

This work was supported by the Canadian Institutes of Health Research (CIHR) and the Robert Packard for ALS Research at Johns Hopkins. Vivek Swarup is a recipient of Merit Scholarship for foreign students from the Fonds québécois de la recherche sur la nature et les technologies (FQRNT). J.-P. Julien holds a Canadian Research Chair in Neurodegeneration.

References

Andersen PM. Amyotrophic lateral sclerosis associated with mutations in the CuZn superoxide dismutase gene. Curr Neurol Neurosci Rep 2006;6:37–46.
Andersen PM, Sims KB, Xin WW, Kiely R, O'Neill G, Ravits J, et al. Sixteen novel mutations in the Cu/Zn superoxide dismutase gene in amyotrophic lateral sclerosis: a decade of discoveries, defects and disputes. Amyotroph Lateral Scler Other Motor Neuron Disord 2003;4:62–73.
Audet JN, Gowing G, Julien JP. Wild-type human SOD1 overexpression does not accelerate motor neuron disease in mice expressing murine Sod1 G86R. Neurobiol Dis 2010. doi:10.1016/j.nbd.2010.05.031.
Batulan Z, Shinder GA, Minotti S, He BP, Doroudchi MM, Nalbantoglu J, et al. High threshold for induction of the stress response in motor neurons is associated with failure to activate HSF1. J Neurosci 2003;23:5789–98.
Beaulieu JM, Jacomy H, Julien JP. Formation of intermediate filament protein aggregates with disparate effects in two transgenic mouse models lacking the neurofilament light subunit. J Neurosci 2000;20:5321–8.
Beaulieu JM, Julien JP. Peripherin-mediated death of motor neurons rescued by overexpression of neurofilament NF-H proteins. J Neurochem 2003;85:248–56.
Bommel H, Xie G, Rossoll W, Wiese S, Jablonka S, Boehm T, et al. Missense mutation in the tubulin-specific chaperone E (Tbce) gene in the mouse mutant progressive motor neuronopathy, a model of human motoneuron disease. J Cell Biol 2002;159:563–9.
Bruijn LI, Becher MW, Lee MK, Anderson KL, Jenkins NA, Copeland NG, et al. ALS-linked SOD1 mutant G85R mediates damage to astrocytes and promotes rapidly progressive disease with SOD1-containing inclusions. Neuron 1997;18:327–38.
Bruijn LI, Houseweart MK, Kato S, Anderson KL, Anderson SD, Ohama E, et al. Aggregation and motor neuron toxicity of an ALS-linked SOD1 mutant independent from wild-type SOD1. Science 1998;281:1851–4.
Cai H, Lin X, Xie C, Laird FM, Lai C, Wen H, et al. Loss of ALS2 function is insufficient to trigger motor neuron degeneration in knock-out mice but predisposes neurons to oxidative stress. J Neurosci 2005;25:7567–74.
Cairns NJ, Neumann M, Bigio EH, Holm IE, Troost D, Hatanpaa KJ, et al. TDP-43 in familial and sporadic frontotemporal lobar degeneration with ubiquitin inclusions. Am J Pathol 2007;171:227–40.
Chen YZ, Bennett CL, Huynh HM, Blair IP, Puls I, Irobi J, et al. DNA/RNA helicase gene mutations in a form of juvenile amyotrophic lateral sclerosis (ALS4). Am J Hum Genet 2004;74:1128–35.
Clement AM, Nguyen MD, Roberts EA, Garcia ML, Boillee S, Rule M, et al. Wild-type nonneuronal cells extend survival of SOD1 mutant motor neurons in ALS mice. Science 2003;302:113–7.
Cleveland DW. From Charcot to SOD1: mechanisms of selective motor neuron death in ALS. Neuron 1999;24:515–20.
Corbo M, Hays AP. Peripherin and neurofilament protein coexist in spinal spheroids of motor neuron disease. J Neuropathol Exp Neurol 1992;51:531–7.
Corrado L, Ratti A, Gellera C, Buratti E, Castellotti B, Carlomagno Y, et al. High frequency of TARDBP gene mutations in Italian patients with amyotrophic lateral sclerosis. Hum Mutat 2009;30:688–94.
Cote F, Collard JF, Julien JP. Progressive neuronopathy in transgenic mice expressing the human neurofilament heavy gene: a mouse model of amyotrophic lateral sclerosis. Cell 1993;73:35–46.
Daoud H, Valdmanis PN, Kabashi E, Dion P, Dupre N, Camu W, et al. Contribution of TARDBP mutations to sporadic amyotrophic lateral sclerosis. J Med Genet 2009;46:112–4.
Deng HX, Jiang H, Fu R, Zhai H, Shi Y, Liu E, et al. Molecular dissection of ALS-associated toxicity of SOD1 in transgenic mice using an exon-fusion approach. Hum Mol Genet 2008;17:2310–9.
Deng HX, Shi Y, Furukawa Y, Zhai H, Fu R, Liu E, et al. Conversion to the amyotrophic lateral sclerosis phenotype is associated with intermolecular linked insoluble aggregates of SOD1 in mitochondria. Proc Natl Acad Sci USA 2006;103:7142–7.
Dennis JS, Citron BA. Wobbler mice modeling motor neuron disease display elevated transactive response DNA binding protein. Neuroscience 2009;158:745–50.
Devon RS, Orban PC, Gerrow K, Barbieri MA, Schwab C, Cao LP, et al. Als2-deficient mice exhibit disturbances in endosome trafficking associated with motor behavioral abnormalities. Proc Natl Acad Sci USA 2006;103:9595–600.
Durham HD, Roy J, Dong L, Figlewicz DA. Aggregation of mutant Cu/Zn superoxide dismutase proteins in a culture model of ALS. J Neuropathol Exp Neurol 1997;56:523–30.
Eymard-Pierre E, Lesca G, Dollet S, Santorelli FM, di Capua M, Bertini E, et al. Infantile-onset ascending hereditary spastic paralysis is associated with mutations in the alsin gene. Am J Hum Genet 2002;71:518–27.
Gitcho MA, Baloh RH, Chakraverty S, Mayo K, Norton JB, Levitch D, et al. TDP-43 A315T mutation in familial motor neuron disease. Ann Neurol 2008;63:535–8.
Greenway MJ, Andersen PM, Russ C, Ennis S, Cashman S, Donaghy C, et al. ANG mutations segregate with familial and 'sporadic' amyotrophic lateral sclerosis. Nat Genet 2006;38:411–3.
Gros-Louis F, Kriz J, Kabashi E, McDearmid J, Millecamps S, Urushitani M, et al. Als2 mRNA splicing variants detected in KO mice rescue severe motor dysfunction phenotype in Als2 knock-down zebrafish. Hum Mol Genet 2008;17:2691–702.
Gros-Louis F, Meijer IA, Hand CK, Dube MP, MacGregor DL, Seni MH, et al. An ALS2 gene mutation causes hereditary spastic paraplegia in a Pakistani kindred. Ann Neurol 2003;53:144–5.
Gros-Louis F, Soucy G, Lariviere R, Julien JP. Intracerebroventricular infusion of monoclonal antibody or its derived Fab fragment against misfolded forms of SOD1 mutant delays mortality in a mouse model of ALS. J Neurochem 2010;113:1188–99.

Gurney ME, Pu H, Chiu AY, Dal Canto MC, Polchow CY, Alexander DD, et al. Motor neuron degeneration in mice that express a human Cu, Zn superoxide dismutase mutation. Science 1994;264:1772–5.

Hadano S, Benn SC, Kakuta S, Otomo A, Sudo K, Kunita R, et al. Mice deficient in the Rab5 guanine nucleotide exchange factor ALS2/alsin exhibit age-dependent neurological deficits and altered endosome trafficking. Hum Mol Genet 2006;15:233–50.

Hadano S, Hand CK, Osuga H, Yanagisawa Y, Otomo A, Devon RS, et al. A gene encoding a putative GTPase regulator is mutated in familial amyotrophic lateral sclerosis 2. Nat Genet 2001;29:166–73.

Hafezparast M, Klocke R, Ruhrberg C, Marquardt A, Ahmad-Annuar A, Bowen S, et al. Mutations in dynein link motor neuron degeneration to defects in retrograde transport. Science 2003;300:808–12.

Hasegawa M, Arai T, Nonaka T, Kametani F, Yoshida M, Hashizume Y, et al. Phosphorylated TDP-43 in frontotemporal lobar degeneration and amyotrophic lateral sclerosis. Ann Neurol 2008;64:60–70.

Hirano A, Nakano I, Kurland LT, Mulder DW, Holley PW, Saccomanno G. Fine structural study of neurofibrillary changes in a family with amyotrophic lateral sclerosis. J Neuropathol Exp Neurol 1984;43:471–80.

Jaarsma D, Teuling E, Haasdijk ED, De Zeeuw CI, Hoogenraad CC. Neuron-specific expression of mutant superoxide dismutase is sufficient to induce amyotrophic lateral sclerosis in transgenic mice. J Neurosci 2008;28:2075–88.

Johnston JA, Dalton MJ, Gurney ME, Kopito RR. Formation of high molecular weight complexes of mutant Cu, Zn-superoxide dismutase in a mouse model for familial amyotrophic lateral sclerosis. Proc Natl Acad Sci USA 2000;97:12571–6.

Jonsson PA, Graffmo KS, Andersen PM, Brannstrom T, Lindberg M, Oliveberg M, et al. Disulphide-reduced superoxide dismutase-1 in CNS of transgenic amyotrophic lateral sclerosis models. Brain 2006;129:451–64.

Kabashi E, Lin L, Tradewell ML, Dion PA, Bercier V, Bourgouin P, et al. Gain and loss of function of ALS-related mutations of TARDBP (TDP-43) cause motor deficits in vivo. Hum Mol Genet 2010;19:671–83.

Kabashi E, Valdmanis PN, Dion P, Spiegelman D, McConkey BJ, Vande Velde C, et al. TARDBP mutations in individuals with sporadic and familial amyotrophic lateral sclerosis. Nat Genet 2008;40:572–4.

Kraemer BC, Schuck T, Wheeler JM, Robinson LC, Trojanowski JQ, Lee VM, et al. Loss of murine TDP-43 disrupts motor function and plays an essential role in embryogenesis. Acta Neuropathol 2010.

Kwiatkowski Jr TJ, Bosco DA, Leclerc AL, Tamrazian E, Vanderburg CR, Russ C, et al. Mutations in the FUS/TLS gene on chromosome 16 cause familial amyotrophic lateral sclerosis. Science 2009;323:1205–8.

Laird FM, Farah MH, Ackerley S, Hoke A, Maragakis N, Rothstein JD, et al. Motor neuron disease occurring in a mutant dynactin mouse model is characterized by defects in vesicular trafficking. J Neurosci 2008;28:1997–2005.

LaMonte BH, Wallace KE, Holloway BA, Shelly SS, Ascano J, Tokito M, et al. Disruption of dynein/dynactin inhibits axonal transport in motor neurons causing late-onset progressive degeneration. Neuron 2002;34:715–27.

Lee MK, Marszalek JR, Cleveland DW. A mutant neurofilament subunit causes massive, selective motor neuron death: implications for the pathogenesis of human motor neuron disease. Neuron 1994;13:975–88.

Li Y, Ray P, Rao EJ, Shi C, Guo W, Chen X, et al. A Drosophila model for TDP-43 proteinopathy. Proc Natl Acad Sci USA 2010;107:3169–74.

Lino MM, Schneider C, Caroni P. Accumulation of SOD1 mutants in postnatal motoneurons does not cause motoneuron pathology or motoneuron disease. J Neurosci 2002;22:4825–32.

Liu J, Lillo C, Jonsson PA, Vande Velde C, Ward CM, Miller TM, et al. Toxicity of familial ALS-linked SOD1 mutants from selective recruitment to spinal mitochondria. Neuron 2004;43:5–17.

Mackenzie IR, Bigio EH, Ince PG, Geser F, Neumann M, Cairns NJ, et al. Pathological TDP-43 distinguishes sporadic amyotrophic lateral sclerosis from amyotrophic lateral sclerosis with SOD1 mutations. Ann Neurol 2007;61:427–34.

Maekawa S, Leigh PN, King A, Jones E, Steele JC, Bodi I, et al. TDP-43 is consistently co-localized with ubiquitinated inclusions in sporadic and Guam amyotrophic lateral sclerosis but not in familial amyotrophic lateral sclerosis with and without SOD1 mutations. Neuropathology 2009.

Martin N, Jaubert J, Gounon P, Salido E, Haase G, Szatanik M, et al. A missense mutation in Tbce causes progressive motor neuronopathy in mice. Nat Genet 2002;32:443–7.

Millecamps S, Robertson J, Lariviere R, Mallet J, Julien JP. Defective axonal transport of neurofilament proteins in neurons overexpressing peripherin. J Neurochem 2006;98:926–38.

Neumann M, Sampathu DM, Kwong LK, Truax AC, Micsenyi MC, Chou TT, et al. Ubiquitinated TDP-43 in frontotemporal lobar degeneration and amyotrophic lateral sclerosis. Science 2006;314:130–3.

Nishimura AL, Mitne-Neto M, Silva HC, Richieri-Costa A, Middleton S, Cascio D, et al. A mutation in the vesicle-trafficking protein VAPB causes late-onset spinal muscular atrophy and amyotrophic lateral sclerosis. Am J Hum Genet 2004;75:822–31.

Pasinelli P, Belford ME, Lennon N, Bacskai BJ, Hyman BT, Trotti D, et al. Amyotrophic lateral sclerosis-associated SOD1 mutant proteins bind and aggregate with Bcl-2 in spinal cord mitochondria. Neuron 2004;43:19–30.

Pramatarova A, Laganiere J, Roussel J, Brisebois K, Rouleau GA. Neuron-specific expression of mutant superoxide dismutase 1 in transgenic mice does not lead to motor impairment. J Neurosci 2001;21:3369–74.

Puls I, Jonnakuty C, LaMonte BH, Holzbaur EL, Tokito M, Mann E, et al. Mutant dynactin in motor neuron disease. Nat Genet 2003;33:455–6.

Raoul C, Estevez AG, Nishimune H, Cleveland DW, deLapeyriere O, Henderson CE, et al. Motoneuron death triggered by a specific pathway downstream of Fas. potentiation by ALS-linked SOD1 mutations. Neuron 2002;35:1067–83.

Reaume AG, Elliott JL, Hoffman EK, Kowall NW, Ferrante RJ, Siwek DF, et al. Motor neurons in Cu/Zn superoxide dismutase-deficient mice develop normally but exhibit enhanced cell death after axonal injury. Nat Genet 1996;13:43–7.

Reid E, Kloos M, Ashley-Koch A, Hughes L, Bevan S, Svenson IK, et al. A kinesin heavy chain (KIF5A) mutation in hereditary spastic paraplegia (SPG10). Am J Hum Genet 2002;71:1189–94.

Rosen DR, Siddique T, Patterson D, Figlewicz DA, Sapp P, Hentati A, et al. Mutations in Cu/Zn superoxide dismutase gene are associated with familial amyotrophic lateral sclerosis. Nature 1993;362:59–62.

Saxena S, Cabuy E, Caroni P. A role for motoneuron subtype-selective ER stress in disease manifestations of FALS mice. Nat Neurosci 2009;12:627–36.

Schroer TA. Dynactin. Annu Rev Cell Dev Biol 2004;20:759–79.

Sephton CF, Good SK, Atkin S, Dewey CM, Mayer 3rd P, Herz J, et al. TDP-43 is a developmentally regulated protein essential for early embryonic development. J Biol Chem 2010;285:6826–34.

Sreedharan J, Blair IP, Tripathi VB, Hu X, Vance C, Rogelj B, et al. TDP-43 mutations in familial and sporadic amyotrophic lateral sclerosis. Science 2008;319:1668–72.

Stallings NR, Puttaparthi K, Luther CM, Elliott JL. Generation and characterization of wild-type and mutant TDP-43 transgenic mice. Abstract Book. Society For Neuroscience; 2009.

Subramaniam JR, Lyons WE, Liu J, Bartnikas TB, Rothstein J, Price DL, et al. Mutant SOD1 causes motor neuron disease independent of copper chaperone-mediated copper loading. Nat Neurosci 2002;5:301–7.

Sumi H, Kato S, Mochimaru Y, Fujimura H, Etoh M, Sakoda S. Nuclear TAR DNA binding protein 43 expression in spinal cord neurons correlates with the clinical course in amyotrophic lateral sclerosis. J Neuropathol Exp Neurol 2009;68:37–47.

Tudor EL, Galtrey CM, Perkinton MS, Lau KF, De Vos KJ, Mitchell JC, et al. Amyotrophic lateral sclerosis mutant vesicle-associated membrane protein-associated protein-B transgenic mice develop TAR-DNA-binding protein-43 pathology. Neuroscience 2010;167:774–85.

Urushitani M, Ezzi SA, Julien JP. Therapeutic effects of immunization with mutant superoxide dismutase in mice models of amyotrophic lateral sclerosis. Proc Natl Acad Sci USA 2007;104:2495–500.

Urushitani M, Ezzi SA, Matsuo A, Tooyama I, Julien JP. The endoplasmic reticulum–Golgi pathway is a target for translocation and aggregation of mutant superoxide dismutase linked to ALS. FASEB J 2008;22:2476–87.

Urushitani M, Kurisu J, Tsukita K, Takahashi R. Proteasomal inhibition by misfolded mutant superoxide dismutase 1 induces selective motor neuron death in familial amyotrophic lateral sclerosis. J Neurochem 2002;83:1030–42.

Van Deerlin VM, Leverenz JB, Bekris LM, Bird TD, Yuan W, Elman LB, et al. TARDBP mutations in amyotrophic lateral sclerosis with TDP-43 neuropathology: a genetic and histopathological analysis. Lancet Neurol 2008;7:409–16.

Vance C, Rogelj B, Hortobagyi T, De Vos KJ, Nishimura AL, Sreedharan J, et al. Mutations in FUS, an RNA processing protein, cause familial amyotrophic lateral sclerosis type 6. Science 2009;323:1208–11.

Wang J, Farr GW, Zeiss CJ, Rodriguez-Gil DJ, Wilson JH, Furtak K, et al. Progressive aggregation despite chaperone associations of a mutant SOD1-YFP in transgenic mice that develop ALS. Proc Natl Acad Sci USA 2009;106:1392–7.

Wang J, Xu G, Gonzales V, Coonfield M, Fromholt D, Copeland NG, et al. Fibrillar inclusions and motor neuron degeneration in transgenic mice expressing superoxide dismutase 1 with a disrupted copper-binding site. Neurobiol Dis 2002;10:128–38.

Wang J, Xu G, Li H, Gonzales V, Fromholt D, Karch C, et al. Somatodendritic accumulation of misfolded SOD1-L126Z in motor neurons mediates degeneration: alphaB-crystallin modulates aggregation. Hum Mol Genet 2005a;14:2335–47.

Wang J, Xu G, Slunt HH, Gonzales V, Coonfield M, Fromholt D, et al. Coincident thresholds of mutant protein for paralytic disease and protein aggregation caused by restrictively expressed superoxide dismutase cDNA. Neurobiol Dis 2005b;20:943–52.

Wegorzewska I, Bell S, Cairns NJ, Miller TM, Baloh RH. TDP-43 mutant transgenic mice develop features of ALS and frontotemporal lobar degeneration. Proc Natl Acad Sci USA 2009;106:18809–14.

Wils H, Kleinberger G, Janssens J, Pereson S, Joris G, Cuijt I, et al. TDP-43 transgenic mice develop spastic paralysis and neuronal inclusions characteristic of ALS and frontotemporal lobar degeneration. Proc Natl Acad Sci USA 2010;107:3858–63.

Wu LS, Cheng WC, Hou SC, Yan YT, Jiang ST, Shen CK. TDP-43, a neuro-pathosignature factor, is essential for early mouse embryogenesis. Genesis 2010;48:56–62.

Xia CH, Roberts EA, Her LS, Liu X, Williams DS, Cleveland DW, et al. Abnormal neurofilament transport caused by targeted disruption of neuronal kinesin heavy chain KIF5A. J Cell Biol 2003;161:55–66.

Xiao S, Tjostheim S, Sanelli T, McLean JR, Horne P, Fan Y, et al. An aggregate-inducing peripherin isoform generated through intron retention is upregulated in amyotrophic lateral sclerosis and associated with disease pathology. J Neurosci 2008;28:1833–40.

Yamanaka K, Boillee S, Roberts EA, Garcia ML, McAlonis-Downes M, Mikse OR, et al. Mutant SOD1 in cell types other than motor neurons and oligodendrocytes accelerates onset of disease in ALS mice. Proc Natl Acad Sci USA 2008;105:7594–9.

Yang Y, Hentati A, Deng HX, Dabbagh O, Sasaki T, Hirano M, et al. The gene encoding alsin, a protein with three guanine-nucleotide exchange factor domains, is mutated in a form of recessive amyotrophic lateral sclerosis. Nat Genet 2001;29:160–5.

Zhao C, Takita J, Tanaka Y, Setou M, Nakagawa T, Takeda S, et al. Charcot-Marie-Tooth disease type 2A caused by mutation in a microtubule motor KIF1Bbeta. Cell 2001;105:587–97.

Zhou H, Huang C, Chen H, Wang D, Landel CP, Xia PY, et al. transgenic rat model of neurodegeneration caused by mutation in the TDP gene. PLoS Genet 2010;6:e1000887.

Pathological hallmarks of amyotrophic lateral sclerosis/frontotemporal lobar degeneration in transgenic mice produced with TDP-43 genomic fragments

Brain Advance Access published July 13, 2011

doi:10.1093/brain/awr159 Brain 2011: Page 1 of 17 | 1

BRAIN
A JOURNAL OF NEUROLOGY

Pathological hallmarks of amyotrophic lateral sclerosis/frontotemporal lobar degeneration in transgenic mice produced with TDP-43 genomic fragments

Vivek Swarup,[1] Daniel Phaneuf,[1] Christine Bareil,[1] Janice Robertson,[2] Guy A. Rouleau,[3] Jasna Kriz[1] and Jean-Pierre Julien[1]

1 Centre de Recherche du Centre Hospitalier Universitaire de Québec, Department of Psychiatry and Neuroscience of Laval University, Québec, QC G1V 4G2, Canada
2 Department of Laboratory Medicine and Pathobiology, Centre for Research in Neurodegenerative Diseases, University of Toronto, Tanz Neuroscience Building, Toronto, ON M5S 3H2, Canada
3 Ste-Justine Hospital Research Center and Department of Medicine, University of Montreal, 3175 Cote Ste-Catherine, Montreal, Quebec H3T 1C5, Canada

Correspondence to: Dr Jean-Pierre Julien,
Centre de Recherche du Centre Hospitalier Universitaire de Québec,
Pavillon CHUL,
2705 Boulevard Laurier,
Quebec,
QC G1V 4G2, Canada
E-mail: jean-pierre.julien@crchul.ulaval.ca

Correspondence may also be addressed to: Dr Jasna Kriz. E-mail: jasna.kriz@crchul.ulaval.ca

Transactive response DNA-binding protein 43 ubiquitinated inclusions are a hallmark of amyotrophic lateral sclerosis and of frontotemporal lobar degeneration with ubiquitin-positive inclusions. Yet, mutations in *TARDBP*, the gene encoding these inclusions are associated with only 3% of sporadic and familial amyotrophic lateral sclerosis. Recent transgenic mouse studies have revealed a high degree of toxicity due to transactive response DNA-binding protein 43 proteins when overexpressed under the control of strong neuronal gene promoters, resulting in early paralysis and death, but without the presence of amyotrophic lateral sclerosis-like ubiquitinated transactive response DNA-binding protein 43-positive inclusions. To better mimic human amyotrophic lateral sclerosis, we generated transgenic mice that exhibit moderate and ubiquitous expression of transactive response DNA-binding protein 43 species using genomic fragments that encode wild-type human transactive response DNA-binding protein 43 or familial amyotrophic lateral sclerosis-linked mutant transactive response DNA-binding protein 43 (G348C) and (A315T). These novel transgenic mice develop many age-related pathological and biochemical changes reminiscent of human amyotrophic lateral sclerosis including ubiquitinated transactive response DNA-binding protein 43-positive inclusions, transactive response DNA-binding protein 43 cleavage fragments, intermediate filament abnormalities, axonopathy and neuroinflammation. All three transgenic mouse models (wild-type, G348C and A315T) exhibited impaired learning and memory capabilities during ageing, as well as motor dysfunction. Real-time imaging with the use of biophotonic transactive response DNA-binding protein 43 transgenic mice carrying a glial fibrillary acidic protein-luciferase reporter revealed that the behavioural defects were preceded by induction of astrogliosis, a finding consistent with a role for reactive astrocytes in amyotrophic lateral sclerosis pathogenesis. These novel transactive response DNA-binding protein 43 transgenic mice mimic several characteristics

Received January 26, 2011. Revised June 2, 2011. Accepted June 5, 2011.

of human amyotrophic lateral sclerosis-frontotemporal lobar degeneration and they should provide valuable animal models for testing therapeutic approaches.

Keywords: amyotrophic lateral sclerosis; motor neuron; neurodegeneration; TDP-43; inclusions

Abbreviations: FTLD-U = frontotemporal lobar degeneration with ubiquitin inclusions; GFAP = glial fibrillary acidic protein; luc = luciferase; PCR = polymerase chain reaction; TDP-43 = transactive response DNA-binding protein 43

Introduction

Amyotrophic lateral sclerosis is an adult-onset neurological disorder that is characterized by the selective loss of motor neurons leading to progressive weakness and muscle atrophy with eventual paralysis and death within 5 years of clinical onset. Frontotemporal lobar degeneration with ubiquitin inclusions (FTLD-U) is a relatively common cause of dementia among patients with onset before the age of 65, typically manifesting with behavioural changes or language impairment due to degeneration of subpopulations of cortical neurons in the frontal, temporal and insular regions (Seeley, 2008). Interestingly, 50% of patients with amyotrophic lateral sclerosis develop varying degrees of cognitive impairment (Lomen-Hoerth *et al.*, 2003), and ~15% of patients with FLTD-U also develop amyotrophic lateral sclerosis (Hodges *et al.*, 2004) and these two diseases co-segregate in some families (Talbot and Ansorge, 2006). The discovery that transactive response DNA-binding protein 43 (TDP-43) is present in cytoplasmic aggregates both in amyotrophic lateral sclerosis and FTLD-U provided the first conclusive molecular evidence that the two disorders share a common underlying mechanism (Neumann *et al.*, 2006).

Identified first as a regulator of HIV gene expression (Ou *et al.*, 1995), TDP-43 is a DNA/RNA-binding (Buratti *et al.*, 2001) protein that contains an N-terminal domain, two RNA-recognition motifs and a glycine-rich C-terminal domain thought to be important for mediating protein–protein interactions (Forman *et al.*, 2007; Lagier-Tourenne and Cleveland, 2009). Although TDP-43 has been implicated as a key factor regulating RNA splicing of human cystic fibrosis transmembrane conductance regulator (Buratti *et al.*, 2001), apolipoprotein A-II (Mercado *et al.*, 2005) and survival motor neuron protein (Bose *et al.*, 2008), the concept that TDP-43 can play a direct role in neurodegeneration was strengthened by recent reports that dominantly inherited missense mutations in TDP-43 are found in patients with familial amyotrophic lateral sclerosis (Gitcho *et al.*, 2008; Kabashi *et al.*, 2008; Rutherford *et al.*, 2008; Sreedharan *et al.*, 2008; Van Deerlin *et al.*, 2008; Yokoseki *et al.*, 2008). Mutations in TDP-43 are associated with the amyotrophic lateral sclerosis cluster in the C-terminal glycine-rich region, which is involved in protein–protein interactions between TDP-43 and other heterogeneous nuclear ribonuclear proteins (Lagier-Tourenne and Cleveland, 2009). The two TDP-43 mutations used in this study, A315T and G348C, have previously been reported (Gitcho *et al.*, 2008; Kabashi *et al.*, 2008). In neurodegenerative diseases, TDP-43 can be found in cytoplasmic ubiquitinated inclusions, where the protein is poorly soluble, hyperphosphorylated and cleaved into small fragments, making TDP-43 aggregates a hallmark pathology of amyotrophic lateral sclerosis and FTLD-U cases (Neumann *et al.*, 2006). Many of the transgenic mouse lines expressing wild-type or mutant TDP-43 reported to date have exhibited early paralysis followed by death (Wegorzewska *et al.*, 2009; Stallings *et al.*, 2010; Wils *et al.*, 2010). The available TDP-43 transgenic mouse models are based on high-level neuronal expression of TDP-43 transgenes. Transgenic mice expressing either wild-type or mutant TDP-43 (A315T and M337V) showed aggressive paralysis accompanied by increased ubiquitination (Stallings *et al.*, 2010; Wegorzewska *et al.*, 2009; Wils *et al.*, 2010; Xu *et al.*, 2010) but the lack of ubiquitinated TDP-43 inclusions raises concerns about their validity as models of human amyotrophic lateral sclerosis (Wegorzewska *et al.*, 2009). Another concern is the restricted expression of TDP-43 species with the use of Thy1.2 and prion promoters.

To better mimic the ubiquitous and moderate levels of TDP-43 occurring in the human context, we describe here the generation of new transgenic mouse models of amyotrophic lateral sclerosis/FTLD based on the expression of genomic TDP-43 fragments resulting in moderate and ubiquitous expression of wild-type and mutant TDP-43 species (A315T and G348C).

Materials and methods

DNA constructs and generation of wild-type, A315T and G348C TDP-43 transgenic mice

TARDBP (NM_007375) was amplified by polymerase chain reaction (PCR) from a human bacterial artificial chromosome clone (clone RPCI-11, number 829B14) along with the endogenous promoter (~4 kb). A315T and G348C mutations in TDP-43 were inserted using site-directed mutagenesis (Supplementary Fig. 1). The full-length genomic *TARDBP* (wild-type TDP-43, TDP-43^{A315T} and TDP-43^{G348C}) was linearized by Swa1 restriction enzyme and an 18-kb DNA fragment microinjected into 1-day-old mouse embryos (having a background of C3H X C57Bl/6). Founders were identified by Southern blotting (Supplementary Fig. 1) and were bred with non-transgenic C57Bl/6 mice to establish stable transgenic lines. The transgenic mice were identified by PCR amplification of the human *TARDBP* gene using the primer pairs listed in Table 1. The messenger RNA was analysed in brain and spinal cord by real-time PCR and protein analysed by western blot using monoclonal human TDP-43 antibody (Clone E2-D3, Abnova). To avoid the effects of genetic background, all experiments were performed on age-matched littermates. The use and maintenance of the mice described in this article were performed

Table 1 Primers for genotyping transgenic mice

Gene symbol	Forward primer	Reverse primer
Wild-type TDP-43	CTCTTTGTGGAGAGGAC	CCCCAACTGCTCTGTAG
TDP-43^{A315T}	CTCTTTGTGGAGAGGAC	TTATTACCCGATGGGCA
TDP-43^{G348C}	CTCTTTGTGGAGAGGAC	GGATTAATGCTGAACGT
GFAP-luc	GAAATGTCCGTTCGGTTGGCAGAAGC	CCAAAACCGTGATGGAATGGAACAACA

in accordance to the Guide of Care and Use of Experimental Animals of the Canadian Council on Animal Care.

Co-immunoprecipitation and western blot assays

Snap-frozen spinal cords of mice were harvested with lysis buffer containing 25 mM HEPES–NaOH (pH 7.9), 150 mM NaCl, 1.5 mM $MgCl_2$, 0.2 mM ethylenediaminetetraacetic acid, 0.5% Triton-X100, 1 mM dithiothreitol and protease inhibitor cocktail. Protein samples were estimated using the Bradford method. The lysate was incubated with 50 µl of Dynabeads (Protein-G beads, Invitrogen), anti-TDP-43 polyclonal (ProteinTech) or anti-peripherin polyclonal antibody (AB1530, Chemicon). After subsequent washing, the beads were incubated overnight at 4°C with 400 µg of tissue lysate. Antibody-bound complexes were eluted by boiling in Laemmli sample buffer. Supernatants were resolved by 10% sodium dodecyl sulphate polyacrylamide gel electrophoresis and transferred onto nitrocellulose membrane (Biorad). The membrane was incubated with anti-ubiquitin antibody (1:1000, Abcam). For other western blot assays, blots were incubated with primary antibodies against human monoclonal transactive response DNA-binding protein antibody (1:1000, Abnova, clone E2-D3), peripherin polyclonal antibody (1:1000, Chemcion, AB1530), peripherin monoclonal antibody (1:500, Chemicon, AB1527), Clone NR4 for light molecular weight neurofilament protein (1:1000, Sigma), Clone NN18 for medium molecular weight neurofilament protein (1:1000, Millipore) and Clone N52 for heavy molecular weight neurofilament protein (1:1000, Millipore). Immunoreactive proteins were then visualized by chemiluminescence (Perkin and Elmer) as described previously (Dequen *et al.*, 2008). Actin (1:10000, Chemicon) was used as a loading control.

Immunohistochemistry/ immunofluorescence microscopy

Paraformaldehyde (4%) fixed spinal cord and brain sections of mice were sectioned and fixed on slides. For immunohistochemistry, tissues were treated with hydrogen peroxide solution before permeabilization. After blocking with 5% normal goat serum for 1 h at room temperature, primary antibody incubations were performed in 1% normal goat serum in phosphate buffered solution with Tween-20 overnight, followed by an appropriate Alexa Fluor 488 or 594 secondary antibody (1:500, Invitrogen) for 1 h at room temperature. For immunohistochemistry, tissues were incubated in biotinylated secondary antibodies (1:500, Vector Labs), incubated in avidin–biotin complex and developed using DAB Kit (Vector labs). *Z*-stacked sections were viewed using ×40 or ×60 oil immersion objectives on an Olympus Fluoview™ Confocal System (Olympus).

Neurofilament enzyme-linked immunosorbent assay

Wells of microtitre plates were coated with 0.1% NaN_3/Tris-buffered saline including the primary antibodies (NR4; 1:600, N52; 1:1000, NN18; 1:500). The coated wells were incubated with 10% normal goat serum/0.2% Tween 20/Tris-buffered saline for 30 min at 37°C. After washing twice with Tris-buffered saline, an aliquot (100 µl) of the diluted samples was placed in each well and incubated overnight at 4°C. Further enzyme-linked immunosorbent assays were performed using standard procedure as described elsewhere (Noto *et al.*, 2010).

Quantitative real-time reverse transcription polymerase chain reaction

Real-time reverse transcription PCR was performed with a LightCycler 480 (Roche Diagnostics) sequence detection system using LightCycler SYBR Green I at the Quebec genomics Centre. Total RNA was extracted from frozen spinal cord or brain tissues using TRIzol® reagent (Invitrogen). Total RNA was treated with DNase (Qiagen) to get rid of genomic DNA contaminations. Total RNA was then quantified using a NanoDrop spectrophotometer and its purity verified by Bioanalyzer 2100 (Agilent Technologies). Gene-specific primers were constructed using the GeneTools (Biotools Inc.) software v.3. Genes *Atp5* and *GAPDH* were used as internal controls. The primers used for the analysis of genes are given in Table 2. The presence of glial fibrillary acidic protein (GFAP)-luciferase (luc) transgene was assessed by PCR with HotStar Taq Mastermix Kit (Quiagen, Mississauga, ON, Canada) in 15 mM $MgCl_2$ PCR buffer with the following primers: 5′GAAATGTCCGTTCGGTTGGCAGAAGC and 5′CCAAAACCGTGATGGAATGGAACAACA (Keller *et al.*, 2009, 2010).

Barnes maze task

For spatial learning test, the Barnes maze task was performed as described previously (Prut *et al.*, 2007). The animals were subjected to four trials per session with an intertrial interval of 15 min. The probe trial takes 90 s (half of the time used for the training trials) per mouse. Twelve days after the first probe, trial mice are tested again in a second probe trial that takes 90 s per mouse. Mice are not tested between the two probe trials. The time taken by the individual mice to reach the platform was recorded as the primary latency period using video tracking software (ANY-maze).

Step-through passive avoidance test

A two-compartment step-through passive avoidance apparatus (Ugo Basile) was used. The apparatus is divided into bright and dark compartments by a wall with a guillotine door. The bright compartment was illuminated by a fluorescent light (8 W). Mice at various ages were

Table 2 Primers for quantitative real-time PCR

Gene symbol	Forward primer sequences	Reverse primer sequences
Tumour necrosis factor-α	CCAGACCCTCACACTCAGATCATC	CCTTGAAGAGAACCTGGGAGTAGAC
Interleukin-6	GTCCTTCCTACCCCAATTTCCAA	GAATGTCCACAAACTGATATGCTTAGG
Interleukin-1β	GCCCATCCTCTGTGACTCAT	CGACAAAATACCTGTGGCCT
Nox2	TTGGAATTGCAGATGAGGAAGCGAG	CGATCCTGGGCATTGGTGAGT
Interleukin-4	AGATCATCGGCATTTTGAACGAGG	CACTCTCTGTGGTGTTCTTCGTTG
Interleukin-2	CAGCAGCAGCAGCAGCAGCAGC	CCTGGGGAGTTTCAGGTTCCTGTAAT
MCP-1	CCAGATGCAGTTAACGCCCCACTCACCT	TGCTGGTGATCCTCTTGTAGCTCTCCA
Per61	AGAGGAGTGGTATAAGTCGAAATATGC	CCCATCCACCTCGCACATCAG
Per58	TGGCCCTGGACATCGAGATAG	GCTCCATCTCAGGCACAGTCG
Per56	GGATCTCAGTGCCGGTTCATT	GGACTCTGTCACCACCTCCC
Human TDP-43	TTGACCCTTTTGAGATGGAACTTT	ATTTGACTTGAGACAACTTTTCAAATAAGT
Mouse TDP-43	ATTTGAGTCTCCAGGTGGGTGTGG	GTTTCACTATACCCAGCCCACTTTTCTTAGG
Atp5	GCTATGCAACCGCCCTGTACTCTG	ACGGTGCGCTTGATGTAGGGATTC
GAPDH	GGCTGCCCAGAACATCATCCCT	ATGCCTGCTTCACCACCTTCTTG

placed in the bright compartment and allowed to explore for 30 s, at which point the guillotine door was raised to allow the mice to enter the dark compartment. When the mice entered the dark compartment, the guillotine door was closed and an electrical foot shock (0.6 mA) was delivered for 4 s on the second day. On the test (third) day, mice were placed in the bright compartment, no shock was given, and their delay in latency to enter the dark compartment was recorded. The procedure was repeated every month to test the mice at different ages.

Neuromuscular junction staining and count

For monitoring the neuromuscular junctions, 25 mm thick muscle sections were incubated for 1 h in 0.1 M glycine in phosphate buffered saline for 2 h at room temperature and then stained with Alexa Fluor 594-conjugated α-bungarotoxin (1:2000, Molecular Probes/Invitrogen Detection Technologies) diluted in 3% bovine serum albumin in phosphate buffered saline for 3 h at room temperature. After washing in phosphate buffered saline, the muscle sections were blocked in 3% bovine serum albumin, 10% goat serum and 0.5% Triton X-100 in phosphate buffered saline overnight at 48°C. The next day, the sections were incubated with mouse anti-neurofilament antibody 160 K (1:2000, Temecula) and mouse anti-synaptophysin (Dako) in the same blocking solution overnight at 48°C. After washing for 5 h, muscle sections were incubated with goat anti-mouse Alexa Fluor 488-conjugated secondary antibody (Probes/Invitrogen Detection Technologies) diluted 1:500 in blocking buffer for 3 h at room temperature. Three hundred neuromuscular junctions were counted per animal sample, discriminating both innervated and denervated junctions as described above. Frequencies of innervation, partial denervation and denervation were then converted to percentages for statistical analyses ($n = 5$, two-way ANOVA with Bonferroni post-test).

Accelerating rotarod

Accelerating rotarod was performed on mice at 4 rpm speed with 0.25 rpm/s acceleration as described elsewhere (Gros-Louis *et al.*, 2008). Mice were subjected to three trials per session and every 2 weeks.

In vivo bioluminescence imaging

As previously described (Keller *et al.*, 2009, 2010), the images were gathered using IVIS® 200 Imaging System (CaliperLS, Xenogen). Twenty-five minutes prior to the imaging session, the mice received intraperitoneal injection of the luciferase substrate D-luciferine [150 mg/kg for mice between 20 and 25 g; 150–187.5 ml of a solution of 20 mg/ml of D-luciferine dissolved in 0.9% saline was injected (CaliperLS, Xenogen)].

Statistical analysis

For statistical analysis, the data obtained from independent experiments are presented as the mean ± SEM. A two-way ANOVA with repeated measures was used to study the effect of group (transgenic and non-transgenic mice) and time (in months or weeks) on latency to fall (accelerating rotarod test), latency to go to the dark chamber (passive avoidance test), primary errors and primary latency (Barnes maze test). Two-way ANOVA with repeated measures was also used for axonal calibre distribution and total flux of photons for *in vivo* imaging. The mixed procedure of the SAS software version 9.2 (SAS Institute Inc.) was used with a repeated statement and covariance structure that minimize the Akaike information criterion. The method of Kenward–Roger was used to calculate degrees of freedom. Pairwise comparisons were made using Bonferroni adjustment. A one-way ANOVA was performed using GraphPad Prism software version 5.0 for real-time inflammation array, real-time reverse transcription PCR and neurofilament enzyme-linked immunosorbent analysis. *Post hoc* comparisons were performed by Tukey's test, with a statistical significance of $P < 0.05$.

Results

Generation of transgenic mice carrying genomic TDP-43 fragments

We generated three transgenic mouse models using genomic DNA fragments coding for either wild-type TDP-43, TDP-43^{A315T} or TDP-43^{G348C} carrying mutations linked to human familial

amyotrophic lateral sclerosis (Kabashi *et al.*, 2008). The transgenic mice (wild-type, A315T and G348C) were generated by injection of DNA fragments into one-cell embryos, subcloned from *TARDBP* bacterial artificial chromosomes using the endogenous ~4 kB promoter. The A315T and G348C mutations were inserted using site-directed mutagenesis (Fig. 1A). Founder TDP-43 transgenic mice were identified by the presence of the 1.8-kb EcoRV fragment on the Southern blot (Supplementary Fig. 1A). Real-time PCR analysis of the spinal cord lysates of wild-type TDP-43, TDP-43^{A315T} and TDP-43^{G348C} mice revealed bands corresponding to human TDP-43 (Supplementary Fig. 1B). As shown by immunoblot analysis, the human TDP-43 transgenes (wild-type and mutants) were expressed in all the tissues examined (Fig. 1B). Real-time reverse transcription PCR showed that the messenger RNA expression of human TDP-43 in the spinal cord was elevated by ~3-fold in 3-month-old wild-type TDP-43, TDP-43^{A315T} and TDP-43^{G348C} transgenic mice as compared with the endogenous mouse TDP-43 (Fig. 1C). Whereas expression of human TDP-43 messenger RNA transcripts remained constant with age, the levels of endogenous mouse TDP-43 messenger RNA transcripts were decreased significantly in 10-month-old transgenic mice (wild-type TDP-43, TDP-43^{A315T} and TDP-43^{G348C}) as compared with 3-month-old mice (*$P < 0.01$, Supplementary Fig. 1E). This is consistent with TDP-43 autoregulation through TDP-43 binding and splicing-dependent RNA degradation as described previously (Polymenidou *et al.*, 2011). Next, we examined whether we can detect pathological cytosolic TDP-43 in our transgenic models, characteristic of amyotrophic lateral sclerosis.

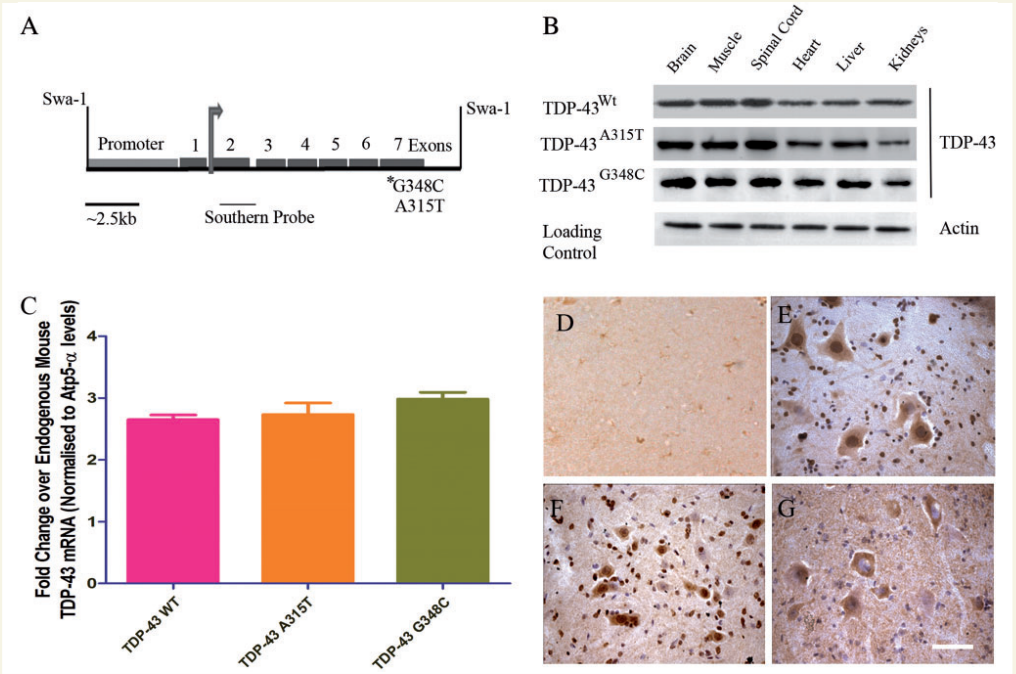

Figure 1 Generation and characterization of TDP-43 transgenic mice. (**A**) Map of human *TARDBP* gene (Gene ID: 23435) showing upstream ~4 kb promoter (uncharacterized) and various exons (numbered 1–7) and introns. The orientation of transcription is shown by arrow. Asterisk denotes position of two mutations G348C (1176G>T) and A315T (1077G>A). The approximate locations of the Southern blotting probes are also indicated. (**B**) Western blots from lysates of various tissues from wild-type TDP-43, TDP-43^{A315T} and TDP-43^{G348C} transgenic mice at 2 months of age using mouse monoclonal TDP-43 antibody that detect human TDP-43 only. Actin is shown as loading control. (**C**) Quantitative real-time PCR analysis of human TDP-43 messenger RNA expression in the spinal cord of wild-type TDP-43, TDP-43^{A315T} and TDP-43^{G348C} transgenic mice at 2 months of age compared individually to their wild-type littermates and normalized to Atp-5α levels. Data shown are means ± SEM of five different mice from each group. (**D–G**) Immunohistochemistry shows human TDP-43 expression pattern in the spinal cord of ~8-month-old wild-type TDP-43, TDP-43^{A315T} and TDP-43^{G348C} transgenic mice using TDP-43 monoclonal antibody. It is noteworthy that the expression of TDP-43 is mostly nuclear in wild-type TDP-43 mice (**E**), but TDP-43 is localized in the cytoplasm in TDP-43^{G348C} mice (**G**), and to a lesser extent in TDP-43^{A315T} mice (**F**). TDP-43 monoclonal antibody does not recognize endogenous mouse TDP-43 in non-transgenic control mice (**D**). Scale bar = 20 µm.

The immunohistochemical staining with anti-human TDP-43 antibodies of spinal cord sections from 10-month-old transgenic mice revealed a cytoplasmic accumulation of TDP-43 in TDP-43^{G348C} mice and to a lower extent in TDP-43^{A315T} mice (Fig. 1D–G and Supplementary Fig. 3A and B). In contrast, the TDP-43 localization remained mostly nuclear in wild-type TDP-43 and non-transgenic mice.

Overexpression of wild-type and mutant TDP-43 is associated with the formation of cytosolic aggregates

Biochemically, amyotrophic lateral sclerosis and FTLD-U cases are characterized by 25 kDa C-terminal deposits that might contribute to pathogenesis (Cairns *et al.*, 2007). Similar to amyotrophic lateral sclerosis cases, TDP-43^{G348C} and TDP-43^{A315T} mice had ~25 kDa fragments in the spinal cord (Fig. 2A and B). This ~25 kDa fragment was more prominent at 10 months of age (Fig. 2B) than at 3 months of age (Fig. 2A). Blots probed with human TDP-43-specific monoclonal antibody reveal increased cytotoxic ~25 kDa TDP-43 fragments in the brain (Supplementary Fig. 1E and F) and spinal cord (Supplementary Fig. 1C and D) lysates of TDP-43^{G348C} and TDP-43^{A315T} mice at 10 months of age as compared with 3-month-old mice. Using immunofluorescence and monoclonal TDP-43 antibody, we detected the presence of cytoplasmic TDP-43 aggregates in TDP-43^{G348C} mice (Fig. 2H) and TDP-43^{A315T} (Fig. 2G) mice at around 10 months of age, but not in wild-type TDP-43 mice (Fig. 2F). Cytoplasmic localization as well as aggregates of TDP-43 were age dependent as they were absent in the spinal cord sections of 3-month-old mice (Fig. 2C–E). In order to determine if the TDP-43 aggregates were ubiquitinated, we performed double immunofluorescence with TDP-43 and anti-ubiquitin antibodies. We found that ubiquitin specifically co-localized with cytoplasmic TDP-43 aggregates in the spinal cord (Fig. 2L–N), hippocampal (Fig. 2O–Q) and cortical sections (Fig. 2R–T) of 10-month-old TDP-43^{G348C} mice, but not in the spinal cord sections of 3-month-old (Fig. 2I–K) TDP-43^{G348C} mice. Ubiquitination of TDP-43-positive inclusions was further confirmed by the co-immunoprecipitation of ubiquitin (poly-ubiquitin) with human TDP-43. This immunoprecipitation experiment clearly demonstrates that proteins associated with TDP-43 inclusions especially in 10-month-old TDP-43^{G348C} and TDP-43^{A315T} mice are massively ubiquitinated (Fig. 2U). However, probing the blot with anti-human TDP-43 monoclonal antibody (Fig. 2U) or with polyclonal antiTDP-43 (data not shown) did not reveal high molecular weight forms of TDP-43, suggesting that TDP-43 itself was not ubiquitinated. To further address this question, we carried out immunoprecipitation of spinal cord extracts with anti-ubiquitin and probed the blot with anti-TDP-43 monoclonal antibody (Fig. 2U). As expected, TDP-43 was co-immunoprecipitated with anti-ubiquitin. However, only a small amount of high molecular weight forms of TDP-43 (i.e. poly-ubiquitinated) could be detected (Fig. 2V). This result is consistent with a report that TDP-43 is not, in fact, the major ubiquitinated target in ubiquitinated inclusions of amyotrophic lateral sclerosis (Sanelli *et al.*, 2007).

Peripherin overexpression and neurofilament disorganization in TDP-43 transgenic mice

A pathological hallmark of both sporadic and familial amyotrophic lateral sclerosis is the presence of abnormal accumulations of neurofilament and peripherin proteins in motor neurons (Carpenter, 1968; Corbo and Hays, 1992; Migheli *et al.*, 1993). Here, we investigated whether such cytoskeletal abnormalities appear in the large motor neurons of TDP-43 transgenic mice. Immunofluorescence analysis of the spinal cord sections by anti-peripherin polyclonal antibody revealed the presence of peripherin aggregates in large motor neurons of TDP-43^{G348C}, TDP-43^{A315T} and, to a lesser extent, in wild-type TDP-43 mice at 10 months of age as compared with 3-month-old mice (Fig. 3A–E and Supplementary Fig. 2A–D). Further analysis revealed that peripherin aggregates were also present in the brain. The aggregates in TDP-43^{G348C} and, to a lesser extent, in TDP-43^{A315T} and wild-type TDP-43 mice were localized in the hippocampus (Fig. 3F–J) and cortex (Fig. 3K–O). Western blot analysis of the brain lysates of transgenic mice using polyclonal antibody against peripherin revealed abnormal splicing variants of peripherin in TDP-43^{G348C} and TDP-43^{A315T} transgenic mice, including a toxic Per61 fragment (Fig. 3P) along with other fragments like Per56 and the normal Per58. The use of anti-peripherin monoclonal antibody revealed overexpression of the peripherin ~58 kDa fragment in TDP-43^{G348C}, TDP-43^{A315T} and to a lower extent in wild-type TDP-43 mice compared with non-transgenic mice.

Earlier reports have shown that Per61 is neurotoxic and is present in spinal cords of patients with amyotrophic lateral sclerosis (Robertson *et al.*, 2003). We then determined the messenger RNA expression levels in the spinal cord extracts of various peripherin transcripts (Per61, Per58 and Per56) using real-time PCR. Though the levels of Per58 and Per56 are not significantly different between various transgenic mice, the levels of Per61 are significantly upregulated (~2.5-fold, $P < 0.01$) in TDP-43^{G348C} mice compared with wild-type TDP-43 mice (Fig. 3Q). Per61 was also upregulated in TDP-43^{A315T} mice (~1.5-fold) compared with wild-type TDP-43 mice. Antibody specifically recognizing Per61 was used to detect Per61 in the spinal cord sections of TDP-43^{G348C} mice (Fig. 3S) and in wild-type TDP-43 mice (Fig. 3R). As expected, Per61 antibody stained Per61 aggregates in the axons and cell bodies in human amyotrophic lateral sclerosis spinal cord sections (Fig. 3U) but not control spinal cord tissues (Fig. 3T).

The TDP-43 transgenic mice also exhibit altered levels of peripherin and neurofilament protein expression. As shown in Fig. 4A, western blotting revealed that heavy neurofilament protein is downregulated by ~1.5-fold and light neurofilament protein by ~2-fold in the spinal cord extracts of 10-month-old TDP-43^{G348C} mice as compared with non-transgenic mice (Fig. 4A). The levels of medium neurofilament protein on the other hand were not significantly altered in any of the transgenic mice. We determined neurofilament levels in the spinal cords of 10-month-old transgenic and non-transgenic mice using enzyme-linked immunosorbent assay. Usual enzyme-linked immunosorbent assay methods are not suitable for the quantitative measurement of

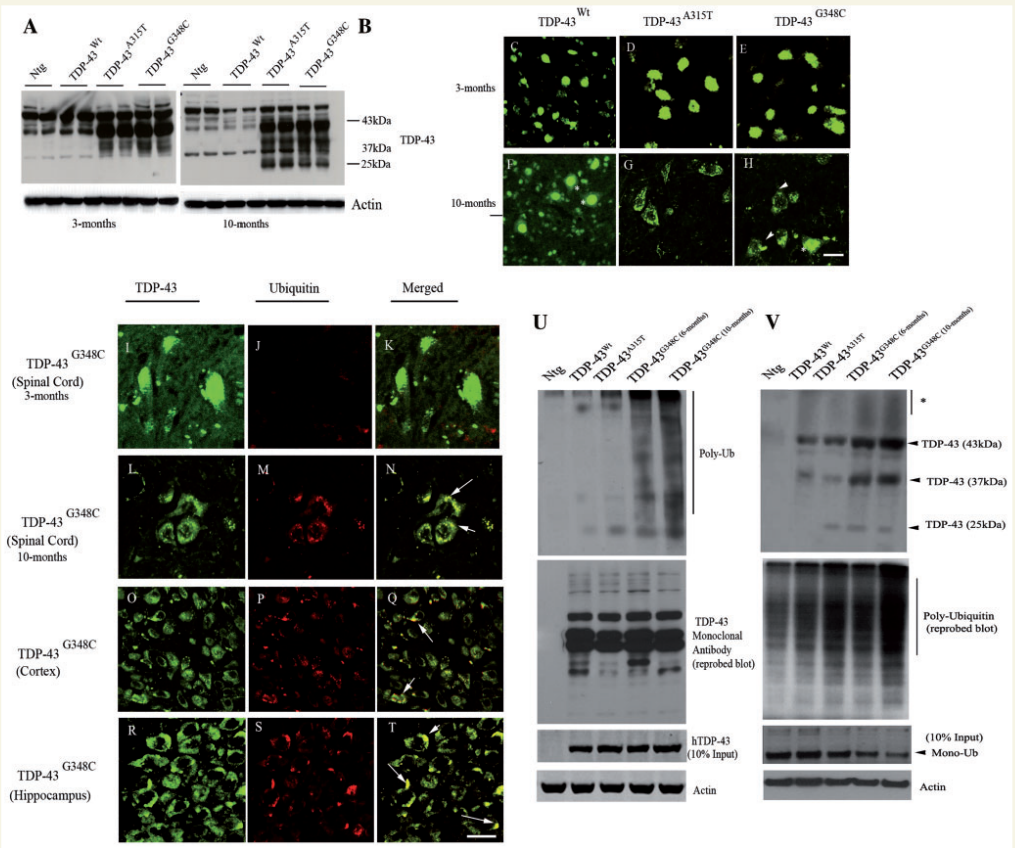

Figure 2 Biochemical and pathological features of amyotrophic lateral sclerosis/FTLD in TDP-43 transgenic mice. (**A** and **B**) Western blot of spinal cord lysates from Ntg (non-transgenic), wild-type (Wt) TDP-43, TDP-43^{A315T} and TDP-43^{G348C} mice using polyclonal TDP-43 antibody at 3 and 10 months show that TDP-43 (both G348C and A315T mutants) have ~35 and ~25 kDa fragments that increase with age. Actin is shown as a loading control. (**C–H**) Immunofluorescence of the spinal cord of 10-month-old wild-type TDP-43 (**F**), TDP-43^{A315T} (**G**) and TDP-43^{G348C} mice (**H**) using TDP-43 monoclonal antibody show cytoplasmic human TDP-43 aggregates (arrowheads) especially in the spinal cord sections of TDP-43^{G348C} transgenic mice. Some of the TDP-43 is still in nucleus (asterisk). On the other hand, spinal cord sections of 3-month-old transgenic mice show nuclear staining exclusively (**C–E**). (**I–T**) Double immunofluorescence of the brain and spinal cord sections of 10-month-old TDP-43^{G348C} mice using monodonal TDP-43 antibody and anti-ubiquitin antibody show ubiquitinated TDP-43 aggregates (arrows) in spinal cord (**L–N**), cortex (**O–Q**) and hippocampal (**R–T**) regions. (**I–K**) Spinal cord sections of 3-month-old TDP-43^{G348C} mice do not show intense ubiquitination. Background intensities were matched with 10-month-old mice for consistency. (**U**) Co-immunoprecipitation of ubiquitin using mouse monoclonal TDP-43 from spinal cord lysates of transgenic mice show that proteins associated with human TDP-43 are poly-ubiquitinated (Poly-Ub) more in TDP-43^{G348C} mice. Note that the ubiquitination is higher in 10-month-old mice than in 6-month old TDP-43^{G348C} mice. Re-probed western blot is shown for TDP-43 using monoclonal antibody. Western blot of human TDP-43 using monoclonal antibody is shown as 10% input and actin as loading control. (**V**) Reverse co-immunoprecipitation with anti-ubiquitin antibody shows that TDP-43 was co-immunoprecipitated with anti-ubiquitin. However, only a small amount of high molecular weight forms of TDP-43 (i.e. poly-ubiquitinated) could be detected. Western blot of ubiquitin using polyclonal antibody is shown as 10% input and actin as loading control. Scale bar = 50 μm (**C–H**); 25 μm (**I–T**).

neurofilament proteins because of their insolubility. However, neurofilament proteins are dissolved in urea at high concentration. Standard curves of light, medium and heavy neurofilament proteins dissolved in various concentrations of urea diluted with the dilution buffer were prepared as described elsewhere (Lu *et al.*, 2011) (Supplementary Fig. 4A–C). A suitable concentration of urea for detection was estimated to be ~0.3 mol/l, because the sensitivity was higher in 0.3 mol/l urea than in the other concentrations

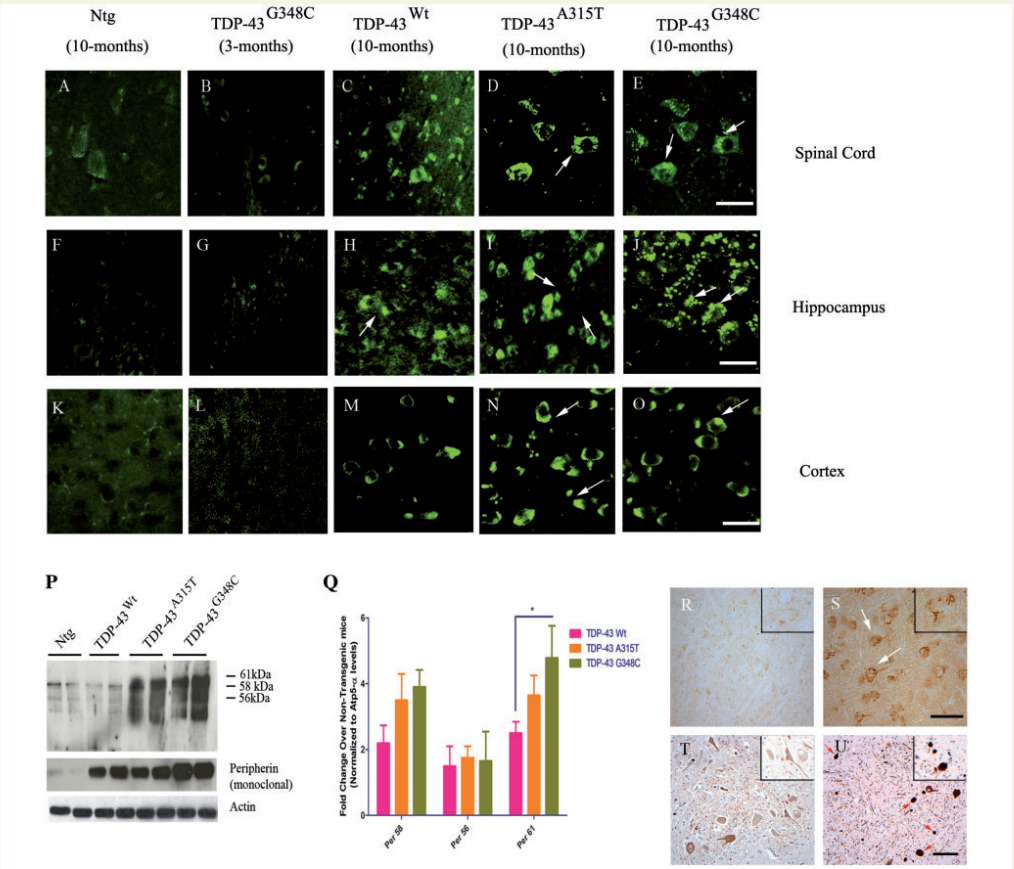

Figure 3 Peripherin abnormalities in TDP-43 transgenic mice. (**A**–**O**) Immunofluorescence of the brain (**F**–**O**) and spinal cord (**A**–**E**) sections of 10-month-old non-transgenic (Ntg), wild-type (Wt) TDP-43, TDP-43^{A315T} and TDP-43^{G348C} transgenic mice using polyclonal anti-peripherin antibody. Peripherin immunofluorescence of the spinal cord sections show peripherin aggregates more in TDP-43^{G348C} mice (**E**) (arrow), and also some in TDP-43^{A315T} mice (**C**) and much less in wild-type TDP-43 mice (**C**) as compared with non-transgenic control (**A**). Spinal cord sections of 3-month-old TDP-43^{G348C} mice do not show peripherin overexpression or aggregates (**B**). (**F**–**J**) Hippocampal region of the brain of 10-month-oldTDP-43^{G348C} mice show abundant peripherin aggregates (**J**). Peripherin aggregates are also seen to a lesser extent in TDP-43^{A315T} mice (**I**) and much less in wild-type TDP-43 mice (**H**) as compared with non-transgenic control (**F**) and 3-month-old TDP-43G348C mice (**G**). (**K**–**O**) Similarly, peripherin immunofluorescence in 10-month-old TDP-43^{G348C} mice (**O**) in the cortical region of the brain show peripherin aggregates. These aggregates are also seen to a lesser extent in TDP-43^{A315T} mice (**N**) and much less in wild-type TDP-43 mice (**M**) as compared with non-transgenic control (**K**) and 3-month-old TDP-43G348C mice (**L**). (**P**) Western blot analysis of the brain lysates of 10-month-old non-transgenic, wild-type TDP-43, TDP-43^{A315T} and TDP-43^{G348C} transgenic mice using polyclonal peripherin antibody reveal various peripherin splice variants including the Per61, Per58 and Per56 fragments especially in TDP-43^{G348C} mice. Monoclonal peripherin antibody revealed overexpression of peripherin in TDP-43^{G348C}, TDP-43^{A315T} and to a lesser extent in wild-type TDP-43 mice as compared with non-transgenic control. Actin is shown as loading control. (**Q**) Quantitative real-time PCR analysis of messenger RNA levels of peripherin splice variants Per61, Per58 and Per56 in the spinal cord lysates show that TDP-43^{G348C} mice had ~2.5-fold higher Per61 transcript levels than in wild-type TDP-43 spinal cord. Per58 levels are also higher in TDP-43^{G348C} mice compared with wild-type TDP-43 mice, but no significant differences are observed in Per56 levels between different transgenic mice. Peripherin transcript levels are expressed as fold change over non-transgenic controls normalized to Atp-5α levels. One-way ANOVA was used with Tukey's *post hoc* comparison for statistical analysis ($n = 3$), $^{*}P < 0.01$ (**R**–**U**) Immunohistochemistry on spinal cord tissues using Per61-specific antibody reveal Per61-specific aggregates in TDP-43^{G348C} mice (**S**) similar to sporadic amyotrophic lateral sclerosis spinal cord tissues (**U**). In contrast, Per61 antibody yielded weak staining of the spinal cord in human control (**T**) and in wild-type TDP-43 transgenic mice (**R**). Inset showing higher magnification images. Scale bars = 25 µm (**A**–**O**); 50 µm (**R**–**U**).

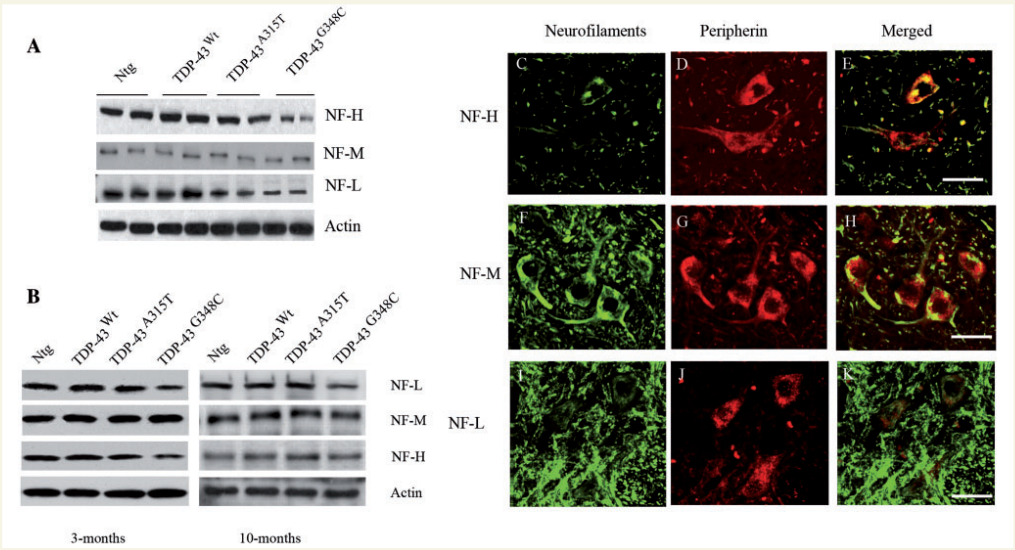

Figure 4 Neurofilament abnormalities in TDP-43 transgenic mice. (**A**) Western blots of various neurofilament proteins on the spinal cord lysates of 10-month-old non-transgenic (Ntg), wild-type (Wt) TDP-43, TDP-43^{A315T} and TDP-43^{G348C} transgenic mice using heavy neurofilament protein (NF-H), medium neurofilament protein (NF-M) and light neurofilament protein (NF-L) specific antibodies. Note the sharp reduction in the protein levels of light neurofilament protein and heavy neurofilament protein in TDP-43^{G348C} spinal cord lysates as compared with wild-type TDP-43 lysates. Actin is shown as loading control. (**B**) Western blots of various neurofilament proteins on the spinal cord lysates of 3-month and 10-month-old non-transgenic, wild-type TDP-43, TDP-43^{A315T} and TDP-43^{G348C} transgenic mice using heavy neurofilament protein, medium neurofilament protein and light neurofilament protein-specific antibodies. Actin is shown as loading control. (**C–K**) Double immunofluorescence of various neurofilaments (green)—heavy neurofilament protein (**C**), medium neurofilament protein (**F**) and light neurofilament protein (**I**) with polyclonal peripherin antibody (red) on the TDP-43^{G348C} spinal cord sections reveal that heavy neurofilament protein is recruited to peripherin aggregates (arrows, **E**), and to a lesser extent heavy neurofilament protein (**H**), but not light neurofilament protein (**K**). Scale bar = 25 μm.

examined. Analysis of enzyme-linked immunosorbent assay revealed that light neurofilament protein levels are significantly reduced in 10-month-old TDP-43G348C mice as compared with age-matched non-transgenic controls (**$P < 0.001$, Supplementary Fig. 4D). Ten-month-old spinal cord samples were fractionated in detergent soluble and insoluble fractions. Though most of the neurofilament proteins were in detergent insoluble fraction, peripherin levels could be detected in both soluble and insoluble fractions (Supplementary Fig. 5A and B). We also determined the heavy neurofilament protein, medium neurofilament protein and light neurofilament protein levels in the sciatic nerve of 3 and 10-month-old transgenic mice. We observed a slight decrease in light neurofilament protein levels in 3-month-old TDP-43^{G348C} mice as compared with age-matched wild-type TDP-43 and TDP-43^{A315T} mice, which had levels similar to non-transgenic mice (Fig. 4B). At 10 months of age, TDP-43^{G348C} mice had ~50% reduction in light neurofilament protein levels in the sciatic nerve (Fig. 4B) as compared with wild-type TDP-43 mice. We then used double immunofluorescence techniques to determine which neurofilament forms part of the aggregates with peripherin in TDP-43^{G348C} spinal cord sections. We found that heavy neurofilament protein clearly forms part of the aggregates (Fig. 4C–E), followed by medium neurofilament protein to a lesser extent (Fig. 4F–H) and light neurofilament protein (Fig. 4I–K) does not form part of the aggregates. TDP-43 aggregates co-localize partially with heavy neurofilament protein and medium neurofilament protein, but not with light neurofilament protein (Supplementary Fig. 6A–C).

Smaller calibre of peripheral axons in TDP-43 transgenic mice

Our previous work has demonstrated that overexpression of the wild-type peripherin, especially in context of light neurofilament protein loss, leads to a late onset motor neuron disease and axonal degeneration (Beaulieu *et al.*, 1999). To investigate whether similar pathology was associated with peripherin induction in TDP-43 transgenic mice, we analysed at different time points the number of axons, the distribution of axonal calibre and their morphology. Axonal counts of the L5 ventral root from TDP-43 transgenic mice at 10 months of age failed to reveal any significant differences in the number of motor axons (Fig. 5A–E). Normal mice exhibit a

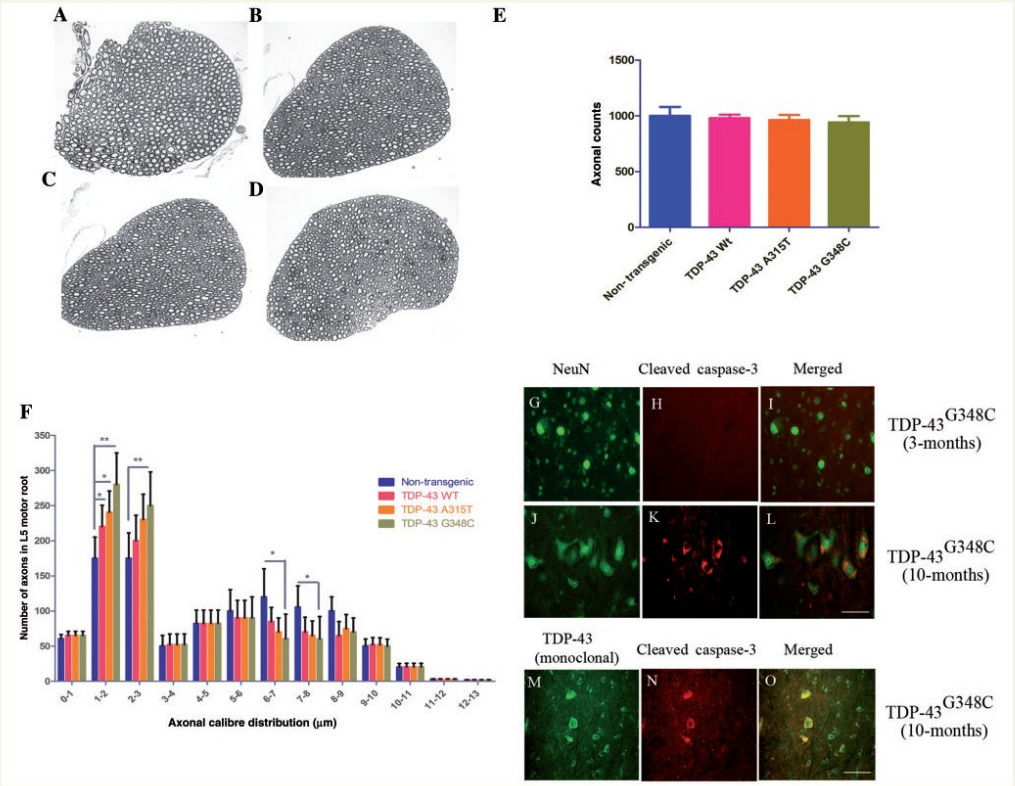

Figure 5 Reduced axonal calibre in ventral roots of TDP-43 transgenic mice. (**A**–**D**) Toluidine blue staining of thin sections of L5 ventral root axons from non-transgenic (**A**), wild-type TDP-43 (**B**), TDP-43^{A315T} (**C**) and TDP-43^{G348C} (**D**) mice showing no significant differences in the motor neuron count. (**E**) Axonal counts of transgenic mouse at 10 months of age failed to reveal any significant differences in the number of motor axons in the L5 ventral root. (**F**) Cumulative axon calibre distribution of axons at L5 ventral root of 10-month-old non-transgenic and transgenic mice showing increased number of 1–3 μm axons and reduced number of 6–9 μm axons in TDP-43^{G348C} mice. A two-way ANOVA with repeated measures was used to study the effect of group (transgenic and non-transgenic mice) on axonal calibre distribution. Pairwise comparisons were made using Bonferroni adjustment $^{*}P < 0.01$ and $^{**}P < 0.001$. Data shown are means ± SEM of five different mice from each group. (**G**–**L**) Double immunofluorescence using neuronal nuclei (NeuN; a neuronal marker) and cleaved caspase-3 show many cleaved caspase-3 positive neurons in the spinal cord of TDP-43^{G348C} mice at 10 months of age (**L**) compared with 3-month-old TDP-43^{G348C} mice (**I**). (**M**–**O**) Double immunofluorescence using human-specific TDP-43 and cleaved caspase-3 show many cleaved caspase-3 positive neurons in the spinal cord of TDP-43^{G348C} mice at 10 months of age. Scale bar = 25 μm.

bimodal distribution of axonal calibre with peaks at ~2 and ~7 μm in diameter (Fig. 5F). In contrast, a skewed bimodal distribution is observed in TDP-43 transgenic mice. There was a 10% increase (an increase of 100 axons, $P < 0.001$) in the number of motor axons with 1–3 μm calibre and a 12% decrease (a decrease of 120 axons) in the number of motor axons with 6–9 μm calibre in 10-month-old TDP-43^{G348C} mice compared with non-transgenic mice (Fig. 5F). There was a similar 7% increase (an increase of 70 axons, $P < 0.01$) in the number of motor axons with 1–3 μm calibre and an 8% decrease (a decrease of 80 axons) in the number of motor axons with 6–9 μm calibre in 10-month-old TDP-43^{A315T} mice as compared with non-transgenic mice. The increase in the number of motor axons with 1–3 μm calibre was less (~5%) and a slight decrease of 6% in 10-month-old wild-type TDP-43 mice compared with non-transgenic mice (Fig. 5F). We have quantified the functional neuromuscular junctions through fluorescence staining for pre- and postsynaptic markers. Neuromuscular junction count revealed that 5 ± 4% of the analysed neuromuscular junctions were denervated in 10-month-old wild-type TDP-43 mice and 10 ± 5% were denervated in age-matched TDP-43^{G348C} mice as compared with non-transgenic controls (Supplementary Fig. 7D). Furthermore, over 20% of

neuromuscular junctions were partially denervated in both wild-type TDP-43 mice and TDP-43^{G348C} mice.

The severe alterations in motor axon morphology of TDP-43^{G348C} mice prompted us to examine whether this phenomenon was associated with caspase-3 activation, a sign of neuronal damage. Using double immunofluorescence and antibodies against cleaved caspase-3 and neuronal nuclei (NeuN; a neuronal marker), we found many cleaved caspase-3 positive neurons in the spinal cord of TDP-43^{G348C} mice at 10 months of age (Fig. 5J–L) compared with 3-month-old TDP-43^{G348C} mice (Fig. 5G–I). Cleaved caspase-3 positive cells were also positive for cytoplasmic TDP-43 (Fig. 5M–O). However, no caspase-3 positive neurons were detected in wild-type TDP-43 and TDP-43^{A315T} mice at 10 months of age (data not shown).

TDP-43 transgenic mice develop motor dysfunction and cognitive deficits

Behavioural analysis of the TDP-43 transgenic mice revealed age-related cognitive defects, particularly learning and memory deficits. We used passive avoidance test to detect deficiencies in contextual memory. No defects were detected until 7 months of age. However, after 7 months, wild-type TDP-43, TDP-43^{A315T} and TDP-43^{G348C} mice exhibited severe cognitive impairments, especially in the 11th and 13th months (Fig. 6A). The most robust memory deficit occurred in TDP-43^{G348C} mice. We then conducted Barnes maze test to specifically discern the spatial learning and memory deficits in these mice. The TDP-43^{G348C} and, to a lesser extent, wild-type TDP-43 mice had significant learning impairment in the Barnes maze test at 10 months of age (Fig. 6B and C) as depicted by significant reduction in the time spent in the target quadrant and increased primary errors. In the probe trial (Day 5), TDP-43^{G348C} and wild-type TDP-43 mice showed a significant reduction in the time spent in the target quadrant and increase in the total number of errors as compared with age-matched non-transgenic mice (Fig. 6B and C). Thus, 10-month-old TDP-43^{G348C} mice had severe spatial learning and memory deficits. Transgenic mice overexpressing TDP-43^{G348C}, TDP-43^{A315T} or wild-type TDP-43 also exhibited age-related motor deficits as depicted by significant reductions in latency in the accelerating rotarod tests starting at ~42 weeks of age (Fig. 6D).

Age-related neuroinflammatory changes in TDP-43 mice precede behavioural defects

The microgliosis and astrogliosis were assessed in spinal cord and brain sections of different transgenic mice at presymptomatic stage (3 months) and after appearance of behavioural and sensorimotor deficits (10 months). Antibodies against ionized calcium binding adaptor molecule 1 (Iba-1), a marker for microglial ion channels, revealed the existence of microgliosis in the brain and spinal cord sections of 10-month-old TDP-43 transgenic mice (Fig. 7A–J). The microgliosis in the brain and spinal cord sections of 10-month-old wild-type TDP-43 and TDP-43^{A315T} mice was less pronounced than in 10-month-old TDP-43^{G348C} mice (Fig. 7E–H). Microgliosis was age dependent as both spinal cord and brain sections of 3-month-old wild-type TDP-43, TDP-43^{A315T} (data not shown) and TDP-43^{G348C} mice (Fig. 7B and G) had far less microglial activation than 10-month-old mice of the same genotype. We also used antibodies against glial fibrillary acidic protein to detect astrogliosis in the brain (Fig. 7P–T) and spinal cord (Fig. 7K–O) sections of 10-month-old TDP-43 transgenic mice. Again, astrogliosis in wild-type TDP-43 and TDP-43^{A315T} mice was less severe than in TDP-43^{G348C} mice. Similar to microgliosis, astrogliosis was also age dependent as both spinal cord and brain sections of 3-month-old wild-type TDP-43, TDP-43^{A315T} (data not shown) and TDP-43^{G348C} mice (Fig. 7L and Q) had far less astroglial activation than 10-month-old mice of same genotype. We then quantified messenger RNA levels of various pro-inflammatory cytokines and chemokines in the spinal cord of 10-month-old transgenic mice using quantitative real-time PCR. The messenger RNA levels of all studied cytokines and chemokines were upregulated in wild-type TDP-43, TDP-43^{A315T} and TDP-43^{G348C} mice when compared with their non-transgenic littermates. For instance, the levels of tumour necrosis factor-α (2.7-fold), interleukin-6 (2-fold) and monocyte chemotactic protein-1 (MCP-1; 2.5-fold) were all upregulated in TDP-43^{G348C} mice as compared with wild-type TDP-43 mice (Fig. 7U).

Next, we asked the question whether neuroinflammatory signals can be detected in early, pre-onset stages of the disease. Previous results, using the sensitive live imaging approaches in SOD1 mutant models, revealed that one of the first signs of the disease is the transient induction of the GFAP signals (Keller *et al.*, 2009). To investigate the temporal induction of gliosis and to relate it to sensorimotor and learning deficits, we generated by breeding double transgenic mice carrying a TDP-43 transgene and a GFAP-luc transgene consisting of the luciferase reporter driven by the murine GFAP promoter.

To analyse the spatial and temporal dynamics of astrocytes activation/GFAP induction in TDP-43 mouse model, we performed series of live imaging experiments, starting at early 4–5 weeks of age until 52 weeks. Quantitative analysis of the imaging signals revealed an early (~20 weeks) and significant upregulation of GFAP promoter activity (Fig. 8A–H) in the brain of TDP-43^{G348C}/GFAP-luc mice. Starting at 20 weeks of age, the light signal intensity from the brain of TDP-43^{A315T}/GFAP-luc mice and wild-type TDP-43/GFAP-luc mice was also significantly elevated when compared with wild-type littermates, but the intensity was less than in GFAP-luc/TDP-43^{G348C} mice. The GFAP promoter activity in the brain progressively increased with age until it peaked at ~50 weeks for GFAP-luc/TDP-43^{G348C}, and at ~46 weeks for GFAP-luc/TDP-43^{A315T} (Supplementary Fig. 8) and GFAP-luc/wild-type TDP-43mice (Fig. 8Q). It is noteworthy that the induction of gliosis at 20 weeks in the brain of TDP-43 transgenic mice preceded the cognitive deficits first detected at ~28 weeks (Fig. 6). Likewise, in the spinal cord of all three TDP-43 mouse models, the induction of GFAP promoter activity signals at ~30 weeks of age (Fig. 8I–P and R and Supplementary Fig. 8) preceded the motor dysfunction first detected by the rotarod test at ~36 weeks of age. Hence, TDP-43-mediated pathogenesis is associated with an early induction of astrogliosis/GFAP signals and age-dependent neuroinflammation.

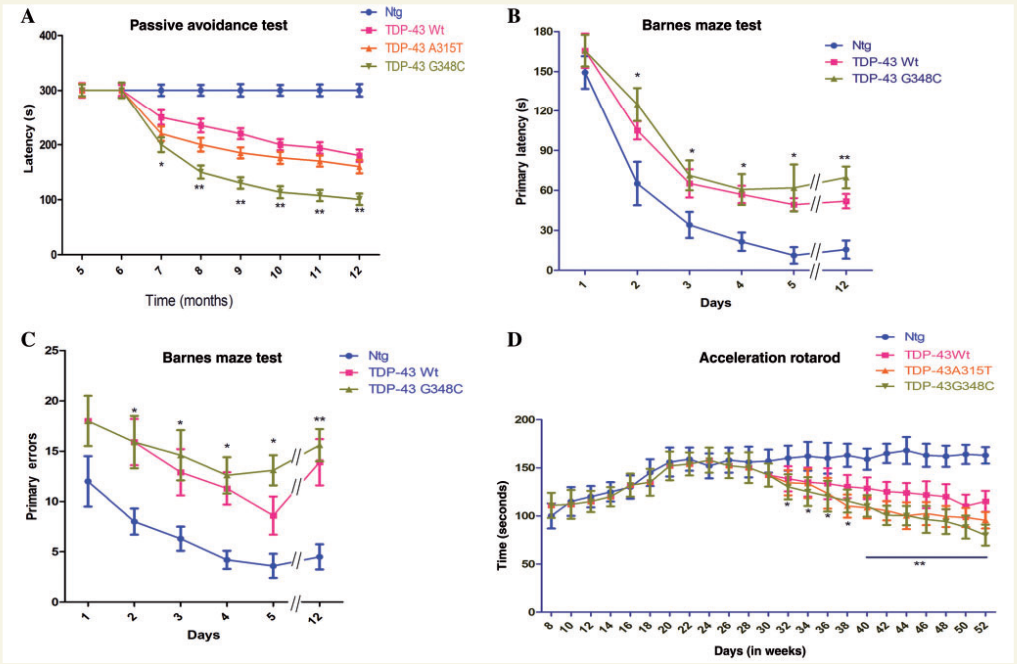

Figure 6 TDP-43 transgenic mice develop cognitive defects and motor dysfunction. (**A**) Passive avoidance test of various transgenic mice was performed every month from 5 to 12 months. Mice were placed in the light chamber, and mice entering in the dark chamber received a small shock. Each test set lasted for 2 days and on the third day, contextual learning/memory of the mice was evaluated based on latency (in s) to enter the dark chamber. A two-way ANOVA with repeated measures was used to study the effect of group (transgenic and non-transgenic mice) and time (in months) on latency to go to the dark chamber. Pairwise comparisons were made using Bonferroni adjustment. TDP-43^{G348C} mice showed significant deficits in contextual learning/memory at 7 months of age ($^{*}P < 0.01$), while TDP-43^{A315T} and wild-type (Wt) TDP-43 mice showed significant deficiencies at 9 months of age ($^{**}P < 0.001$) as compared with non-transgenic controls (Ntg). The cut off time was 300 s; data shown are means ± SEM of 10 different mice from each group. (**B**) Barnes maze test was performed on 10-month-old mice (wild-type TDP-43, TDP-43^{G348C} and non-transgenic). The spatial learning/memory capabilities are expressed as the primary latencies (latency to enter the target quadrant) exhibited in five consecutive sessions and one session at Day 12 of the test for long-term learning/memory analysis. A two-way ANOVA with repeated measures followed by Bonferroni adjustment was used for statistical analysis. TDP-43^{G348C} and to a lesser extent wild-type TDP-43 transgenic mice have severe spatial learning/memory deficits even at Day 2, which became increasingly prominent at Day 5. Long-term memory of TDP-43^{G348C} and wild-type TDP-43 mice are also severely impaired as assessed at Day 12 ($^{*}P < 0.01$, $^{**}P < 0.001$). Results represent means ± SEM of three independent trials ($n = 6$ mice/group). (**C**) The spatial learning/memory capabilities are also expressed as the primary errors (number of errors before entering the target quadrant) exhibited in five consecutive sessions and one session at Day 12 of the test for long-term learning/memory analysis. TDP-43^{G348C} and to a lesser extent wild-type TDP-43 transgenic mice have severe spatial learning/memory deficits even at Day 2, which became increasingly prominent at Day 5. Long-term memory of TDP-43^{G348C} and wild-type TDP-43 mice are also severely impaired as assessed at Day 12 ($^{*}P < 0.01$, $^{**}P < 0.001$). Results represent means ± SEM of three independent trials ($n = 6$ mice/group). (**D**) Accelerating rotarod analysis of mice at various ages from 8 weeks to 52 weeks reveal that TDP-43^{G348C} mice had significant differences in rotarod latencies at 36 weeks of age, TDP-43^{A315T} at 38 weeks and wild-type TDP-43 at 42 weeks of age as compared with non-transgenic control mice. A two-way ANOVA with repeated measures followed by Bonferroni adjustment was used for statistical analysis, $^{*}P < 0.01$, $^{**}P < 0.001$. Data represent means ± SEM of three independent trials ($n = 12$ mice/group).

Discussion

Here we report the generation and characterization of novel transgenic mouse models of amyotrophic lateral sclerosis-FTLD based on expression of genomic fragments encoding wild-type TDP-43 or mutants (A315T and G348C). The mouse models reported here carry TDP-43 transgenes under their own promoters resulting in ubiquitous and moderate expression (~3-fold) of human TDP-43 messenger RNA species. Most of the mouse models of TDP-43 reported previously have shown early paralysis followed by death.

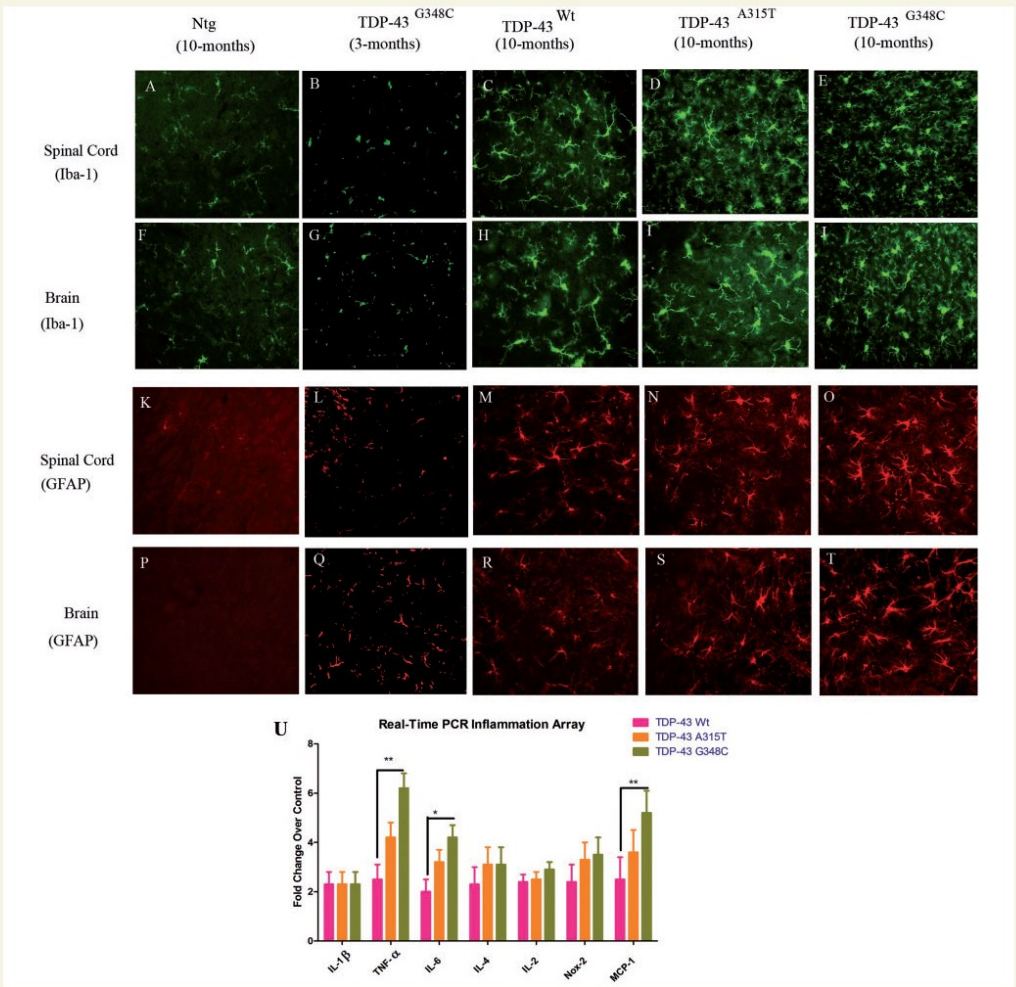

Figure 7 Neuroinflammation in TDP-43 transgenic mice. (**A**–**H**) Immunofluorescence of the spinal cord (**A**–**E**) and brain (**F**–**J**) sections of non-transgenic (Ntg), wild-type (Wt) TDP-43, TDP-43^{A315T} and TDP-43^{G348C} mice was performed using anti-Iba-1 antibody. In the spinal cord, microglial proliferation was abundant in 10-month-old TDP-43^{G348C} mice (**E**), followed by age-matched TDP-43^{A315T} (**D**) and wild-type TDP-43 mice (**C**) as compared with non-transgenic control mice (**A**) and 3-month-old TDP-43^{G348C} mice (**B**). In brain sections also, microgliosis was intense in TDP-43^{G348C} mice (**J**) as well as in age-matched TDP-43^{A315T} (**I**) and wild-type TDP-43 (**H**) as compared with non-transgenic control mice (**F**) and 3-month-old TDP-43^{G348C} mice (**G**). (**K**–**T**) Immunofluorescence of the spinal cord (**K**–**O**) and brain (**P**–**T**) sections of non-transgenic, wild-type TDP-43, TDP-43^{A315T} and TDP-43^{G348C} mice was performed using anti-GFAP antibody. In the spinal cord, astroglial proliferation was abundant in 10-month-old TDP-43^{G348C} mice (**O**), followed by age-matched TDP-43^{A315T} (**N**) and wild-type TDP-43 (**M**) as compared with non-transgenic control mice (**K**) and 3-month-old TDP-43^{G348C} mice (**L**). In brains sections also, microgliosis was abundant in TDP-43^{G348C} mice (**T**) followed by age-matched TDP-43^{A315T} (**S**) and wild-type TDP-43 (**R**) as compared with non-transgenic control mice (**P**) and 3-month-old TDP-43^{G348C} mice (**Q**). (**U**) Quantitative real-time PCR was performed on spinal cord tissue samples from 10-month-old wild-type TDP-43, TDP-43^{A315T} and TDP-43^{G348C} transgenic mice and expressed as fold change over non-transgenic control littermates normalized to Atp-5α levels. One-way ANOVA was used with Tukey's *post hoc* comparison for statistical analysis ($n = 5$ mice/group), $^{*}P < 0.01$, $^{**}P < 0.001$. The levels of tumour necrosis factor-α (TNF-α; 2.7-fold, $^{**}P < 0.001$), interleukin-6 (IL-6; 2-fold, $^{*}P < 0.01$) and monocyte chemotactic protein-1 (MCP-1; 2.5-fold, $^{**}P < 0.001$) were upregulated in TDP-43^{G348C} mice as compared with wild-type TDP-43 mice. Data represent means ± SEM of three independent experiments. Scale bars = 50 µm (**A**–**T**).

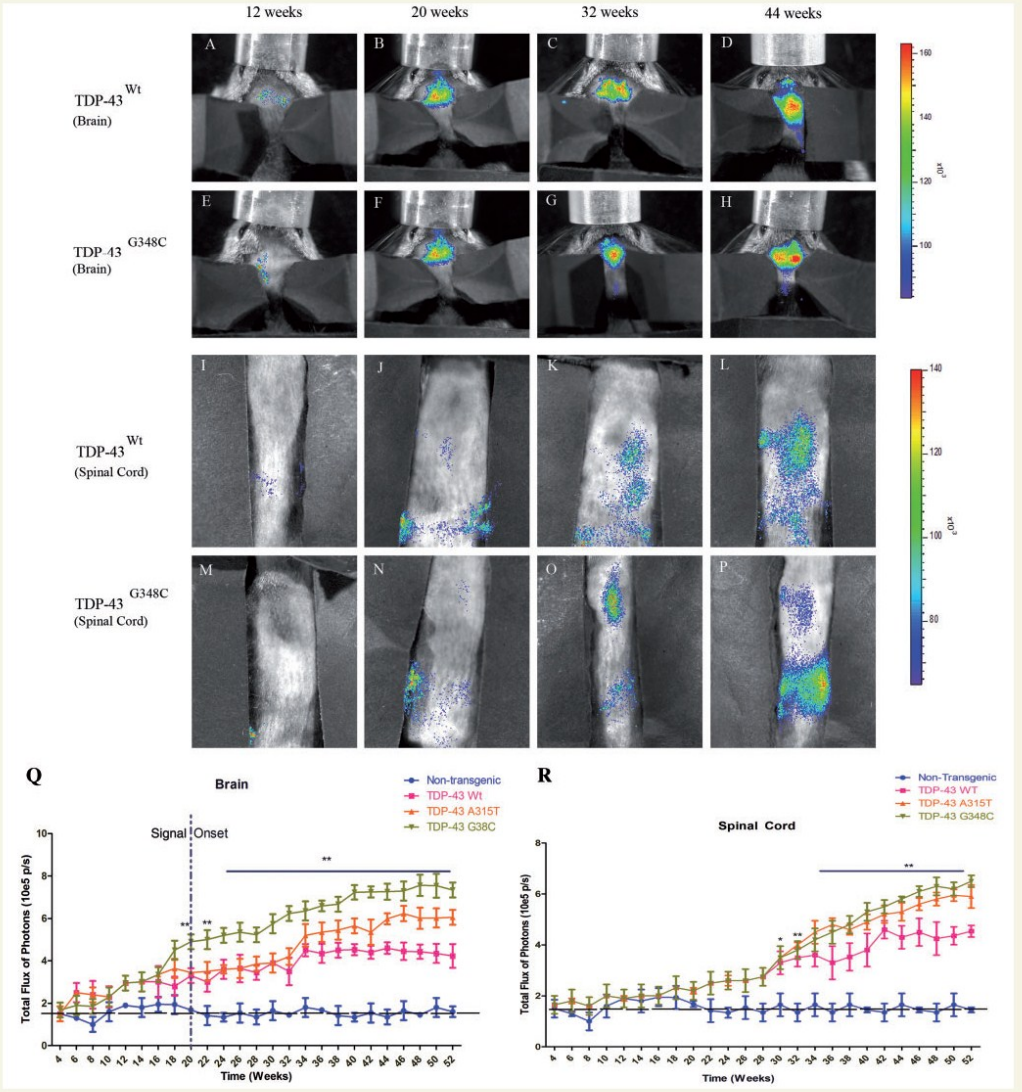

Figure 8 *In vivo* imaging revealed onset of astrocytosis before onset of behavioural impairments in doubly transgenic mice TDP-43/GFAP-luc. (**A–H**) *In vivo* bioluminescence imaging of astrocytes activation was studied at various time points in the brain of GFAP-luc/wild-type TDP-43 (**A–D**) and GFAP-luc/TDP-43^{G348C} (**E–H**) mice. Note that the GFAP-luc/TDP-43^{G348C} (**F**) mice had significant increase of GFAP promoter activity at 5 months (20 weeks) of age compared with GFAP-luc/wild-type TDP-43 (**B**) mice. (**I–P**) Typical sequence of images of the spinal cord area obtained from of GFAP-luc/wild-type TDP-43 (**I–L**) and GFAP-luc/TDP-43^{G348C} (**M–P**) mice at different time points by *in vivo* imaging. Significant GFAP promoter activity can be observed in GFAP-luc/wild-type TDP-43 (**K**) and GFAP-luc/TDP-43^{G348C} (**O**) mice at 8 months (32 weeks) of age. (**Q–R**) Longitudinal quantitative analysis of the total photon GFAP-signal/bioluminescence (total flux of photon/s) in GFAP-luc/wild-type TDP-43, GFAP-luc/TDP-43^{A315T} and GFAP-luc/TDP-43^{G348C} mice in the brain (**Q**) and spinal cord (**R**). A two-way ANOVA with repeated measures followed by Bonferroni adjustment was used for statistical analysis, $*P < 0.01$, $**P < 0.001$. Data represent means ± SEM of three independent experiments ($n = 12$ mice/group).

However, these mouse models are based on high expression levels of TDP-43 transgenes that can mask age-dependent pathogenic pathways. Mice expressing either wild-type or mutant TDP-43 (A315T and M337V) showed aggressive paralysis accompanied by increased ubiquitination (Wegorzewska *et al.*, 2009; Stallings *et al.*, 2010; Wils *et al.*, 2010; Xu *et al.*, 2010), but the lack of ubiquitinated TDP-43-positive inclusions raises concerns about their validity as models of human amyotrophic lateral sclerosis disease. Another concern is the restricted expression of TDP-43 species with the use of Thy1.2 and prion promoters. To better mimic the ubiquitous and moderate levels of TDP-43 occurring in the human context, it seems more appropriate to generate transgenic mice with genomic DNA fragments of TDP-43 gene with its own promoter. As in human neurodegenerative disease, our TDP-43 transgenic mice exhibited age-related phenotypic defects including impairment in contextual learning/memory and spatial learning/memory as determined by the passive avoidance and Barnes maze tests. Long-term memory of 10-month-old TDP-43^{G348C} transgenic mice was severely impaired according to the Barnes maze test. The TDP-43^{G348C}, TDP-43^{A315T} and, to a lesser extent, wild-type TDP-43 mice also exhibited motor deficits as depicted by significant reductions in latency in the accelerating rotarod test.

Cognitive and motor deficits in TDP-43 transgenic mice prompted us to test the underlying pathological and biochemical changes in these mice. Western blot analysis of spinal cord lysates of transgenic mice revealed ~25 kDa and ~35 kDa TDP-43 cleavage fragments that increased in levels with age. Previous studies demonstrated cytotoxicity of the ~25 kDa fragment (Zhang *et al.*, 2009). Immunofluorescence studies with human TDP-43-specific monoclonal antibodies revealed TDP-43 cytoplasmic aggregates in the spinal cord of TDP-43^{G348C}, TDP-43^{A315T} and to a lesser extent in wild-type TDP-43 mice. The cytoplasmic TDP-43-positive inclusions were ubiquitinated. The TDP-43-positive ubiquitinated cytoplasmic inclusions, along with ~25 kDa cytotoxic fragments, are reminiscent of those described in studies on patients with amyotrophic lateral sclerosis and FTLD-U (Neumann *et al.*, 2006). The co-immunoprecipitation of ubiquitin with anti-TDP-43 antibody and inversely of TDP-43 with anti-ubiquitin antibody (Fig. 2U and V) using spinal cord samples from TDP-43^{G348C} mice further confirmed the association of TDP-43 with ubiquitinated protein aggregates. However, TDP-43 itself was not extensively ubiquitinated. A thorough survey of articles on TDP-43 led us to the conclusion that there is no compelling biochemical evidence in literature supporting the general belief that TDP-43 is the major poly-ubiquitinated protein in the TDP-43-positive inclusions. We could find only one blot from one amyotrophic lateral sclerosis case in one paper (Neumann *et al.*, 2006) that revealed a very weak detection of high molecular weight smear with anti-TDP-43 after TDP-43 immunoprecipitation. A subsequent paper (Sanelli *et al.*, 2007) concluded from 3D-deconvolution imaging that TDP-43 is not, in fact, the major ubiquitinated target in ubiquitinated inclusions of amyotrophic lateral sclerosis.

The TDP-43 transgenic mice described here exhibit perikaryal and axonal aggregates of intermediate filaments, another hallmark of degenerating motor neurons in amyotrophic lateral sclerosis (Carpenter, 1968; Corbo and Hays, 1992; Migheli *et al.*, 1993). Before the onset of behavioural changes in these mice, peripherin aggregates form in the spinal cord and brain sections of TDP-43^{G348C} as well as in TDP-43^{A315T} transgenic mice. These peripherin inclusions were also seen in the hippocampal region of the brain of TDP-43^{G348C} mice. Normally, peripherin is not expressed in brain. However, it is known that peripherin expression in the brain can be upregulated after injury or stroke (Beaulieu *et al.*, 2002). The enhanced peripherin levels in these mice are probably due to an upregulation of interleukin-6, a cytokine that can trigger peripherin expression (Sterneck *et al.*, 1996). Sustained peripherin overexpression by >4-fold in transgenic mice was found previously to provoke progressive motor neuron degeneration during aging (Beaulieu *et al.*, 1999). In addition, we detected in TDP-43 transgenic mice the presence of abnormal splicing variants of peripherin, such as Per61, that can contribute to formation of intermediate filament aggregates (Robertson *et al.*, 2003). Using Per61-specific antibodies, we detected peripherin inclusions in the spinal cord sections of TDP-43^{G348C} mice, but not in wild-type TDP-43 mice (Fig. 3). The occurrence of specific splicing peripherin variants has also been reported in human amyotrophic lateral sclerosis cases (Xiao *et al.*, 2008).

In addition, we detected neurofilament protein anomalies in TDP-43^{G348C} mice. Double immunofluorescence revealed the detection of heavy neurofilament protein and medium neurofilament protein in inclusion bodies with peripherin in the spinal cord of TDP-43^{G348C} mice. Moreover, we found that light neurofilament protein is downregulated in the spinal cord lysates of TDP-43^{G348C} mice, a phenomenon that has also been observed in motor neurons of amyotrophic lateral sclerosis cases (Wong *et al.*, 2000). A decrease in light neurofilament protein levels may explain in part the age-related axonal atrophy detected in TDP-43 mice. Previous studies with light neurofilament protein knockout mice demonstrated that such substantial shift in calibres of large myelinated axons provokes a reduction of axon conduction velocity by ~3-fold (Kriz *et al.*, 2000). In large animals with long peripheral nerves, this would cause neurological disease. A loss of neurofilaments due to a homozygous recessive mutation in the *NEFL* gene was found recently to cause a severe early-onset axonal neuropathy (Yum *et al.*, 2009).

Age-related neuroinflammation constitutes another striking feature of the TDP-43 transgenic mice. *In vivo* imaging of biophotonic doubly transgenic mice bearing TDP-43 and GFAP-luc transgenes showed that astrocytes are activated as early as 20 weeks in the brain of GFAP-luc/TDP-43^{G348C} mice followed by activation in the spinal cord at ~30 weeks of age. The signal intensity for astrocytosis in GFAP-luc/TDP-43^{A315T} and GFAP-luc/wild-type TDP-43 was less than in GFAP-luc/TDP-43^{G348C} mice. It is noteworthy that the induction of astrogliosis in the brain and spinal cord in all three TDP-43 mouse models preceded by 6–8 weeks the appearance of cognitive and motor defects. This finding is in line with the recent view of an involvement of reactive astrocytes in amyotrophic lateral sclerosis pathogenesis (Barbeito *et al.*, 2004; Di Giorgio *et al.*, 2007, 2008; Julien, 2007; Nagai *et al.*, 2007).

In conclusion, the TDP-43 transgenic mice described here mimic several aspects of the behavioural, pathological and biochemical features of human amyotrophic lateral sclerosis/FTLD including

age-related development of motor and cognitive dysfunction, cytoplasmic TDP-43-positive ubiquitinated inclusions, intermediate filament abnormalities, axonopathy and neuroinflammation. Why is there no overt degeneration in our TDP-43 mouse models? Unlike previous TDP-43 transgenic mice, these transgenics were made with a genomic fragment that contains 3′ sequence autoregulating TDP-43 synthesis (Polymenidou *et al.*, 2011). So, the TDP-43 levels remain moderate. The ubiquitous TDP-43 ~3-fold overexpression in these mice mimics the ~2.5-fold increase of TDP-43 messenger RNA measured in the spinal cord of human sporadic amyotrophic lateral sclerosis by quantitative real-time PCR (V. Swarup, D. Phaneuf, N. Dupré, S. Petri, M. Strong, J. Kriz and J-P. Julien, unpublished results). In human amyotrophic lateral sclerosis cases carrying TDP-43 mutations, it takes many decades before amyotrophic lateral sclerosis disease onset. The factors that trigger the onset are unknown but perhaps future studies with TDP-43 mouse models might provide some insights. In any case, our new TDP-43 mouse models should provide valuable tools for unravelling pathogenic pathways of amyotrophic lateral sclerosis/FTLD and for preclinical drug testing.

Acknowledgements

We thank Genevieve Soucy for technical assistance. We are grateful to Jean-Nicolas Audet and the transgenic facility of Centre Hospitalier Universitaire de Québec (CHUQ) for generating and maintaining transgenic mice.

Funding

Canadian Institutes of Health Research (CIHR); Amyotrophic lateral sclerosis Society of Canada; Muscular Dystrophy of Canada; Fondation André-Delambre. J.-P.J. holds a Canada Research Chair Tier 1 in mechanisms of neurodegeneration. J.K. holds a R and D/HRF/CIHR Career Award. V.S. is the recipient of the Merit Scholarship for Foreign Students (FQRNT, Quebec, Canada).

Supplementary material

Supplementary material is available at *Brain* online.

References

Barbeito LH, Pehar M, Cassina P, Vargas MR, Peluffo H, Viera L, et al. A role for astrocytes in motor neuron loss in amyotrophic lateral sclerosis. Brain Res Brain Res Rev 2004; 47: 263–74.

Beaulieu JM, Kriz J, Julien JP. Induction of peripherin expression in subsets of brain neurons after lesion injury or cerebral ischemia. Brain Res 2002; 946: 153–61.

Beaulieu JM, Nguyen MD, Julien JP. Late onset of motor neurons in mice overexpressing wild-type peripherin. J Cell Biol 1999; 147: 531–44.

Bose JK, Wang IF, Hung L, Tarn WY, Shen CK. TDP-43 overexpression enhances exon 7 inclusion during the survival of motor neuron pre-mRNA splicing. J Biol Chem 2008; 283: 28852–9.

Buratti E, Dork T, Zuccato E, Pagani F, Romano M, Baralle FE. Nuclear factor TDP-43 and SR proteins promote in vitro and in vivo CFTR exon 9 skipping. EMBO J 2001; 20: 1774–84.

Cairns NJ, Neumann M, Bigio EH, Holm IE, Troost D, Hatanpaa KJ, et al. TDP-43 in familial and sporadic frontotemporal lobar degeneration with ubiquitin inclusions. Am J Pathol 2007; 171: 227–40.

Carpenter S. Proximal axonal enlargement in motor neuron disease. Neurology 1968; 18: 841–51.

Corbo M, Hays AP. Peripherin and neurofilament protein coexist in spinal spheroids of motor neuron disease. J Neuropathol Exp Neurol 1992; 51: 531–7.

Dequen F, Bomont P, Gowing G, Cleveland DW, Julien JP. Modest loss of peripheral axons, muscle atrophy and formation of brain inclusions in mice with targeted deletion of gigaxonin exon 1. J Neurochem 2008; 107: 253–64.

Di Giorgio FP, Boulting GL, Bobrowicz S, Eggan KC. Human embryonic stem cell-derived motor neurons are sensitive to the toxic effect of glial cells carrying an ALS-causing mutation. Cell Stem Cell 2008; 3: 637–48.

Di Giorgio FP, Carrasco MA, Siao MC, Maniatis T, Eggan K. Non-cell autonomous effect of glia on motor neurons in an embryonic stem cell-based ALS model. Nat Neurosci 2007; 10: 608–14.

Forman MS, Trojanowski JQ, Lee VM. TDP-43: a novel neurodegenerative proteinopathy. Curr Opin Neurobiol 2007; 17: 548–55.

Gitcho MA, Baloh RH, Chakraverty S, Mayo K, Norton JB, Levitch D, et al. TDP-43 A315T mutation in familial motor neuron disease. Ann Neurol 2008; 63: 535–8.

Gros-Louis F, Kriz J, Kabashi E, McDearmid J, Millecamps S, Urushitani M, et al. Als2 mRNA splicing variants detected in KO mice rescue severe motor dysfunction phenotype in Als2 knock-down zebrafish. Hum Mol Genet 2008; 17: 2691–702.

Hodges JR, Davies RR, Xuereb JH, Casey B, Broe M, Bak TH, et al. Clinicopathological correlates in frontotemporal dementia. Ann Neurol 2004; 56: 399–406.

Julien JP. ALS: astrocytes move in as deadly neighbors. Nat Neurosci 2007; 10: 535–7.

Kabashi E, Valdmanis PN, Dion P, Spiegelman D, McConkey BJ, Vande Velde C, et al. TARDBP mutations in individuals with sporadic and familial amyotrophic lateral sclerosis. Nat Genet 2008; 40: 572–4.

Keller AF, Gravel M, Kriz J. Live imaging of amyotrophic lateral sclerosis pathogenesis: disease onset is characterized by marked induction of GFAP in Schwann cells. Glia 2009; 57: 1130–42.

Keller AF, Gravel M, Kriz J. Treatment with minocycline after disease onset alters astrocyte reactivity and increases microgliosis in SOD1 mutant mice. Exp Neurol 2010; 228: 69–79.

Kriz J, Meier J, Julien JP, Padjen AL. Altered ionic conductances in axons of transgenic mouse expressing the human neurofilament heavy gene: a mouse model of amyotrophic lateral sclerosis. Exp Neurol 2000; 163: 414–21.

Lagier-Tourenne C, Cleveland DW. Rethinking ALS: the FUS about TDP-43. Cell 2009; 136: 1001–4.

Lomen-Hoerth C, Murphy J, Langmore S, Kramer JH, Olney RK, Miller B. Are amyotrophic lateral sclerosis patients cognitively normal? Neurology 2003; 60: 1094–7.

Lu CH, Kalmar B, Malaspina A, Greensmith L, Petzold A. A method to solubilise protein aggregates for immunoassay quantification which overcomes the neurofilament 'hook' effect. J Neurosci Methods 2011; 195: 143–50.

Mercado PA, Ayala YM, Romano M, Buratti E, Baralle FE. Depletion of TDP 43 overrides the need for exonic and intronic splicing enhancers in the human apoA-II gene. Nucleic Acids Res 2005; 33: 6000–10.

Migheli A, Pezzulo T, Attanasio A, Schiffer D. Peripherin immunoreactive structures in amyotrophic lateral sclerosis. Lab Invest 1993; 68: 185–91.

Nagai M, Re DB, Nagata T, Chalazonitis A, Jessell TM, Wichterle H, Przedborski S. Astrocytes expressing ALS-linked mutated SOD1 release factors selectively toxic to motor neurons. Nat Neurosci 2007; 10: 615–22.

Neumann M, Sampathu DM, Kwong LK, Truax AC, Micsenyi MC, Chou TT, et al. Ubiquitinated TDP-43 in frontotemporal lobar degeneration and amyotrophic lateral sclerosis. Science 2006; 314: 130–3.

Noto YI, Shibuya K, Sato Y, Kanai K, Misawa S, Sawai S, et al. Elevated CSF TDP-43 levels in amyotrophic lateral sclerosis: Specificity, sensitivity, and a possible prognostic value. Amyotroph Lateral Scler 2010.

Ou SH, Wu F, Harrich D, Garcia-Martinez LF, Gaynor RB. Cloning and characterization of a novel cellular protein, TDP-43, that binds to human immunodeficiency virus type 1 TAR DNA sequence motifs. J Virol 1995; 69: 3584–96.

Polymenidou M, Lagier-Tourenne C, Hutt KR, Huelga SC, Moran J, Liang TY, et al. Long pre-mRNA depletion and RNA missplicing contribute to neuronal vulnerability from loss of TDP-43. Nat Neurosci 2011; 14: 459–68.

Prut L, Abramowski D, Krucker T, Levy CL, Roberts AJ, Staufenbiel M, Wiessner C. Aged APP23 mice show a delay in switching to the use of a strategy in the Barnes maze. Behav Brain Res 2007; 179: 107–10.

Robertson J, Doroudchi MM, Nguyen MD, Durham HD, Strong MJ, Shaw G, et al. A neurotoxic peripherin splice variant in a mouse model of ALS. J Cell Biol 2003; 160: 939–49.

Rutherford NJ, Zhang YJ, Baker M, Gass JM, Finch NA, Xu YF, et al. Novel mutations in TARDBP (TDP-43) in patients with familial amyotrophic lateral sclerosis. PLoS Genet 2008; 4: e1000193.

Sanelli T, Xiao S, Horne P, Bilbao J, Zinman L, Robertson J. Evidence that TDP-43 is not the major ubiquitinated target within the pathological inclusions of amyotrophic lateral sclerosis. Journal of neuropathology and experimental neurology 2007; 66: 1147–53.

Seeley WW. Selective functional, regional, and neuronal vulnerability in frontotemporal dementia. Curr Opin Neurol 2008; 21: 701–7.

Sreedharan J, Blair IP, Tripathi VB, Hu X, Vance C, Rogelj B, et al. TDP-43 mutations in familial and sporadic amyotrophic lateral sclerosis. Science 2008; 319: 1668–72.

Stallings NR, Puttaparthi K, Luther CM, Burns DK, Elliott JL. Progressive motor weakness in transgenic mice expressing human TDP-43. Neurobiol Dis 2010; 40: 404–14.

Sterneck E, Kaplan DR, Johnson PF. Interleukin-6 induces expression of peripherin and cooperates with Trk receptor signaling to promote neuronal differentiation in PC12 cells. J Neurochem 1996; 67: 1365–74.

Talbot K, Ansorge O. Recent advances in the genetics of amyotrophic lateral sclerosis and frontotemporal dementia: common pathways in neurodegenerative disease. Hum Mol Genet 2006; 15: R182–7.

Van Deerlin VM, Leverenz JB, Bekris LM, Bird TD, Yuan W, Elman LB, et al. TARDBP mutations in amyotrophic lateral sclerosis with TDP-43 neuropathology: a genetic and histopathological analysis. Lancet Neurol 2008; 7: 409–16.

Wegorzewska I, Bell S, Cairns NJ, Miller TM, Baloh RH. TDP-43 mutant transgenic mice develop features of ALS and frontotemporal lobar degeneration. Proc Natl Acad Sci USA 2009; 106: 18809–14.

Wils H, Kleinberger G, Janssens J, Pereson S, Joris G, Cuijt I, et al. TDP-43 transgenic mice develop spastic paralysis and neuronal inclusions characteristic of ALS and frontotemporal lobar degeneration. Proc Natl Acad Sci USA 2010; 107: 3858–63.

Wong NK, He BP, Strong MJ. Characterization of neuronal intermediate filament protein expression in cervical spinal motor neurons in sporadic amyotrophic lateral sclerosis (ALS). J Neuropathol Exp Neurol 2000; 59: 972–82.

Xiao S, Tjostheim S, Sanelli T, McLean JR, Horne P, Fan Y, et al. An aggregate-inducing peripherin isoform generated through intron retention is upregulated in amyotrophic lateral sclerosis and associated with disease pathology. J Neurosci 2008; 28: 1833–40.

Xu YF, Gendron TF, Zhang YJ, Lin WL, D'Alton S, Sheng H, et al. Wild-type human TDP-43 expression causes TDP-43 phosphorylation, mitochondrial aggregation, motor deficits, and early mortality in transgenic mice. J Neurosci 2010; 30: 10851–9.

Yokoseki A, Shiga A, Tan CF, Tagawa A, Kaneko H, Koyama A, et al. TDP-43 mutation in familial amyotrophic lateral sclerosis. Ann Neurol 2008; 63: 538–42.

Yum SW, Zhang J, Mo K, Li J, Scherer SS. A novel recessive Nefl mutation causes a severe, early-onset axonal neuropathy. Ann Neurol 2009; 66: 759–70.

Zhang YJ, Xu YF, Cook C, Gendron TF, Roettges P, Link CD, et al. Aberrant cleavage of TDP-43 enhances aggregation and cellular toxicity. Proc Natl Acad Sci USA 2009; 106: 7607–12.

Deregulation of TDP-43 in amyotrophic lateral sclerosis triggers nuclear factor-κB–mediated pathogenic pathways

Published November 14, 2011

JEM

Article

Deregulation of TDP-43 in amyotrophic lateral sclerosis triggers nuclear factor κB–mediated pathogenic pathways

Vivek Swarup,[1] Daniel Phaneuf,[1] Nicolas Dupré,[2] Susanne Petri,[3] Michael Strong,[4] Jasna Kriz,[1] and Jean-Pierre Julien[1]

[1]Department of Psychiatry and Neuroscience, Research Centre of the University Hospital Centre of Quebec; and [2]Department of Neurological Sciences, Faculty of Medicine, Enfant-Jesus Hospital; Laval University, Quebec City, Quebec G1V 0A6, Canada
[3]Department of Neurology, Hannover Medical School, 30625 Hannover, Germany
[4]Molecular Brain Research Group, Robarts Research Institute, London, Ontario N6A 5K8, Canada

TDP-43 (TAR DNA-binding protein 43) inclusions are a hallmark of amyotrophic lateral sclerosis (ALS). In this study, we report that TDP-43 and nuclear factor κB (NF-κB) p65 messenger RNA and protein expression is higher in spinal cords in ALS patients than healthy individuals. TDP-43 interacts with and colocalizes with p65 in glial and neuronal cells from ALS patients and mice expressing wild-type and mutant TDP-43 transgenes but not in cells from healthy individuals or nontransgenic mice. TDP-43 acted as a co-activator of p65, and glial cells expressing higher amounts of TDP-43 produced more proinflammatory cytokines and neurotoxic mediators after stimulation with lipopolysaccharide or reactive oxygen species. TDP-43 overexpression in neurons also increased their vulnerability to toxic mediators. Treatment of TDP-43 mice with Withaferin A, an inhibitor of NF-κB activity, reduced denervation in the neuromuscular junction and ALS disease symptoms. We propose that TDP-43 deregulation contributes to ALS pathogenesis in part by enhancing NF-κB activation and that NF-κB may constitute a therapeutic target for the disease.

CORRESPONDENCE
Jean-Pierre Julien:
jean-pierre.julien@crchul.ulaval.ca

Abbreviations used: ALS, amyotrophic lateral sclerosis; ANOVA, analysis of variance; BMM, BM-derived macrophage; EMSA, electrophoretic mobility shift assay; GFAP, glial fibrillary acidic protein; HA, hemagglutinin; LDH, lactate dehydrogenase; mRNA, messenger RNA; NMJ, neuromuscular junction; PDL, poly-D-lysine; ROS, reactive oxygen species; siRNA, small interfering RNA; VCP, vasolin-containing protein; WA, Withaferin A.

Amyotrophic lateral sclerosis (ALS) is an adult-onset neurodegenerative disorder characterized by the progressive degeneration of motor neurons in the brain and spinal cord. Approximately 10% of ALS cases are familial and 90% are sporadic. Recently, TDP-43 (TAR DNA-binding protein 43) has been implicated in ALS (Neumann et al., 2006). TDP-43 is a DNA/RNA-binding 43-kD protein that contains an N-terminal domain, two RNA recognition motifs and a glycine-rich C-terminal domain, characteristic of the heterogeneous nuclear RNP class of proteins (Dreyfuss et al., 1993). TDP-43, normally observed in the nucleus, is detected in pathological inclusions in the cytoplasm and nucleus of both neurons and glial cells of ALS and frontotemporal lobar degeneration with ubiquitin inclusions (FTLD-U) cases (Arai et al., 2006; Neumann et al., 2006). The inclusions consist prominently of TDP-43 C-terminal fragments of ∼25 kD. The involvement of TDP-43 with ALS cases led to the discovery of TDP-43 mutations found in ALS patients. Dominant mutations in *TARDBP*, which codes for TDP-43, were reported by several groups as a primary cause of ALS (Gitcho et al., 2008; Kabashi et al., 2008; Sreedharan et al., 2008; Van Deerlin et al., 2008; Corrado et al., 2009; Daoud et al., 2009) and may account for ∼3% of familial ALS cases and ∼1.5% of sporadic cases.

Neuronal overexpression at high levels of WT or mutant TDP-43 in transgenic mice caused a dose-dependent degeneration of cortical and spinal motor neurons but with no cytoplasmic TDP-43 aggregates (Wegorzewska et al., 2009; Stallings et al., 2010; Wils et al., 2010; Xu et al., 2010), raising up the possibility that an up-regulation of TDP-43 in the nucleus rather than TDP-43 cytoplasmic aggregates may contribute to neurodegeneration. The physiological role of TDP-43 and the pathogenic pathways of TDP-43 abnormalities are not well

The Rockefeller University Press $30.00
J. Exp. Med.
www.jem.org/cgi/doi/10.1084/jem.20111313

Published November 14, 2011

JEM

understood. TDP-43 is essential for embryogenesis (Sephton et al., 2010), and postnatal deletion of the TDP-43 gene in mice caused down-regulation of *Tbc1d1*, a gene which alters body fat metabolism (Chiang et al., 2010). Proteins known to interact with TDP-43 have also been implicated in protein refolding or proteasomal degradation, including ubiquitin, proteasome-β subunits, SUMO-2/3, and Hsp70 (Seyfried et al., 2010).

Because TDP-43 is ubiquitously expressed and several studies have supported the importance of glial cells in mediating motor neuron injury (Clement et al., 2003; Boillée et al., 2006a,b), we have searched for additional proteins that might interact with TDP-43 in LPS-stimulated microglial (BV-2) cells. Our rationale for choosing microglial BV-2 cells was that TDP-43 deregulation may occur not only in neurons but also in microglial cells. Moreover, there are recent reports of increased levels of LPS in the blood of ALS patients (Zhang et al., 2009a) and of an up-regulation of LPS/TLR-4 signaling–associated genes in peripheral blood monocytes from ALS patients (Zhang et al., 2011). Accordingly, we have biased our search for proteins interacting with TDP-43 when microglia are activated by LPS. Surprisingly, coimmunoprecipitation assays and mass spectrometry led us to identify the p65 subunit of NF-κB as a binding partner of TDP-43. Furthermore, we discovered that TDP-43 messenger RNA (mRNA) was abnormally up-regulated in the spinal cord of ALS subjects. The results reported here led us to further explore the physiological significance of the interaction between TDP-43 and p65 NF-κB.

RESULTS

TDP-43 interacts with the p65 subunit of NF-κB

Mass spectrometry analysis and coimmunoprecipitation experiments were performed to identify proteins that interact with TDP-43 in mouse microglia (BV-2) cells after LPS stimulation, as described in Materials and methods. Many proteins were coimmunoprecipitated with TDP-43, including proteins responsible for RNA granule transport (kinesin), molecular chaperones (Hsp70), and cytoskeletal proteins (unpublished data). In addition, our analysis revealed p65 (*REL-A*) as a novel protein interacting with TDP-43. An interaction between TDP-43 with p65 NF-κB was confirmed by a coimmunoprecipitation assay with a polyclonal antibody against TDP-43 using spinal cord extracts from transgenic mice overexpressing human TDP-43^{WT} and TDP-43^{G348C} mutant (Swarup et al., 2011) by threefold (Fig. 1 B). Additional coimmunoprecipitation experiments performed using BV-2 cells that were transiently transfected with pCMV–TD-P43^{WT} and pCMV-p65 plasmids clearly showed that TDP-43 interacts with p65.

To further determine the significance of TDP-43 interaction with p65 in the context of human ALS, TDP-43 was pulled down with the polyclonal anti–TDP-43 antibody using spinal cord extracts from nine sporadic ALS cases and six control subjects (Fig. 1 A). In protein extracts from ALS cases, p65 NF-κB was coimmunoprecipitated with TDP-43. In contrast, no p65 was pulled down with TDP-43 using extracts of control spinal cords. To further validate TDP-43–p65 interaction, we performed reverse coimmunoprecipitation using p65 antibody to immunoprecipitate TDP-43 in human spinal cord tissues. Indeed, p65 was able to coimmunoprecipitate TDP-43 in all nine ALS cases but not in six control cases (Fig. S1 A). Along with p65, p50 was also coimmunoprecipitated with TDP-43 from the spinal cord samples of TDP-43^{WT} and TDP-43^{G348C} mice and ALS samples but not from nontransgenic or control spinal cord tissues, suggesting that TDP-43, p50, and p65 are a part of a complex (Fig. 1 B). To determine whether TDP-43 interacts directly with p65 or p50, we have performed overexpression experiments using pCMV expression vectors transfected into mouse neuroblastoma Neuro2a cells (Fig. 1 C). Neuro2a cells were transfected with pCMV-p65 or pCMV-p50 expression vectors along with vectors encoding either hemagglutinin (HA)-tagged TDP-43^{WT} or TDP-43$^{\Delta NR.1\text{-}30}$, a deletion mutant lacking the region required for binding to p65 as described in the section p65 interacts with the N-terminal and RRM-1 domains of TDP-43. It should be noted that the cells were not stimulated by LPS or any other means. After overexpression of p65 and TDP-43^{WT} in the Neuro2a cells, p65 was coimmunoprecipitated with TDP-43^{WT} but not with TDP-43$^{\Delta NR.1\text{-}30}$ using anti-HA antibody. In contrast, p50 was not coimmunoprecipitated with TDP-43^{WT} when overexpressed alone with TDP-43. These results suggest that TDP-43 interacts directly with p65 but not directly with p50. Immunofluorescence microscopy corroborated these results. In the spinal cord of sporadic ALS subjects, p65 was detected predominantly in the nucleus of cells in colocalization with TDP-43 (Fig. 1 D). On the contrary, in control spinal cord, there was an absence of p65 in the nucleus, reflecting a lack of p65 activation (Fig. 1 D). It is remarkable that microscopy of the spinal cord from TDP-43^{WT} transgenic mice revealed ALS-like immunofluorescence with active p65 that colocalized perfectly with TDP-43 in the nuclei of cells (Fig. 1 D). To elucidate which cell types in the spinal cord of ALS cases express TDP-43 and p65, we performed three-color immunofluorescence with CD11b as a microglial-specific marker and glial fibrillary acidic protein (GFAP) as an astroglial marker. We found that TDP-43 and p65 colocalized in many microglial and astroglial cells (Fig. 2, D–F, insets). We have quantified our data and found that 20 ± 5% of microglia and 8 ± 3% of astrocytes had TDP-43–p65 colocalization. We also found that many of the TDP-43 p65 colocalization was in neurons, and some also in motor neurons in many ALS cases (Fig. 2, A–C). In many ALS cases in which TDP-43 formed aggregates in the cytoplasm, p65 was still in the nucleus (Fig. 2, A–C, arrowheads). In nontransgenic C57BL/6 mice, the lack of p65 activation resulted in partial colocalization of TDP-43 with p65 mainly in cytoplasm (Fig. 1 D). LPS-stimulated BV-2 cells transfected with pCMV-p65 and pCMV–TDP-43^{WT} had most p65 colocalized with nuclear TDP-43^{WT}, whereas in unstimulated cells, p65 did not colocalize with nuclear TDP-43^{WT}. Although p65 was mainly

Published November 14, 2011

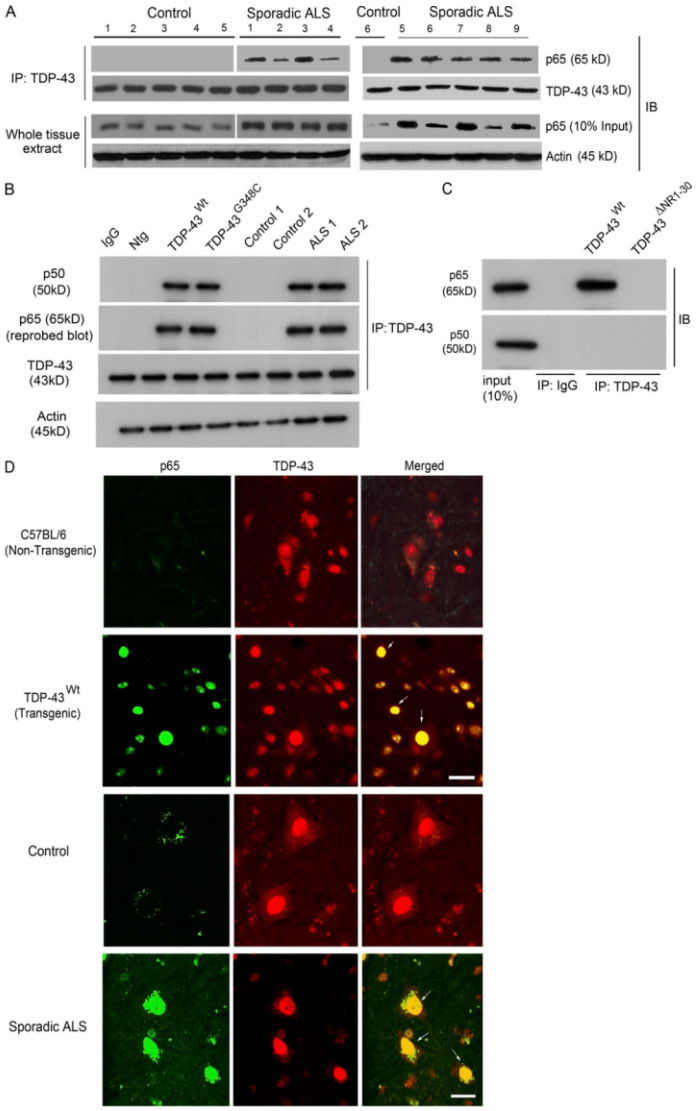

Figure 1. TDP-43 interacts with NF-κB p65. (A) Protein extracts from the spinal cords of nine sporadic ALS subjects (1–9) and six control individuals (1–6) were used for the immunoprecipitation (IP) with TDP-43–specific polyclonal antibody where indicated. Immunoprecipitates or whole cells extracts were subjected to immunoblot (IB) with the indicated antibodies. Two experiments were performed (one with controls 1–5 and ALS patients 1–4, and the other with control 6 and ALS patients 5–9). (B) Total protein extract from spinal cords of TDP-43^{WT} and TDP-43^{G348C} transgenic mice, B6 nontransgenic mice (Ntg), two control individuals, and two sporadic ALS patients were subjected to immunoprecipitation and immunoblot where indicated. (C) Neuro2a cells were transfected with pCMV-p65 and pCMV-p50 expression vectors along with TDP-43^{WT} or TDP-43$^{\Delta NR1\text{-}30}$. Extracts were immunoprecipitated with anti–TDP-43 or control IgG where indicated and immunoblotted with anti-p65 and anti-p50. (B and C) A representative blot from two independent experiments is shown. (D) Spinal cords of B6 nontransgenic or TDP-43^{WT} transgenic mice or control or ALS patients were stained with anti-p65 and anti–TDP-43 and analyzed by immunofluorescence. Brightness and contrast adjustments were made to the whole image to make background intensities equal in control and ALS cases. The images represent at least four sections from two experiments using ALS and control patient material. Arrows indicate colocalization of TDP-43 with p65. Bars, 20 µm.

cytoplasmic in 3-mo-old TDP-43^{WT} spinal cord, there was gradual age-dependent p65 activation in 6- and 10-mo-old TDP-43^{WT} spinal cord (Fig. S1 D).

TDP-43 acts as a co-activator of p65

A gene reporter assay was performed to study the effect of TDP-43 on NF-κB–dependent gene expression. The effect of TDP-43 was studied on gene expression of the reporter plasmid 4κB^{WT}-luc by transfecting pCMV–TDP-43^{WT} in BV-2 cells with or without cotransfection of pCMV-p65 (Fig. 3 A). When expressed alone, TDP-43 had no detectable effect on the basal transcription level of plasmid 4κB^{WT}-luc, suggesting that TDP-43 does not alter the basal transcription level of NF-κB. However, in coexpression with p65, TDP-43 augmented the gene expression of plasmid 4κB^{WT}-luc in a dose-dependent manner. 20 ng pCMV-p65 alone activated gene expression of 4κB^{WT}-luc by 10-fold (Fig. 3 A). However, upon cotransfection with 20 ng pCMV–TDP-43^{WT}, the extent of gene activation was elevated to 22-fold (2.2-fold augmentation by the effect of TDP-43). A further increase in NF-κB–dependent gene expression was recorded as the levels of TDP-43^{WT} were elevated to 50 ng (2.8-fold activation) and 100 ng (3.2-fold activation; $n = 4$; $P < 0.05$). When using a

Published November 14, 2011

JEM

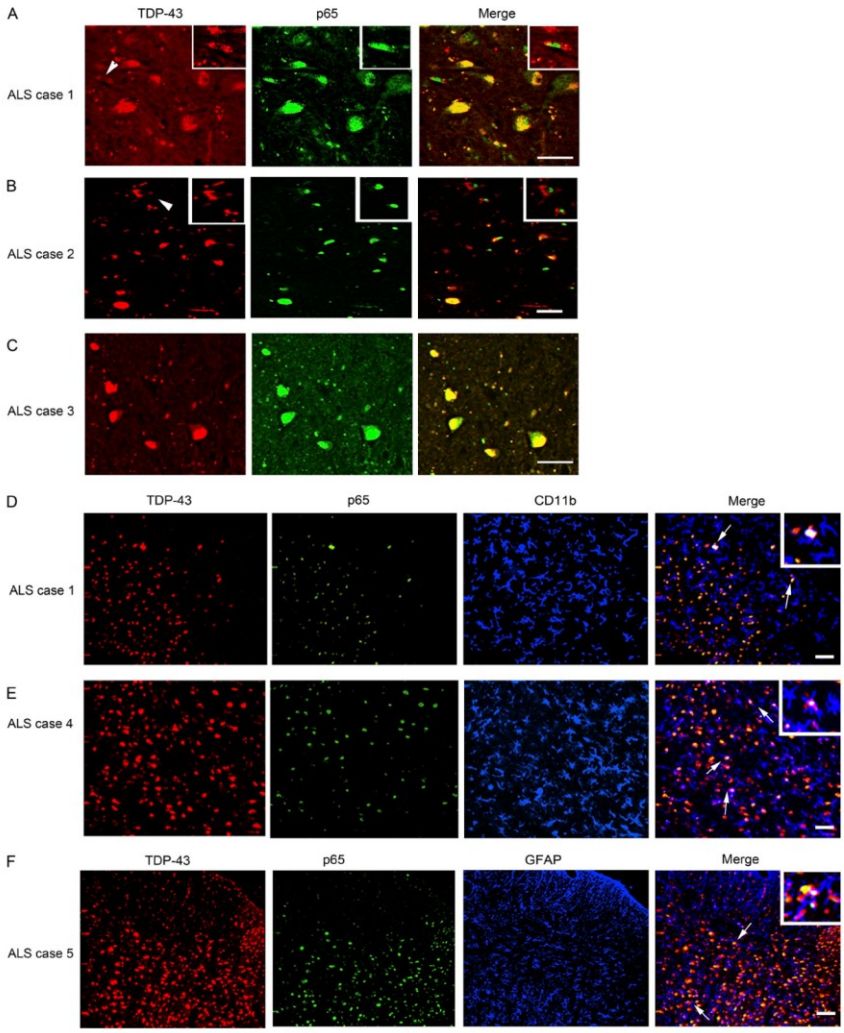

Figure 2. TDP-43 colocalizes with p65 in neuronal and glial cells. (A–C) TDP-43 and p65 double immunofluorescence was performed in different sporadic ALS cases as indicated. Double immunofluorescence pictures were taken at various magnifications. Arrowheads represent cytoplasmic localization of TDP-43 and nuclear p65 staining. Insets of higher magnification show cytoplasmic localization of TDP-43 and nuclear p65 staining. (D and E) A three-color immunofluorescence was performed using rabbit TDP-43, mouse p65, and rat CD11b (marker for microglia) as primary antibodies and Alexa Fluor 488 (green), 594 (red), and 633 (far-red, pseudo-color blue) as secondary antibody. Insets of higher magnification show triple colocalization (white) of TDP-43–, p65-, and CD11b-positive cells (arrows). (F) A three-color immunofluorescence was performed using rabbit TDP-43, mouse p65, and rat GFAP (marker for astrocytes) as primary antibodies and Alexa Fluor 488 (green), 594 (red), and 633 (far-red, pseudo-color blue) as secondary antibody. An inset of higher magnification shows triple colocalization (white) of TDP-43–, p65-, and GFAP-positive cells (arrows). (A–F) The images shown are representative of at least four sections from two experiments from ALS patients. Bars, 20 µm.

control luciferase reporter construct, $4\kappa B^{mut}$-luc, in which all four κB sites were mutated, neither the activation by pCMV-p65 nor the effect of cotransfection of pCMV–TDP-43^{WT} was detected. The boosting effects of TDP-43 were not caused by increased levels in p65 as shown by immunoblotting (Fig. 3 B). Similarly, pCMV–TDP-43^{A315T} and

Published November 14, 2011

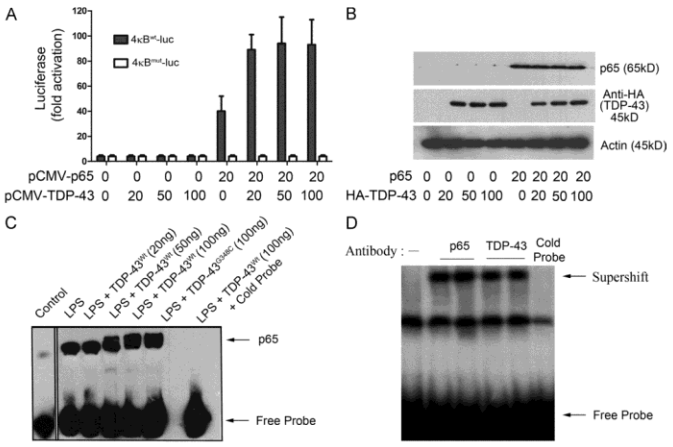

Figure 3. TDP-43 acts as a co-activator of NF-κB p65. (A) BV-2 cells were transfected with 20 ng $4κB^{WT}$-luc (containing WT NF-κB-binding sites) or $4κB^{mut}$-luc (containing mutated NF-κB-binding sites) together with the indicated amounts of pCMV-TDP-43^{WT} expression plasmid. Cells were harvested 48 h after transfection, and luciferase activity was measured. Values represent the luciferase activity mean ± SEM of three independent transfections, and statistical analysis was performed by two-way ANOVA with Bonferroni adjustment. TDP-43–transfected BV-2 cells were treated with 100 ng/ml LPS. (B) BV-2 cells were transfected with 20 ng pCMV-p65 and various concentrations of pCMV-TDP-43^{WT}. TDP-43 levels are shown when blotted with anti-HA antibody (Sigma-Aldrich), and actin is shown as a loading control. (C) 48 h after transfection, BV-2 cells were harvested, and nuclear extracts were then incubated with NF-κB p65-binding site–specific oligonucleotides coated with streptavidin. EMSA was then performed using the NF-κB EMSA kit. The specificity of the assay was ascertained by adding cold probe. The control lane was performed on a separate EMSA experiment and added. EMSA shown is a representative image of two independent experiments. (D) Supershift assay was performed by adding anti-HA antibody, which specifically recognizes human TDP-43, during the EMSA assay. p65 antibody was also added in a separate lane as a positive control. Note that all the samples were TDP-43 and p65 transfected and LPS stimulated. Supershift EMSA shown is a representative image of two independent experiments.

pCMV–TDP-43^{G348C} augmented p65-mediated gene expression from the reporter plasmid $4κB^{WT}$-luc (not depicted).

To further examine the effect of TDP-43 on the activation of p65, we performed p65 electrophoretic mobility shift assays (EMSAs). Transfection in BV-2 cells of pCMV-p65 with pCMV–TDP-43^{WT} or pCMV–TDP-43^{G348C} and LPS treatment was followed by extraction of nuclear proteins. Subsequently, the interaction between p65 in the protein extract and DNA probe was investigated using the EMSA kit from Panomics according to the manufacturer's instructions. TDP-43 increased the binding of p65 to the NF-κB DNA probe in a dose-dependent manner. LPS alone induced the binding of p65 to the DNA probe by about twofold as compared with control (Fig. 3 C). The cotransfection of 50 and 100 ng TDP-43^{WT} or of 100 ng TDP-43^{G348C} resulted in a significant dose-dependent increase in the DNA binding of p65. The specificity of the gel shift assay was assessed by adding a cold probe. TDP-43 alone did not bind to p65 EMSA probes (Fig. S1 B). Moreover, adding an anti-HA antibody that recognizes the transfected TDP-43 or an anti-p65 antibody caused supershifts of bands in the p65 EMSA (Fig. 3 D). Along with p65 and TDP-43, p50 is also part of the activated complex as seen by supershifts of bands in p65 EMSA experiments in BV-2 cells using antibodies specific to p65, TDP-43, and p50 (Fig. S1 C).

p65 interacts with the N-terminal and RRM-1 domains of TDP-43

To determine which domains of TDP-43 interact with p65, we constructed a series of deletion mutants of various TDP-43 domains. Various pCMV-HA–tagged deletion mutants like TDP-$43^{ΔN}$ (1–105 aa), TDP-$43^{ΔRRM-1}$ (106–176 aa), TDP-$43^{ΔRRM-2}$ (191–262 aa), and TDP-$43^{ΔC}$ (274–414 aa) were transfected in BV-2 cells with pCMV-p65 (Fig. 4 A). TDP-$43^{ΔRRM-1}$ coimmunoprecipitated p65 partially, whereas TDP-$43^{ΔRRM-2}$ and TDP-$43^{ΔC}$ interacted well with p65, suggesting that RRM-1 is important but RRM-2 and C-terminal domains are dispensable for interaction with p65. After transfection, we found that TDP-$43^{ΔN}$ had much reduced interaction with p65 (Fig. 4 B), thereby suggesting that the N-terminal domain of TDP-43 is essential for the interaction of TDP-43 with p65. Because the nuclear localization signal is in the N terminus, the reduced interaction of TDP-$43^{ΔN}$ to p65 could have been the result of a mislocalization of TDP-$43^{ΔN}$. To address this issue and to further define the interacting domain, we constructed a series of N-terminal and RRM-1 deletion mutants, TDP-$43^{ΔNR1-81}$ (98–176 aa), TDP-$43^{ΔNR1-50}$ (51–81 and 98–176 aa), and TDP-$43^{ΔNR1-30}$ (31–81 and 98–176 aa), with the nuclear localization signal attached so that the mutant proteins are able to be directed to the nucleus. Coimmunoprecipitation with these constructs suggested that even though TDP-$43^{ΔNR1-30}$ is in the nucleus (Fig. 4 C), it cannot effectively interact with p65, TDP-$43^{ΔNR1-81}$, and TDP-$43^{ΔNR1-50}$, whereas it can interact with p65 (Fig. 4 B). These results indicate that TDP-43 interacts with p65 through its N-terminal domain (31–81 and 98–106 aa) and RRM-1 (107–176 aa) domain.

To assess the effect of these deletion mutants on the activation of NF-κB gene, we used the gene reporter assay. Various deletion mutants of TDP-43 were cotransfected along with $4κB^{WT}$-luc or $4κB^{mut}$-luc. When compared with full-length TDP-43^{WT}, TDP-$43^{ΔN}$ had reduced effect (twofold; $n = 3$; $P < 0.05$) on the gene activation. TDP-$43^{ΔRRM-1}$ also exhibited attenuation of gene activation but to a lesser extent than TDP-$43^{ΔN}$ (Fig. 4 D). In contrast, TDP-$43^{ΔRRM-2}$ and

Published November 14, 2011

JEM

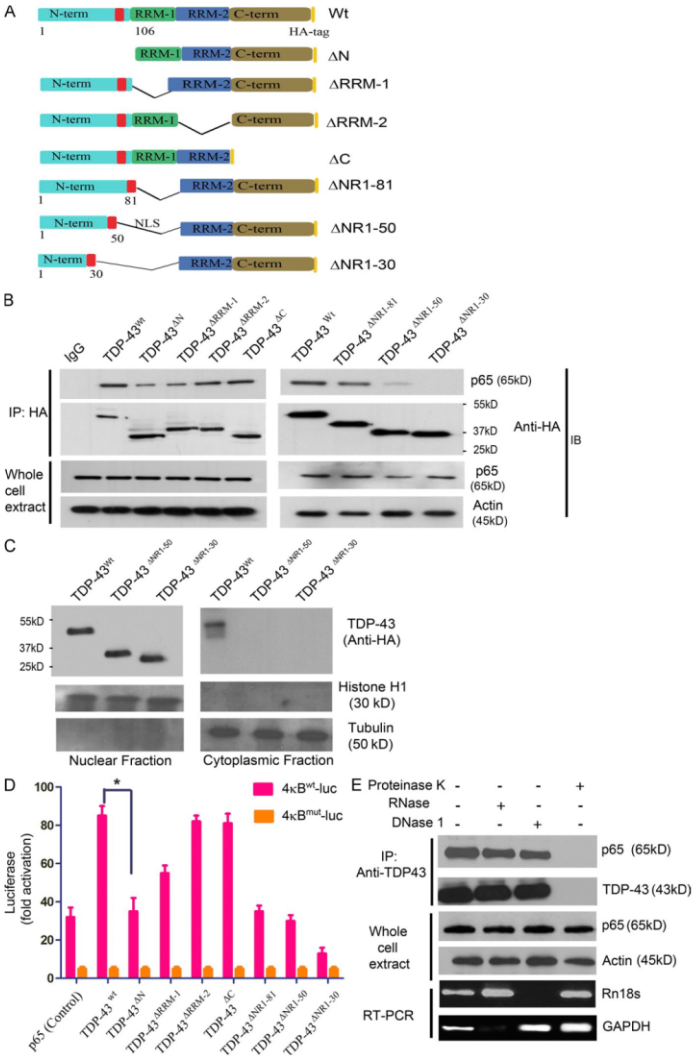

Figure 4. The N-terminal and RRM-1 domains of TDP-43 are crucial for interaction with p65. (A) Two-dimensional cartoon of TDP-43 protein showing various deletion mutants used in this study. Deletion mutants TDP-43$^{\Delta N}$ (1–105 aa), TDP-43$^{\Delta RRM-1}$ (106–176 aa), TDP-43$^{\Delta RRM-2}$ (191–262 aa), and TDP-43$^{\Delta C}$ (274–414 aa) and full-length TDP-43 (TDP-43^{WT}) are shown. Serial N-terminal and RRM-1 domain deletion mutants are also shown. TDP-43$^{\Delta NR1-81}$ (98–176 aa), TDP-43$^{\Delta NR1-50}$ (51–81 and 98–176 aa), and TDP-43$^{\Delta NR1-30}$ (31–81 and 98–176 aa) were generated. (B) All constructs (WT and deletion mutants) were cloned in pcDNA3.0 with HA tag at the extreme C terminus of the encoded protein. BV-2 cells were transfected with TDP-43^{WT} or deletion constructs and pCMV-p65. 24 h after transfection, cells were harvested and immunoprecipitated (IP) with anti-HA antibody. Immunoprecipitates or whole cells extracts were subjected to immunoblot (IB) with the indicated antibodies. A representative gel from three independent experiments is shown. (C) BV-2 cells transfected with TDP-43^{WT}, TDP-43$^{\Delta NR1-50}$, or TDP-43$^{\Delta NR1-30}$ were fractionated into nuclear and cytoplasmic fractions using sucrose density gradient centrifugation. These fractions were then probed with anti-HA antibody for the expression of transfected TDP-43 species. Histone H1 is used as a nuclear and tubulin as a cytoplasmic marker. A representative gel from two independent experiments is shown. (D) Various deletion mutants of TDP-43 were co-transfected along with 4κB^{WT}-luc (containing WT NF-κB–binding sites) or 4κB^{mut}-luc (containing mutated NF-κB–binding sites). 48 h after transfection, luciferase activity was measured. Statistical analysis was performed by two-way ANOVA with Bonferroni adjustment (*, $P < 0.05$). Error bars represent mean ± SEM from three independent experiments. (E) TDP-43 antibody was added to BV-2–transfected cell lysates, and proteins were immunoprecipitated with the indicated antibody. After TDP-43 immunoprecipitation, samples were treated with 1 µg/ml proteinase K, 1 µg/ml RNase, or 1 µg/ml DNase 1. To monitor the effectiveness of RNase and DNase digestion, RNase or DNase was added to cell lysates before immunoprecipitation and subjected to PCR. GAPDH RT-PCR was used to monitor RNase digestion, whereas Rn18s gene (which codes for 18SrRNA) genomic PCR was used to monitor DNase digestion. Representative blots and gels from three different experiments are shown.

TDP-43$^{\Delta C}$ deletion mutants had effects similar to full-length TDP-43^{WT}. As expected, because TDP-43$^{\Delta NR1-30}$ does not effectively interact with p65, the level of NF-κB activation detected by the 4κB^{WT}-luc reporter assay was extremely low, sixfold lower than full-length TDP-43^{WT} ($n = 3$; $P < 0.001$; Fig. 4 D). p65 and luciferase vectors were used as controls for the experiment. Note that the amount of pCMV-p65 vector transfected in control was more than in other experiments to keep similar amounts of total transfected DNA. Transfection of a control luciferase reporter construct, 4κB^{mut}-luc, in which all four κB sites were mutated, had no effect on the basal level activation of p65. To determine whether the interaction between TDP-43 and p65 is a protein–protein interaction, we performed immunoprecipitation experiments

Published November 14, 2011

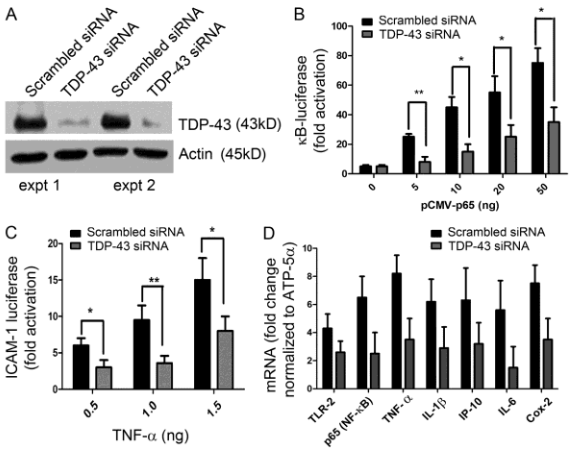

Figure 5. TDP-43 siRNA inhibits activation of NF-κB. BV-2 cells were transfected either with mouse TDP-43 siRNA or scrambled siRNA. 72 h after transfection, some of the cells were either stimulated with 100 ng/ml LPS or mock stimulated for 12 h. (A) Protein extracted from the siRNA experiment was subjected to Western blot analysis. Mouse endogenous TDP-43 levels in TDP-43 siRNA or scrambled siRNA were compared in two different experiments (expt 1 and expt 2) as determined by rabbit polyclonal TDP-43 antibody. (B) Additionally, BV-2 cells were transfected with pCMV-p65 (concentrations as indicated) and $4\kappa B^{WT}$-luc vector, and luciferase assay was performed. (C) We transfected BV-2 cells with ICAM-1–luc vector in addition to TDP-43 siRNA or scrambled siRNA in three different experiments. 72 h after transfection, cells were stimulated with varying concentrations (as indicated) of TNF. (D) Real-time quantitative PCR levels of various mRNAs were compared with TDP-43 siRNA–transfected (and LPS stimulated) BMMs and scrambled siRNA–transfected (and LPS stimulated) BMMs. (B-D) Statistical analysis was performed by two-way ANOVA with Bonferroni adjustment (*, $P < 0.05$; **, $P < 0.01$). Error bars represent mean ± SEM from three different experiments.

by adding proteinase K, RNase A, or DNase 1 (Fig. 4 E). The addition of proteinase K abolished the TDP-43–p65 interaction, whereas RNase A or DNase 1 had no effect, suggesting that the interaction is not DNA/RNA dependent.

TDP-43 small interfering RNA (siRNA) inhibits activation of NF-κB

If it is correct that TDP-43 acts as a co-activator of p65, then reducing the levels of TDP-43 should attenuate p65 activation. To reduce the expression levels of TDP-43, microglial BV-2 cells were transfected with either TDP-43 siRNA or scrambled siRNA together with $4\kappa B^{WT}$-luc vectors. 72 h after transfection, some of the cells were either stimulated with 100 ng/ml LPS or mock stimulated for 12 h. As shown in Fig. 5 A, TDP-43 siRNA reduced the endogenous mouse TDP-43 levels significantly as compared with scrambled siRNA–transfected cells in two different experiments. To examine the effect of reducing TDP-43 levels on NF-κB activation, BV-2 cells were transfected with pCMV-p65 and $4\kappa B^{WT}$-luc vectors. TDP-43 siRNA decreased activation of NF-κB reporter gene in transfected cells. The decrease in NF-κB activation was about threefold for 5 ng pCMV-p65 ($n = 4$; $P < 0.01$), ~2.5-fold for 10 and 20 ng pCMV-p65 ($n = 4$; $P < 0.05$), and twofold for 50 ng pCMV-p65 ($n = 4$; $P < 0.05$) as compared with scrambled siRNA–transfected cells (Fig. 5 B). To examine the physiological significance of TDP-43 inhibition by siRNA, we transfected BV-2 cells with ICAM-1–luc vector together with TDP-43 siRNA or scrambled siRNA. 72 h after transfection, cells were stimulated with varying concentrations of TNF. When stimulated with 0.5 ng/ml TNF, TDP-43 siRNA–transfected cells exhibited a twofold decrease in ICAM-1 luciferase activity ($n = 4$; $P < 0.05$) as compared with cells transfected with scrambled siRNA. Similarly, TDP-43 siRNA–transfected BV-2 cells exhibited at 1.0- and 1.5-ng/ml TNF concentrations a decrease of 2.5-fold ($n = 4$; $P < 0.01$) and twofold ($n = 4$; $P < 0.05$) in ICAM-1 luciferase activity, respectively (Fig. 5 C). We also tested the effect of TDP-43 siRNA transfected in BM-derived macrophages (BMMs) from normal mice. We compared the level of innate immunity activation when stimulated with LPS. BMMs transfected with TDP-43 siRNA had reduced levels of TLR2 mRNA (1.5-fold; $P < 0.05$), p65 (threefold; $P < 0.01$), TNF (threefold; $P < 0.01$), IL-1β (twofold; $P < 0.05$), IP-10 (twofold; $P < 0.05$), IL-6 (2.5-fold; $P < 0.01$), and Cox-2 (cyclooxygenase-2; twofold; $P < 0.05$) as compared with scrambled siRNA–transfected BMMs (Fig. 5 D).

TDP-43 and p65 mRNA levels are up-regulated in the spinal cord of sporadic ALS patients

The findings that TDP-43 can interact with p65 and that TDP-43 overexpression in transgenic mice was sufficient to provoke abnormal nuclear colocalization of p65 as observed in sporadic ALS (Fig. 1 D) prompted us to compare the levels of mRNA coding for TDP-43 and p65 NF-κB in spinal cord samples from sporadic ALS cases and control individuals. Real-time RT-PCR data revealed that the levels of TDP-43 mRNA in the spinal cord of sporadic ALS cases ($n = 16$) were up-regulated by ~2.5-fold ($P < 0.01$) compared with controls ($n = 6$; Fig. 6 A). It is also noteworthy that the levels of p65 NF-κB mRNA were up-regulated by about fourfold ($P < 0.001$) in ALS cases as compared with controls. Because TDP-43 forms many bands in Western blot analysis, we quantified the total level of TDP-43 protein using sandwich ELISA as described in Materials and methods. The ELISA results suggest that TDP-43 protein levels are in fact up-regulated in total spinal cord protein extracts of ALS cases ($n = 16$) by 1.82-fold (241.2 ± 8.5 pg/μg of total protein) as compared with control cases (132.8 ± 5.6 pg/μg of total protein; $n = 6$; Fig. 6 B). For human p65 ELISA, we used an ELISA kit from QIAGEN. The levels of p65 were also up-regulated in total spinal cord extracts of ALS cases ($n = 16$) by 3.5-fold (222.5 ± 11.5 pg/μg of total protein) as compared with control cases (62.83 ± 3.8 pg/μg of total protein; $n = 6$; Fig. 6 C).

Published November 14, 2011

JEM

TDP-43 overexpression in glia or macrophages causes hyperactive inflammatory responses to LPS

Because NF-κB is involved in proinflammatory and innate immunity response, we tested the effects of increasing TDP-43 mRNA expression in BV-2 cells. Because LPS is a strong proinflammatory stimulator (Horvath et al., 2008), we used it to determine the differences in levels of proinflammatory cytokines produced by TDP-43–transfected or mock-transfected BV-2 cells. BV-2 cells were transiently transfected with pCMV–TDP-43^{WT}, pCMV–TDP-43^{A315T}, pCMV–TDP-43^{G348C}, or empty vector. 48 h after transfection and 12 h after 100-ng/ml LPS challenge, RNA extracted from various samples was subjected to real-time quantitative RT-PCR to determine the mRNA levels of various proinflammatory genes. As expected, there was a fourfold increase in mRNA levels of TNF after LPS stimulation of BV-2 cells compared with controls (Fig. 7 A). However, in LPS-treated cells transfected with WT TDP-43, there was an additional threefold (n = 5; $P < 0.05$) increase in TNF levels. TDP-43 harboring the A315T and G348C mutations had similar effects on boosting the levels of TNF upon LPS stimulation.

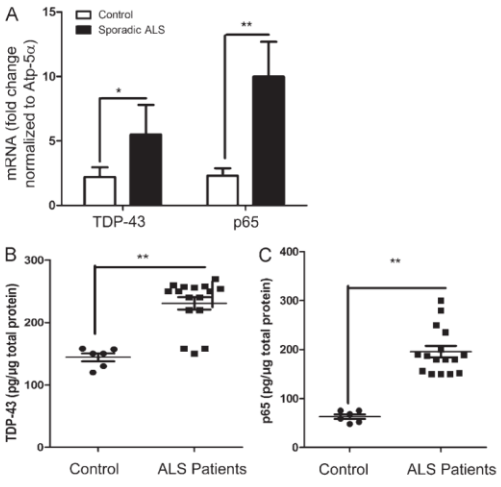

Figure 6. Analysis of TDP-43 and NF-κB p65 mRNA expression in sporadic ALS spinal cord. (A) Spinal cord tissue samples from 16 different sporadic ALS patients and 6 controls were subjected to real-time RT-PCR analysis using primers specific for TDP-43 (TARDBP) and p65 (RELA). All real-time RT-PCR values are normalized to Atp-5α levels. (B) Sandwich ELISA was performed for TDP-43 using TDP-43 monoclonal and polyclonal antibodies. After coating the ELISA plates with TDP-43 monoclonal antibody, the plates were incubated with the protein lysates (containing both soluble and insoluble fragments in between) followed by TDP-43 polyclonal antibody and subsequent detection. (C) For p65 ELISA, an ELISA kit from QIAGEN was used. (A–C) Statistical analysis was performed using the unpaired Student's t test with Welch's correction (*, $P < 0.01$; **, $P < 0.001$). Error bars represent mean ± SEM from three different experiments.

Similarly, in response to LPS, the extra levels of TDP-43 species in transfected microglial cells caused a significant fivefold increase (n = 5; $P < 0.001$) in the mRNA levels of IL-1β (Fig. 8 A) and ninefold increase in mRNA levels of IL-6 (n = 5; $P < 0.001$; Fig. 7 B) as compared with LPS-treated mock-transfected cells. The levels of NADPH oxidase 2 (Nox-2 gene) was increased by ∼2.8-fold (n = 5; $P < 0.05$; Fig. 8 B) in LPS-challenged TDP-43–transfected cells as compared with LPS-treated mock-transfected cells. Remarkably, overexpression of TDP-43 species resulted in a 10-fold (n = 5; $P < 0.001$) increase in levels of p65 (RELA) mRNA in LPS-treated transfected cells as compared with LPS-treated mock-transfected cells (Fig. 7 C). Note that, in the absence of LPS stimulation, microglial cells transfected with TDP-43 species (both WT and mutants) exhibited no significant differences in levels of TNF, IL-1β, Nox-2, and NF-κB when compared with mock-transfected controls.

To further evaluate the effect of LPS stimulation in TDP-43–overexpressing microglia, we prepared primary microglial cultures from C57BL/6 mice and from transgenic mice overexpressing TDP-43^{WT} by threefold. Primary microglial cells were challenged with LPS at a concentration of 100 ng/ml of media. 12 h after LPS challenge, cells were harvested, and total protein was extracted and used for multianalyte ELISA. LPS-treated TDP-43^{WT} transgenic microglia had significantly higher levels of TNF (2.5-fold; $P < 0.01$), IL-1β (2.3-fold; $P < 0.01$), IL-6 (twofold; $P < 0.05$), and IFN-γ (twofold; $P < 0.05$) as compared with LPS-treated microglia from C57BL/6 nontransgenic mice (Fig. 7 D). However, in the absence of LPS stimulation, no significant differences in cytokines levels were detected between microglia from TDP-43^{WT} transgenic mice and from nontransgenic mice (not depicted). The p65 level was significantly higher (threefold; $P < 0.01$) in LPS-treated TDP-43^{WT} microglia as compared with nontransgenic microglia (Fig. 7 D). We also treated primary microglial cultures with 1 mM H_2O_2 for 1 h (and incubated in serum-free media for 12 h) to study the effect of reactive oxygen species (ROS) on primary microglial cultures. H_2O_2-treated TDP-43^{WT} transgenic microglia had significantly higher levels of TNF (threefold; $P < 0.01$), IL-1β (2.5-fold; $P < 0.01$), IL-6 (1.7-fold; $P < 0.05$), IFN-γ (twofold; $P < 0.05$), and p65 (RELA) levels (2.2-fold; $P < 0.05$) when compared with H_2O_2-treated microglia from C57BL/6 nontransgenic mice (Fig. 7 E) as determined by multianalyte ELISA.

LPS stimulation of primary microglial cells caused degradation of IκB-α as shown in Fig. 7 G. The decrease in IκB-α levels was more pronounced in microglia overexpressing TDP-43 species. After LPS treatment, the increases in levels of p65, phospho-p65^{Ser536}, p50, and phospho-p50^{Ser337} were also more robust in transgenic microglia overexpressing TDP-43 species (Fig. 7 G). Similarly, H_2O_2 treatment led to a reduction in IκB-α levels and increase in levels of p65 and phospho-p65^{Ser536} in TDP-43^{WT} (Fig. 8 C). Again, the effects were more pronounced in transgenic microglia overexpressing TDP-43 species (Fig. 8 C). We then treated primary astrocytes with LPS and studied their

Published November 14, 2011

response to LPS using real-time RT-PCR. LPS-treated TDP-43^{WT} transgenic astrocytes had significantly higher levels of IL-α (1.75-fold; $P < 0.05$), IL-1β (1.67-fold; $P < 0.05$), IL-6 (2.8-fold; $P < 0.01$), IL-18 (1.8-fold; $P < 0.05$), and chemokines like CSF (1.6-fold; $P < 0.05$), CCL5 (1.9-fold; $P < 0.05$), and CXCL12 (2.67-fold; $P < 0.01$) as compared with LPS-treated microglia from C57BL/6 nontransgenic mice (Fig. 7 F).

To further evaluate the innate immune response in TDP-43^{WT} transgenic mice, we isolated BMMs from TDP-43^{WT} transgenic mice and from C57BL/6 nontransgenic mice. In LPS-stimulated TDP-43^{WT} macrophages, there

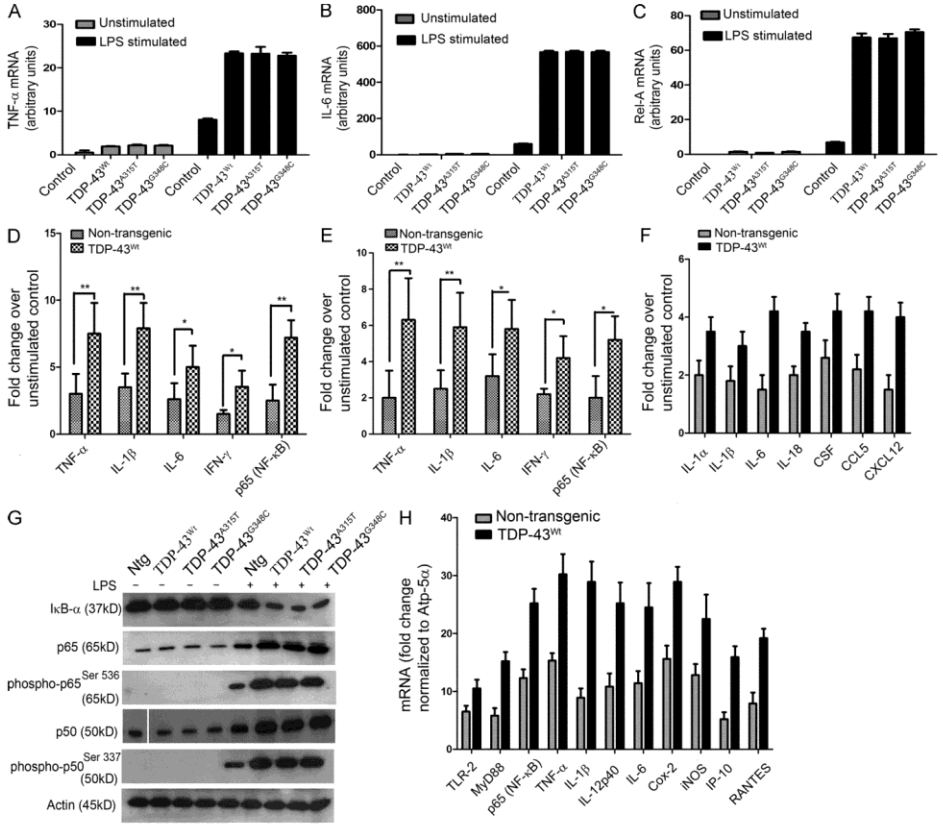

Figure 7. Analysis of genes involved in inflammation of mouse microglial and macrophage cells overexpressing human TDP-43. (A–C) Mouse microglial cells BV-2 were either transfected with pCMV–TDP-43^{WT}, pCMV–TDP-43^{A315T}, and pCMV–TDP-43^{G348C} or with empty vectors for 48 h. These cells were then either stimulated with LPS at a concentration of 100 ng/ml or unstimulated (as indicated). 12 h after stimulation, total RNA was extracted with TRIZOL. The total RNA samples were then subjected to real-time quantitative RT-PCR for TNF (A), IL-6 (B), and Rel-A (p65; C). Error bars represent mean ± SEM from five different experiments. (D) Primary microglial cultures from TDP-43^{WT} and B6 nontransgenic mice were stimulated with 100 ng/ml LPS. Proteins from LPS-stimulated microglial cultures were subjected to multianalyte ELISA for inflammatory cytokines and p65. Error bars represent mean ± SEM from four different experiments. (E) Primary microglial cultures from TDP-43^{WT} and B6 nontransgenic mice were treated with 1 mM H_2O_2 for 1 h and incubated in serum-free media for 12 h to study the effect of ROS. (F) Pure (>90%) primary astrocytes from TDP-43^{WT} and B6 nontransgenic mice were stimulated with LPS and their response studied using real-time PCR for various genes as indicated. (E and F) Error bars represent mean ± SEM from three different experiments. (G) Primary microglial cells from TDP-43^{WT}, TDP-43^{A315T}, TDP-43^{G348C}, and B6 nontransgenic mice (Ntg) were stimulated or unstimulated with LPS. Immunoblots were run to determine the levels of various proteins using specific antibodies as indicated. A representative blot from two independent experiments is shown. (H) BMMs isolated from TDP-43^{WT} and B6 nontransgenic mice were stimulated with 100 ng/ml LPS for 12 h. Total RNA samples were then subjected to real-time quantitative RT-PCR for various genes as indicated. Results are displayed as fold change over unstimulated control. All real-time RT-PCR values are normalized to Atp-5α levels. Error bars represent mean ± SEM from four different experiments. (A–F and H) Statistical analysis was performed by two-way ANOVA with Bonferroni adjustment (*, $P < 0.05$; **, $P < 0.01$).

Published November 14, 2011

JEM

was an increase of 1.6-fold ($P < 0.05$) in TLR2 mRNA levels, 1.8-fold ($P < 0.05$) in MyD88 levels, and 2.6-fold ($P < 0.01$) in p65 (RELA; $P < 0.01$) levels as compared with LPS-stimulated control (nontransgenic) macrophages (Fig. 7 H). We also found in LPS-stimulated TDP-43^{WT} macrophages that there was an increase of 3.2-fold ($P < 0.01$) in TNF, 3.5-fold in IL-1β ($P < 0.01$), and 2.6-fold in IL-12p40 levels, 2.5-fold ($P < 0.01$) in IL-6 levels, twofold ($P < 0.05$) in Cox-2 and iNOS levels, threefold in IP-10 levels ($P < 0.01$), and 2.1-fold in RANTES ($P < 0.05$) mRNA levels as compared with LPS-stimulated control (nontransgenic) macrophages (Fig. 7 H).

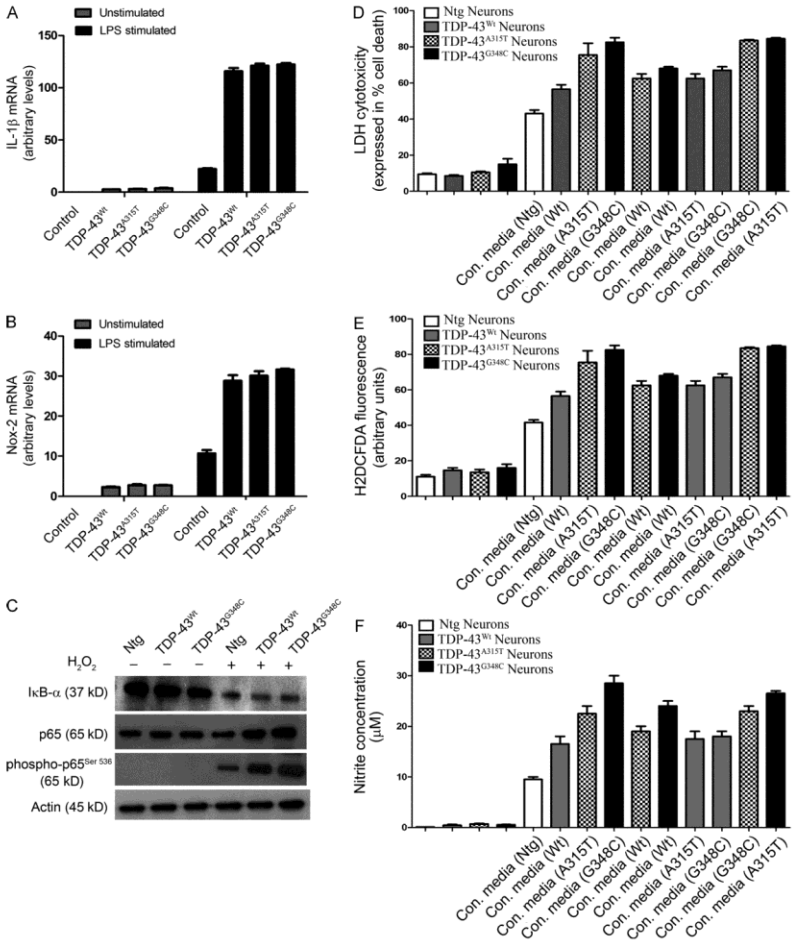

Figure 8. TDP-43 up-regulation enhances neuronal vulnerability to death by microglia-mediated cytotoxicity. (A and B) TDP-43 (WT and mutants)-transfected BV-2 cells were stimulated with LPS. 12 h after stimulation, total RNA was extracted with TRIZOL. The total RNA samples were then subjected to real-time quantitative RT-PCR for IL-1β (A) and Nox-2 (B). Error bars represent mean ± SEM from five different experiments. Statistical analysis was performed by two-way ANOVA with Bonferroni adjustment. (C) Primary microglial cells from TDP-43^{WT}, TDP-43^{A315T}, TDP-43^{G348C}, and B6 nontransgenic mice (Ntg) were stimulated or unstimulated with H_2O_2. Immunoblots were run to determine the levels of various proteins using specific antibodies as indicated. A representative blot from two independent experiments is shown. (D–F) Primary cortical neurons from TDP-43^{WT}, TDP-43^{A315T}, TDP-43^{G348C}, and control B6 nontransgenic mice were incubated with the conditioned media (con. media) derived from primary microglial cells treated with 100 ng/ml LPS. 12 h after challenging cortical cells, cell culture supernatants were used for LDH assay (D). ROS production was determined by H2D-CFDA fluorescence (E), and nitrite production was evaluated by Griess reagent (F). Error bars represent mean ± SEM from four independent experiments.

Published November 14, 2011

TDP-43 up-regulation increases microglia-mediated neurotoxicity

We then examined the effect of TDP-43 overexpression on toxicity of microglia toward neuronal cells. This was done with the use of primary microglia and of cortical neurons derived from transgenic mice overexpressing TDP-43 species (TDP-43^{WT}, TDP-43^{A315T}, or TDP-43^{G348C}) and C57BL/6 nontransgenic mice. Primary cortical neurons were cultured for 12 h in conditioned media from LPS-stimulated microglial cells. All conditioned media from LPS-challenged microglia increased the death of cortical neurons in culture (Fig. 8 D). The media from LPS-stimulated nontransgenic microglial cells increased the neuronal death of nontransgenic mice by 3.5-fold ($P < 0.01$). However, there were marked increases of neuronal death caused by conditioned media from LPS-challenged microglia (of same genotype) overexpressing TDP-43 species: 5.5-fold ($P < 0.001$) for TDP-43^{WT}, 6.5-fold ($P < 0.001$) for TDP-43^{A315T}, and 7.5-fold ($P < 0.001$) for TDP-43^{G348C}. The increased neurotoxicity of the conditioned media was associated with increased ROS and NO production. The ROS production, as determined by H2DCFDA fluorescence, was significantly higher in conditioned media–challenged neurons from TDP-43^{WT} (1.5-fold; $P < 0.05$), TDP-43^{A315T} (1.8-fold; $P < 0.05$), or TDP-43^{G348C} (twofold; $P < 0.05$) as compared individually with conditioned media–challenged nontransgenic control neurons (Fig. 8 E). Similarly, the nitrite (NO) production was significantly higher in TDP-43^{WT} (1.5-fold; $P < 0.05$), TDP-43^{A315T} (2.3-fold; $P < 0.05$), or TDP-43^{G348C} (threefold; $P < 0.01$) as compared individually with nontransgenic control (Fig. 8 F).

Inhibition of NF-κB activation reduces vulnerability of TDP-43–overexpressing neurons to toxic injury

The aforementioned experiments also revealed that the presence of TDP-43 transgenes in cortical neurons increased their vulnerability to microglia-mediated toxicity. NF-κB is known to modulate p53-p38MAPK–dependent apoptosis in neurons when treated with DNA damage–inducing chemicals like camptothecin (Aleyasin et al., 2004), glutamate excitotoxicity (Pizzi et al., 2005), or general bystander-mediated killing of neurons by microglia (Sephton et al., 2010). To assess the potential contribution of NF-κB to the death of TDP-43–overexpressing neurons exposed to toxic injury, we prepared cultures of primary cortical neurons and microglia from transgenic mice overexpressing TDP-43^{WT} or TDP-43 mutants. Cortical neurons were exposed to 10 µM glutamate for 15 min, with or without 1 µM Withaferin A (WA), a known inhibitor of NF-κB (Oh et al., 2008). The lactate dehydrogenase (LDH) cytotoxicity was determined 24 h later (see Fig. 10 A). We found that neurons overexpressing TDP-43 species were more vulnerable than nontransgenic neurons to glutamate cytotoxicity and that inhibition of NF-κB by WA resulted in a marked decrease in cell death: TDP-43^{WT} (twofold; $P < 0.01$), TDP-43^{A315T} (threefold; $P < 0.01$), and TDP-43^{G348C} (threefold; $P < 0.01$). The addition of WA inhibited NF-κB, as detected by reduced levels of phospho-$p65^{Ser536}$ (see Fig. 10 B). We then incubated cortical neurons with the conditioned media from primary microglial culture, which were challenged with LPS at a concentration of 100 ng/ml of media. Treatment of neuronal cultures with WA resulted in substantial decrease in microglia-mediated death of neurons overexpressing TDP-43^{WT} (twofold; $P < 0.01$), TDP-43^{A315T} (threefold; $P < 0.01$), or TDP-43^{G348C} (threefold; $P < 0.01$). As WA might exert multiple pharmacological actions, we tested a more specific molecular approach for inhibiting NF-κB. Because activation of NF-κB requires its dissociation from the inhibitory molecule, IκB, we expressed a stable mutant super-repressive form of IκB-α (Ser32/Ser36 to alanine mutant; $IκB^{SR}$) and evaluated its effects on neuronal death. Cultured cortical neurons from TDP-43 transgenic and nontransgenic mice were transfected with a plasmid construct, expressing $IκB^{SR}$, and exposed to either 10 µM glutamate for 30 min or incubated in conditioned media from LPS-stimulated microglia of the same genotype. Similar to WA treatment, we found that $IκB^{SR}$ inhibited NF-κB activation and it attenuated the glutamate-induced or microglia-mediated death of neurons overexpressing TDP-43^{WT} (1.3-fold; $P < 0.01$), TDP-43^{A315T} (1.5-fold; $P < 0.01$), and TDP-43^{G348C} (twofold; $P < 0.01$; Fig. 9, A and D).

NF-κB inhibition by WA treatment reduces inflammation and ameliorates motor impairment of TDP-43 transgenic mice

To study the in vivo effect of NF-κB inhibition on disease progression, we injected TDP-43^{WT};GFAP-luc double transgenic mice with 3 mg/kg body weight of WA twice a week for 10 wk starting at 30 wk. The pharmacokinetic parameters of WA have been published recently (Thaiparambil et al., 2011), and we have determined that this compound passes the blood–brain barrier (unpublished data). We used TDP-43^{WT};GFAP-luc double transgenic mice because the reporter luciferase allowed the longitudinal and noninvasive biophotonic imaging with charge-coupled device camera of the GFAP promoter activity, which is a target of activated NF-κB. To analyze the spatial and temporal dynamics of astrocyte activation/GFAP induction in the TDP-43 mouse model, we performed a series of live imaging experiments. These live imaging experiments revealed that treatment of TDP-43^{WT}; GFAP-luc mice with WA caused progressive reduction in GFAP-luc expression in the spinal (Fig. 9, B and C) compared with untreated TDP-43^{WT} mice, which continued to exhibit high GFAP-luc expression. The down-regulation of GFAP promoter activity was further confirmed in these mice using GFAP immunofluorescence of spinal cord sections of TDP-43^{WT} mice (both drug treated and untreated; Fig. 9 F). This down-regulation of GFAP in WA-treated mice was actually caused by a reduced amount of active p65 in the nucleus of cells as indicated by p65 EMSA (Fig. 10 C). Down-regulation of GFAP along with reduction in active p65 levels in WA-treated mice prompted us to analyze behavioral changes in these mice. Analysis of motor behavior using accelerating rotarod showed that WA-treated TDP-43^{WT} mice had significantly better motor performance compared with untreated TDP-43^{WT} mice as indicated by improved

Published November 14, 2011

JEM

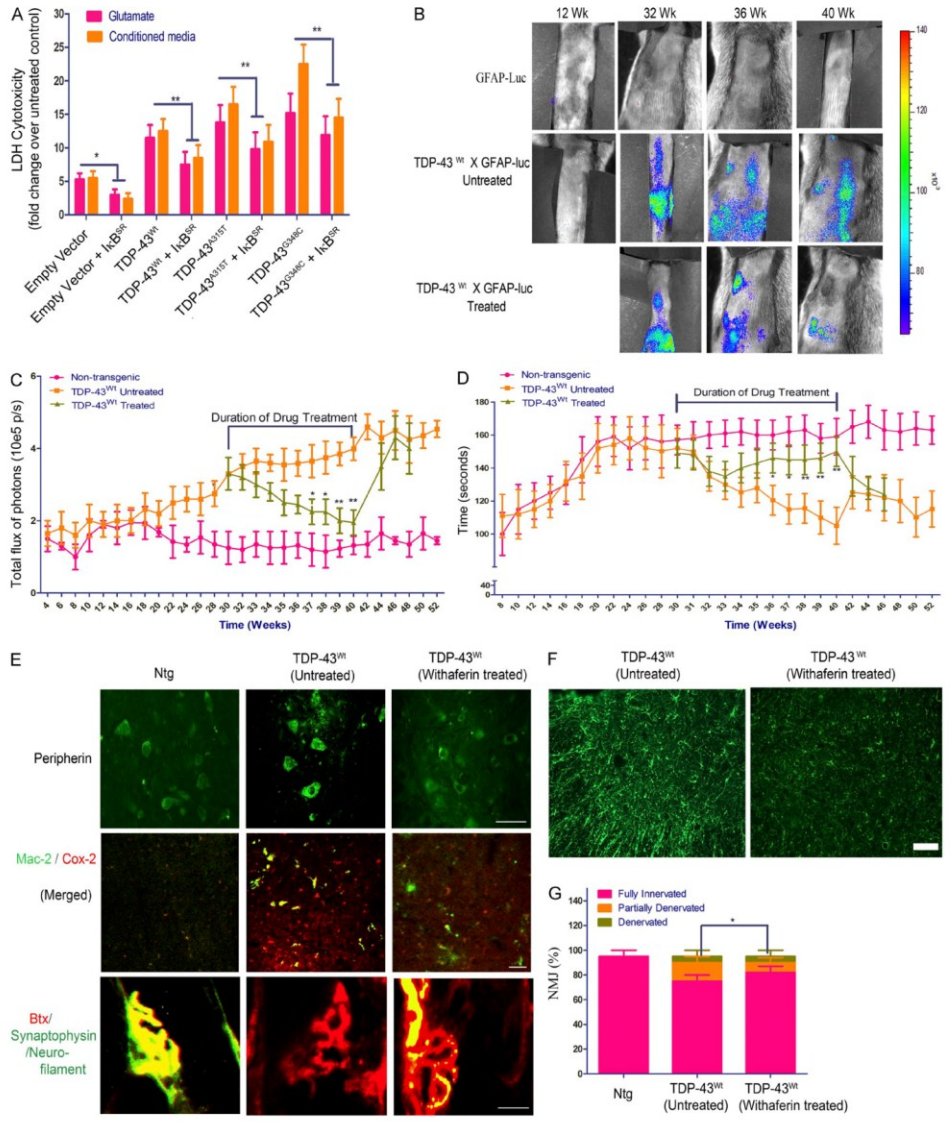

Figure 9. Inhibition of NF-κB reduces neuronal vulnerability to toxic injury and ameliorates disease phenotypes in TDP-43 transgenic mice. (A) A stable mutant super-repressive form of IκB-α (IκB^{SR}) was expressed, and its effects on neuronal death were evaluated. The phosphorylation-defective IκB-αS32A/S36A acts by sequestering the cytoplasmic NF-κB pool in a manner that is insensitive to extracellular stimuli. Cultured cortical neurons from TDP-43^{WT}, TDP-43^{A315T}, TDP-43^{G348C}, and B6 nontransgenic mice were transfected with a plasmid construct, expressing IκB^{SR}, and exposed to either 10 µM glutamate for 30 min or incubated in conditioned media from LPS-stimulated microglia of the same genotype. Cytotoxicity to the cells was measured by LDH assay using a commercially available kit. Statistical analysis was performed by two-way ANOVA with Bonferroni adjustment (*, $P < 0.05$; **, $P < 0.01$). Data represent mean ± SEM from three independent experiments. (B) In vivo bioluminescence imaging of astrocyte activation was analyzed at various time points in the spinal cord of GFAP-luc/TDP-43^{WT} mice. Typical sequence of images of the spinal cord area obtained from of GFAP-luc/TDP-43^{WT} mice at different time points (12, 32, 36, and 40 wk) by in vivo imaging ($n = 10$ each group). WA was injected in GFAP-luc/TDP-43^{WT} for 10 wk starting at

Published November 14, 2011

rotarod testing times (Fig. 9 D). We performed peripherin immunofluorescence and found reduction of peripherin aggregates in WA-treated TDP-43^{WT} mice (Fig. 9 E). Peripherin levels were also reduced in WA-treated TDP-43^{WT} mice as seen by immunoblot (Fig. 10 E). Double immunofluorescence of activated microglial marker Mac-2 and Cox-2 showed a marked reduction in activated microglia in WA-treated TDP-43^{WT} mice (Figs. 9 E and 10 F). The WA-treated mice also had a 40% reduction in the number of partially denervated neuromuscular junctions (NMJs; Fig. 9, E and G).

DISCUSSION

From the data presented in this study, we propose that a TDP-43 deregulation in ALS may contribute to pathogenic pathways through abnormal activation of p65 NF-κB. Several lines of evidence support this scheme: (a) proof of a direct interaction between TDP-43 and p65 NF-κB was provided by immunoprecipitation experiments using protein extracts from cultured cells, from TDP-43 transgenic mice, and from human ALS spinal cord samples; (b) reporter gene transcription assays and gel shift experiments demonstrated that TDP-43 was acting as a co-activator of p65 NF-κB through binding of its N-terminal and RRM-1 domains to p65; (c) the levels of mRNAs for both TDP-43 and p65 NF-κB were substantially elevated in the spinal cord of ALS subjects as compared with non-ALS subjects, whereas immunofluorescence microscopy of ALS spinal cord samples revealed an abnormal nuclear localization p65 NF-κB; (d) cell transfection experiments demonstrated that an overexpression of TDP-43 can provoke hyperactive innate immune responses with ensuing enhanced toxicity on neuronal cells, whereas in neurons TDP-43 overexpression increased their vulnerability to toxic environment; and (e) in vivo treatment of TDP-43 transgenic mice with an inhibitor of NF-κB reduced inflammation and ameliorated motor deficits.

This is the first report of an up-regulation of mRNAs encoding TDP-43 in postmortem frozen spinal cords of sporadic ALS. A recent study has provided evidence of increased TDP-43 immunodetection in the skin of ALS patients (Suzuki et al., 2010), but it failed to demonstrate whether this was caused by up-regulation in TDP-43 mRNA expression. The process that underlies a 2.5-fold increase in TDP-43 mRNA levels in ALS, whether it is transcriptional or mRNA stability, remains to be investigated. It seems unlikely that copy number variants could explain an increase of TDP-43 gene transcription as variations in copy number of *TARDBP* have not been detected in cohorts of ALS (Guerreiro et al., 2008; Bäumer et al., 2009; Gitcho et al., 2009). Actually, the pathogenic pathways of TDP-43 abnormalities in ALS are not well understood. To date, much attention has been focused on cytoplasmic C-terminal TDP-43 fragments that can elicit toxicity in cell culture systems (Johnson et al., 2008; Dormann et al., 2009; Igaz et al., 2009; Zhang et al., 2009b). However, it is noteworthy that neuronal overexpression at high levels of WT or mutant TDP-43 in transgenic mice caused a dose-dependent degeneration of cortical and spinal motor neurons but without massive cytoplasmic TDP-43 aggregates (Wils et al., 2010). This suggests that an up-regulation of TDP-43 in the nucleus rather than TDP-43 cytoplasmic aggregates may contribute to neurodegeneration in these mouse models. As shown in this study, an overexpression of TDP-43 can trigger pathogenic pathways via NF-κB activation.

The transcription factor NF-κB is a key regulator of hundreds of genes involved in innate immunity, cell survival, and inflammation. Because the nuclear translocation and DNA binding of NF-κB are not sufficient for gene induction (Yoza et al., 1996; Bergmann et al., 1998), it has been suggested that interactions with other protein molecules through the transactivation domain (Schmitz et al., 1995b; Gerritsen et al., 1997; Perkins et al., 1997) as well as its modification by phosphorylation (Schmitz et al., 1995a) might play a critical role. It has been reported that transcriptional activation of NF-κB requires multiple co-activator proteins including CBP (CREB-binding protein)/p300 (Gerritsen et al., 1997; Perkins et al., 1997), CBP-associated factor, and steroid receptor co-activator 1 (Sheppard et al., 1999). These co-activators have histone acetyltransferase activity to modify the chromatin structure and also provide molecular bridges to the basal transcriptional machinery. NF-κB p65 was also found to interact specifically with FUS (fused in sarcoma) protein, another DNA/RNA-binding protein

30 wk of age until 40 wk. Representative images are shown. (C) Longitudinal quantitative analysis of the total photon GFAP signal/ bioluminescence (total flux of photon/s) in WA-treated and untreated GFAP-luc/TDP-43^{WT} mice and control GFAP-luc mice in the spinal cord is displayed. Duration of drug treatment is indicated. (D) Accelerating rotarod analysis was performed in GFAP-luc/TDP-43^{WT} mice at various ages from 8 wk to 52 wk, and time taken by the mice to fall from the rotarod is used as rotarod performance. WA treatment period is marked as drug treatment period. (C and D) Asterisks represent a statistically significant difference between treated and untreated groups (*, $P < 0.05$; and **, $P < 0.01$) using repeated measures two-way ANOVA. (C and D) Error bars represent mean ± SEM ($n = 10$ each group). (E) Immunofluorescence of spinal cord sections of nontransgenic (Ntg; control), TDP-43^{WT} (untreated), and TDP-43^{WT} (WA treated) mice with polyclonal peripherin antibody is shown. Double immunofluorescence of spinal cord sections with activated microglial marker Mac-2 and Cox-2 is shown. Representative images from four different mice per genotype are shown. NMJ staining was performed using anti-synaptophysin/neurofilament antibodies (green) and α-bungarotoxin (BTX; red). Representative images from four different mice per genotype showing fully innervated muscle in 10-mo-old nontransgenic mice, fully denervated muscle in TDP-43^{WT} mice (untreated), and partially denervated muscle in age-matched WA-treated TDP-43^{WT} mice. (F) Immunofluorescence using GFAP antibody was performed in the spinal cord sections of WA-treated and untreated GFAP-luc/TDP-43^{WT} mice. Representative images from five different mice per genotype are shown. (G) 300 NMJs were counted per animal sample. Frequencies of innervation, partial denervation, and denervation were then converted to percentages and plotted as a graph. Statistical analysis was performed by the Student's *t* test. The asterisk represents a statistically significant difference between treated and untreated groups (*, $P < 0.01$) using repeated measures two-way ANOVA. Error bars represent mean ± SEM from three different experiments. Bars, 20 µm.

Published November 14, 2011

JEM

which is involved in ALS (Kwiatkowski et al., 2009; Vance et al., 2009; Deng et al., 2010).

Our results revealed robust effects of TDP-43 on the activation of NF-κB and innate immune responses. After transfection with TDP-43 species, microglial cells challenged with LPS exhibited much higher mRNA levels for proinflammatory cytokines, Nox-2, and NF-κB mRNA when compared with untransfected cells after LPS stimulation. TDP-43 overexpression makes microglia hyperactive to immune stimulation, resulting in enhanced toxicity toward neighboring neuronal cells with involvement of ROS and increased nitrite levels (NO). Moreover, the adverse effects of TDP-43 up-regulation are not limited to microglial cells. TDP-43 overexpression in transgenic astrocytes caused exaggerated responses to LPS (Fig. 7 F), whereas primary cortical neurons overexpressing TDP-43 transgenes by approximately threefold exhibited increased susceptibility to the toxic effects of excess glutamate or LPS-activated microglia (Figs. 8 D and 9 A).

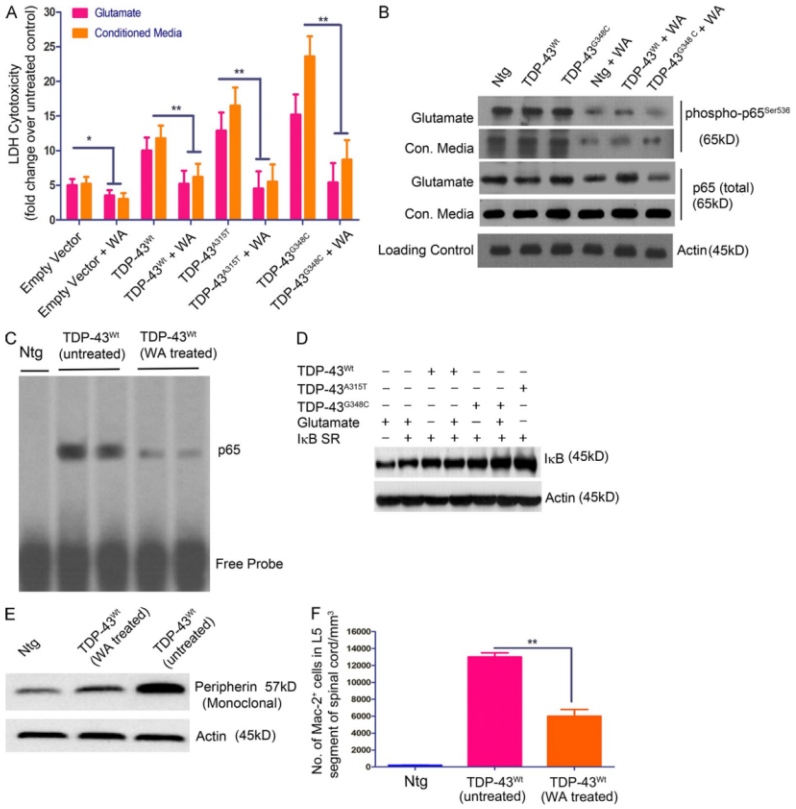

Figure 10. WA ameliorates TDP-43–mediated toxicity. (A) Primary cortical neurons from TDP-43^{WT}, TDP-43^{A315T}, TDP-43^{G348C}, and B6 nontransgenic mice were exposed to 10 µM glutamate for 15 min or incubated in conditioned media from LPS-stimulated microglia of the same genotype with or without 1 µM WA and were evaluated for LDH cytotoxicity 24 h later. Asterisks represent a statistically significant difference between treated and untreated groups (*, $P < 0.05$; and **, $P < 0.01$) using repeated measures two-way ANOVA. Error bars represent mean ± SEM from three independent experiments. (B) Protein samples from cortical neurons (isolated from TDP-43^{WT}, TDP-43^{A315T}, TDP-43^{G348C}, and B6 nontransgenic [Ntg] mice) were subjected to immunoblot against various antibodies as indicated. (C) p65 EMSA was performed on the spinal cord tissue nuclear lysates from WA-treated and untreated GFAP-luc/TDP-43^{WT} mice. A representative EMSA of two independent experiments is shown. (D) IκB levels were measured by Western blot analysis of the cell lysates from cortical neurons of various genotypes as indicated. Actin is shown as loading control. Various conditions are also shown. (E) Western blot analysis of spinal cord sections of nontransgenic (control), TDP-43^{WT} (untreated), and TDP-43^{WT} (WA treated) mice with monoclonal peripherin antibody. (D and E) A representative blot from two different experiments is shown. (F) Quantification of microglial Mac-2–positive cells in the spinal cord sections of nontransgenic (control), TDP-43^{WT} (untreated), and TDP-43^{WT} (WA treated) mice. Mac-2$^+$ cells in TDP-43^{WT} (untreated) L5 spinal cord, 13,000 ± 500/mm^3; and TDP-43^{WT} (WA treated) L5 spinal cord, 6,000 ± 300/mm^3 (**, $P < 0.001$). Error bars represent mean ± SEM for four mice of each genotype.

Published November 14, 2011

The presence of ALS-linked mutations in TDP-43 (A315T or G348C) did not affect the binding and activation of p65 NF-κB. This is not surprising because our deletion mutant analysis revealed that a region spanning part of the N-terminal domain and RRM-1 of TDP-43 is responsible for interaction with p65, whereas most TDP-43 mutations in ALS occur in the C-terminal domain, which is dispensable for p65 NF-κB activation (Fig. 4). In fact, our cytotoxicity assays with primary cells from TDP-43 transgenic mice revealed that, at similar levels of mRNA expression, the adverse effects of mutant TDP-43 were more pronounced than TDP-43^{WT}. These results could be explained by the observation that ALS-linked mutations in TDP-43 increase its protein stability (Ling et al., 2010). From the data presented here, we propose the involvement in ALS of a pathogenic pathway caused by nuclear increase in TDP-43 levels (Fig. 6). This scheme does not exclude adverse effects caused by cytoplasmic TDP-43 aggregates that might occur concomitantly or later on during the disease process. A recent TDP-43 study with *Drosophila melanogaster* suggested that the TDP-43 toxicity may occur in the absence of inclusions formation and that neurotoxicity requires the TDP-43 RNA–binding domain (Voigt et al., 2010). These results are consistent with our model of TDP-43 toxicity and with data demonstrating the interaction of TDP-43 with p65 via the RNA recognition motif RMM-1.

Our finding that TDP-43 acts as co-activator of p65 suggests a key role for NF-κB signaling in ALS pathogenesis. This is corroborated by the abnormal fourfold increase of p65 NF-κB mRNA in the spinal cord of human ALS (Fig. 6) and by the nuclear localization of p65 (Fig. 1 D and Fig. 2, insets). Remarkably, an overexpression of TDP-43 species by approximately threefold in transgenic mice (Swarup et al., 2011), at levels similar to the human ALS situation (2.5-fold), was sufficient to cause nuclear translocation of p65 NF-κB in the spinal cord during aging (Fig. 1 D). It should be noted that TDP-43 itself does not cause NF-κB activation (Fig. 7) and that it does not up-regulate p65. It seems that a second hit is required. For example, LPS or other inducers such as pathogen-associated molecular patterns can trigger through TLR signaling p65 NF-κB nuclear localization. Cytokines such as TNF and IL-1β can also trigger p65 activation. In ALS, the second hits triggering innate immune responses remain to be identified. There is recent evidence for involvement of LPS in ALS (Zhang et al., 2009a, 2011) and of endogenous retrovirus (HEVR-K) expression (Douville et al., 2011). In this study, we show that aging is associated with p65 nuclear translocation in the spinal cord of TDP-43 transgenic mice (Fig. S1 D), but the exact factors underlying this phenomenon remain to be defined

There is a recent report of mutations in the gene coding for vasolin-containing protein (VCP) associated with 1–2% of familial ALS cases (Johnson et al., 2010). It is well established that VCP is involved in the control of the NF-κB pathway through regulation of ubiquitin-dependent degradation of IκB-α. For instance, mutant VCP expression in mice resulted in increased TDP-43 levels and hyperactivation of NF-κB signaling (Badadani et al., 2010; Custer et al., 2010). Moreover, some ALS-linked mutations have been discovered in the gene coding for optineurin, a protein which activates the suppressor of NF-κB (Maruyama et al., 2010), further supporting a convergent NF-κB pathogenic pathway. Thus, the data presented in our paper as well as ALS-linked mutations in the VCP and optineurin genes (Badadani et al., 2010; Johnson et al., 2010; Maruyama et al., 2010) are all supporting a convergent NF-κB pathogenic pathway in ALS. Recently, the NF-κB signaling complex was identified as a major contributor of astrocyte mediated toxicity to motor neurons (Haidet-Phillips et al., 2011). In this study, we show that inhibitors of NF-κB activation are able to attenuate the vulnerability of cultured neurons overexpressing TDP-43 species to glutamate-induced or microglia-mediated toxicity. Moreover, pharmacological inhibition of NF-κB by WA treatment attenuated disease phenotypes in TDP-43 transgenic mice. From these results, we propose that NF-κB signaling should be considered as a potential therapeutic target in ALS treatment.

MATERIALS AND METHODS

Human subjects. The spinal cords of 16 subjects with sporadic ALS and 6 control cases were used in this study. The diagnosis of ALS was made on both clinical and pathological grounds. The ages at death ranged from 42 to 79 yr, and the duration of illness ranged from 21 to 48 mo (Table S3). TDP-43–positive inclusions were found in all ALS cases. We also used spinal cord samples from six neurologically normal individuals (normal controls), aged between 55 and 84 yr. For routine histological examination, the spinal cord of each subject was fixed with 10% buffered formalin for 3 wk and then embedded in paraffin; 4-µm-thick sections were cut and stained with hematoxylin. The use of the human tissue samples described in this article was performed in accordance to the Committee on Research Ethics of Enfant-Jesus Hospital.

Generation of TDP-43 transgenic mice. *TARDBP* (GenBank/EMBL/DDBJ accession no. NM_007375) was amplified by PCR from a human BAC clone (clone RPCI-11, clone number 829B14) along with the endogenous promoter (~4 kB). A315T and G348C mutations in TDP-43 were inserted using site-directed mutagenesis. The full-length genomic *TARDBP* (TDP-43^{WT} and TDP-43^{G348C}) was linearized by Swa1 restriction enzyme and 18-kb DNA fragment microinjected in 1-d-old mouse embryos (having a background of C3H × C57BL/6). The embryos were implanted in pseudo-pregnant mothers (having ICR CD1 background). Founders were bred with nontransgenic C57BL/6 mice to establish stable transgenic lines (Swarup et al., 2011). Transgene expression was analyzed in brain and spinal cord by real-time PCR and in brain, spinal cord, muscle, and liver by Western blotting using monoclonal human TDP-43 antibody (clone E2-D3; Abnova). All experimental procedures were approved by the Laval University Animal Care Ethics Committee and are in accordance with the Guide to the Care and Use of Experimental Animals of the Canadian Council on Animal Care.

WA treatment. WA (Enzo Life Sciences) was injected intraperitoneally twice a week for 10 consecutive weeks at 3 mg/kg body weight in 30-wk-old TDP-43^{WT} mice (n = 10). Age-matched control nontransgenic animals (n = 10) and TDP-43^{WT} (n = 10) littermates were injected twice a week with 0.9% saline intraperitoneally. All of the behavioral and imaging experiments were conducted in a double blind manner, and as such the experimenter had no knowledge of the drug treatment or the genotype of animals.

Plasmids. Mammalian expression vector plasmids pCMV-p65, pCMV-p50, and ICAM1–luc (positions −340 to −25) and luciferase reporter plasmids 4κB^{WT}-luc or 4κB^{mut}-luc, containing four tandem copies of the human immunodeficiency virus-κB sequence upstream of minimal SV40 promoter,

Published November 14, 2011

JEM

and mutant IκB-α ($IκB^{SR}$), containing Ser32 and Ser36 to alanine mutations, were gifts from the laboratory of M.J. Tremblay (Centre de Recherche du Centre Hospitalier Universitaire de Quebec, Quebec City, Quebec, Canada). To create a human pCMV–TDP-43, the cDNA library from human myeloid cells was amplified by PCR using primers as described in Table S1. These products were subcloned into TOPO vector (Invitrogen) and later digested with Kpn1–BamHI restriction enzymes and subcloned in frame into pcDNA3.0 vector to form pCMV–TDP-43^{WT}. The HA tag was later added by PCR. HA-tagged TDP-$43^{\Delta N}$, TDP-$43^{\Delta RRM-1}$, TDP-$43^{\Delta RRM-2}$, and TDP-$43^{\Delta C}$ deletion mutants were constructed by PCR amplification and cloned between Kpn1–BamHI sites using the primers described in Table S1. Point mutations (pCMV–TDP-43^{A315T} and pCMV–TDP-43^{G348C}) were inserted by PCR using site-directed mutagenesis.

Cell culture and transfection. Mouse microglial BV-2 and mouse neuroblastoma N2a cells were maintained in DME (Invitrogen) with 10% FBS and antibiotics. Cells were transfected using Lipofectamine 2000 transfection reagent (Invitrogen) according to the manufacturer's instructions. At 48 h after transfection, the cells were harvested, and the extracts were prepared for downstream assays.

Primary cell cultures. Primary microglial culture from brain tissues of neonatal (P0-P1) C57BL/6, TDP-43^{WT}, TDP-43^{A315T}, and TDP-43^{G348C} mice were prepared as described previously (Weydt et al., 2004). In brief, the brain tissues were stripped of their meninges and minced with scissors under a dissecting microscope in DME. After trypsinization (0.5% trypsin, 10 min, 37°C/5% CO_2), the tissue was triturated. The cell suspension was washed in culture medium for glial cells (DME supplemented with 10% FBS [Invitrogen], 1 mM L-glutamine, 1 mM Na pyruvate, 100 U/ml penicillin, and 100 mg/ml streptomycin) and cultured at 37°C/5% CO_2 in 75-cm^2 Falcon tissue culture flasks (BD) coated with 10 mg/ml poly-D-lysine (PDL; Sigma-Aldrich) in borate buffer (2.37 g borax and 1.55 g boric acid dissolved in 500 ml of sterile water, pH 8.4) for 1 h and then rinsed thoroughly with sterile, glass-distilled water. Half of the medium was changed after 6 h in culture and every second day thereafter, starting on day 2, for a total culture time of 10–14 d. Microglia were shaken off the primary mixed brain glial cell cultures (150 rpm, 37°C, 6 h) with maximum yields between days 12 and 16, seeded (10^5 cells per milliliter) onto PDL-pretreated 24-well plates (1 ml per well), and grown in culture medium for microglia (DME supplemented with 10% FBS, 1 mM L-glutamine, 1 mM Na pyruvate, 50 mM 2-mercaptoethanol, 100 U/ml penicillin, and 100 mg/ml streptomycin). The cells were allowed to adhere to the surface of a PDL-coated culture flask (30 min, 37°C/5% CO_2). After removal of primary microglial culture, the remaining cells were mainly astrocytes. Purity of the astrocytes was >90%. Astrocytes were maintained in a medium consisting of DME supplemented with 10% FBS, 1 mM L-glutamine, 1 mM Na pyruvate, 50 mM 2-mercaptoethanol, 100 U/ml penicillin, and 100 mg/ml streptomycin. Primary cortical cultures from brain tissues of gestation day 16 (E16) C57BL/6, TDP-43^{WT}, TDP-43^{A315T}, and TDP-43^{G348C} mice were prepared as described previously (Hilgenberg and Smith, 2007). In brief, dissociated cortical cells (2.5–3.5 hemispheres) were plated onto PDL-coated 24-well plates, containing DME supplemented with 20 mM glucose, 2 mM glutamine, 5% FBS, and 5% horse serum. Cytosine arabinoside was added 4–5 d after the plating to halt the growth of nonneuronal cells. Cultures were maintained at 37°C in a humidified CO_2 incubator and used for experiments between 14 and 21 d in vitro. Cells were treated with WA at a final concentration of 1 µM for 24 h. BMMs were isolated and cultured using established protocols as described previously (Davies and Gordon, 2005).

Coimmunoprecipitation and Western blot assays. After transfection of plasmids, BV-2 cells were cultured for 48 h and then harvested with lysis buffer (25 mM Hepes-NaOH, pH 7.9, 150 mM NaCl, 1.5 mM $MgCl_2$, 0.2 mM EDTA, 0.5% Triton X-100, 1 mM dithiothreitol, and protease inhibitor cocktail). Alternatively, spinal cords from TDP-43 transgenic mice or sporadic ALS subjects along with controls were lysed in the buffer. The lysate was incubated with 50 µl Dynabeads (protein G beads; Invitrogen), anti–TDP-43 polyclonal (ProteinTech), and anti-HA antibody (clone 3F10; Roche). After subsequent washing, the beads were incubated overnight at 4°C with 400 µg of cell lysate. Antibody-bound complexes were eluted by boiling in Laemmli sample buffer. Supernatants were resolved by 10% SDS-PAGE and transferred on nitrocellulose membrane (Bio-Rad Laboratories). The membrane was incubated with anti-p65 antibody, and immunoreactive proteins were visualized by chemiluminescence (PerkinElmer) as described previously (Dequen et al., 2008). In some cases, phospho-$p65^{Ser536}$ (Cell Signaling Technology) and phospho-$p50^{337}$ (Santa Cruz Biotechnology, Inc.) were used at a concentration of 1:1,000.

Mass spectrometer analysis. BV-2 microglial cells were transiently transfected with plasmid vector pCMV–TDP-43^{WT} coding for TDP-43^{WT} tagged with HA and subsequently treated with LPS. 48 h after transfection, the LPS-challenged BV-2 cells were then harvested, and cell extracts were coimmunoprecipitated with anti-HA antibody. Proteins were resolved in 4–20% Tris-glycine gels (Precast gels; Bio-Rad Laboratories) and stained with Sypro-Ruby (Bio-Rad Laboratories). Protein bands from the gel were excised and subjected to mass spectrometer analysis at the Proteomics Platform, Quebec Genomics Centre. The experiments were performed on a Thermo Surveyor MS pump connected to an LTQ linear ion trap mass spectrometer (Thermo Fisher Scientific) equipped with a nanoelectrospray ion source (Thermo Fisher Scientific). Scaffold (version 1.7; Proteome Software Inc.) was used to validate tandem mass spectrometry–based peptide and protein identifications. Peptide identifications were accepted if they could be established at >90.0% probability as specified by the Peptide Prophet algorithm (Keller et al., 2002).

Immunofluorescence microscopy. Cells were grown to 70% confluence on glass coverslips and fixed in 2% paraformaldehyde for 30 min. In some cases, BV-2 cells were transiently transfected with the pCMV-TDP-43^{WT} and pCMV-p65 vectors using the Lipofectamine 2000 reagent. After fixation with 4% paraformaldehyde, cells were washed in PBS, and permeabilized with 0.2% Triton X-100 in PBS for 15 min. After blocking coverslips with 5% normal goat serum for 1 h at room temperature, primary antibody incubations were performed in 1% normal goat serum in PBS overnight, followed by an appropriate Alexa Fluor 488 or 594 secondary antibody (Invitrogen) for 1 h at room temperature. Similar procedures were used for staining spinal cord sections from TDP-43 transgenic mice and sections of sporadic ALS cases. Cells were viewed using a 40× or 63× oil immersion objective on a DM5000B microscope (Leica).

Quantitative real-time RT-PCR. Real-time RT-PCR was performed with a LightCycler 480 (Roche) sequence detection system using LightCycler SYBR green I at the Quebec Genomics Centre. Total RNA was extracted from cell culture experiments using TRIZOL reagent (Invitrogen). Total RNA was treated with DNase (QIAGEN) to get rid of genomic DNA contaminations. Total RNA was the quantified using Nanodrop, and its purity was verified by Bioanalyzer 2100 (Agilent Technologies). Gene-specific primers were constructed using the GeneTools software (Biotools Inc.). Three genes, Atp5, Hprt1, and GAPDH, were used as internal control genes. The primers used for the analysis of genes are given in Table S2.

Cytotoxicity assay. N2a cells were transfected with pCMV–hTDP-43 (both WT and mutants). 48 h after transfection, cells were treated with the conditioned media derived from BV-2 cells, some of which were treated with LPS (0111:B4 serotype; Sigma-Aldrich). 24 h after challenging N2a cells, culture supernatants were assayed for CytoTox-ONE Homogeneous Membrane Integrity Assay (Promega), a fluorimetric assay which depends on the levels of LDH released as the result of cell death (Swarup et al., 2007a). The assay was performed according to the manufacturer's protocol. Fluorescence was measured using a SpectraMAX Gemini EM fluorescence plate reader (Molecular Devices) at an excitation wavelength of 560 nm and an emission wavelength of 590 nm. Similar techniques were used for primary cortical neurons derived from TDP-43 transgenic mice.

Published November 14, 2011

ELISA. The levels of TNF, IL-1β, IL-6, and IFN-γ were assayed by multi-analyte ELISA and MIX-N-MATCH ELISAarray kits (mouse inflammatory cytokine array; SABiosciences). Mouse p65 ELISA (Stressgen) and human p65 ELISA (SABiosciences) were performed according to manufacturer's instructions. For TDP-43 ELISA, we used the sandwich-ELISA protocol. In brief, ELISA plates were incubated in mouse monoclonal antibody against TDP-43 (clone E2-D3; Abnova) overnight, and the total protein extracts (both soluble and insoluble fractions) were incubated in precoated plates. A second TDP-43 polyclonal antibody (ProteinTech) was further added, and ELISA was performed as described previously (Kasai et al., 2009; Noto et al., 2011). The standard curve for the ELISA assay was performed with triplicate measurements using 100 µl/well of recombinant TDP-43 protein (molecular mass 54.3 kD, AAH01487, recombinant protein with GST tag; Abnova) solution at different concentrations (0.24, 0.48, 0.97, 1.9, 3.9, 7.8, 15.6, 31.2, 62.5, 125, 250, 500, 1,000, and 1,250 ng/ml) of the protein in PBS. The relative concentration estimates of TDP-43 were calculated according to each standard curve.

Nitrite and ROS assays. The cell culture supernatants from cortical neurons or N2a cells were assayed for nitrite concentration using Griess reagent (Invitrogen) as described previously (Swarup et al., 2007b). The supernatants were also assayed for ROS using H2DCFDA (Sigma-Aldrich).

EMSA. 48 h after transfection of CMV-p65 with pCMV–TDP-43^{WT} or pCMV–TDP-43^{G348C} and treatment with LPS, BV-2 cells were harvested, and nuclear extracts were prepared. Nuclear proteins were extracted using a protein extraction kit (Panomics) as per the manufacturer's instructions. Concentrations of nuclear proteins were determined on diluted samples using a Bradford assay (Bio-Rad Laboratories). Interaction between p65 in the protein extract and DNA probe was investigated using the EMSA kit (Panomics) as per the manufacturer's instructions. These nuclear extracts were incubated with NF-κB–binding site–specific oligonucleotides coated with streptavidin. EMSA was then performed using the NF-κB EMSA kit. For supershift assays, antibodies against p50, p65, or TDP-43 were added during the sample preparation step.

Reporter gene assays. BV-2 cells were harvested in 120 µl of cell lysis buffer (Promega), and an ensuing 1-min centrifugation step (20,000 *g*) yielded a luciferase-containing supernatant. In both cases, aliquots of 20-µl supernatant were tested for luciferase activity (luciferase assay kit; Promega) and for β-galactosidase activity (β-galactosidase assay kit; Promega) to adjust for transfection efficiency.

RNA interference. To selectively prevent TDP-43 expression, we used the RNA interference technology. A double-stranded RNA (siRNA) was used to degrade TDP-43 mRNA and thus to limit the available protein. The siRNA experiments were designed and conducted as described previously (Swarup et al., 2007a). The siRNAs directed against the murine TDP-43 mRNA (GenBank accession no. NM_145556.4) consisted of sequences with symmetrical 3′-UU overhangs using siRNA Target Finder (Invitrogen). The sequence of the most effective TDP-43 siRNAs represented is as follows: 5′-AGGAAUCAGCGUGCAUAUAUU-3′ and 5′-UAUAUGCACGCUGAUUCCUUU-3′. To account for the nonsequence-specific effects, scrambled siRNA was used. The sequence of scrambled siRNA is as follows: 5′-GUGCACAUGAGUGAGAUUU3′ and 5′-CACGUGUACUCACUCUAAA-3′. TDP-43 siRNAs or the scrambled siRNAs were suspended in diethyl pyro-carbonate water to yield the desired concentration. For in vitro transfection, cells were plated in 24-well plates and transfected with 0.6 µmol/l siRNAs with 2 µl Lipofectamine 2000. The cells were then kept for 72 h in OptiMEM medium (Invitrogen).

Accelerating rotarod. Accelerating rotarod was performed on mice at 4-rpm speed with 0.25-rpm/s acceleration as described previously (Gros-Louis et al., 2008). Mice were subjected to three trials per session and every 2 wk.

In vivo bioluminescence imaging. As previously described (Maysinger et al., 2007; Cordeau et al., 2008), the images were gathered using the IVIS 200 Imaging System (Caliper Life Sciences). 25 min before imaging session, the mice received intraperitoneal injection of the luciferase substrate D-luciferine (150 mg/kg for mice between 20 and 25 g, 150–187.5 ml of a solution of 20 mg/ml of D-luciferine dissolved in 0.9% saline was injected; Caliper Life Sciences).

Statistical analysis. For statistical analysis, the data obtained from independent experiments are presented as the mean ± SEM; they were analyzed using a paired Student's *t* test with Mann-Whitney test, one-way analysis of variance (ANOVA) with Kruskal-Wallis test, or two-way ANOVA with Bonferroni adjustment for multiple comparisons using Prism software version 5.0 (GraphPad Software). For rotarod and GFAP imaging experiments, repeated measures ANOVA was used. In some experiments, an unpaired Student's *t* test followed by a Welch's test was performed. Differences were considered significant at $P < 0.05$.

Online supplemental material. Fig. S1 demonstrates reverse immunoprecipitation of TDP-43 with p65 antibody and EMSA supershift assay and describes how p65 activation is age dependent in TDP-43^{WT} transgenic mice. Table S1 lists the primers used for TDP-43 cloning. Table S2 lists the primers used for quantitative R.T-PCR. Table S3 gives details of patients examined during the study. Online supplemental material is available at http://www.jem.org/cgi/content/full/jem.20111313/DC1.

We thank Christine Bareil and Genevieve Soucy for technical assistance. We are grateful to the laboratory of Dr. Michel J. Tremblay for p65, IκB^{SR}, and luciferase plasmids.

This work was supported by the Canadian Institutes of Health Research and Neuromuscular Research Partnership, the Robert Packard Center for ALS Research at Johns Hopkins and the Fondation André-Delambre. J.-P. Julien holds a Canada Research Chair Tier 1 in mechanisms of neurodegeneration. V. Swarup is the recipient of the Merit Scholarship for foreign students (Fonds Québécois de la Recherche sur la Nature et les Technologies, Quebec, Canada).

The authors have no conflicting financial interests.

Submitted: 28 June 2011
Accepted: 18 October 2011

REFERENCES

Aleyasin, H., S.P. Cregan, G. Iyirhiaro, M.J. O'Hare, S.M. Callaghan, R.S. Slack, and D.S. Park. 2004. Nuclear factor-(kappa)B modulates the p53 response in neurons exposed to DNA damage. *J. Neurosci.* 24:2963–2973. http://dx.doi.org/10.1523/JNEUROSCI.0155-04.2004

Arai, T., M. Hasegawa, H. Akiyama, K. Ikeda, T. Nonaka, H. Mori, D. Mann, K. Tsuchiya, M. Yoshida, Y. Hashizume, and T. Oda. 2006. TDP-43 is a component of ubiquitin-positive tau-negative inclusions in frontotemporal lobar degeneration and amyotrophic lateral sclerosis. *Biochem. Biophys. Res. Commun.* 351:602–611. http://dx.doi.org/10.1016/j.bbrc.2006.10.093

Badadani, M., A. Nalbandian, G.D. Watts, J. Vesa, M. Kitazawa, H. Su, J. Tanaja, E. Dec, D.C. Wallace, J. Mukherjee, et al. 2010. VCP associated inclusion body myopathy and paget disease of bone knock-in mouse model exhibits tissue pathology typical of human disease. *PLoS ONE.* 5:e13183. http://dx.doi.org/10.1371/journal.pone.0013183

Bäumer, D., N. Parkinson, and K. Talbot. 2009. TARDBP in amyotrophic lateral sclerosis: identification of a novel variant but absence of copy number variation. *J. Neurol. Neurosurg. Psychiatry.* 80:1283–1285. http://dx.doi.org/10.1136/jnnp.2008.166512

Bergmann, M., L. Hart, M. Lindsay, P.J. Barnes, and R. Newton. 1998. IkappaBalpha degradation and nuclear factor-kappaB DNA binding are insufficient for interleukin-1beta and tumor necrosis factor-alpha-induced kappaB-dependent transcription. Requirement for an additional activation pathway. *J. Biol. Chem.* 273:6607–6610. http://dx.doi.org/10.1074/jbc.273.12.6607

Boillée, S., C. Vande Velde, and D.W. Cleveland. 2006a. ALS: a disease of motor neurons and their nonneuronal neighbors. *Neuron.* 52:39–59. http://dx.doi.org/10.1016/j.neuron.2006.09.018

Boillée, S., K. Yamanaka, C.S. Lobsiger, N.G. Copeland, N.A. Jenkins, G. Kassiotis, G. Kollias, and D.W. Cleveland. 2006b. Onset and

Published November 14, 2011

JEM

progression in inherited ALS determined by motor neurons and microglia. *Science.* 312:1389–1392. http://dx.doi.org/10.1126/science.1123511

Chiang, P.M., J. Ling, Y.H. Jeong, D.L. Price, S.M. Aja, and P.C. Wong. 2010. Deletion of TDP-43 down-regulates Tbc1d1, a gene linked to obesity, and alters body fat metabolism. *Proc. Natl. Acad. Sci. USA.* 107: 16320–16324. http://dx.doi.org/10.1073/pnas.1002176107

Clement, A.M., M.D. Nguyen, E.A. Roberts, M.L. Garcia, S. Boillée, M. Rule, A.P. McMahon, W. Doucette, D. Siwek, R.J. Ferrante, et al. 2003. Wild-type nonneuronal cells extend survival of SOD1 mutant motor neurons in ALS mice. *Science.* 302:113–117. http://dx.doi.org/10.1126/science.1086071

Cordeau, P. Jr., M. Lalancette-Hébert, Y.C. Weng, and J. Kriz. 2008. Live imaging of neuroinflammation reveals sex and estrogen effects on astrocyte response to ischemic injury. *Stroke.* 39:935–942. http://dx.doi.org/10.1161/STROKEAHA.107.501460

Corrado, L., A. Ratti, C. Gellera, E. Buratti, B. Castellotti, Y. Carlomagno, N. Ticozzi, L. Mazzini, L. Testa, F. Taroni, et al. 2009. High frequency of TARDBP gene mutations in Italian patients with amyotrophic lateral sclerosis. *Hum. Mutat.* 30:688–694. http://dx.doi.org/10.1002/humu.20950

Custer, S.K., M. Neumann, H. Lu, A.C. Wright, and J.P. Taylor. 2010. Transgenic mice expressing mutant forms VCP/p97 recapitulate the full spectrum of IBMPFD including degeneration in muscle, brain and bone. *Hum. Mol. Genet.* 19:1741–1755. http://dx.doi.org/10.1093/hmg/ddq050

Daoud, H., P.N. Valdmanis, E. Kabashi, P. Dion, N. Dupré, W. Camu, V. Meininger, and G.A. Rouleau. 2009. Contribution of TARDBP mutations to sporadic amyotrophic lateral sclerosis. *J. Med. Genet.* 46:112–114. http://dx.doi.org/10.1136/jmg.2008.062463

Davies, J.Q., and S. Gordon. 2005. Isolation and culture of murine macrophages. *Methods Mol. Biol.* 290:91–103.

Deng, H.X., H. Zhai, E.H. Bigio, J. Yan, F. Fecto, K. Ajroud, M. Mishra, S. Ajroud-Driss, S. Heller, R. Sufit, et al. 2010. FUS-immunoreactive inclusions are a common feature in sporadic and non-SOD1 familial amyotrophic lateral sclerosis. *Ann. Neurol.* 67:739–748. http://dx.doi.org/10.1002/ana.22051

Dequen, F., P. Bomont, G. Gowing, D.W. Cleveland, and J.P. Julien. 2008. Modest loss of peripheral axons, muscle atrophy and formation of brain inclusions in mice with targeted deletion of gigaxonin exon 1. *J. Neurochem.* 107:253–264. http://dx.doi.org/10.1111/j.1471-4159.2008.05601.x

Dormann, D., A. Capell, A.M. Carlson, S.S. Shankaran, R. Rodde, M. Neumann, E. Kremmer, T. Matsuwaki, K. Yamanouchi, M. Nishihara, and C. Haass. 2009. Proteolytic processing of TAR DNA binding protein-43 by caspases produces C-terminal fragments with disease defining properties independent of progranulin. *J. Neurochem.* 110:1082–1094. http://dx.doi.org/10.1111/j.1471-4159.2009.06211.x

Douville, R., J. Liu, J. Rothstein, and A. Nath. 2011. Identification of active loci of a human endogenous retrovirus in neurons of patients with amyotrophic lateral sclerosis. *Ann. Neurol.* 69:141–151. http://dx.doi.org/10.1002/ana.22149

Dreyfuss, G., M.J. Matunis, S. Piñol-Roma, and C.G. Burd. 1993. hnRNP proteins and the biogenesis of mRNA. *Annu. Rev. Biochem.* 62:289–321. http://dx.doi.org/10.1146/annurev.bi.62.070193.001445

Gerritsen, M.E., A.J. Williams, A.S. Neish, S. Moore, Y. Shi, and T. Collins. 1997. CREB-binding protein/p300 are transcriptional coactivators of p65. *Proc. Natl. Acad. Sci. USA.* 94:2927–2932. http://dx.doi.org/10.1073/pnas.94.7.2927

Gitcho, M.A., R.H. Baloh, S. Chakraverty, K. Mayo, J.B. Norton, D. Levitch, K.J. Hatanpaa, C.L. White III, E.H. Bigio, R. Caselli, et al. 2008. TDP-43 A315T mutation in familial motor neuron disease. *Ann. Neurol.* 63:535–538. http://dx.doi.org/10.1002/ana.21344

Gitcho, M.A., E.H. Bigio, M. Mishra, N. Johnson, S. Weintraub, M. Mesulam, R. Rademakers, S. Chakraverty, C. Cruchaga, J.C. Morris, et al. 2009. TARDBP 3′-UTR variant in autopsy-confirmed frontotemporal lobar degeneration with TDP-43 proteinopathy. *Acta Neuropathol.* 118:633–645. http://dx.doi.org/10.1007/s00401-009-0571-7

Gros-Louis, F., J. Kriz, E. Kabashi, J. McDearmid, S. Millecamps, M. Urushitani, L. Lin, P. Dion, Q. Zhu, P. Drapeau, et al. 2008. Als2 mRNA splicing variants detected in KO mice rescue severe motor dysfunction phenotype in Als2 knock-down zebrafish. *Hum. Mol. Genet.* 17:2691–2702. http://dx.doi.org/10.1093/hmg/ddn171

Guerreiro, R.J., J.C. Schymick, C. Crews, A. Singleton, J. Hardy, and B.J. Traynor. 2008. TDP-43 is not a common cause of sporadic amyotrophic lateral sclerosis. *PLoS ONE.* 3:e2450. http://dx.doi.org/10.1371/journal.pone.0002450

Haidet-Phillips, A.M., M.E. Hester, C.J. Miranda, K. Meyer, L. Braun, A. Frakes, S. Song, S. Likhite, M.J. Murtha, K.D. Foust, et al. 2011. Astrocytes from familial and sporadic ALS patients are toxic to motor neurons. *Nat. Biotechnol.* 29:824–828. http://dx.doi.org/10.1038/nbt.1957

Hilgenberg, L.G., and M.A. Smith. 2007. Preparation of dissociated mouse cortical neuron cultures. *J. Vis. Exp.* 2007:562.

Horvath, R.J., N. Nutile-McMenemy, M.S. Alkaitis, and J.A. Deleo. 2008. Differential migration, LPS-induced cytokine, chemokine, and NO expression in immortalized BV-2 and HAPI cell lines and primary microglial cultures. *J. Neurochem.* 107:557–569. http://dx.doi.org/10.1111/j.1471-4159.2008.05633.x

Igaz, L.M., L.K. Kwong, A. Chen-Plotkin, M.J. Winton, T.L. Unger, Y. Xu, M. Neumann, J.Q. Trojanowski, and V.M. Lee. 2009. Expression of TDP-43 C-terminal fragments in vitro recapitulates pathological features of TDP-43 proteinopathies. *J. Biol. Chem.* 284:8516–8524. http://dx.doi.org/10.1074/jbc.M809462200

Johnson, B.S., J.M. McCaffery, S. Lindquist, and A.D. Gitler. 2008. A yeast TDP-43 proteinopathy model: Exploring the molecular determinants of TDP-43 aggregation and cellular toxicity. *Proc. Natl. Acad. Sci. USA.* 105:6439–6444. http://dx.doi.org/10.1073/pnas.0802082105

Johnson, J.O., J. Mandrioli, M. Benatar, Y. Abramzon, V.M. Van Deerlin, J.Q. Trojanowski, J.R. Gibbs, M. Brunetti, S. Gronka, J. Wuu, et al. 2010. Exome sequencing reveals VCP mutations as a cause of familial ALS. *Neuron.* 68:857–864. http://dx.doi.org/10.1016/j.neuron.2010.11.036

Kabashi, E., P.N. Valdmanis, P. Dion, D. Spiegelman, B.J. McConkey, C. Vande Velde, J.P. Bouchard, L. Lacomblez, K. Pochigaeva, F. Salachas, et al. 2008. TARDBP mutations in individuals with sporadic and familial amyotrophic lateral sclerosis. *Nat. Genet.* 40:572–574. http://dx.doi.org/10.1038/ng.132

Kasai, T., T. Tokuda, N. Ishigami, H. Sasayama, P. Foulds, D.J. Mitchell, D.M. Mann, D. Allsop, and M. Nakagawa. 2009. Increased TDP-43 protein in cerebrospinal fluid of patients with amyotrophic lateral sclerosis. *Acta Neuropathol.* 117:55–62. http://dx.doi.org/10.1007/s00401-008-0456-1

Keller, A., A.I. Nesvizhskii, E. Kolker, and R. Aebersold. 2002. Empirical statistical model to estimate the accuracy of peptide identifications made by MS/MS and database search. *Anal. Chem.* 74:5383–5392. http://dx.doi.org/10.1021/ac025747h

Kwiatkowski, T.J. Jr., D.A. Bosco, A.L. Leclerc, E. Tamrazian, C.R. Vanderburg, C. Russ, A. Davis, J. Gilchrist, E.J. Kasarskis, T. Munsat, et al. 2009. Mutations in the FUS/TLS gene on chromosome 16 cause familial amyotrophic lateral sclerosis. *Science.* 323:1205–1208. http://dx.doi.org/10.1126/science.1166066

Ling, S.C., C.P. Albuquerque, J.S. Han, C. Lagier-Tourenne, S. Tokunaga, H. Zhou, and D.W. Cleveland. 2010. ALS-associated mutations in TDP-43 increase its stability and promote TDP-43 complexes with FUS/TLS. *Proc. Natl. Acad. Sci. USA.* 107:13318–13323. http://dx.doi.org/10.1073/pnas.1008227107

Maruyama, H., H. Morino, H. Ito, Y. Izumi, H. Kato, Y. Watanabe, Y. Kinoshita, M. Kamada, H. Nodera, H. Suzuki, et al. 2010. Mutations of optineurin in amyotrophic lateral sclerosis. *Nature.* 465:223–226. http://dx.doi.org/10.1038/nature08971

Maysinger, D., M. Behrendt, M. Lalancette-Hébert, and J. Kriz. 2007. Real-time imaging of astrocyte response to quantum dots: in vivo screening model system for biocompatibility of nanoparticles. *Nano Lett.* 7:2513–2520. http://dx.doi.org/10.1021/nl071611t

Neumann, M., D.M. Sampathu, L.K. Kwong, A.C. Truax, M.C. Micsenyi, T.T. Chou, J. Bruce, T. Schuck, M. Grossman, C.M. Clark, et al. 2006. Ubiquitinated TDP-43 in frontotemporal lobar degeneration and amyotrophic lateral sclerosis. *Science.* 314:130–133. http://dx.doi.org/10.1126/science.1134108

Published November 14, 2011

Noto, Y.I., K. Shibuya, Y. Sato, K. Kanai, S. Misawa, S. Sawai, M. Mori, T. Uchiyama, S. Isose, S. Nasu, et al. 2011. Elevated CSF TDP-43 levels in amyotrophic lateral sclerosis: specificity, sensitivity, and a possible prognostic value. *Amyotroph. Lateral Scler.* 12:140–143. http://dx.doi.org/10.3109/17482968.2010.541263

Oh, J.H., T.J. Lee, J.W. Park, and T.K. Kwon. 2008. Withaferin A inhibits iNOS expression and nitric oxide production by Akt inactivation and down-regulating LPS-induced activity of NF-kappaB in RAW 264.7 cells. *Eur. J. Pharmacol.* 599:11–17. http://dx.doi.org/10.1016/j.ejphar.2008.09.017

Perkins, N.D., L.K. Felzien, J.C. Betts, K. Leung, D.H. Beach, and G.J. Nabel. 1997. Regulation of NF-kappaB by cyclin-dependent kinases associated with the p300 coactivator. *Science.* 275:523–527. http://dx.doi.org/10.1126/science.275.5299.523

Pizzi, M., I. Sarnico, F. Boroni, A. Benetti, M. Benarese, and P.F. Spano. 2005. Inhibition of IkappaBalpha phosphorylation prevents glutamate-induced NF-kappaB activation and neuronal cell death. *Acta Neurochir. Suppl. (Wien).* 93:59–63. http://dx.doi.org/10.1007/3-211-27577-0_8

Schmitz, M.L., M.A. dos Santos Silva, and P.A. Baeuerle. 1995a. Transactivation domain 2 (TA2) of p65 NF-kappa B. Similarity to TA1 and phorbol ester-stimulated activity and phosphorylation in intact cells. *J. Biol. Chem.* 270:15576–15584. http://dx.doi.org/10.1074/jbc.270.26.15576

Schmitz, M.L., G. Stelzer, H. Altmann, M. Meisterernst, and P.A. Baeuerle. 1995b. Interaction of the COOH-terminal transactivation domain of p65 NF-kappa B with TATA-binding protein, transcription factor IIB, and coactivators. *J. Biol. Chem.* 270:7219–7226. http://dx.doi.org/10.1074/jbc.270.13.7219

Sephton, C.F., S.K. Good, S. Atkin, C.M. Dewey, P. Mayer III, J. Herz, and G. Yu. 2010. TDP-43 is a developmentally regulated protein essential for early embryonic development. *J. Biol. Chem.* 285:6826–6834. http://dx.doi.org/10.1074/jbc.M109.061846

Seyfried, N.T., Y.M. Gozal, E.B. Dammer, Q. Xia, D.M. Duong, D. Cheng, J.J. Lah, A.I. Levey, and J. Peng. 2010. Multiplex SILAC analysis of a cellular TDP-43 proteinopathy model reveals protein inclusions associated with SUMOylation and diverse polyubiquitin chains. *Mol. Cell. Proteomics.* 9:705–718. http://dx.doi.org/10.1074/mcp.M800390-MCP200

Sheppard, K.A., D.W. Rose, Z.K. Haque, R. Kurokawa, E. McInerney, S. Westin, D. Thanos, M.G. Rosenfeld, C.K. Glass, and T. Collins. 1999. Transcriptional activation by NF-kappaB requires multiple coactivators. *Mol. Cell. Biol.* 19:6367–6378.

Sreedharan, J., I.P. Blair, V.B. Tripathi, X. Hu, C. Vance, B. Rogelj, S. Ackerley, J.C. Durnall, K.L. Williams, E. Buratti, et al. 2008. TDP-43 mutations in familial and sporadic amyotrophic lateral sclerosis. *Science.* 319:1668–1672. http://dx.doi.org/10.1126/science.1154584

Stallings, N.R., K. Puttaparthi, C.M. Luther, D.K. Burns, and J.L. Elliott. 2010. Progressive motor weakness in transgenic mice expressing human TDP-43. *Neurobiol. Dis.* 40:404–414. http://dx.doi.org/10.1016/j.nbd.2010.06.017

Suzuki, M., H. Mikami, T. Watanabe, T. Yamano, T. Yamazaki, M. Nomura, K. Yasui, H. Ishikawa, and S. Ono. 2010. Increased expression of TDP-43 in the skin of amyotrophic lateral sclerosis. *Acta Neurol. Scand.* 122:367–372. http://dx.doi.org/10.1111/j.1600-0404.2010.01321.x

Swarup, V., S. Das, S. Ghosh, and A. Basu. 2007a. Tumor necrosis factor receptor-1-induced neuronal death by TRADD contributes to the pathogenesis of Japanese encephalitis. *J. Neurochem.* 103:771–783. http://dx.doi.org/10.1111/j.1471-4159.2007.04790.x

Swarup, V., J. Ghosh, R. Duseja, S. Ghosh, and A. Basu. 2007b. Japanese encephalitis virus infection decrease endogenous IL-10 production: correlation with microglial activation and neuronal death. *Neurosci. Lett.* 420:144–149. http://dx.doi.org/10.1016/j.neulet.2007.04.071

Swarup, V., D. Phaneuf, C. Bareil, J. Robertson, G.A. Rouleau, J. Kriz, and J.P. Julien. 2011. Pathological hallmarks of amyotrophic lateral sclerosis/frontotemporal lobar degeneration in transgenic mice produced with TDP-43 genomic fragments. *Brain.* 134:2610–2626. http://dx.doi.org/10.1093/brain/awr159

Thaiparambil, J.T., L. Bender, T. Ganesh, E. Kline, P. Patel, Y. Liu, M. Tighiouart, P.M. Vertino, R.D. Harvey, A. Garcia, and A.I. Marcus. 2011. Withaferin A inhibits breast cancer invasion and metastasis at sub-cytotoxic doses by inducing vimentin disassembly and serine 56 phosphorylation. *Int. J. Cancer.* 129:2744–2755. http://dx.doi.org/10.1002/ijc.25938

Van Deerlin, V.M., J.B. Leverenz, L.M. Bekris, T.D. Bird, W. Yuan, L.B. Elman, D. Clay, E.M. Wood, A.S. Chen-Plotkin, M. Martinez-Lage, et al. 2008. TARDBP mutations in amyotrophic lateral sclerosis with TDP-43 neuropathology: a genetic and histopathological analysis. *Lancet Neurol.* 7:409–416. http://dx.doi.org/10.1016/S1474-4422(08)70071-1

Vance, C., B. Rogelj, T. Hortobágyi, K.J. De Vos, A.L. Nishimura, J. Sreedharan, X. Hu, B. Smith, D. Ruddy, P. Wright, et al. 2009. Mutations in FUS, an RNA processing protein, cause familial amyotrophic lateral sclerosis type 6. *Science.* 323:1208–1211. http://dx.doi.org/10.1126/science.1165942

Voigt, A., D. Herholz, F.C. Fiesel, K. Kaur, D. Müller, P. Karsten, S.S. Weber, P.J. Kahle, T. Marquardt, and J.B. Schulz. 2010. TDP-43-mediated neuron loss in vivo requires RNA-binding activity. *PLoS ONE.* 5:e12247. http://dx.doi.org/10.1371/journal.pone.0012247

Wegorzewska, I., S. Bell, N.J. Cairns, T.M. Miller, and R.H. Baloh. 2009. TDP-43 mutant transgenic mice develop features of ALS and frontotemporal lobar degeneration. *Proc. Natl. Acad. Sci. USA.* 106:18809–18814. http://dx.doi.org/10.1073/pnas.0908767106

Weydt, P., E.C. Yuen, B.R. Ransom, and T. Möller. 2004. Increased cytotoxic potential of microglia from ALS-transgenic mice. *Glia.* 48:179–182. http://dx.doi.org/10.1002/glia.20062

Wils, H., G. Kleinberger, J. Janssens, S. Pereson, G. Joris, I. Cuijt, V. Smits, C. Ceuterick-de Groote, C. Van Broeckhoven, and S. Kumar-Singh. 2010. TDP-43 transgenic mice develop spastic paralysis and neuronal inclusions characteristic of ALS and frontotemporal lobar degeneration. *Proc. Natl. Acad. Sci. USA.* 107:3858–3863. http://dx.doi.org/10.1073/pnas.0912417107

Xu, Y.F., T.F. Gendron, Y.J. Zhang, W.L. Lin, S. D'Alton, H. Sheng, M.C. Casey, J. Tong, J. Knight, X. Yu, et al. 2010. Wild-type human TDP-43 expression causes TDP-43 phosphorylation, mitochondrial aggregation, motor deficits, and early mortality in transgenic mice. *J. Neurosci.* 30:10851–10859. http://dx.doi.org/10.1523/JNEUROSCI.1630-10.2010

Yoza, B.K., J.Y. Hu, and C.E. McCall. 1996. Protein-tyrosine kinase activation is required for lipopolysaccharide induction of interleukin 1beta and NFkappaB activation, but not NFkappaB nuclear translocation. *J. Biol. Chem.* 271:18306–18309. http://dx.doi.org/10.1074/jbc.271.31.18306

Zhang, R., R.G. Miller, R. Gascon, S. Champion, J. Katz, M. Lancero, A. Narvaez, R. Honrada, D. Ruvalcaba, and M.S. McGrath. 2009a. Circulating endotoxin and systemic immune activation in sporadic amyotrophic lateral sclerosis (sALS). *J. Neuroimmunol.* 206:121–124. http://dx.doi.org/10.1016/j.jneuroim.2008.09.017

Zhang, R., K.G. Hadlock, H. Do, S. Yu, R. Honrada, S. Champion, D. Forshew, C. Madison, J. Katz, R.G. Miller, and M.S. McGrath. 2011. Gene expression profiling in peripheral blood mononuclear cells from patients with sporadic amyotrophic lateral sclerosis (sALS). *J. Neuroimmunol.* 230:114–123. http://dx.doi.org/10.1016/j.jneuroim.2010.08.012

Zhang, Y.J., Y.F. Xu, C. Cook, T.F. Gendron, P. Roettges, C.D. Link, W.L. Lin, J. Tong, M. Castanedes-Casey, P. Ash, et al. 2009b. Aberrant cleavage of TDP-43 enhances aggregation and cellular toxicity. *Proc. Natl. Acad. Sci. USA.* 106:7607–7612. http://dx.doi.org/10.1073/pnas.0900688106